ELBOW JOINT PROSTHESIS DESIGN:

BIOMECHANICAL ASPECTS

Thesis presented for

The Degree of Doctor of Philosophy in Bioengineering

from

The University of Strathclyde

by

Alexander C. Nicol, B.Sc.

February, 1977

to:

Sheila

ABSTRACT

A three-dimensional biomechanical analysis of elbow joint function is presented. Eating, dressing, pulling a heavy object and assisted standing from the seated position were investigated for healthy males in the age group 21-25 years. Three cine cameras recorded the motion of specially designed markers taped to the upper limb and the forces transmitted between the hand and the environment were measured using a versatile force transducer. Muscle activity was recorded electromyographically.

A simplified model of the anatomical structures of the elbow joint was formulated and four computer programs were developed for the subsequent calculation of muscle, ligament and joint forces. Calculations showed that during the eating and dressing activities, compressive loads of 300 N were acting on the trochlear notch and in the other activities, the joint forces maximum values were 2000 N.

Using several of the results from the theoretical analysis, a set of design criteria was established in connection with the development of a new elbow prosthesis. A detailed study of the geometry of the articular surfaces of the elbow was undertaken and a large series of X-rays was measured in order to determine the geometrical configuration of the distal humerus and the proximal ulna. Chapter 9 contains a full report on the design study and some of the more important aspects of the prototype prosthesis are discussed.

ACKNOWLEDGEMENTS

The work presented in this thesis was carried out in the laboratories of the Bioengineering Unit, University of Strathclyde and I am very grateful to Professor R.M. Kenedi for the use of these facilities.

Professor J.P. Paul initiated and supervised the project and I am grateful for his constructive criticism and advice throughout the project.

Thanks are also due to Mr W.A. Souter of Princess Margaret Rose Orthopaedic Hospital, Edinburgh for his professional advice during the design and development of the elbow prosthesis.

I am especially grateful to Dr. N. Berme for his guidance and assistance which contributed to the final form of the work.

The computer processing of the large amount of numerical data was undertaken with the excellent help of my wife, Sheila. It is also a pleasure to record my gratitude to Ms M. Jordan who assisted in the processing of analogue signals from the force transducer.

I would also like to thank Ms J.M. Bowen for her assistance in the preparation of diagrams for this thesis: Mr A.J. Tullis for his help and good humour during the acquisition of the cine film records: Mr D. Smith for his assistance during the mechanical testing of bone specimens: and my friends and colleagues who kindly volunteered as test subjects.

The project was financed by the Arthritis and Rheumatism Council to whom I am particularly indebted.

Finally I would like to thank Mrs L. Peedle who effectively typed this thesis.

CONTENTS

NOTATION INDEX

A	Inclination of Y_u to $Y_g - Z_g$ plane.
AREAL, AREAM	Trochlear notch contact areas.
B	Inclination of Y_u to $Z_g - X_g$ plane.
$BA_{x,y,z}$	"Joint" coordinates of brachioradialis insertion.
$BI_{x,y,z}$	"Joint" coordinates of biceps insertion.
$BR_{x,y,z}$	"Joint" coordinates of brachialis insertion.
BT	M-L thickness of upper arm.
C	Inclination of Y_u to $X_g - Y_g$ plane.
CG	"Centre of Gravity" of forearm + hand + ball.
CM	"Centre of Gravity" of forearm + hand.
D	A-P "diameter" of gleno-humeral joint.
DFL	Resultant joint force on lateral trochlear notch.
DFM	Resultant joint force on medial trochlear notch.
DIFF	Residual force in Z_i direction.
EB	Distance between EC and ball centre.
EC	"Centre" of the elbow joint.
EL	Distance from base of olecranon to EC.
EP	Epicondylar width.
F	Force.
F_{ba}	Force produced in brachioradialis muscle.
F_{bi}	Force produced in biceps muscle.
F_{br}	Force produced in brachialis muscle.
F_L	Lateral joint force ($Y_i - Z_i$ plane).
F_M	Medial joint force ($Y_i - Z_i$ plane).
F_{rad}	Radial head contact force ($Y_i - Z_i$ plane).
F_{tr}	Force produced in triceps muscle.
FB	Overall length of forearm plus hand.
$FG_{ux,uy,uz}$	Ulnar components of gravitational forces.
$FP_{ux,uy,uz}$	Ulnar components of transducer forces.
g	"gravity" or subscript for "grid" axis system.

h	Subscript for "humeral" axis system.
I	Moment of inertia.
I_{tot}	Moment of inertia of forearm assembly.
i	Subscript for "joint" axis system.
KL	Radius of gyration of forearm + hand.
l_1	Distance between EC and CM.
l_2	As for EB.
LEQ	Distance between EC and CG.
LGXX	Direction cosine - see section 6.6.
M	Mass.
M	Moment.
M	"Centre" of lead ball.
M_1	Mass of forearm + hand.
M_2	Mass of lead ball.
MGXX	Direction cosine - see section 6.6.
MT	Total body mass.
NGXX	Direction cosine - see section 6.6.
p	Subscript for "transducer" axis system.
P	"Centre" of transducer.
P_L	Pressure on lateral surface of trochlear notch.
P_M	Pressure on medial surface of trochlear notch.
R_L	Lateral joint force (Y_i - Z_i plane).
R_M	Medial joint force (Y_i - Z_i plane).
R_{x1}	Distance from grid origin to left camera lens.
R_{x2}	Distance from grid origin to right camera lens.
R_z	Distance from grid origin to front camera lens.
SS	"Centre" of shoulder joint.
$\theta_{x,y,z}$	Inclination of forearm to grid axes.
T_L	Tension developed in the lateral ligament.
T_M	Tension developed in the medial ligament.

$TI_{x,y,z}$	"Joint" coordinates of triceps insertion.
$TL_{x,y,z}$	"Joint" coordinates of insertion of lateral ligament.
$TM_{x,y,z}$	"Joint" coordinates of insertion of medial ligament.
u	Subscript for "ulnar" axis system.
W	Thickness of wrist.
W	"Centre" of wrist (distal ulna).
X_{1-14}	Grid coordinates of marker points.
X_h, Y_h, Z_h	Humeral axes.
X_i, Y_i, Z_i	Joint axes.
X_p, Y_p, Z_p	Transducer axes.
X_u, Y_u, Z_u	Ulnar axes.
X_{ar}, Y_{ar}, Z_{ar}	"Apparent" grid coordinates of marker points.
X_{gr}, Y_{gr}, Z_{gr}	"Actual" grid coordinates of marker points.
$(X,Y,Z)_b$	Coordinates of point B (grid).
$(X,Y,Z)_{CG}$	Coordinates of point CG (grid).
$(X,Y,Z)_{EC}$	Coordinates of point EC (grid).
$(X,Y,Z)_M$	Coordinates of point M (grid).
$(X,Y,Z)_{SS}$	Coordinates of point SS (grid).
$(X,Y,Z)_W$	Coordinates of point W (grid).
X_{FT}, Y_{FT}, Z_{FT}	Components of triceps force in ulnar axis system.
X_{FB}, Y_{FB}, Z_{FB}	Components of biceps force in ulnar axis system.
XC, YC	Calibration factors for film measurement.
$XF_{BA}, YF_{BA}, ZF_{BA}$	Components of brachioradialis force in joint axis system.
$XF_{bi}, YF_{bi}, ZF_{bi}$	Components of biceps force in joint axis system.
$XF_{br}, YF_{br}, ZF_{br}$	Components of brachialis force in joint axis system.
$XF_{tr}, YF_{tr}, ZF_{tr}$	Components of triceps force in joint axis system.
XT_L, YT_L, ZT_L	Components of lateral ligament tension (joint axes).
XT_M, YT_M, ZT_M	Components of medial ligament tension (joint axes).

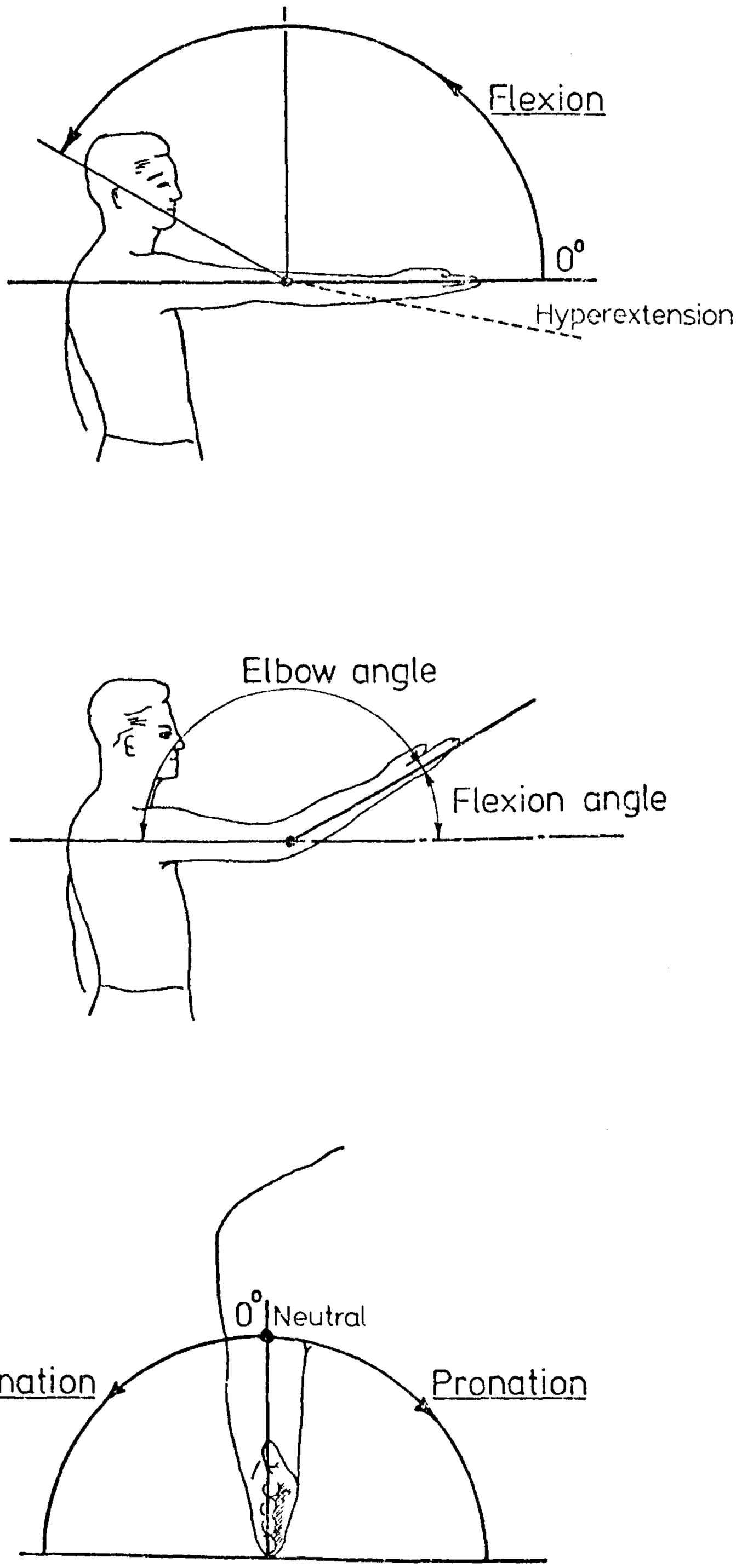

Definition of Forearm Movements

INTRODUCTION

The relatively high success of total joint replacements in the lower limb in recent years has encouraged surgeons and engineers to undertake the design and development of prosthetic joints for the upper limb. Around 64% of all patients suffering from rheumatoid arthritis have affected elbow joints compared to 27% and 82% having affected hip joints and knee joints respectively, (Wright and Amis, 1975). Personal activities such as eating, dressing and toileting functions can become extremely difficult to perform without the aid of a second person.

To aggravate the situation, current hinge arthroplasties for the elbow joint have inherent technical problems and frequently result in surgical complications (Souter, 1974). Modern designs of elbow prostheses include a variety of concepts but have failed to overcome the majority of problems.

Although hinged elbow prostheses can provide the necessary stability at the elbow region, the dynamic load carrying characteristics of the rigid assembly are questionable. It is now accepted that clearance is desirable between the two components of knee prostheses to produce a certain degree of joint "laxity".

The stability of two of the new generation of "unrestrained" elbow prostheses (see section 8.6) is dependent on the normal function of intact ligamentous structures around the elbow joint. To the author's knowledge, no data has been published regarding the load carrying characteristics of the collateral ligaments of the elbow joint or the loads imposed on the articular surfaces during "everyday" activities.

The following work was undertaken to study the kinematics and kinetics of the elbow joint and to develop an improved total elbow prosthesis using the biomechanical data so obtained.

1. ANATOMY

The information contained in the following chapter was collected from literature by Romanes (1969), Gray (1973) and Kendal et al (1971). The diagrams are based on figures by the two latter authors.

1. ANATOMY

1.1 Introduction:

Originally a locomotive structure, the upper limb has evolved over many thousands of years to become a highly mobile, skilled and sensory limb. The basic "design principle" may be described as providing the most efficient use of the hand.

Having its proximal boundary at the shoulder joint, the upper limb consists of hand, forearm and upper arm. The hand is of comparatively minor significance to this thesis and, consequently, only the more essential details relating to the elbow region are described.

1.2 Skeletal Structures:

Leaving aside those of the wrist and hand, the three important bones of the upper limb are the humerus, the ulna and the radius.

The upper arm contains the longest and strongest bone of the upper limb; the humerus, shown in figure 1.1. Generally, the upper half of the humeral shaft is circular in cross section, beginning with the bulbous, partly hemi-spherical, humeral head. The shaft commences after the surgical neck; appropriately named due to the frequency of fracture at that site. At mid length, the shaft deforms at the deltoid tuberosity laterally, and the radial groove posteriorly. The lower half of the shaft becomes increasingly triangular in section terminating, after bifurcation, in two epicondyles. Situated between the so formed medial and lateral epicondyles is the articular cartilage of the saddle-shaped trochlea, and the convex capitulum (figure 1.3). Superiorly, the medial and lateral supracondylar ridges enclose three fossae; the radial and coronoid fossae anteriorly and the olecranon fossa posteriorly. The thickness of hard tissue between the two latter fossae is very small and in some cases the space may be void.

Articulating with the trochlea of the humerus, the ulna provides the hingeing between upper arm and forearm. As shown in figure 1.2, the trochlear notch is formed anteriorly between the coronoid process and the olecranon.

2a

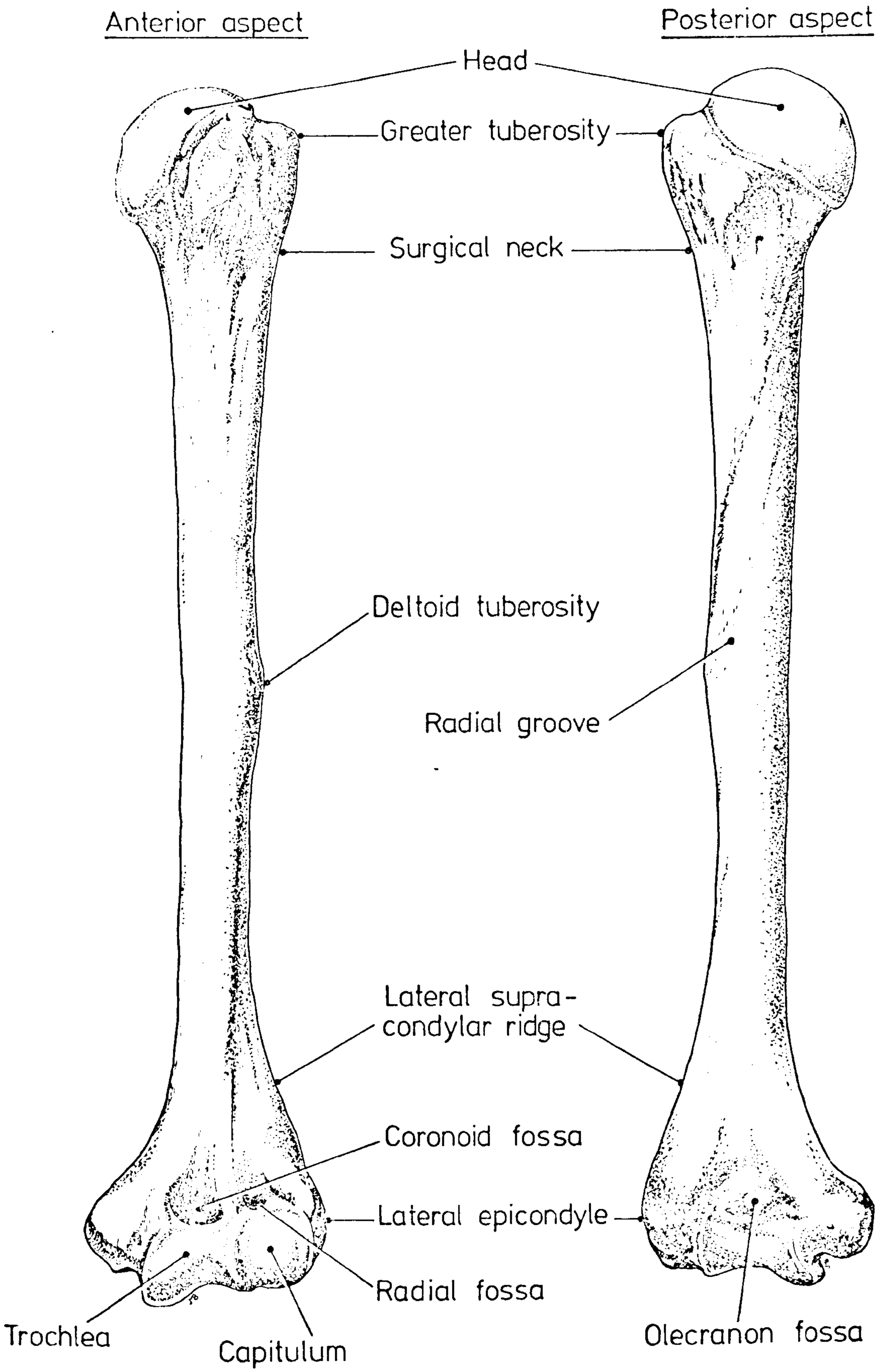

Figure 1·1: The left humerus.

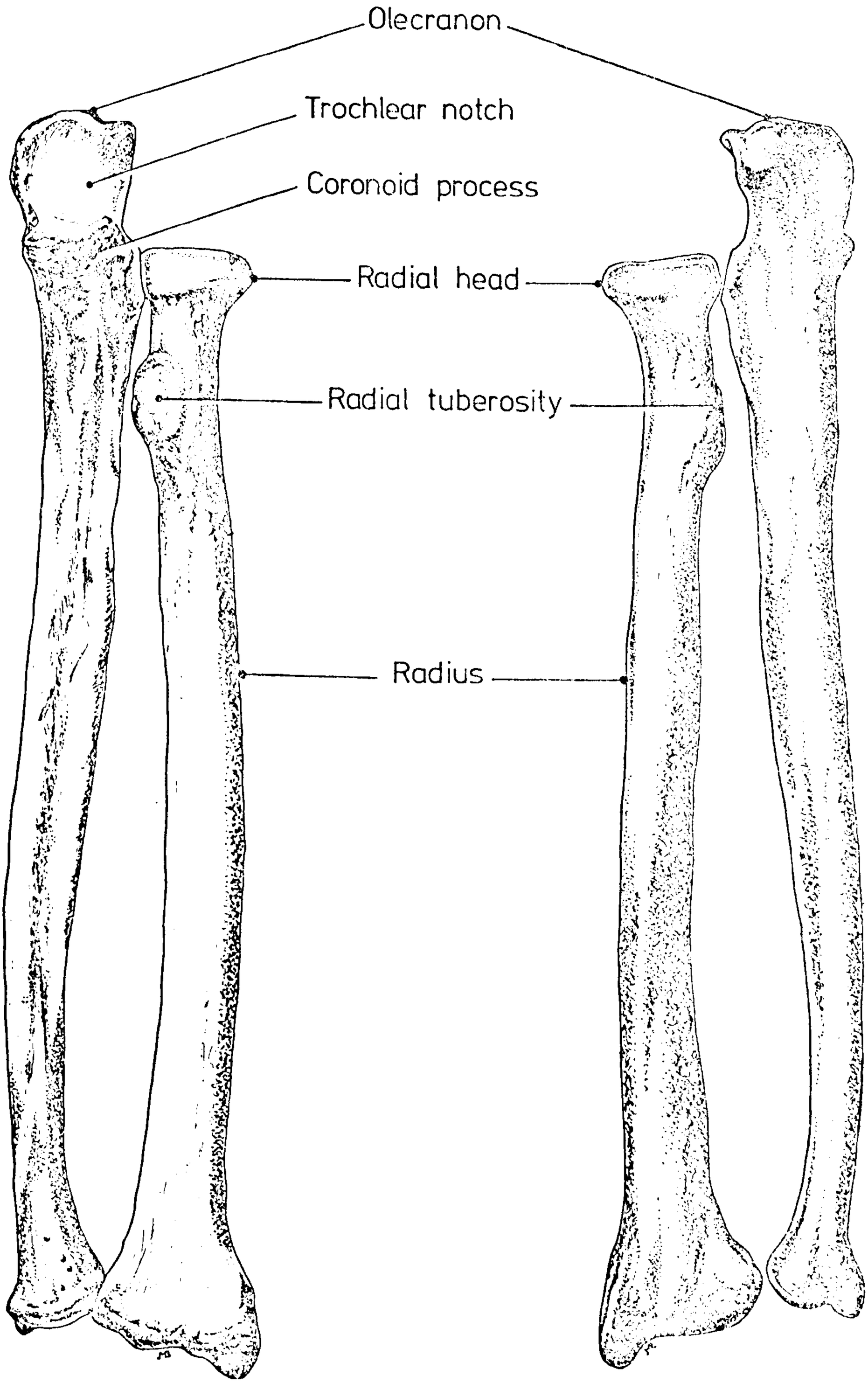

Figure 1·2: The left ulna and radius.

3a

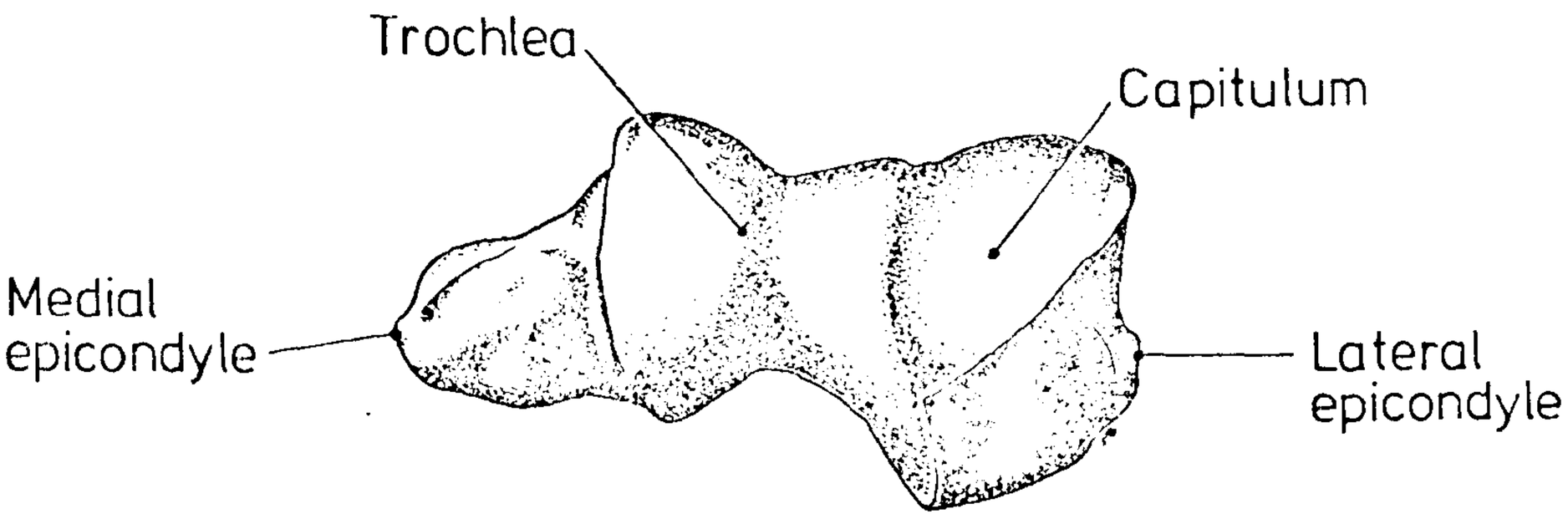

Figure 1·3: Details of the left distal humerus (inferior aspect).

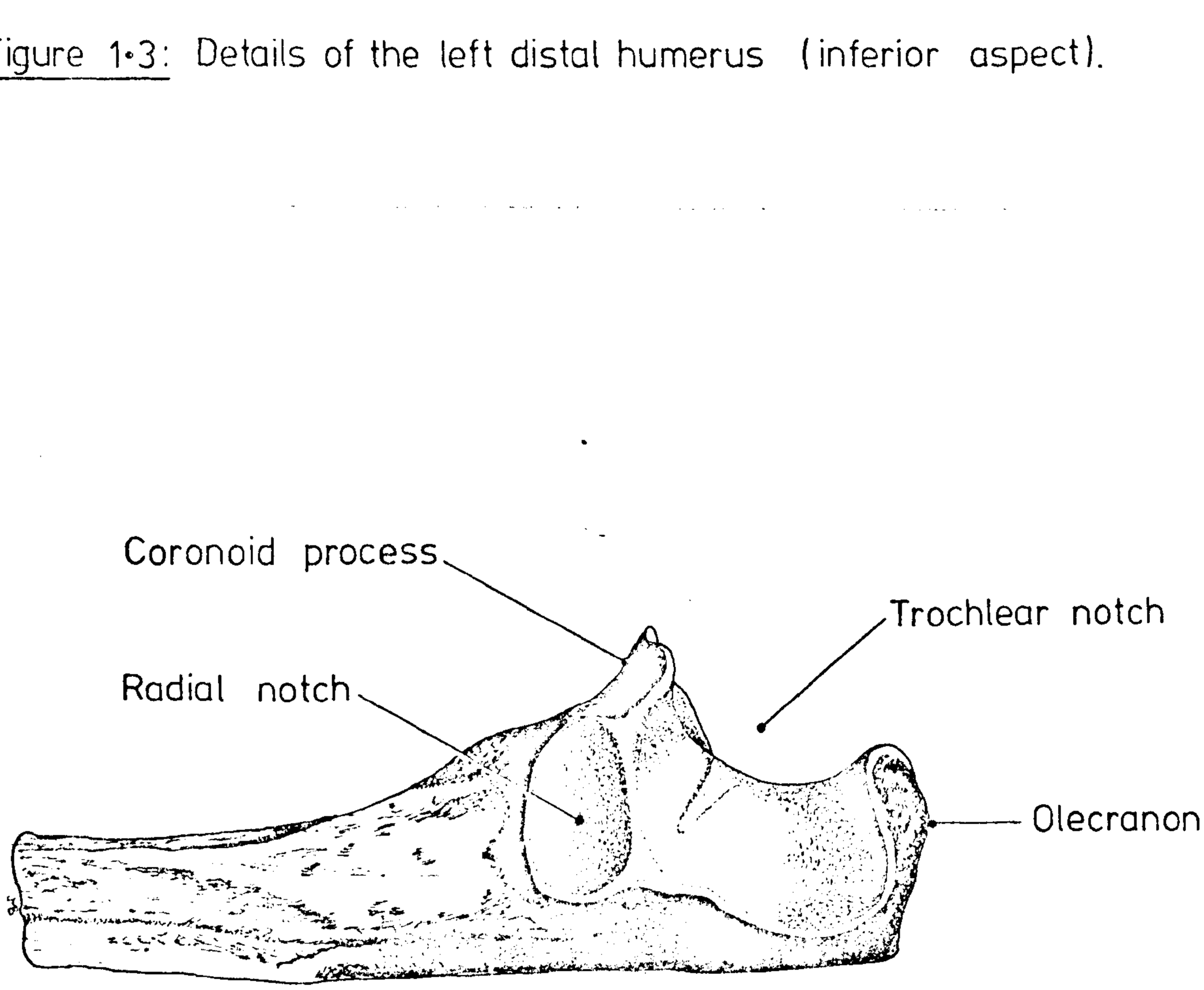

Figure 1·4: Details of the left proximal ulna (lateral aspect)

Laterally, the radial notch (figure 1.4) provides articulation with the head of the radius. Along its length, the ulna has a distinct medial curve and reduces its cross sectional area distally to form the compact, ulnar head at the wrist.

Lengthwise, the radius is the inverse of the ulna having its slim head proximally and a lateral curve to its shaft (see figure 1.2). The radial head forms a slightly concave disc which articulates with the capitulum of the humerus. The periphery of the radial head articulates with the ulna in the radial notch, the majority of cartilage being on the medial side of the disc. Distally, articulation with the ulnar head is provided by the small strip of cartilage in the ulnar notch.

To ensure stability of the elbow joint during activity, the ligamentous structures which surround the assembled joint are numerous and complex. The fibrous capsule integrates with the ligaments and certain muscle tendons to completely surround the articular region and provide many restraining actions. Medial and lateral aspects of the structures are shown in figures 1.5 and 1.6 respectively.

Medially, the ulnar collateral ligament consists of anterior, posterior and oblique bands arranged triangularly. From the medial epicondyle, the anterior band inserts into the medial side of the coronoid process and the posterior band attaches along the medial margin of the olecranon. Usually there is a thin sheet of intermediate fibres running from the medial epicondyle to the weak oblique band stretching between the coronoid process and olecranon.

Laterally, the radial collateral ligament runs from the lateral epicondyle to join the annular ligament which surrounds the radial head. A few of the most posterior fibres unite with the ulna, adjacent to the annular ligament, in an intimate blend of ligaments and forearm muscle origins.

The radius and ulna are additionally bound together by the interosseous membrane shown in figure 1.5. The fibres run medially downward from medial radius to lateral ulna for most of the forearm length.

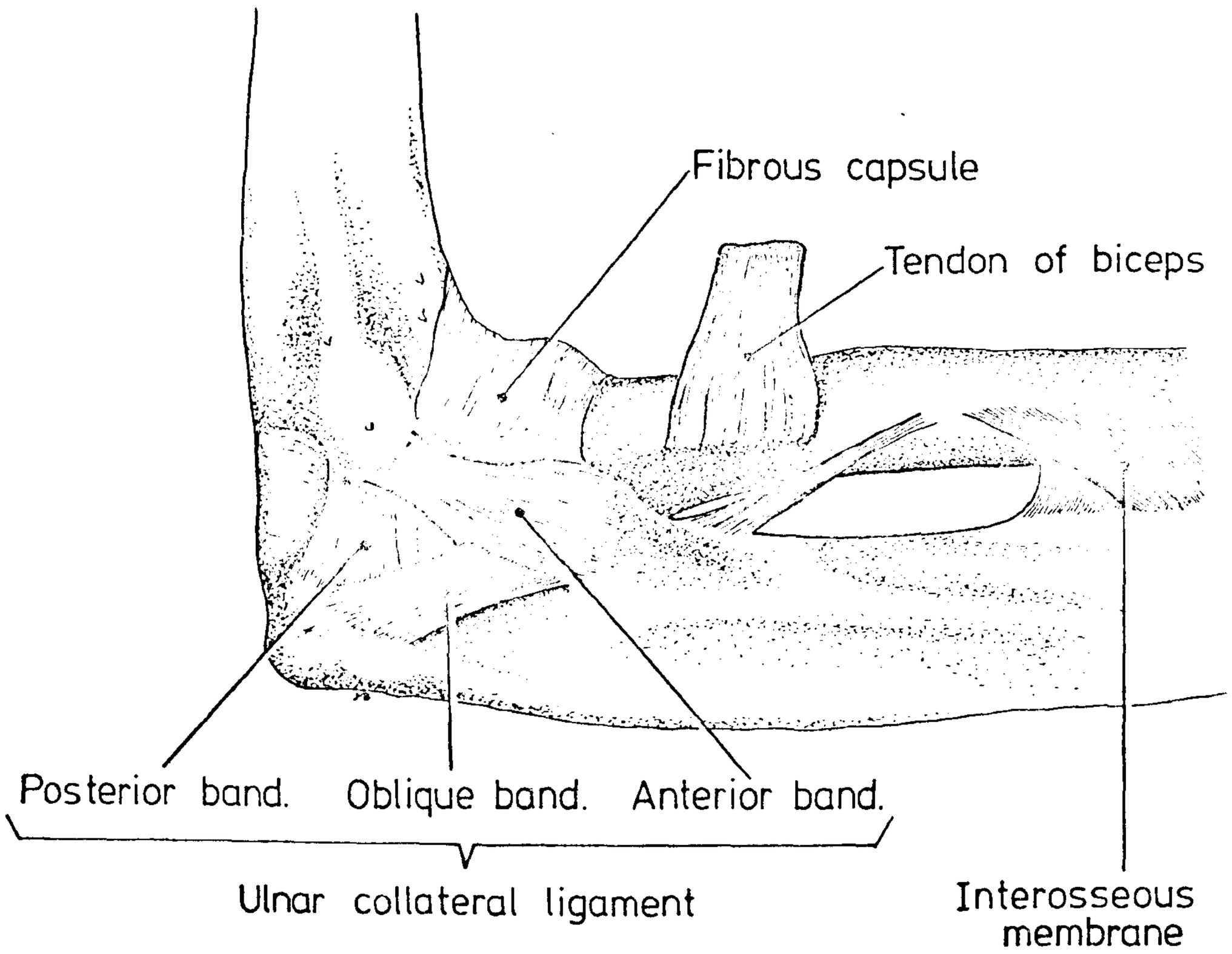

Figure 1•5: Medial ligamentous structures of the left elbow.

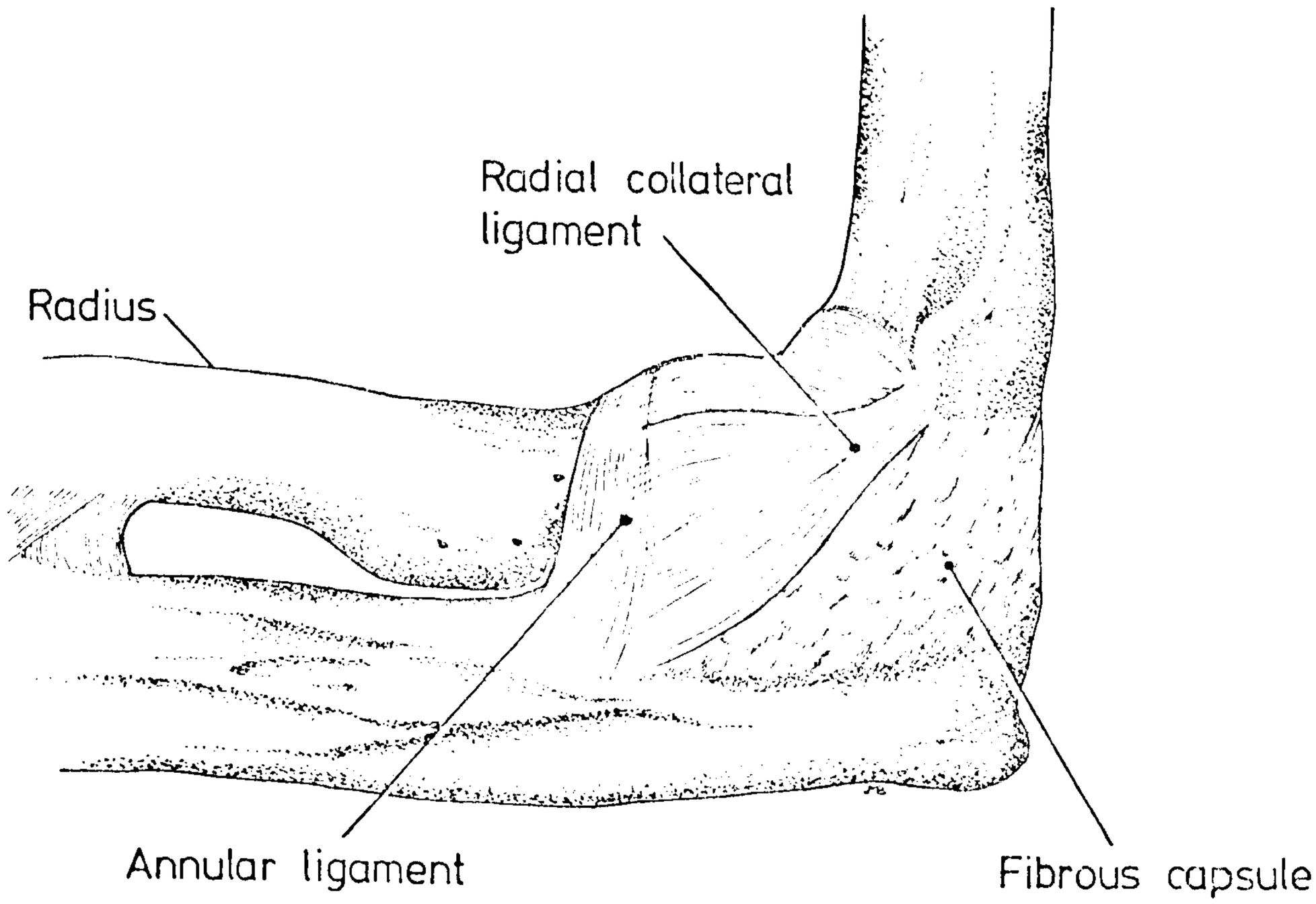

Figure 1·6: Lateral ligamentous structures of the left elbow joint.

1.3 Musculature:

The upper arm contains three important muscles which can act upon the elbow joint; triceps, brachialis and biceps brachii. Excepting brachialis, the upper arm muscles serve both shoulder and elbow joints and have several sections or "heads".

The large biceps brachii receives its name from the fact that it is composed of two heads; the short head originating from the coracoid process on the scapula and the long head arising from the apex of the shoulder joint glenoid cavity (see figure 1.8). A single thick tendon inserts onto the radial tuberosity of the radius but, in addition, the bicepetal aponeurosis branches from the origin of the main tendon to fuse with the medial forearm flexors.

The brachialis muscle originates on the anterior lower half of the humerus and lies directly behind the biceps brachii (figure 1.8). Its thick and broad tendon inserts immediately inferior to the coronoid process.

As its name suggests, the triceps muscle is composed of three parts; the long, medial and lateral heads. As shown in figure 1.9, the long head originates from the inferior glenoid capsule and the adjacent scapula whereas the medial and lateral heads arise from the humeral shaft. Superior to the radial groove, the lateral head has its origin which extends for a few centimetres towards the medial side of the surgical neck. The medial head arises from a large area on the lower three quarters of the posterior humerus. Occupying the entire posterior compartment of the upper arm, the three heads produce a large tendon beginning around the middle of the muscle and inserting on the olecranon of the ulna.

The muscles of the forearm are divided into two sections; the flexors and extensors which are further subdivided into deep and superficial structures.

The flexors occupy the anterior region of the forearm and provide flexion of the wrist and digits and pronation of the forearm.

Of the superficial flexors, all five have part of their origin on the common flexor tendon on the medial epicondyle of the humerus. With the exception of the pronator teres, all the flexors have long, slim tendons which extend to the wrist and hand. The group consists of the following:

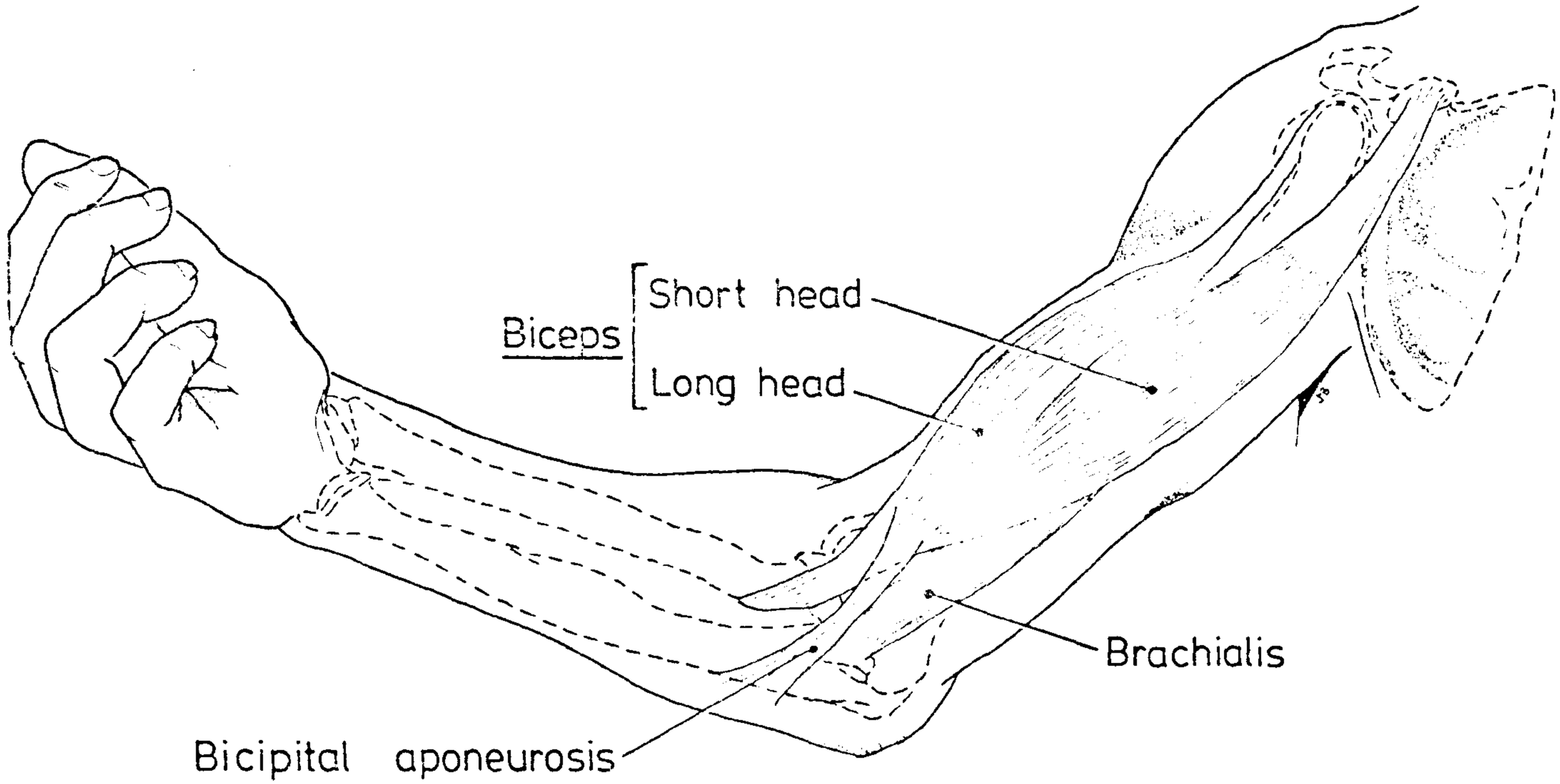

Figure 1·8: The elbow flexors of the upper arm.

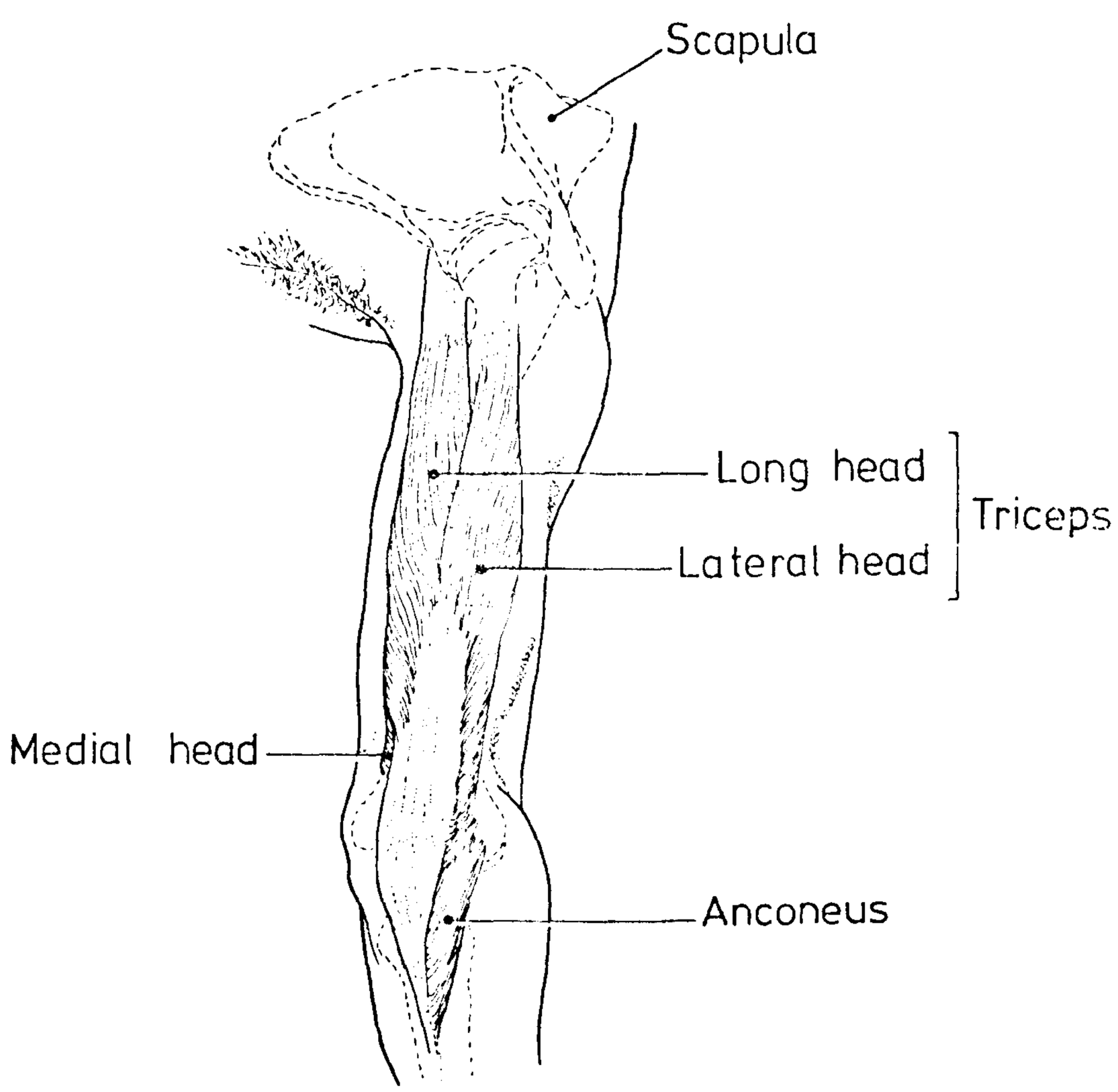

Figure 1·9: The elbow extensors.

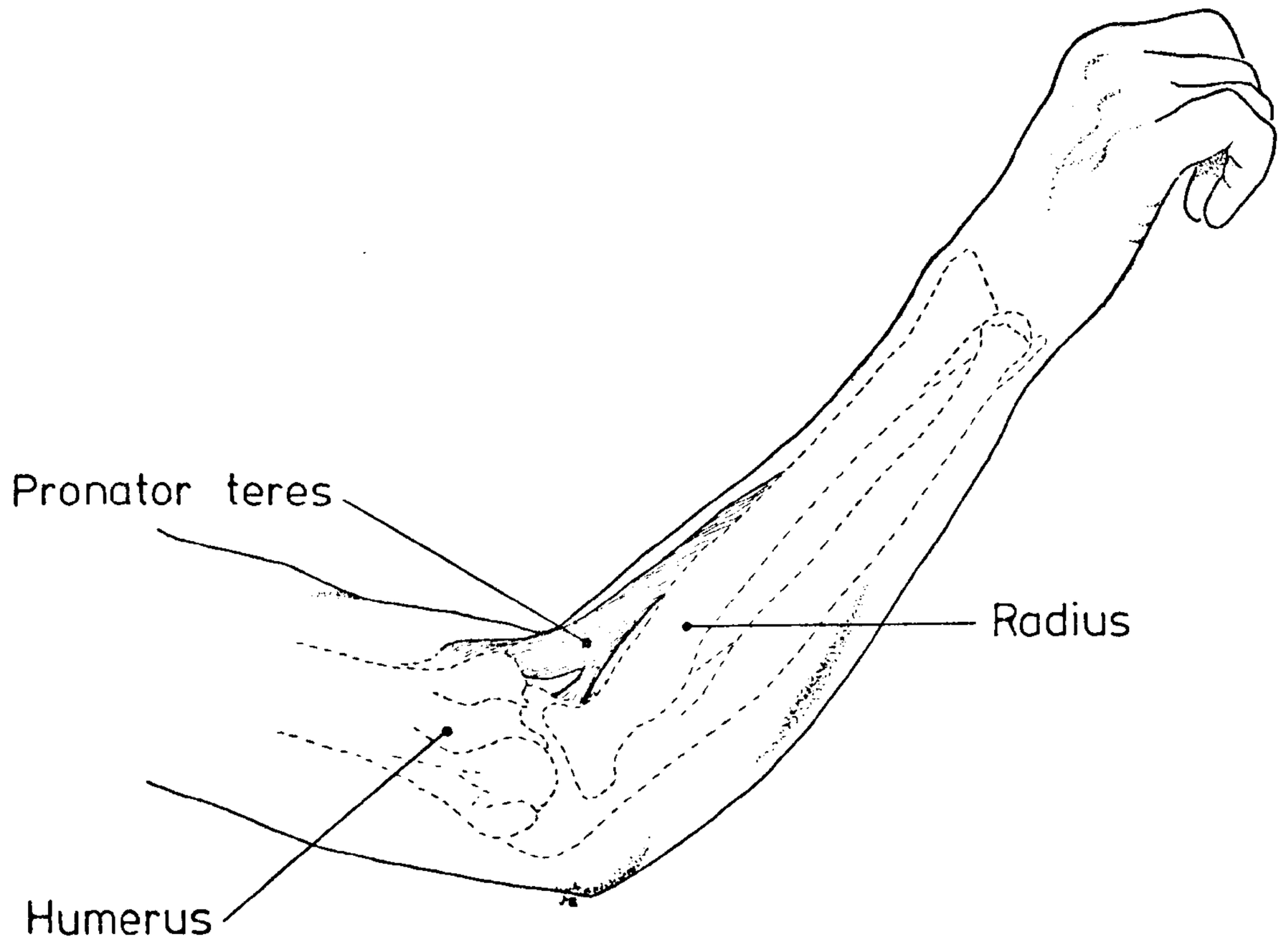

Figure 1·10: The pronator teres muscle.

Pronator teres (figure 1.10)

Flexor carpi radialis (figure 1.11)

Palmaris longus (figure 1.11)

Flexor carpi ulnaris (figure 1.11)

Flexor digitorum superficialis (figure 1.11)

The pronator teres crosses the proximal half of the anterior forearm arising by humeral and ulnar heads. Originating from the medial side of the coronoid process, the ulnar head unites with the humeral head, from the common tendon, at an acute angle. The common insertion tendon leads to the middle of the lateral surface of the radius.

Arising almost totally from the common flexor tendon, the flexor carpi radialis produces a tendon which extends down the lateral anterior surface of the forearm. Insertion occurs chiefly at the base of the index metacarpal bone.

From the common flexor tendon, the palmaris longus has a short muscle belly and a long thin tendon inserted into the palmaris aponeurosis.

Originating by humeral and ulnar heads, from the common flexor tendon and olecranon respectively, the flexor carpi ulnaris is the most medial of the group and runs down the medial side of the forearm. Insertion occurs on the pisiform bone of the wrist.

Lying below the superficial group, the deep flexors of the forearm consist of:- (see figure 1.12)

Flexor digitorum profundus

Flexor pollicis longus

Pronator quadratus.

The chief origin of the thick flexor digitorum profundus is along the upper three quarters of the medial and anterior surfaces of the ulna. Although four tendons are issued, only the forefinger tendon is separate. Each tendon inserts into the terminal phalanx of a finger.

Arising from the proximal two thirds of the anterior surface of the radius, the flexor pollicus longus runs down the forearm, turns after the wrist and inserts into the terminal phalanx of the thumb.

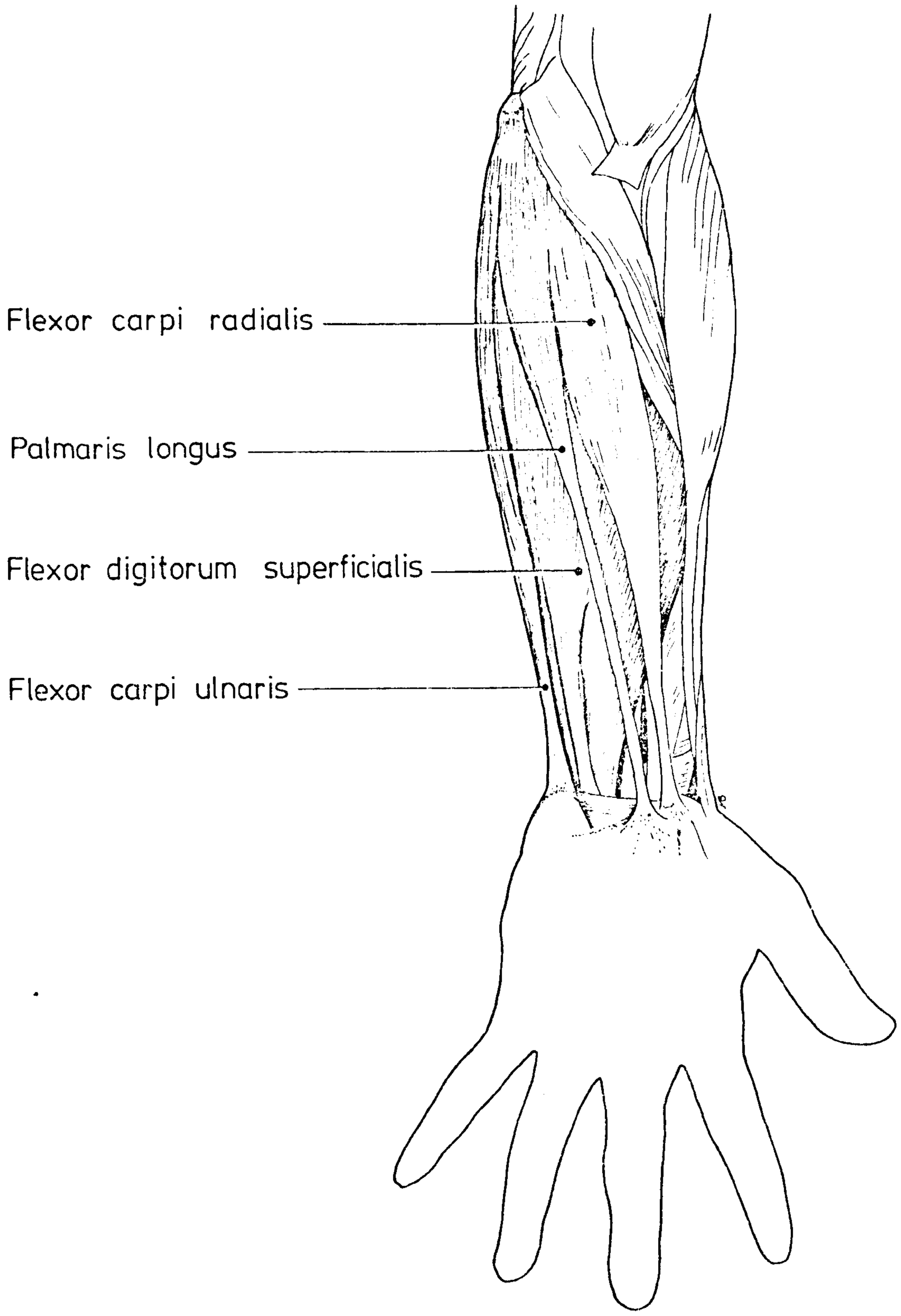

Figure 1·11: Superficial flexors of the forearm.

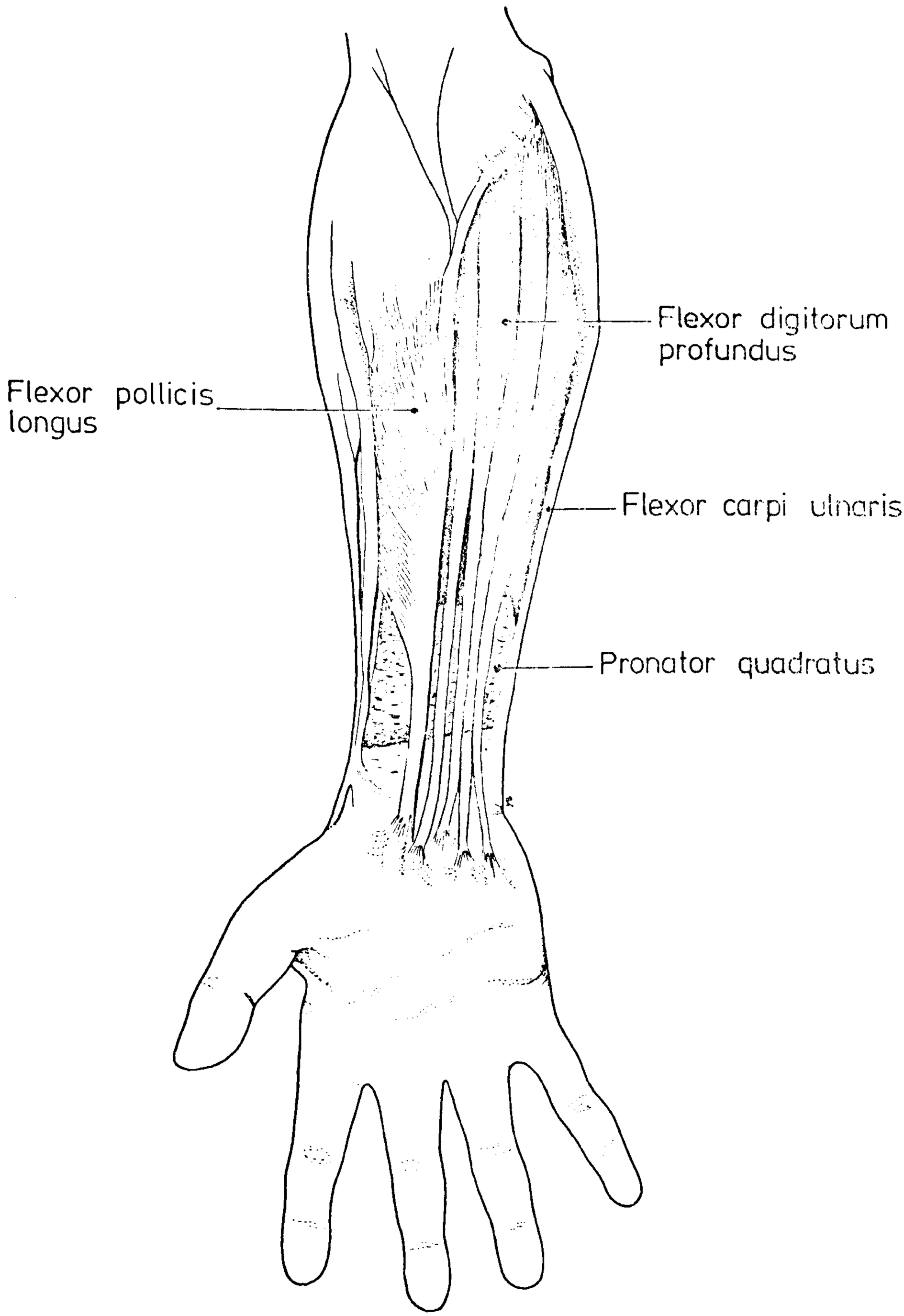

Figure 1·12: The deep flexors of the forearm.

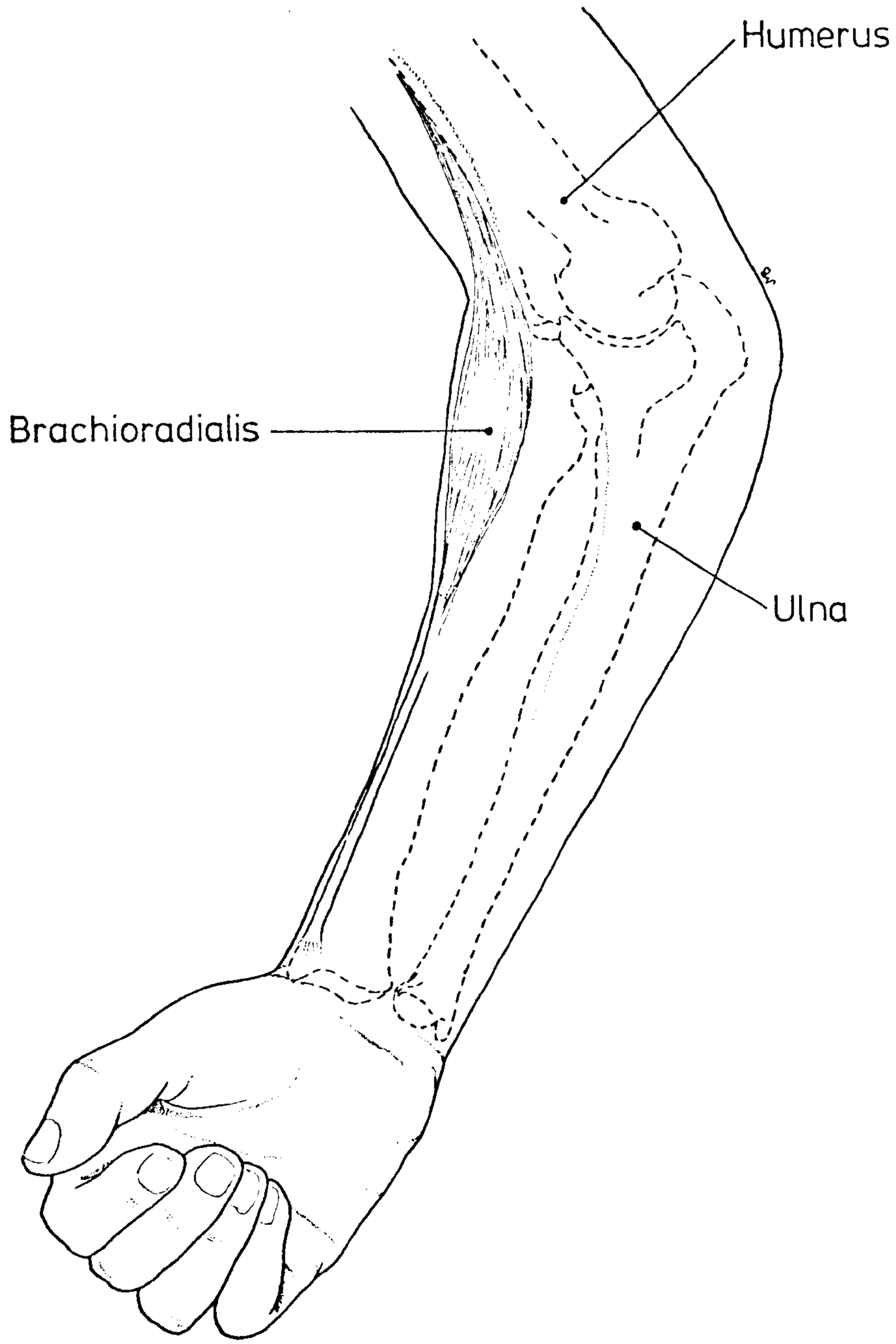

Figure 1·13: Layout of Brachioradialis

The pronator quadratus lies deep in the distal quarter of the forearm and takes origin from the anterior surface of the ulna. Insertion is made, laterally, on the anterior surface of the distal quarter of the radius.

Occupying the posterior compartment of the forearm, the extensor group, like the flexors, is divided into superficial and deep groups.

The seven superficial extensors, from medial to lateral sides, are as follows:

Brachioradialis	(figure 1.13)
Extensor carpi radialis longus	(figure 1.14)
Extensor carpi radialis brevis	(figure 1.14)
Extensor digitorum	(figure 1.15)
Extensor digiti minimi	
Extensor carpi ulnaris	(figure 1.14)
Anconeus	(figure 1.9)

Originating on the lateral supracondylar ridge, the fibres of the brachioradialis extend to the mid forearm level. Insertion, by a long tendon, takes place at the lateral side of the distal radius. Although having innervation in common with wrist flexors, this muscle is an elbow flexor and is seen to best advantage during forced flexion of the forearm with zero supination or pronation.

Arising from the lower third of the lateral supracondylar ridge, the extensor carpi radialis longus issues a long tendon which inserts into the base of the second metacarpal bone. Lying immediately posterior to this muscle, the extensor carpi radialis brevis originates from the common extensor tendon and inserts into the base of the third metacarpal bone.

From the common extensor tendon and the posterior border of the ulna, the extensor carpi ulnaris gradually issues a relatively thick tendon near the wrist. Insertion occurs at the base of the fifth metacarpal bone.

The extensor digitorum and extensor digiti minimi both have their origins in the common extensor tendon and their fibres are usually connected longitudinally. The tendons issued from the extensor digitorum insert into the bases of the middle and terminal phalanges via the extensor expansions. United with a tendon from the extensor digitorum, the tendon of extensor digiti minimi

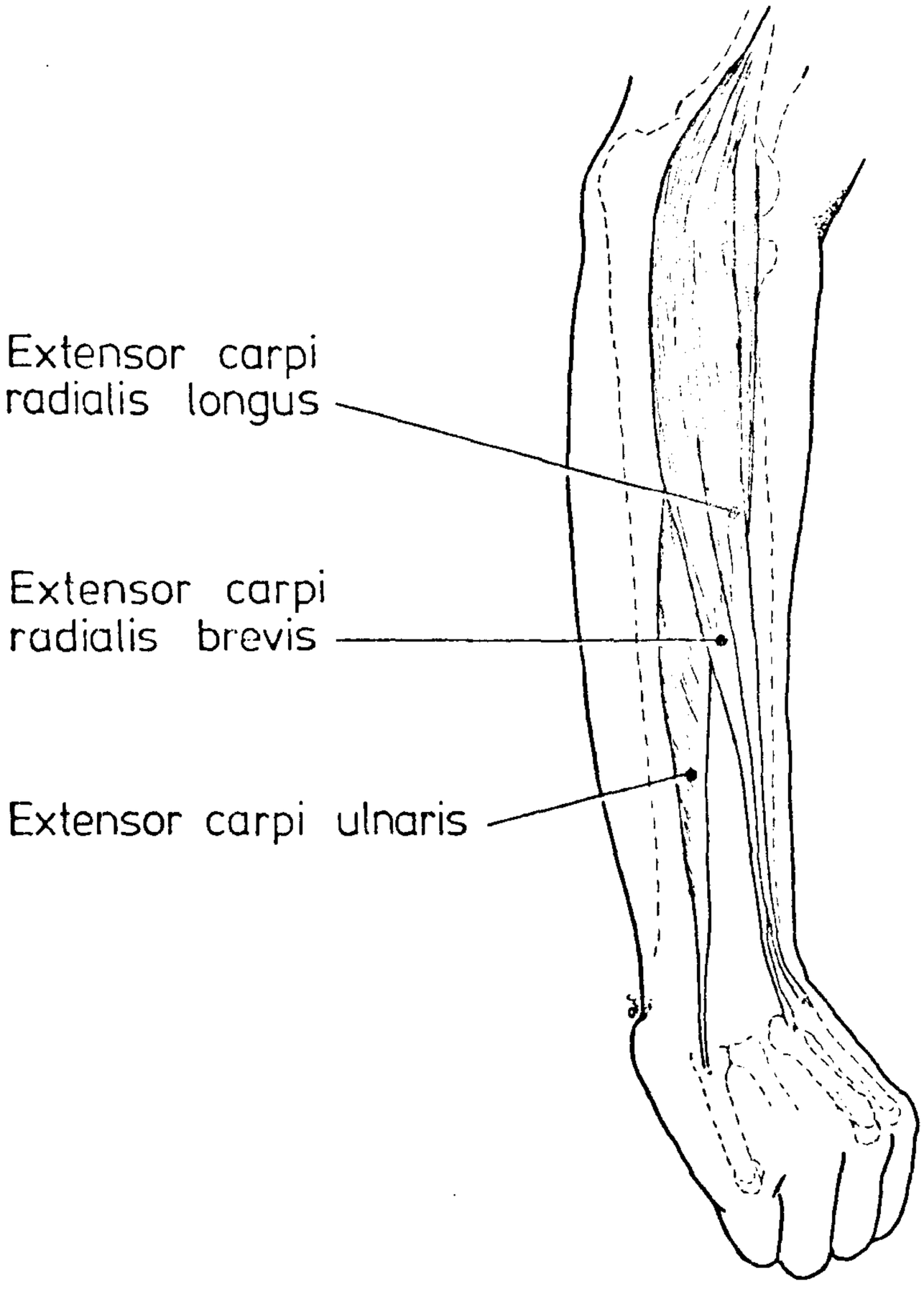

Figure 1·14: Three of the forearm extensor muscles.

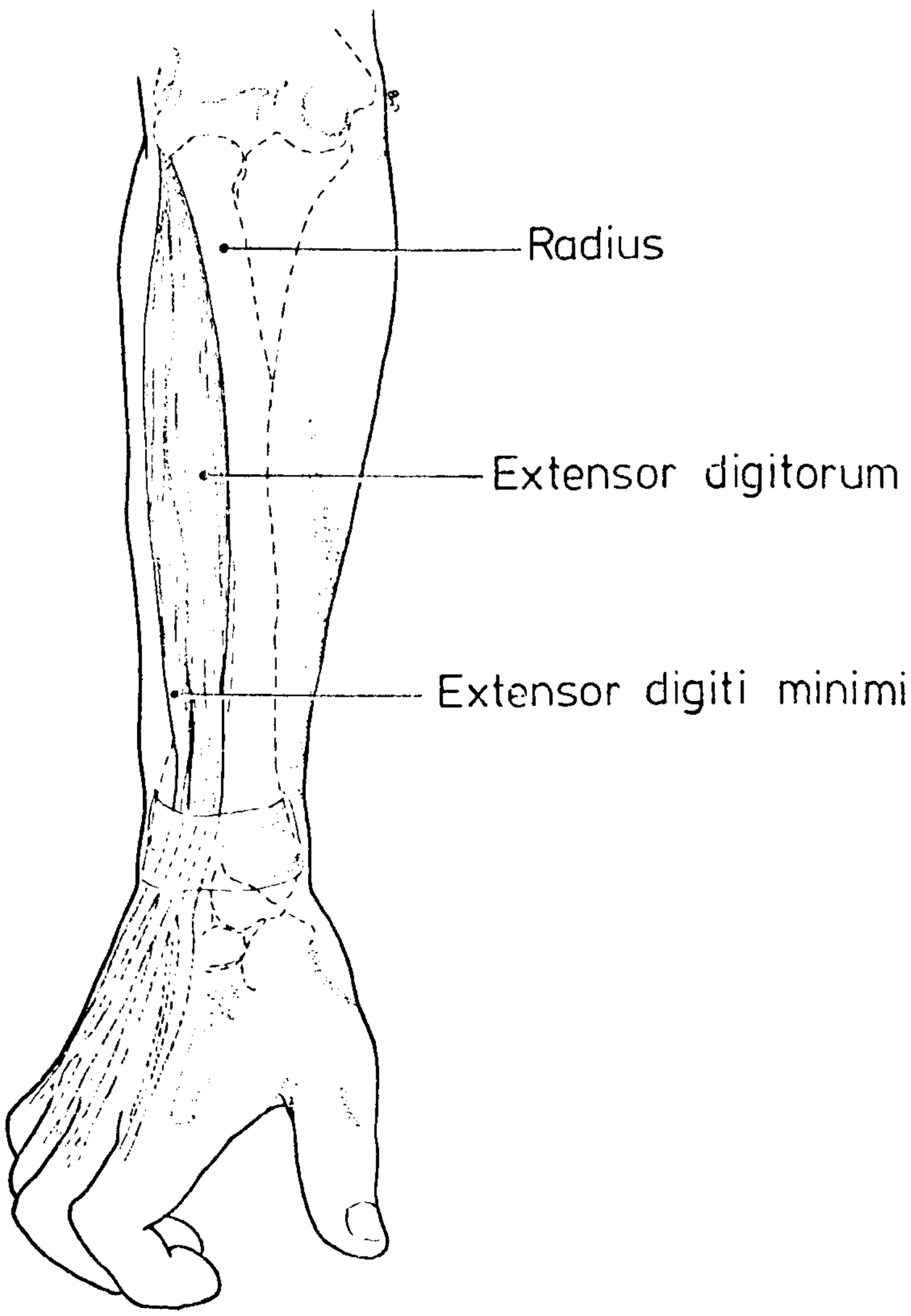

Figure 1·15: Two extensors of the wrist and digits

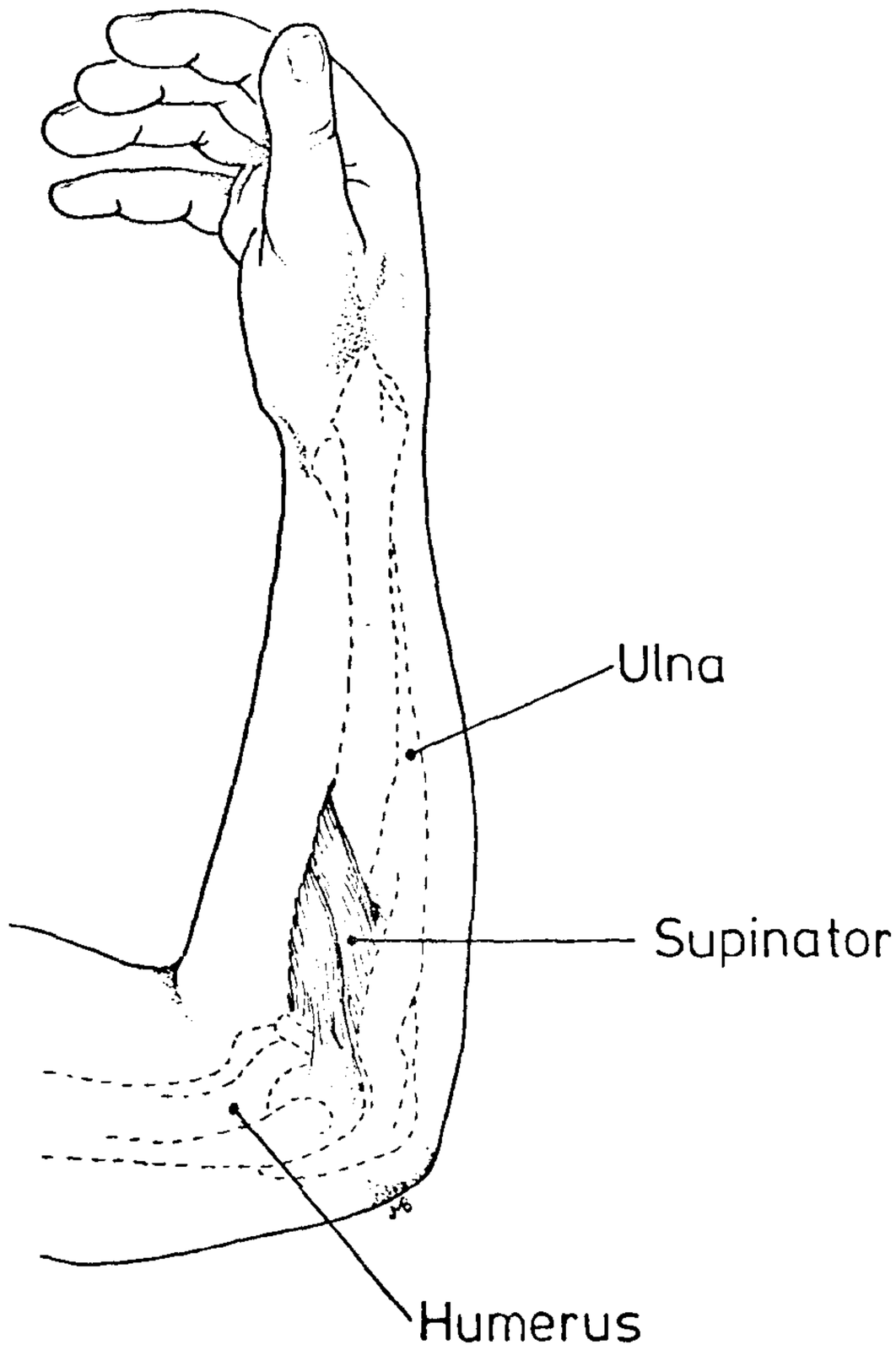

Figure 1·16: The Supinator muscle

is confined to the phalanges of the fifth digit.

Triangular in overall shape, the anconeus runs from behind the lateral epicondyle of the humerus to the lateral side of the olecranon and upper fourth of the posterior ulna.

The deep extensors are composed of the following:

Supinator	(figure 1.16)
Abductor pollicis longus	(figure 1.17)
Extensor pollicis longus	(figure 1.17)
Extensor pollicis brevis	(figure 1.17)
Extensor indices	(figure 1.17)

From their main origin on the lateral proximal ulna the supinator fibres sweep round and envelop the neck and proximal shaft of the radius. The tendon has its insertion on the lateral proximal third of the radius.

The abductor pollicis longus arises from the posterior surfaces of the interosseous membrane, the ulna and the radius. Crossing the two radial extensors' tendons, the tendon weaves its way to the insertion at the base of the metacarpal bone of the thumb.

The short extensor pollicis brevis lies alongside the distal border of the preceding muscle and originates from the posterior interosseous membrane and radius. This muscle closely follows its neighbour but inserts into the proximal phalanx of the thumb.

Taking origin from the posterior surface of the middle third of the ulna and the interosseous membrane, the extensor pollicis longus overlaps the extensor pollicis brevis to a certain extent. The tendon alters direction at the wrist and runs along the back of the thumb to insert into the base of the distal phalanx.

The extensor indicis arises from a limited area on the posterior ulna and interosseous membrane. Its tendon accompanies the extensor digitorum to the back of the hand, thereafter inserting into the first phalanx of the index finger.

1.4 Blood Vessels:

Supplied solely by the axillary artery from the shoulder region, the upper limb receives a generous quantity of blood; the important vessels being shown in figures 1.18 and 1.19.

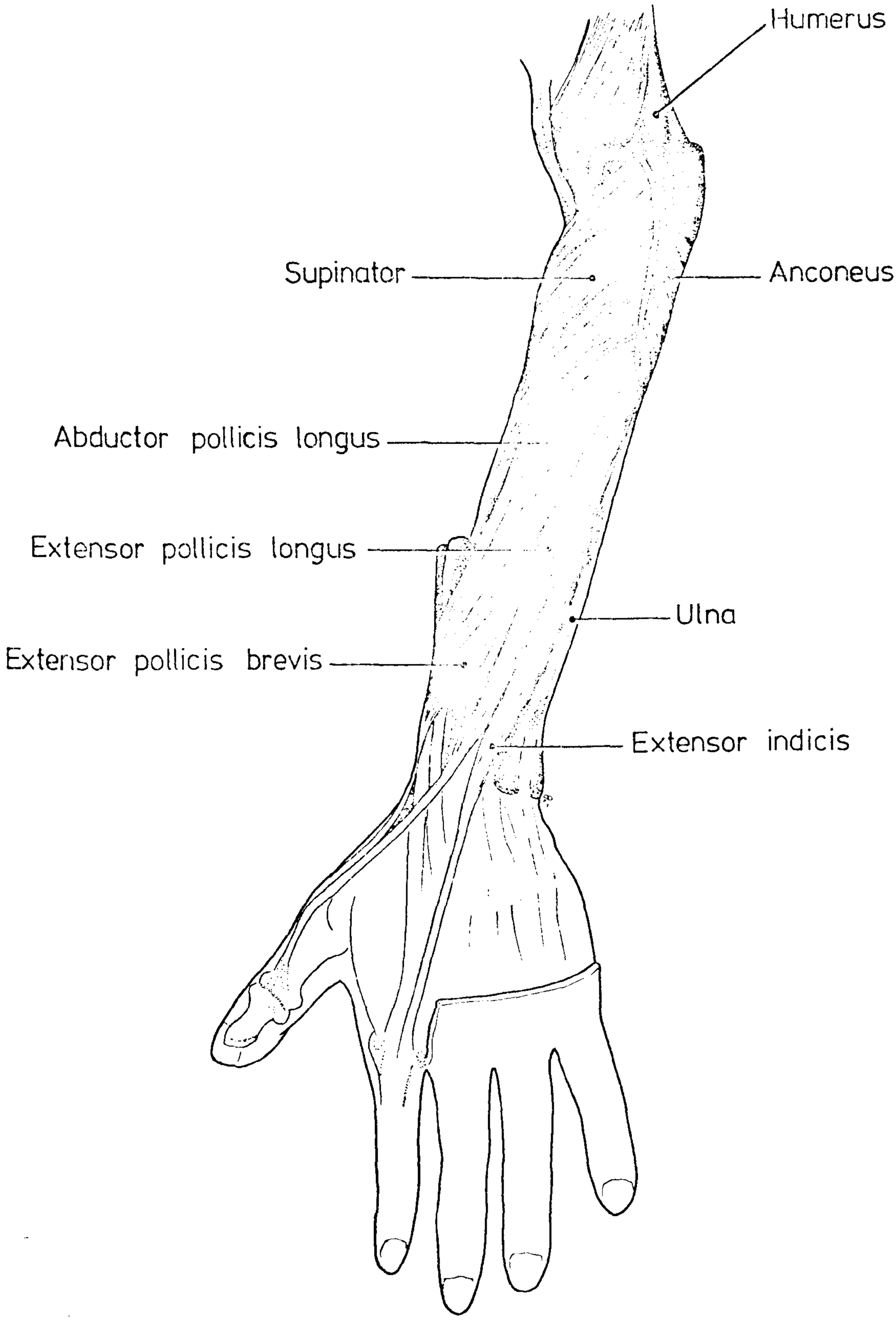

Figure 1·17: The deep extensors of the forearm.

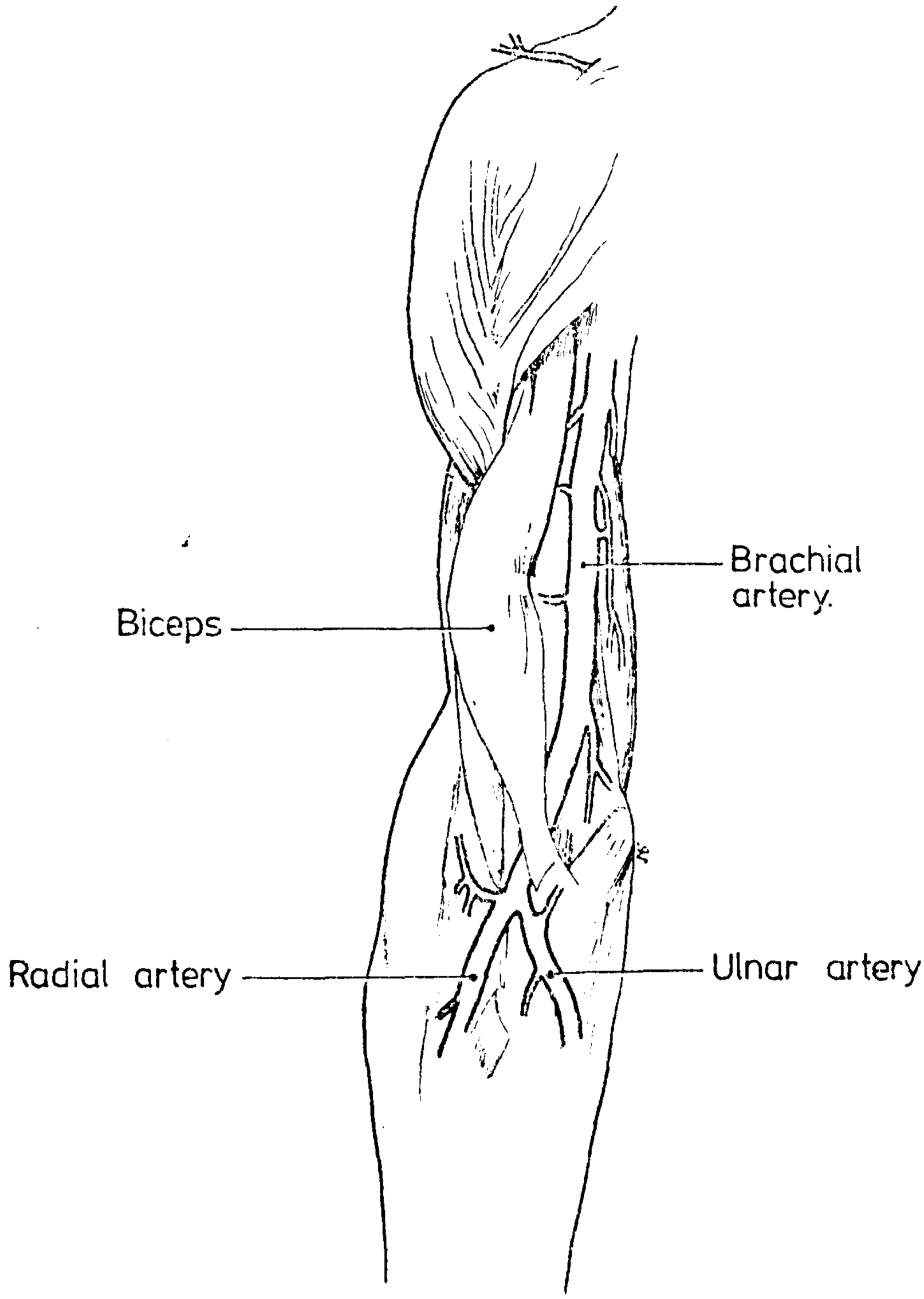

Figure 1·18: Arteries of the right arm [anterior aspect].

Figure 1·19: Superficial veins of the right arm (anterior)

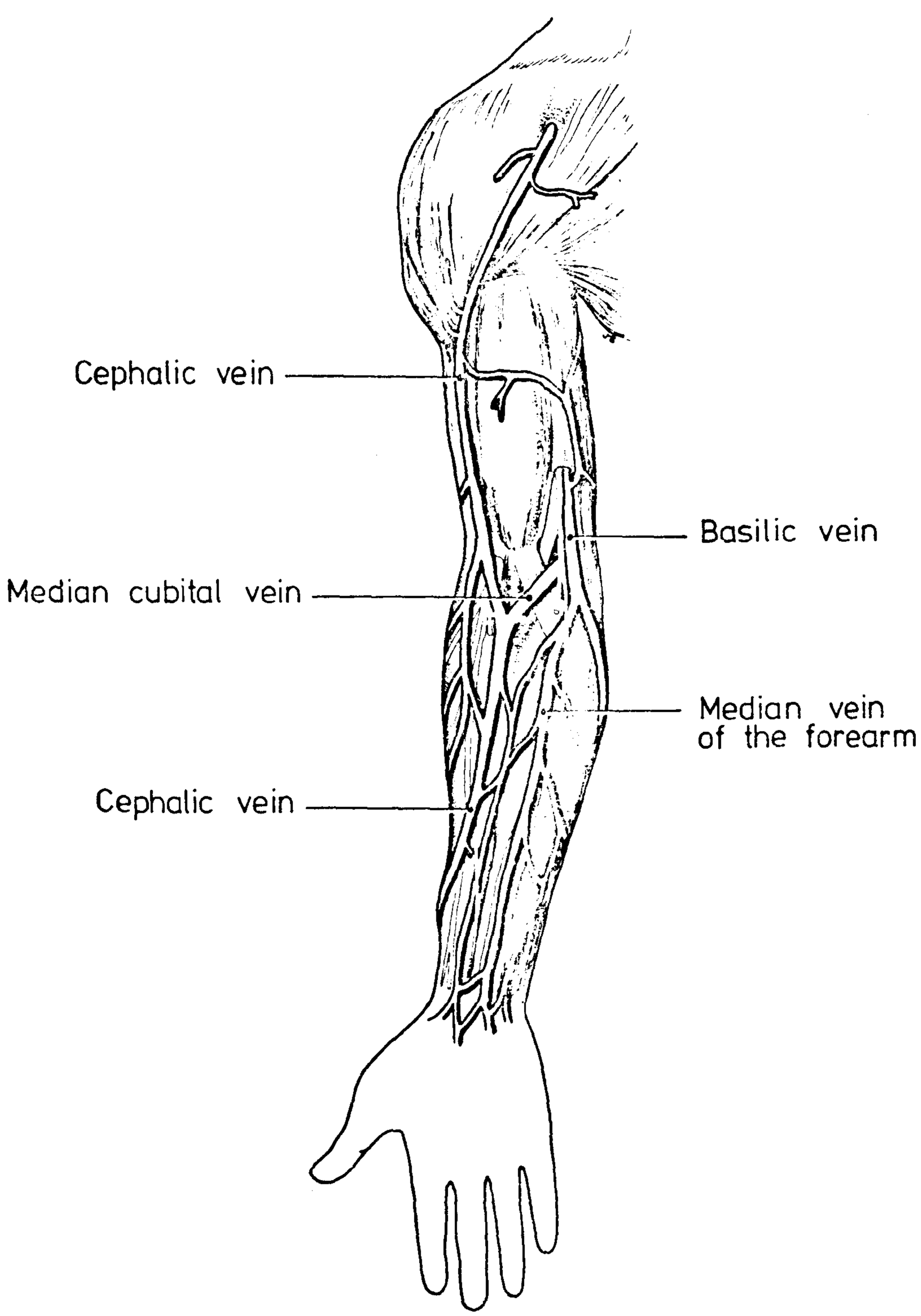

The main artery of the upper arm, the brachial artery, is a continuation of the axillary artery and spirals down the humerus from the proximal medial surface to the distal anterior region. Several branches issue from this vessel; the superior and inferior ulnar collateral arteries being of importance in relation to the elbow region. The former vessel branches quite proximally and supplies the back of the elbow whereas the inferior ulnar collateral artery arises much nearer the elbow, supplying the anterior proximal forearm.

Crossing in front of the elbow, the brachial artery bifurcates to produce the radial and ulnar arteries. The radial artery has its origin opposite the neck of the radius and travels down the lateral side of the forearm whereas the ulnar artery runs down the medial surface. Both arteries have branches which anastomose with brachial artery branches. Being derived from the origin of the ulnar artery, the anterior and posterior interosseous arteries supply the anterior and posterior regions of the membrane respectively.

The venous system of the upper limb consists of deep and superficial vessels which anastomose freely with each other (figure 1.19).

Superficially, the forearm and hand are drained by the cephalic, basilic and median veins. The deeper forearm veins accompany the main arteries and are consequently named the ulnar and radial veins.

In the upper arm, the two deep veins unite to form the brachial vein which drains into the large axillary vein. The basilic vein is joined by the median and the median cubital vein and runs along the medial side of the biceps muscle. On the lateral side, the cephalic vein travels upwards and bends across the anterior superficial region of the shoulder joint.

1.5 Innervation:

The complexity of innervation of the upper limb dictates that only a very brief description of the layout of important nerves is applicable to this thesis. Figure 1.20 shows the general arrangement of such items considered relevant to the elbow region.

Originating from the lower cervical and upper dorsal vertebrae, the brachial plexus of the shoulder region consists of amalgamations of several

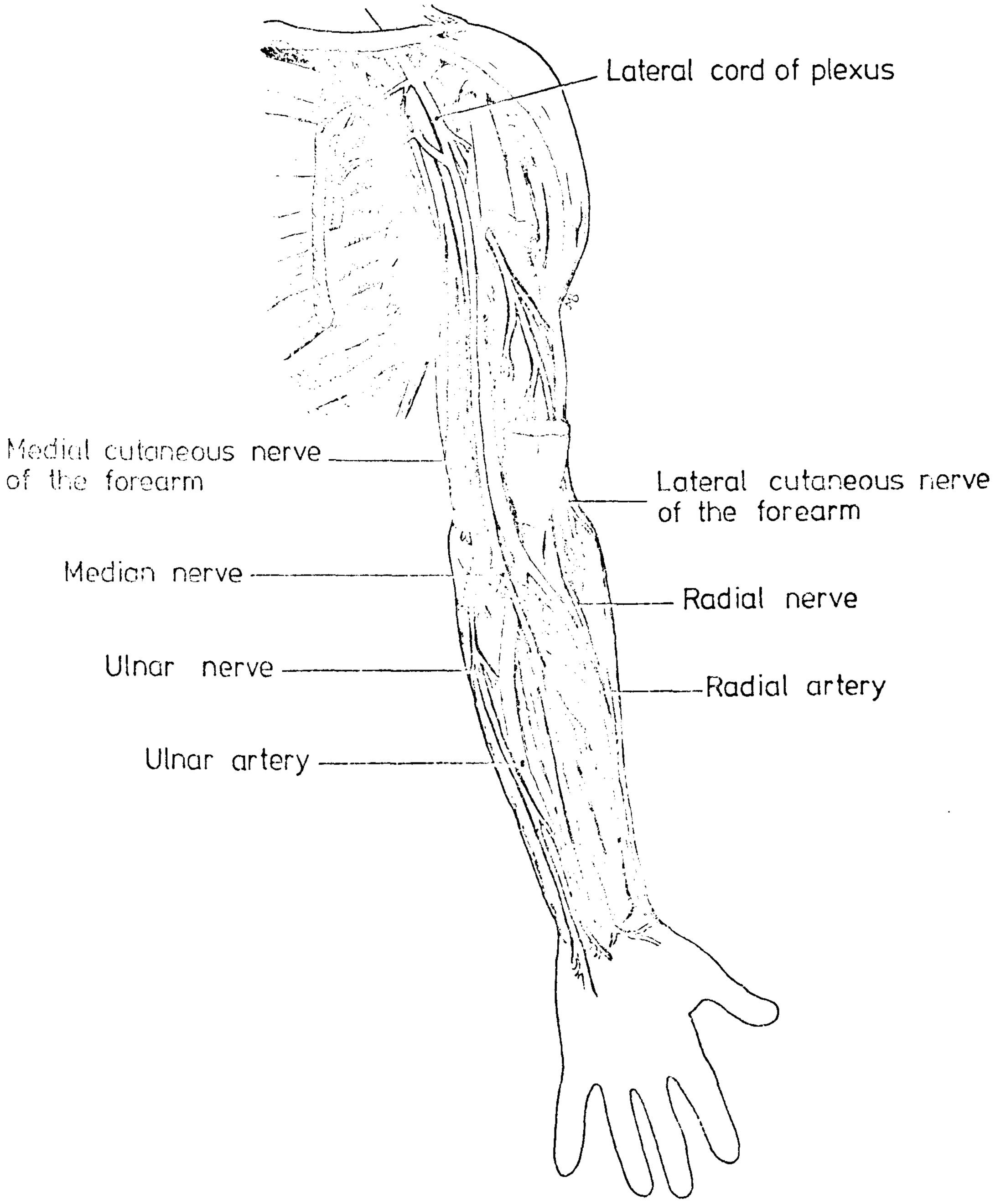

Figure 1·20: Nerves of the left arm [anterior aspect].

origins to produce the upper limb nerves. A brief description of five principal nerves is as follows:-

After descending deep to the cephalic vein, the lateral cutaneous nerve of the forearm crosses the lateral side of the elbow and supplies the lateral half of the anterior forearm.

The medial cutaneous nerve descends next to the brachial artery and divides above the elbow joint. The larger anterior branch supplies the medial side of the forearm whereas the posterior branch twists round and supplies the posterior forearm.

Accompanying the brachial artery in crossing the elbow joint, the median nerve proceeds along the middle of the anterior forearm to supply the lateral side of the palm and digits.

Again descending with the brachial artery, the ulnar nerve crosses the elbow joint, from a groove on the medial epicondyle, and travels along the medial side of the forearm supplying some flexor muscles and the medial side of the hand.

The radial nerve is the thickest branch of the brachial plexus and passes between the lateral and medial heads of the triceps to a groove on the humerus. Several branches appear in the upper arm and the important superficial branch crosses the elbow joint in front of the lateral epicondyle to supply the lateral half of the back of the hand. (See figure 1.21)

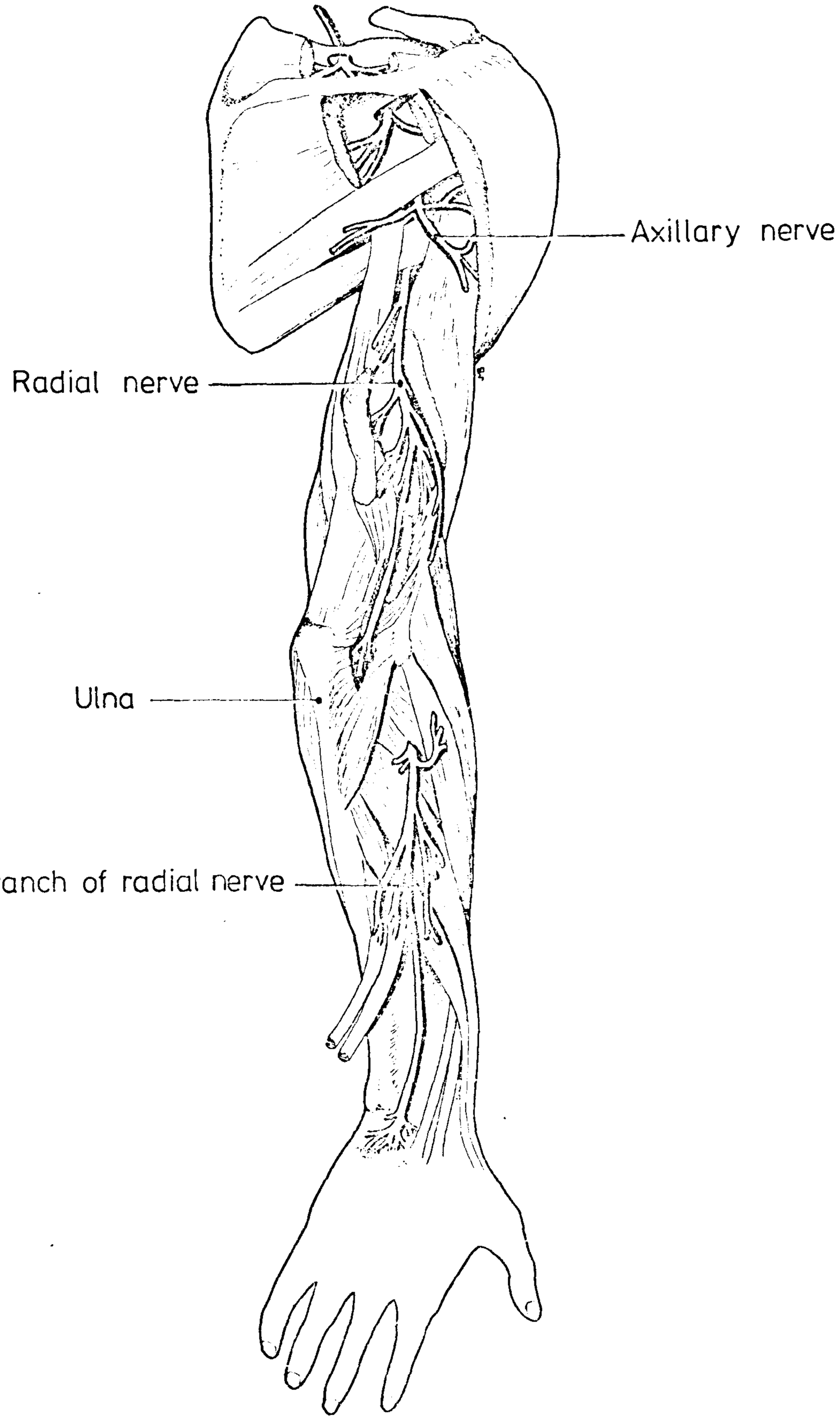

Figure 1·21: Nerves of the right arm – posterior aspect.

2. FUNCTIONAL ANATOMY

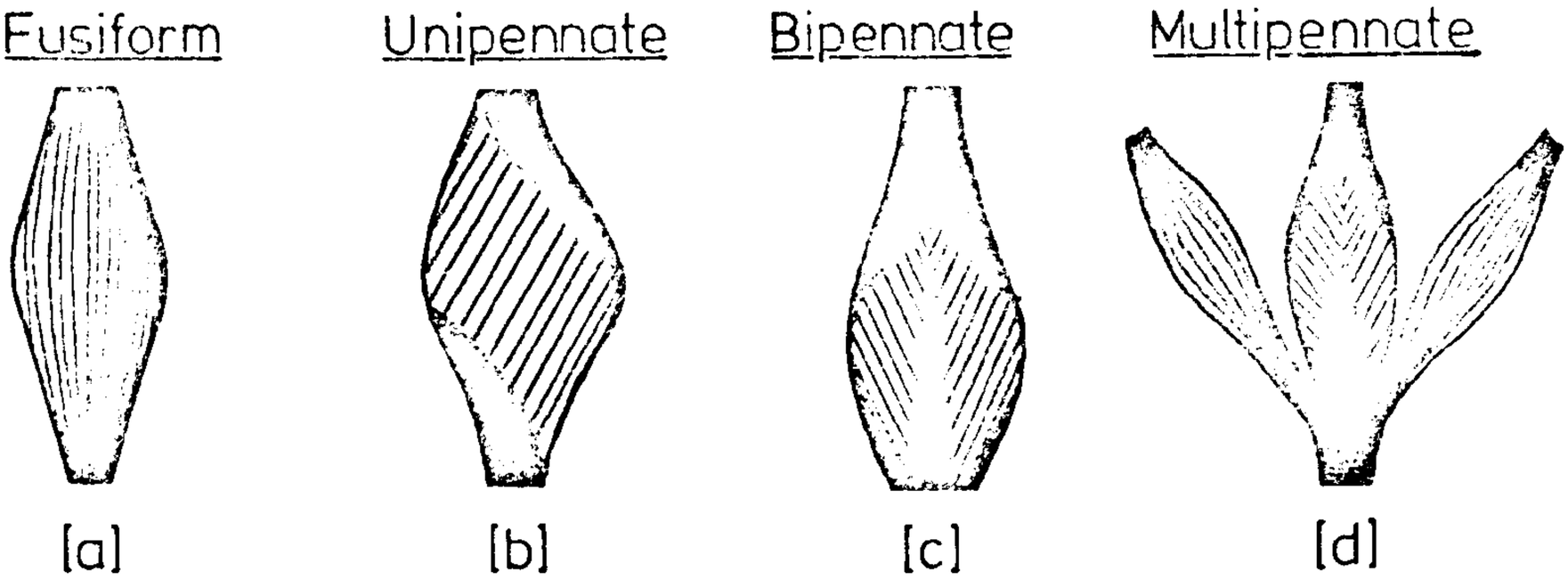

Figure 2·1: Types of muscle structure

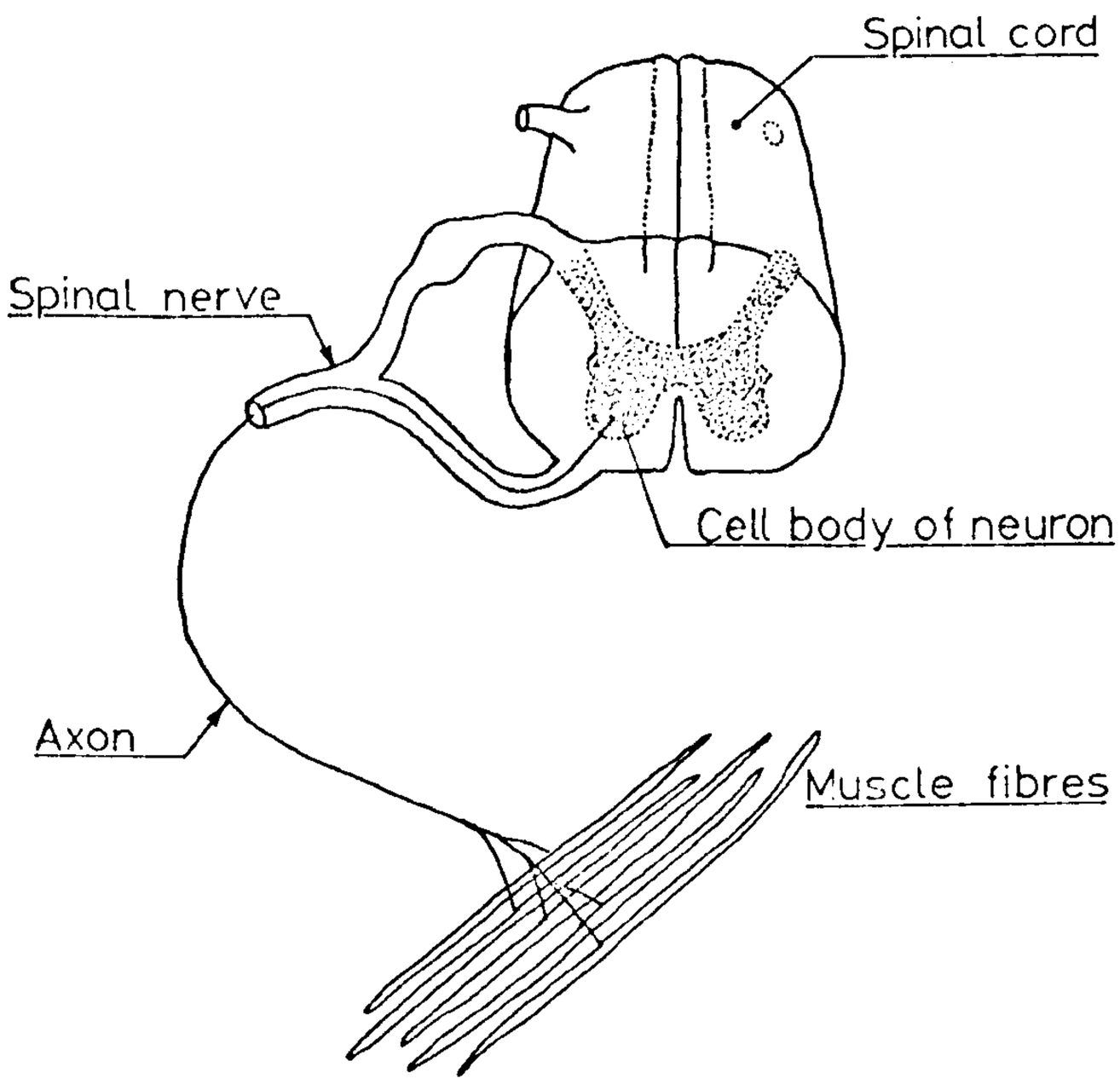

Figure 2·2: The "Motor Unit"

2. FUNCTIONAL ANATOMY

2.1 Muscle Physiology:

Mechanical actions in every part of the body rely on muscles for their effective execution. Such an important system is, understandably, very complex in its layout and structure. Accordingly, only a brief description of the principles of muscle action is given.

2.1.1 Skeletal muscle: Three types of muscle exist; cardiac muscle of the heart which suffers no effects of fatigue, involuntary smooth muscle, and skeletal muscle which powers the limbs by voluntary action. The arrangement of fibres and the design of the muscle body are determined by the function of the muscle and a compromise is often made between power, speed and range of movement (Bourne, 1972). The bulk, or belly, of the muscle is usually positioned to minimise interference with movement around the skeletal joint. The flexors of the hand are typical of the use of long tendons to transfer muscle action to regions of restricted volume.

The muscle fibres join the tendon in several ways to give a variety of muscle performance. Where the tendon blends with the muscle fibres longitudinally, the muscle is termed fusiform and is shown diagrammatically in figure 2.1a. Unipennate muscles have their fibres attached along one edge of the tendon (figure 2.1b), whereas bipennate muscle fibres are joined to both sides of the tendon (figure 2.1c). In cases where several tendons join the muscle fibres, as in figure 2.1d, the muscle is termed multipennate.

Muscles are stimulated by electrochemical signals from the brain which travel down the spinal cord and through long nerve fibres or "neurones". The cell body of the neuron is contained in the anterior horn of the spinal grey matter and each axon supplies several muscle fibres as shown in figure 2.2. The combination of neuron and the muscle fibres supplied by the neuron is termed a motor unit and is the functional unit of skeletal muscle. The motor end-plate, the junction of nerve with muscle fibre, is a thin flat plate composed of acetylcholine and provides the neuromuscular transmission mechanism (see figure 2.3).

The number of muscle fibres contained in each motor unit determines the finesse of overall muscle action. Leg muscles have a high number per unit whereas eye muscles, which require accurate control, have very few fibres

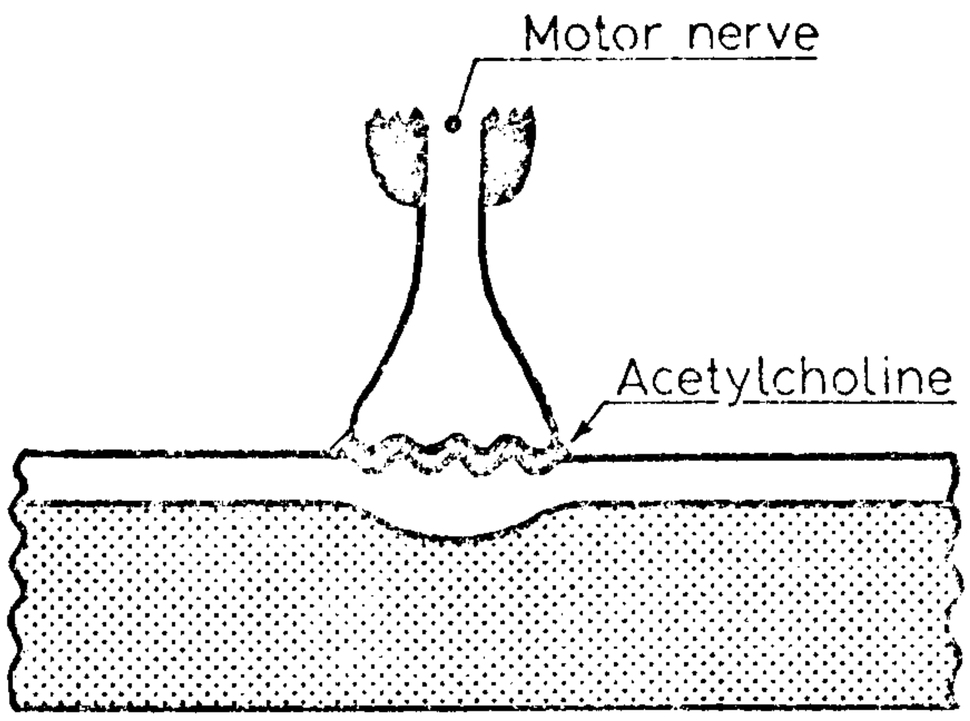

Figure 2·3: The "motor end plate"

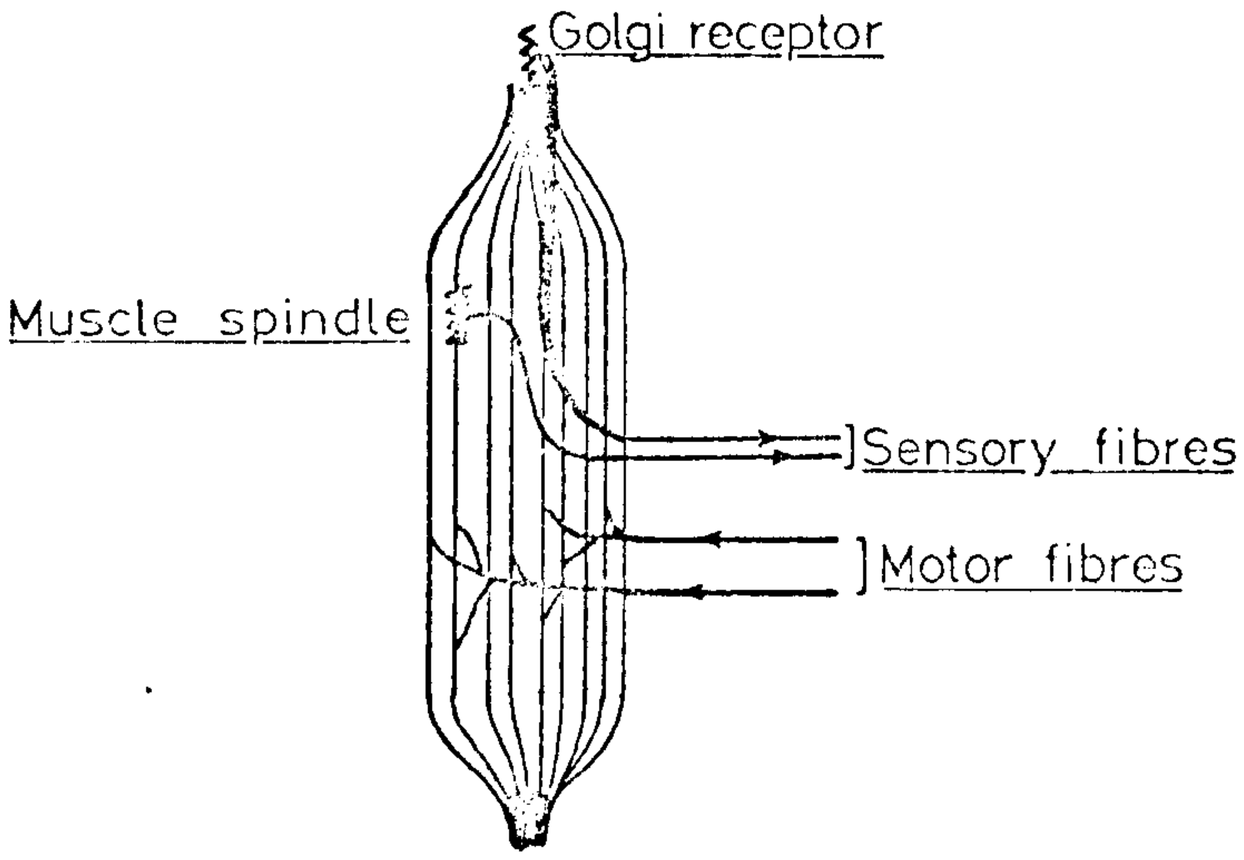

Figure 2·4: Feedback mechanism for muscle

per motor unit (Basmajian 1974). To achieve accurate function of muscular contraction, provision is made for a continuous feedback of information relating to muscle actions. Sensory organs are incorporated into muscles and tendons and are called muscle spindles and Golgi receptors respectively. The information sent to the brain from the sensory organs controls the impulses which activate the muscle. Several subtle refinements are built into the feedback system giving smooth, accurate and automatic control (Katz, 1966). A generalised diagram of the system is shown in figure 2.4.

2.1.2 Electromyography: As its name suggests, electromyography is the recording of the electrical discharges or action potentials, from muscles. The science of electromyography dates back to the 18th century but it was not widely used until amplifiers and sophisticated recording equipment became available. The electromyogram (EMG) can be obtained superficially or intramuscularly.

Small disc electrodes are applied to the skin in the former method and the resulting EMG represents the activity of the muscle masses in the adjacent underlying tissue. More localised recording is achieved by using intramuscular electrodes in the form of hypodermic needles or very fine wires. Detailed descriptions of the manufacture and use of the various types of electrodes are contained in literature by Basmajian (1974 and 1973) and O'Connell and Gardner (1962).

2.1.3 Length-tension relation: The most fundamental property of skeletal muscle is the relation between its length and the tension which it can produce (Elftman 1966). In simple mechanical terms, muscle is composed of a contractile unit (filaments) in parallel with an elastic component in the form of the surrounding connective tissue. (Morrison 1970). In series with both these units, the connective tendon represents a second elastic element. The force produced by a muscle at maximal stimulation will, therefore, depend on two factors; the amount of stretch in the parallel elastic component and the shift from the resting length, L_o. The contractile element has a tension/length curve as shown in figure 2.7 where the tension is zero at about 60% extension. However, since the parallel elastic component exhibits tension

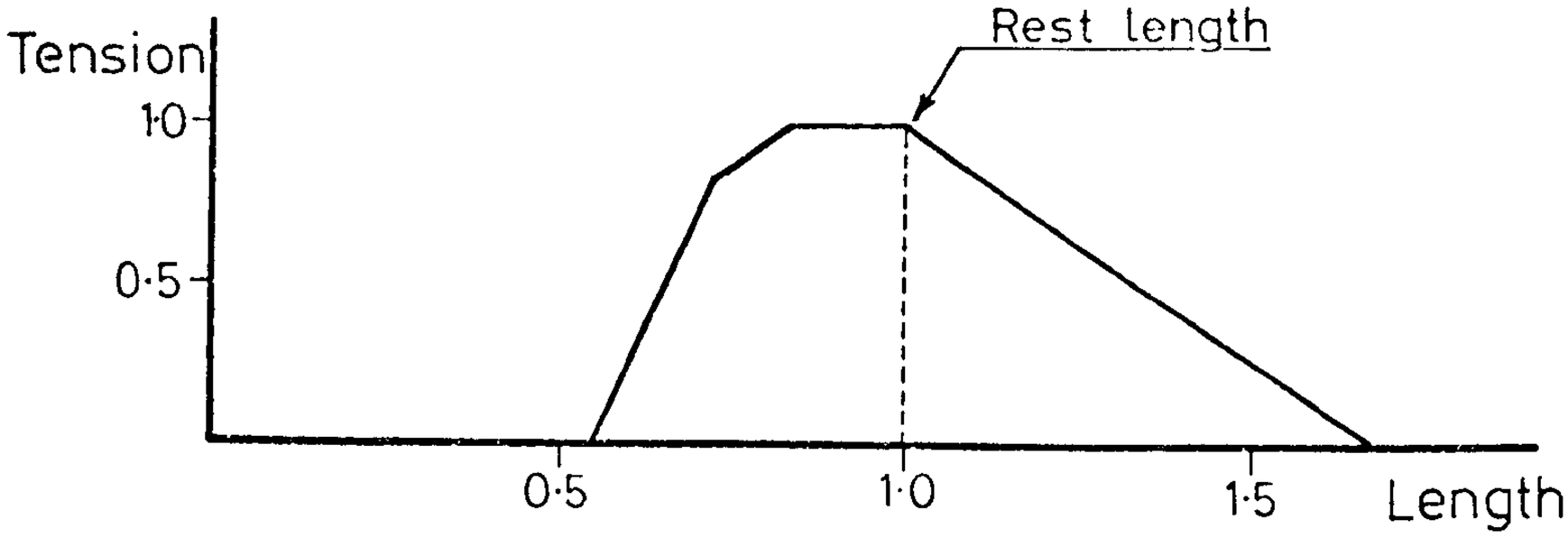

Figure 2·7: Length - tension relation of muscle.

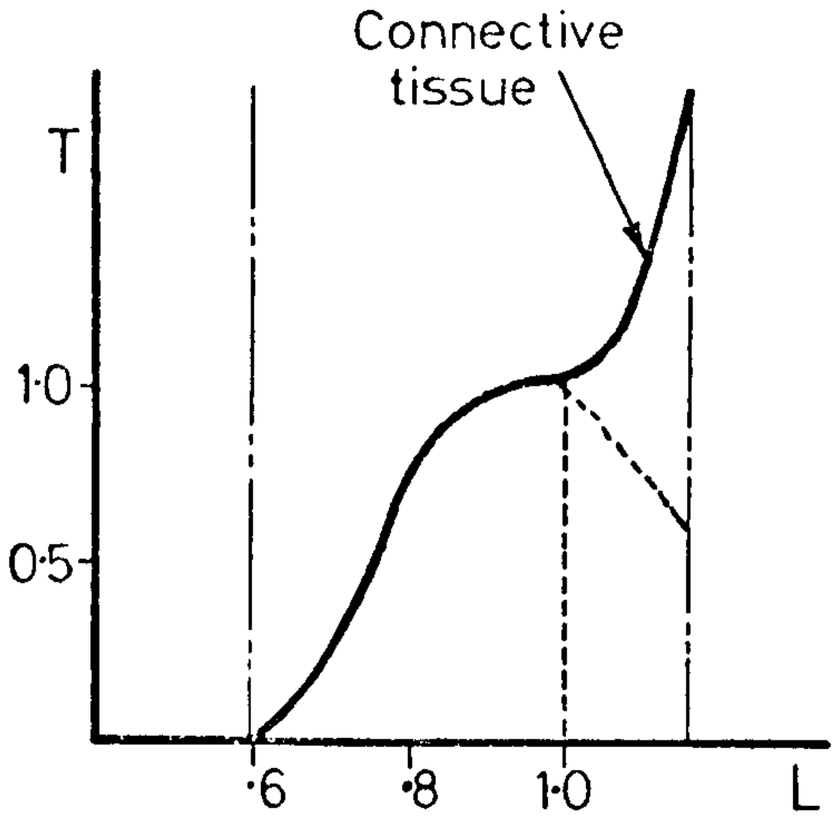

[a] Isometric Contraction

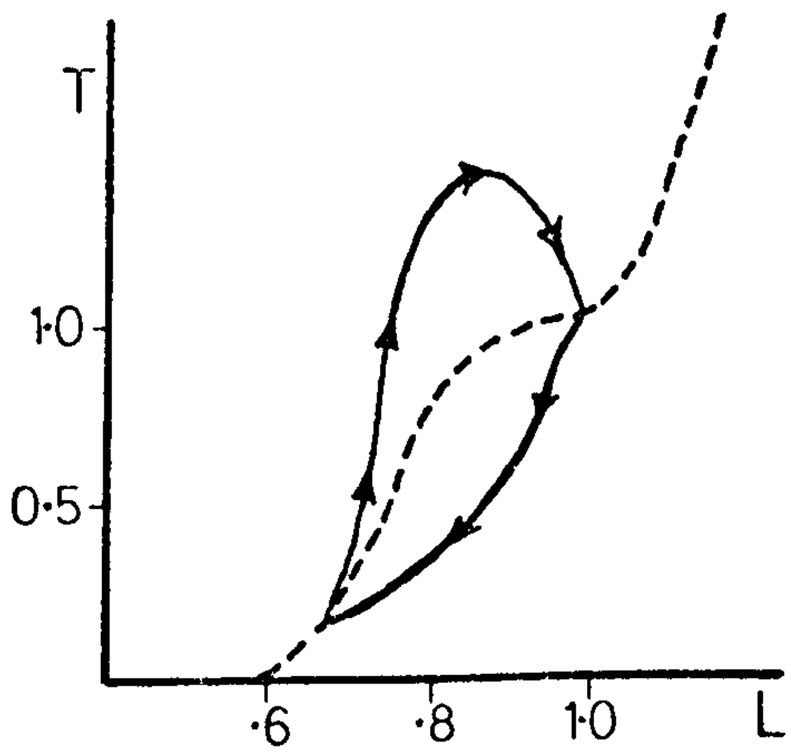

[b] Fast Contraction

Figure 2·8: Dynamic characteristics of muscle

at this length, the overall "muscle tension" is greater (Elftman 1966).

Anatomically, limits are imposed on the distances between origins and insertions when dealing with two-joint muscles. "Active insufficiency" occurs when the muscle contracts fully before the range of joint movement is complete. "Passive insufficiency" results in the muscle reaching its limit of extension before the completion of joint movement (e.g. hamstrings group). Thus the length of a muscle has a limit of around 25% extension, as shown in figure 2.8a. (Elftman 1966). Accordingly, the parallel elastic tension has a great effect on the gross force in a muscle under extension.

2.1.4 Velocity - tension relation: In addition to the length of a muscle, the velocity of contraction affects the tension which may be produced. Figure 2.8a shows the force/length relation for isometric "contractions" where no change in length is observed. Figure 2.8b shows the alterations to the muscle force if extension or contraction occurs. The interesting point is that a muscle produces less force when it contracts than when undergoing isometric contraction.

Hill (1970, 1950 and 1938) produced an empirical relationship between tension and velocity of contraction from studies with frog muscle undergoing maximal stimulation as follows:-

$$v = b(p_o - p)/(p + a)$$

where, p = contractile force

p_o = isometric contractile force

v = velocity of shortening

a, b are constants

It was postulated that the constant "a" represented the heat produced during contraction. Combined with the velocity of contraction, the product $(p + a) * v$ represented the power emitted by the muscle. Hill (1951) also showed that energy was absorbed, in addition to the heat generated, when active muscle was lengthened. Matsumoto (1966) performed mathematical validity tests using Hill's equation for various lengths of muscle. For constant loads, the results verified the relationship between isotonic contraction tension and the velocity of contraction.

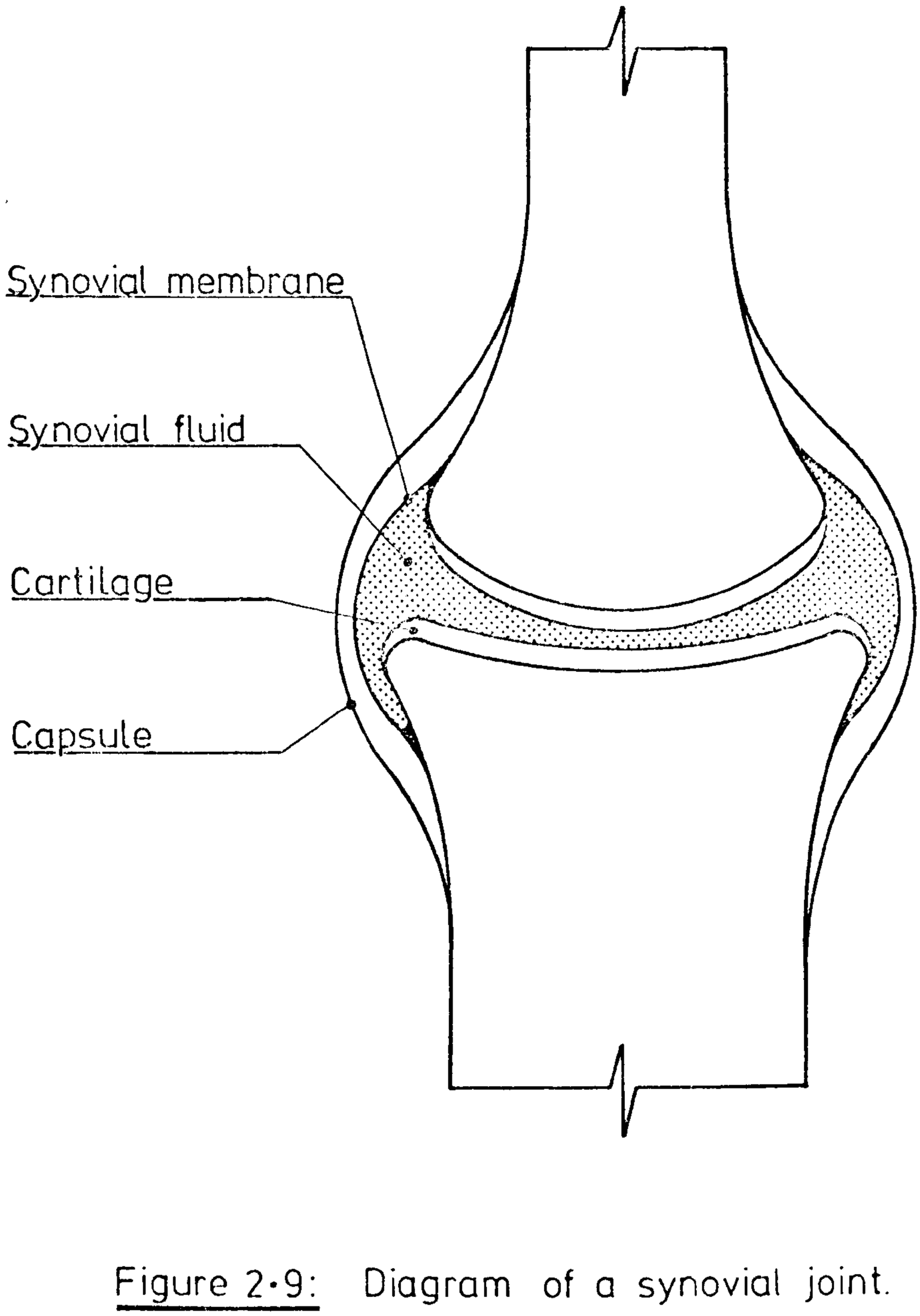

Figure 2·9: Diagram of a synovial joint.

2.1.5 E.M.G. - tension relation: Muscle tension and the corresponding E.M.G. signals are directly related to one another (Basmajian 1967) but the precise quantitative assessment has yet to be performed.

"Integrated" action potentials have been obtained by Ralston et al (1947, 1948) and Inman et al (1952) where the averaged signal amplitude was taken. For surface, needle and wire electrodes, parallelism was concluded between the curves describing both the processed E.M.G. and isometric muscle tension. However, an inverse relationship appeared between muscle length and electrical output with the short muscle length giving increased electrical output. Moreover, for the same tension, muscle undergoing extension gave a lower electrical output than muscle in isometric contraction.

By using a planimeter to measure the area enveloped by the E.M.G. trace, Lippold (1952) showed that a definite linear relationship exists between isometric force and the "integrated" E.M.G. Shortly afterwards, Bigland and Lippold (1954) concluded that tension, velocity and electrical output were interrelated and that the relationship between tension and integrated E.M.G. was linear.

More recent investigations into the relations between muscular tension and processed E.M.G. signals have followed the empirical approach which involves the comparison of the electrical "output" with dynamic mechanical quantities. The various problems involved in quantitative electromyography are outlined in Desmedt (1973), together with details of recent investigations.

2.2 Joint Physiology:

2.2.1 Synovial joints: Joints are designed to permit location of, and articulation between two or more members of an endoskeletal structure and can be of three types; fibrous, cartilaginous or synovial (Gray 1973). The unions between segments of the skull are typical of one type of fibrous joint where no appreciable movement is possible. Where cartilage, or fibrocartilage, forms the uniting medium the joint is termed fibrocartilaginous and slight movement is possible by deformation of the connecting pad of fibrocartilage. All the joints of the limbs, excluding the tibiofibular syndemosis, are of the synovial type (see figure 2.9).

20a

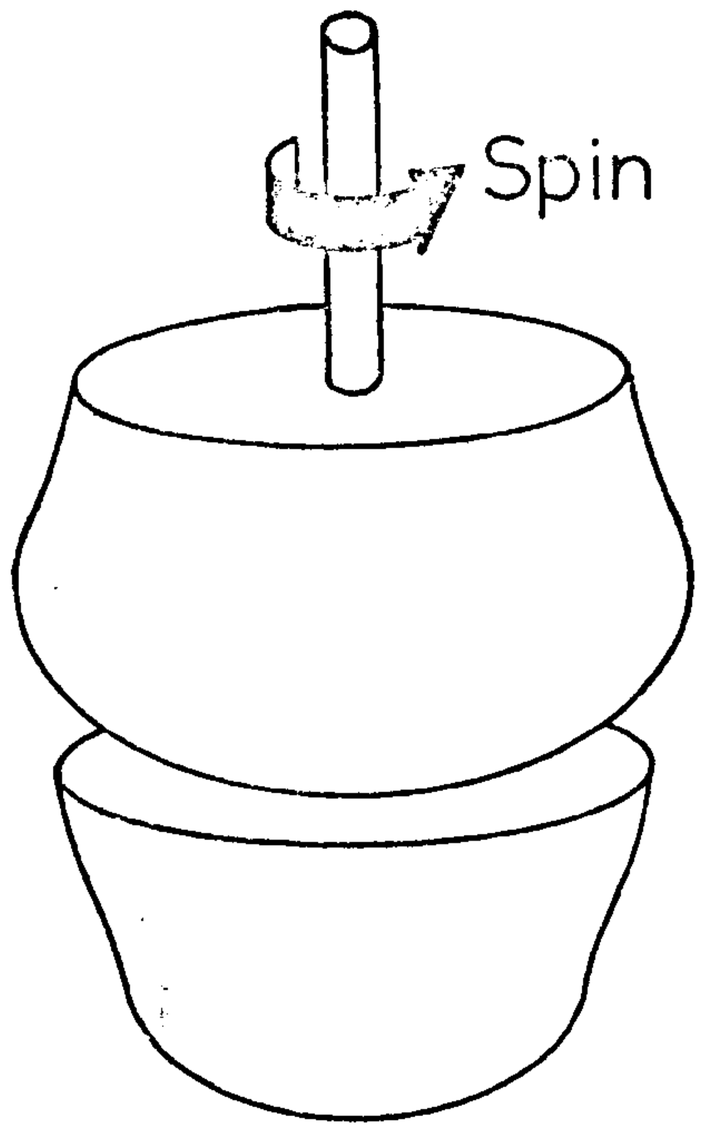

[a]

[b]

[c]

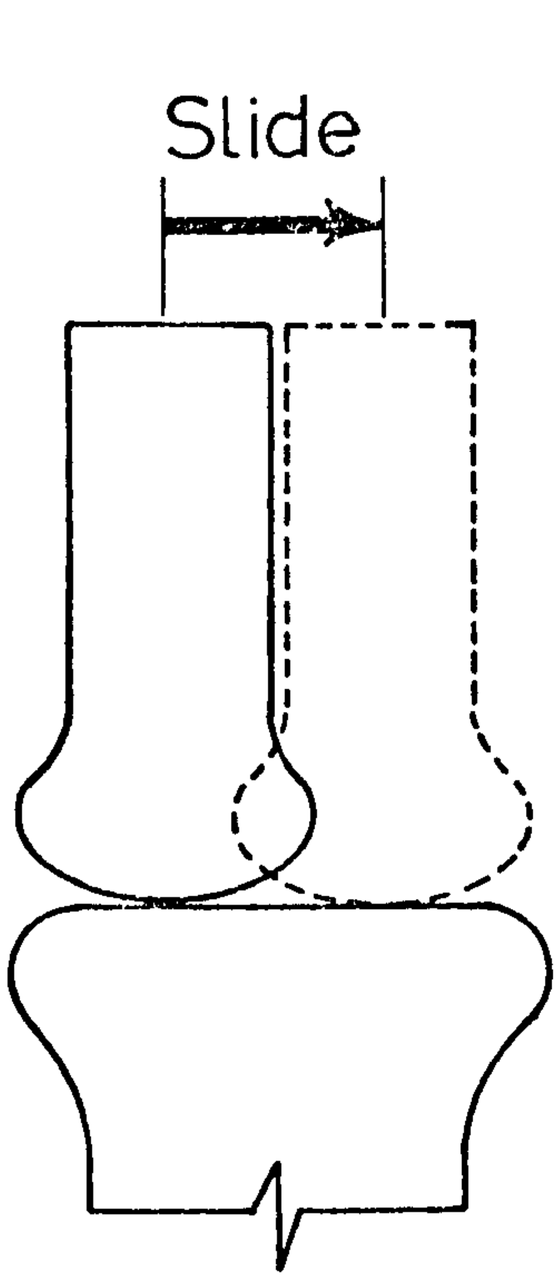

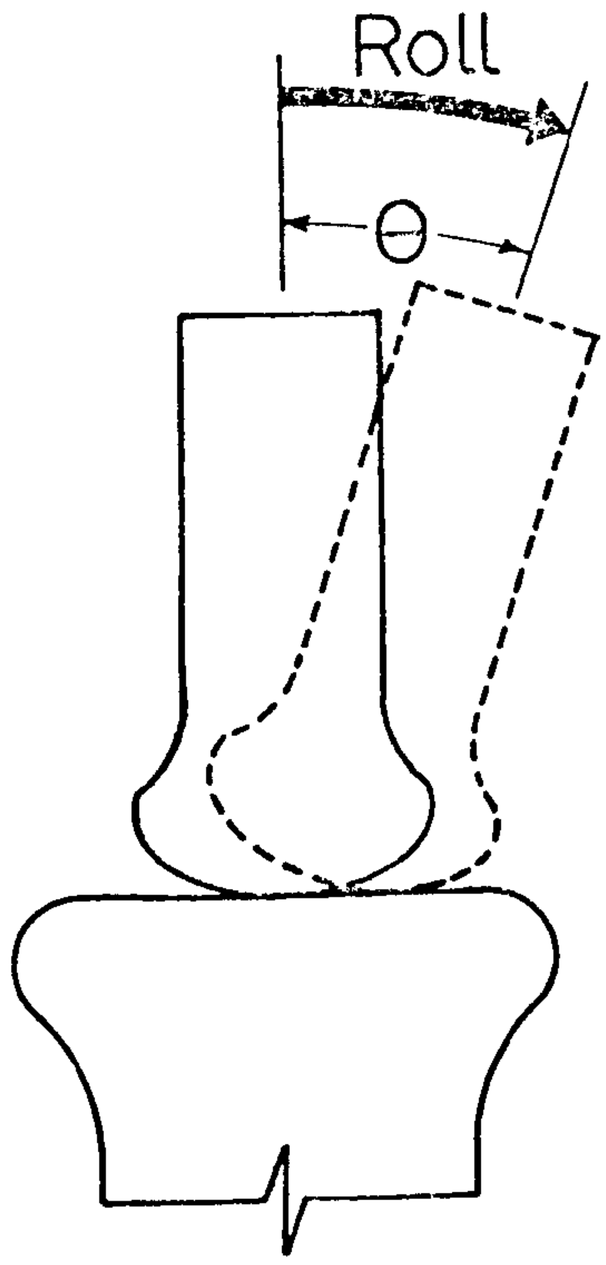

Figure 2·10: Fundamental movements of a synovial joint.

Synovial joints consist of at least one pair of mating surfaces completely enclosed by the articular capsule. The capsule consists of an outer fibrous medium with an inner lining (synovial membrane) which lines the whole of the interior of the joint cavity, excluding the articular surfaces, and contains and produces the lubricating medium, synovial fluid (MacConail 1967). In this way a healthy synovial joint has a complete self-maintenance mechanism.

Although the fibrous capsule can connect the various bones, it is usual to find a number of ligaments providing additional strength. Any tendency to overload the structures is usually opposed by reflex muscle action (Gray 1973).

2.2.2 Joint motion: There are three fundamental movements of one joint surface upon another; spinning, sliding and rolling. Normal joint activities consist of various combinations of these basic modes.

Where rotation occurs about the long axis of the moving segment, spinning will be dominant. Theoretically, pure spinning involves zero displacement of the idealised point of contact and zero slip of one surface over the other as shown in figure 2.10a.

Given two contacting surfaces, "pure sliding" occurs when the point of contact on the moving surface undergoes a displacement relative to the other surface and remains the point of contact (figure 2.10b).

"Pure rolling" exists when one surface is displaced relative to the other but no slip occurs at the point of contact. This action is always accompanied by a relative angular displacement as indicated by θ in figure 2.10c.

2.2.3 Mechanical characteristics: The remarkable ability of synovial joints to function for many years under frequently severe loading conditions can be attributed to the geometry of the joint surfaces, the structure of the articular cartilage, and the dynamic lubrication properties of synovial fluid (Dowson 1973).

It has been shown by Saha (1957) and Wright et al (1971b) that the male components of the shoulder and hip joints respectively have a greater radius of sphericity than the female part. For the weight bearing hip joint, the radial difference is of the order of 500μm and provides a marked increase in the load bearing area for increased joint loadings. In other joints, for example the knee, the relative "fit" of the components is very loose and consequently large areas of cartilage are provided for load transmission by

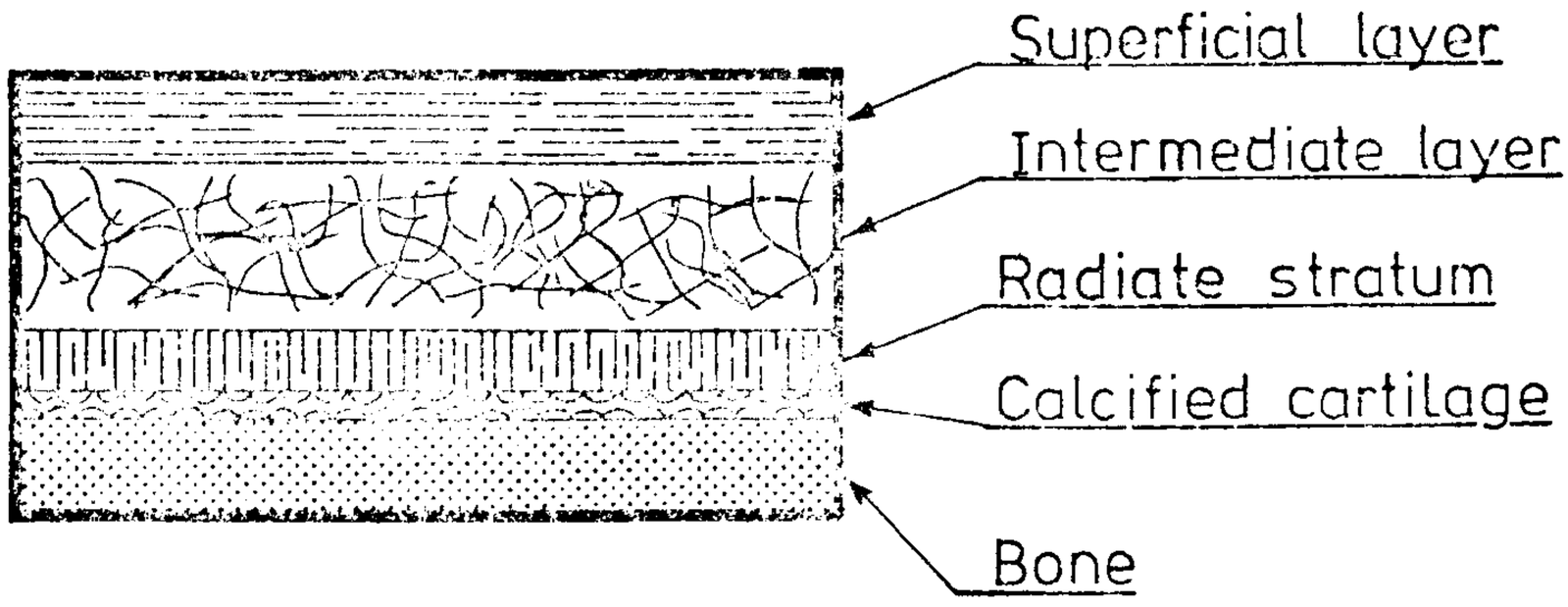

Figure 2·11: Micro-structure of articular cartilage

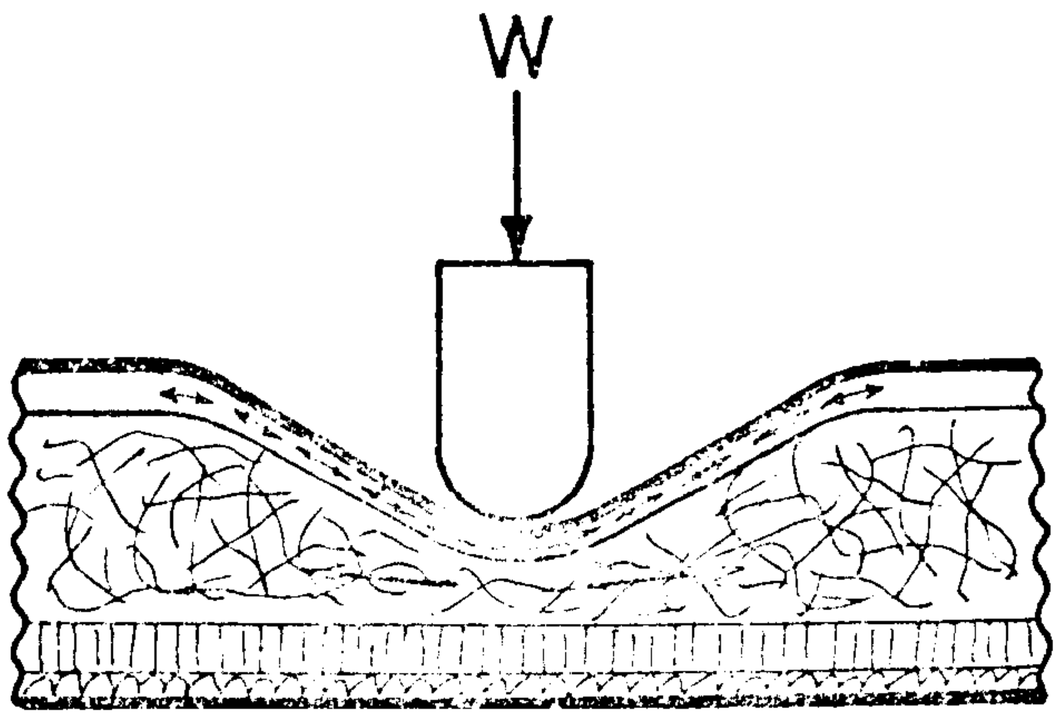

Figure 2·12: Load bearing mechanism of cartilage

normal deflection around the point of contact.

Articular cartilage is composed of cells, the chondrocytes, which lie in cavities contained in an intracellular matrix. The cartilage covering the articular surfaces of most synovial joints is of hyaline or glass-like appearance and suggests a perfectly smooth bearing surface. The cartilage varies in thickness from 1 mm in small joints up to 7 mm in the large joints of healthy adults (Barnett et al, 1961). It is generally accepted that the layer is thicker where higher pressures are experienced and that periods of exercise produce significant swelling. From electron microscope studies it is now known that cartilage consists of bundles of two types of collagen fibres in the form of fine fibrils of 400 $\mathring{A}$ diameter and cross-banded fibres which lie approximately 700 $\mathring{A}$ apart (Barnett et al 1961). The four visible layers, or strata, commence with "calcified cartilage" which lies adjacent to the subchondral bone and binds the second layer, the "radiate stratum", to the bone tissue. Large tightly packed fibrils make up this radial stratum and are perpendicular to the bone surface as shown in figure 2.11. Above the radiate stratum, the intermediate layer consists of large fibres arranged in a tangled open network. The superficial layer covers all other layers and has lightly packed fibrils arranged tangentially in relation to the bearing surface. When the cartilage is compressed, only the structure of the open intermediate layer is affected (Wright et al 1971b). The arrangement of the tangled fibres becomes disrupted and the fibres tend to uncoil and orientate themselves at right angles to the direction of loading. Tension is therefore produced perpendicular to the load direction and gives the required support. (see figure 2.12).

In engineering terms, synovial joints are lubricated by synovial fluid which is a clear or slightly yellow viscid fluid (Barnett et al, 1961). Synovial fluid is a dialysate of blood plasma and contains protein hyaluronic acid which is a mucopolysaccharide with high molecular weight (approx. 10^6). The viscosity of synovial fluid is due to the hyaluronic acid and it has been postulated that the protein constituent serves as the mediator for the adsorption of synovial fluid to articular cartilage (Wright et al 1971b). The fluid is

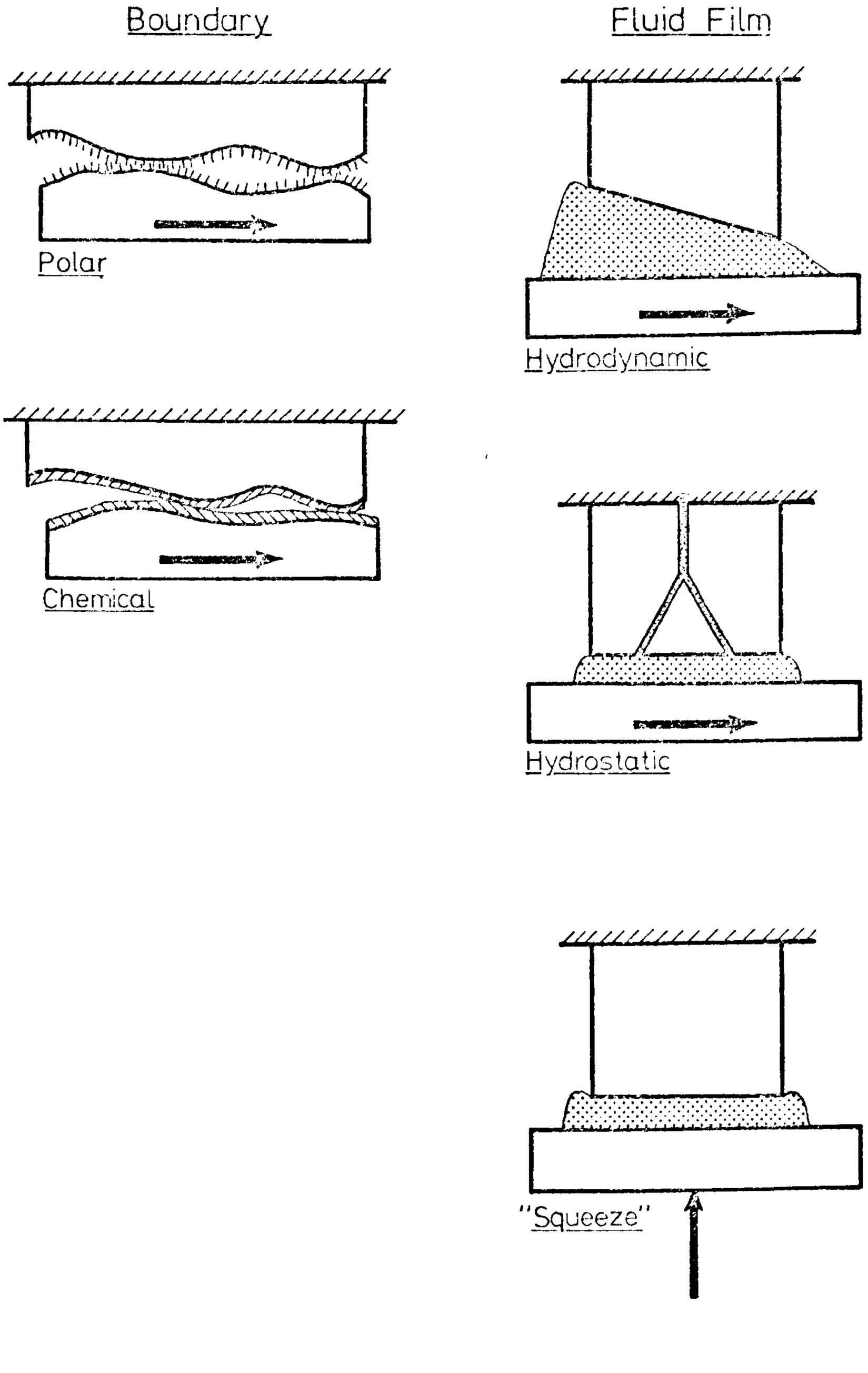

Figure 2·13: Several modes of joint lubrication.

characteristically non-Newtonian in so far as its viscosity drops as the rate of shear increases. Elasticity is also present which produces a tensile force in the direction of motion. The lubrication properties of synovial fluid are of particular significance to engineering studies. The high viscosity and good adsorption properties of synovial fluid suggest that a film of fluid exists between the articulating surfaces. The precise nature of the film, especially its thickness, has been the topic of many investigations and experiments. Two modes of lubrication have become apparent, namely: fluid film and boundary lubrication.

Boundary lubrication exists when the fluid is attached to the bearing surfaces by polar or chemical mechanisms. The system follows the usual frictional relationships and if the film of fluid remains unperforated, the wear rate would be zero. Under certain local contact stresses however, the fluid film would almost certainly break down, resulting in contact between bearing surfaces. It has been shown that for low physiological rubbing speeds, boundary lubrication exists in synovial joints (Swanson 1975).

To prevent wear during normal loading situations, the film of fluid must be considerably thicker than that produced by adsorption methods. Fluid film lubrication produces an unbroken film of fluid which can be maintained by several methods shown in figure 2.13.

Hydrodynamic lubrication exists where surface incongruities of human joints can produce a wedge of pressurised fluid if the rubbing speeds are appropriate. Unfortunately high loads during low sliding speeds would lead to breakdown of the film.

Hydrostatic lubrication, where the fluid film is maintained by an external pressurising unit, may be obtained during cartilage compression. In such cases the pressure is produced by fluid being squeezed out of the compressed cartilage and is known as "squeeze-film" lubrication. The low porosity of the cartilage, however, would produce a slow dispersion of synovial fluid and therefore diminish the efficacy of such a mechanism.

Wright et al (1971a) postulated a squeeze-film lubrication mechanism supplemented by "boosted lubrication". Pressurisation of synovial fluid trapped

in the bearing surface undulations during high loads would cause the low molecular weight constituents to escape through pores into the cartilage. The heavy constituents which remain would form layers inclined to the surface of the cartilage. Under additional load actions the layers would flatten to cover and protect the bearing surfaces.

Despite the number of investigations into the precise nature of synovial joint lubrication, no single description has been universally accepted. Swanson (1975) reviewed the progress made so far and suggested that studies of synovial fluid composition in a wide range of joints could provide the necessary information.

2.3 Joint Pathology:

2.3.1 Introduction: Excluding traumatic injuries, the two most common diseases of human joints are rheumatoid arthritis and osteoarthrosis. Surgery in various forms can be performed to relieve pain and restore the use of the limb to near normal. Unfortunately, only the hip arthroplasty can be termed completely "successful", although knee joint replacement is presently at an advanced stoge of development. Other joints are troublesome and functional normality remains a distant objective.

2.3.2 Rheumatoid arthritis: In 1941 the term "rheumatoid arthritis" was introduced and defined as a "systemic disease affecting primarily connective tissue" (Marmor 1967). Non articular arthritis refers to primary involvement of the soft tissues but this is of minor relevance to joint studies.

The science of rheumatic diseases is extremely complex since their aetiology is at present unknown. One current theory describes rheumatoid arthritis as an "autoimmune" disease. Referring to the basic principle of self distinction, discovered by Ehrlich and Morgenroth at the turn of the century, no antibodies harmful to self can be produced. From immunity principles however, the formation of the antibody in rheumatoid arthritis is understandable. This antibody-like factor, called rheumatoid factor, is a macroglobulin and forms an important test in the clinical diagnosis of rheumatoid arthritis (Marmor, 1967). However, the clinical, pathological and radiological observations can only offer information relating to the severity of the disease and effectiveness of applied therapy.

The fundamental disease process is rheumatoid synovitis where the mono-cellular synovial lining becomes markedly hypertrophied and thickened. Tendons and fascial tissues which are lined with synovium can also be affected, but structures around synovial joints are by far the most susceptible (Byers, 1969).

Abnormalities are seen first in the synovial membrane. The infiltration of inflammatory cells into the synovial membrane precedes and accompanies the process of forming a layer of proteinaceous material, called "fibrinoid", over part of the surface. The next stage involves prolifering fibroblasts and capillaries entering the fibrinoid material and increasing the bulk of inflamed material and this results in the stretching of the articular capsule and ligaments. Simultaneously, the disease progresses to affect adjacent tissues and structures. X-rays show a narrowing of the joint space as the articular cartilage is removed by the agency of the vascular tissue which spreads over it. The vascular tissue is believed to be of the same form as that involved with the synovial membrane. The cartilage below the spreading tissue or pannus, is resorbed and disappears, exposing the subchondral bone to the pannus. With the fibrous tissue covering the joint surfaces and the lack of joint motion, the surfaces can form a union and effectively solidify the joint. On the other hand, the subchondral bone may become grossly exposed by the degenerative changes which follow, resulting in an osteoarthrotic joint.

2.3.3 Osteo-arthrosis: It will be noted that the term osteo-arthrosis does not contain "arthritis" which helps to distinguish this degenerative disease from inflammatory disorders. Osteo-arthrosis is the most common of all the arthritic diseases (Carson Dick, 1972).

Generally, the disorder is primarily a degeneration of articular cartilage with tissue softening followed by surface flaking and a matt surface finish (Freeman 1972). Thereafter, deep clefts develop with chondrocytes around their perimeter. Exposure of the cartilage to synovial fluid enzymes, and chondrocyte enzymes, has been put forward as an explanation of the rapid destruction of cartilage (Carson-Dick, 1972).

Many changes occur in the synovial fluid including an increase in volume which may be attributable to dilution of the fluid which in turn produces a decrease in viscosity. Many

engineering studies are underway to investigate lubrication characteristics of synovial fluid and "artificial" lubricants which may overcome cartilage flaking. It has been shown that osteo-arthrotic joints possess increased friction and abnormal methods of lubrication (Freeman 1972). On the other hand, the onset of osteo-arthrosis could be due to changes in the load carrying properties of the articular cartilage. Many of the investigations involving the properties of cartilage are discussed briefly by Freeman (1972).

2.4 Bone Characteristics:

Bone is a dense matrix in which spidery cells, osteocytes, are embedded. The matrix material is composed of collagen fibres, crystals of calcium-phosphate complexes and a ground substance containing mucopolysaccharides (Pritchard, 1972). The nucleated body of the cell occupies a very small cavity but the cytoplasmic processes lie in long thin tunnels, or canaliculi, interconnected with other canaliculi. During bone formation, osteoblasts (modified cells of connective tissue) secrete a material which becomes densely fibrous and is known as "osteoid". Deposition of calcium phosphate crystals then changes the osteoid into the bone matrix. Bone is therefore permeated throughout by an extremely rich system of communicating canals and cavities (osteones).

There are three specific structural types of bone; fine cancellous, compact, and coarse cancellous bone.

Fine cancellous bone is characteristic of new bone whether foetal or pathologically induced and can be of cartilage or membrane origin. Compact bone consists almost entirely of fine-fibred bone, riddled with vascular canals. Its formation arises from the production of cylinders of new bone, within existing bone, or by direct primary formation of solid bone on the periosteal and medullary surfaces of the bone shaft. Coarse cancellous bone is similar to compact bone in its fine structure except that complete osteones are rarely present.

A great number of investigations have been performed relating to the mechanical properties of bone and whole bones. Relationships, both qualitative and quantitative, have been sought between bone mineral content, trabecular pattern, cortical bone thickness, degree of osteoporosis and bone strength.

For the various standard engineering strength tests of bone as a material, specimens are usually taken from the large long bones for example; human and bovine femurs. Sweeney et al (1965), Evans (1957), Currey (1970) and Yamada (1970) all report ranges of tensile, compressive and shear strengths under specified tissue conditions.

Currey (1959) investigated the variation in strength between primary and Haversian (mature) ox bone. An empirical relationship was formulated as follows:

$$y = (16368 - 56.5x) \text{ lbs/sq.in}$$ where y = ultimate tensile strength
x = % Haversian system.

The equation clearly shows the effect of age on bone strength and increased porosity of older bone was suggested as a probable cause. Currey (1970) again reported the effect of maturity in relation to strength, stating that trabecular bone will tolerate less and less stress with age.

Yamada (1970) reported tests performed on femoral shafts under various loadings and Evans (1957) reported more relevant tests performed on whole bones using a stress sensitive laquer ("stresscoat"). Using this substance, the critical areas of stress can be viewed and subsequent intensive testing can be carried out although it is a very cumbersome procedure.

More theoretical analyses have been performed on bone structures by Pugh et al (1973) in which they used Finite Element Analysis techniques. The authors approximated the trabecular geometry of the distal femur to a hypothetical analytical network and were able to postulate several conclusions regarding the properties of the trabecular tissue.

Saha (1973) also analysed bone from a theoretical standpoint but, in addition, he gave consideration to the anisotropic construction of the material. However, the analysis involved a considerable number of assumptions and approximations which diminished the validity of the preliminary results.

McElhaney (1965) studied the dynamic behaviour of bone using an "air gun" type testing machine which was capable of developing constant velocity compression with strain rates up to 4000 s^{-1}. The results obtained from several bone specimens clearly showed the influence of the rate of loading on the

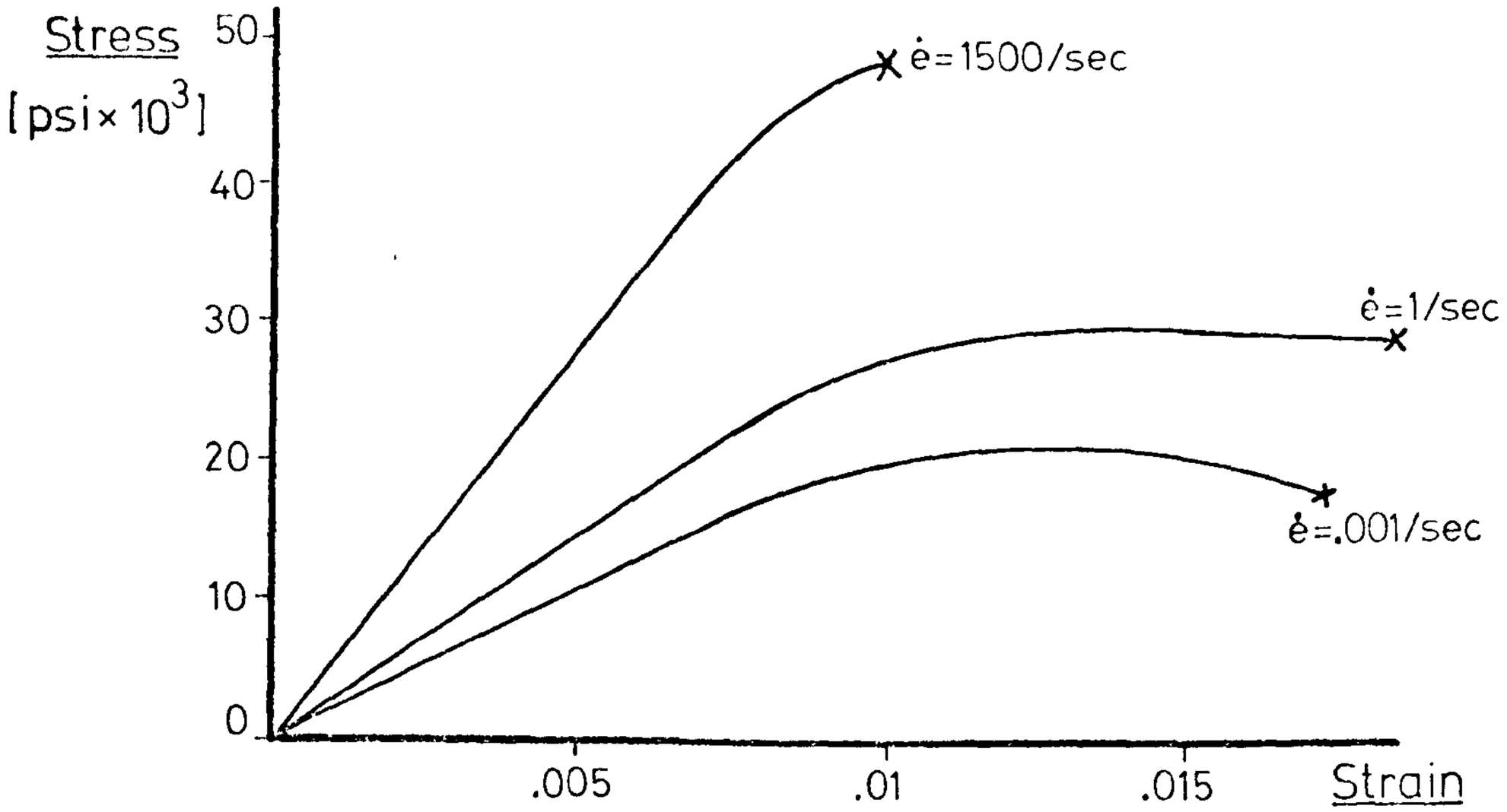

Figure 2·14: Effect of strain rate on bone characteristics.

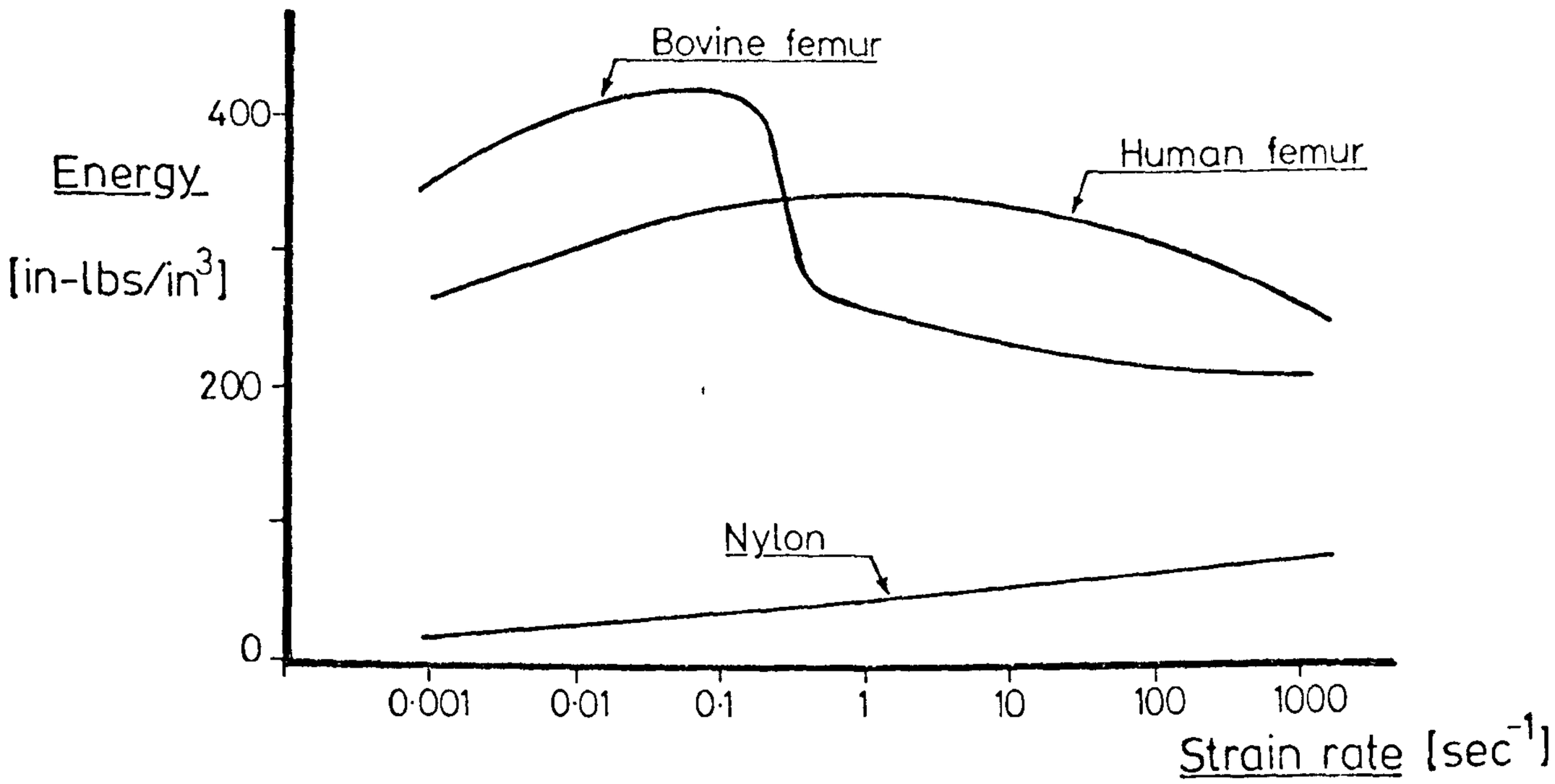

Figure 2·15: Energy absorption of bone.

stress-strain relationship. (see figure 2.14). In addition, the results indicated the existence of a "critical velocity" for bone. This phenomenon occurs when the mechanical properties of a material exhibit large variations over a small range of strain rates. Figure 2.15 shows the large drop in the energy absorption capacity for bovine bone between strain rates of 0.1 and 1.0 s^{-1}. A number of similar investigations are in progress at present and it is hoped that a practical dynamic model of bone will eventually be formulated.

3. REVIEW OF ANALYTICAL TECHNIQUES

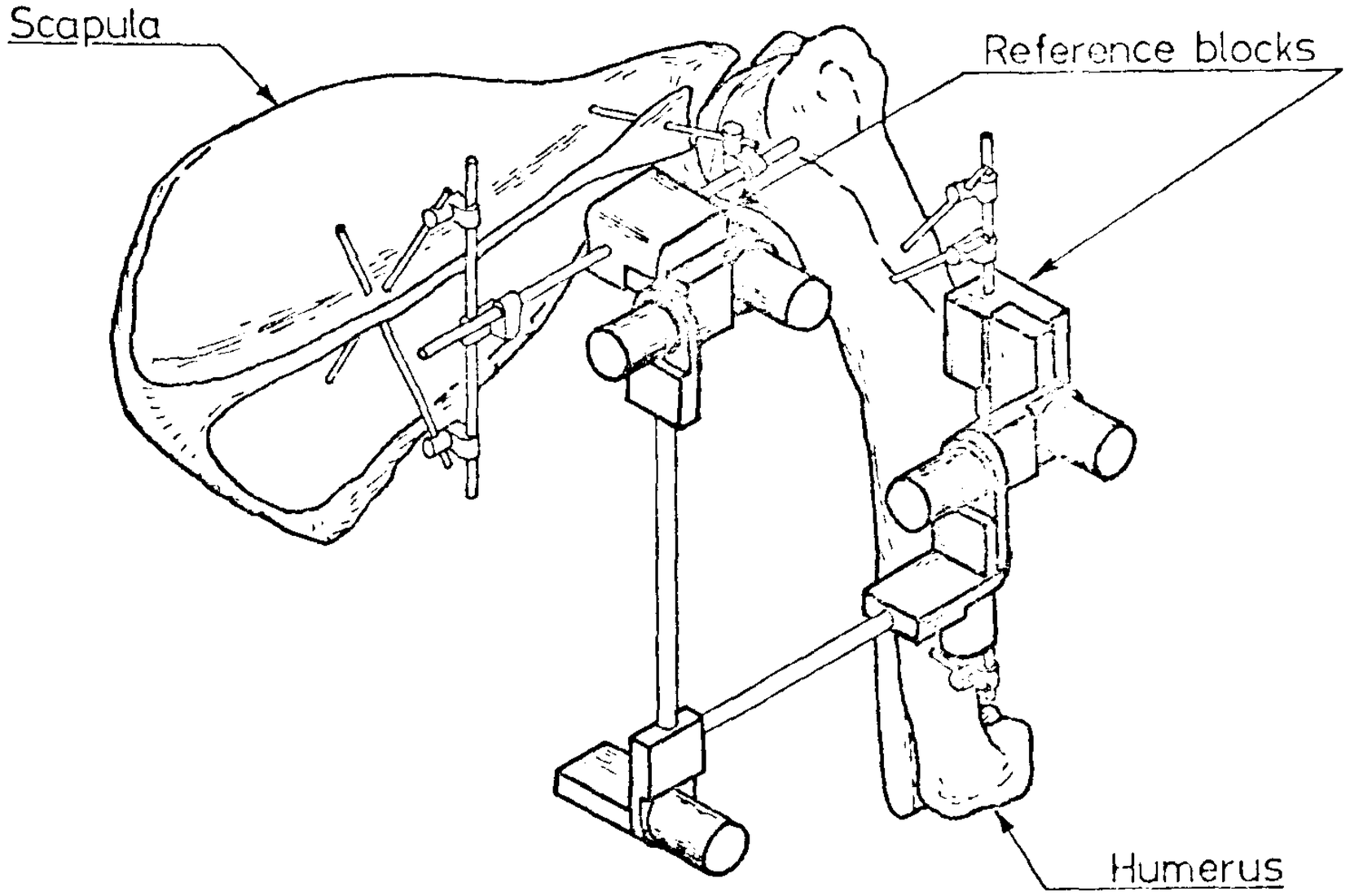

Figure 3·1: Seven bar linkage used by Kinzel et al (1972)

3. REVIEW OF ANALYTICAL TECHNIQUES

3.1 Introduction:

As a prelude to the review of analyses directly related to the elbow joint (see Chapter 4), this section describes the techniques used in the acquisition and analysis of biomechanical data.

3.2 Motion Analysis:

3.2.1 Electrogoniometry: The angle between two segments of any limb can be monitored using electronic potentiometers. A simple electrogoniometer consists of two light metal arms which can be strapped to the appropriate parts of the limb. The change in electrical resistance of the potentiometer is a measure of the angular displacements of the joint in question.

Sophisticated electrogoniometers have been developed by Lamoreux (1971) to monitor hip, knee, and ankle motion during walking. Problems encountered in the fixation of the devices to the pelvis, thigh, and shank were overcome with the construction of special frameworks from tubular aluminium. For the pelvis, the tubular structure was located by nine bony prominences whereas thigh fixation was achieved using a "velcro" cuff. Three potentiometers and suitable linkages provided measurements of flexion-extension, adduction-abduction and internal-external rotation of the hip. The knee and ankle attachments presented fewer problems but the polycentricity of these joints required the use of a parallelogram system of linkages. One of the three knee rotations was absorbed by the "self-aligning" design of this linkage but knee flexion and tibial rotation were monitored. A suitable linkage was attached to the ankle region to measure similar parameters. Precision potentiometers were used throughout and the apparatus was calibrated regularly.

To monitor the total 3-dimensional movement at any joint, Kinzel and his colleagues (1972) developed a seven-bar linkage system having six measurement axes. The complete motion between the humerus and scapula of a dog was measured during several activities. Rigid fixation of the base links was obtained using threaded Steinman pins drilled into the bones. Figure 3.1 shows the basic arrangement diagrammatically. By defining Cartesian axes

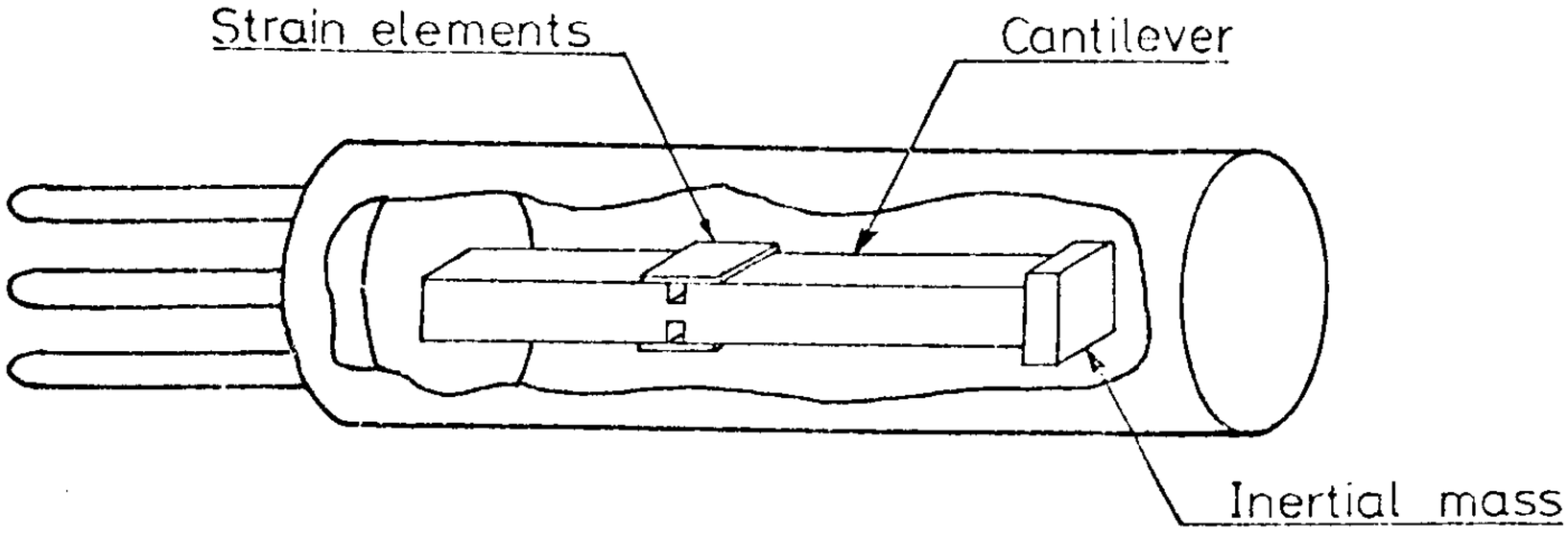

Figure 3·2: Diagrammatic accelerometer (Morris, 1973)

for each segment of the system, it was possible to compute the total motion of one segment relative to another.

In some cases, however, it is useful to measure the motion of limb segments using the Earth's gravitational axis as reference. A pendulum type electrogoniometer was developed by Peat et al (1976) where two rotations were monitored using a freely suspended mass. The two axes ensured a vertical plane for the counterbalanced pendulum and a horizontal position for the pivot axis. The device was developed for clinical use and provided rapid and accurate measurements of the angular orientation of the upper arm. However, critical quantities must be carefully selected such as the degree of pendulum damping and the natural frequency of the whole assembly.

To use electrogoniometry for the analysis of elbow function would necessitate the measurement of the movements of the upper arm and forearm with respect to the trunk. The complexity of the shoulder region would require the use of equally complex linkage systems and the final instrumentation would limit the normal movement of the arm. Limitations would also have to be imposed on the movements of the trunk.

3.2.2 Accelerometry: Accelerometry is the art of measuring body accelerations and the subsequent calculation of velocities and displacements. A typical transducer which measures accelerations consists essentially of a cantilever with strain elements and an inertial mass (see figure 3.2). Under accelerations about the sensitive axis of the transducer, the mass resists motion and the strain elements give a change of electrical resistance proportional to the strain of the cantilever. Since the deflection is produced by direct inertial force actions, the electrical signal is proportional to the linear acceleration along the specified axis.

Morris (1973) described the use of five accelerometers in the analyses of shank movements during walking. It was stated that transducers for bio-mechanical studies must contain cantilevers which deform elastically under inertial force actions. Morris also detailed the integration methods whereby the complete spatial analysis of a segment was computed from acceleration data.

As with electrogoniometry, the analysis of elbow movements using accelerometry would require the full quantification of both upper arm and

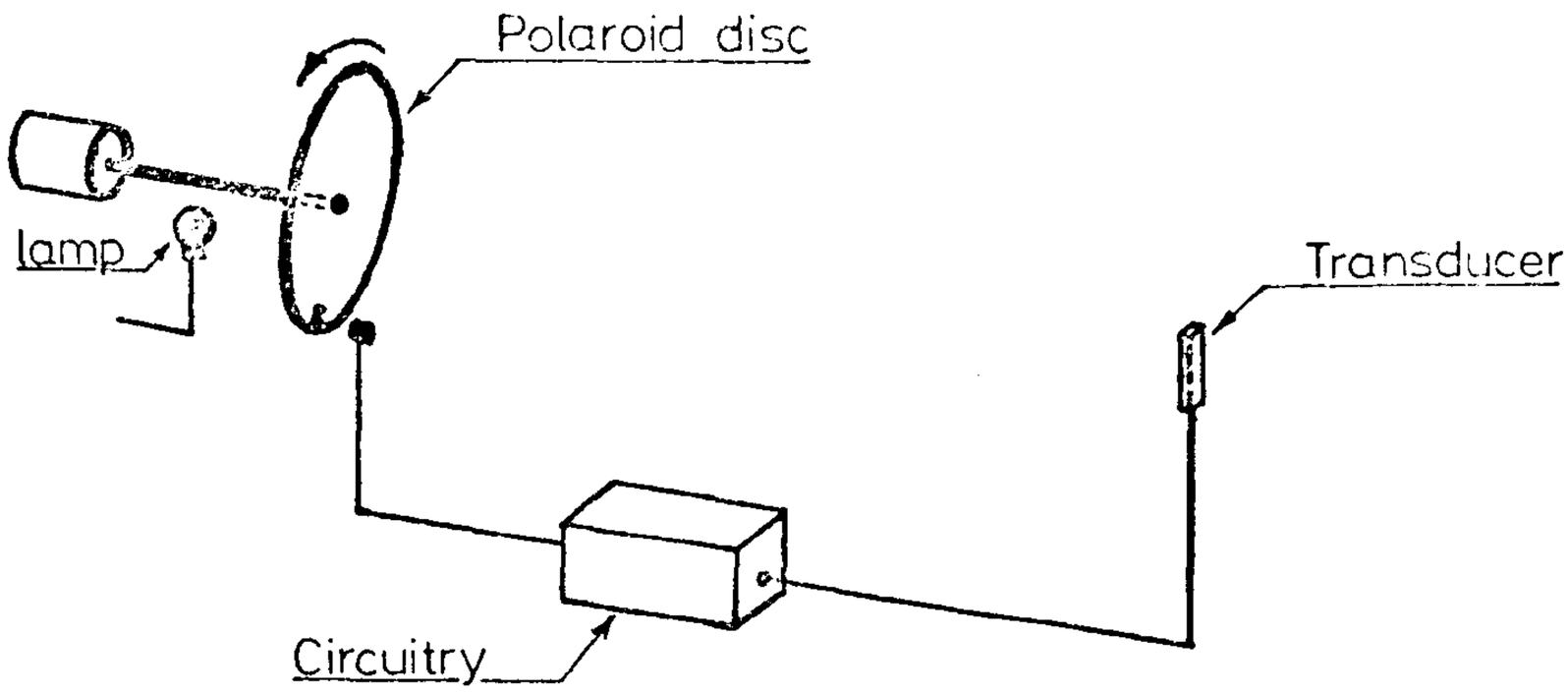

Figure 3·3: Basic arrangement of "POLGON"

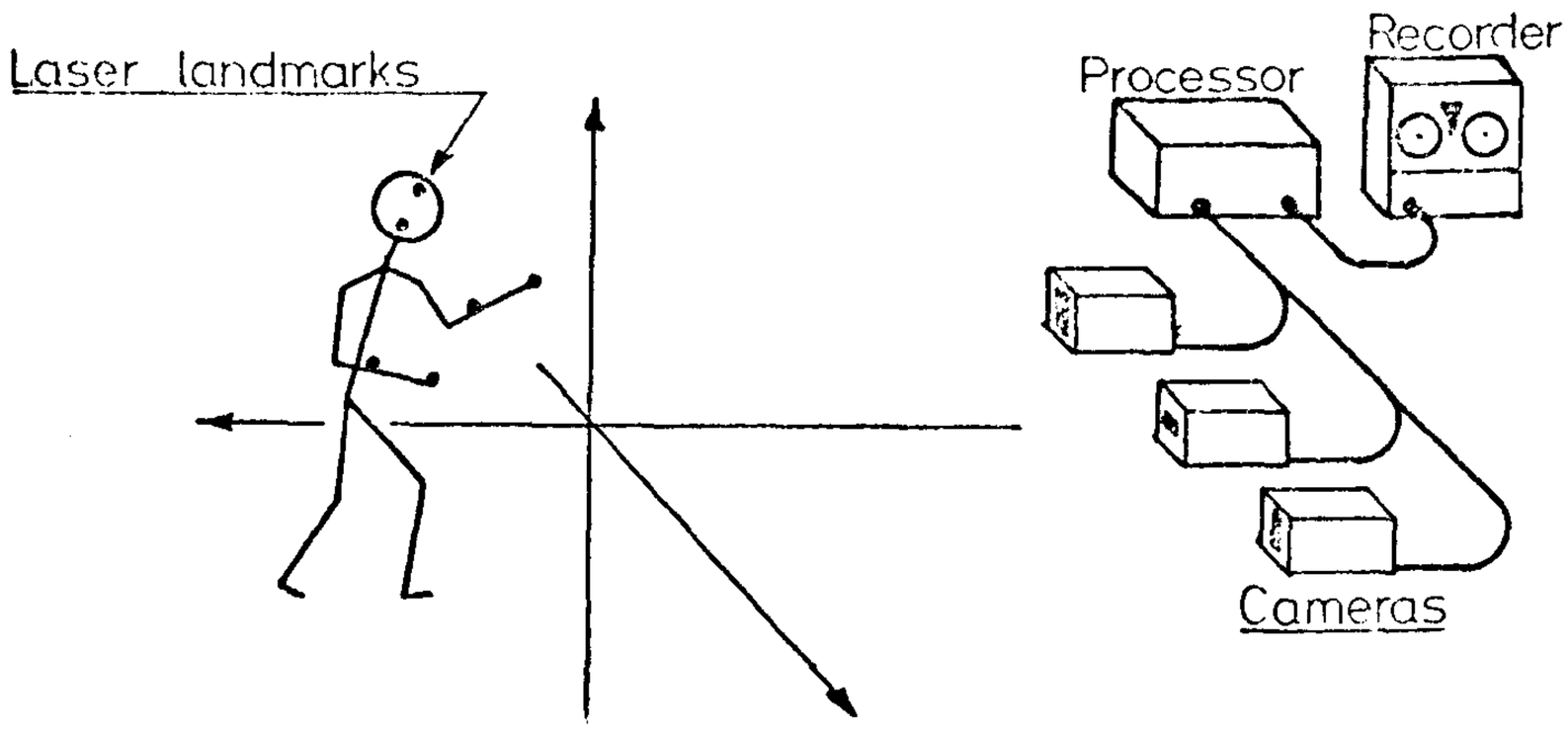

Figure 3·4: Basic arrangement of "CODA"

forearm movements. The subsequent motion analysis was therefore considered to be impracticable for the elbow movements which were contemplated.

3.2.3 Future techniques:

Polgon: Grieve has developed a new device called the Polarised Light Goniometer ("POLGON") which has been described in Grieve et al (1975). Referring to figure 3.3, a D.C. light supply is polarised via a rotating disc of linearly polarising filter material. The transducer which receives the light is mounted on the limb segment and consists of a photo cell situated behind a disc of similar polarising material. As the drive disc rotates, the photo cell produces a sinusoidal signal corresponding to the alternate transmission and extinction of light. An opaque mark on the driven disc provides a reference event by triggering a second photo cell positioned close to the disc. Electronic circuitry measures the time elapsed between the reference event and zero transducer output. This time is proportional to the angular displacement of the polarising axis of the transducer filter with respect to the reference photo cell.

Sophisticated circuitry can provide the angular velocity of the transducer assembly and although the device is limited to simple movements at present, the system shows much potential for future development.

Coda: "CODA" is the abbreviation used for a "cartesian opto-electric dynamic anthropometer" being developed by Mitchelson (1975). Basically, the device is an optical instrument which simultaneously measures the 3-dimensional Cartesian coordinates of several body landmarks. The markers are miniature infra-red light sources in the form of gallium arsenide lasers, and their motion is monitored using a specially designed electronic camera system (see figure 3.4).

By using cylindrical lenses, the camera receives a line image of the body marker. An optical mask is positioned in the focal plane of the camera and an array of silicon photodetectors records the position of the line image. The central camera is sensitive to vertical movements and the two outer cameras are only sensitive to horizontal movements.

With a fixed distance between the outer cameras, the 3-dimensional coordinates of the body marker are obtained from the signal processor unit.

The special design features of CODA over existing techniques are high resolution (1 in 4000) and high frequency response (200 Hz). Although development of the system is in the preliminary stages, it is hoped that useful measurements will be obtained in the near future.

Television: Over recent years it has become possible to use television for the measurement of human movements. Using special markers, one coordinate is obtained by reference to a particular television rastor line while the second coordinate can be obtained from the position of the marker point along the same line. The whole movement activity is sampled by the sequential scanning of the television camera. Problems of marker identification have been overcome by extrapolation of marker positions between time samples. The computer is manually operated for the first few events and subsequent locations of the markers are estimated by the computer.

A versatile television measurement system has recently been developed at the University of Strathclyde and reference is made to Jarrett (1976) for further information.

3.3 Photographic Measurement Techniques:

There are three fundamental methods by which photographic records of human motion may be obtained; namely, stroboscopic photography, stereo-photogrammetry and cine photography.

3.3.1 Stroboscopic photography: This method involves the long exposure of a single plate of high resolution film with an interrupted light supply. Special markers are illuminated at a known frequency and their path of motion is recorded on the film.

The technique was pioneered using continuously illuminated subject markers and interrupted exposure at a predetermined frequency. The locomotion studies of Bresler (1950) were performed using small marker lamps attached to relevant parts of the body. A black disc, containing a radial aperture, was rotated in front of the lens. The field of view of the camera was consequently limited to the instances when the slot was in line with the lens. The resulting photographic record consisted of points situated in relation to the movement of the marker.

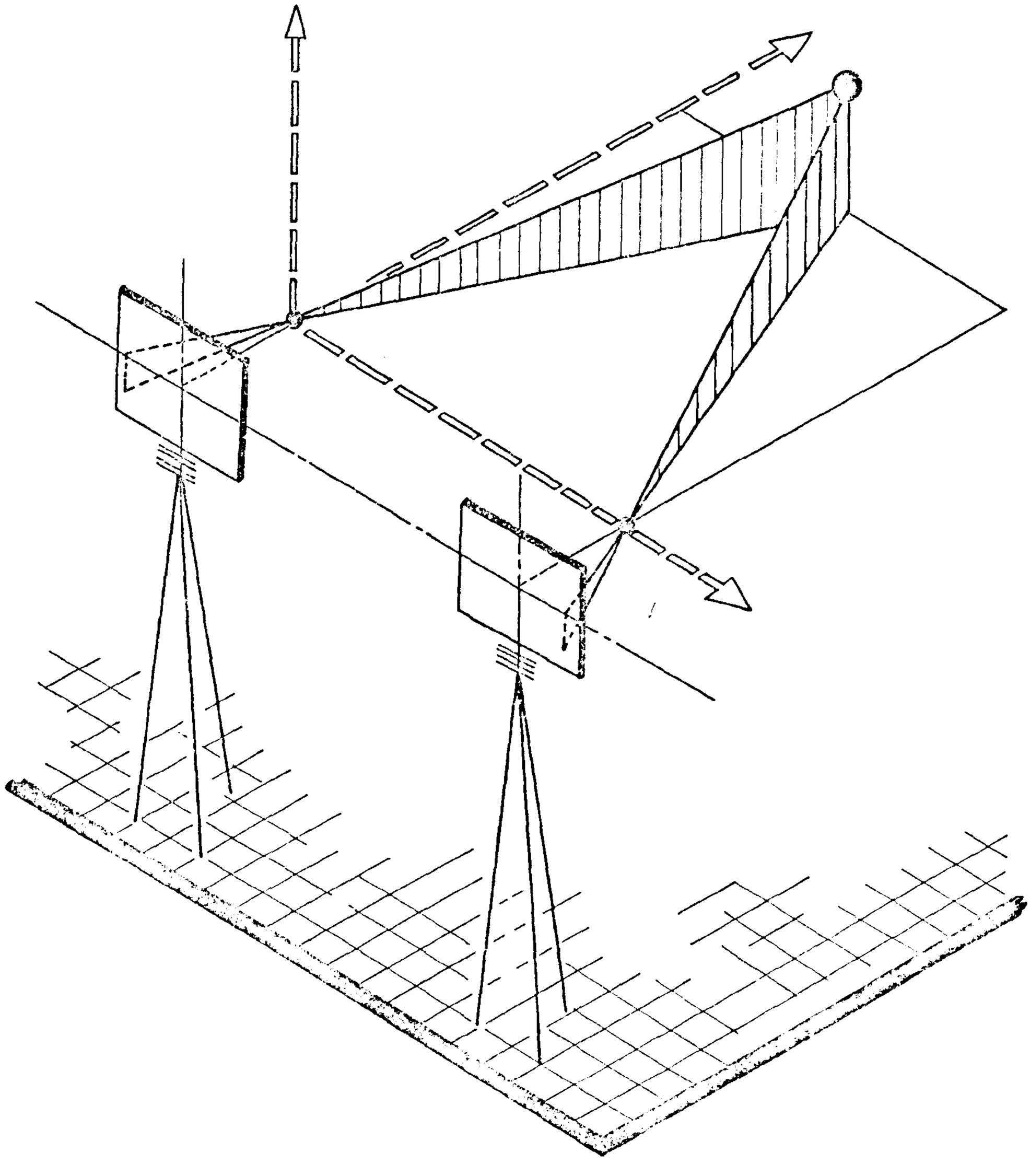

Figure 3·5: Stereophotogrammetry geometry (Ayoub et al)

In place of continuously illuminated subject markers, modern stroboscopic photography involves continual exposure of film with stroboscopic illumination of the markers. Nelson et al (1969) used this method to study elbow flexion and extension. All items were blackened with the exception of a white line running the length of an aluminium forearm splint. The motion record contained a series of lines corresponding to forearm movements. Marker spacing was dependent on stroboscope frequency and it was found that frequencies of 100 to 150 flashes/second were suitable for such studies. The angular positions were easily measured and velocities and accelerations were calculated using double differentiation.

The above technique becomes inaccurate during slow movements when the individual marker records become indistinguishable. Complex human motions produce similar difficulties if the position of several markers coincide. In extreme cases it becomes impossible to recognise motion pathways owing to the high number of points and lines. In addition, the method is extremely involved for 3-dimensional studies and was therefore considered to be of little value for the analysis of elbow function.

3.3.2 Stereophotogrammetry: The technique of stereophotogrammetry enables 3-dimensional measurements to be made from two camera pictures taken in the same plane. The principle of operation is the same as binocular vision.

Ayoub et al (1970) described a two camera system where the cameras were separated by a known distance and accurately aligned with each other. The geometry of the stereophotographs is shown in figure 3.5 and the coordinates of any point were given by straightforward trigonometrical equations.

The accuracy of the procedure depended on the "internal" geometry of the cameras (focal length, distortion etc.) and the orientation of one camera relative to the other. Ayoub and his associates performed static and dynamic tests using the principles of stroboscopic photography for motion recording. For comparison, an accelerometer was incorporated into the dynamic testing of a crank-slider assembly. It was found that the accelerations calculated from the photographic measurements lay between the theoretical values and the accelerometer results. The system was also used for the analysis of a simple arm movement.

"Meaningful" results were obtained for the velocities and accelerations of the hand.

An increase in measurement accuracy was obtained by Guteworth (1971) with the use of small light flashes for body markers in place of stroboscopic methods. Measurements of the photographs were performed to an accuracy of $\pm$ 1.6 to 2.5 μm, using a comparator. The system returned overall accuracies of approximately 0.1% for velocity trials compared to 5% for cine film studies (32 frames/sec.).

Although the procedure can give accurate results, stereophotogrammetry suffered the same limitations, for speed and complexity of movements, as found with stroboscopic photography. The method was therefore rejected for elbow function analysis.

3.3.3 Cine photography: Cine photography has been used to study human motion for many years but it was only recently that accurate 3-dimensional measurements were made possible.

Paul (1967) succeeded in combining versatility of motion with a high degree of measurement accuracy. Using two cine cameras, he obtained "front" and "side" film records of subjects during walking. The cameras were driven at a constant speed of 50 frames/second using synchronous motors and appropriate gearing. By firing a flash bulb in the field of view of both cameras, a reference event for each test was recorded on both films. This ensured correct camera synchronization during subsequent film measurement.

After filming several walking cycles, the films were rewound and a reference grid positioned at the intersection of the camera axes. Each camera was run in turn giving a superimposed grid on the original film record. Calibration and distortion errors were therefore minimal and a measurement accuracy of $\pm$ 1 mm was claimed. It was emphasised that the measurement process was extremely tedious since all measurements of the projected film were done by hand. Trace analysers have greatly reduced the time factor and have provided an increase in measurement accuracy.

With such equipment, the film is projected onto a glass table and a "pencil" is positioned at each marker point in turn. The X and Y coordinates relative to the table origin are punched out on paper tape for future computer

TOP
[inverse]

FRONT
[normal]

SIDE
[inverse]

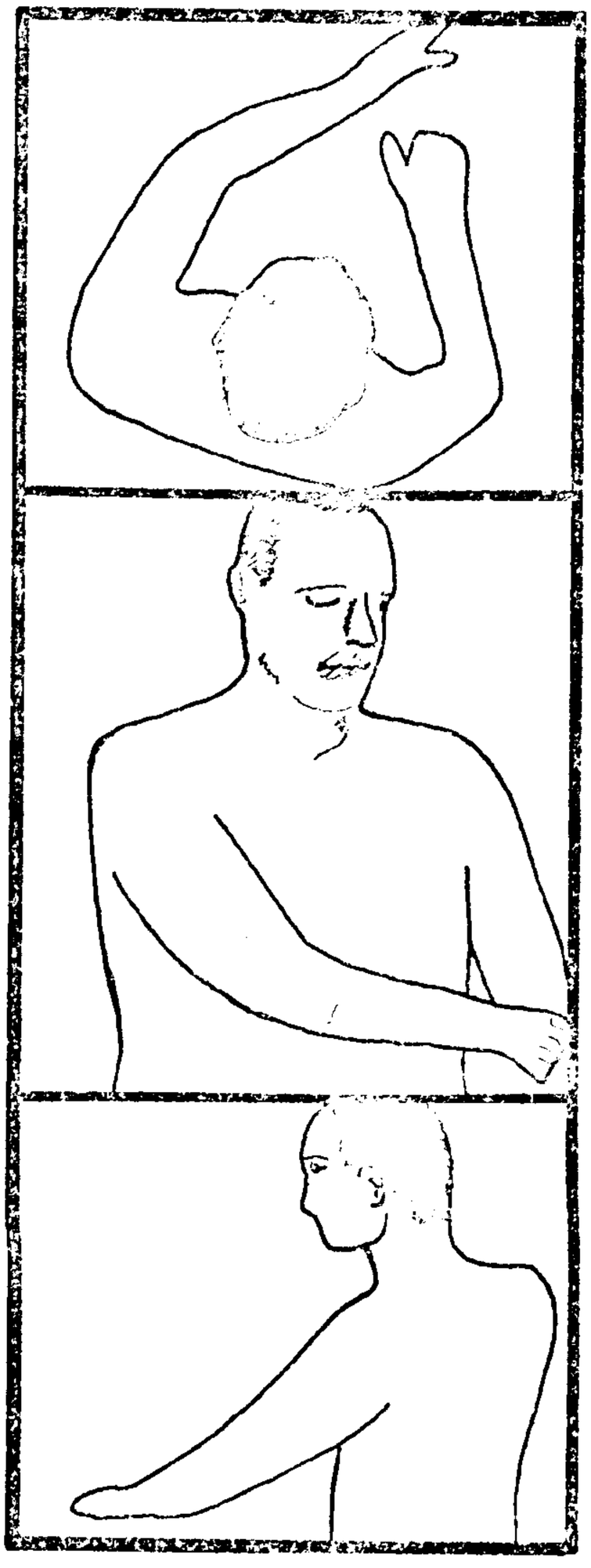

Figure 3·6: Triple image cine photography (Engen + Spencer)

analysis. Grid reference point must therefore be measured so that the correct datum can be established.

For a similar camera arrangement, Sutherland (1972) investigated the range of measurement errors, during the analysis of lower limb motion, using a Vanguard Motion Analyser. Two independent observers measured the same piece of film and comparisons were made of results for rotations at the hip, knee and ankle.

It was found that the percentage discrepancies were high for small ranges of movement. Errors as high as 50% of the total range of movement were recorded for rotations of the pelvis and corresponded to an actual error of 6.3^{o}. On average, however, the measurement error was 2.6^{o} which lowered the discrepancy to around 20%.

Taking knee movement to be 60^{o} in total, the average error of 3.1^{o} was equivalent to 5% which was within an acceptable range. It is interesting to note that repeatability tests performed by one observer produced discrepancies of 0^{o} to 2.5^{o}.

A novel approach to cine photography was developed by Engen and Spencer (1968) where body markers were again used to define limb positions. In place of using a number of cameras to analyse the required number of dimensions, the authors used one 35 mm cine camera and two mirrors, tilted at 45^{o}, to give front, side, and top views (see figure 3.6). Each frame of film therefore contained three images in predetermined positions. The marker spots of shoulder, elbow and wrist were joined by two lines and the motion characteristics were obtained by reference to time clocks in the field of view.

Although the accuracy and versatility of this method are inferior to the photographic procedures described by Paul, the convenient presentation of data is worthy of note.

3.4 Force Measurement:

The external force applied by any part of the body can be measured using two fundamental methods. The equilibrium method can be used whereby springs, weights or fluid pressure balance the limb action. As an alternative,

the deformation of an elastic structural system can be measured.

Conventional strength tests have utilised systems based on the former method and are both numerous and varied (see Hunsicker (1955)). For the measurement of forces produced in normal activities, the force transducer must exhibit minimal mechanical displacement and provide facilities for continuous data recording. Paul (1975) suggested that a movement of around 0.001" can be detected in ground/foot force transducers and, consequently, the equilibrium method has not been widely used for biomechanical studies.

Modern transducer design is dependent on the type and number of parameters to be measured. Numerous dynamometers have been developed over recent years but only two of the most pertinent will be described.
Force platforms: In locomotion studies, the forces transmitted between the ground and the foot have been measured using "force plates" and several designs have been developed corresponding to the particular type of study (Paul, 1975). A typical dynamometer consists of a rigid platform mounted on several strain gauged columns. Modern designs employ load cells operating on the "Piezo-electric" principle and are now in use in many research establishments.
"Pylon" transducer: A more compact dynamometer can be produced using a single strain gauged column. Berme et al (1975) developed a short tubular transducer for the measurement of forces and moments transmitted through lower limb prostheses. Shear forces in a transverse direction were measured at a single level, which enabled the length of the unit to be kept small. Bolted adaptors provided a very versatile fixation mechanism.

For these reasons the transducer described by Berme and his associates was incorporated into specially designed equipment for the measurement of hand/environment forces during selected activities. Details of the design and employment of the device are given in section 5.3.

3.5 Analytical Methods:

3.5.1 Introduction: Once the resultant force actions and spatial orientations of the particular limb segments have been calculated, the analysis of muscle, ligament and joint forces can be undertaken. In practically all joint analyses, the number of unknown quantities (muscle forces etc.) exceeds the number of

equilibrium equations.

By postulating certain functional conditions regarding anatomical structures, the problem can be reduced to one having a singular solution. The results must not be regarded as being unique since they are dependent on the choice of simplification parameters. Accordingly, two fundamentally different approaches to biomechanical problems have evolved over recent years. One method involves the minimisation of selected parameters, such as muscle force or energy, after studying the gross anatomical behaviour of the joint. As an alternative, the number of unknown quantities can be sufficiently reduced by studying the precise functional anatomy of certain anatomical structures and applying logical constraints to these structures (e.g. ligaments cannot transmit compressive forces etc.).

3.5.2 Minimisation techniques: Problems of indeterminability have been solved in many branches of science and have given rise to the methods of "least work" in engineering and "least squares" in statistical analyses. In the field of biomechanics, the situation can be overcome by considering several constraints; namely, energy, total muscle force, joint loads etc.

Nubar and Contini (1961) minimised the total muscular force produced during locomotion and postulated that "a mentally normal individual will, in all likelihood, move (or adjust his posture) in such a way as to reduce his total muscular force to a minimum". To prevent negative results for muscle tensions, the square of the muscle force was used throughout the equations.

$$E = (c_1 M_1^2 + c_2 M_2^2 + \ldots\ldots\ldots) \Delta t + A_o$$

where E = muscular effort ($cM^2 \Delta t$) at all body points

c = numerical factor

M_1 = muscle force

A_o = an initial constant.

The restraints were assumed to be a general type of function for muscle effort and were equated to zero:

$$f_1(M_1, M_2, M_3 \ldots\ldots\ldots) = 0$$

$$f_2(M_1, M_2, M_3 \ldots\ldots\ldots) = 0$$

The unknown forces were found from normal equilibrium equations plus the necessary number of constraint equations. In other words, the constraint equations supplemented the number of equilibrium equations to render the system determinate.

By way of illustration, Nubar and Contini used their technique to analyse the mechanics of several joints during a hypothetical walking cycle. The sum of the squares of the joint moments was taken as a measure of the total muscle force. Their results were compared to two cases obtained without minimisation and large discrepancies were found. No further quantitative comparison was made.

Several years later, Beckett and Chang (1968) studied the kinematics of gait by applying principles of "minimum energy" to the indeterminate system of the leg. The kinetic and potential energies of the system were calculated from a simplified model of the limb. The hip joint was assumed to move along a sinusoidal curve and the activity of the two muscle groups (quadriceps and hamstrings) was simplified to discrete rectangular forms.

The condition of restraint for the "toe-off/swing" phase was taken as an interrelation between the angular velocities of the thigh and shank. For "toe-off", the shank was considered to describe an arc having its centre at the point of toe contact. Therefore, it was possible to construct an equation relating the angular positions, hence angular velocities, of the thigh and shank. The motion of toe during swing phase was described by a 4th order polynomial and a similar constraint equation was obtained.

The equations of motion were constructed by a method similar to that used by Nubar and Contini (1961). Solutions were obtained for body weights of 120 and 150 lbs and for several walking speeds (60, 70, 80, 90 and 100 steps/min.). The results of the angular velocity and limb position were found to be similar to results from earlier investigations. A comparison was also made of computed knee moments with those produced from accelerometer data. It was concluded that the analytical method involving minimum energy was acceptable for plane gait analyses.

The above techniques boih depended on "artificial" paths of motion for the derivation of equations of motion. Barbenel (1972) achieved a great deal more versatility by using linear programming techniques which provided a method of minimising (or maximising) a linear function. The so called "objective function" was subject to constraints of inequality, or equality, together with the overall condition that the variable could not be negative. Barbenel studied two functions at the temperomandibular joint; namely, minimum joint force and minimum total muscle force. The results predicted that, although a lower limit of joint force was feasible, no upper limit existed. Results of total muscle force analysis indicated that only one muscle would be active during biting. Electromyograph and palpation tests showed that three muscles were definitely active during activity and it was concluded that minimisation techniques were inapplicable.

Following the failure of total muscular force as a minimisation criterion, Seireg and Arvikar (1973) studied several objective functions of the lower limb using a similar analysis to the above. "Leaning" and "stooping" movements were performed which produced 21 equations representing the gross mechanical system of the body. 29 muscle force and 12 reaction/ligament forces were required and linear programming methods provided solutions for the minimisation of muscle forces, muscle work, vertical reactions or moments carried by the ligaments. It was discovered that not one of four conditions agreed with experimental findings.

On further analysis, a weighted combination of muscle force and joint moment was found to give reasonable agreement with previous data.

3.5.3 Reduction techniques: By studying the functional anatomy of muscles, ligaments and joint forces, it is usually possible to reduce the number of unknown quantities to equal the number of equilibrium equations. As examples, two locomotion studies are discussed.

The force actions transmitted by the human hip joint during normal walking were analysed by Paul (1967) using cine film and force plate records. Moments about the long axis of ihe femur were not included and five equilibrium equations were constructed. Three joint forces, together with six muscle tensions,

resulted in an excess of four unknown quantities. To overcome this indeterminability, antagonistic muscle activity was neglected and the muscles were grouped according to their action.

The effective lines of action of the various muscles were obtained from cadaveric measurements of origins and insertions within predetermined measurement axes. Muscle activity was chosen according to the nature of the appropriate moment actions on the hip joint.

Having reduced the unknowns to three orthogonal joint forces and two muscle forces, the system became statically determinate and singular solutions were obtained.

A similar analysis was performed by Morrison (1968) for the forces transmitted by the knee joint during locomotion. Again, cine film and force plate records were used to calculate the external forces and moments around the joint in question. In this case the analysis was complicated by the ligamentous structures around the joint and the non-sphericity of the joint surfaces. The unknown quantities reduced to four ligament tensions, three muscle tensions and one compressive joint force (resultant of standardised pressure distribution). Muscle activity was selected from flexion-extension moments whereas the anterior-posterior force actions provided tension in one of the cruciate ligaments. Similarly, the adduction-abduction effect produced tension in one of the collateral ligaments with a compressive joint force on the opposite side of the joint.

By applying specified functional logic, the number of unknown quantities was again reduced to that required for a determinate system. In conclusion, it can be seen that this analytical method required a higher degree of selective combinations of unknown quantities than was found in the hip joint analysis.

With this in mind, the analysis of force actions across the elbow joint was based on Morrison's work. Minimisation techniques were considered inappropriate since no relevant biomechanical data was available for comparison purposes.

4. REVIEW OF UPPER LIMB BIOMECHANICS

4. REVIEW OF UPPER LIMB BIOMECHANICS

4.1 Introduction:

The purpose of this review is to present a brief description of publications over the past forty years which are of particular relevance to the study of elbow joint biomechanics. Although there is an abundance of literature in respect of arm movements, athletic events, and electromyograph investigations, there are very few reports concerning the forces transmitted by the elbow joint. This chapter is therefore subdivided into four sections; namely, electromyography, arm mechanics, muscle forces and joint forces.

4.2 Electromyography of Arm Muscles:

Electromyographical studies of elbow flexors and extensors have been so numerous and varied that careful study of the available literature is required if the correct function of these muscles is to be obtained. Basmajian and Latif (1957) reported a comprehensive range of carefully planned electromyographic experiments on elbow flexors. Since that date, various athletic activities have undergone similar rigorous experimentation but only two reports of the general function of elbow joint musculature were used. From the work of Basmajian (1974) and Rasch and Burke (1974) the analysis of muscle function was as follows.

4.2.1 Flexor group: In general, the flexor group of the elbow joint is considered to be composed of the brachialis, biceps brachii (long and short heads) and brachioradialis.

Brachialis: The true "muscle of the upper arm", the brachialis has been described by Basmajian as the "workhorse" among the elbow flexors. Its line of pull does not change with forearm rotation and the muscle acts in all elbow positions. Maintenance of posture and slow and fast elbow flexion also give rise to brachialis activity.

Biceps brachii: The function of the biceps brachii is relatively complex as it can act on the shoulder, elbow and radio-ulnar articulations. Both the "long" and "short" heads are designed to flex the elbow. When the hand is in extreme pronation, the radial tuberosity is turned inwards and downwards,

which causes the muscle tendon to wrap round the radius. Subsequent biceps action would have the combined effect of elbow flexion and wrist supination. When the forearm is pronated, the biceps brachii muscle has a reduced contribution to elbow "torque".

In positions of supination, the muscle is an elbow flexor under all conditions but supination of the extended forearm does not produce activity in the muscle. Action of the long head of the muscle also produces movement at the shoulder joint but the precise activity is dependent on numerous factors.

Brachioradialis: Rasch and Burke described this muscle as an elbow flexor having a greater mechanical advantage than the biceps brachii. Basmajian, on the other hand, has found the brachioradialis to play no part in the maintenance of flexion of the unloaded forearm. Moderate activity was recorded when a weight was lifted with the forearm pronated whereas only slight activity was monitored for loaded flexion with a supinated forearm.

The brachioradialis was found to be active for all forearm positions during quick flexion and extension and it was therefore suggested that the muscle acts as a reserve for rapid elbow movements.

The pronator teres, although mainly a forearm pronator, does show signs of activity during resisted elbow flexion and it can be concluded that the muscle counteracts the supination effects of biceps brachii.

4.2.2 Extensors: It is generally accepted that the medial head of the triceps is the prime extensor of the elbow joint. The lateral and long heads become active during resisted elbow extension and comparisons have been made of the medial head and brachialis. Each muscle is considered to be the "workhorse" of its associated muscle group. The long head of triceps has been reported by Basmajian to be the weakest of the three heads, due to the lack of fixation at its scapular origin.

The function of the anconeus muscle has been the subject of much controversy for many years. Reports clearly state that it is an extensor of the elbow but in positions of supination and pronation no agreement has been reached concerning its precise activity.

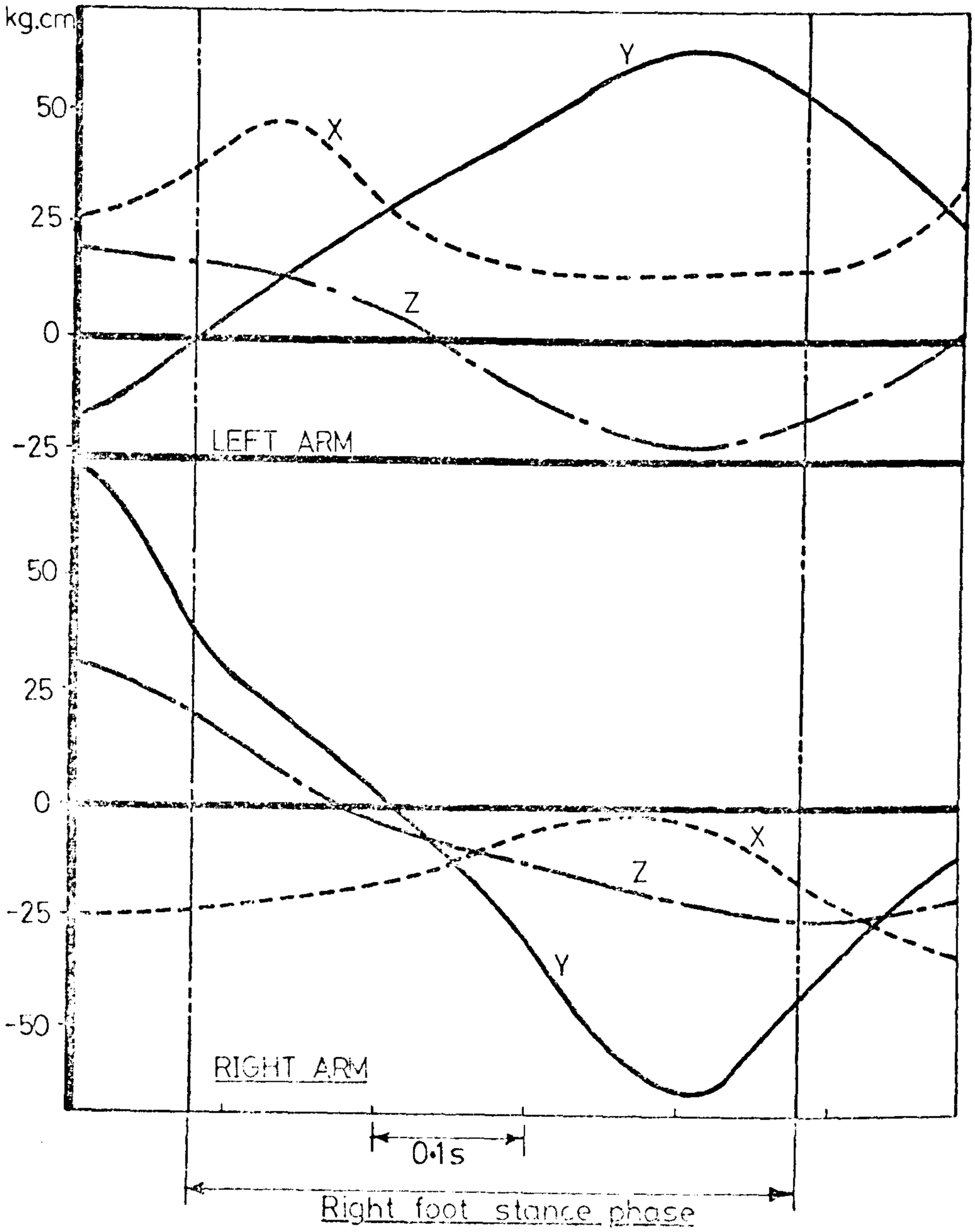

Figure 4·1: Shoulder moments during locomotion (Elftman, 1939)

From the foregoing reports of muscle action, brachialis, biceps brachii and brachioradialis were chosen to represent the flexor muscles of the elbow whereas extension was considered to be the direct result of triceps activity.

4.3 Arm Biomechanics:

The first analytical study of arm motion was performed by Elftman (1939) when he analysed the action of arm muscles, and the three dimensional momentum effects of the arm, during the stance phase of walking. From the summation of these momentum quantities, the kinematic effects of the arm were calculated in relation to whole body equilibrium. Results showed that the arm did not act as a simple pendulum but in fact experienced controlled muscle activity and produced significant moments about the shoulder joint as shown in figure 4.1. The actual energy changes occurring at the shoulder joint were also calculated and it was concluded that arm movements reduced the rotations of the body as a whole and provided lower rotational accelerations of the body during locomotion.

Dern and his associates (1947) investigated arm movements in an attempt to test Hill's experiments on isolated muscle. Three voluntary elbow flexion tests were performed for different types of loading and consisted of inertial loads, isotonic torques and constant forces parallel to the line of action of the flexor muscle. Using results from the last type of flexion test, they calculated the force-velocity relationships of the flexor muscle and compared them directly to Hill's relations for isolated cat muscle. Their results proved meaningless since no account was taken of antagonistic or synergistic muscle activity.

Hunsicker (1955) performed the most rigorous and comprehensive tests on arm strength to date. A "machine" was constructed which enabled measurements to be made of elbow flexion-extension efforts in almost all possible body positions. In particular, the maximum hand force was recorded at elbow angles of 180°, 150, 120, 90° and 60°. Six movements were performed for each position; namely, pull, push, lift up, push down, abduction and adduction.

Right and left arms were tested on 55 aircrew volunteers in the sitting and prone body positions. The amount of data produced was so great that reference is made to Hunsicker (1955) for details of the quantitative results. It is, however, worth mentioning the more important qualitative observations.

1) A large variation of individual "strength" was found in that it was not uncommon for one subject to exert ten times as much force as another.

2) The strength of the left arm was found to be approximately 10% lower than the strength of the right arm and a reduction of 28% occurred over the complete flexion range.

3) For the sitting position, the order of maximum effort was pull, push, up, down, adduction, abduction. "Abduction" forces were found to be around 1/3rd of the "pull" forces.

The mechanics of falling on an outstretched arm were studied by Carlsoo and Johansson (1962) using a force plate positioned 25 cms above floor level. Forward, backward and sideward falls were examined and EMG apparatus was used to study the timing of muscle activity in relation to the fall and the subsequent braking force. Results clearly indicated that the elbow flexors contracted strongly just before contact was made with the force plate. At an elbow angle of approximately 160°, the EMG equipment recorded interrupted muscle activity during the "braking" period. The elbow extensors usually acted much sooner than the flexors and their activity was very strong at the beginning of the braking period.

It was concluded that the orientation of the elbow joint did not produce the most stable joint configuration but that the anatomical structures appeared to cater for all force actions experienced during the fall. Muscular stability was well developed at the braking period and it was postulated that muscle activity was the dominant factor in the prevention of bone fractures.

Larson et al (1969) conducted a general set of experiments to study the strength, velocity and acceleration of resisted and non-resisted elbow flexion. Sixteen student volunteers participated in speed tests with wrist cuff forces of 0, 6, 15 + 30 lbs f. Isometric strength tests for 0, 15 and 45° elbow flexion were also conducted. The elbow motion was recorded using stroboscopic photography.

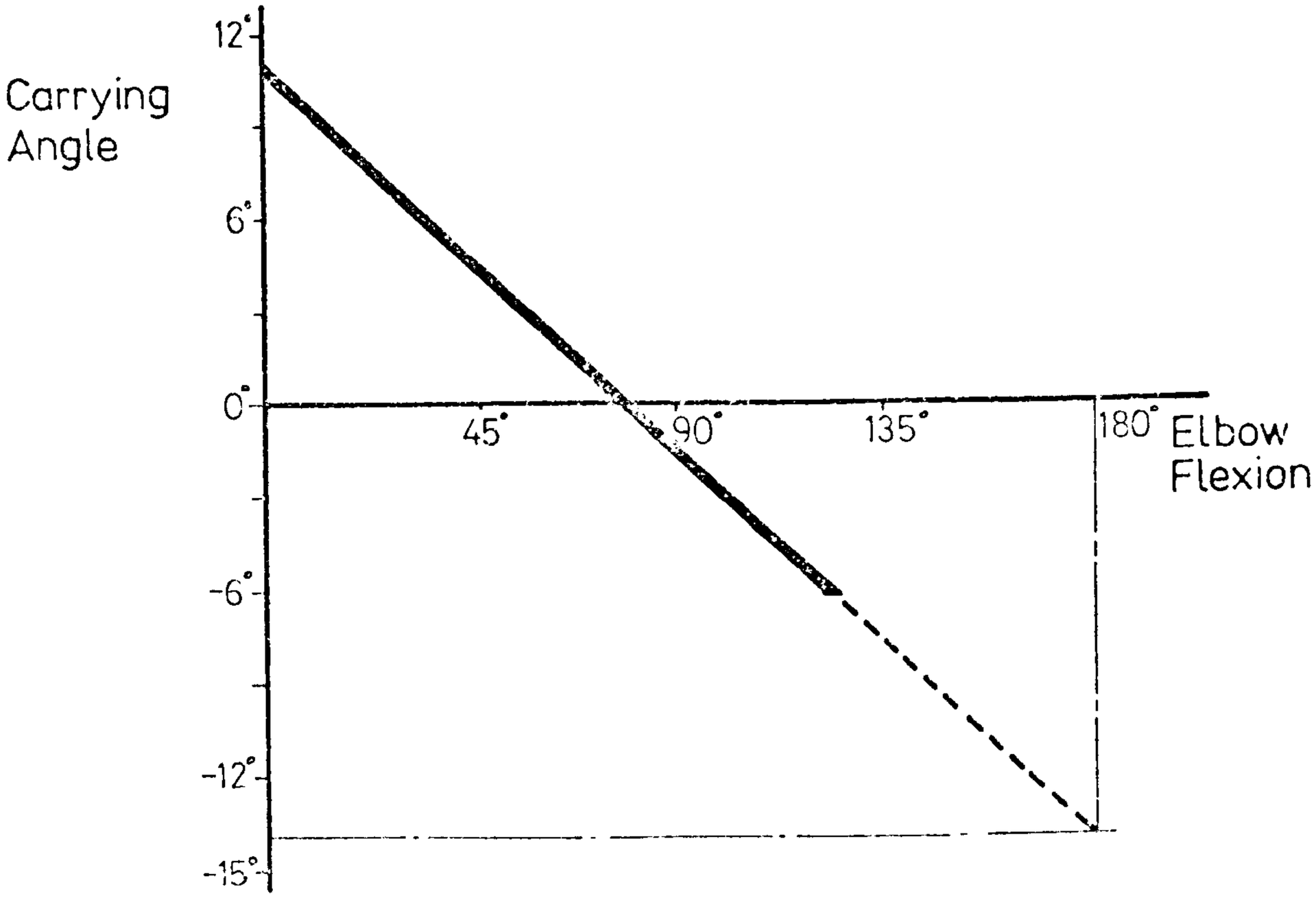

Figure 4·2: Variation of carrying angle v elbow flexion. (Morrey + Chao)

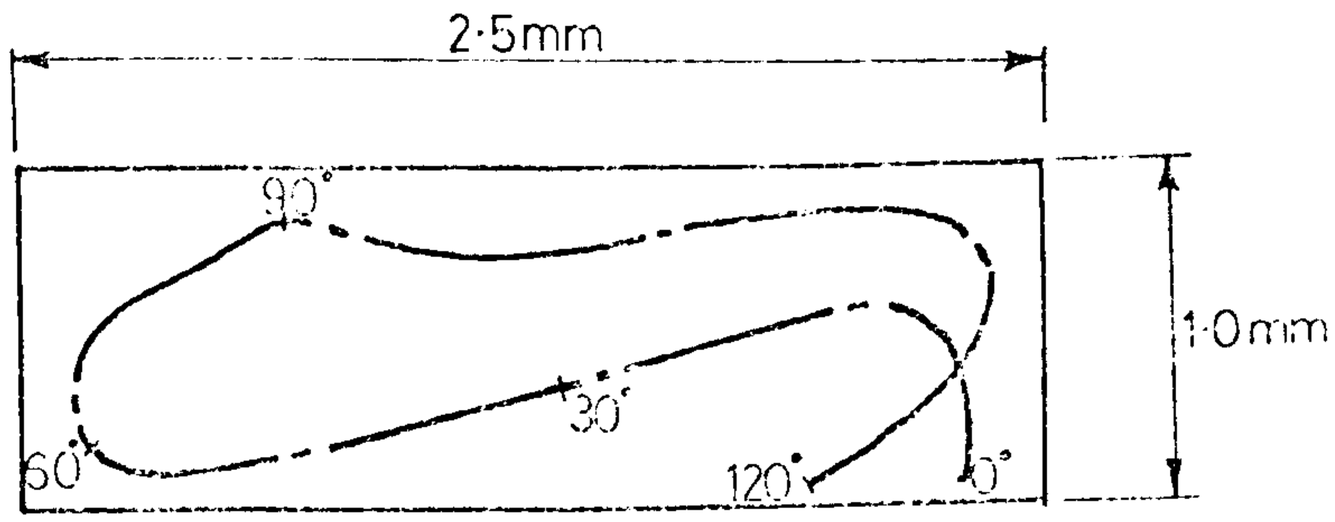

Figure 4·3: Locus of elbow joint "centre" from Fischer's work [Morrey & Chao]

Angular displacements were measured every 15° of elbow flexion and the corresponding velocities were used to obtain the accelerations at 15, 45 and 90° of elbow flexion.

As a conclusion to this section the work of Morrey and Chao (1976) is of particular interest. Detailed measurements of elbow motion during passive elbow flexion and passive forearm rotation were obtained using two unembalmed cadaveric arms and biplanar X-rays. Metal pins were fixed to the humerus, ulna and radius to provide their three dimensional orientation in relation to a reference grid system.

For the flexion study, the carrying angle was measured at 20° intervals of elbow flexion and was found to vary in a linear fashion as shown in figure 4.2. If this straight line is extrapolated to 180° of flexion, the resulting deviation becomes -14°. Since the angle varies linearly with the angle of flexion, it can be seen that the humero-ulnar joint possesses a linear axis of flexion which is inclined at approximately 12.5° to the long axis of the humerus. These values agree with visual estimations from several bone specimens.

Measurements of forearm rotation revealed that zero valgus deviation of the ulna occurred during pronation with the elbow fully extended. On the other hand the long axis of the radius was displaced between 6° and 10° medially in relation to the long axis of the humerus. These displacements were to be expected from anatomical observations.

From the collected data the authors studied the movement of the instantaneous centres of rotation of the elbow joint. For the humero-ulnar articulation the locus of the centres occupied an area within 2.5 mm * 1.0 mm which agreed with Fischer's earlier study (see figure 4.3.).

It must be remembered that the measurements were obtained from passive activities and that the elbow joint movements were controlled by ligament tension and joint surface pressure. During full extension of the elbow joint Morrey and Chao noted a gap on the lateral side of the humero-ulnar articulation. A similar situation occurred on the medial side during full flexion of the elbow. If the skeletal movement had resulted from muscle activity the articular surfaces would have been pressed together and stresses applied to the

ligamentous structures. This in turn would reduce the linear displacements of the articular surfaces and reduce the area occupied by the locus of the instantaneous centres.

For the purpose of prosthetic design the elbow joint should therefore be treated as a uniaxial joint as far as flexion-extension motion is concerned. In the transverse plane however, a certain degree of joint laxity is necessary to ensure the correct function of the ligamentous structures during activity.

4.4 Muscle Forces: Investigations involving the forces produced in human muscle have been numerous and varied since Hill's pioneering experiments around 1920. Elbow flexion activities have been chosen by many investigators because of the simplicity of the measurement of hand forces. In recent years, serious attention has been drawn to arm strength and the corresponding muscular forces produced around the elbow joint. The most relevant of these investigations are briefly described.

Provins and Salter (1955) undertook a study of the factors affecting the strength of elbow flexion and extension with particular regard to the degree of elbow flexion and the orientation of the forearm. They used a strain gauged dynamometer with a 1" diameter grip handle, or a wrist cuff, for force measurement of the fully pronated, neutral and fully supinated forearm positions. For the grip handle tests, elbow angles of 45, 90 and 135° were used, whereas the wrist cuff tests were limited to 90° of flexion. In all tests the upper arm was abducted horizontally in order to exclude gravitational effects from the computations. Maximal flexion and extension efforts were performed after a five second "build-up" and minimal movements of the apparatus enabled the muscular contractions to be considered "isometric". The peak galvonometer readings were noted and a one minute relaxation period allowed between tests. The volume of the subject's hand, forearm and upper arm were measured after the series of tests using the water displacement principle.

The test results were obtained statistically using the method of analysis of variance and good correlations were obtained between tests at 90° of elbow flexion. Overall mean values of 3.97 and 4.25 kg m were obtained for handle and cuff tests respectively. A mean value of 4.45 kg m was returned

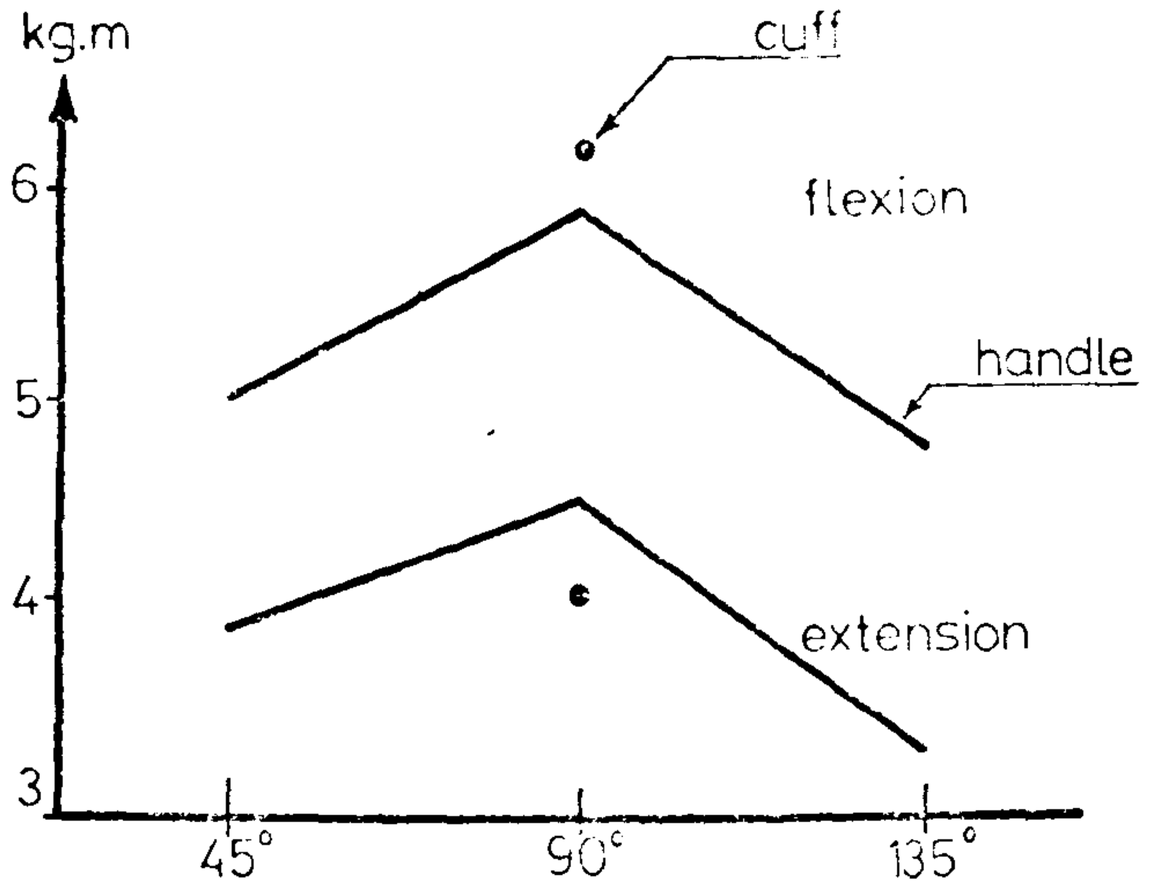

Figure 4·4: Elbow torque v elbow flexion. (Provins and Salter)

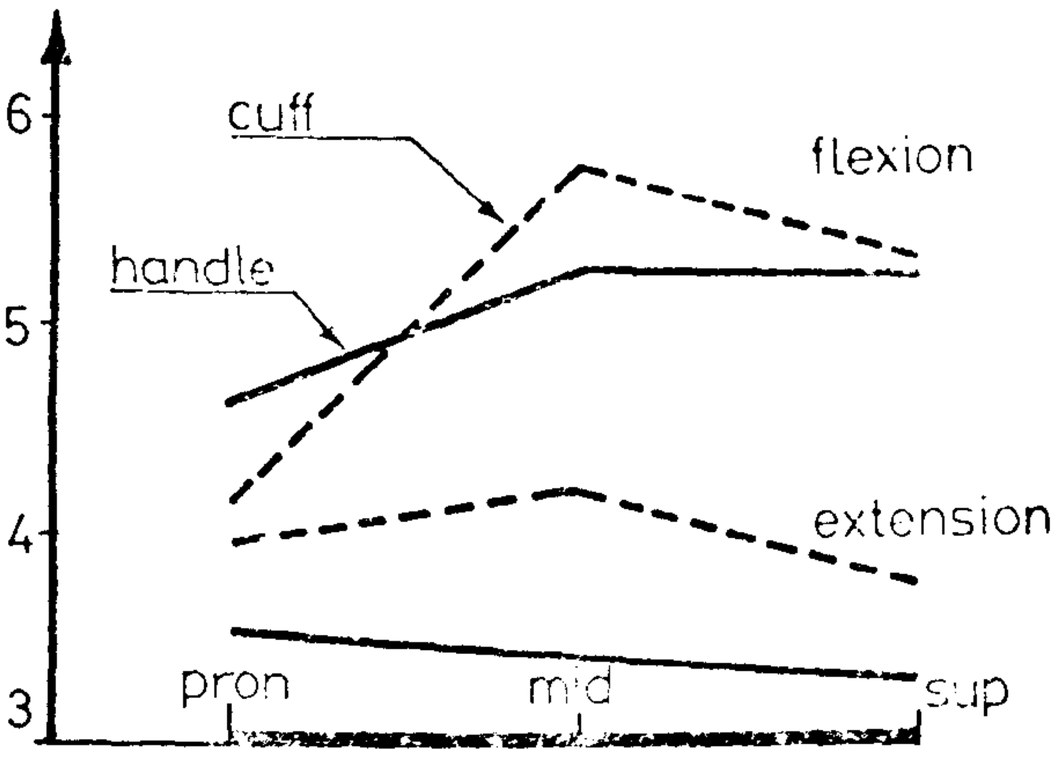

Figure 4·5: Elbow torque v forearm position. (Provins and Salter)

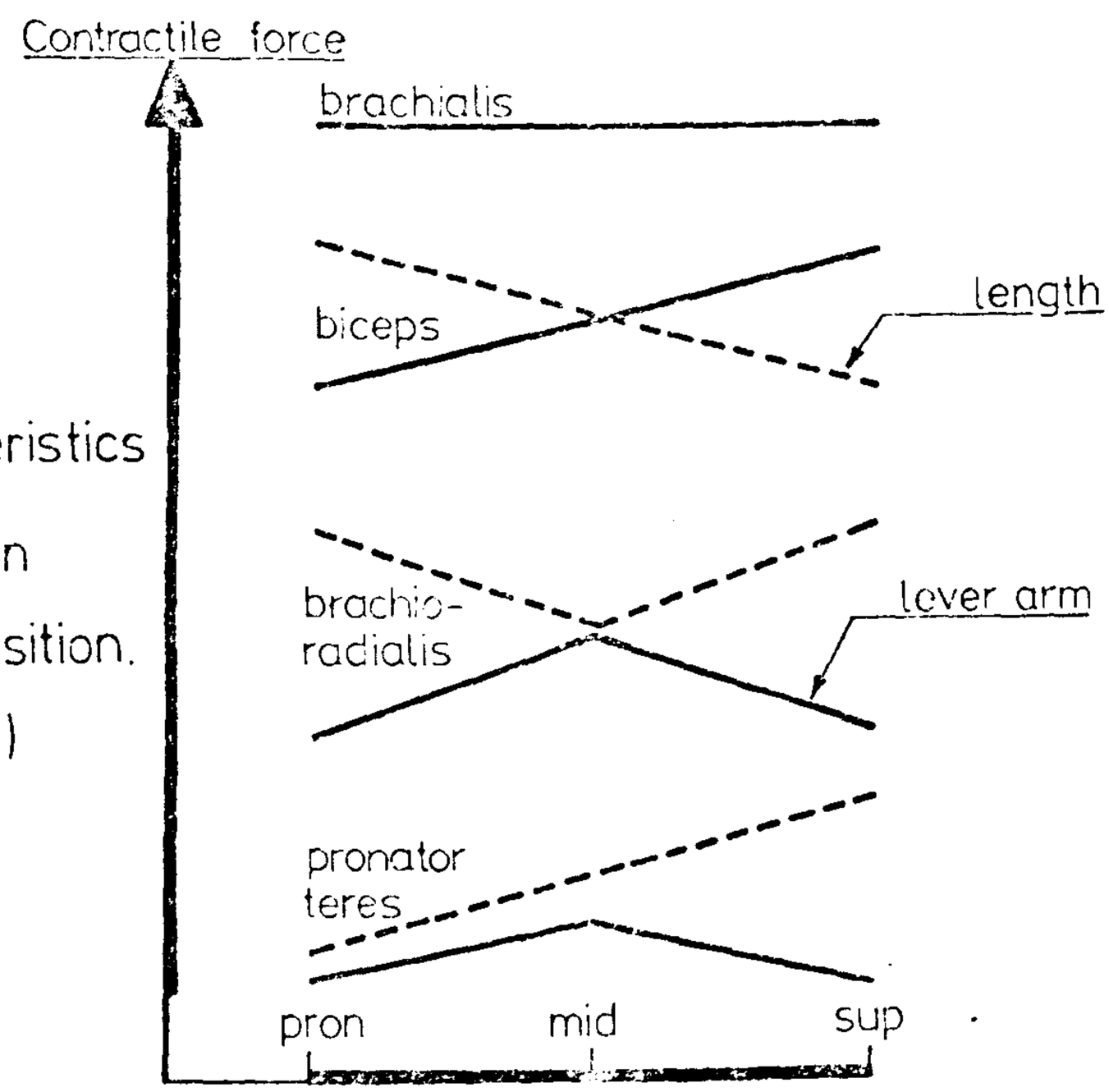

Figure 4·6: Characteristics of the elbow flexors in relation to forearm position. (Provins and Salter)

for a handle test for 90° of flexion. Figure 4.4 shows the effect of elbow angle on the torques produced and figure 4.5 details the corresponding effect of forearm positions. Low positive correlation was obtained between arm strength and arm volume but was accounted for by the large number of variables inherent in the investigation.

By considering muscle lengths and the appropriate lever arms, Provins and Salter concluded that the mechanical advantage of biceps and brachioradialis increased and that their length decreased in going from full pronation to full supination. Referring to figure 4.6, the effect of forearm position on the lever arm of the pronator teres clearly imitated the form of elbow torque variation and it was suggested that the pronator teres was responsible for the inverted "V" form of the graph. They postulated that the variation in strength was due to "some change in the efficiency or number of the muscles involved".

Rasch and Pierson (1960) investigated the relationship between maximum isometric strength and the "breaking" strength of the elbow flexors. This "breaking" strength was obtained by steadily increasing an applied torque on on the elbow joint until the static position was lost. A "Y" handle connected to a cable tensiometer provided the method of measuring the forces applied by the hand with 90° of flexion. The maximum voluntary isometric effort was recorded as 49.5 lbs whereas a break point of 50.9 lbs was obtained. Their tests therefore indicated that a slight fundamental difference existed between the force which could be applied, and that which could be resisted (concentric and eccentric muscle activity respectively).

As a dynamic extension of the above investigation, Doss and Karpovich (1965) studied the differences between isometric, isotonic, concentric and eccentric elbow flexion tests. The problem of producing constant torques for the isotonic activity was overcome by designing the apparatus shown diagrammatically in figure 4.7. The volunteer subject pulled on a cable which was attached to a floor-mounted load cell. The resistive motion was obtained by the examiner turning the windlass and observing the load cell output. Since the disc/windlass ratio was 9 : 1, the method was considered to be of "sufficient" accuracy for the tests undertaken.

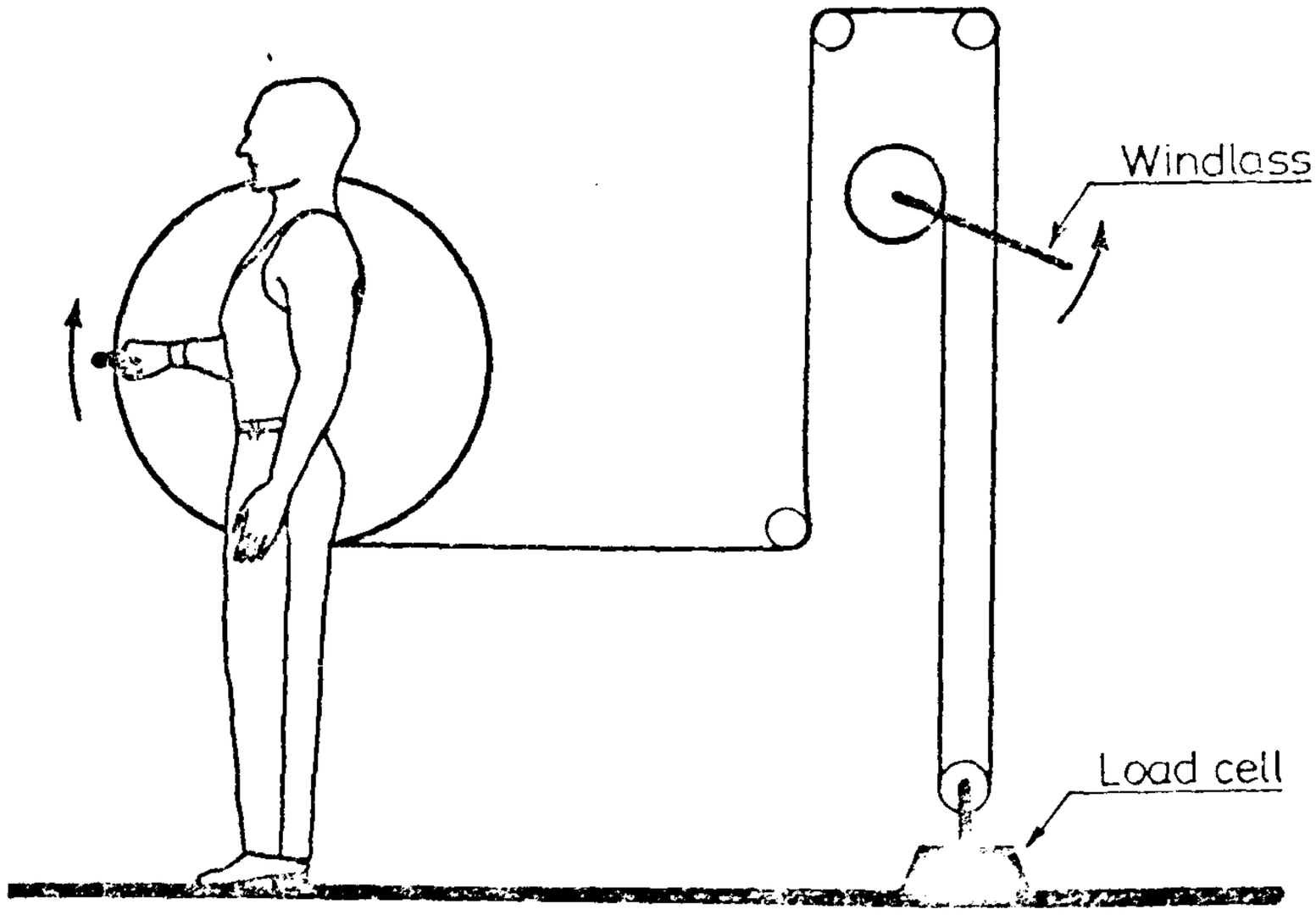

Figure 4·7: Apparatus used by Doss and Karpovich.

For the 37 male subjects tested, the eccentric force was 13.5% greater than the isometric force and the concentric force was found to be 23% smaller than the eccentric force. Correlation between these forces was statistically significant at the 0.01 level and empirical relations were developed as follows:

$$F_{conc} = -0.22\,A^2 + 4.54\,A + 15.23$$

and: $$F_{ecc} = -0.161\,A^2 + 2.91\,A + 37.65$$

where A = elbow angle.

The above terms did not account for such items as hand grip musculature and antagonistic muscle activity and, consequently, the results must be treated with the appropriate reservations.

On a different front, it is possible to determine maximal muscle tensions by measuring the cross-sectional area of the muscle belly. Care must be exercised regarding the line of pull of individual muscle fibres together with the inclusion of non-muscular tissue in the computations of cross-sectional areas. Ikai and Fukunaga (1968) measured the cross-sectional area of the muscles of the upper arm using ultrasonic methods. The arm was held in water while the ultrasonic scanner encircled the container. A "picture" was obtained which clearly indicated soft tissue boundaries. Strength tests were performed and high correlation was obtained between arm strength and the cross-sectional area of muscles. The absolute force of the muscle group was calculated using lever arms obtained from X-ray measurements. Unfortunately, only biceps was considered for the flexor group of the elbow which makes the range of muscle strength of 4.5 to 9.5 kg/cm^2 questionable, even although these values fall close to results from earlier investigators.

In an attempt to clarify conflicting reports of elbow flexor strength, various investigations were conducted into the effect of forearm position on the degree of muscle stimulation. Larson (1969) performed strength/E.M.G. tests on 30 subjects for the usual three forearm positions. The elbow was flexed to 65° for maximal effort against a cable tensiometer and the results were obtained by analysis of variance. From the results of the surface electromyography it was found that the greatest stimulation of biceps and brachioradialis occurred in the fully pronated position. Pronator teres was

stimulated almost constantly with a slight reduction toward full pronation. Results showed that the force exerted in full supination (87.6 lbs f) was significantly less than that measured for the neutral and fully pronated positions (96.8 and 95.1 lb f respectively).

Bankov and Jorgensen (1969) extended the study of E.M.G. activity to include static and dynamic tests. Three male volunteers performed reference isometric flexion tests together with concentric and eccentric movements between 45^{o} and 135^{o} of flexion. A motor driven lever system provided the necessary resistance to movement and the force applied to a wrist cuff was measured using a strain gauged dynamometer. Three velocities of flexion were tested and surface electrodes recorded the electromyographical activity of biceps brachii and brachioradialis.

A "reference" test was performed by measuring the maximum isometric strength of elbow flexion with the elbow in 90^{o} of flexion. It was found that the isometric strengths at flexion angles of 45^{o} and 135^{o} were only about 75% of the reference strength. These values agreed with the findings of Doss and Karpovich (1965). In addition, the results indicated that the strength of flexion with the forearm pronated was 85% of the flexion torque produced with the supinated forearm.

No statistically significant difference in electrical activity was recorded for biceps brachii throughout the selected range of elbow flexion. However, a 50% drop in biceps stimulation was recorded when the forearm was rotated from pronated to supinated positions.

Similarly, no difference was recorded for brachioradialis stimulation except for a very slight increase in activity when the muscle was shortened.

For the dynamic series of tests, the maximum torques were developed corresponding to the 90^{o} elbow position and the torque-velocity curves agreed with the results of earlier investigations. The values of flexion torque for the pronated forearm were 10 to 15% lower than those for the supine position whereas electrical activity was reduced by 30 to 40%. No difference in electrical activity was recorded for the various flexion velocities or for the concentric and eccentric movements.

	X-Sect [cm]	Lever arm [cm]	Torque	Relative torque [%]
Pronator teres	2·7	1·34	3·62	4
Ext. carp. rad. longus	3·0	3·46	10·38	12
Brachialis	8·7	3·22	28·01	32
Biceps brachii	6·7	4·44	29·75	34
Brachioradialis	2·1	7·93	16·65	19

Table 4·1: Summary of results from Bankov and Jorgensen (1969).

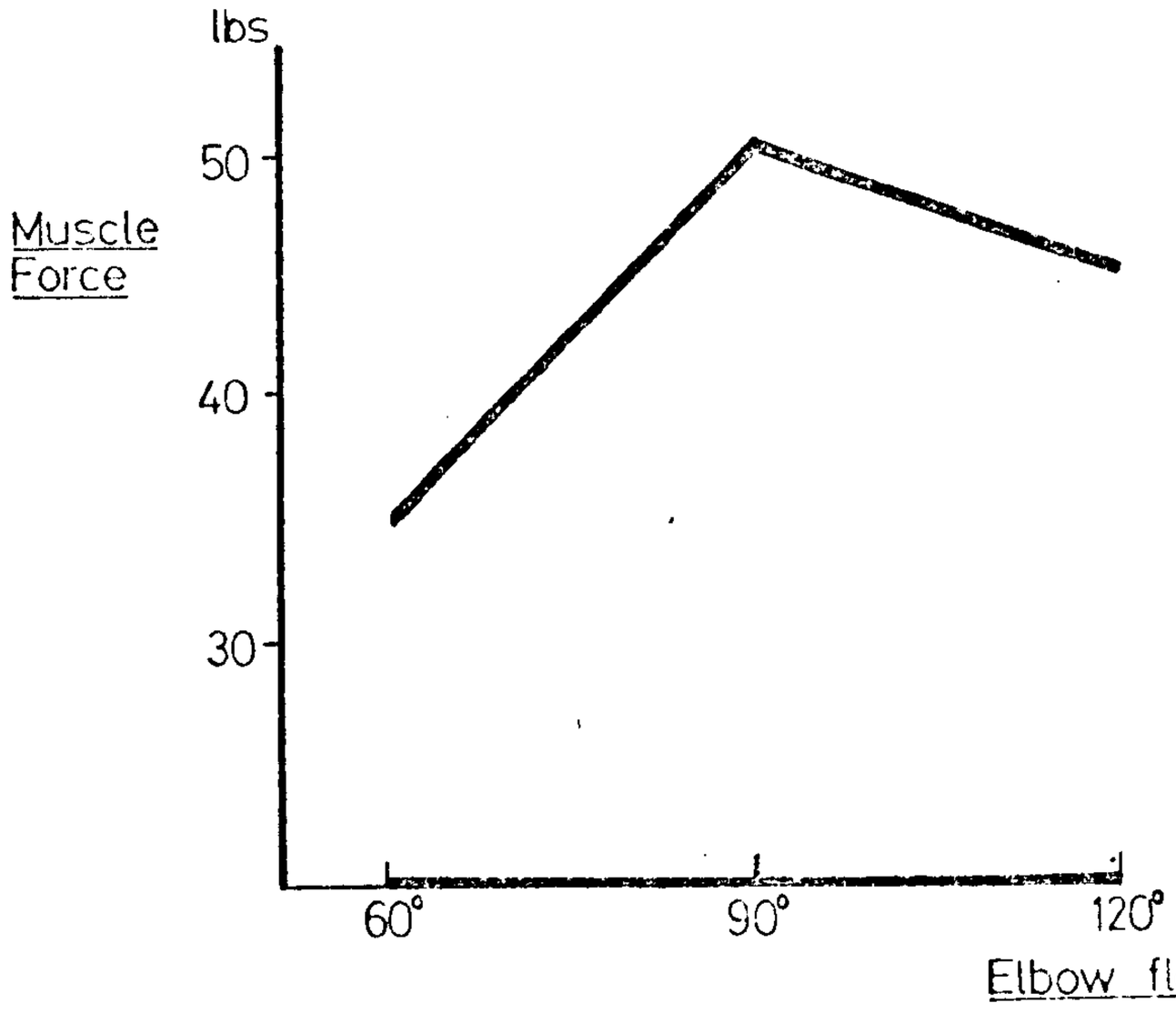

Figure 4·8: Maximum triceps force during extension (Currier ,1972)

Bankov and Jorgensen studied the lever arms and cross-sectional areas of the muscles at the 90° elbow position in an attempt to estimate the individual contribution of each muscle to the overall torque produced at the elbow. It was assumed that the muscles underwent maximal stimulation and that the forearm was in the supinated position. The results of their calculations are detailed in Table 4.1.

A few years later, several refinements were incorporated in the investigation of flexor muscle strength by Messier et al (1971). Using strings and nails to model the muscles and connective tissue around the elbow joint, empirical equations were produced relating the muscle lever arms to the angle of elbow flexion.

Measurements of flexor strength were made using a wrist cuff and freely suspended weights. Surface electrodes recorded the electrical activity of biceps and triceps and five muscle lengths were investigated, corresponding to θ = 30, 45, 60, 75 and 90°. A high significance was obtained for direct proportionality between muscle tension, wrist force and "averaged" E.M.G. The relationships were found to be independent of both muscle tension and muscle length.

Using the records of "averaged" E.M.G., Messier and his associates analysed the antagonistic activity of the triceps muscle. The forces in both muscle groups were found to increase as the external load was increased and it was therefore postulated that the need for control of elbow position over-powered the pre-requisite of simple mechanical efficiency. In addition, the ratio of forces in opposing muscle groups was found to be dependent on the elbow angle. This ratio doubled from 90° to 30° of elbow flexion irrespective of flexion or extension force actions.

The mechanics of the extensor compartment of the elbow joint were studied by Currier (1972) using a wrist cuff and a cable tensiometer. Forty-one male subjects were instructed to exert extensive forces for elbow angles of 60, 90 and 120°. Maximum isometric force was applied at all times with the cable held at right angles to the forearm. Figure 4.8 indicates that Currier's findings were similar in nature to those of Provins and Salter for flexor strength.

More recently, attention has been focussed on the contribution of individual flexor muscles to the overall "torque" produced at the elbow joint. Cnockaert et al (1975) undertook an electromyographic study of elbow muscles to ascertain the relative contributions made by biceps brachii and brachioradialis to the isometric flexion strength.

The elbow joint was flexed to 75° corresponding to the accepted "equilibrium position" of the muscles and connective tissue. A constant torque was applied to the adducted limb using pulleys and weights. Pronation and supination torques were measured using a strain gauged beam mounted on the back of the hand. The latter torques were controlled by observation of the bridge circuit galvanometer and the E.M.G. of biceps, triceps and brachioradialis were rectified, integrated and recorded.

Three test conditions were defined; namely, pure flexion, flexion associated with pronation, and flexion associated with supination. The total flexor torque was written as:

$$T = T_{biceps} + T_{brachioradialis}$$

$$= P_b Q_b + P_{br} Q_{br}$$

where: P = ratio between E.M.G. and individual muscle torque.

Q = quantified integrated E.M.G.

The above test conditions provided three ratios between Q_b and Q_{br}, for each of three flexor torques, corresponding to the various forearm actions. Very high correlation was obtained between flexion torques and the integrated E.M.G. and good correlation was indicated between the computed muscle torques (T_b and T_{br}) and the total flexion torque "T".

From the results presented, it appears that the decomposition of flexor torques could be a useful analytical technique. However, a comprehensive study of all muscle activity related to elbow flexion and extension would be necessary to test the efficacy of the procedure and it is envisaged that the subsequent analyses would be rather cumbersome for practical applications.

Another method of decomposition of total muscular effort was described

by Yeo (1976) and involved the application of "minimisation" principles to the musculature of the elbow joint. Maintenance of elbow position and a simple elbow flexion movement were mathematically modelled using the straight line joining muscle ends as the effective line of action for biceps brachii, brachialis and brachioradialis.

The minimisation techniques were applied to the moment equilibrium equations about the elbow axes but results indicated a complete contradiction of the findings of Basmajian and Latif (1957). Yeo found that brachioradialis stimulation would reach saturation before biceps stimulation which, in turn, preceded brachialis stimulation. Earlier research proved that all the flexors were active together. It was therefore concluded that minimisation of total muscular force, as applied to elbow flexor muscles, was an invalid technique.

4.5 Elbow Joint Forces:

4.5.1 Introduction: After an exhaustive search of the available literature, very few reports were found regarding the force actions transmitted across the human elbow joint. Two types of investigations have been reported and involve the distribution of forces applied to isolated cadaveric specimens and the measurement of external forces involved in selected arm movements with the subsequent computation of joint forces.

4.5.2 Cadaveric studies: To determine the forces transmitted by the two weight-bearing components of the fully extended elbow joint, Hall and Travill (1964) used specially designed pressure transducers made from 0.125 mm thick brass and coated with pressure sensitive paint. Seven human cadaveric arms were held vertically upright in the test rig and a downward force of 15 kp was applied to the hand. The compressive actions on the humerus and ulna and the humerus and radius were recorded. In all cases the humero-radial joint transmitted a slightly greater proportion of the load than that carried by the ulnar joint; namely 57% compared to 43%. It is interesting to note that Hall and Travill found that 43% of the applied load was transmitted by the humero-ulnar joint even when the interosseous membrane was severed. It was concluded that the ligamentous structures at the wrist joint, and not the

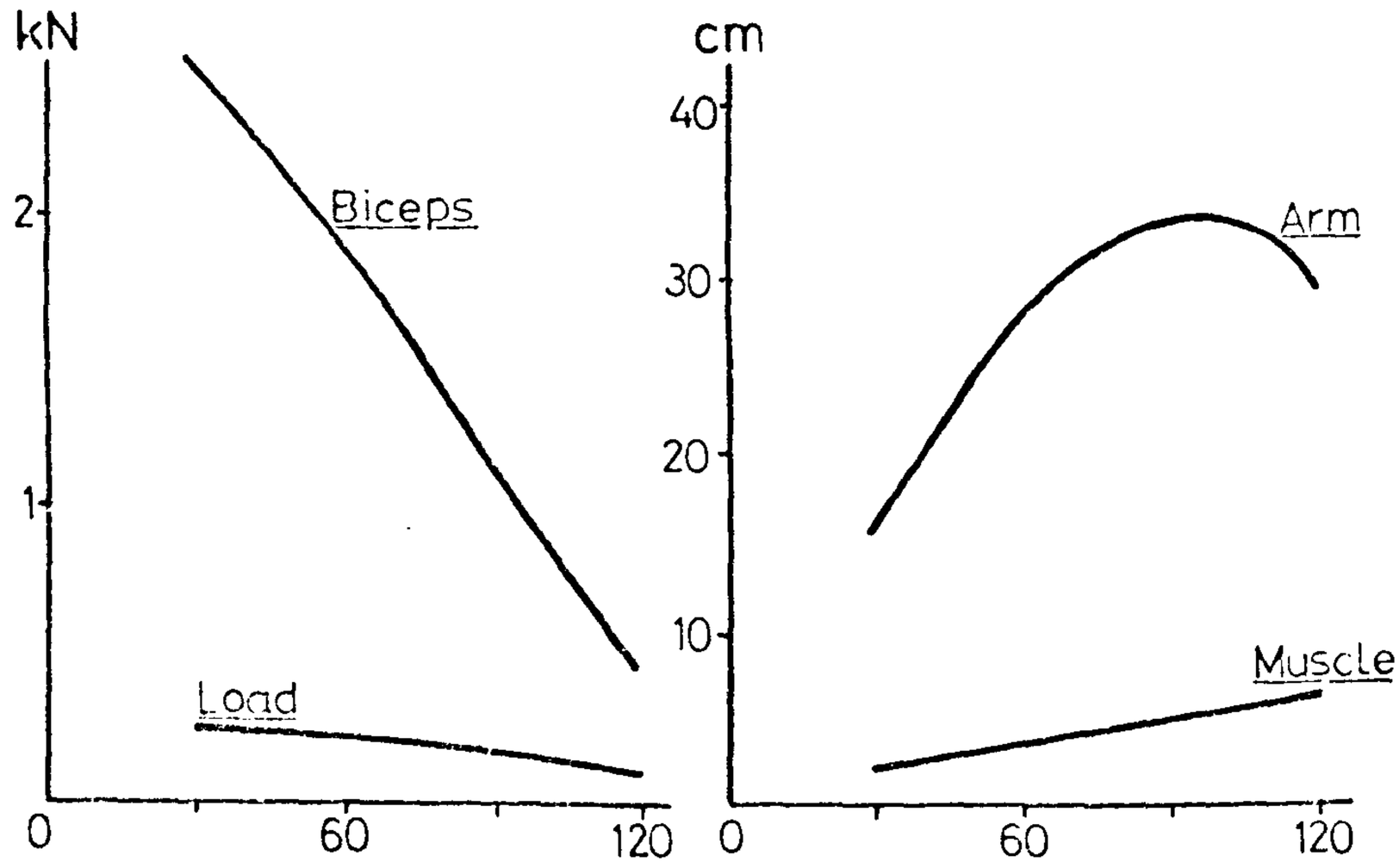

Figure 4·10: Forces and lever arms during elbow flexion (Groh, 1973).

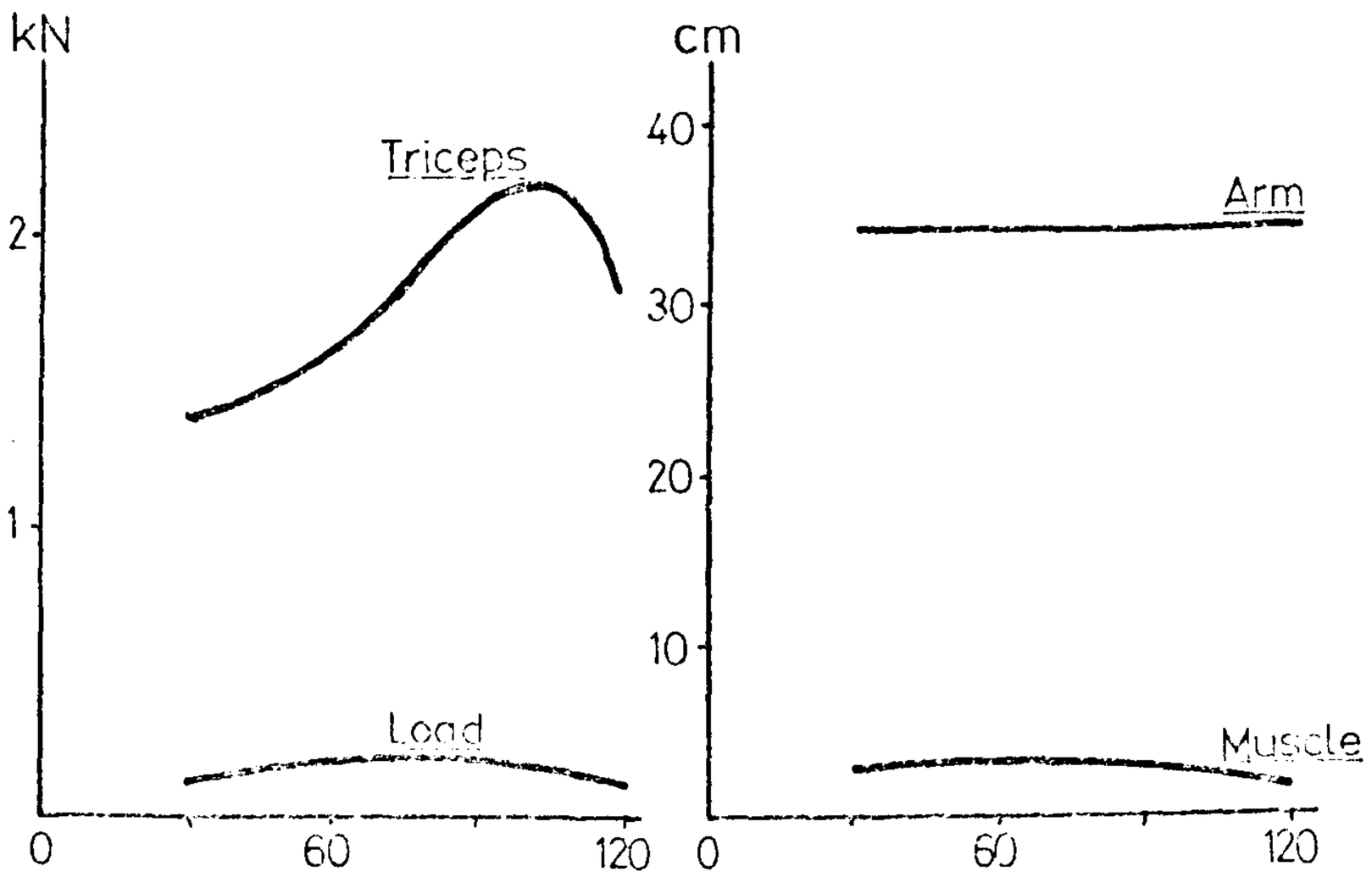

Figure 4·11: Forces and lever arms for elbow extension (Groh, 1973)

interosseous membrane were responsible for the transmission of forces from the hand to the ulna and radius.

Following the work of the previous authors, Walker (1975) undertook a series of tests to clarify the role of the two articulations and the interosseous membrane. Eight fresh arms were loaded sinusoidally in a vertical direction, with the humerus rigidly fixed to the test machine. Accurate measurements were made of the movement of the machine cross head, and loads and deflections as high as 500 N and 0.69 mm were recorded. Palpation of the interosseous membrane was performed in all tests and it was found that the initial tautness in the neutral forearm position was increased on application of load. In supination the fibres were initially taut and, in some cases, the applied load created greater tension. However, in positions of pronation the membrane fibres were slack in all conditions.

From tests in which the membrane had been severed, it was postulated that the interosseous membrane serves to reduce the stress in the radial shaft during heavy activity. A mechanical analogy was developed for the bone and ligament assembly but no correlation with "normal" activity was found.

4.5.3 Theoretical analyses: Pauwels (Groh, 1973) studied the force and pressure quantities transmitted by the elbow joint during voluntary flexion and extension. The upper arm was always vertical and the simplified analysis was restricted to two dimensions. The maximum load which the hand could support in flexion or extension was measured at 15° intervals of elbow flexion from 30-120.

For flexion of the elbow, the loads were found to range from 24 kp at 30° to 9 kp at 120°. Using muscle geometry reported by Braune and Fischer in 1889, the corresponding biceps tensions were calculated as 225 kp and 50 kp (see figure 4.10).

In extension, the load carrying capacity of the arm ranged between 10 kp and 16 kp as shown in figure 4.11 and the maximum muscle force was reported to be 213 kp at 105° of flexion.

The joint reactions were estimated from vectorial summations of muscle force and arm load. In the example illustrated in figure 4.12, a flexor force

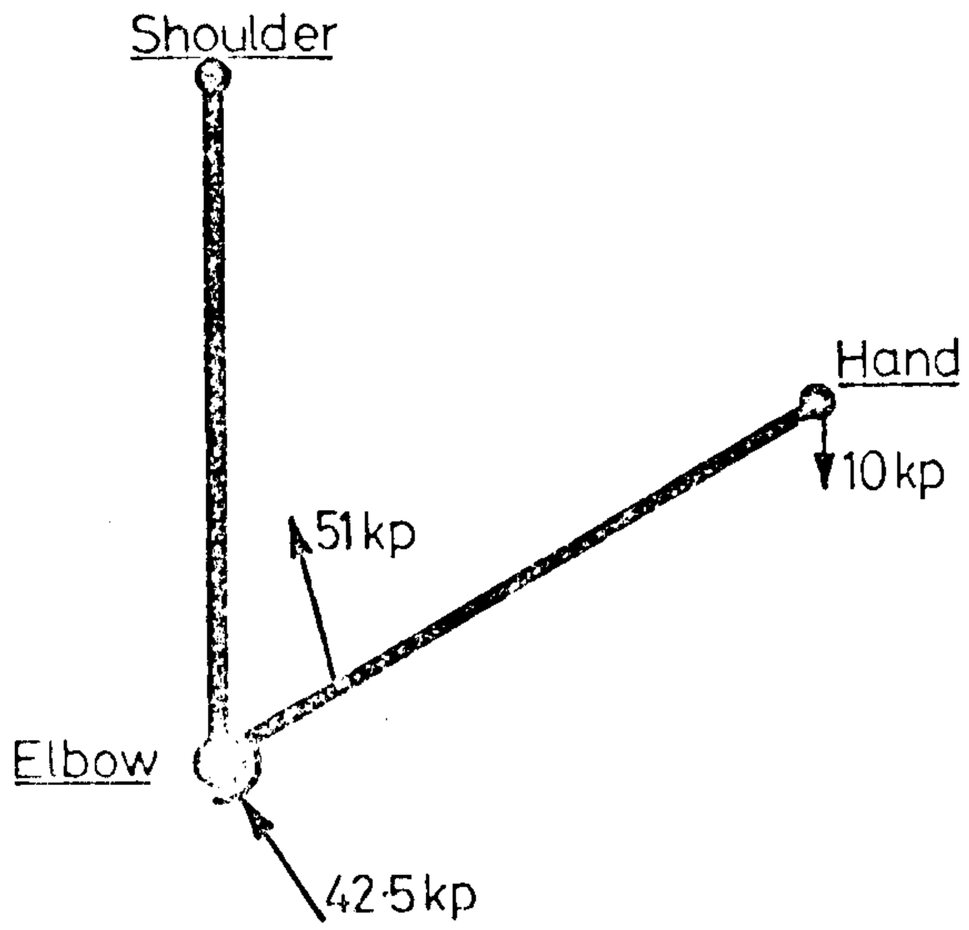

Figure 4.12: Statics of elbow flexion. (Groh, 1973)

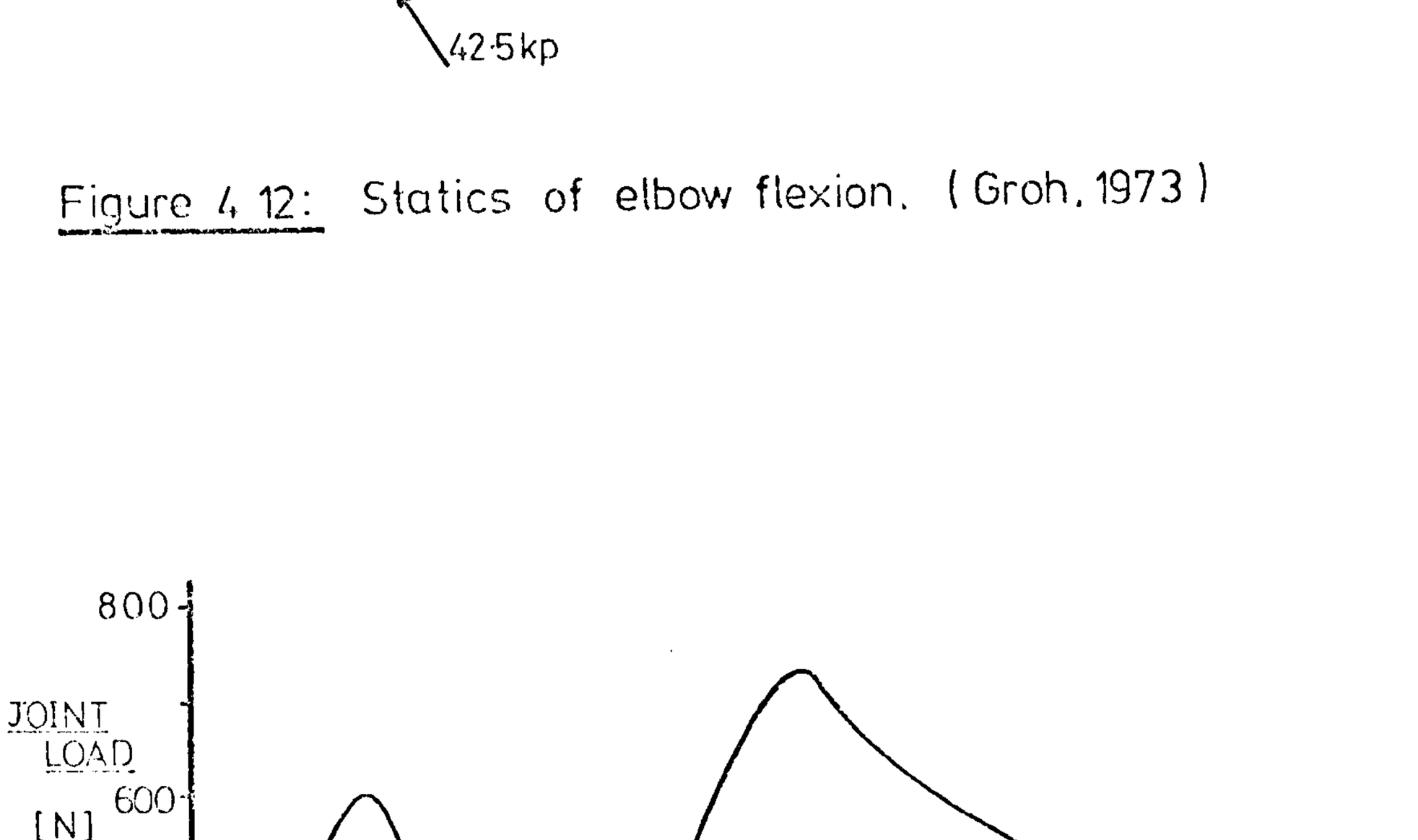

Figure 4·13: Joint forces produced during elbow flexion. (Simpson, 1975)

of 51 kp and arm load of 10 kp produced a resultant compressive joint force of 42.5 kp. Pauwels also performed a purely theoretical study of pressure distribution for the elbow joint, and the pressures obtained were of the order of 350 kp/cm^2 for "edge" loading but significantly lower for normal articulation.

For similar limited arm positions, Simpson (1975) performed a 3-dimensional analysis of joint loading during pure flexion movements. The flexor muscles were grouped together and consisted of brachialis, biceps brachii and brachio-radialis. The lines of action of these muscles were calculated from measurements of the appropriate origins and insertions on cadaveric specimens. Standard body segment parameters were used throughout the computations. An electrogoniometer was used to monitor the angular displacements of the elbow joint and the angular velocities and accelerations were obtained by graphical differentiation.

Two series of tests were performed as follows:

(a) Static analysis:

The arms of seven male volunteers were measured and the force actions on the elbow joint calculated for hand loads of 1, 2, 3, 4 and 5 kg. A range of 150° of flexion was examined for pure flexion with the upper arm in a vertical position. For the loading conditions chosen, values of joint force approached 700N for 5 kg and around 200N for the unloaded arm.

(b) Dynamic tests:

To simulate normal activity, three tests were performed with active flexion of the elbow. Slow flexion, rapid flexion and rapid flexion with a 2 kg mass were studied using one subject. Graphs of angular velocity and acceleration were obtained and the inertial effects of the movements were included in the subsequent analysis. Results of total joint force for the latter activity are given in figure 4.13 and it can be seen that forces in excess of 700N were obtained.

The foregoing analyses of elbow joint mechanics have a common failing in so far as the activities were of a completely artificial and even "pure" nature. In lower limb studies the adoption of the walking cycle as a reference activity is internationally recognised. For the upper limb no attempt has been

made to standardise "normal" movements. The work presented in this thesis was undertaken to bring together the results of previous investigations and to provide some basis for the design of a replacement elbow joint.

5. EXPERIMENTAL WORK

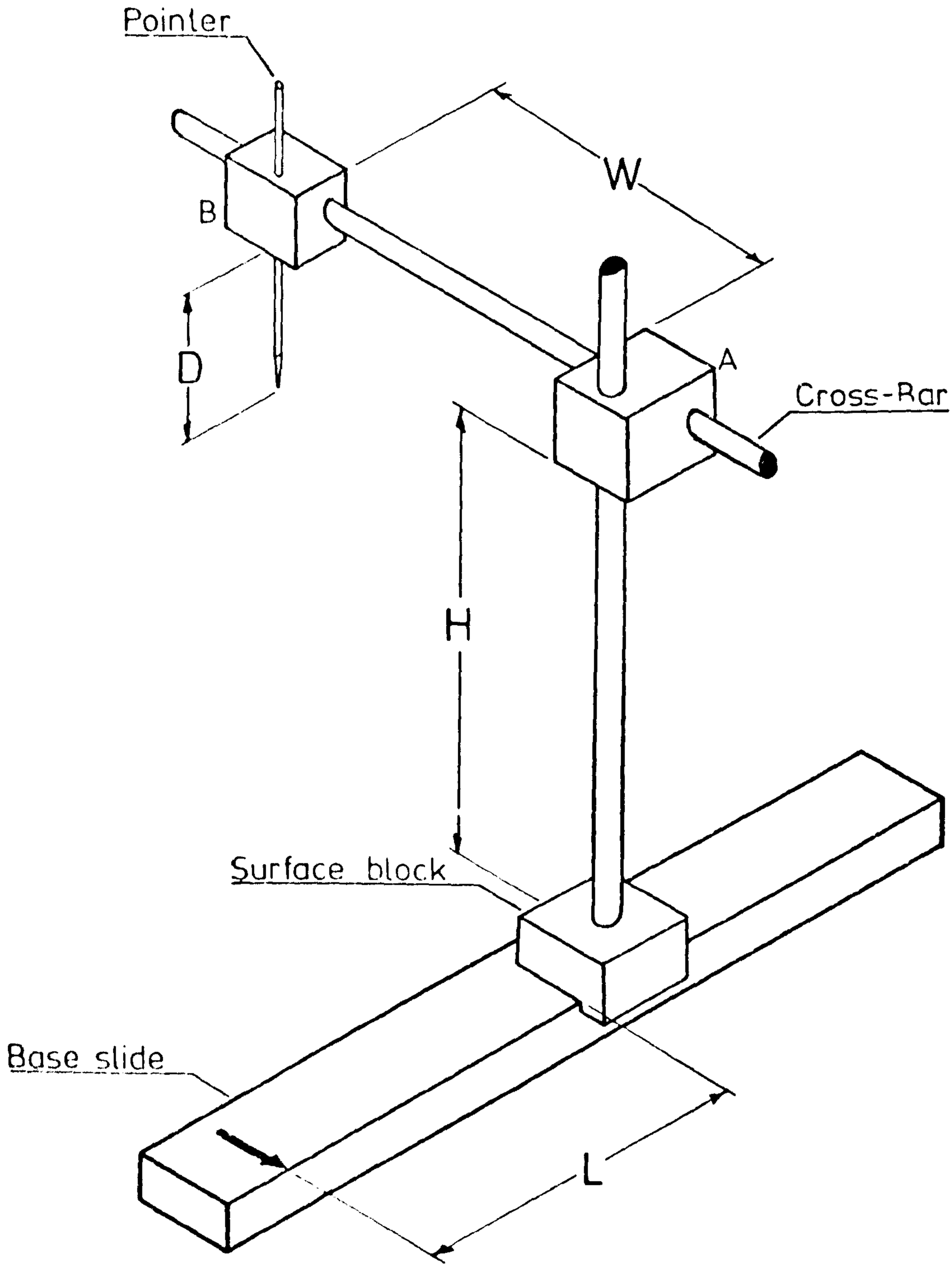

Figure 5•1: Fundamentals of anatomical measurement apparatus.

5. EXPERIMENTAL WORK

5.1 Introduction:

Tests have been carried out to assess the joint forces for various upper limb activities. This section describes the equipment used to obtain displacement data and the forces acting on the arm.

The experiment design criteria and experimental procedures are presented for several "everyday" activities with particular reference to patients suffering from rheumatoid arthritis. The steps involved in the collection of data are also detailed.

5.2 Anatomical Studies:

For the determination of muscle, ligament and joint forces, a knowledge of certain anatomical parameters was required. The effective lines of action of the muscles and ligaments were calculated from measurements obtained from cadaveric limbs, and transverse sections of the distal humerus and proximal ulna provided geometric details of the humero-ulnar articular surfaces. The humero-radial joint was considered to be part-spherical and did not warrant detailed measurement.

5.2.1: Anatomical measurements: Apparatus was designed and built to measure the three-dimensional coordinates of muscle and ligament origins and insertions for the upper arm and forearm. The basic unit consisted of a base slide and proprietary surface block shown diagrammatically in figure 5.1. Two aluminium blocks were suitably drilled to make sliders A and B, and small thumb screws provided a rapid and convenient system of clamping to the relevant cross bars.

The embalmed arm was disarticulated at the shoulder region and partially dissected to reveal all the necessary measurement points. Two retort stands supported the appropriate limb segment with its axes parallel to the measurement axes while a third stand supported the free end of the arm. The neutral position of the hand was adopted to minimise errors arising from pronation/supination effects. Figure 5.2 shows the measurement of a forearm in progress. For each landmark the pointer was locked in the appropriate location and the orthogonality of the apparatus was checked, and adjusted if necessary. Base

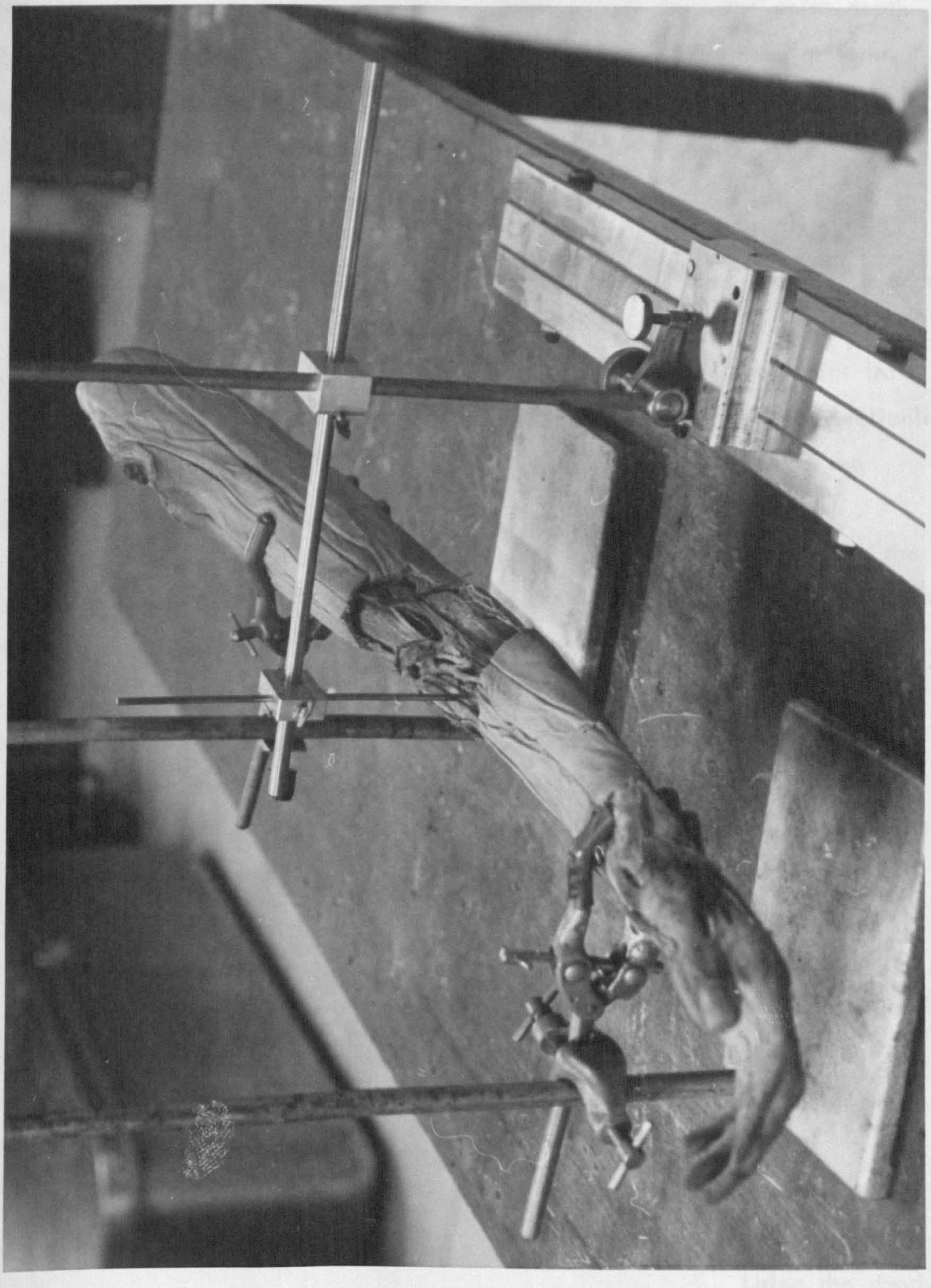

Figure 5.2: The three dimensional measurement of a forearm.

slide travel (L), cross bar height (H), cross bar reach (W), and point depth (D) were measured with a 300 mm steel rule and recorded in tabular form. To check the accuracy of the measurement system a repeatability test was performed on several marked points and a maximum error of $\pm$ 1 mm was recorded.

5.2.2 Bone slicing: After studying literature by Seedhom et al (1972a) describing geometrical studies of the human knee joint it was decided to undertake a similar investigation for the articular surfaces of the elbow joint. Seedhom obtained sagittal sections of the components of the knee joint from plastic models of the bones. For the smaller joint of the elbow the sectioning procedure was performed using a circular sanding disc and recording the transverse profile on tracing paper.

A unit was constructed which held the bone end at right angles to the sanding disc as shown in figure 5.3. Referring to the diagram of figure 5.4 the lead screw had a 180° indexing mechanism which enabled steps of $\frac{1.25}{2}$ mm to be made. The base plate stop "A" registered with the cross-slide groove on the sander table to give reference to the depth and orientation of cut.

Using a synthetic resin, the prepared bone end was embedded in the mounting block with the hinge axis of the elbow joint horizontal and parallel to the cutting plane (see figure 5.4). By slowly advancing the lead screw towards the sanding disc, the first section of bone was removed. Ink was applied to the cut surface using a "rubber-stamp" ink pad and an image of the perimeter of the section was obtained by pressing the surface against a piece of tracing paper which was attached to a special recording jig. From figure 5.5 it can be seen that repeatability was ensured by the use of two marker pins which protruded through the tracing paper.

The lead screw was advanced a full turn (1.25 mm) and the procedure repeated till the geometry of the whole articular surface had been recorded. A typical record of the cut section is shown in figure 5.6. Using the depth of cut as the third dimension, graphs were drawn of the geometry of the articular surfaces for the two remaining planes.

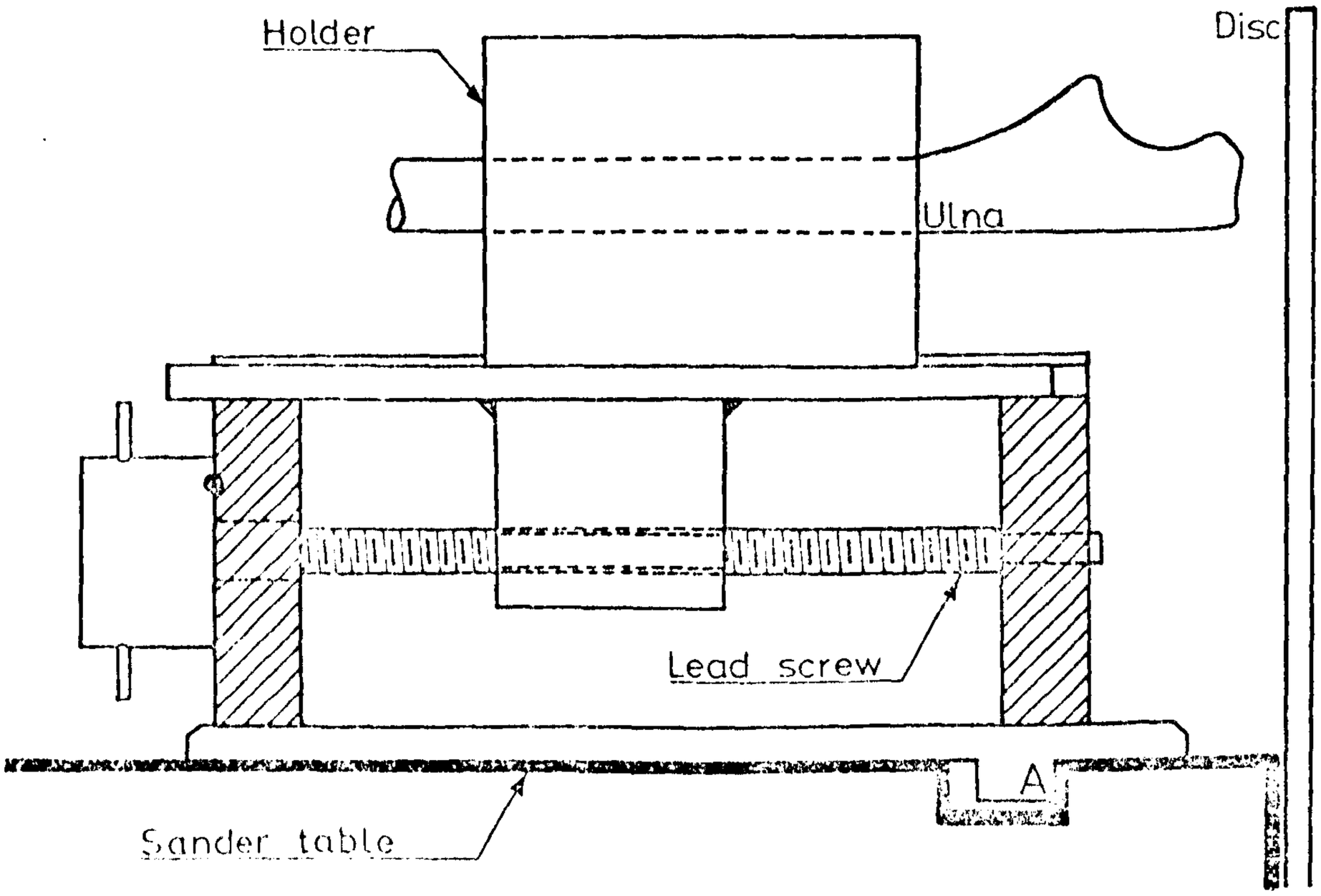

Figure 5•4: Functional details of the bone slicing jig.

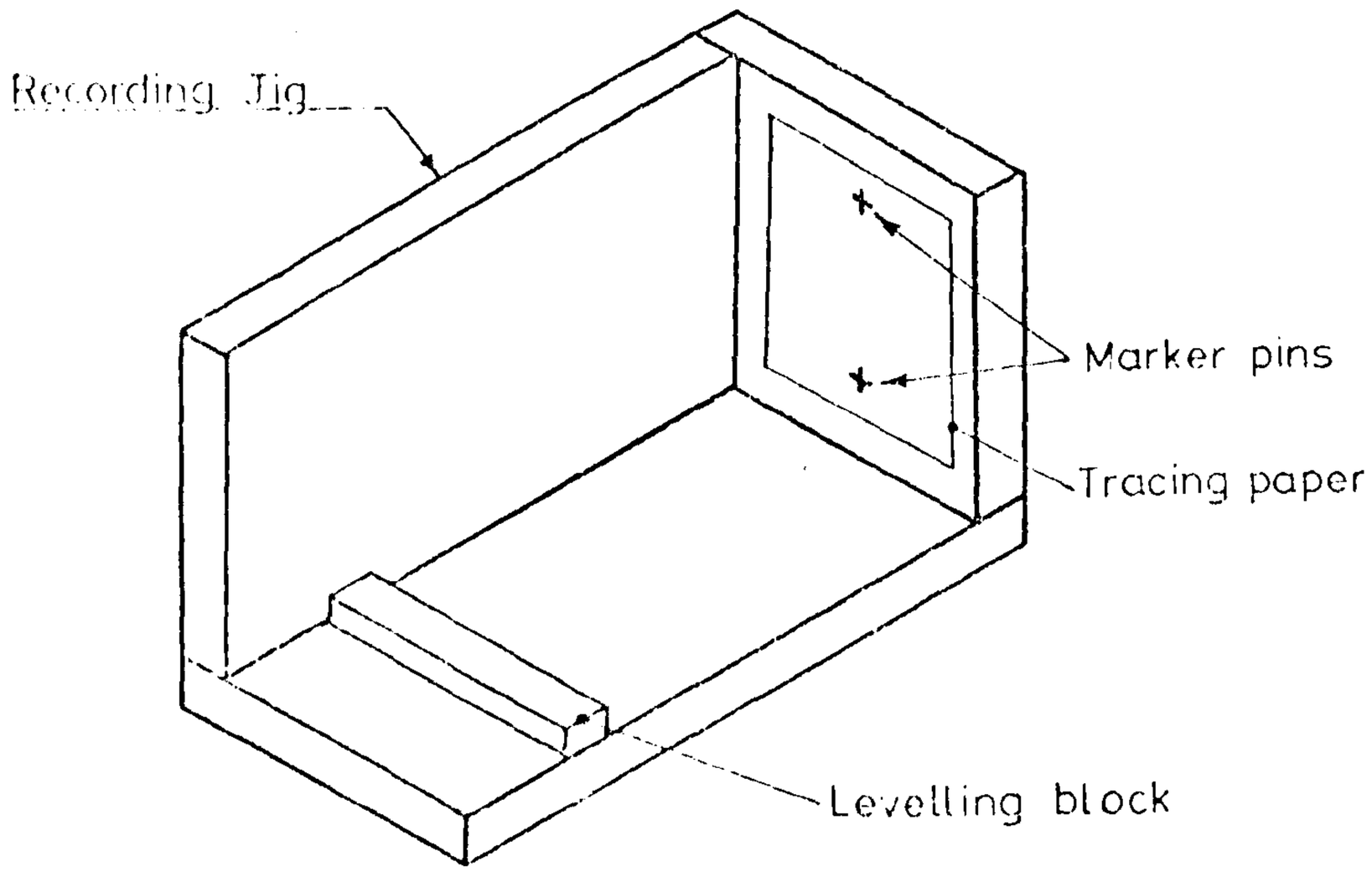

Figure 5•5: Recording jig used during the bone sectioning.

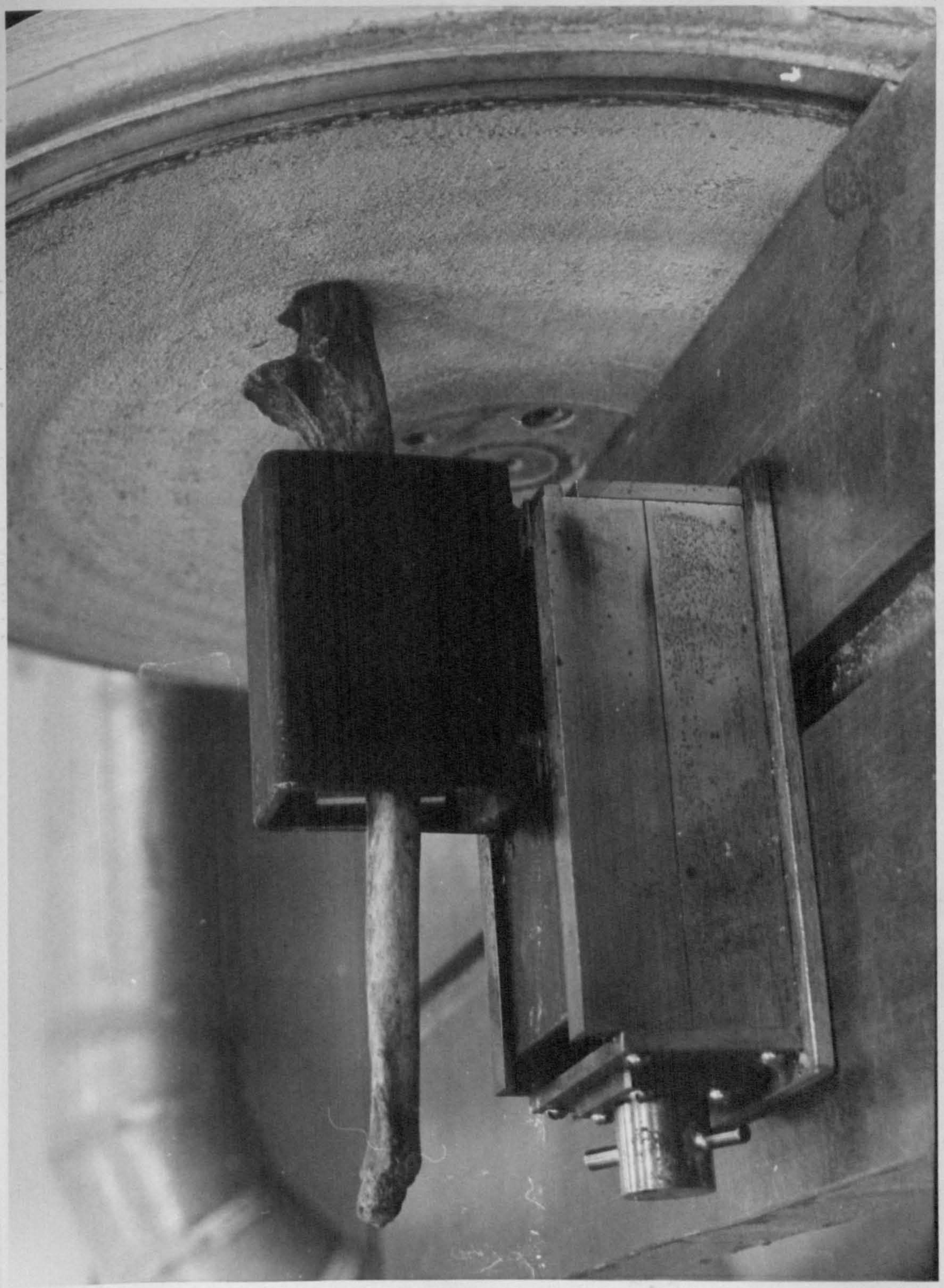

Figure 5.3: The bone sectioning unit in use.

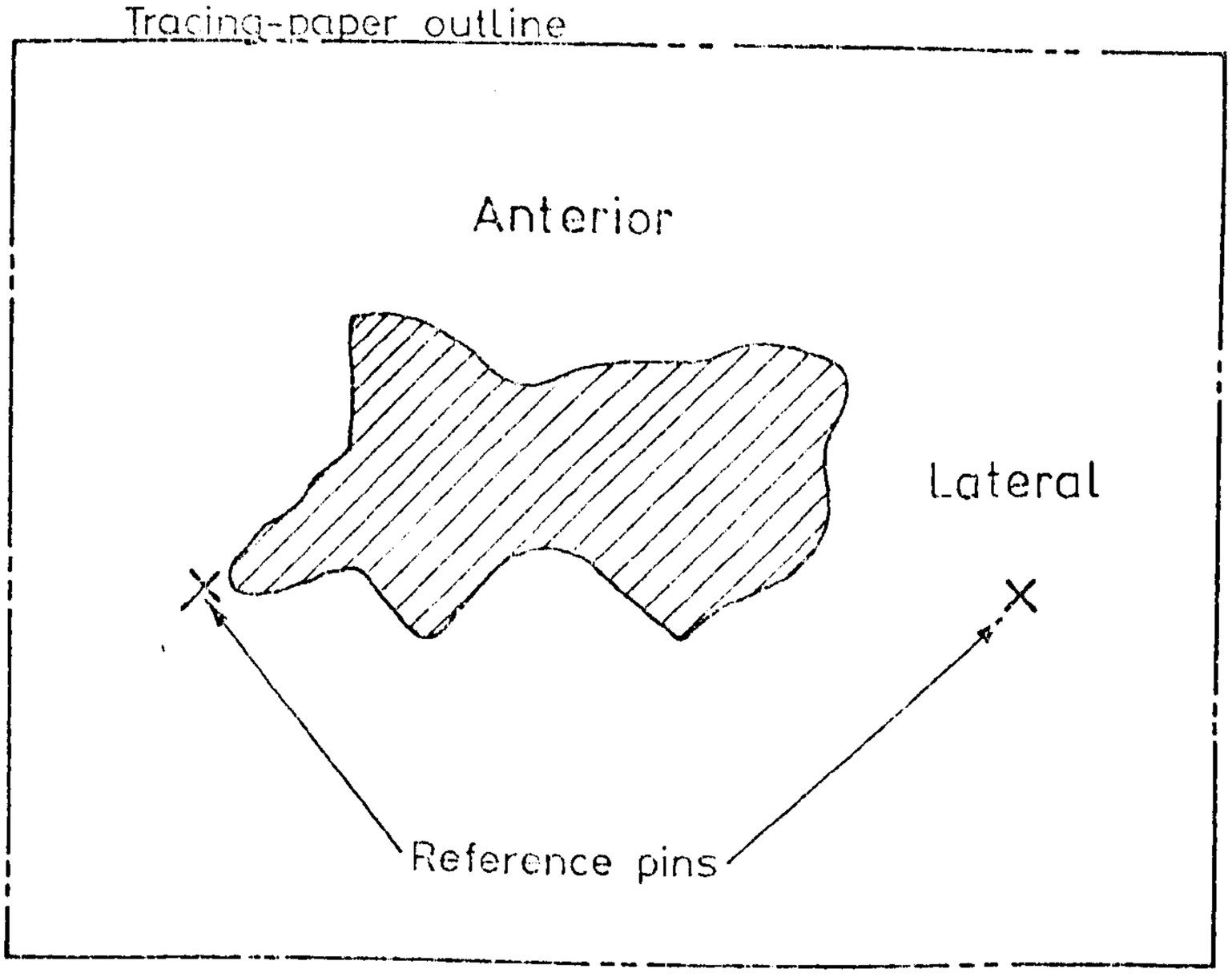

Figure 5·6: Typical cross-section of distal humerus.

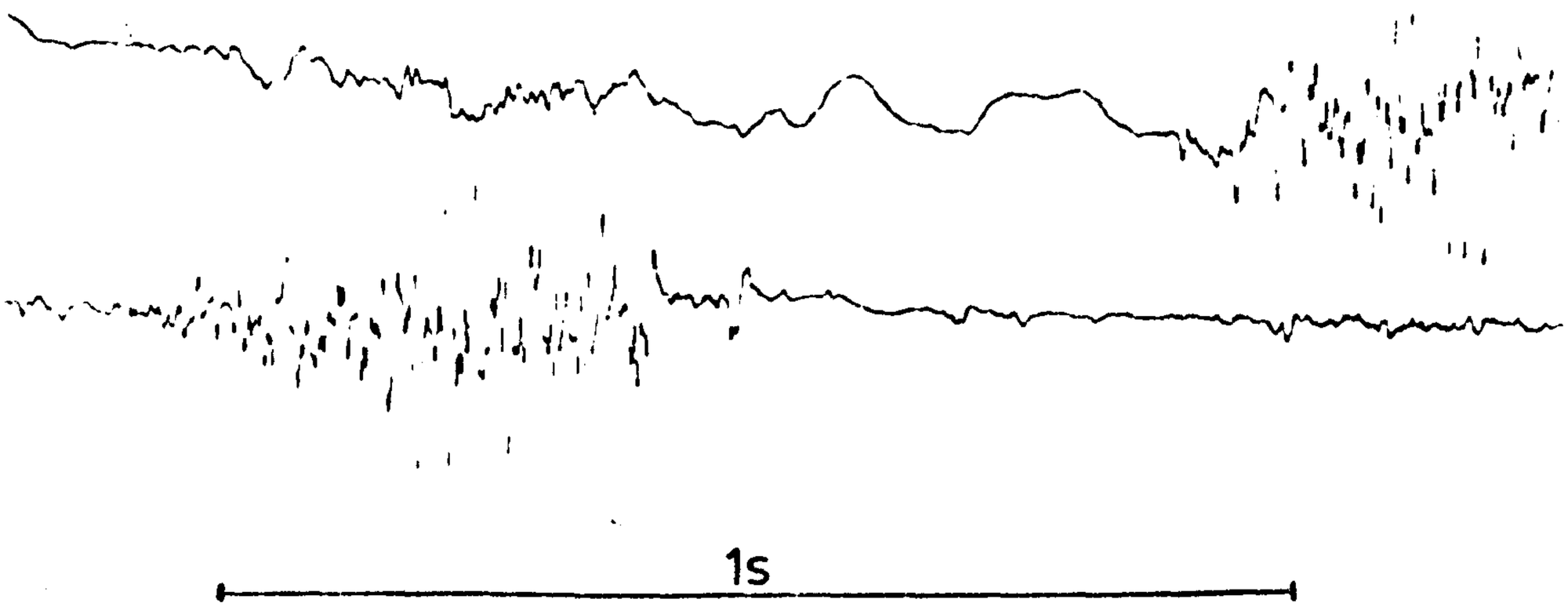

Figure 5·7: Typical electromyographs

5.3 Instrumentation:

This section describes the equipment used to obtain kinematic and dynamic data during activities performed by "normal" male subjects. Three sets of apparatus are discussed; namely electromyography, force measurement and cine photography.

5.3.1 Electromyography: Electromyographic recordings of arm muscle activity were obtained using silver skin electrodes coated with silver chloride to prevent surface polarisation. The electrodes were used in pairs to give a differential input to the amplifiers and, for convenience, special leads were made from 7/0.1 mm miniature screened cable. Suitable preamplifiers were incorporated into the circuitry to boost the physiological signals and were mounted on a special "back-pack" to minimise restrictions on mobility. A bank of seven Medelec A8 amplifiers with individual monitoring oscilloscopes and gain/frequency response controls was used to amplify and display the output from the preamplifiers. A permanent record of the muscle activity was produced on an "S.E. Laboratory" ultra violet galvanometer recorder. A3300 galvonometers were used to cope with the maximum E.M.G. frequencies of around 1 kHz. To synchronise the electromyograms with the cine film records a 20 msec pulse was displayed on the U.V. trace and corresponded to the "flash" signal of the cine cameras.

The appropriate muscle bellies were lightly shaved and degreased using alcohol swabs. Initially, the electrodes were applied to the skin using annular sticky rings. A syringe was used to squeeze electrode jelly through the central hole of the electrode. Results indicated that the conduction area of 19 mm^2 gave too high an electrical resistance and produced 50 Hz "noise" on the E.M.G. signal. To overcome this problem the jelly was applied directly to the inside of the electrode which was then attached to the skin with a piece of surgical tape. With the larger area of 63 mm^2 no noise problem was experienced.

Before connection was completed between electrodes, preamplifiers and the main amplifiers, a reference "earth" electrode was strapped to the left ankle. The E.M.G. signals were finally checked for gain under maximal muscle exertion and modified as required. Figure 5.7 shows a typical test record.

5.3.2 Force measurement: Activities which involved hand force actions required some form of force transducer to measure the three forces and moments transmitted to the environment. A strain gauged column transducer, developed for the evaluation of lower limb prostheses, was used since its sensitivity and size were ideal for upper limb investigations.

The transducer has been described by Berme et al (1975) and consisted of a short tube with integral end flanges (see figure 5.8). The central portion of the tube was strain gauged to measure the three forces and moments applied to the tube ends. End adaptors were fitted to provide simple mounting wherever required.

A 6 volts D.C. bridge supply voltage, together with a bank of six Fylde 154 AB S bridge amplifiers was used to obtain the output signals and a seven channel Bell and Howell instrument tape recorder was used to store the analogue information for future analysis. The seventh channel recorded the synchronising pulse from the camera flash units. The theory concerning the calculation of calibration terms is described in section 6.13.

Before use, the tape recorder channels were zeroed and calibrated. A trial test was performed to check that the output from the tape recorder did not exceed the limiting value of 1000 mV for input to the PDP-12 computer.

Special tubular holders were used to protect the instrument during use and to provide convenient hand grips for the selected activities. Figures 5.9a and 5.9b show the two holders used for the "transducer" series of tests.

5.3.3 Cine photography: Displacement data was obtained from measurements of cine film records of upper limb movements. Three Bolex Paillard 16 mm cameras were used and their configuration in relation to both subject position and reference axes is shown in figure 5.10. Camera nomenclature was adopted from lower limb investigations with the "front" camera being in the direction of walking. Overhead lighting provided suitable illumination of the subject for a shutter speed of 1/250 second and aperture setting of f 2.8.

The cameras were driven at 50 frames/second, through appropriate gearing, by synchronous motors. Synchronisation between the three cameras was achieved

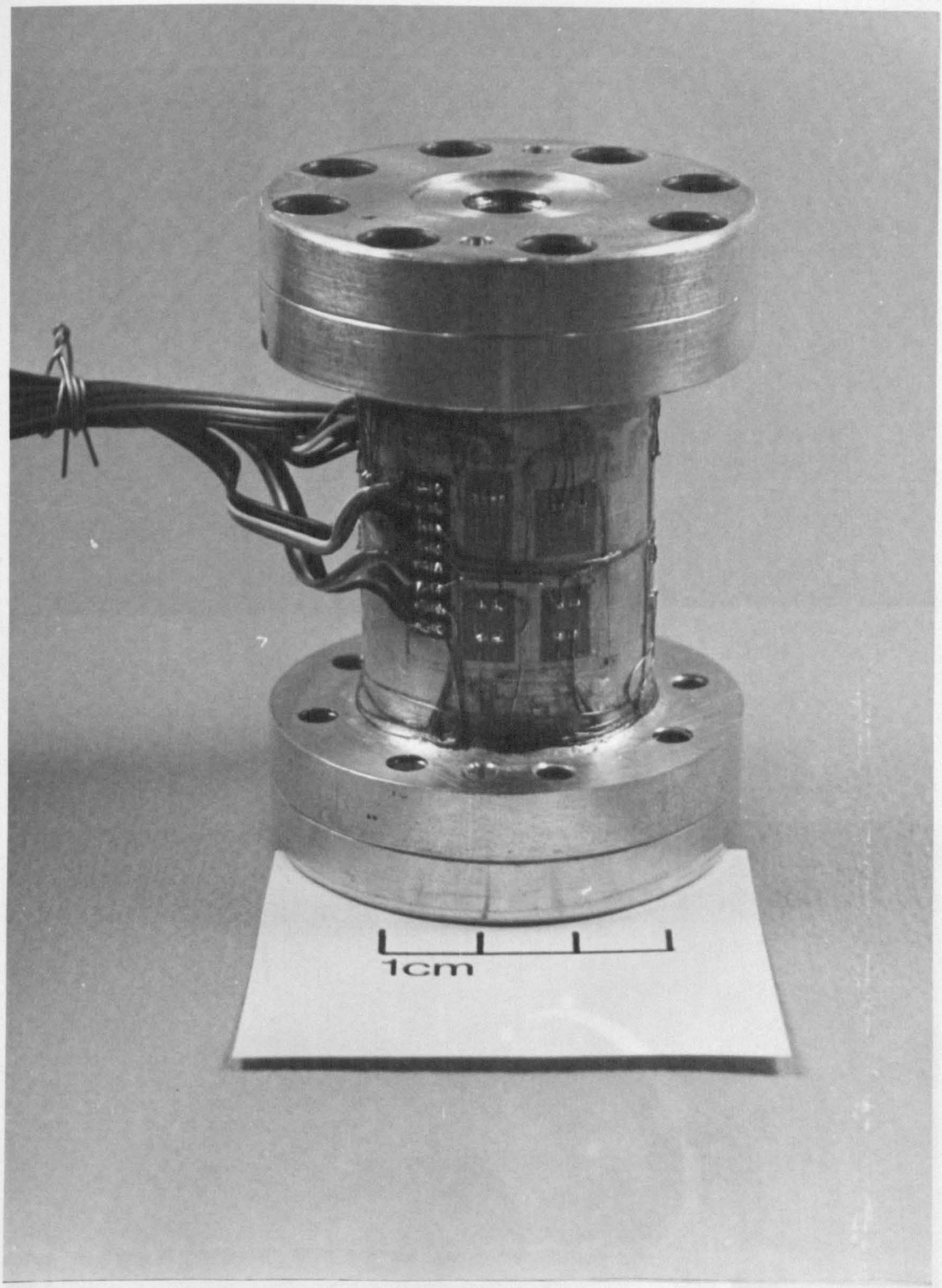

Figure 5.8: The force transducer.

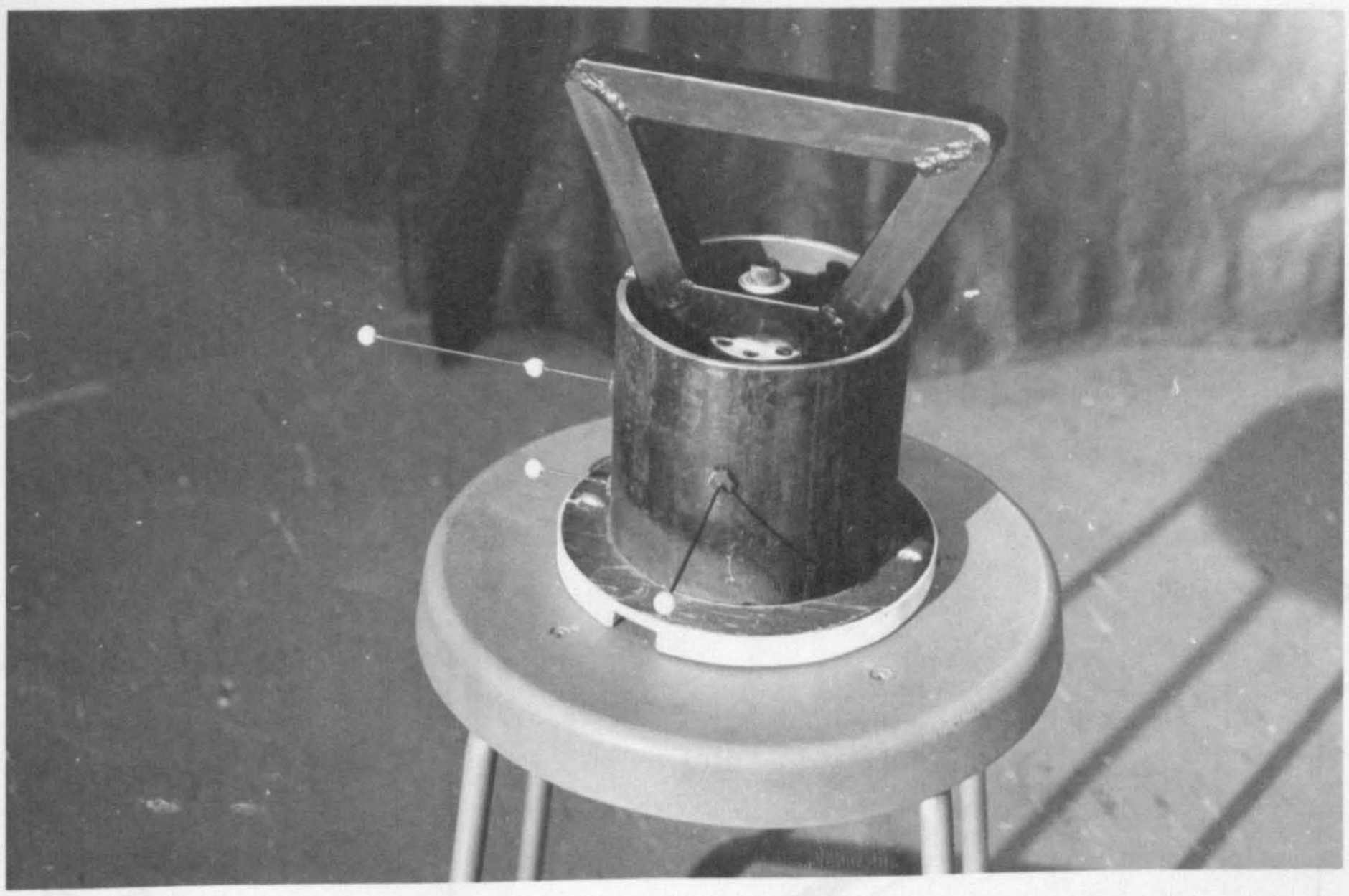

(a)

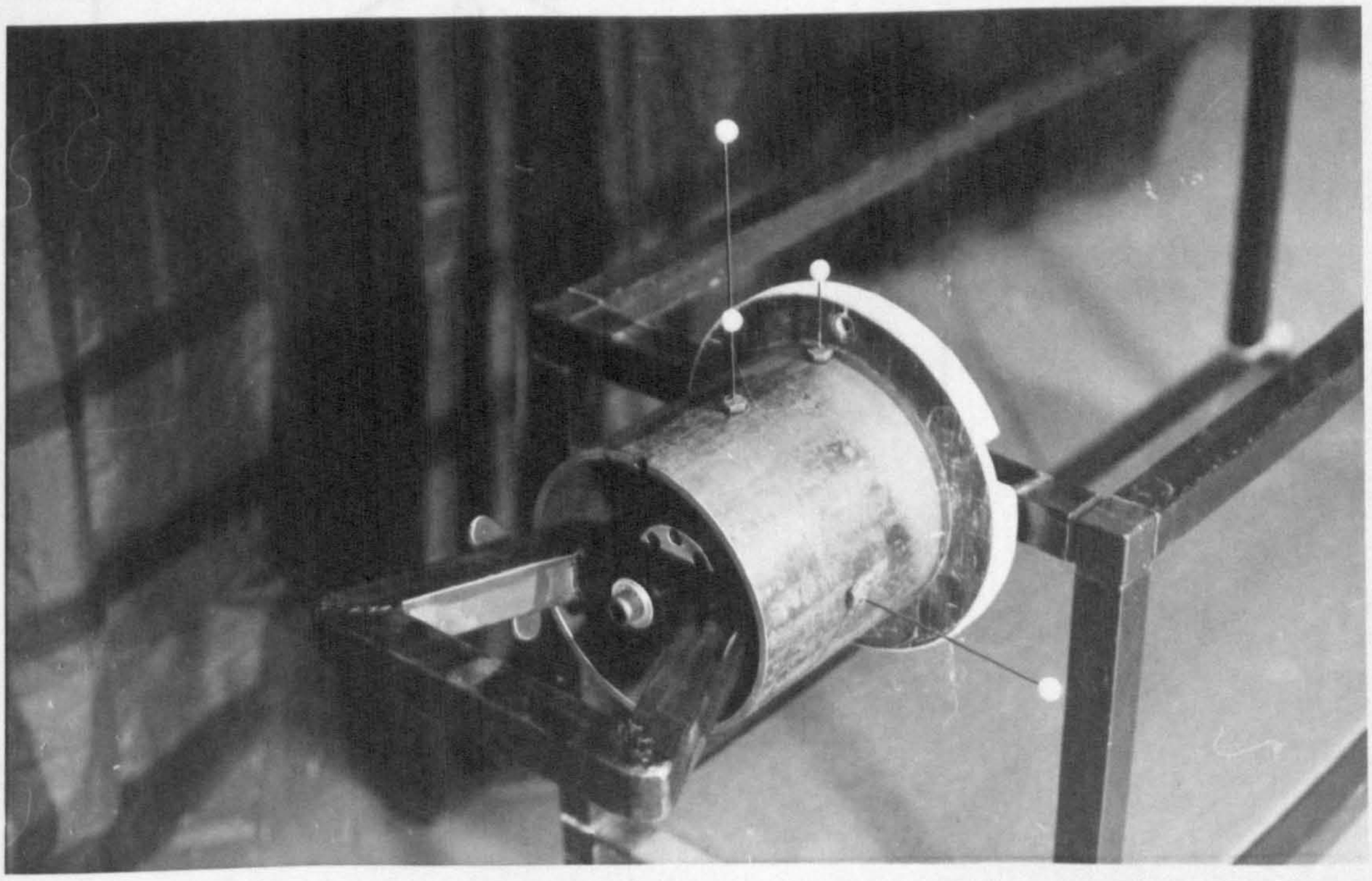

(b)

Figure 5.9: The markers, holder and handle for the transducer.

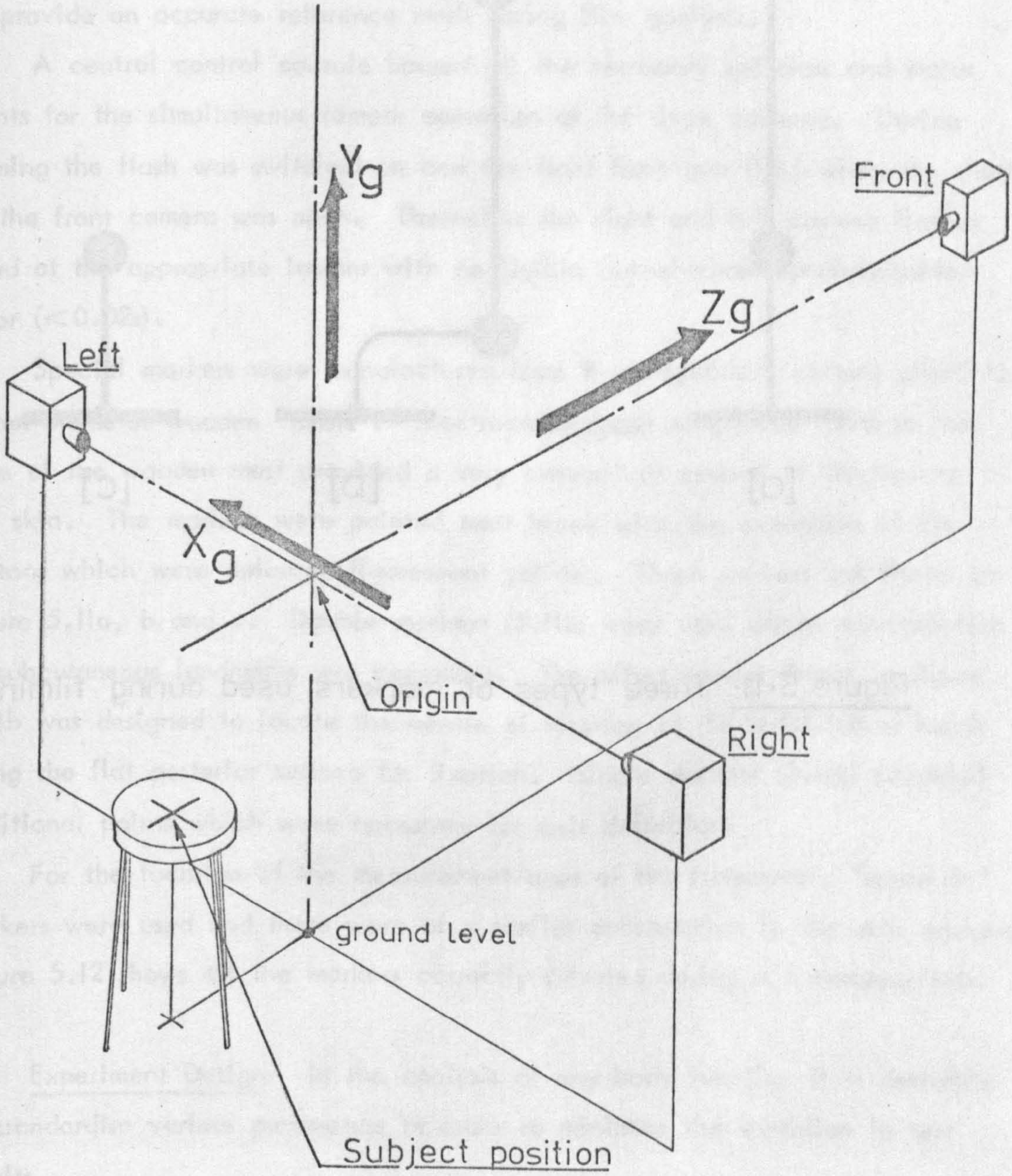

Figure 5·10: Positioning of subject;"grid" and cameras.

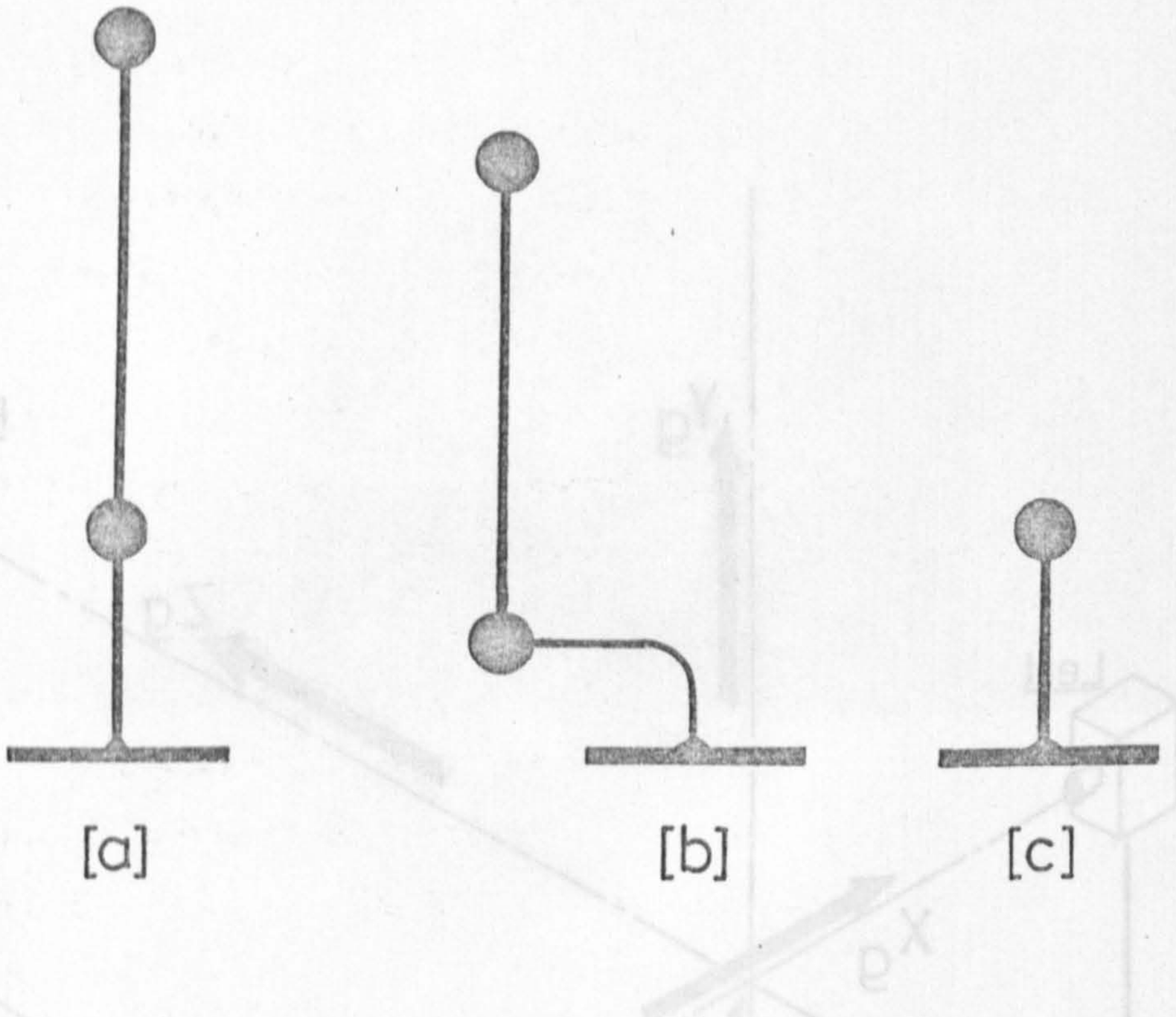

Figure 5•11: Three types of markers used during filming.

using electronic flash guns and strips of white plastic positioned in the field of view of each camera. Shutter opening was recorded electronically using a photo-electric cell and a slotted opaque disc on the end of the drive motor. The flash fired only when the shutter was in the "open" position. Corresponding to the flash event a white band appeared on a single frame of developed film to provide an accurate reference mark during film analysis.

A central control console housed all the necessary switches and status lights for the simultaneous remote operation of the three cameras. During filming the flash was switched on and the front flash gun fired when the shutter of the front camera was open. Thereafter the right and left camera flashes fired at the appropriate instant with negligible out-of-phase synchronisation error ($<0.02s$).

Special markers were manufactured from 9 mm spherical buttons glued to 2 mm diameter wooden "masts". Electrocardiograph electrodes fixed to the base of the wooden mast provided a very convenient method of fixation to the skin. The markers were painted matt black with the exception of the buttons which were coloured fluorescent yellow. Three markers are shown in figure 5.11a, b and c. Double markers (5.11a) were used where extrapolation to subcutaneous landmarks was necessary. The offset marker shown in figure 5.11b was designed to locate the centre of rotation at the wrist (ulnar head) using the flat posterior surface for fixation. Single markers (5.11c) provided additional points which were necessary for axis definition.

For the location of the measurement axes of the transducer, "screw-in" markers were used and these were of a similar construction to the skin markers. Figure 5.12 shows all the markers correctly situated during a transducer test.

5.4 Experiment Design: In the analysis of any body function it is desirable to standardise various parameters in order to minimise the variation in test results.

For the analysis of upper limb movements, the problems relating to standardisation were numerous. In contrast to the activity of locomotion in lower limb investigations, there was no upper limb activity which could be

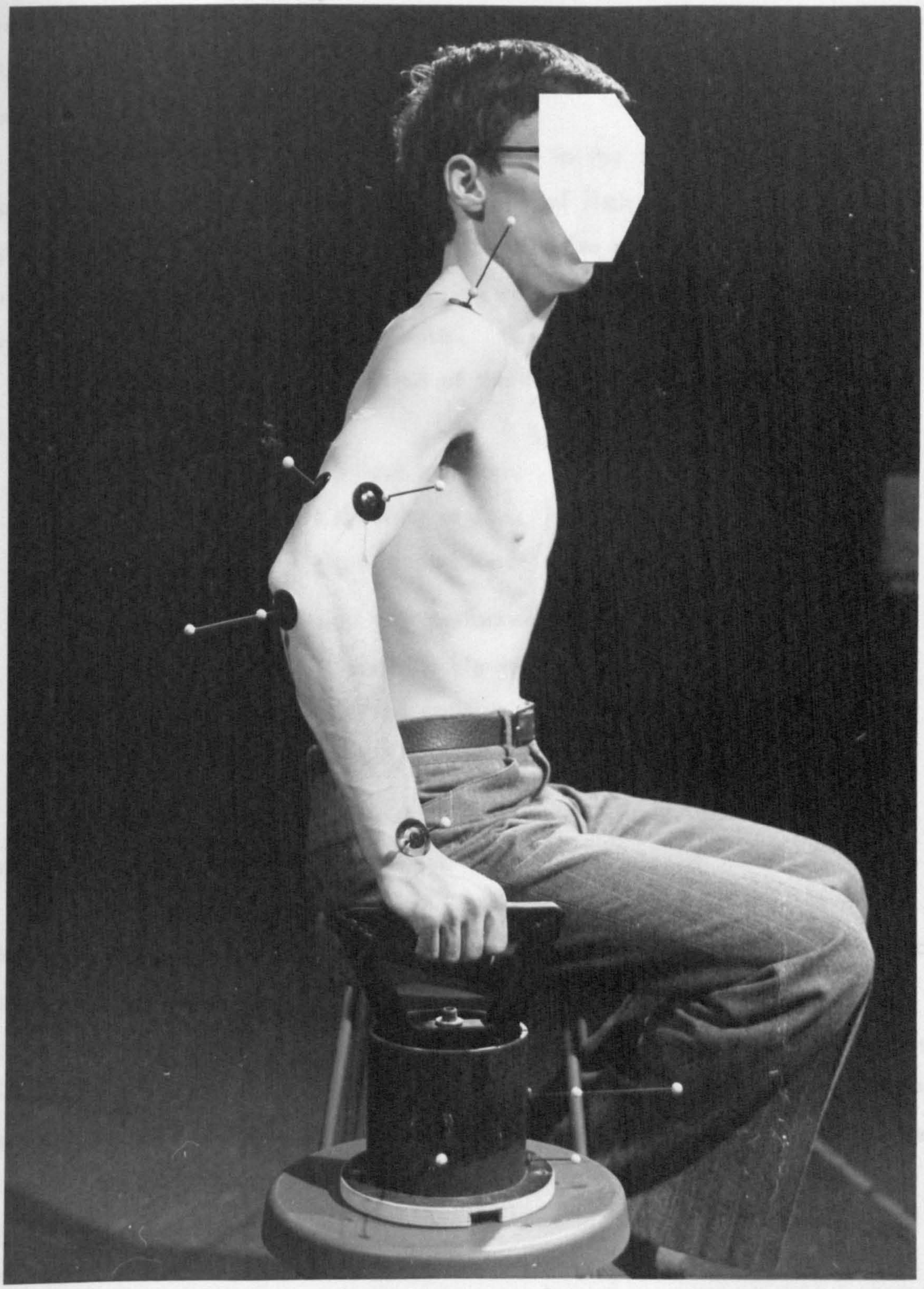

Figure 5.12: Correct positioning of the skin markers.

considered to be functionally "common". It was therefore decided to analyse four activities which were considered to be representative of the majority of arm movements.

Two "inertial" movements were included in the test sequence and they represented activities in which a high degree of limb movement was required with relatively light mechanical effort. Activities such as eating, dressing, washing and many other daily necessities were considered to be represented by "eating" and "reaching" movements.

The "eating" activity consisted of the following manoeuvres (see figure 5.13).

Right arm held in anatomical position.

Swing hand up to left shoulder region.

Reverse procedure to starting position.

The "reaching" movement was performed as shown in figure 5.14:

Right hand held at left anterior hip region.

Swing arm to an outstretched position as if reaching up to a shelf.

Reverse procedure to the starting position.

For both of these activities a 1 kg lead ball was held in the hand and provided considerable inertial effects.

For the more strenuous tasks of everyday life such as lifting, levering and pushing, more consideration was given to the specific problems experienced by rheumatoid patients. In rising from an ordinary chair, for example, a patient will use the arm muscles in addition to the muscle effort from the legs. A "seat rise" movement was therefore included in the test sequence where the subject was seated with outstretched legs while the hands were placed on the arms of the chair (see figure 5.15). To minimise the lifting effect from leg musculature, the subject was instructed to keep his knees fully extended and to maintain heel contact with the ground surface.

To represent the common activity of pulling heavy objects (doors, tables, drawers etc.) the "table-pull" movement consisted of dragging a table along the floor. A 40 kg f weight supplied sufficient frictional force to necessitate "considerable" exertion for completion of the activity (see figure 5.17).

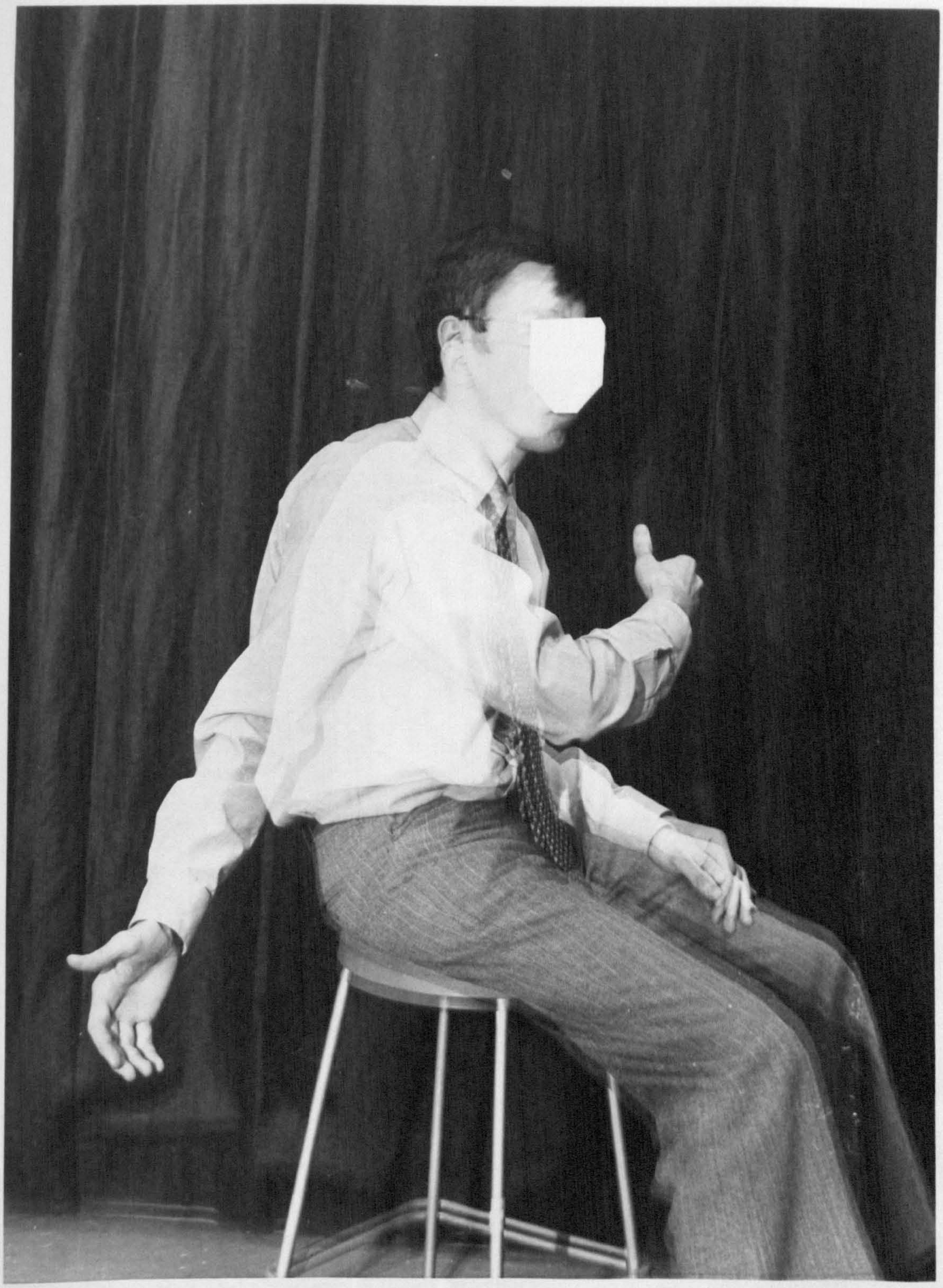

Figure 5.13: The range of movement obtained during the "eating" activity.

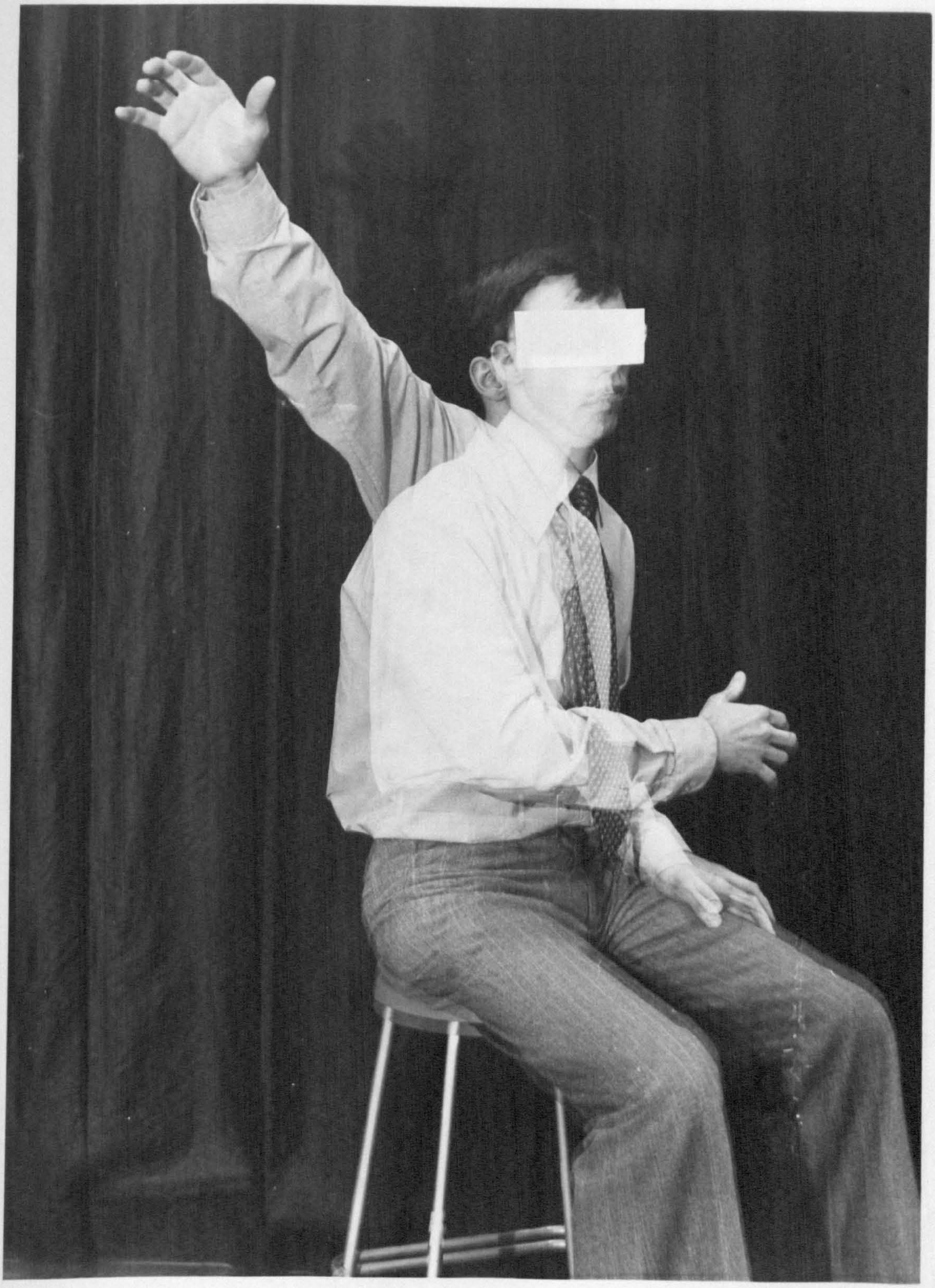

Figure 5.14: The range of movement involved in the "reaching" activity.

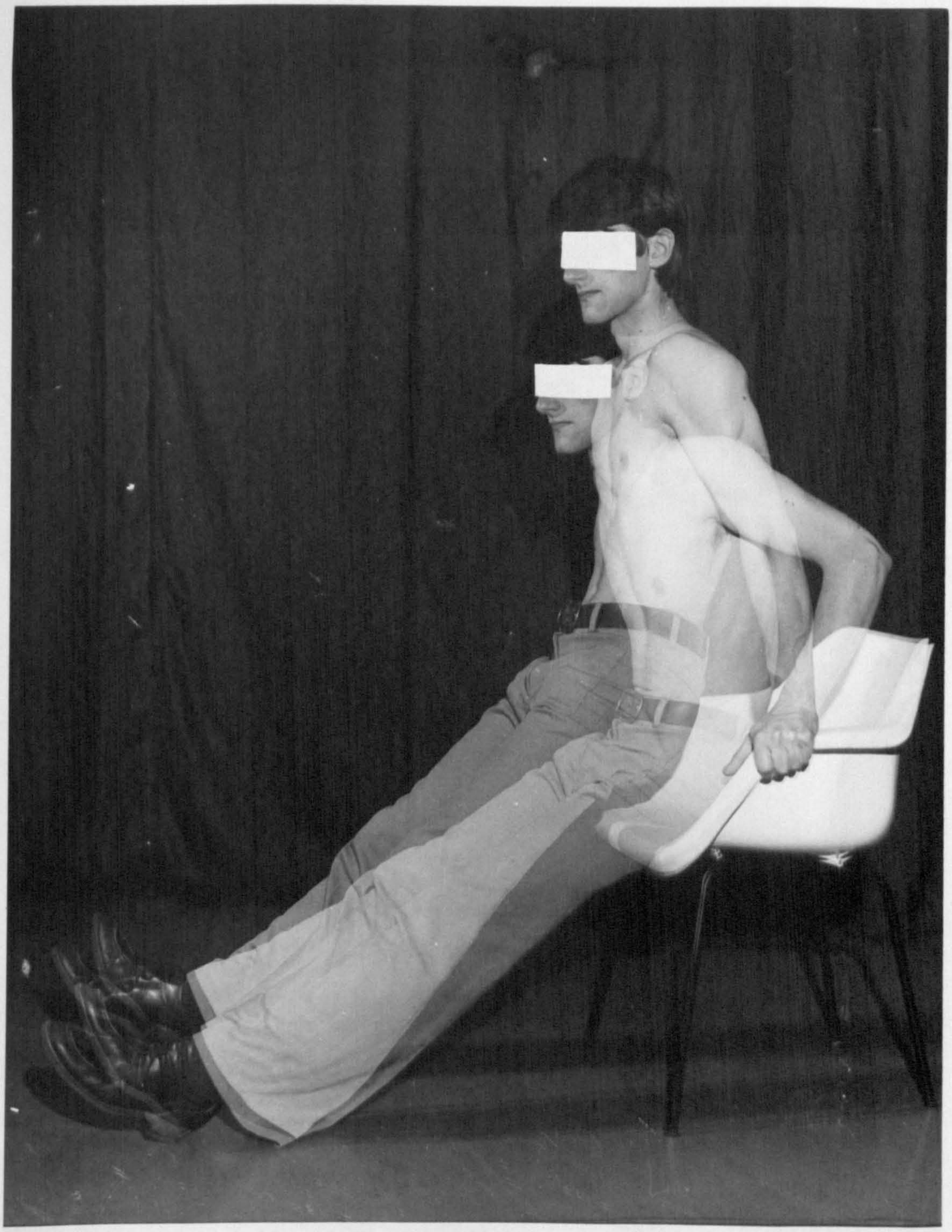

Figure 5.15: The definition of the "seat-rise" exercise.

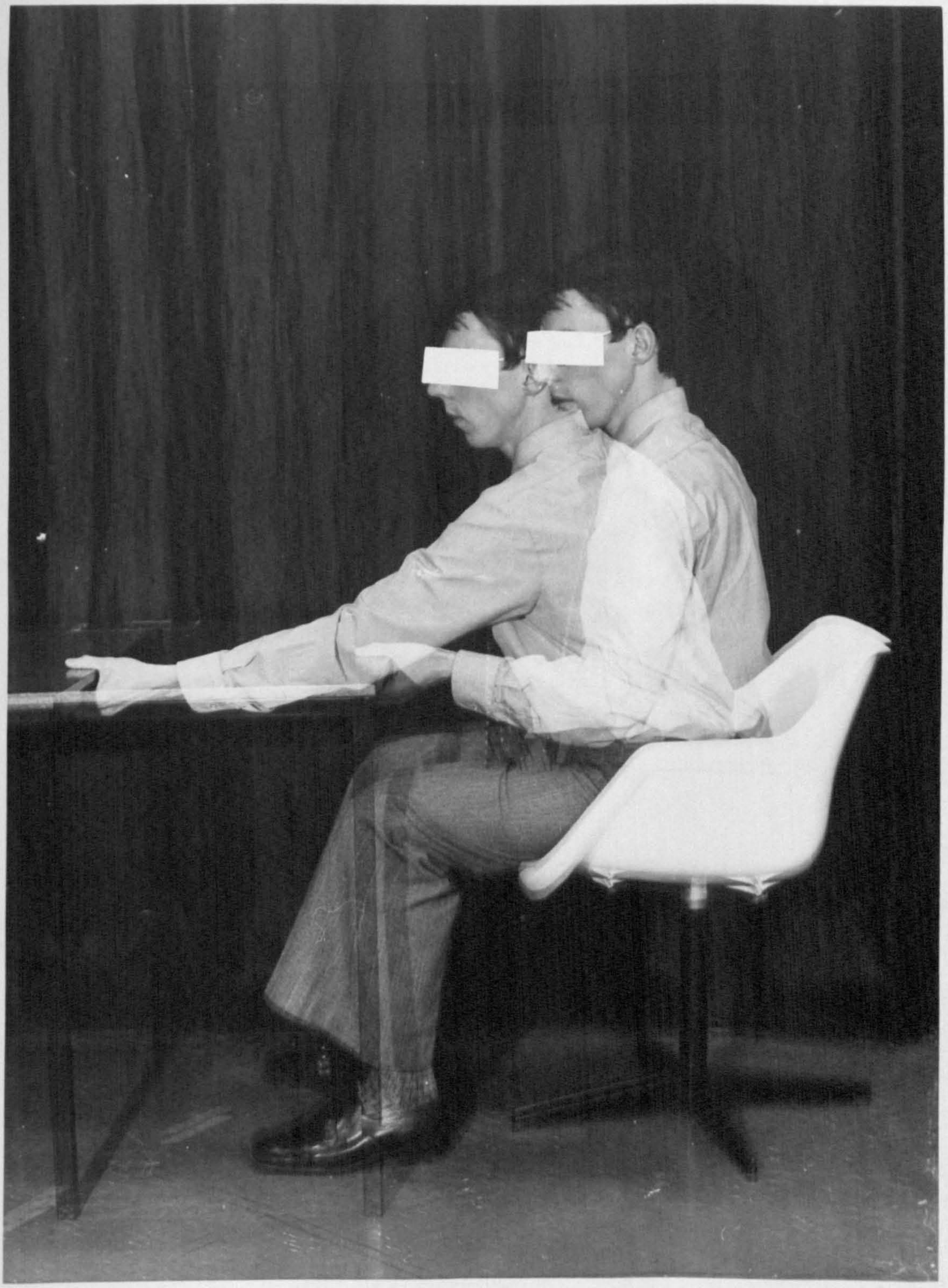

Figure 5.17: The extent of movement for the "table-pull" exercise.

During the two latter activities the force transducer was used to measure the forces and moments transmitted to the hand. Suitable holders were constructed as previously described in section 5.3.

5.5 Experimental Procedure:

Before the subject was due to arrive, the cameras were positioned, tested and loaded with Kodachrome II film, and the overhead floodlights set to the "warm-up" setting. Transducer power supply was set to 6.0 volts for each bridge and allowed to stabilise. Bridge balancing was performed thereafter and the output voltages were set to zero. The tape recorder calibration was noted and a check made of the synchronisation system. The E.M.G. amplifiers and recorders were arranged as previously described and the skin preparation equipment laid out in readiness.

When the subject arrived, his weight and height, together with the required arm dimensions were measured, and recorded in tabular form (see table 5.1). E.M.G. electrodes were applied to representative areas for biceps, triceps and brachioradialis muscles and a reference earth plate was strapped to the left ankle. The subject was then seated facing the left camera with all markers visible to the front camera.

Trial runs of each activity were performed to obtain the correct speed and range of movement so that comparisons could be made between several subjects. To commence the test, the cameras were started and the synchronisation flash was fired. The subject performed the particular movements and the cameras were stopped. This procedure was repeated till all four activities had been filmed.

Once complete, the films were individually rewound to the beginning of the spool and the reference grid shown in figure 5.18 was filmed, which provided a superimposed grid on the developed image.

5.6 Data Collection: Two sources of data were analysed and stored on punched paper tape as input media to a large computer. The film records were measured using a proprietary trace analyser and the results processed by a series of three programs. The analogue signals from the force transducer were converted to digital format using a PDP-12 computer. Program "FORCEPROG" was used

Figure 5.18: Volunteer subject and superimposed grid.

SUBJECT DATA

Test No.		Height	
Arm		Hand → ball	
Weight		EC → ball	
Shoulder diam.		EC → posterior ulna	
Epicondyle width		Upper arm thickness	
Wrist thickness		Forearm length (+ hand)	

TRANSDUCER

Bridge gains	Calibration	Channel	Tape recorder
2000	999.9 mV	1	
5000		2	
2000		3	
200		4	
500		5	
5000		6	
-		7	

ACTIVITIES

No.	Description	Tape start	Tape stop	Load

Table 5.1: Test record form.

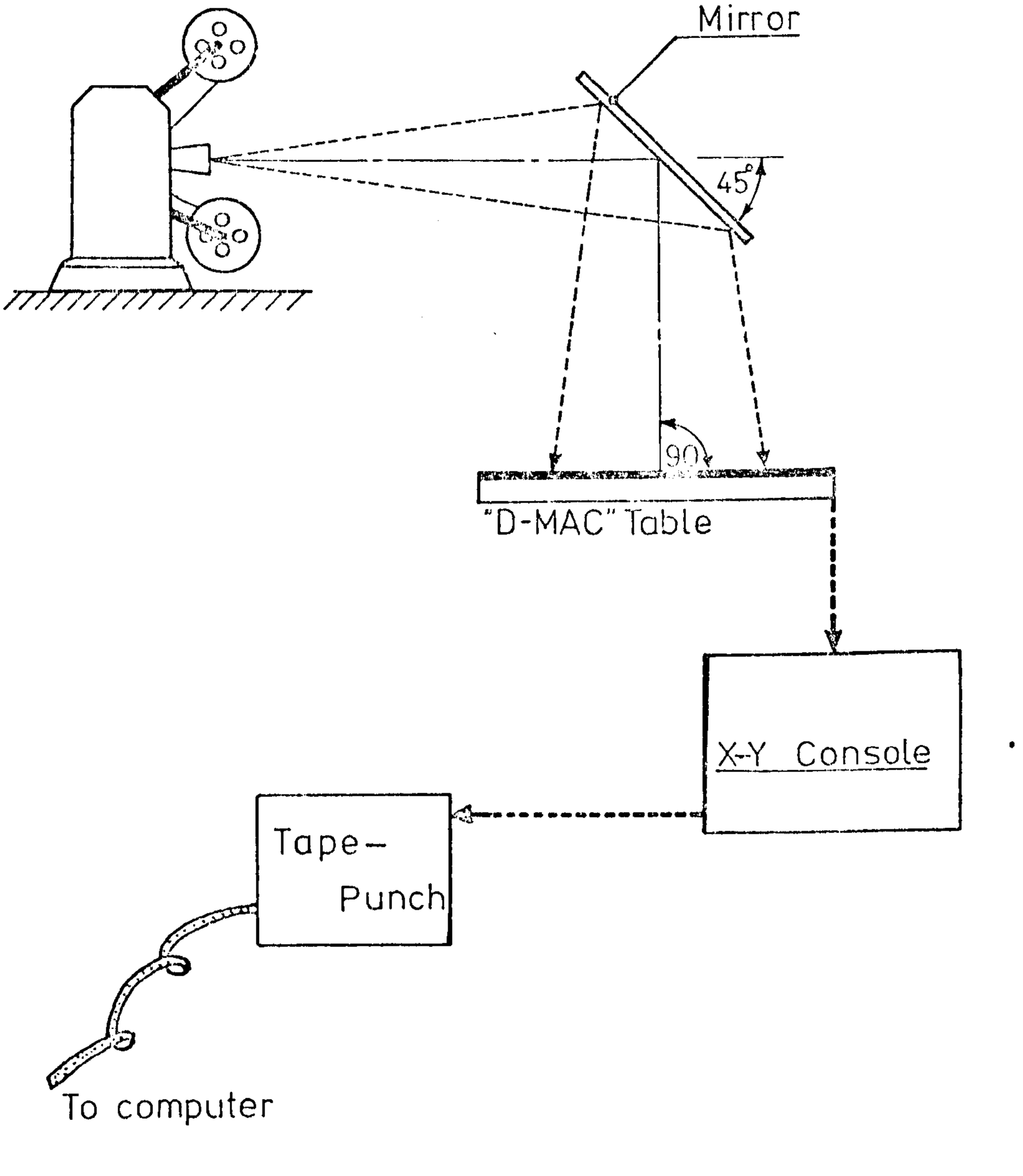

Figure 5·19: Layout of film measurement equipment.

to convert the paper tape results into force actions applied to the transducer, which were later used as input to the final program of the three already mentioned. The complete series of computer programs and running instructions are detailed in Appendix 5.

5.6.1 Photographic data: The developed films were analysed frame by frame using a D-MAC trace analyser with a measurement field of X = 1000 mm and Y = 500 mm. A special "projection pencil" was used to locate the point of interest and, prior to punching on paper tape, the coordinates of X and Y were displayed to an accuracy of $\pm$ 0.1 mm. A keyboard console was used to punch identification characters and error corrections on the paper tape output. The data file was segmented by the automatic insertion of a "line feed" character after every seven measured points (six points for inertial tests).

The projector equipment was positioned so that the image on the D-MAC table was approximately one third full size. The superimposed reference grid was aligned with the measuring axes and test points were taken to check for distortion of the image from the overhead face-silvered mirror (see figure 5.19). After the necessary adjustments had been made, the film was advanced to a predetermined frame which was assigned frame number "1". The number of frames between the flash event and frame number 1 was recorded to ensure correct synchronisation with the transducer data. Subject and activity codes were punched on the console and the four calibration points were measured in order (see section 6.2). The frame number was assigned from the keyboard together with a "muscle" code corresponding to biceps or triceps activity. Measurements of all the marker positions were made with the grid origin position being recorded as point No.1. Figures 5.20a and 5.20b show the order of measurement for transducer and inertial tests respectively. The film was advanced one frame and the sequence of events repeated until the whole activity had been analysed.

Although every marker was visible from the front camera there were many instances when several markers were hidden from the left camera. A code was incorporated into "FILTERPROG" so that values of Y in excess of 8000 signified a "hidden" point. The relevant marker coordinates were therefore obtained from measurements of the right camera record. For such cases it

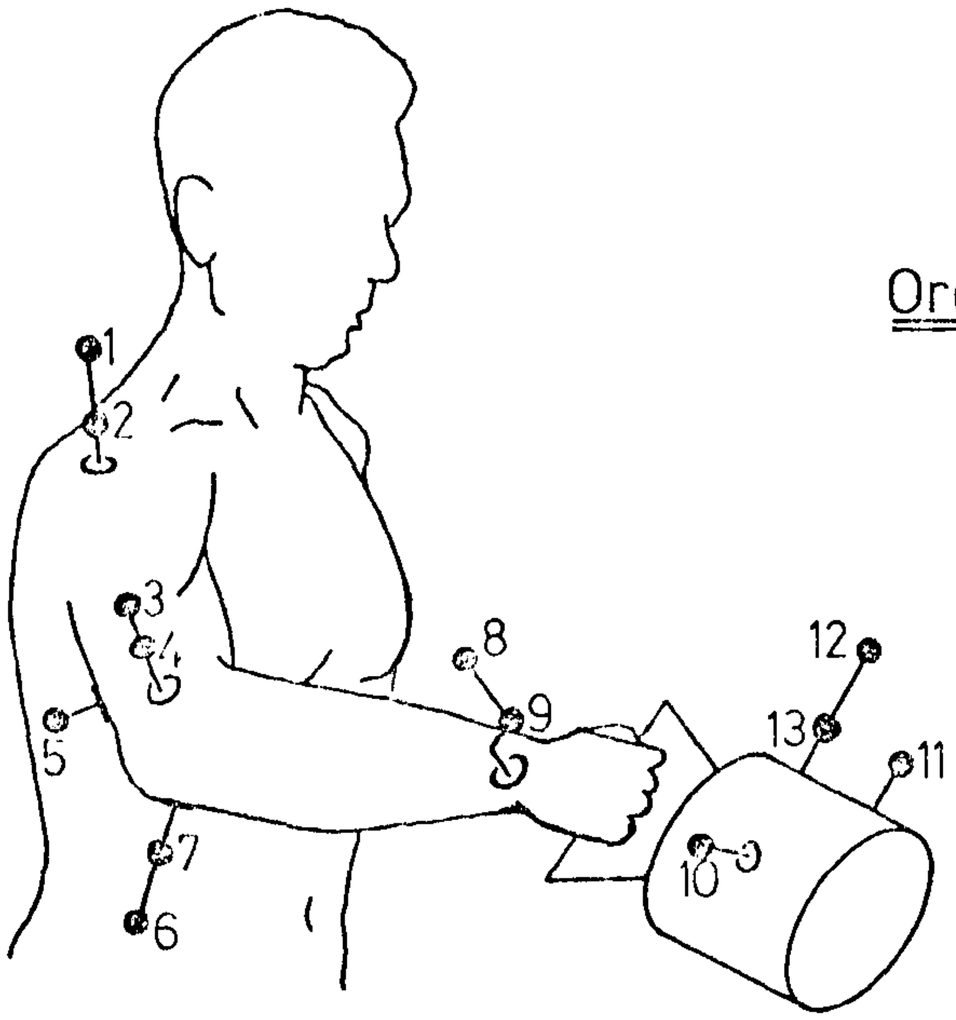

Order: 1→13

Figure 5·20a: Order of measurement for "transducer" tests.

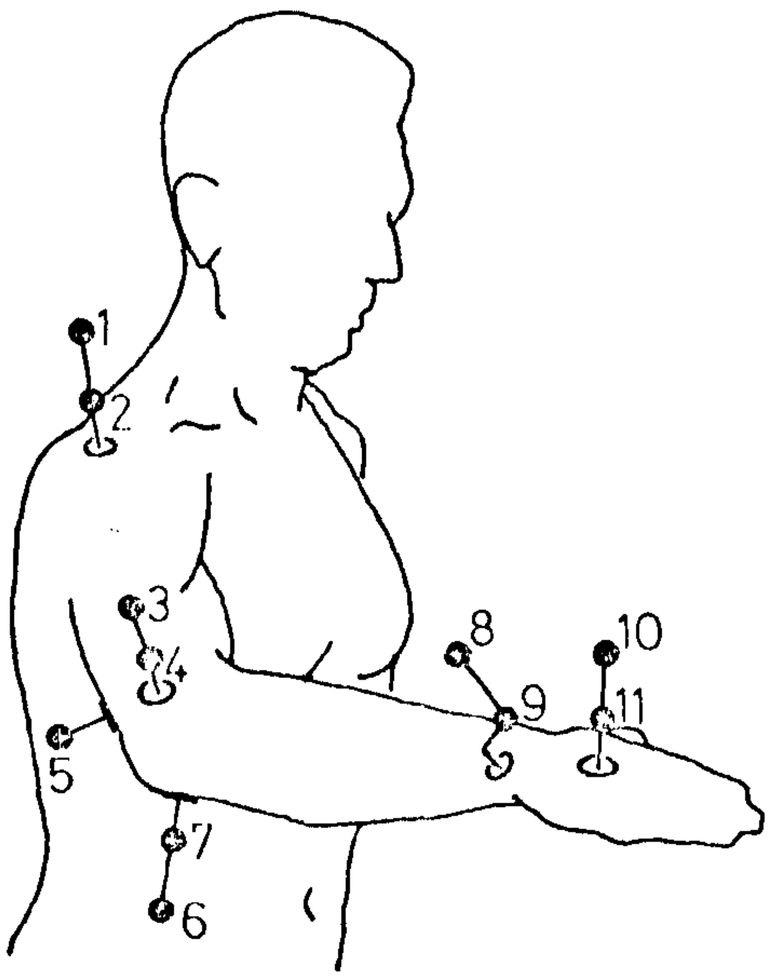

Order: 1→7, 9, 11, 10, 8.

Figure 5·20b: Order of measurement for "inertial" tests

was found useful to position the D-MAC pencil below the Y = 0.0 line and obtain an "overflow" reading of Y = 9999.

5.6.2 Transducer data: The transducer data was required in punched paper tape format for input to an I.C.L. 1904S computer on which subsequent analysis was performed, using the program "FORCEPROG". Conversion of the recorded analogue signals was carried out using the A-D converter of a Digital Equipment Corp. PDP-12 computer housed in the Bioengineering Unit.

Program "BIOMEC2" was loaded and the six channels of the Bell and Howell tape recorder were connected to the inputs of the converter. The synchronisation channel was connected to the input of the "clock" unit and a data block number assigned for the "LINC" tape file.

The tape recorder was set to "replay" just before the start of the relevant activity and sense switch 0 was thrown. On receipt of the synchronisation pulse the machine sampled the six analogue channels at a rate of 50 Hz. When the store was full, sampling ceased and the digital results were transferred to the LINC tape. The contents of channel 1 were displayed on the visual display unit for verification purposes. Subsequent channels were displayed by punching any character on the teletype console.

To output the digital data on paper tape the Program "EDITOR" was loaded and the appropriate LINC tape block number assigned. The contents of the same block were thereafter displayed on the visual display unit. Boundaries were set which enclosed the most relevant part of the signal and output to graph plotter or paper tape was effected by pressing "G" or "O" (not zero) on the teletype keyboard. Character "2" advanced the LINC tape to the next channel for subsequent output.

5.6.3 Sample size: In order to obtain statistically reliable results it would be necessary to analyse a large number of test records for one activity. If several different activities were to be considered, the task of data collection would rapidly become enormous. A compromise was therefore adopted and it was agreed to extend the range of the activities and to decrease the number of test records analysed. For the four activities described previously, the analytical results of three test subjects are presented in Chapter 7.

6. THEORETICAL ANALYSIS

Note:

Throughout this chapter the small counterparts of J (i.e. "j") and L (i.e. "l") have been used as subscripts. It should be noticed that the "IBM Executive" characters produce a certain degree of similarity between small J and small I, and between small L and unity (1).

6. THEORETICAL ANALYSIS

6.1 Introduction:

The following analytical procedures describe the method of calculation of the forces transmitted by the elbow joint during any arm activity. Several separate stages were involved as follows:

a) Rationalisation of cine film data to give the coordinates of each marker point in terms of X, Y and Z reference grid axes.
b) Correction of parallax errors for each point.
c) Digital filtering of each coordinate to minimise the effects of "noise".
d) The analysis of marker points and the calculation of the spatial orientation of various moving axes.
e) Numerical differentiation of displacement data to obtain linear and angular accelerations of the forearm.
f) Calculation of inertial force actions on the forearm using standard body segment parameters.
g) Calculation of transducer force actions on the hand and their subsequent transfer to the elbow joint.
h) Calculation of the lines of action of muscles and ligaments and the position of joint reactions.
i) Full analysis of joint equilibrium involving muscle forces, ligament forces and joint reactions.

Although a single computer program would have been capable of handling the analysis, four programs were developed so that the University's "CAFETERIA" system could be used. Using this system, short "jobs" were run quickly which permitted rapid development of each section of the analysis. In addition, the checking of data was greatly simplified after each of the four program "runs". All programs used in the analysis are listed in Appendix 5.

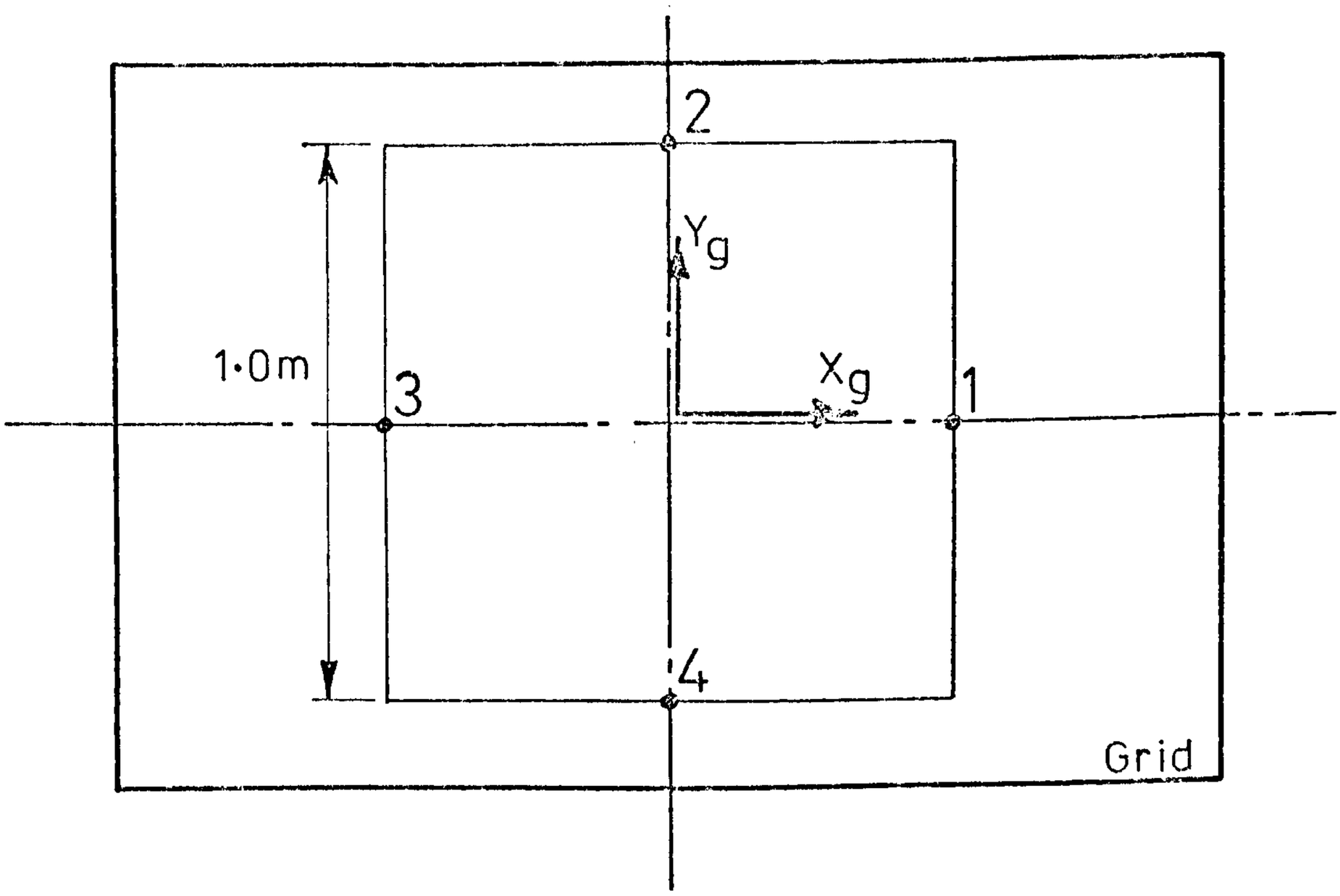

Figure 6·1: Layout of the calibration points

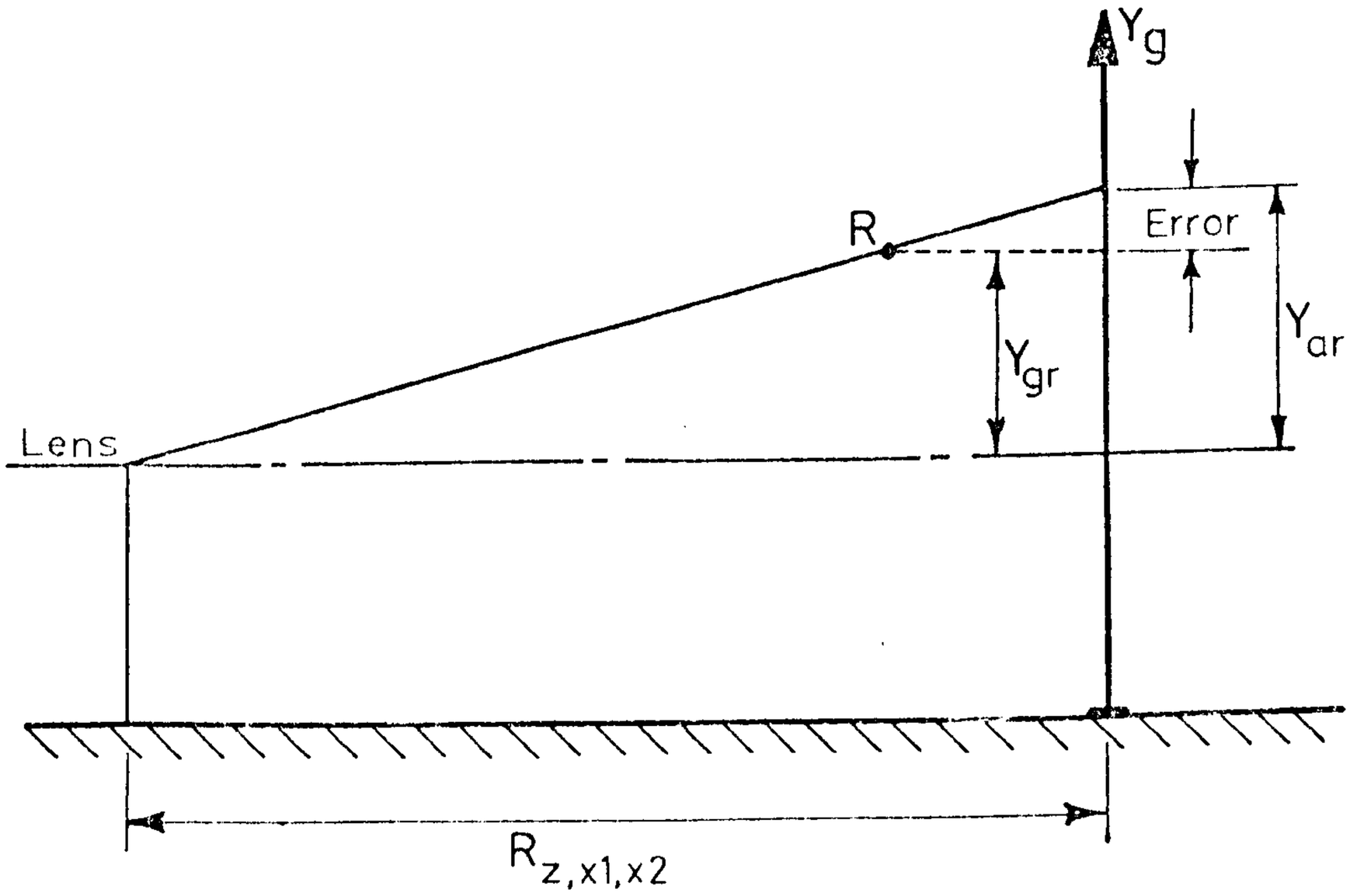

Figure 6·2: Calculation of parallax errors

6.2 Data Rationalisation:

6.2.1 Magnification: The first operation in the analytical procedure was the amplification of the projected film data to the full size of the reference grid. Magnification factors were defined for X and Y directions using a one metre square on the grid board. Referring to figure 6.1, the magnification factors were obtained from

$$XC = 1000/(X_1 - X_3) \qquad 6.1a$$

$$YC = 1000/(Y_2 - Y_4) \qquad 6.1b$$

For each coordinate, the appropriate coordinate of the grid origin was deducted to obtain relative grid coordinates. The relevant magnification factor was applied to obtain the full size grid coordinates

$$\text{eg} \qquad X_{g1} = (X_1 - X_0) * XC$$

No correction terms were incorporated for distortion effects around the perimeter of the camera lens. For the central area of the lens, the error from non-ideal lens function was too small to be determinable.

6.2.2 Parallax corrections: Where the marker points lay outwith the relevant grid reference plane, parallax errors had to be accommodated (see figure 6.2). Knowing the three measured "apparent" coordinates of any point "R" (X_{ar}, Y_{ar}, Z_{ar}), the "true" coordinates (X_{gr}, Y_{gr}, Z_{gr}) were calculated using the distances between the cameras and the grid planes.

$$X_{gr} = \frac{X_{ar}(R_z.R_{x1} - Z_{ar}.R_{x1})}{R_z.R_{x1} - Z_{ar}X_{ar}} \qquad 6.2a$$

$$Z_{gr} = Z_{ar}(1 - \frac{X_{gr}}{R_{x1}}) \qquad 6.2b$$

$$\text{or} \qquad Z_{gr} = Z_{ar}(1 + \frac{X_{gr}}{R_{x2}}) \quad \text{for right camera.} \qquad 6.2c$$

$$Y_{gr} = \frac{Y_{ar}(R_z - Z_{gr})}{R_z} \qquad 6.2d$$

The derivation of equations is detailed in Appendix 2.1.

6.3 Digital Filtering:

The displacement data contained "noise" which resulted from a combination of errors in film measurement, mechanical tolerances on the cine cameras, and marker "vibration". By passing the displacement data through a digital filter, the effect of noise was considerably reduced, without appreciably altering the signal content. A 4th order "Butterworth" filter was used throughout the analyses (see Andrews, 1975). The filter was incorporated in an ALGOL computer procedure which is listed in Appendix 2.2. Sample time interval (TIME), 3dB cut-off frequency (FCUT) and signal length (N) were assigned, from data files, for each test run. It must be emphasised that only the signal component of the data was processed; linear trends and D.C. shifts were removed before, and replaced after filtering (see figure 6.3). In addition, forward and reverse passes of the data were performed to cancel the inherent phase shift of the filter.

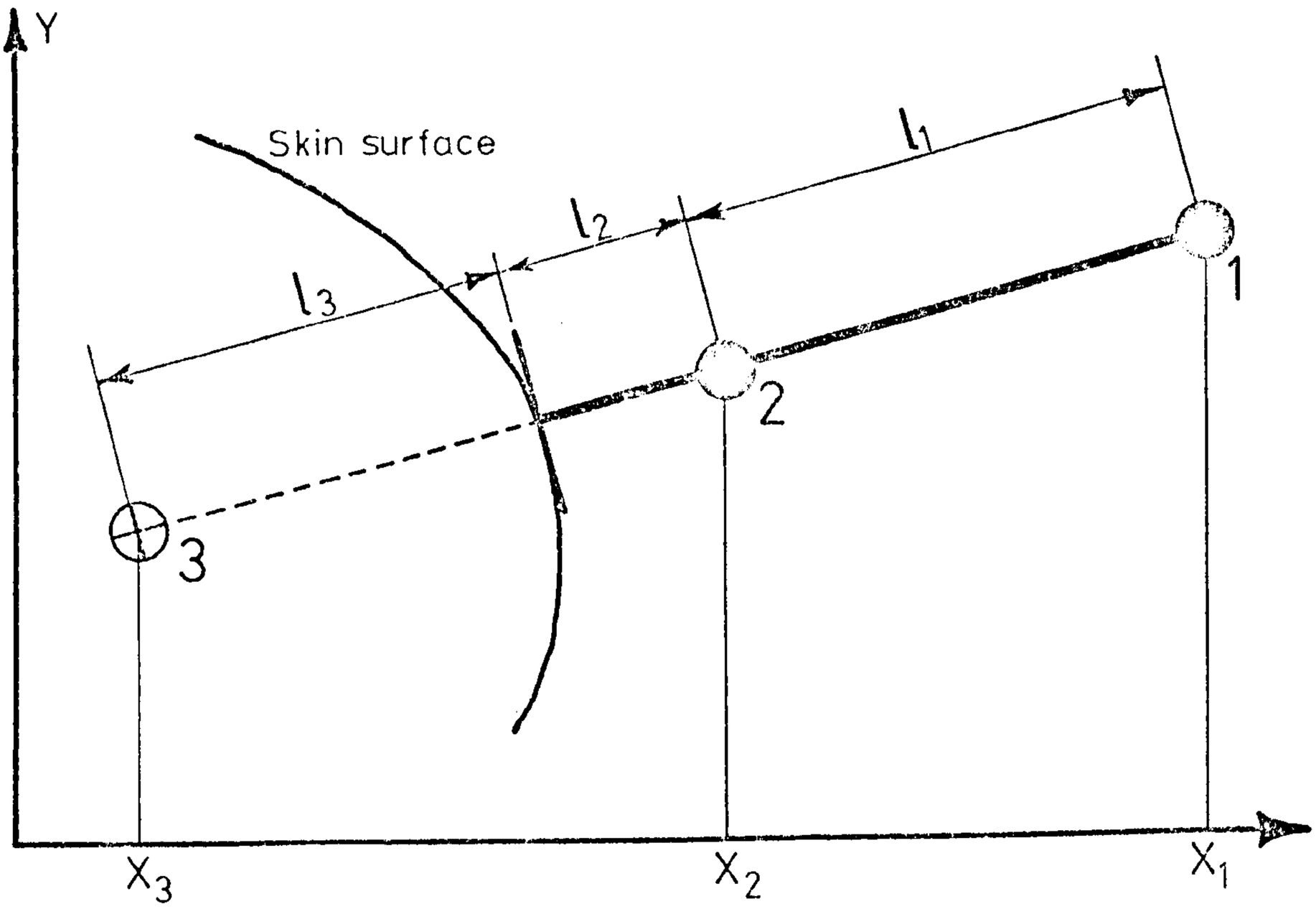

Figure 6·4: General arrangement of skin markers

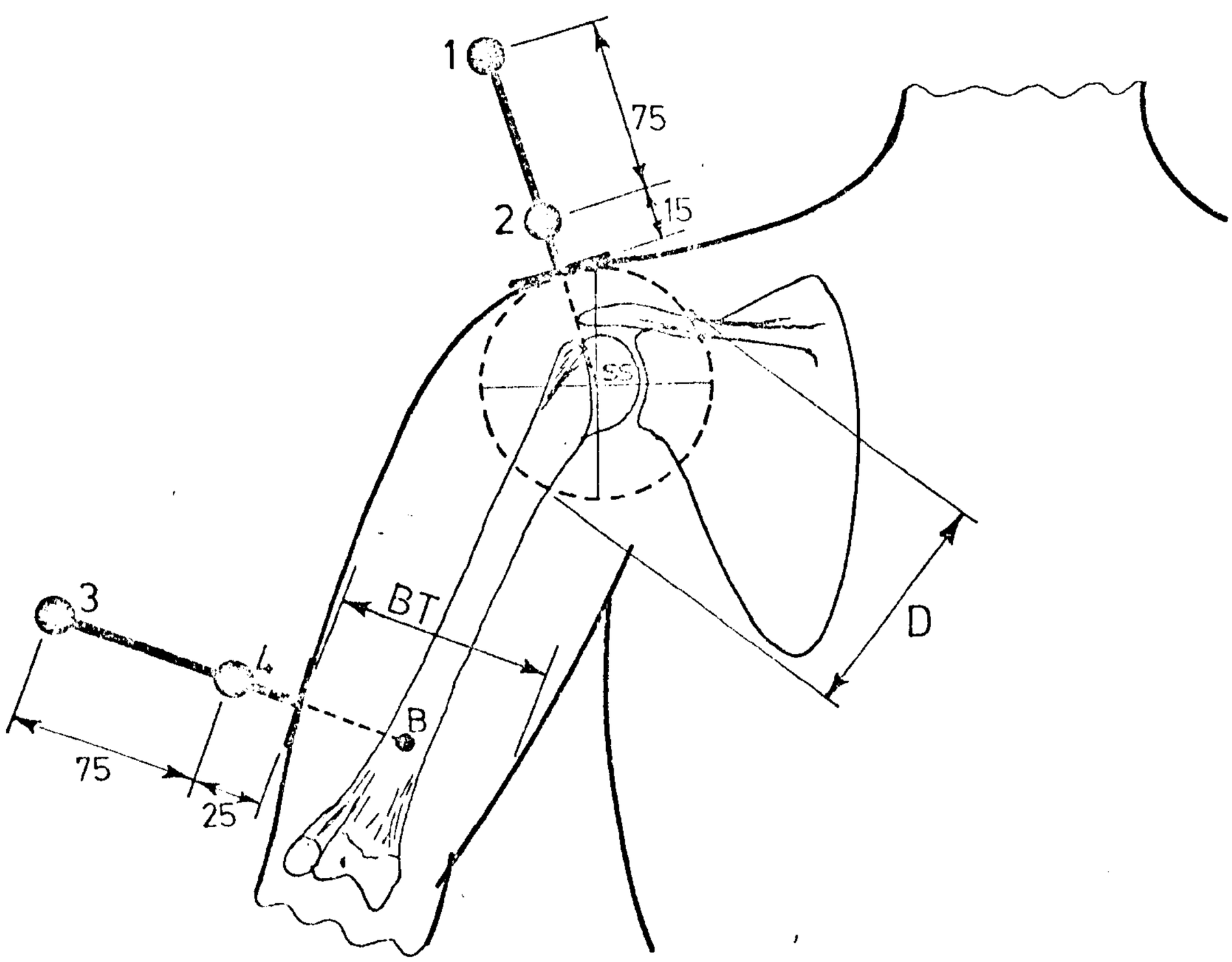

Figure 6·5: Markers for the upper arm

6.4 Marker Analysis:

Referring to the marker system described in Chapter 5, the double ball markers were used to locate subcutaneous reference points. Extrapolation of the line joining the two balls gave the position of such anatomical points with an accuracy of $\pm$ 2 mm. Assuming zero bone/skin displacement, the required coordinate for the generalised situation in figure 6.4 was given by:

$$X_3 = X_1 + (X_2 - X_1) * \frac{l_1 + l_2 + l_3}{l_1} \qquad 6.3$$

Dimensions "l_1" and "l_2" were known from the details of marker construction; l_3 was an estimated depth below the skin level. Prominent anatomical curvatures and landmarks were used for such measurements. Shoulder, upper arm, elbow, wrist and hand regions were analysed as follows. The subscript "g" is omitted in this stage of the analysis since only the grid axis system applies.

The shoulder joint centre (ss) was located by extrapolation of markers number 1 and 2 using the semi-circular form of the surface contour at the shoulder region as shown in figure 6.5. Equation 6.3 therefore became

$$X_{ss} = X_1 + (X_2 - X_1) \frac{180 + D}{150} \qquad 6.4a$$

$$Y_{ss} = Y_1 + (Y_2 - Y_1) \frac{180 + D}{150} \qquad 6.4b$$

$$Z_{ss} = Z_1 + (Z_2 - Z_1) \frac{180 + D}{150} \qquad 6.4c$$

By the same principle, the upper arm reference point "B" was obtained using markers number 3 and 4; half the arm thickness being taken for the extrapolation distance.

$$\text{e.g.} \qquad X_b = X_3 + (X_4 - X_3) \frac{200 + BT}{150} \qquad 6.5$$

For the forearm, the elbow centre (EC) was found by extrapolation of markers no. 6 and 7 (see figure 6.6a). The dimension "EL" was measured as the distance between the posterior ulna and a line joining the humeral epicondyles.

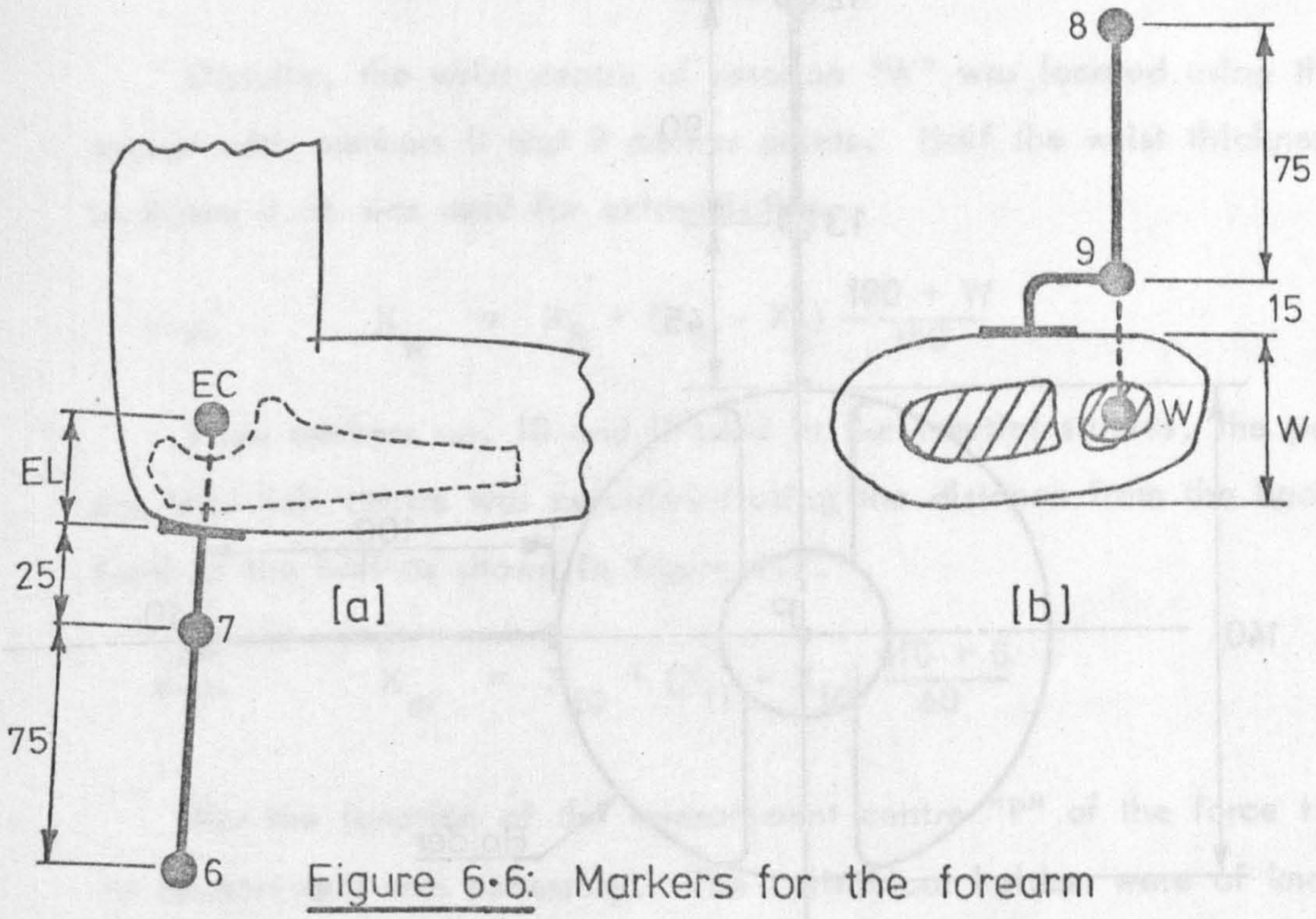

Figure 6·6: Markers for the forearm

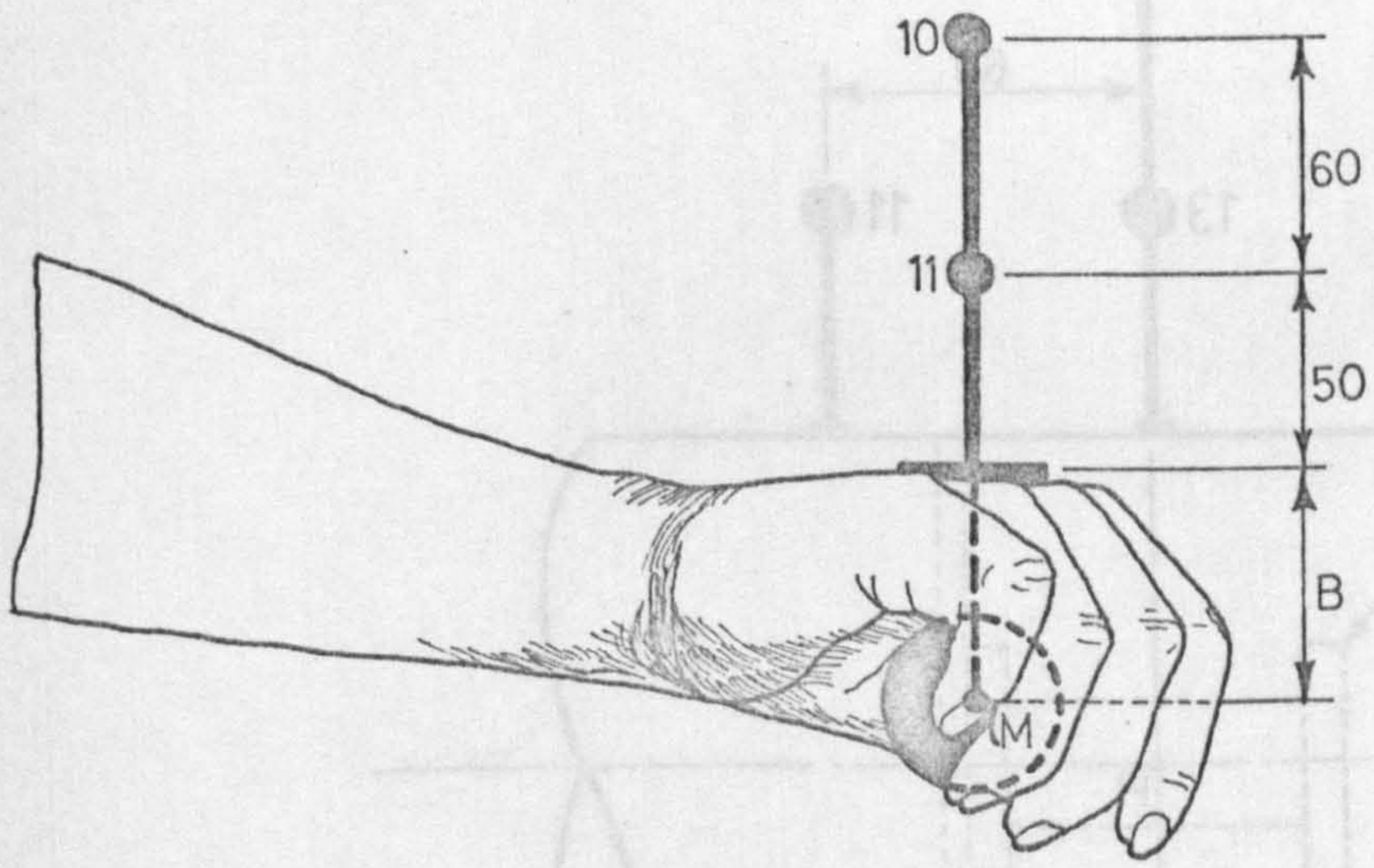

Figure 6·7: Markers for the hand

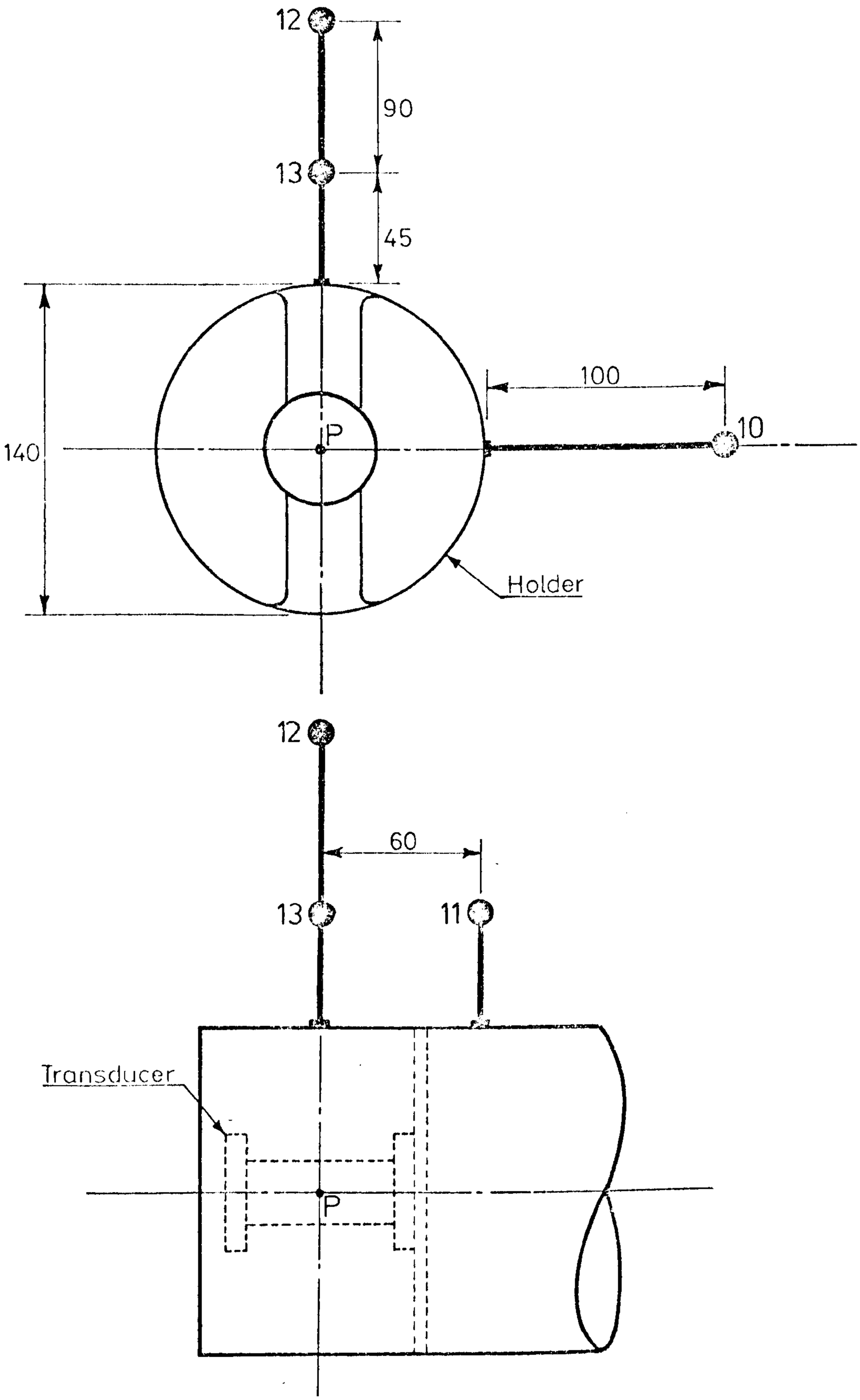

Figure 6·8: Markers for the transducer

$$\text{e.g.} \qquad X_{ec} = X_6 + (X_7 - X_6)\frac{100 + EL}{75} \qquad 6.6$$

Distally, the wrist centre of rotation "W" was located using the special marker with numbers 8 and 9 marker points. Half the wrist thickness shown in figure 6.6b was used for extrapolation.

$$\text{e.g.} \qquad X_w = X_8 + (X_9 - X_8)\frac{180 + W}{150} \qquad 6.7$$

From markers no. 10 and 11 used in the inertial studies, the position of the lead ball centre was calculated using the distance from the back of the hand to the ball as shown in figure 6.7.

$$\text{e.g.} \qquad X_m = X_{10} + (X_{11} - X_{10})\frac{110 + B}{60} \qquad 6.8$$

For the location of the measurement centre "P" of the force transducer, no measurement was necessary. The cylindrical holders were of known dimensions and markers no. 12 and 13 were used as shown in figure 6.8.

$$\text{e.g.} \qquad X_p = X_{12} + (X_{13} - X_{12})\frac{205}{90} \qquad 6.9$$

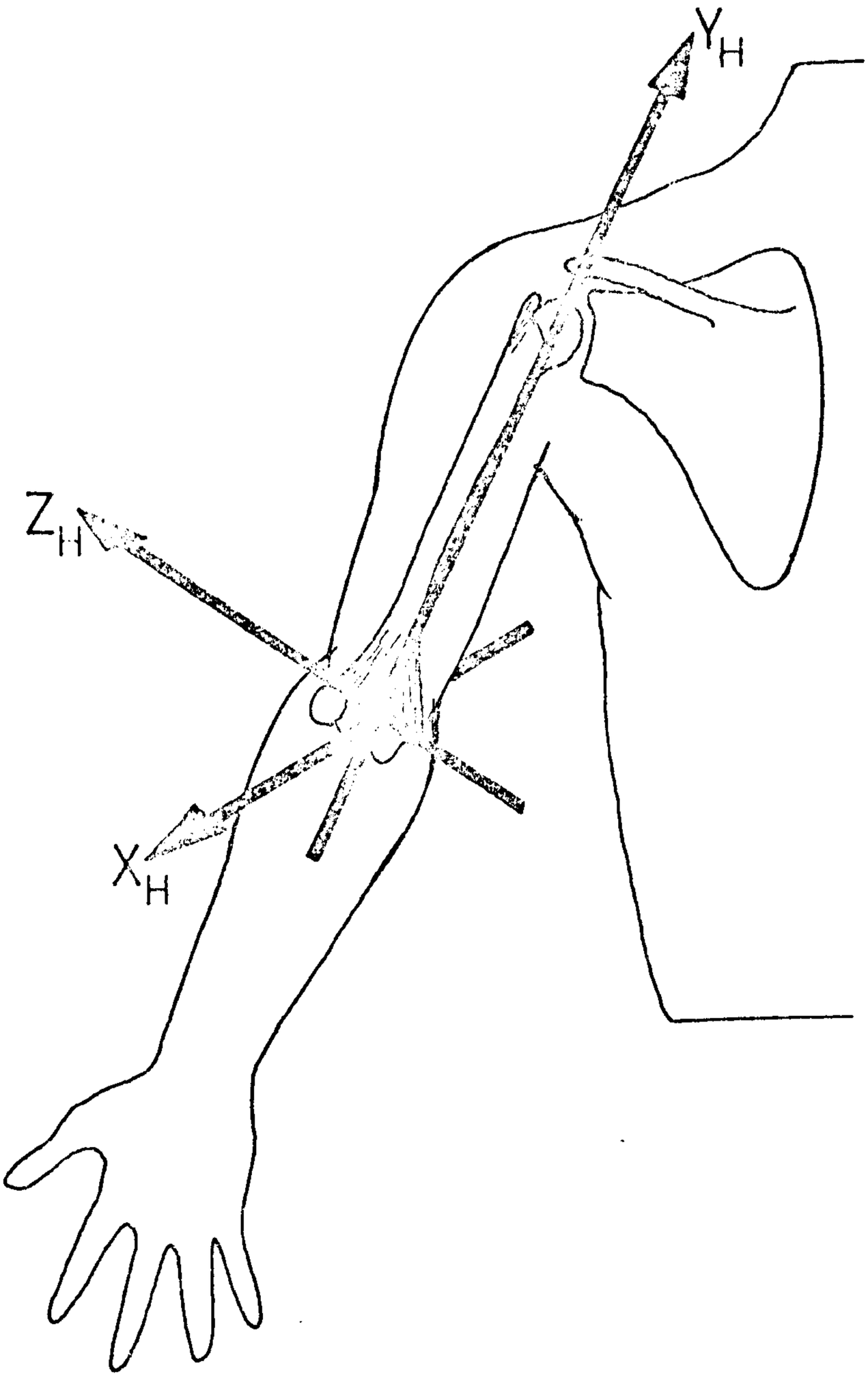

Figure 6·9: Definition of the humeral axis system

6.5 Axis Definition:

Although the cine film measurements provided forearm displacements with respect to the reference grid axes, it was impossible to measure force and anatomical parameters in the same reference system. For this reason, moving axes were defined for the upper arm (humeral), the forearm (ulnar) and transducer measurements.

With the right arm held in the standard anatomical position (see figure 6.9), the humeral axes were defined as follows:

Origin	elbow centre "EC".
Y_h	from EC to shoulder centre "SS"
Z_h	from EC to the right, at right angles to Y_h and parallel to a line joining the epicondyles. (obtained from point B to marker no.3).
X_h	from EC forwards, at right angles to Y_h and Z_h (marker no.5 to point B).

Referring to figure 6.10, the positive directions of the ulnar axes were defined as follows:

Origin	at elbow centre "EC".
Y_u	from wrist centre to EC (point W to EC)
X_u	at right angles to Y_u, pointing forwards (marker no.6 to EC).
Z_u	at right angles to X_u and Y_u, and in general direction of Z_h (obtained from orthogonality relationships).

As a refinement to the theoretical analysis, an additional set of moving axes was defined which related the orientation of the ulnar articular surfaces to the ulnar axes. The "joint" axes represented the inclinations of the trochlear notch. Rotations of $\Theta_z = 30^\circ$ and $\Theta_x = 7^\circ$ were made according to Schlein (1974). Figure 6.21 shows the relative positions of ulnar and joint axes; the numerical relationships are detailed later (section 6.14).

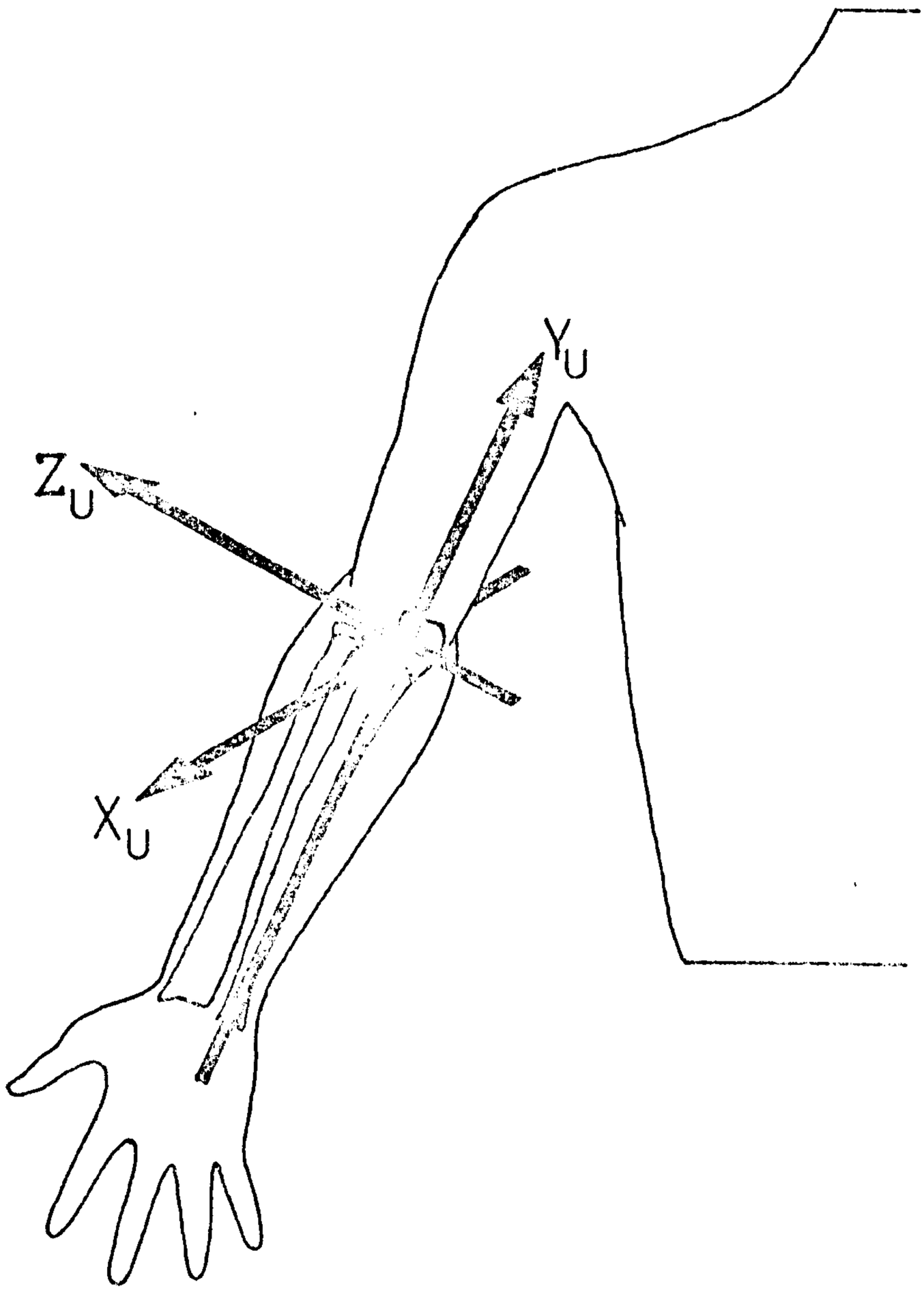

Figure 6·10: Definition of the ulnar axis system

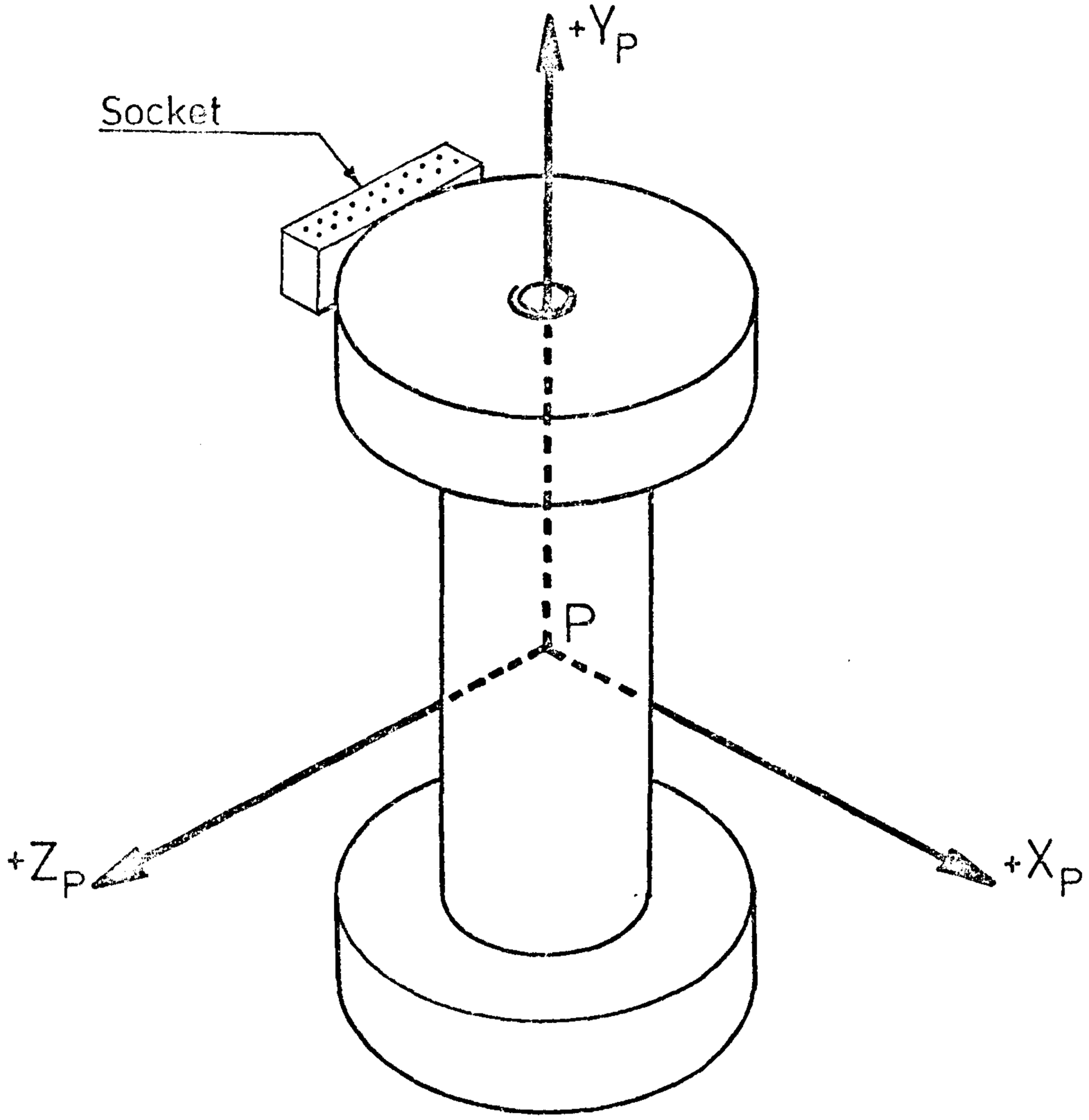

Figure 6·11: Definition of the transducer axis system

The spatial orientations of the transducer were defined using the multi-way connector socket as the only landmark. With the connector at the "top" and "rear" of the unit, the transducer axes were defined as follows (see figure 6.11).

Origin	at point P.
Y_p	vertically upwards. (markers 13 to 11).
X_p	horizontally forwards (markers 12 to 13).
Z_p	horizontally to the right (point P to marker 10).

6.6 Axis Orientation:

For the analysis of joint loadings, it was necessary to define all parameters with respect to a common axis system. The joint axis system was adopted for this purpose. It therefore became essential to have some method of calculating the orientation of one moving axis system relative to another moving system. For this reason, the orientations of the humeral, ulnar and transducer axes were calculated with respect to the reference grid axis system. Inter-axis relationships were then developed to define one moving system relative to another.

Using the previously described markers, it was possible to fully define all three moving axes, relative to the grid axes, by direction cosine principles. The direction cosine of one axis relative to another axis was defined as the cosine of the true angle between the positive directions of the two axes. Four digits were used to define the various direction cosines; the first two digits signifying the reference axis as follows:

"LG" refers to the X_g axis as reference.
"MG" refers to the Y_g axis as reference.

The third digit refers to the moving axis system under consideration, i.e.:

"U" for ulnar axes
"H" for humeral axes
"P" for transducer axes.

The final digit enables the specification of X, Y or Z to be made for the moving axis.

"1" refers to the moving X axis.
"2" refers to the moving Y axis.
"3" refers to the moving Z axis.

Two examples on the classification of direction cosines are helpful. The direction cosine of the Y-axis of the ulnar system, relative to the X-axis of the grid system, is specified by "LGU2". Similarly, "MGP3" would be the direction cosine of the transducer's Z-axis with respect to the Z-axis of the grid system.

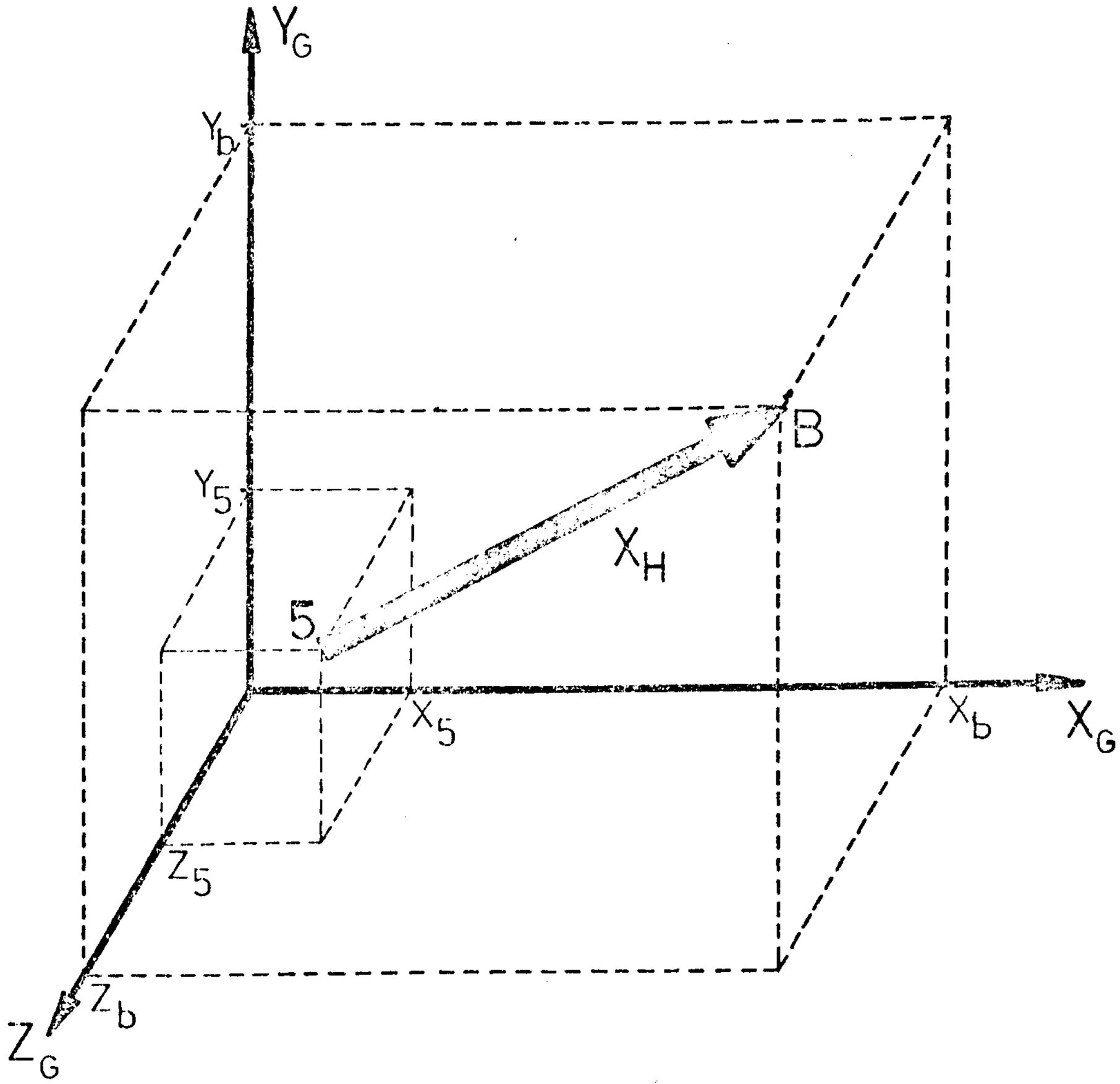

Figure 6·12: Calculation of direction cosines for the X-axis of the humerus in relation to the grid axis system.

The calculation of the nine direction cosines defining the orientation of the humerus, relative to the reference grid axes, follows as an example. The equations of all direction cosines for other axes are detailed in Appendix 2.3.

Referring to figure 6.12, the humeral direction cosines were obtained from the following.

$$DX = \sqrt{[(X_b - X_5)^2 + (Y_b - Y_5)^2 + (Z_b - Z_5)^2]} \qquad 6.10a$$

$$= \text{length of } X_h.$$

$$DY = \sqrt{[(X_b - X_{ss})^2 + (Y_b - Y_{ss})^2 + (Z_b - Z_{ss})^2]} \qquad 6.10b$$

$$= \text{length of } Y_h.$$

$$DZ = \sqrt{[(X_b - X_3)^2 + (Y_b - Y_3)^2 + (Z_b - Z_3)^2]} \qquad 6.10c$$

$$= \text{length of } Z_h.$$

$$LGHI = (X_b - X_5)/DX$$

$$MGHI = (Y_b - Y_5)/DX$$

$$NGHI = (Z_b - Z_5)/DX$$

$$LGH2 = (X_{ss} - X_b)/DY$$

$$MGH2 = (Y_{ss} - Y_b)/DY$$

$$NGH2 = (Z_{ss} - Z_b)/DY$$

$$LGH3 = (X_3 - X_b)/DZ$$

$$MGH3 = (Y_3 - Y_b)/DZ$$

$$NGH3 = (Z_3 - Z_b)/DZ$$

6.7 Orthogonality Relations:

For the Z-axis of the ulna, no skin markers could be used for direct calculation of direction cosines due to the excessive skin movement around the proximal forearm during elbow function. Since the three axes were orthogonal, there were unique values for the orientation of Z_U as follows.

$$LGU3 = MGU1 * NGU2 - MGU2 * NGU1 \quad 6.11a$$

$$MGU3 = NGU1 * LGU2 - NGU2 * LGU1 \quad 6.11b$$

$$NGU3 = LGU1 * MGU2 - LGU2 * MGU1 \quad 6.11c$$

Similarly, for the orientation of the X-axis of the humerus, the accuracy of marker number 5 was considered to be unacceptable for direction cosine computations.

$$LGH1 = MGH2 * NGH3 - MGH3 * NGH2 \quad 6.12a$$

$$MGH1 = LGH3 * NGH2 - LGH2 * NGH3 \quad 6.12b$$

$$NGH1 = LGH2 * MGH3 - MGH2 * LGH3 \quad 6.12c$$

The derivation of the above orthogonality relations are detailed in Appendix 2.4.

6.8 Inter-Axis Relations:

Having defined the moving axes with reference to the grid axis system, it was possible to evaluate all measured parameters in terms of the grid axes. For example, the position of any point R, measured in humeral coordinates, may be defined in grid coordinates by the following:

$$X_{gr} = (X_{hr} * LGH1) + (Y_{hr} * LGH2) + (Z_{hr} * LGH3)$$

$$Y_{gr} = (X_{hr} * MGH1) + (Y_{hr} * MGH2) + (Z_{hr} * MGH3)$$

$$Z_{gr} = (X_{hr} * NGH1) + (Y_{hr} * NGH2) + (Z_{hr} * NGH3)$$

or, in matrix form:

$$\begin{bmatrix} X \\ Y \\ Z \end{bmatrix}_{gr} = [DCHG] \ast \begin{bmatrix} X \\ Y \\ Z \end{bmatrix}_{hr} \qquad 6.13$$

where the matrix [DCHG] contains the nine direction cosines of the humeral axes relative to the grid axis system. In other words

$$[DCHG] = \begin{bmatrix} LGH1 & LGH2 & LGH3 \\ MGH1 & MGH2 & MGH3 \\ NGH1 & NGH2 & NGH3 \end{bmatrix} \qquad 6.14$$

Similar matrices were constructed for ulnar and transducer directions called [DCUG] and [DCPG] respectively. The direction cosines of the joint axes relative to the ulnar axis system were assigned to the matrix [DCJU] . Appendix 2.5 details the calculation of direction cosines contained in the latter matrix.

The calculation of grid coordinates relative to some moving axis system was performed using the inverse of equation 6.13 as follows:

$$\begin{bmatrix} X \\ Y \\ Z \end{bmatrix}_{hr} = [DCHG]^{-1} \ast \begin{bmatrix} X \\ Y \\ Z \end{bmatrix}_{gr} \qquad 6.14$$

By combining the two axis transformations, it therefore became possible to transfer quantities from one moving axis system to another; the reference grid system acting as a mediator. For example, the calculation of muscle origins, on the humerus in terms of ulnar coordinates was performed using the following:

$$\begin{bmatrix} X \\ Y \\ Z \end{bmatrix}_g = [DCHG] \begin{bmatrix} X \\ Y \\ Z \end{bmatrix}_h$$

$$\begin{bmatrix} X \\ Y \\ Z \end{bmatrix}_u = [DCUG]^{-1} \begin{bmatrix} X \\ Y \\ Z \end{bmatrix}_g$$

Combining the two equations:

$$\begin{bmatrix} X \\ Y \\ Z \end{bmatrix}_u = [DCUG]^{-1} [DCHG] \begin{bmatrix} X \\ Y \\ Z \end{bmatrix}_h \qquad 6.15$$

Similar calculations were performed for transducer and joint axes parameters.

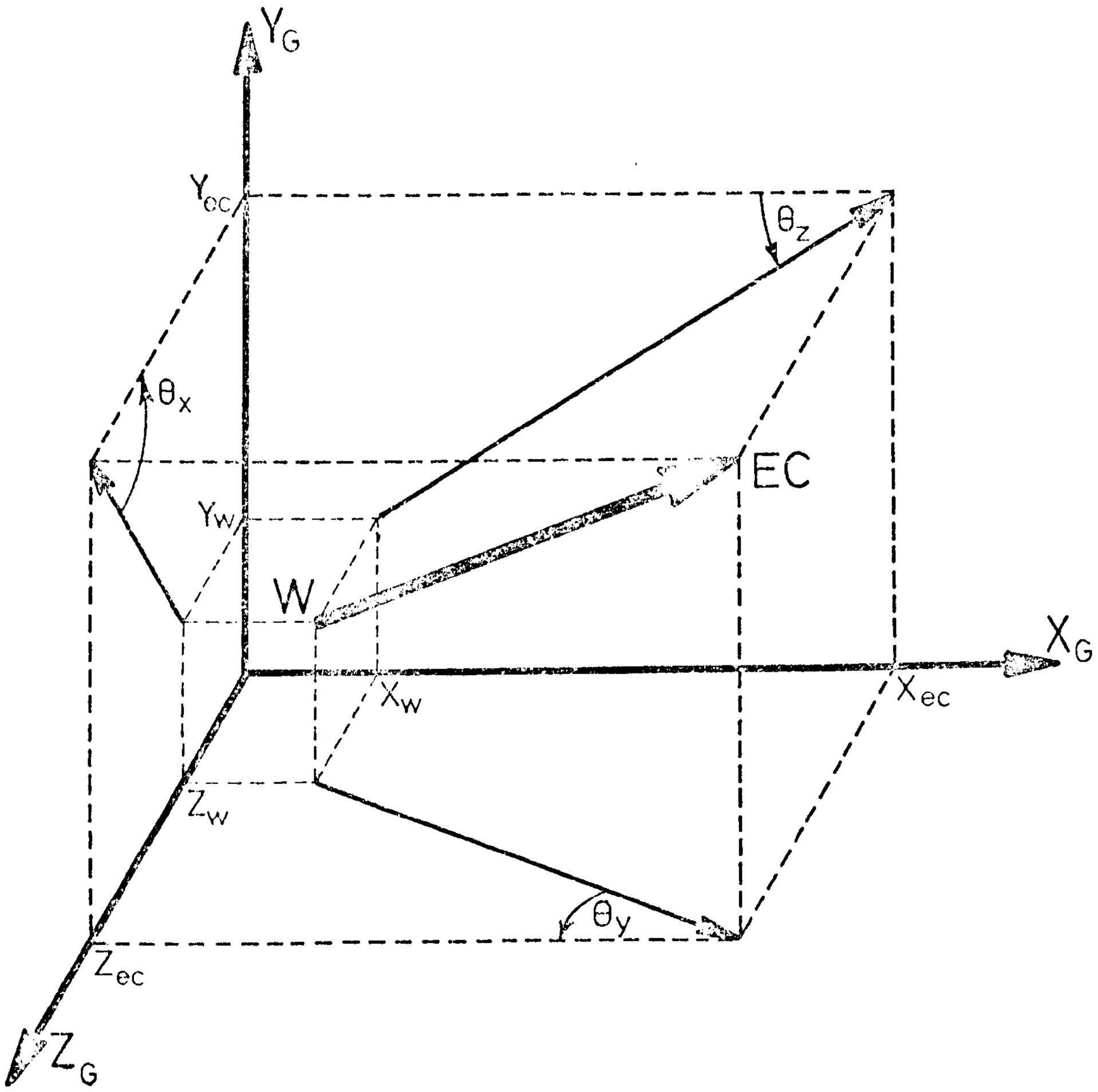

Figure 6·13: Calculation of the position of Y_u

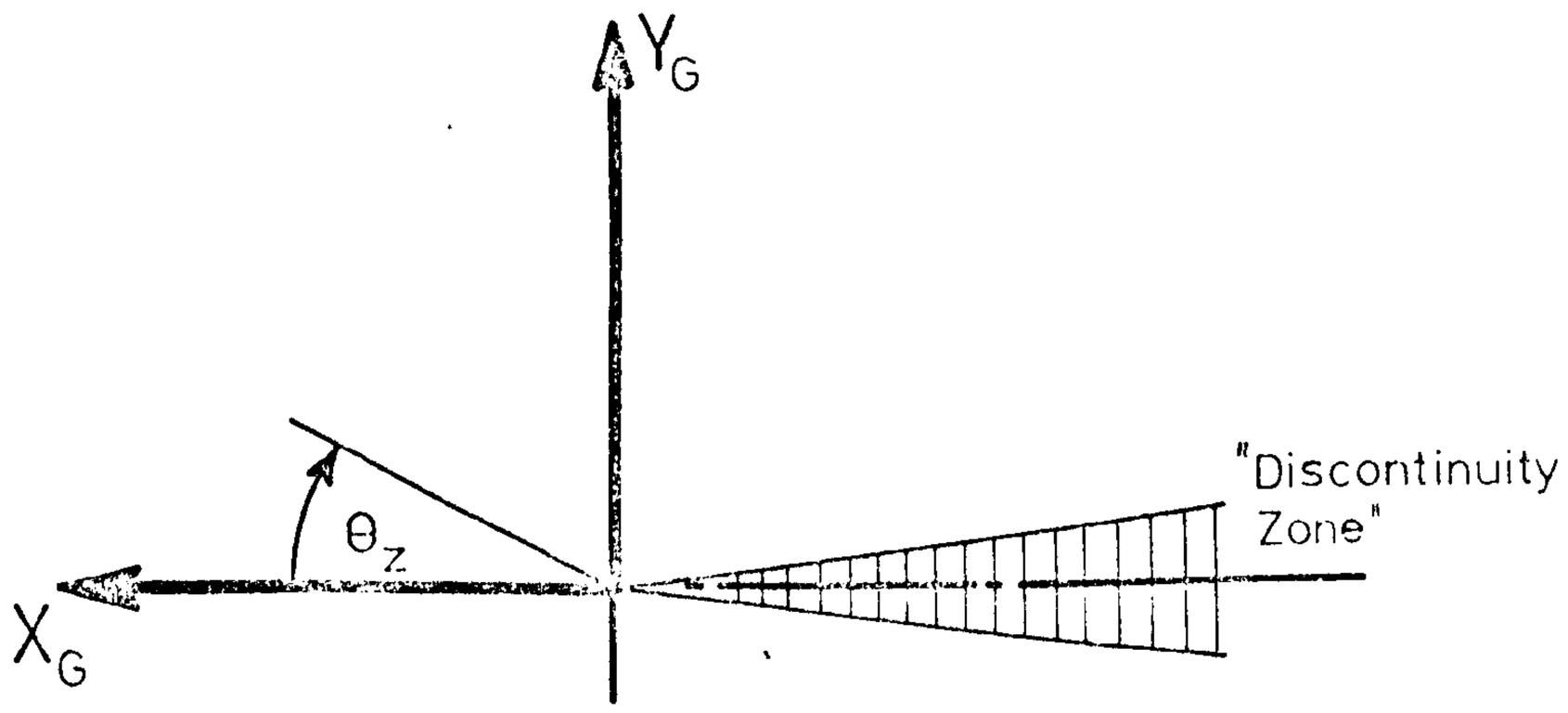

Figure 6·14: Definition of θ_z

6.9 Forearm Orientation:

To calculate the inertial torques acting on the forearm during the "inertial" studies, the angular displacements of the long axis of the forearm (Y_u) were required. Using points "EC" and "W", three angles were defined representing rotations about the grid axes.

The angles Θ_x, Θ_y and Θ_z were the projected rotations of Y_u about X_g, Y_g and Z_g respectively (see figure 6.13).

$$\Theta_x = \tan^{-1} \frac{Z_w - Z_{ec}}{Y_w - Y_{ec}} \qquad 6.16a$$

$$\Theta_y = \tan^{-1} \frac{X_w - X_{ec}}{Z_w - Z_{ec}} \qquad 6.16b$$

$$\Theta_z = \tan^{-1} \frac{Y_w - Y_{ec}}{X_w - X_{ec}} \qquad 6.16c$$

Using standard computer functions, the angles were evaluated for $-\pi/2 < \Theta < \pi/2$. The appropriate quadrant was found from the signs of numerator and denominator in equations 6.16a,b,c. By such a method, the value of Θ would range from -2π to $+2\pi$ depending on its definition. To avoid discontinuities of $\pm 2\pi$ at extreme values of Θ, careful consideration was given to the least probable position of Y_u for the calculations of Θ_x, Θ_y and Θ_z.

Taking Θ_z as an example, the least probable position of Y_u, during any activity, was defined as the $+X_g$ direction. The calculation of Θ_z was as follows (see figure 6.14).

$$\Theta_z = \tan^{-1} \frac{Y_w - Y_{ec}}{X_w - X_{ec}} = \tan^{-1} \frac{\Delta Y}{\Delta X} \qquad 6.17$$

For $\Delta Y > 0$ and $\Delta X > 0$; $\Theta := \Theta$

For $\Delta Y > 0$ and $\Delta X < 0$; $\Theta := \pi + \Theta$

For $\Delta Y < 0$ and $\Delta X > 0$; $\Theta := \Theta$

For $\Delta Y < 0$ and $\Delta X < 0$; $\Theta := -\pi + \Theta$

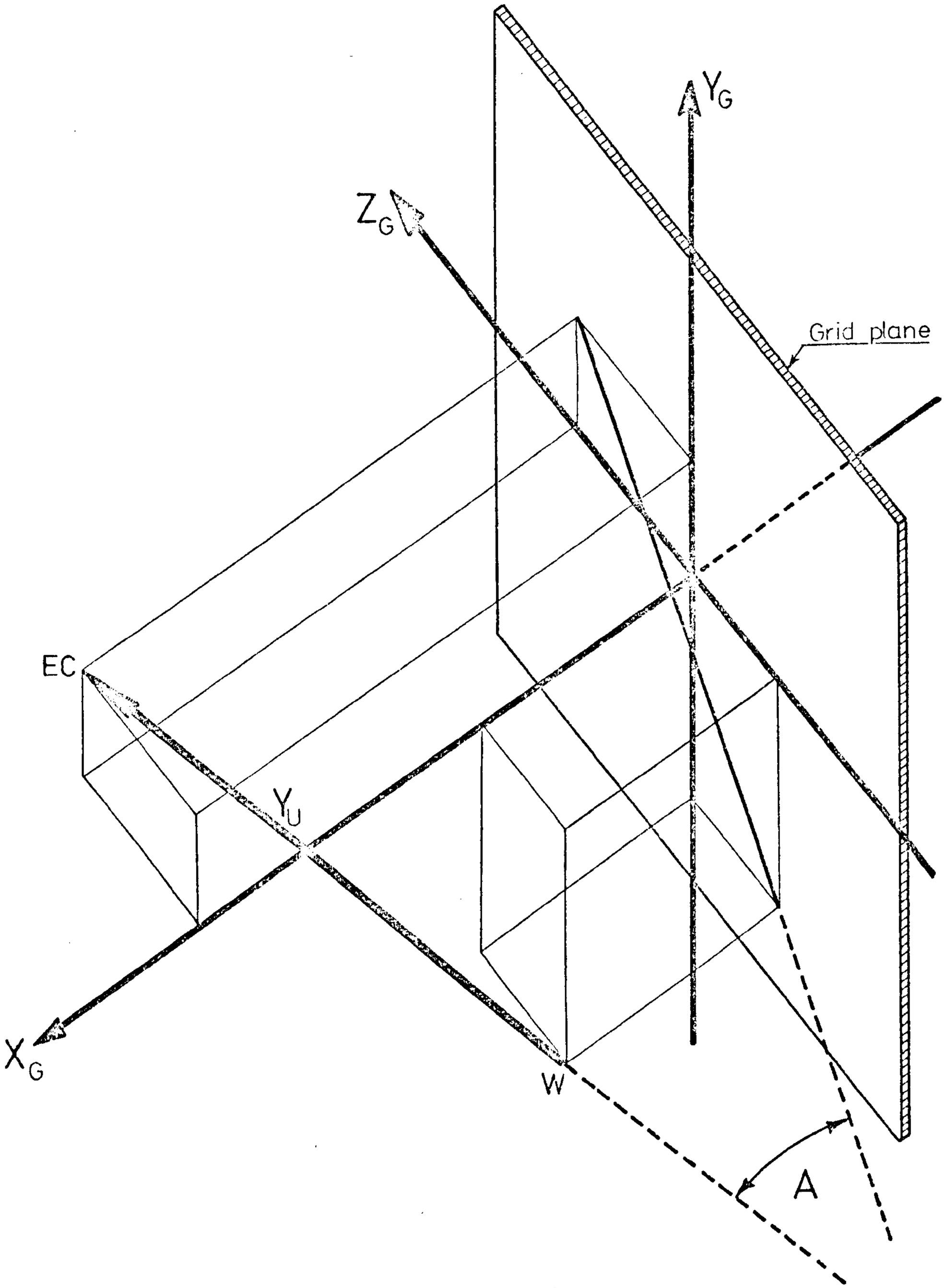

Figure 6·15: Definition of the "true" angle between Y_U and the grid planes.

The corresponding logic applicable to Θ_x and Θ_y is described in Appendix 2.6.

With the forearm lying at an angle to all three grid reference planes, the planar components of the moment of inertia for the forearm will be a percentage of the total amount of inertia. Ignoring inertial effects about Y_u, the three complementary components of the total moment of inertia are defined by the following

$$I_x = I \cos^2 A \qquad 6.18a$$

$$I_y = I \cos^2 B \qquad 6.18b$$

$$I_z = I \cos^2 C \qquad 6.18c$$

where I is the moment of inertia of the forearm about any axis perpendicular to the long axis of the forearm (i.e. $I = I_1 = I_2$). Angles A, B and C are the "true" angles between the long axis of the forearm (Y_u) and the YZ, ZX and XY grid planes respectively (see figure 6.15). Since the square of the cosine was required, the calculations simplified to the following:

$$\cos^2 A = (Y^2 + Z^2)/(X^2 + Y^2 + Z^2) \qquad 6.19a$$

$$\cos^2 B = (X^2 + Z^2)/(X^2 + Y^2 + Z^2) \qquad 6.19b$$

$$\cos^2 C = (X^2 + Y^2)/(X^2 + Y^2 + Z^2) \qquad 6.19c$$

where

$$X = X_w - X_{ec}$$

$$Y = Y_w - Y_{ec}$$

$$Z = Z_w - Z_{ec}$$

6.10 Numerical Differentiation:

The acceleration quantities of the forearm complex were calculated from the displacement data using a Newtonian numerical differentiator. Derived from a 4th order polynomial, the frequency response of the differentiator was exact up to 10 Hz for the sampling frequency of 50 Hz. (Tooth, 1976). Accordingly, the differentiator was incorporated into the analytical procedures with no correction terms.

The polynomial was of the form:

$$y = a_4x^4 + a_3x^3 + a_2x^2 + a_1x + a_0 \qquad 6.20$$

Consider five consecutive points, Y_{-2}, Y_{-1}, Y_0, Y_{+1} and Y_{+2} corresponding to time instants t_{-2}, t_{-1}, t_0, t_{+1} and t_{+2} ($t_{-2} < t_{-1} < t_0 < t_{+1} < t_{+2}$). The five points represent displacement data and the time "t_0" indicates the particular time instant under consideration. Two data samples were therefore required, before and after the arm activity, for full differentiation of the data sequence.

With a time interval "h", the five points became:

$$\begin{bmatrix} Y_{-2} \\ Y_{-1} \\ Y_0 \\ Y_{+1} \\ Y_{+2} \end{bmatrix} = \begin{bmatrix} 16h^4 - 8h^3 + 4h^2 - 2h + 1 \\ h^4 - h^3 + h^2 - h + 1 \\ 0 \quad 0 \quad 0 \quad 0 + 1 \\ h^4 + h^3 + h^2 + h + 1 \\ 16h^4 + 8h^3 + 4h^2 + 2h + 1 \end{bmatrix} \begin{bmatrix} a_4 \\ a_3 \\ a_2 \\ a_1 \\ a_0 \end{bmatrix} \qquad 6.21$$

$$\therefore \quad Y_{-2} + Y_{+2} = 32h^4a_4 + 8h^2a_2 + 2a_0$$

And:

$$Y_{-1} + Y_{+1} = 2h^4a_4 + 2h^2a_2 + 2a_0$$

$$\therefore \quad Y_{-2} - 16Y_{-1} - 16Y_{+1} + Y_{+2} = -24h^2a_2 - 30a_0$$

But $Y_0 = a_0$ from eqn.

$$\therefore \quad Y_{-2} - 16Y_{-1} + 30Y_0 - 16Y_{+1} + Y_{+2} = -24h^2 a_2.$$

$$\therefore \quad a_2 = \left[-Y_{-2} + 16Y_{-1} - 30Y_0 + 16Y_{+1} - Y_{+2}\right] / 24h^2$$

But for time t_0:

$$\ddot{Y}_0 = 2a_2$$

$$\therefore \quad \ddot{Y}_0 = \left[-Y_{-2} + 16Y_{-1} - 30Y_0 + 16Y_{+1} - Y_{+2}\right] / 12h^2. \qquad 6.22$$

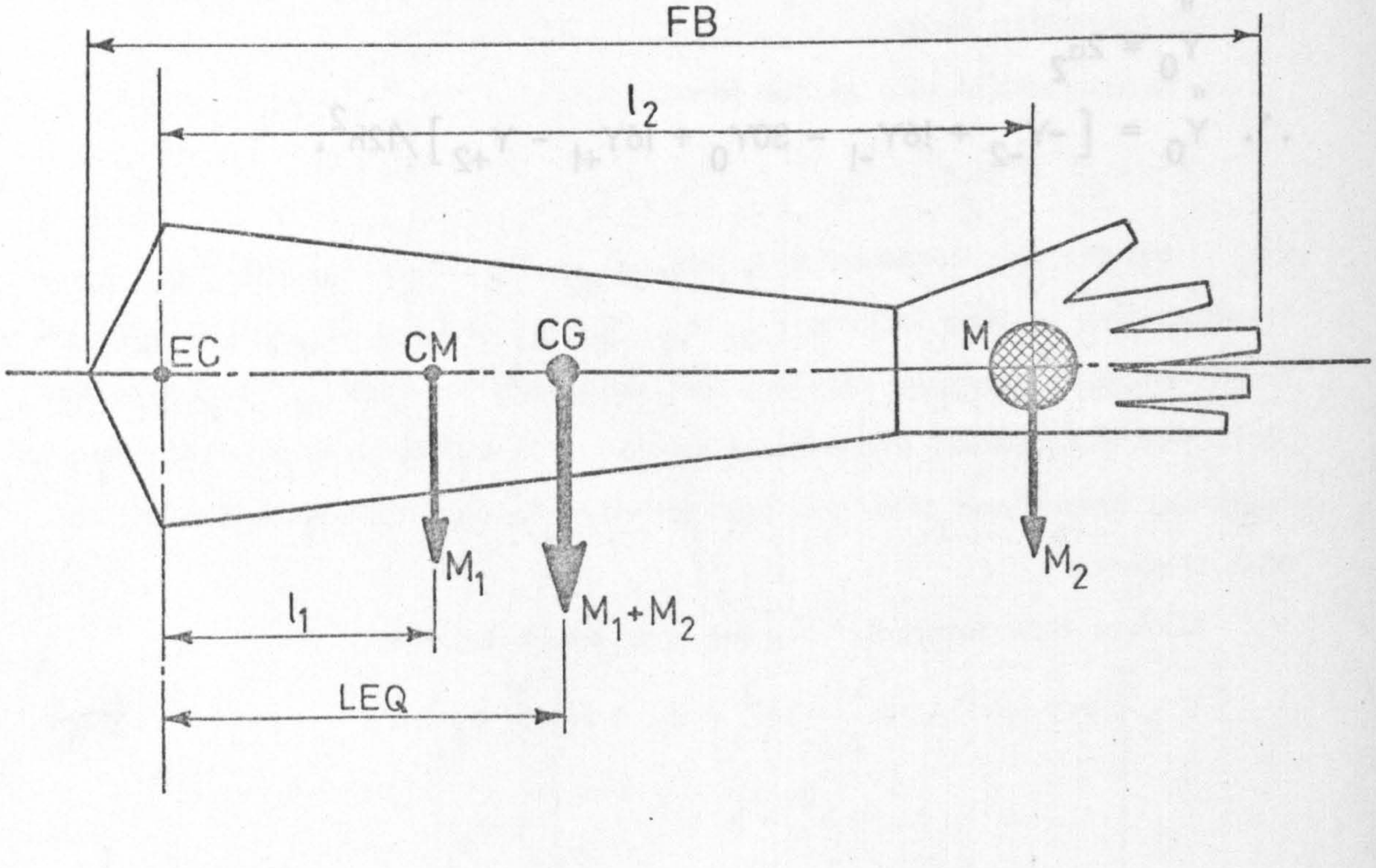

Figure 6·16: Simplified system of forearm, hand and ball.

6.11 Limb Parameters:

To fully analyse forearm movements, the dynamic characteristics of the segment were determined. Mass and inertial properties of the forearm and hand complex were obtained from Contini and Drillis (1966). Their sophisticated measurement techniques solved most of the problems encountered in body parameter investigations by previous workers. The values presented were considered to be sufficiently accurate for this analysis.

The position of the centre of mass "CM" from the elbow, was given as 42% of the overall length "FB". Similarly, the radius of gyration of the assembly was taken as 25% of FB and the segment mass as 2.4% of the total body mass. No radius of gyration about the long axis of the forearm was presented. Consequently, the inertial actions about Y_u were ignored.

Referring to figure 6.16, the position of the centre of total mass of the "forearm plus hand plus ball" complex was obtained as follows. Points EC, CM, CG and M were assumed to be colinear.

LEQ = equivalent mass distance from EC.

$$= \frac{(I_1 * M_1) + (I_2 * M_2)}{M_1 + M_2} \qquad 6.23$$

$$X_{cg} = X_{ec} + \frac{LEQ}{EB}(X_m - X_{ec}) \qquad 6.24a$$

$$Y_{cg} = Y_{ec} + \frac{LEQ}{EB}(Y_m - Y_{ec}) \qquad 6.24b$$

$$Z_{cg} = Z_{ec} + \frac{LEQ}{EB}(Z_m - Z_{ec}) \qquad 6.25c$$

where M_1 = 0.024 * MT (2.4% body mass)

M_2 = mass of ball

I_1 = 0.42 * FB

I_2 = EB (see section 5.5)

The total moment of inertia of the assembly about an axis through CG and perpendicular to Y_u was given by:

$$I_{tot} = M_1(KL^2 + (LEQ - l_1)^2) + M_2(l_2 - LEQ)^2 \qquad 6.26$$

where KL = radius of gyration of forearm

= 0.25 * FB.

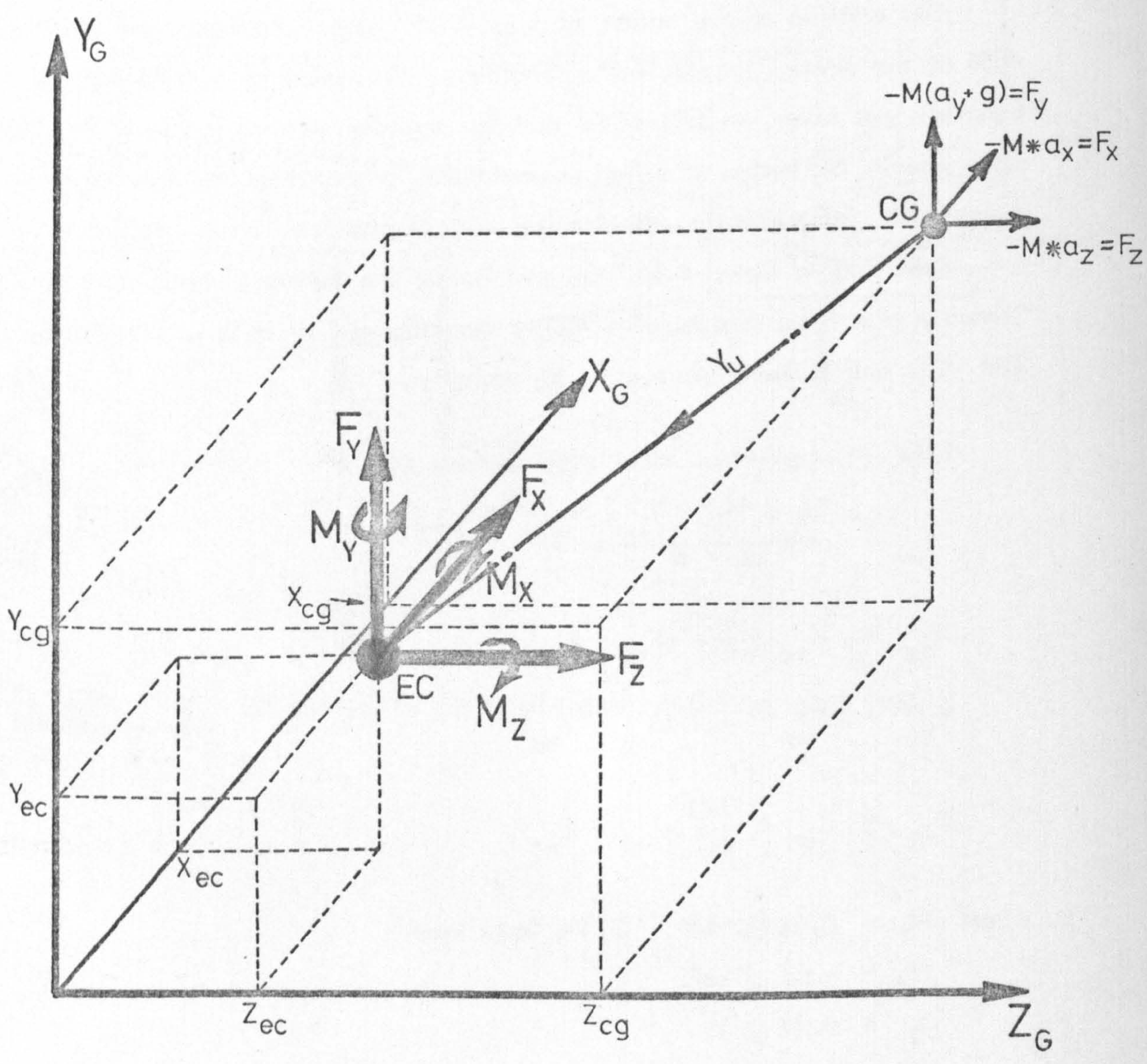

Figure 6·17: Generalised system of forces at the elbow joint.

6.12 Inertial Force Actions:

The linear and rotational displacement data for the forearm were processed by the differentiator to give linear ("a") and angular ("α") accelerations respectively. Knowing the mass and equivalent moment of inertia of the forearm, the inertial forces and torques acting on the forearm were calculated as follows (e.g. for X direction)

$$F_x = -M * a_x \qquad 6.27$$

$$M_x = -I_{tot} * \alpha_x * \cos^2 A \qquad 6.28$$

Referring all actions to the elbow centre "EC", but defined with respect to the grid axes, the force equations became (see figure 6.17)

$$F_x = -M * a_x$$

$$F_y = -M_* (a_y + g) \quad \text{where } g = 9.81 \text{ ms}^{-2}$$

$$F_z = -M * a_z$$

The resulting inertial torques about the elbow joint were given by:

$$M_x = -I_{tot} * \alpha_x * \cos^2 A + F_z(Y_{cg} - Y_{ec}) - F_y(Z_{cg} - Z_{ec})$$

$$M_y = -I_{tot} * \alpha_y * \cos^2 B + F_x(Z_{cg} - Z_{ec}) - F_z(X_{cg} - X_{ec})$$

$$M_z = -I_{tot} * \alpha_z * \cos^2 C + F_x(Y_{cg} - Y_{ec}) - F_y(X_{cg} - X_{ec})$$

All six force actions were thereafter rotated to the ulnar axis coordinate system using:

$$\begin{bmatrix} \text{Forces} \\ \text{or} \\ \text{Torques} \end{bmatrix}_u = [\,\text{DCUG}\,]^{-1} \begin{bmatrix} \text{Forces} \\ \text{or} \\ \text{Torques} \end{bmatrix}_g \qquad 6.29$$

For example:

$$\begin{bmatrix} F_{ux} \\ F_{uy} \\ F_{uz} \end{bmatrix} = [\,\text{DCUG}\,]^{-1} \begin{bmatrix} F_{gx} \\ F_{gy} \\ F_{gz} \end{bmatrix} \qquad 6.30$$

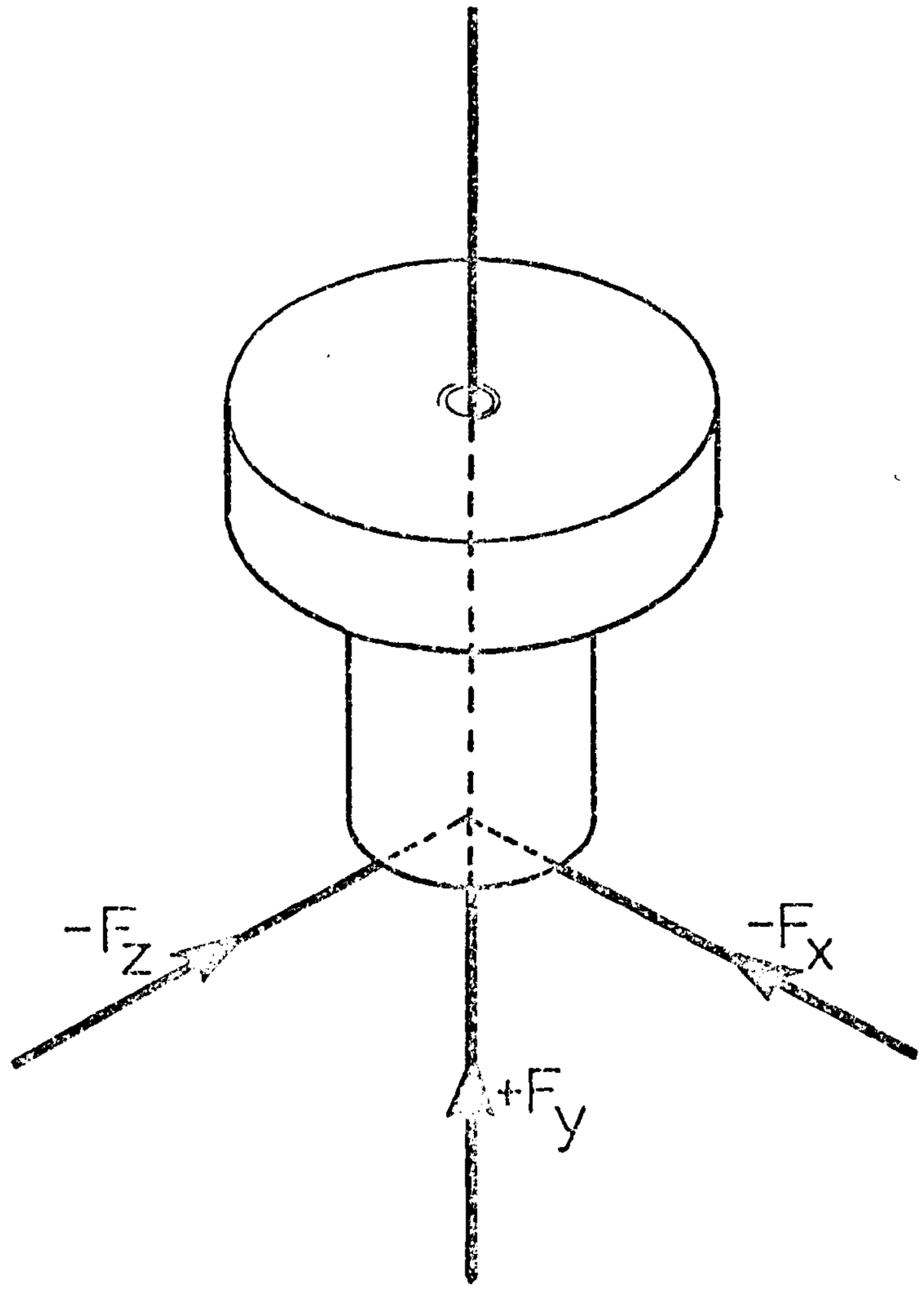

Figure 6·18: Forces acting ON the transducer.

6.13 Transducer Force Actions:

As previously described, the analogue signals from the transducer bridge amplifiers were processed by a PDP-12 computer. Analogue to digital conversion was performed at a sampling frequency of 50 Hz to correspond to cine camera speeds. A limit of 1000 mV signal magnitude was implemented corresponding to a digital value of $2^9(512)$ or 1000000000 in binary form.

The conversion from digital signals back to force quantities necessitated the use of calibration terms. To accommodate the six channels of data, matrix methods were used throughout. By definition

$$[\text{SIGNAL}] = [\text{CALIBRATION}][\text{FORCE}] \qquad 6.31a$$

$$\therefore [\text{FORCE}] = [\text{CALIBRATION}]^{-1}[\text{SIGNAL}] \qquad 6.31b$$

The matrix [CALIBRATION] was the product of three individual matrices; primary calibration, tape recorder attenuation and "cross-effects".

The primary calibration matrix "[CAL]" was obtained from the measurement of bridge amplifier output voltages corresponding to known force actions applied to the transducer. The matrix "[TAPE]" resulted from the attenuation/amplification of the input/output stages of the "Bell and Howell" tape recorder. A "cross-effect" matrix, called [X - TALK], resulted from force actions in one channel having an effect on the signal output of other channels. The content of this correction matrix was obtained from Lawes (1975).

Hence:

$$[\text{CALIBRATION}] = [\text{TAPE}][\text{CAL}][\text{X - TALK}] \qquad 6.32$$

Since the matrix SIGNAL was defined in millivolts, multiplication of values by 1000/512 was necessary to convert the PDP-12 signals to millivolts. The force quantities so obtained were relative to the X_p, Y_p and Z_p directions and were considered to act on the lower side of the central section shown in figure 6.18 at point P (X_p, Y_p, Z_p). Transfer of these actions to the ulnar axis system was performed using equations which were similar to equation 6.15. Gravitational effects were included but all other inertial quantities were considered to be negligible.

The position of point "P" in terms of ulnar coordinates was obtained in a similar manner as was designated by (X_{up}, Y_{up}, Z_{up}). Gravitational effects were included but all other inertial quantities were considered to be negligible. The components of the forearm weight referred to the ulnar axes were given by the following:

$$FG_{ux} = -MGU1 * M_l * 9.81 \text{ (Newtons)}$$

$$FG_{uy} = -MGU2 * M_l * 9.81$$

$$FG_{uz} = -MGU3 * M_l * 9.81$$

The forces and moments acting on the elbow joint were therefore given by:-

$$F_{ux} = FP_{ux} + FG_{ux} \qquad 6.33a$$

$$F_{uy} = FP_{uy} + FG_{uy} \qquad 6.33b$$

$$F_{uz} = FP_{uz} + FG_{uz} \qquad 6.33c$$

$$M_{ux} = MP_{ux} + (FP_{ux} * Y_{up} - FP_{uy} * Z_{up} - FG_{uz} * l_l) * 0.001 \qquad 6.44a$$

$$M_{uy} = MP_{uy} + (FP_{ux} * Z_{up} - FP_{uz} * X_{up}) * 0.001 \qquad 6.44b$$

$$M_{uz} = MP_{uz} + (FP_{uy} * X_{up} - FP_{ux} * Y_{up} - FG_{ux} * l_l) * 0.001 \qquad 6.44c$$

"FP" and "FG" represent the forces produced at the transducer and forearm C of G respectively.

The "external" mechanical actions on the elbow region were therefore completely defined in terms of the ulnar axes.

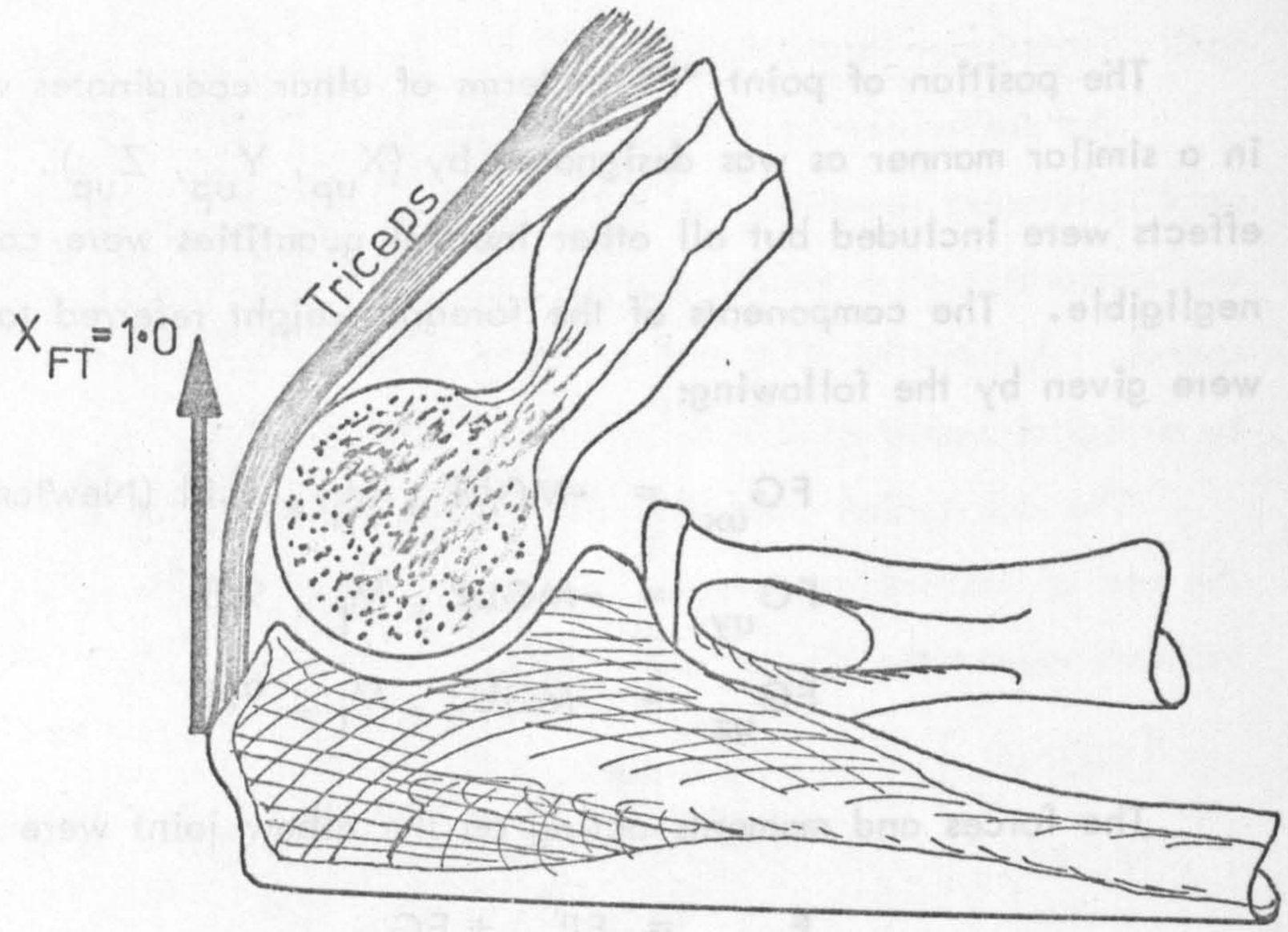

Figure 6·19a: Limit of direction for triceps tension

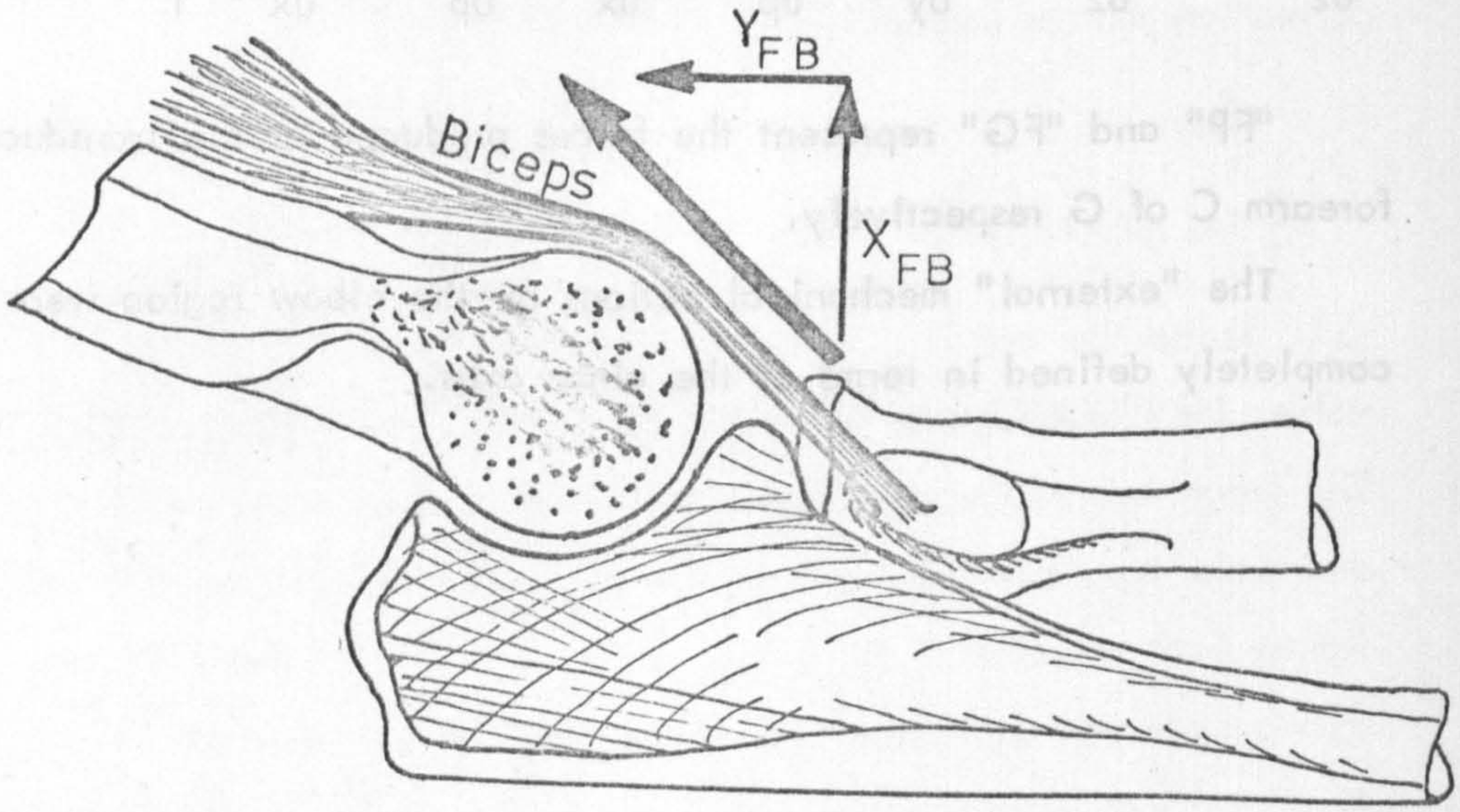

Figure 6·19b: Limit of direction for biceps tension.

6.14 Anatomical Considerations:

6.14.1 Muscle action: From the cadaveric measurements described in section 5.2.1, the origins and insertions of muscles and ligaments were obtained relative to the humeral or ulnar axis system. The coordinates obtained for three specimens are given in Table 6.1. Relationships were calculated with respect to epicondylar width, overall forearm length and elbow depth. These so-called "scaling factors" were used to calculate the fundamental anatomical geometry of each test subject.

Points measured on the humerus had their coordinates transferred to the ulnar axes using equation 6.15. The lines of action of the four relevant muscles were calculated as component values in the X_u, Y_u and Z_u directions. The straight line joining the origin and insertion of the muscles was taken to represent the line of action of the muscle. For example, the triceps components X_{ft}, Y_{ft} and Z_{ft} were obtained as follows

Muscle origin: X_{tr0}, Y_{tr0}, Z_{tr0}

Muscle insertion: X_{trl}, Y_{trl}, Z_{trl}

$$\text{Muscle length} = L_{tr} = \sqrt{[(X_{tr0} - X_{trl})^2 + (Y_{tr0} - Y_{trl})^2 + (Z_{tr0} - Z_{trl})^2]} \qquad 6.45$$

$$X_{ft} = (X_{tr0} - X_{trl})/L_{tr} \qquad 6.46a$$

$$Y_{ft} = (Y_{tr0} - Y_{trl})/L_{tr} \qquad 6.46b$$

$$Z_{ft} = (Z_{tr0} - Z_{trl})/L_{tr} \qquad 6.46c$$

At extreme values of elbow flexion and extension, the soft tissues surrounding the elbow joint disrupted the theoretical line of action of the triceps and the biceps muscles as shown in figures 6.19a and 6.19b. Limiting values of muscle components were therefore imposed to allow flexion and extension lever arms to remain effective.

From consideration of the skeletal and muscular structures surrounding the elbow joint, the Y_u component of the triceps force was limited to positive values. Correspondingly, the limit of X_{ft} approximated to 1.00 for $Y_{ft} = 0.0$;

Structure	Ulna			Humerus		
	X_u	Y_u	Z_u	X_H	Y_H	Z_H
Triceps	-0.4864	0.0692	-0.0694	-0.7297	0.55	-0.1388
	-0.3529	0.0769	-0.1076	-0.8235	0.8576	-0.1538
	-0.40	0.0869	-0.1052	-0.7333	1.021	-0.1228
Average	-0.4131	0.0777	-0.094	-0.7621	0.8095	-0.1384
Biceps	-0.2972	-0.1307	0.1666	0.8378	1.0846	0.1805
	-0.3235	-0.1269	0.2461	0.4411	1.088	0.1076
	-0.3666	-0.1217	0.1921	0.60	1.434	0.0877
Average	-0.3291	-0.1264	0.2018	0.6263	1.105	0.1252
Brachialis	0.2162	-0.0538	0.0277	0.4864	0.6615	0.0138
	0.2058	-0.0576	0.0307	0.5294	0.5230	0
	0.2666	-0.0565	0.0175	0.4666	0.5826	0.0306
Average	0.2295	-0.0559	0.0246	0.4941	0.5890	0.0148
Brachioradialis	0.1081	-0.5461	0.0833	0.1351	0.0538	0.3472
	0.1764	-0.7423	0.0923	0.0588	0.0461	0.2307
	0.20	-0.8608	0.228	0.1333	0.0739	0.3859
Average	0.1615	-0.7164	0.1345	0.1091	0.0579	0.3212
Medial Lig. (coronoid)	-0.1621	-0.073	-0.25	0	0	-0.4305
	-0.1470	-0.069	-0.4153	0	0	-0.4153
	-0.2333	-0.078	-0.2105	0	0	-0.3859
Average	-0.3238	-0.0107	-0.2597	0	0	-0.4105
Medial Lig. (olecranon)	-0.4594	0.05	-0.2083	-	-	-
	-0.4411	0.0538	-0.2461			
	-0.50	0.0521	-0.228			
Lateral Lig.	-0.3243	-0.0884	0.5416	0	0	0.5694
	-0.2941	-0.073	0.4307	0	0	0.5846
	-0.3666	-0.0739	0.5438	0	0	0.6140
Average	-0.3283	-0.0785	0.5053	0	0	0.5893
Forearm (overall size)	37 mm	260 mm	72 mm			
	34 mm	260 mm	65 mm			
	30 mm	230 mm	57 mm			

Table 6.1: "Scaling Factors" defined in terms of forearm thickness (X_u), forearm length (Y_u) and epicondylar width (Z_u).

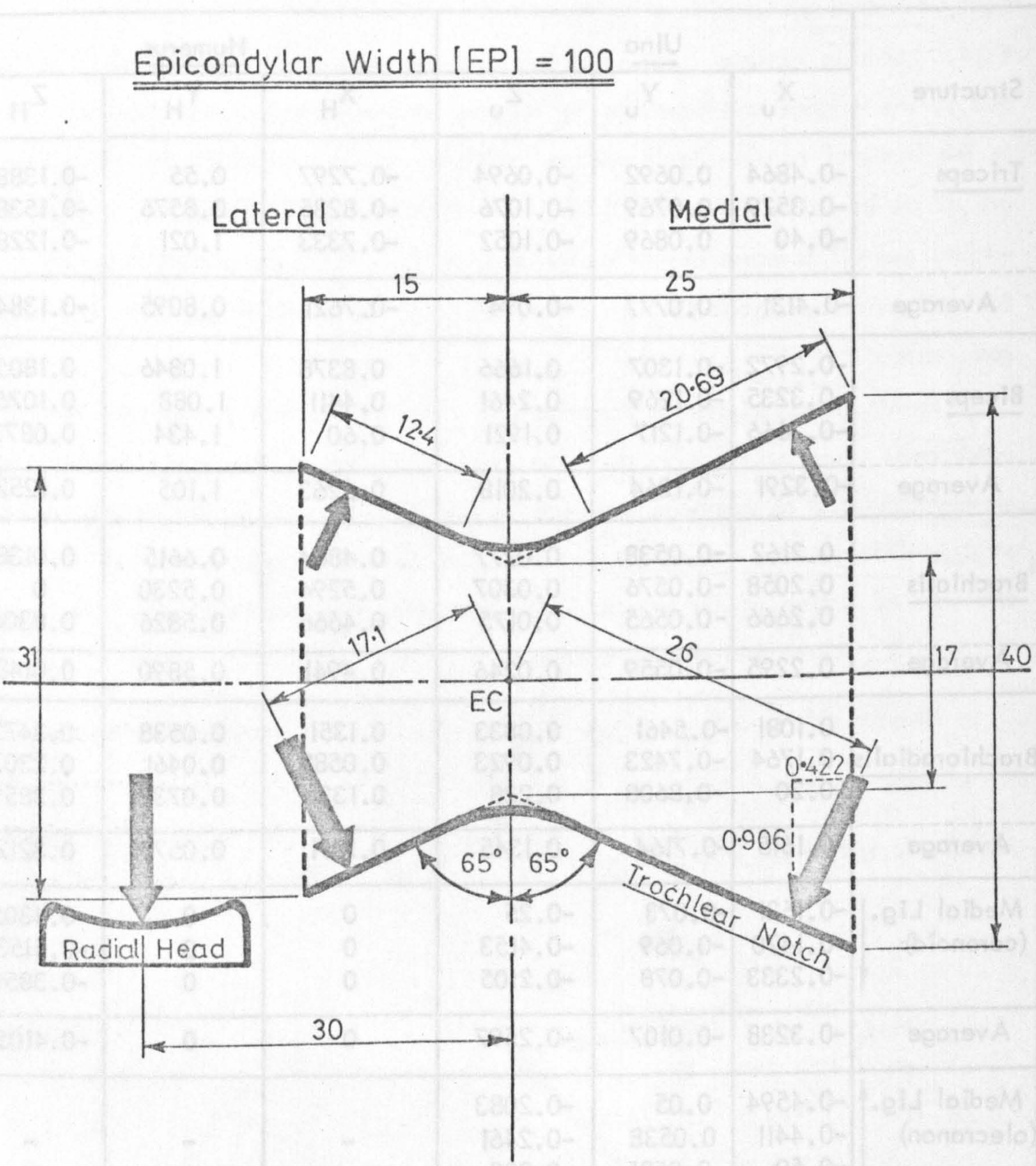

Figure 6·20: Details of the "analytical" elbow joint surfaces

Z_{ft} being unaltered.

With the relatively deep insertion of the biceps brachii tendon, limits of 0.80 and 0.606 were imposed on Y_{fb} and X_{fb} respectively; Z_{fb} remaining as calculated.

The summation of the square of the limiting values obviously exceeded unity but the Z-components were generally less than 0.10 which made the approximations acceptable. Brachialis and brachioradialis were not subject to any restrictions.

The lateral and medial ligament lines of action were calculated by the same method; their origins being defined on the appropriate epicondyle. With the ulnar collateral ligament comprising two bands, the straightforward average of the anatomical coordinates was taken for the ulnar insertion point.

6.14.2 Joint surfaces: From the bone sectioning experiments described in section 5.2.2, it was considered feasible to use a "model" joint consisting of straight sided conical surfaces. The complete joint resembled a split frustrum and is shown in figure 6.20. All dimensions are in terms of the epicondylar width "EP". Details of their derivation are given in Appendix 2.7.

6.14.3 Joint orientation: As previously mentioned, the "joint" axes were defined relative to the ulnar axis system. At this stage in the analysis, all relevant parameters were transferred from the ulnar axis system to the joint axes to simplify future calculations. This step was performed using the inter-axis relations of section 6.8 and the direction cosine of X_i, Y_i and Z_i relative to the ulnar axes. (see figure 6.21).

For rotations of $\Theta_{uy} = 0$, $\Theta_{ux} = 7^\circ$ and $\Theta_{uz} = +30^\circ$ any set of parameters X_u, Y_u, Z_u, relative to the ulnar axes, became

$$X_i = 0.866 * X_u + 0.4692 * Y_u + 0.06089 * Z_u \qquad 6.47a$$

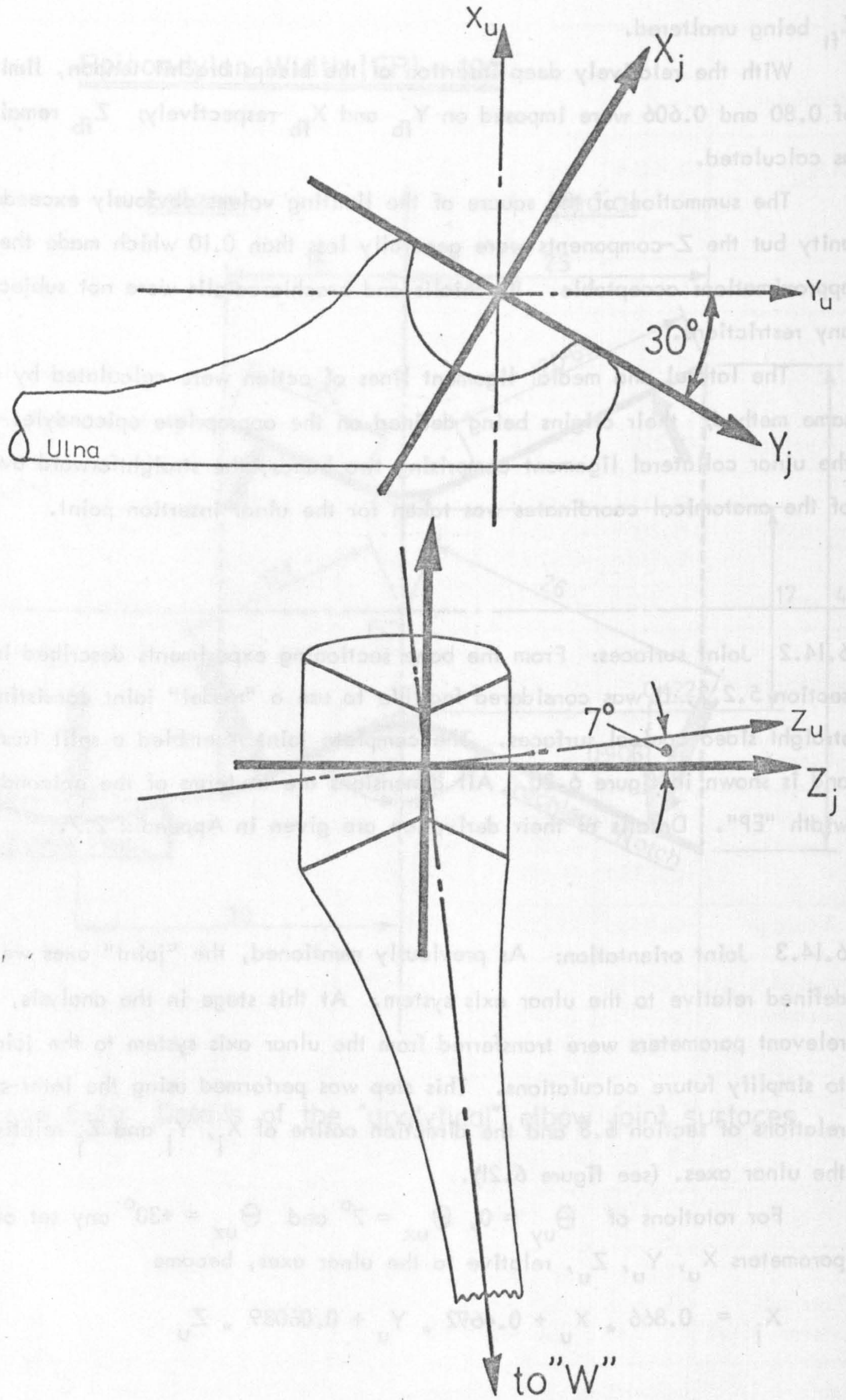

Figure 6·21: Position of the "joint" axes with respect to the "ulnar" axis system.

$$Y_i = -0.50 * X_u + 0.8595 * Y_u + 0.1055 * Z_u \qquad 6.47b$$

$$Z_i = -0.122 * Y_u + 0.9925 * Z_u \qquad 6.47c$$

where X_i, Y_i, Z_i were the values of the said parameters with respect to the joint axes. Details of the formation of equations 6.47a, b, c are given in Appendix 2.5.

From this point, all parameters relating to the joint axis system will be designated without the subscript "J". For example, the "grid" coordinates of the shoulder joint centre were termed X_{ss}, Y_{ss} and Z_{ss}. No subscript "G" was incorporated for reasons previously stated. Transfer of the shoulder centre into "ulnar" coordinates produced X_{uss}, Y_{uss} and Z_{uss}. For convenience, the shoulder joint centre in "joint" coordinates will again be termed X_{ss}, Y_{ss} and Z_{ss}. This method greatly simplifies future equations.

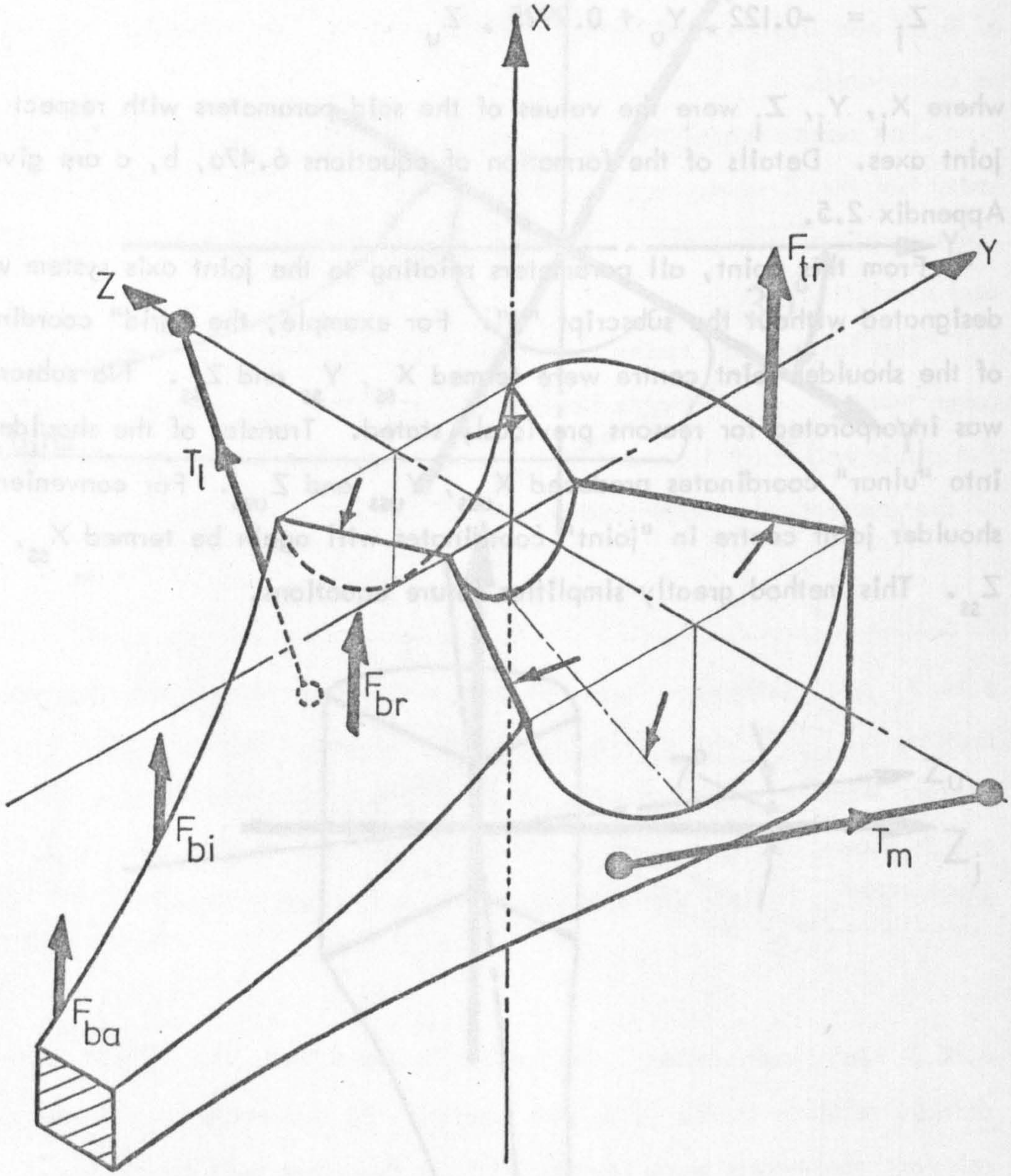

Figure 6·22: Complete system of forces ["internal"] acting on the proximal ulna.

6.15 Joint Equilibrium:

6.15.1 Introduction: At this stage in the computations, all external forces and moments acting on the forearm were fully defined at the elbow centre with respect to the joint axes. Equilibrium was established by the action of muscle, ligament and joint forces on the ulna and radius. Figure 6.22 shows all such force actions.

Initially, the number of unknown parameters far exceeded the six equilibrium equations (3 force plus 3 moment summations). The system was made statically determinate by analysing the function of several anatomical structures. For the following analysis, five unknown quantities were defined; one muscle force, one or two ligament tensions and, correspondingly, three or two joint forces.

The computations were divided into four sections:

i) Consideration of moments about the Z_i axis provided the forces in the flexor or extensor muscle groups (F_{bi} or F_{tr} respectively).

ii) The medial and lateral ligament tensions (T_m and T_l respectively) were derived from the summation of forces and moments in the $X_i - Z_i$ plane. Joint forces in this plane were also calculated (R_m and R_l).

iii) The remaining joint forces (F_m and F_l) were calculated using equilibrium equations from the summation of forces and moments in the $Y_i - Z_i$ plane.

iv) Knowing the loads transmitted by the joint surfaces, antagonistic muscle action was evaluated for limited articular surface pressure (P_m and P_l).

6.15.2 Muscle forces: Assuming, in the first instance, zero antagonistic muscle action, the flexor or extensor muscle force was obtained from the summation of moments around Z_i; joint friction being neglected. To model the true effect of the three flexor muscles, the tensions in biceps brachii and brachialis were assumed equal, while that in brachioradialis was taken as half the tension in biceps brachii. From figures 6.23 and 6.24 the muscles forces were:

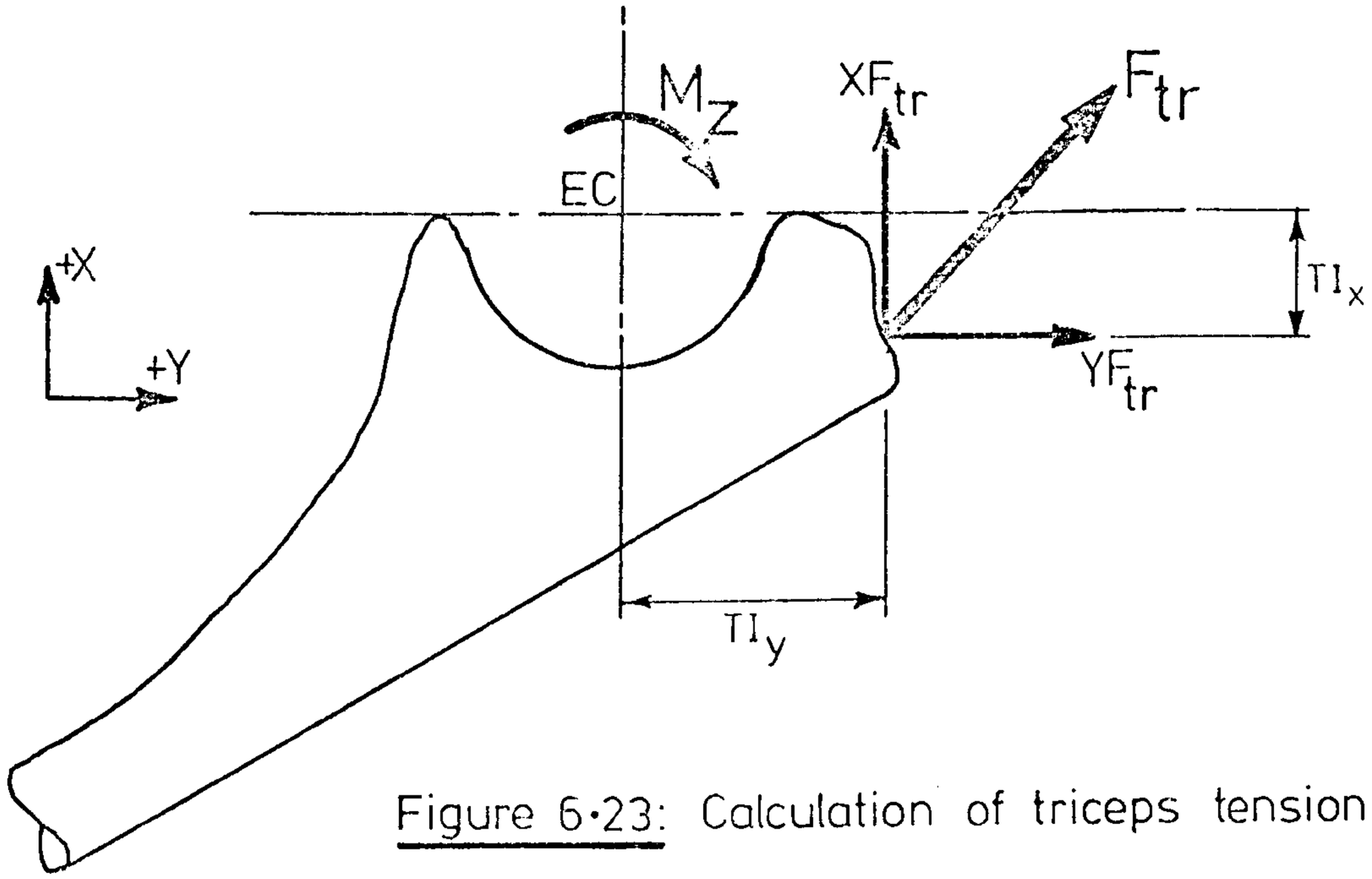

Figure 6·23: Calculation of triceps tension

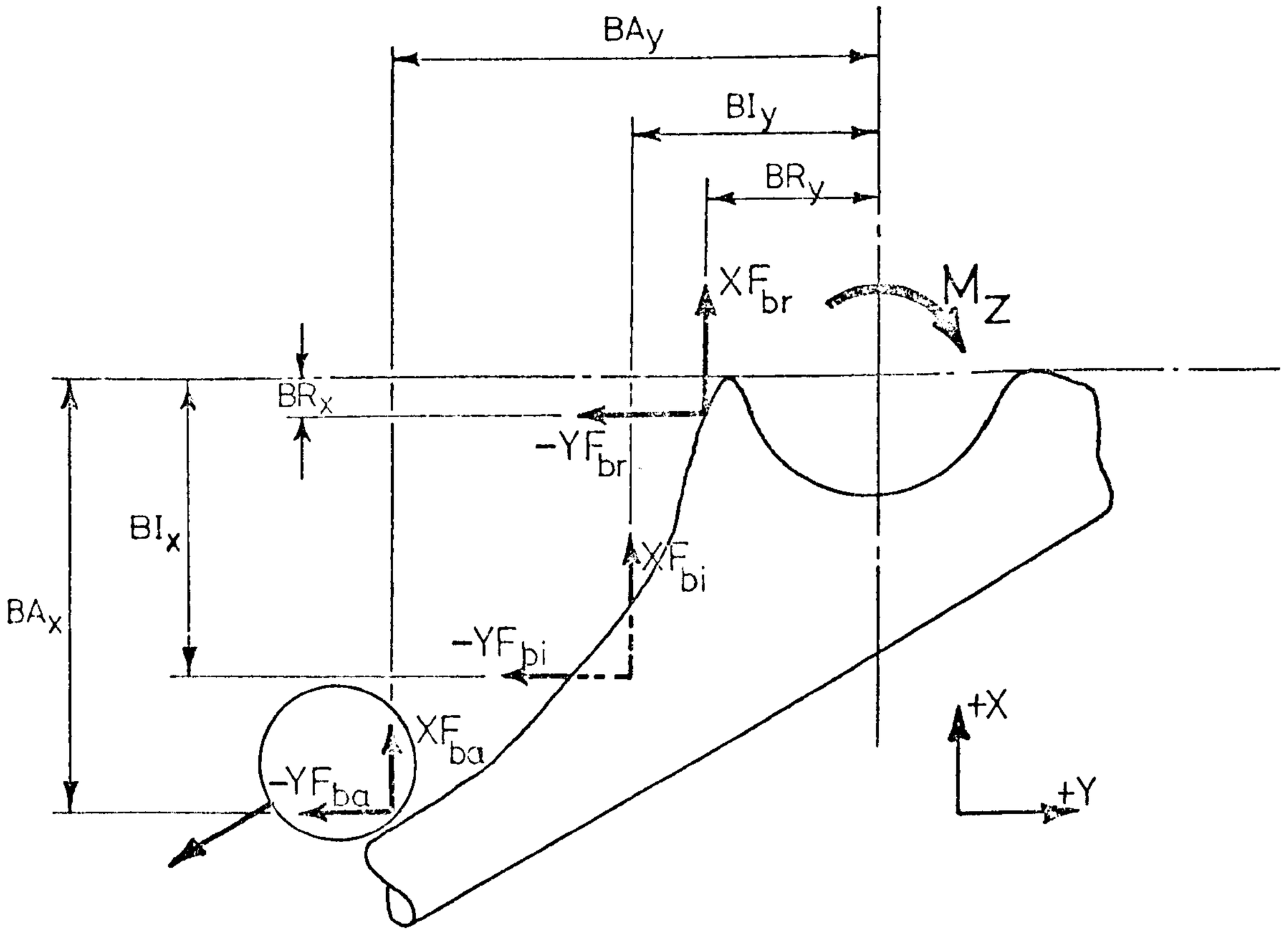

Figure 6·24: Calculation of flexor tensions

$$F_{bi} = F_{br} = 2 * F_{ba} \quad \text{(from Bankov and Jorgensen, 1969)}$$

$$F_{tr} = M_z/(XF_{tr} * TI_y - YF_{tr} * TI_x) \qquad 6.48$$

$$ARM = (XF_{bi} * BI_y - YF_{bi} * BI_x) + (XF_{br} * BR_y - YF_{br} * BR_x) + \tfrac{1}{2}(XF_{ba} * BA_y - YF_{ba} * BA_x) \qquad 6.49$$

$$\therefore \quad F_{bi} = M_z/ARM$$

6.15.3 Ligament tensions: Several attempts were made to calculate the ligament and joint forces using different combinations of the unknown parameters. Too many feasible arrangements resulted, however, and it was found necessary to calculate the ligament tensions before further analysis could be performed.

Since the major components of the ligament action lay in the X-Z plane of the joint axes, moments and forces in that plane were summated to calculate the tension in the ligaments. For convenience, the torque effects of the muscle forces about Y_i were grouped together and termed "TORQUEY" (see figure 6.25).

$$TORQUEY = (XF_{bi} * BI_z - ZF_{bi} * BI_x + XF_{br} * BR_z - ZF_{br} * BR_x + \tfrac{1}{2}(XF_{ba} * BA_z - ZF_{ba} * BA_x)) * F_{bi} + (XF_{tr} * TI_z - ZF_{tr} * TI_x) * F_{tr} \qquad 6.50$$

Similarly, the term "MUSCLEX" contained the summation of muscle contributions to the X_i force equations, thus:

$$MUSCLEX = (XF_{bi} + XF_{br} + \tfrac{1}{2}XF_{ba}) * F_{bi} + (XF_{tr} * F_{tr}) \qquad 6.51$$

As an initial condition, both ligaments were considered to act simultaneously. In such a case, the joint force in the $X_i - Z_i$ plane was zero. This produced a "joint gap" as shown in figure 6.26. The summations of M_y and F_x produced

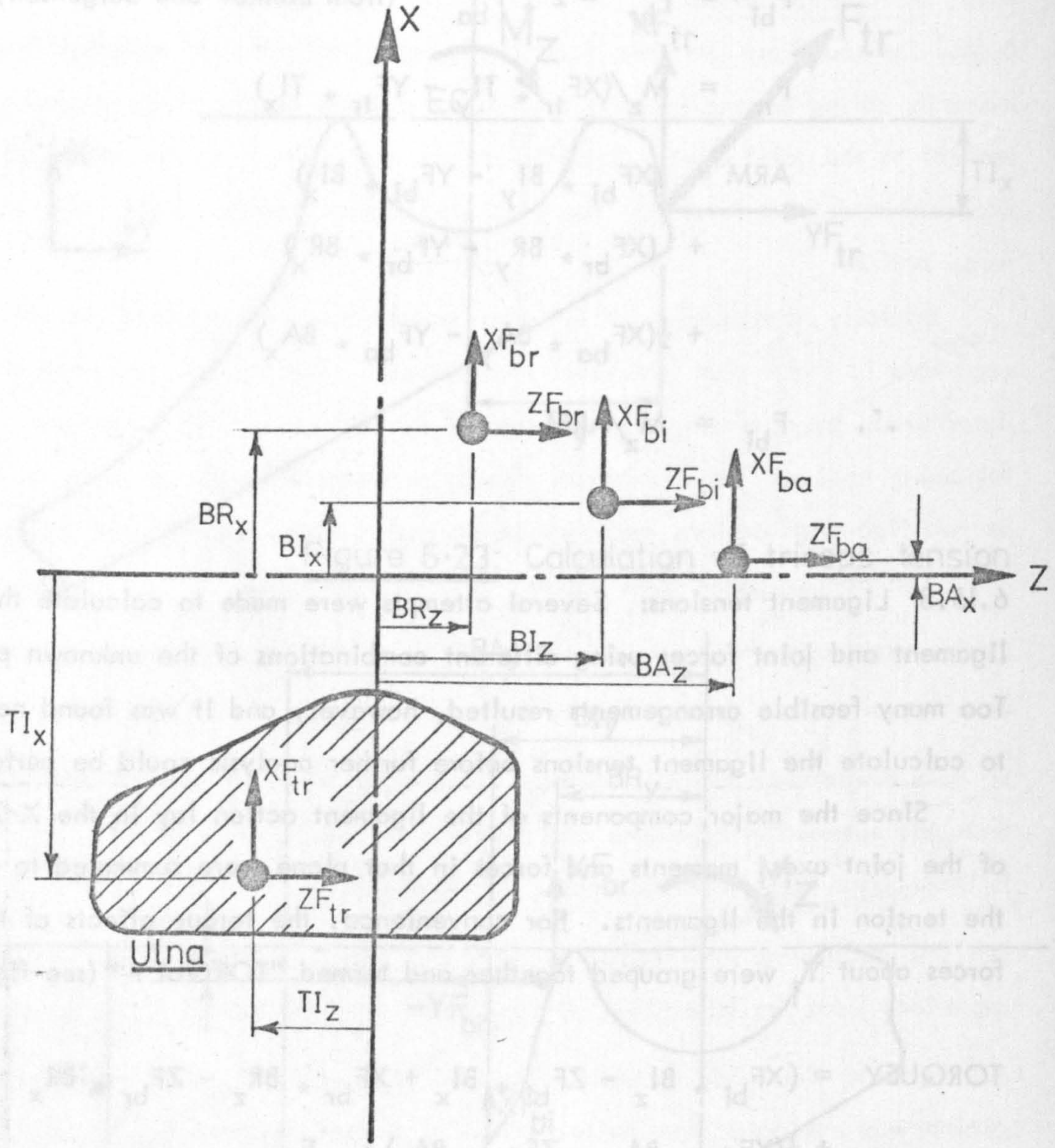

Figure 6·25: Calculation of muscle moments about Y_j

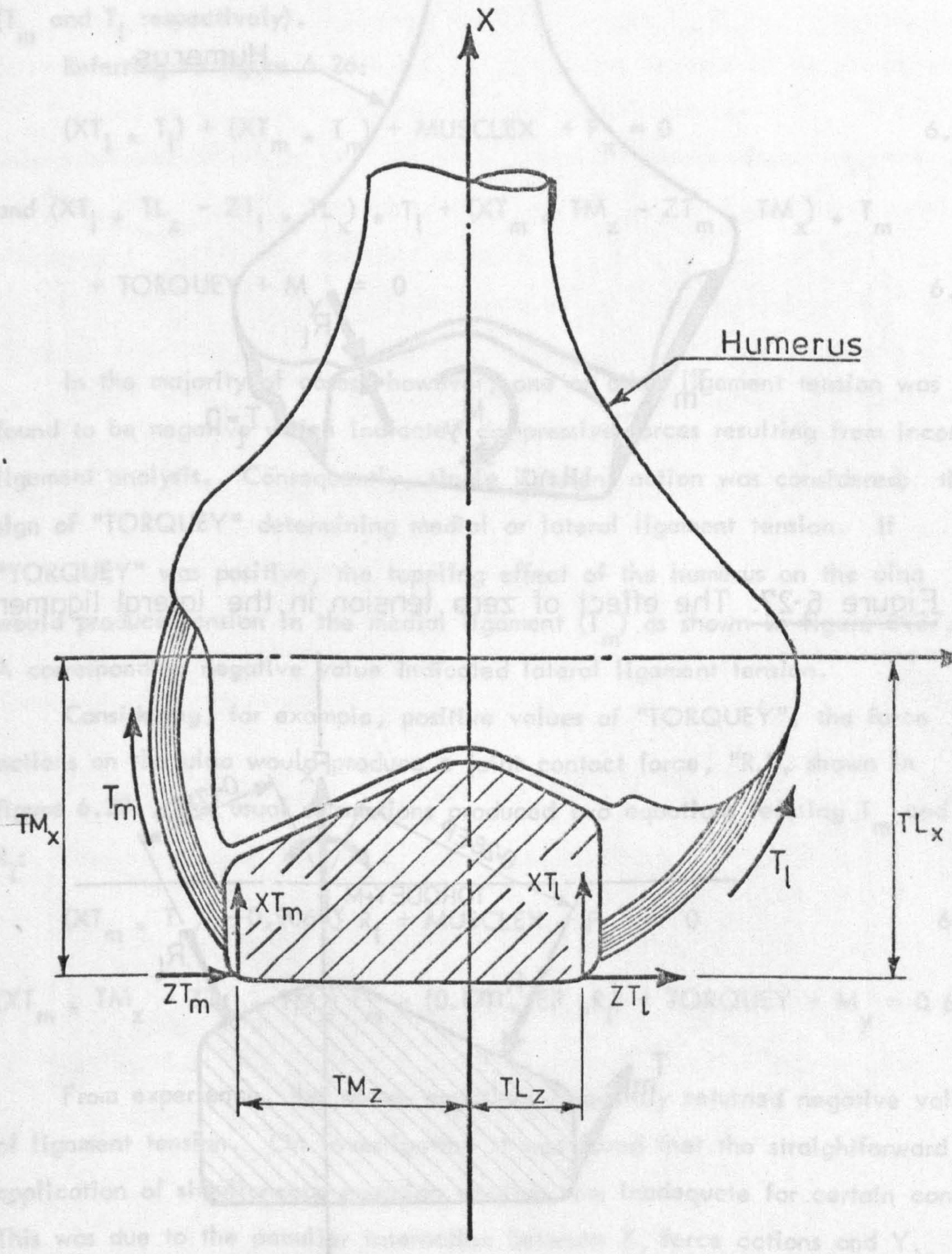

Figure 6·26: The effect of tension in both ligaments

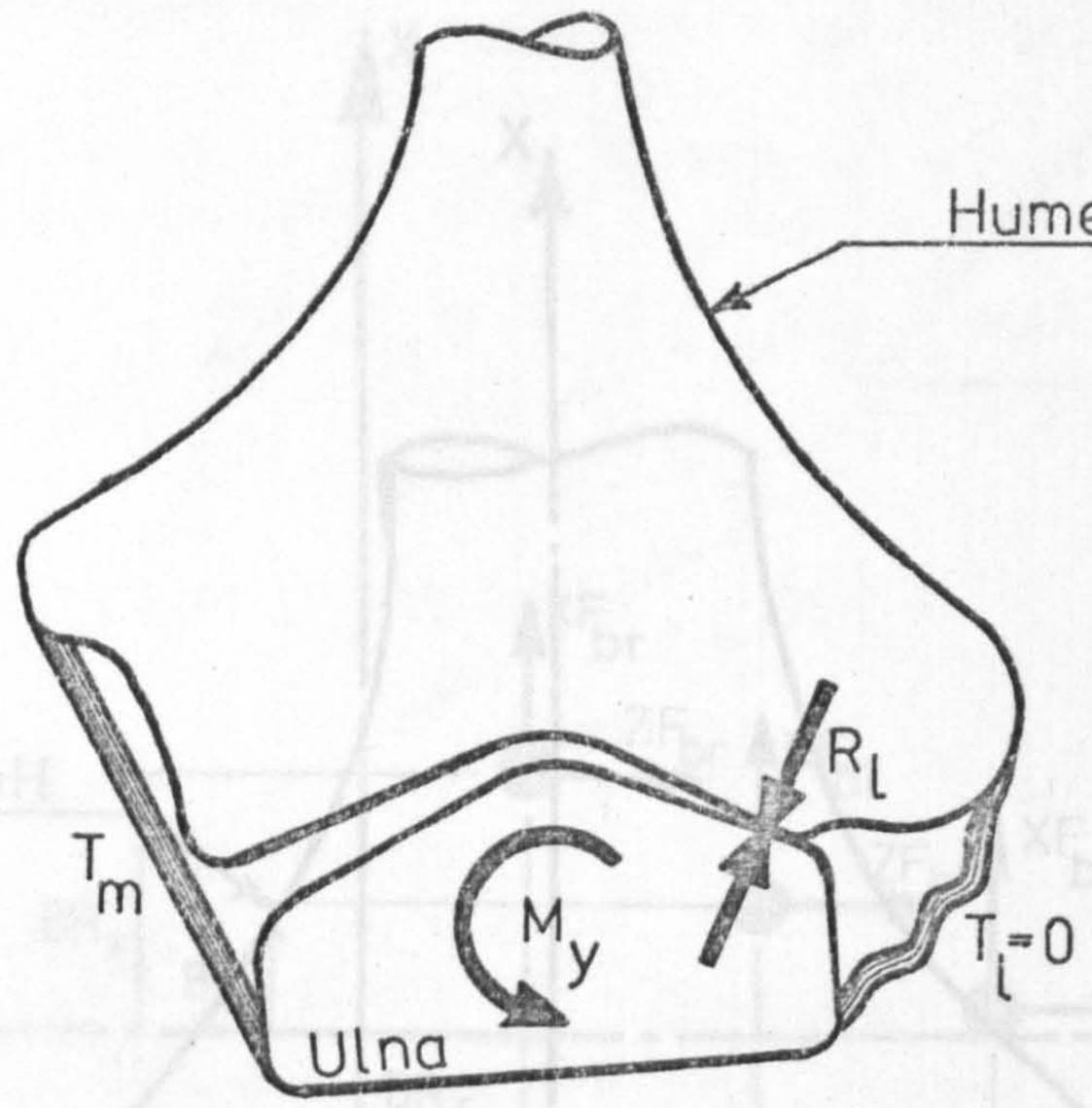

Figure 6·27: The effect of zero tension in the lateral ligament.

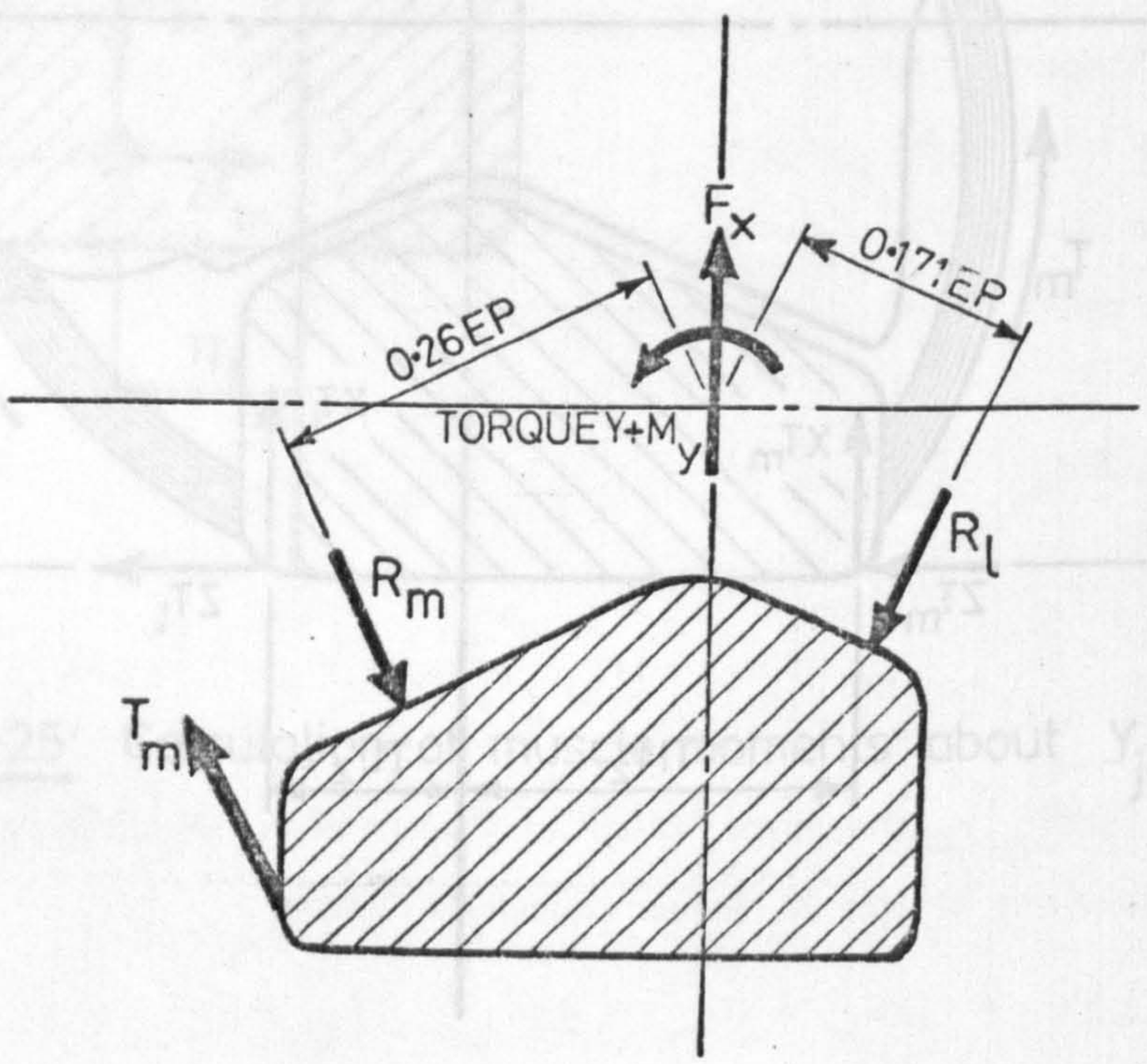

Figure 6·28: Calculation of the tension in the medial ligament and the corresponding joint forces.

two simultaneous equations containing medial and lateral ligament tensions (T_m and T_l respectively).

Referring to figure 6.26:

$$(XT_l * T_l) + (XT_m * T_m) + MUSCLEX + F_x = 0 \qquad 6.52a$$

and $(XT_l * TL_z - ZT_l * TL_x) * T_l + (XT_m * TM_z - ZT_m * TM_x) * T_m$

$$+ TORQUEY + M_y = 0 \qquad 6.52b$$

In the majority of cases, however, one or other ligament tension was found to be negative which indicated compressive forces resulting from incorrect ligament analysis. Consequently, single ligament action was considered; the sign of "TORQUEY" determining medial or lateral ligament tension. If "TORQUEY" was positive, the toppling effect of the humerus on the ulna would produce tension in the medial ligament (T_m) as shown in figure 6.27. A corresponding negative value indicated lateral ligament tension.

Considering, for example, positive values of "TORQUEY", the force actions on the ulna would produce a joint contact force, "R_l", shown in figure 6.28. The usual summations produced two equations relating T_m and R_l:

$$(XT_m * T_m) - 0.906 * R_l + MUSCLEX + F_x = 0 \qquad 6.53a$$

$$(XT_m * TM_z - ZT_m * TM_x) T_m - (0.171 * EP * R_l) + TORQUEY + M_y = 0 \qquad 6.53b$$

From experience, the above equations frequently returned negative values of ligament tension. On investigation it was found that the straightforward application of simultaneous equation routines was inadequate for certain conditions. This was due to the peculiar interaction between X_i force actions and Y_i moment effects.

Consider the situation where the Y_i moment effect produces tension in the medial ligament. The X_i component of T_m has a "negative" contribution to joint surface contact $(XT_m * T_m)$. "R_l" has a contribution to the summation of

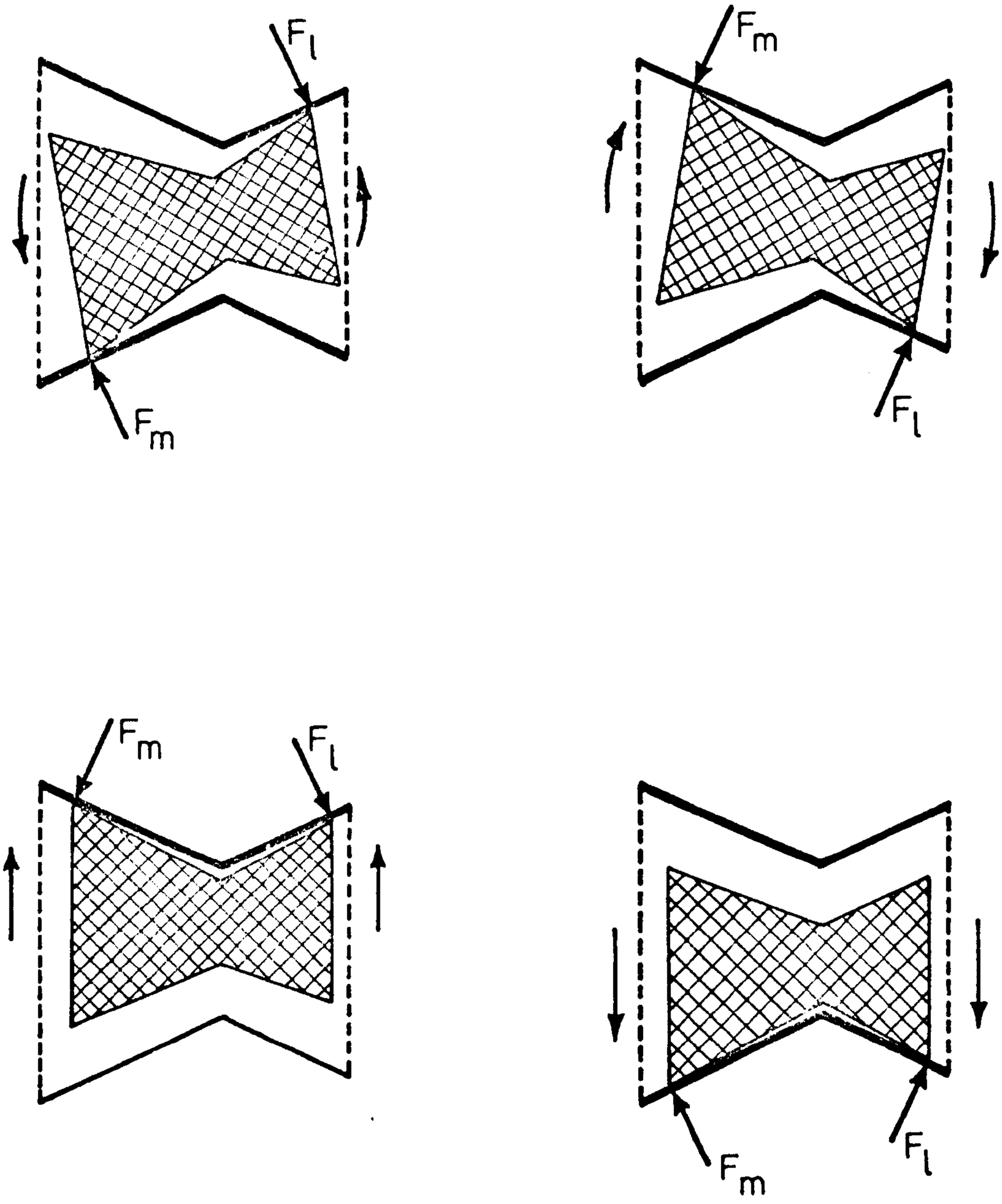

Figure 6·30: Definition of the joint forces in the Y_j-Z_j plane.

moments about Y_i. If the value of (MUSCLEX + F_x) was relatively small, the system of forces would produce equilibrium with $T_m > 0$. However, for increased values of (MUSCLEX + F_x), "R_l" would increase in magnitude while "T_m" would be reduced to maintain moment equilibrium about Y_i. A point would be reached where "R_l" produced sufficient moment effect, about Y_i, to make $T_m = 0$. Further increase of "R_l" would subsequently produce negative values of T_m and render the ulna unstable.

To overcome the above phenomenon, a second contact force "R_m" was introduced to distribute the force actions, along X_i, as shown in figure 6.28. In practical terms, R_m and R_l represented the two surfaces being pressed together to produce contact on both the medial and lateral surfaces. R_l and R_m were related so that the forces produced zero contribution to ΣM_y.

$$\text{i.e. } R_l = 1.32 * R_m$$

The modified value of ligament tension, T'_m, was calculated using the summation of moments about Y_i:

$$(ZT_m * TM_x - XT_m * TM_z)T'_m + TORQUEY + M_y = 0 \qquad 6.54a$$

The value of R_l, hence R_m, was calculated from ΣF_x:

$$(XT_m * T_m) + MUSCLEX - 0.906\,(2.32\,R_l) + F_x = 0 \qquad 6.54b$$

T_m was compared with T'_m to verify the introduction of "R_m". If T'_m was less than T_m, the initial analysis was representative of the joint system of forces. "R_m" was included otherwise.

6.15.4 Joint forces: The various force actions and contact conditions in the $Y_i - Z_i$ plane are shown in figure 6.30. The two forces "F_l" and "F_m" were found to provide equilibrium for all force actions excluding Z_i force effects. The forces were defined positive in the Y_i direction, that is, while acting on the superior surfaces of the trochlear notch. Contact at the inferior surfaces

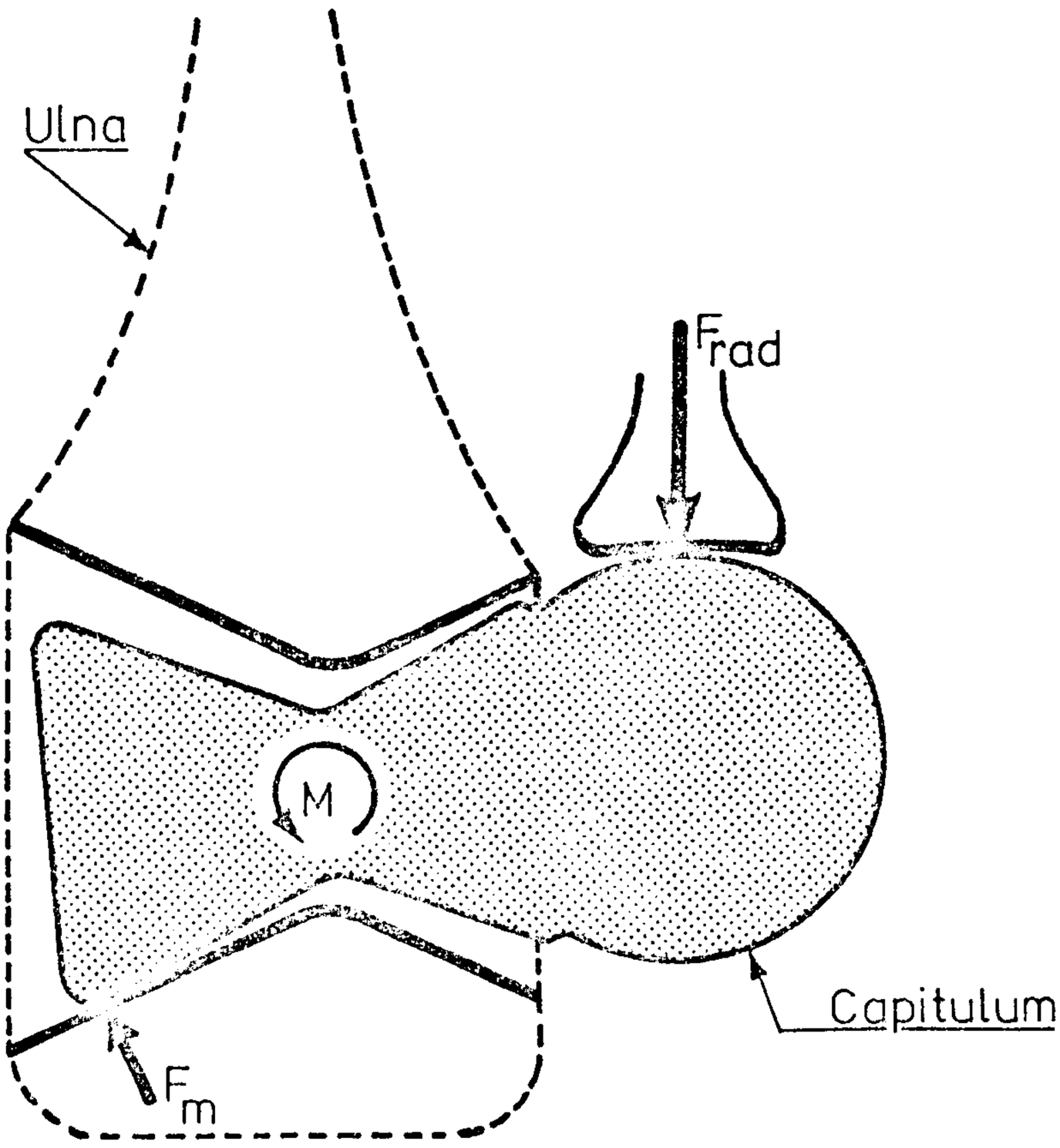

Figure 6•31: Definition of the radial head contact force

produced negative values of F_m. For negative values of F_l, contact was considered to act solely between the radial head and the capitulum (F_{rad}) as shown in figure 6.31. Summations of M_x and F_y produced two equations containing F_l (or F_{rad}) and F_m. As before, repetitive terms were grouped together giving "TORQUEX" and "MUSCLEY" as follows:

$$\begin{aligned} TORQUEX = [&(ZF_{bi} * BI_y - YF_{bi} * BI_z) + (ZF_{br} * BR_y - YF_{br} * BR_z) \\ &+ \tfrac{1}{2}(ZF_{ba} * BA_y - YF_{ba} * BA_z)] * F_{bi} \\ &+ (ZF_{tr} * TR_y - YF_{tr} * TR_z) * F_{tr} \end{aligned} \qquad 6.55$$

$$MUSCLEY = (YF_{bi} + YF_{br} + \tfrac{1}{2}YF_{ba}) * F_{bi} + (YF_{tr} * F_{tr}) \qquad 6.56$$

Thus:

$$0.906(F_l + F_m) + (YT_m * T_m) + MUSCLEY + F_y = 0$$

And:

$$-(0.171 * EP * F_l) + (0.26 * EP * F_m) + (ZT_m * TM_y - YT_m * TM_z)\, TM$$

$$+ TORQUEX + M_x = 0$$

For $F_l < 0$, radial head contact force, "F_{rad}", was considered to act as already described. The equilibrium equations became:

$$F_{rad} + 0.906 * F_m + (YT_m * T_m) + MUSCLEY + F_y = 0 \qquad 6.57a$$

$$(0.30 * EP * F_{rad}) + (0.26 * EP * F_m) + (ZT_m * TM_y - YT_m * TM_z)T_m$$

$$+ TORQUEX + M_x = 0 \qquad 6.57b$$

The remaining equilibrium equation, $F_z = 0$, provided a "difference" across the joint surfaces in the Z_l direction. This term was used as an accuracy check during the developmental stages of the analysis. For the conditions above:

$$\begin{aligned} DIFF = -0.422(&R_l - R_m - |F_m| + |F_l|) + (ZT_m * T_m) \\ &+ (ZF_{bi} + ZF_{br} + \tfrac{1}{2}ZF_{ba})F_{bi} + (ZF_{tr} * F_{tr}) + F_z. \end{aligned} \qquad 6.58$$

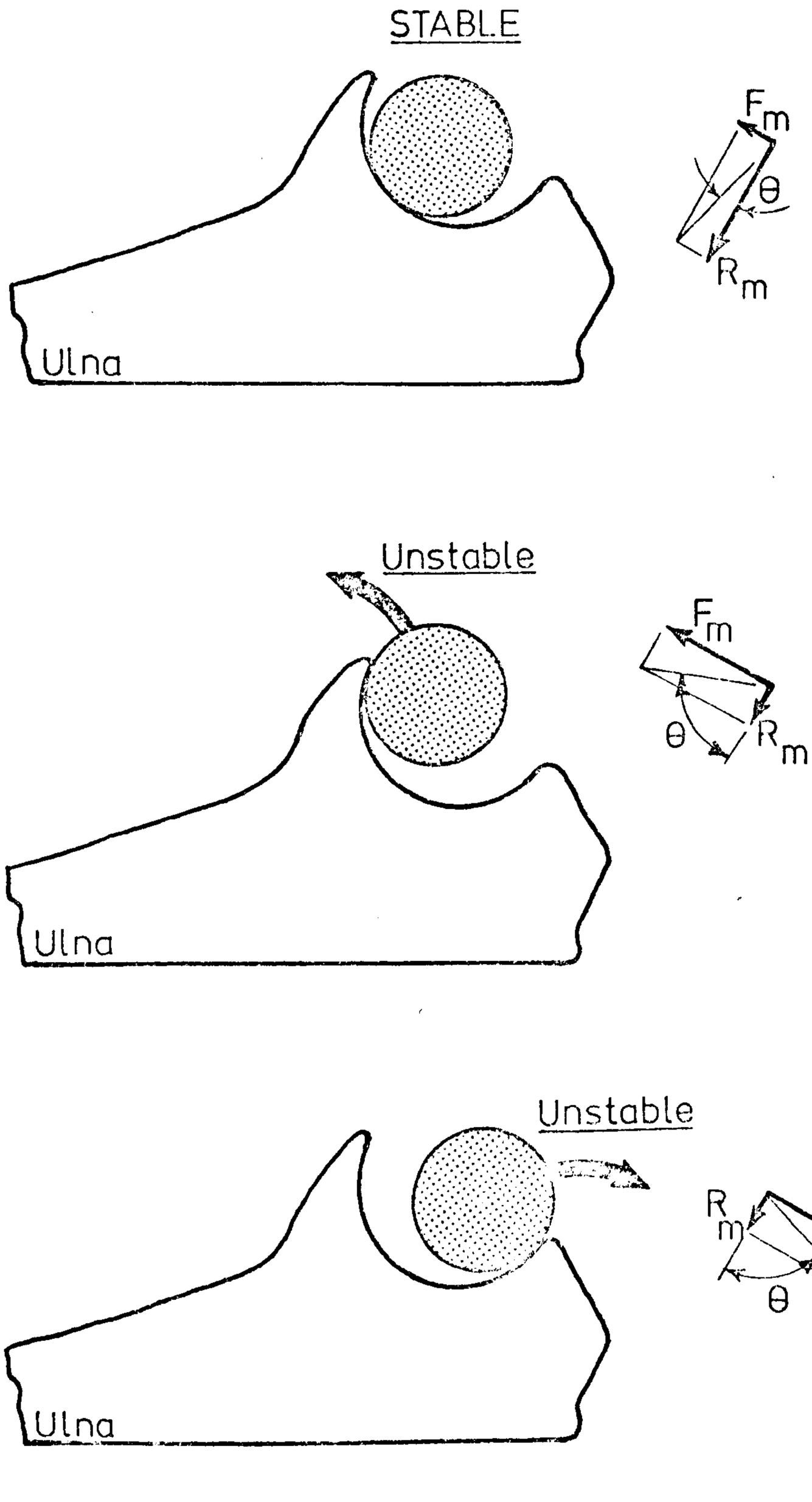

Figure 6·32: "Stability" of the trochlea.

6.15.5 Antagonistic muscle activity: From the electromyographic recordings of the arm activities, antagonistic muscle activity was frequently observed during the "transducer" series of tests. It was therefore postulated that muscular action provided stability of the elbow joint during such load/position configurations. Shoulder joint function would obviously affect the activity of the biceps and triceps muscles but, since no quantitative electromyography was possible, only a simple analysis of elbow joint antagonism was possible.

The critical factor for stability was considered to be the effect of F_l and F_m in the $Y_i - Z_i$ plane. If these forces were very much greater than their complementary joint reactions (R_l and R_m), the trochlea would have a tendency to "roll-out" of the trochlear notch due to cartilage deformation. Figure 6.32 shows the effect of several loading conditions on the medial side of the ulna. The angle Θ of the resultant joint force R_r can be decreased by increasing R_m (or R_l). This was achieved by the introduction of additional muscle force which "pushed" the humerus into the trochlear notch. One exception to this principle was the action of triceps near full extension of the elbow.

The choice of limiting factor for stability control presented many problems. A straightforward ratio of F_m and R_m was initially used but the results were quite arbitrary. A more suitable criterion was later adopted which made use of the articular surface pressures, P_m and P_l. Knowing the inclination of the resultant joint reaction, together with the geometry of each articular surface, the contact area was calculated as follows (see figure 6.33).

$$\text{Area} = 2 * ARC * \text{joint width}$$

From previous investigations (Seedhom et al 1974) the typical pressures in the hip and knee joints can be around 9 and 5 MN/m^2 respectively (1 MN/m^2 = 10 atm). A limit of 5 MN/m^2 was therefore chosen for the non-weight-bearing elbow joint. The distribution of this pressure across the articular surface was assumed to be triangular in form and acting within the bounds shown in figure 6.34. The maximum articular pressures were then calculated from

$$P_m = 2 * DFM/AREAM \qquad 6.59a$$

$$P_l = 2 * DFL/AREAL \qquad 6.59b$$

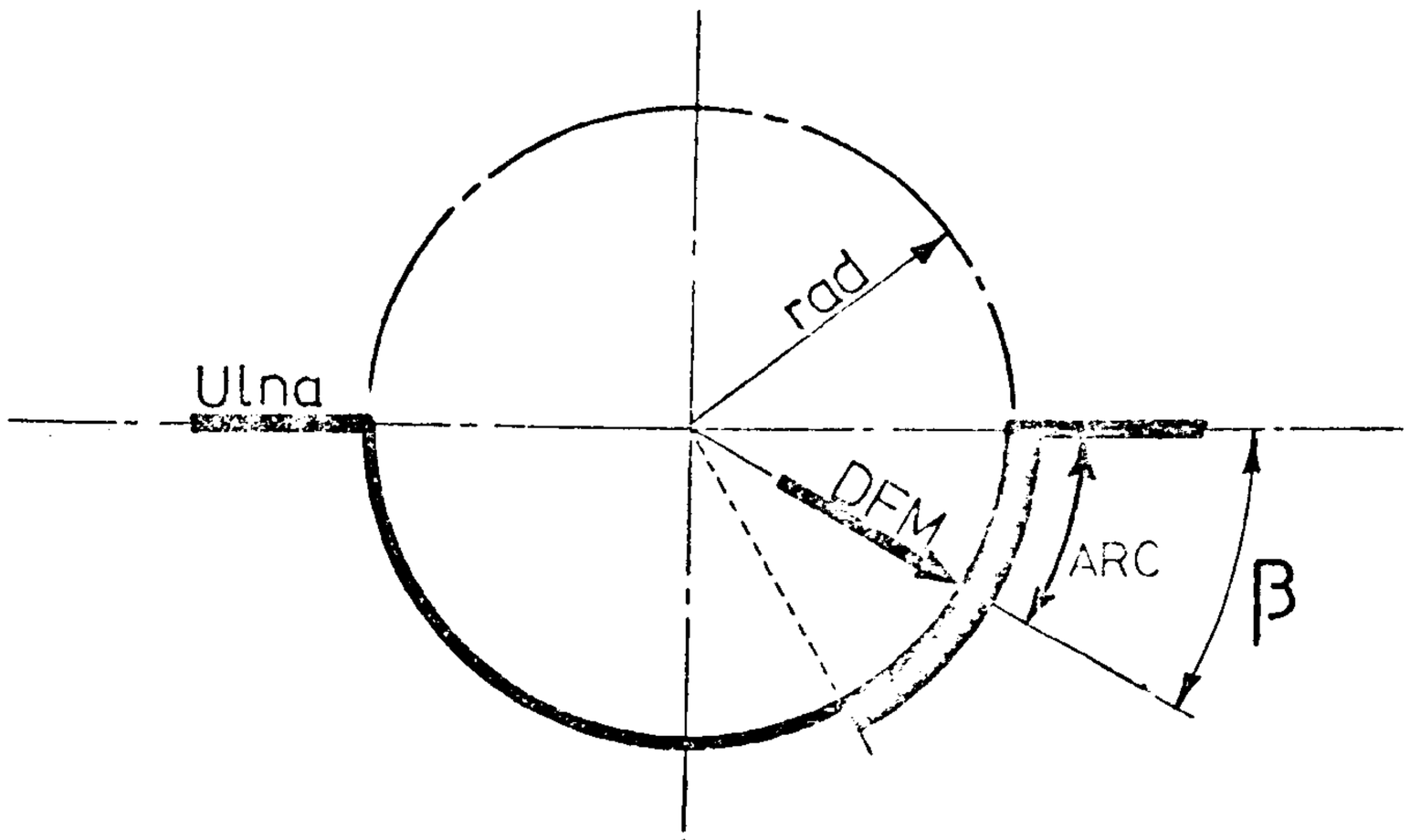

Figure 6·33: Calculation of the area of surface contact.

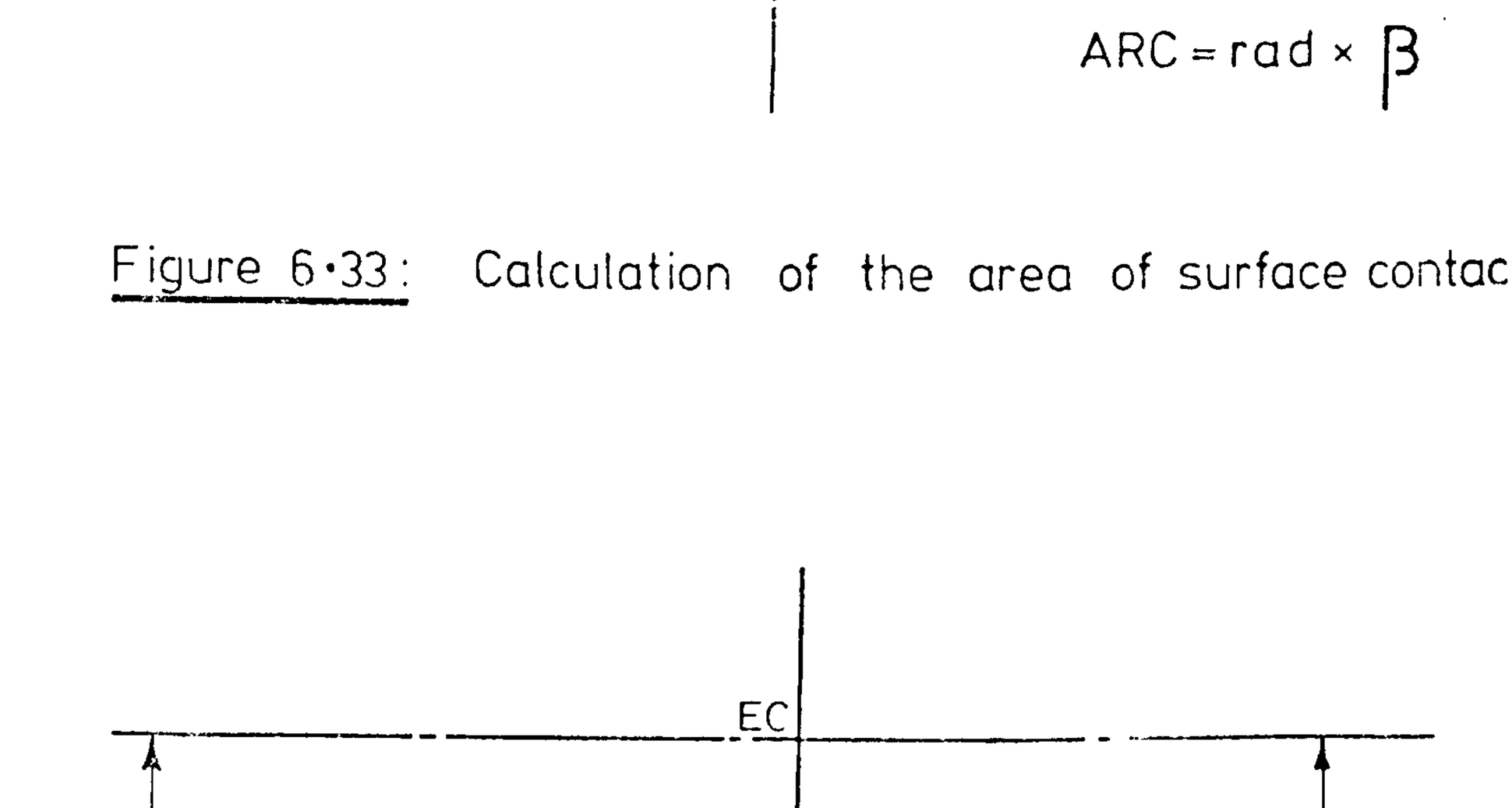

Figure 6·34: Distribution of articular pressure across the ulna.

where DFM and DFL are the resultant forces on the medial and lateral joint surfaces.

If either pressure exceeded the chosen value, the peak pressure was therefore excessive and antagonistic muscle activity was considered. An iterative procedure was adopted with appropriate converging routines. If the pressures were not decreased by the additional muscle force, as mentioned for full extension, the routine was cancelled.

7. RESULTS

7.1 Introduction:

The experimental tests were carried out in four series using a total of six subjects. In the first two series, the elbow joint was analysed for movements involving inertial effects as the major load actions ("eating" and "reaching" activities). In the two remaining series, additional measurements were made regarding the forces and moments transmitted between the hand and the environment ("seat-rise" and "table pull").

The results are presented in four separate sections according to the activity in question. Sections 7.2, 7.3, 7.4 and 7.5 contain the complete solution of the equations derived in Chapter 6 for the eating, reaching, pulling and seat rise activities respectively. For each of these sections, the bio-mechanical results are described and discussed in a predetermined order.

After an introductory description of the important characteristics of the particular activity, the kinematics of the elbow joint are described together with any important movements of the body, or environment, as a whole. Thereafter, the resultant system of "external" forces and moments applied to the elbow joint is discussed. The "internal" force actions (muscle, ligament and joint forces) are then described with particular reference to anatomical considerations. As a conclusion to each section, the complete system of internal force actions for each subject is displayed on a separate graph in order that the phasing of each test can be studied.

The "joint forces" calculated for the lateral and medial surfaces of the trochlear notch are defined as the resultant of the two joint forces described in section 6.15 (F_M and R_M, or F_L and R_L). On the lateral side of the elbow joint, the humero-radial contact force (F_{RAD}) became significant during some parts of the activities and is presented accordingly. In such cases, the "joint force" (DFL) is presented as the resultant of F_{RAD} and R_L.

In the analysis of locomotion data it is accepted practice to present the relevant force actions in terms of the total body weight (e.g. F/BW). In addition, the results of the walking cycle are usually plotted to a "time" base corresponding to percentages of the complete cycle of events. When

considering the biomechanics of the upper limb similar parameters were considered to be inappropriate and all the results were therefore presented as actual values to a base of time (s). All force actions were defined in units consistent with SI definitions (i.e. N and Nm).

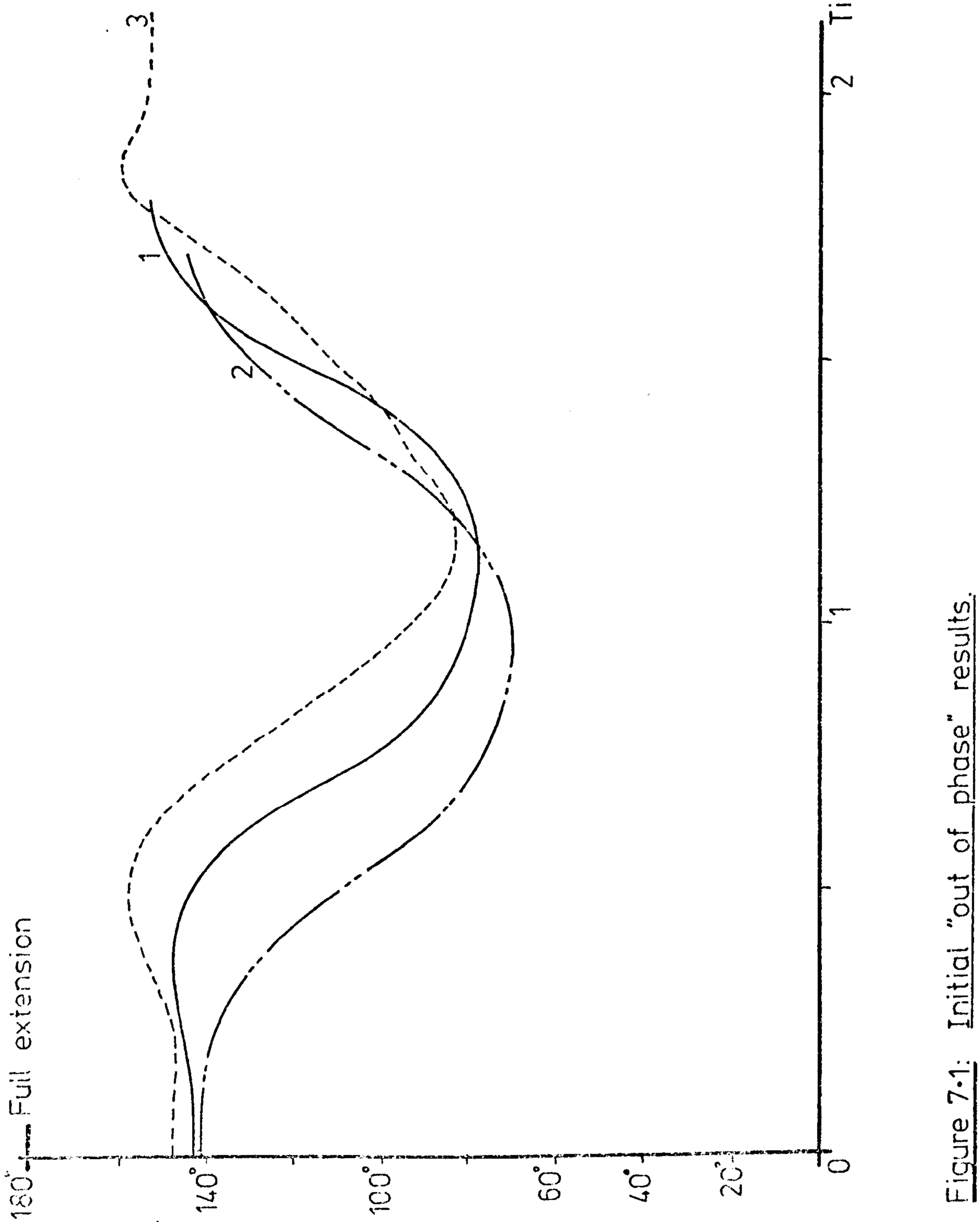

Figure 7·1: Initial "out of phase" results.

7.2 "Eating" Activity:

The "eating" activity was performed by subjects 1, 2 and 3 and had an average duration of approximately 1.3/4 seconds. Film measurements were initiated at the start of arm movement but it was found that the three graphs of elbow motion were "out of phase" with each other (see figure 7.1). An arithmetic modification to the number of frames of film contained in each data sequence corrected this phenomenon.

The complete movement was characterised by the "start" (Δ) which corresponded to the initiation of movement, the "changeover" ($\underline{\Omega}$) period, and the "finish" at the termination of arm motion. Each graph is labelled accordingly.

7.2.1 Movement: Figure 7.3 shows the variation in "elbow angle" for three subjects during the "eating" activity. An overall movement of 70^{o} was produced by each subject but a relative variation of some 15^{o} was recorded between subjects.

As the arm was accelerated forwards at the beginning of the activity (see figure 5.13) the inertial effects on the forearm produced a slight increase in elbow angle. This was immediately followed by forced elbow flexion at an approximate rate of 3 rad/s. After half a second, deceleration actions were applied to the forearm and a stationary position was recorded. Following this "changeover" period (t = 0.9 s) the return movement was performed with rapid elbow extension (approx. 4 rad/s) and a braking phase. Subject No.3 experienced a slight amount of "over-extension" but a stable position was reached after 6^{o} of elbow flexion.

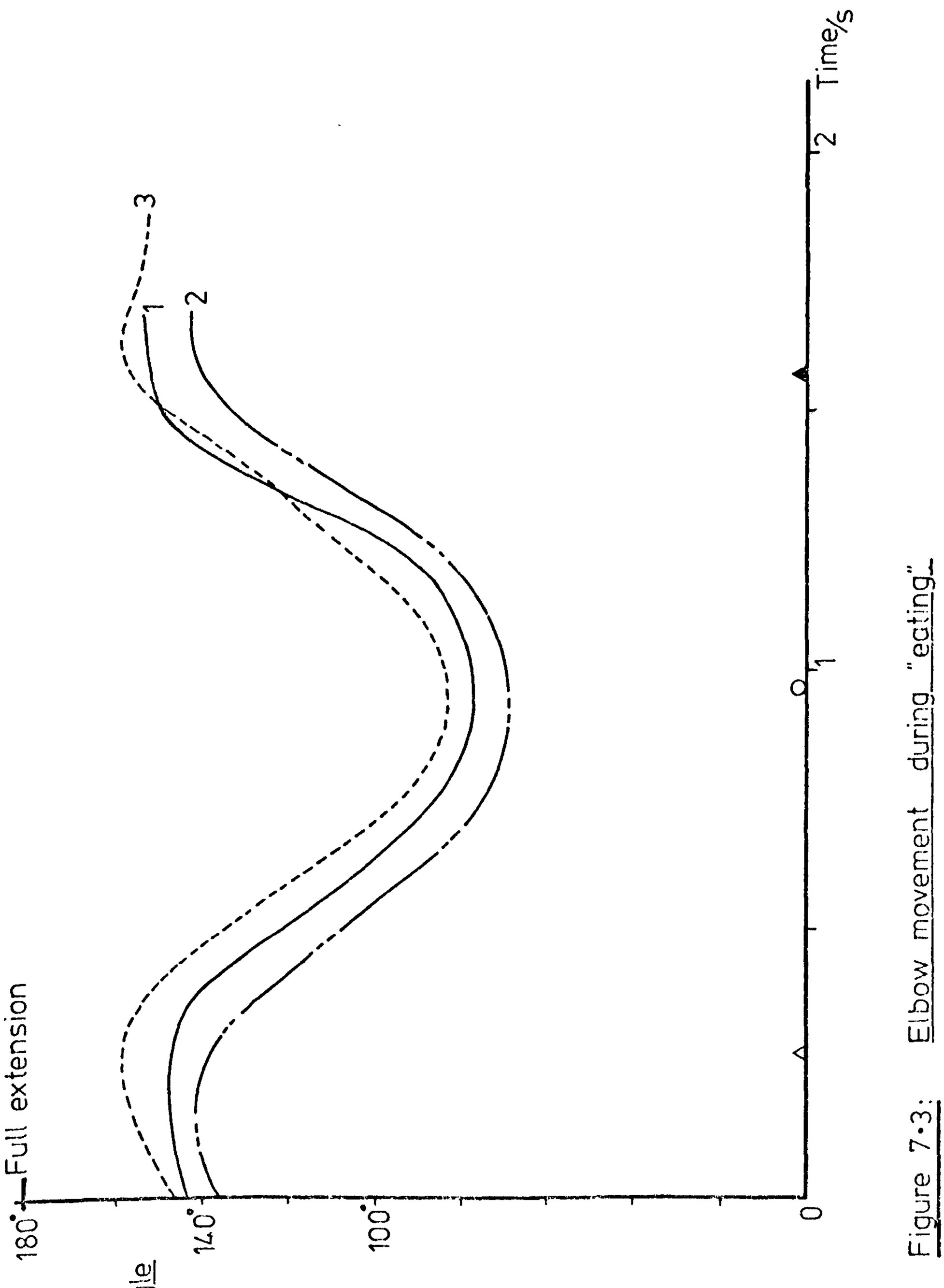

Figure 7·3: Elbow movement during

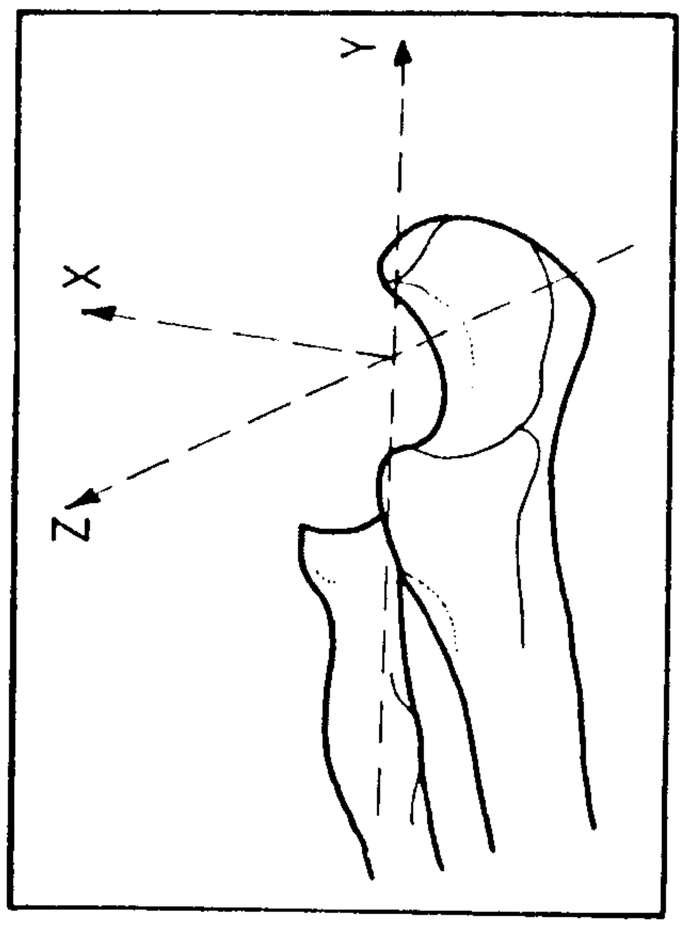

Figure 7·4: Forces acting along Xu during "eating".

7.2.2 External force system: The inertial forces acting on the elbow joint are detailed in figures 7.4, 7.5 and 7.6 and they are defined in terms of the ulnar axis system.

Considering forces in the X_U direction (Figure 7.4), the large negative values occurred when the forearm was accelerated in a forward direction. At that time, the arm was held in the "anatomical" position and the direction of movement was approximately parallel to the X axis of the ulna. Consequently, the forces in the X_U direction were directly related to the inertial actions applied to the forearm. The positive force which was experienced during the "braking" period was decreased as the arm was returned to the initial location. The weight of the forearm assembly (approximately 20-25 N) accounted for the apparent "D.C.-shift" of the traces in figure 7.4 and it is interesting to note that the "over-extension" experienced by Subject No.3 resulted in a significant negative force compared to the other subjects.

A similar situation existed for the forces acting in the Y_U direction (see figure 7.5) in so far as gravitational effects produced an axial "pull" on the forearm when the arm was outstretched at the start of the movement. As the elbow was progressively flexed, the angular movement of the forearm resulted in greater centrifugal forces and produced the minimum values of -30 to -40 N. As the forearm was rotated to a horizontal position, the effects of gravity in the Y_U direction were reduced. At the "changeover" period the Y_U axis was inclined at approximately 45° to the horizontal plane and this produced an axial "thrust" on the elbow as shown by the positive peaks of 10 to 20 N in figure 7.5. Normality was restored (approx - 20N) on completion of the activity.

The force actions in the lateral (Z_U) direction are detailed in figure 7.6 and were negative throughout the exercise. Initially, the position of the forearm produced a component of weight in the $-Z_U$ direction and the magnitude of this force was approximately 50 -75% combined weight of the forearm, hand and lead ball (up to -20 N). At "changeover", the forearm had undergone rotations about all three reference axes and the Z-axis of the ulna was

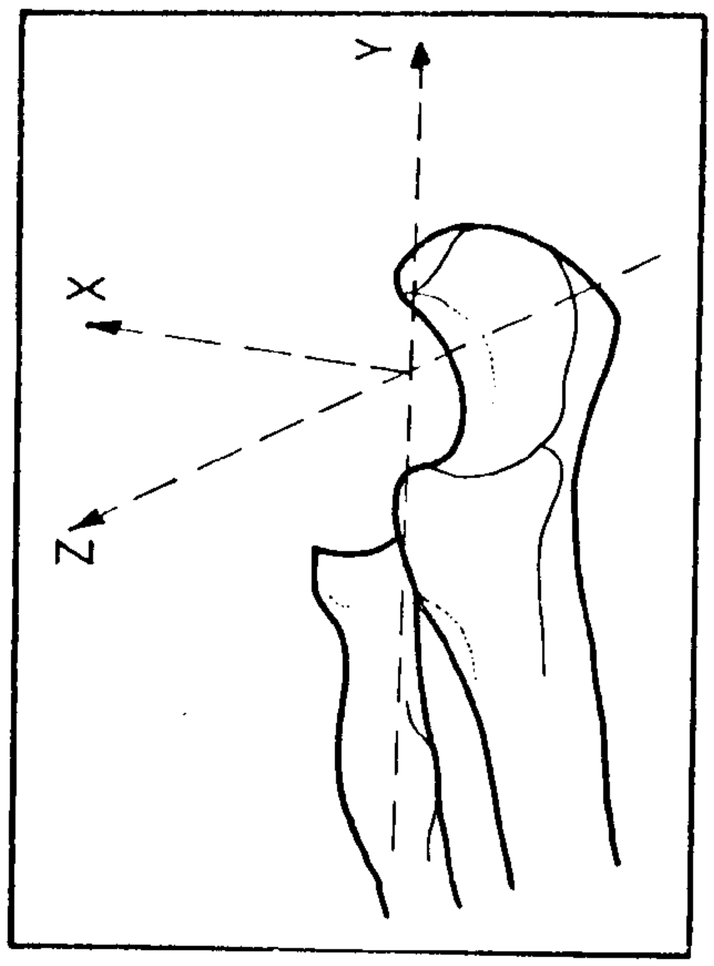

Figure 7•5: Forces acting along Yu during "eating".

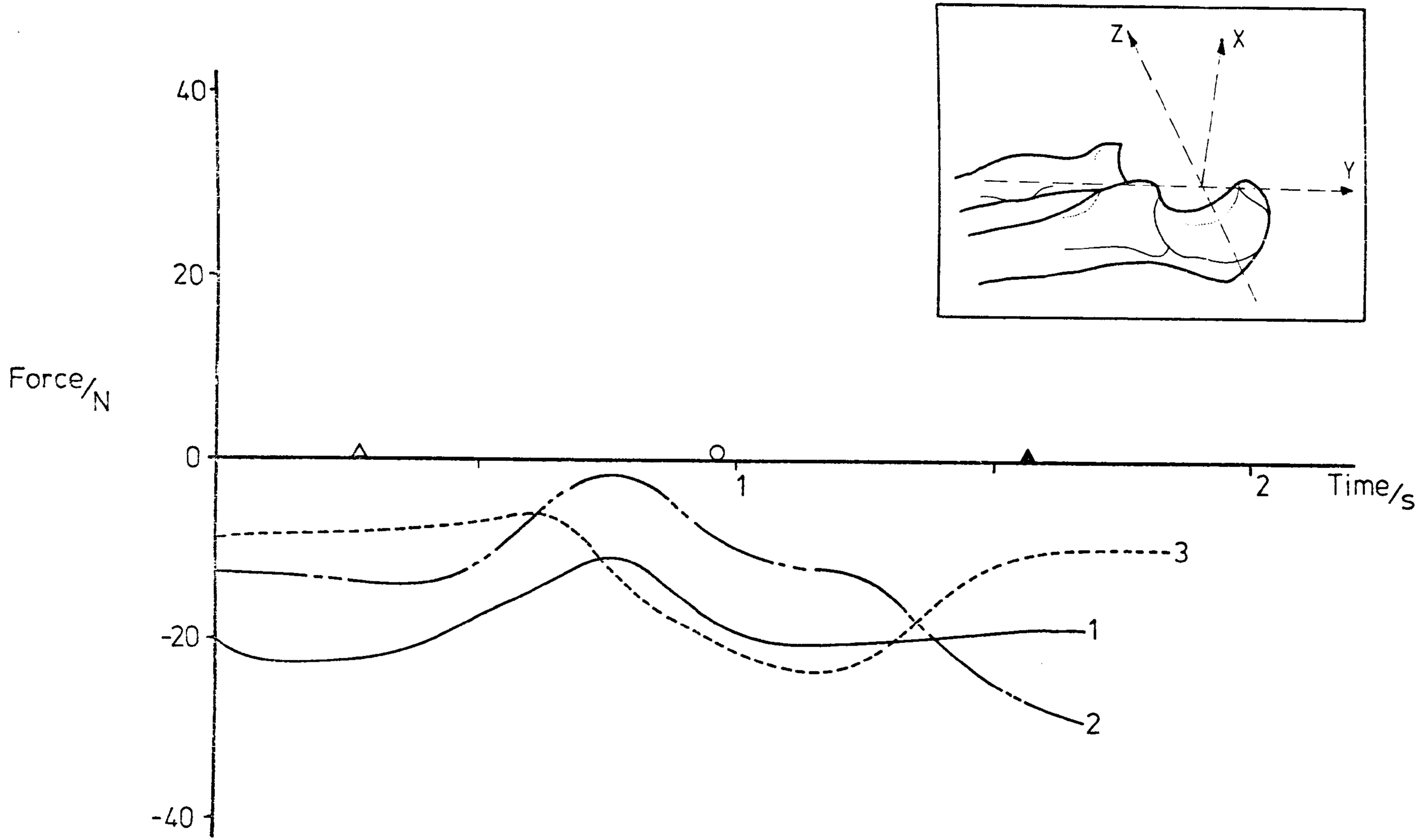

Figure 7·6: Forces acting along Z_U during "eating".

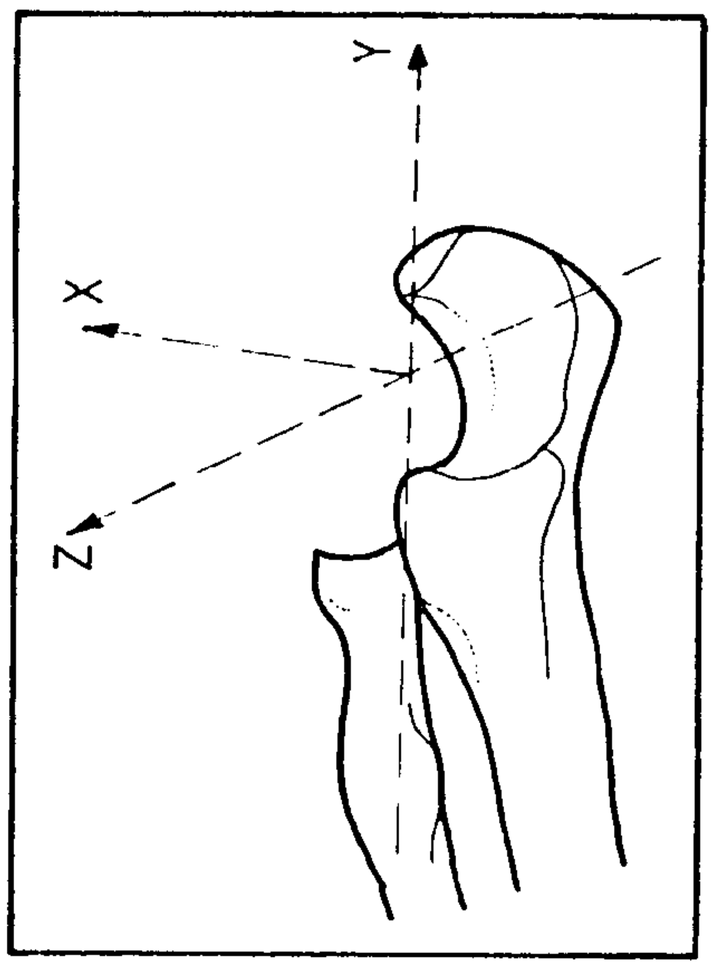

Moments acting about X_u during "eating"

Figure 7·7:

still positioned in an upward direction. Although the effects of gravity produced a negative Z_U force during the deceleration phase as the changeover position was approached, the magnitude of this "weight" was reduced by the direct inertial actions. A peak of -2 N was therefore experienced at t = 0.75 s (approximately).

The moment effects applied to the X, Y and Z axes of the elbow joint are shown in figures 7.7, 7.8 and 7.9. The inertial moments resulting directly from angular accelerations were small and, for this reason, the moments in the X_U and Z_U directions correspond to inertial forces along the Z_U and X_U axes respectively. (Lever arm equals the Y_U coordinate of the forearm C. of G.) Inertial moments of 3 Nm were obtained for moments about the long axis of the forearm (figure 7.8) and were minimal compared to moments about the two other axes.

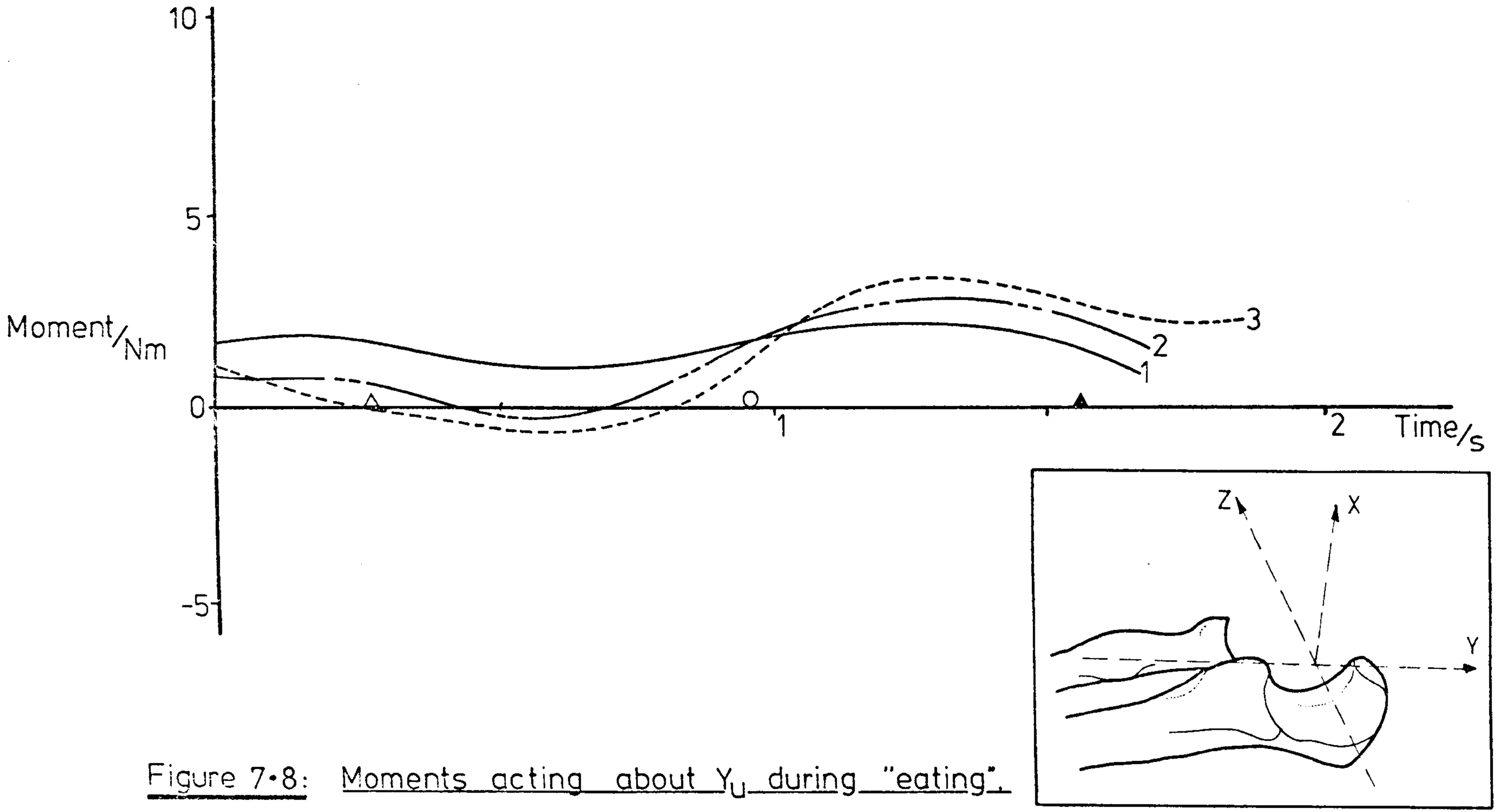

Figure 7·8: Moments acting about Y_U during "eating".

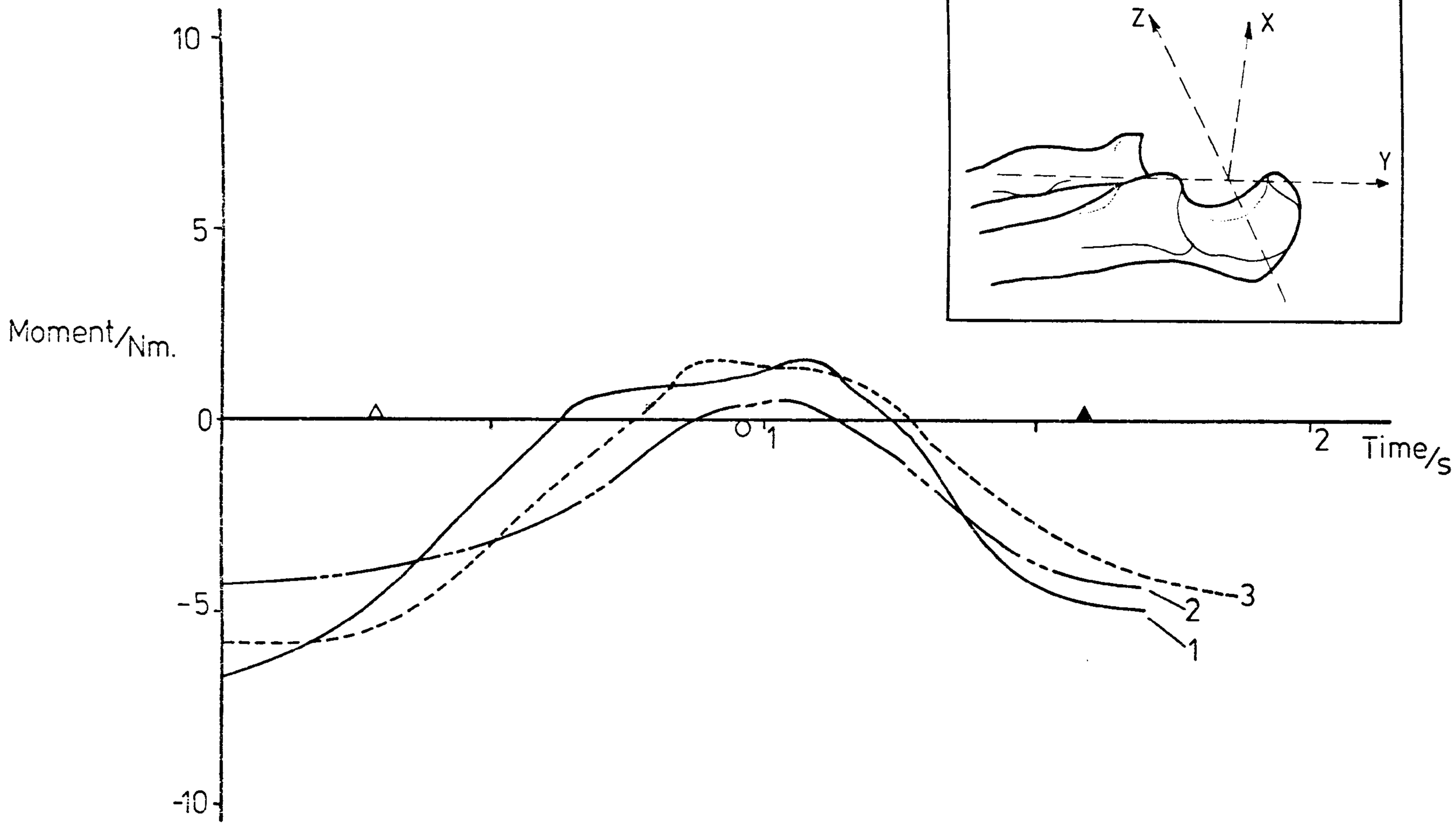

Figure 7·9: Moments acting about Z_u during "eating".

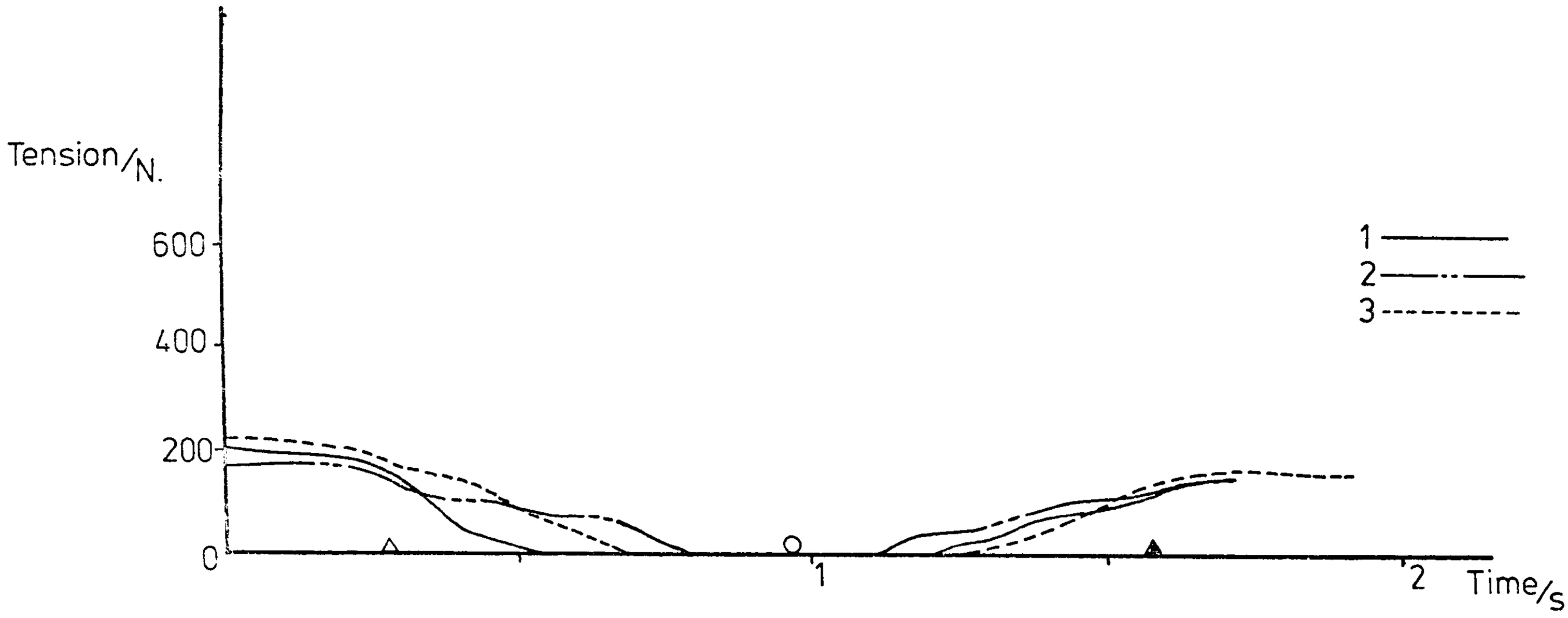

Figure 7·10: Tensions produced in the main flexors during "eating".

7.2.3 Muscle forces: Figures 7.10 and 7.11 show the tensions produced in the flexor group muscles and the triceps muscle respectively.

Flexor activity was dominant during the "lifting" stage of the movement and initial tensions of around 200 N were experienced in biceps and brachialis with half that value in brachioradialis. As the elbow was flexed, the effective lever arms of the muscles became increased and the muscle tension fell off to zero in a linear fashion. The corresponding decrease in M_z followed a similar pattern (figure 7.9).

The deceleration of the forearm (t = 0.75 secs) was executed with triceps activity (see figure 7.11) and corresponded to the positive portion of figure 7.9. Tension remained in the triceps muscle during the acceleration of the forearm at the beginning of the return movement (elbow extension).

Control of the movement of the forearm against gravity was effected by flexor activity which increased during the "braking" phase of the activity. The non-antagonistic action of the flexor and extensor muscle groups of the elbow region is verified by the typical electromyogram shown in figure 7.12.

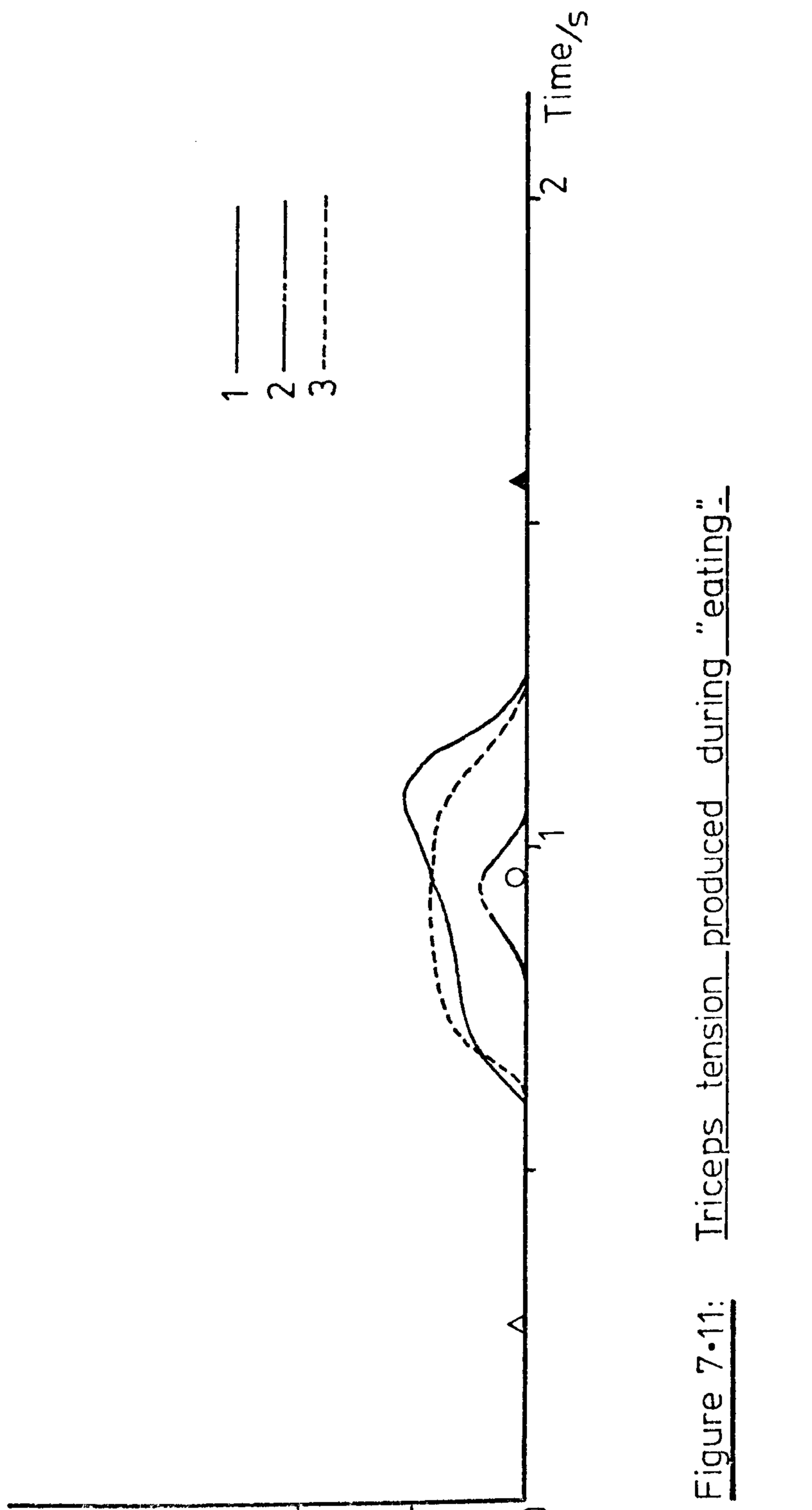

Figure 7·11: Triceps tension produced during "eating".

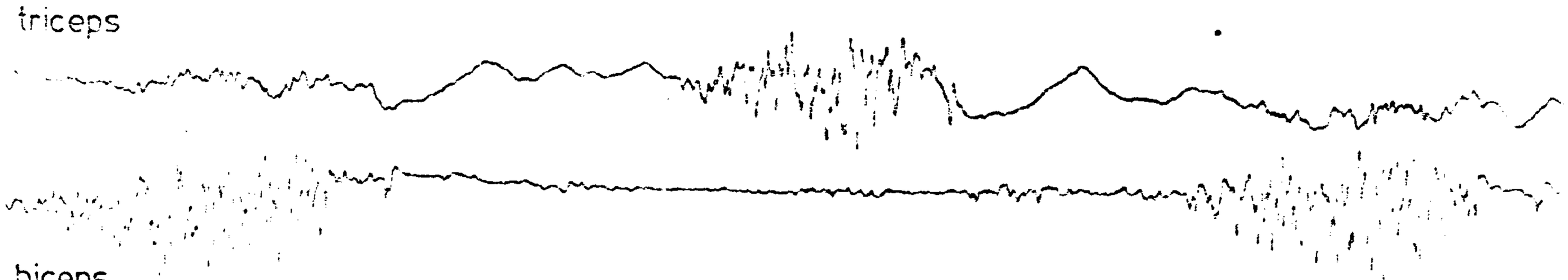

Figure 7-12: Muscle activity recorded during "eating" (pen recorder)

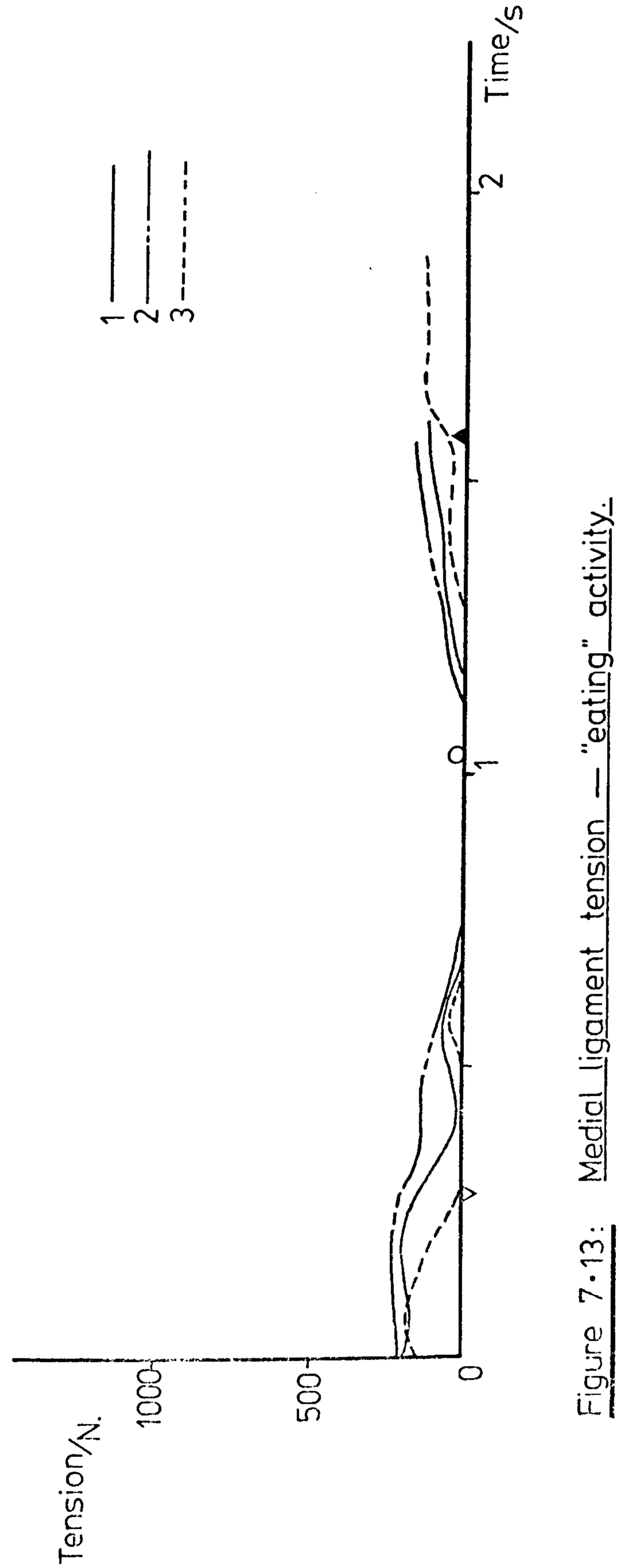
1
2
3
Time/s
0
1
2
Medial ligament tension — "eating" activity.
Tension/N.
1000
500
0

Figure 7·13:

7.2.4 Ligament forces: The ligamentous structures on the medial and lateral sides of the elbow joint transmitted force actions as shown in figures 7.13 and 7.14 respectively. The initial tension of 200 N in the medial collateral ligament reduced to zero as the deceleration of the forearm was initiated (t = 0.75 secs) and lateral ligament action was dominant around the "changeover" period (approximately 100 N). Tensions of 100 N were experienced in the medial ligament for the remainder of the activity.

7.2.5 Joint forces: The joint forces corresponding to the preceding muscle and ligament tensions are shown in figures 7.15 and 7.16. At the start of the activity, slightly larger forces were experienced on the lateral surface of the trochlear notch than those produced on the medial surface (350 N compared to 200 N). For the remainder of the "eating" activity however, the two joint surfaces were loaded uniformly.

As a result of flexor activity at extreme values of elbow angle, the contact force between the radial head and the capitulum was prominent at the beginning and end of the movement. Figure 7.17 shows that compressive forces as high as 200 N were experienced.

Figures 7.18, 7.19 and 7.20 show the complete system of internal force actions for the three subjects.

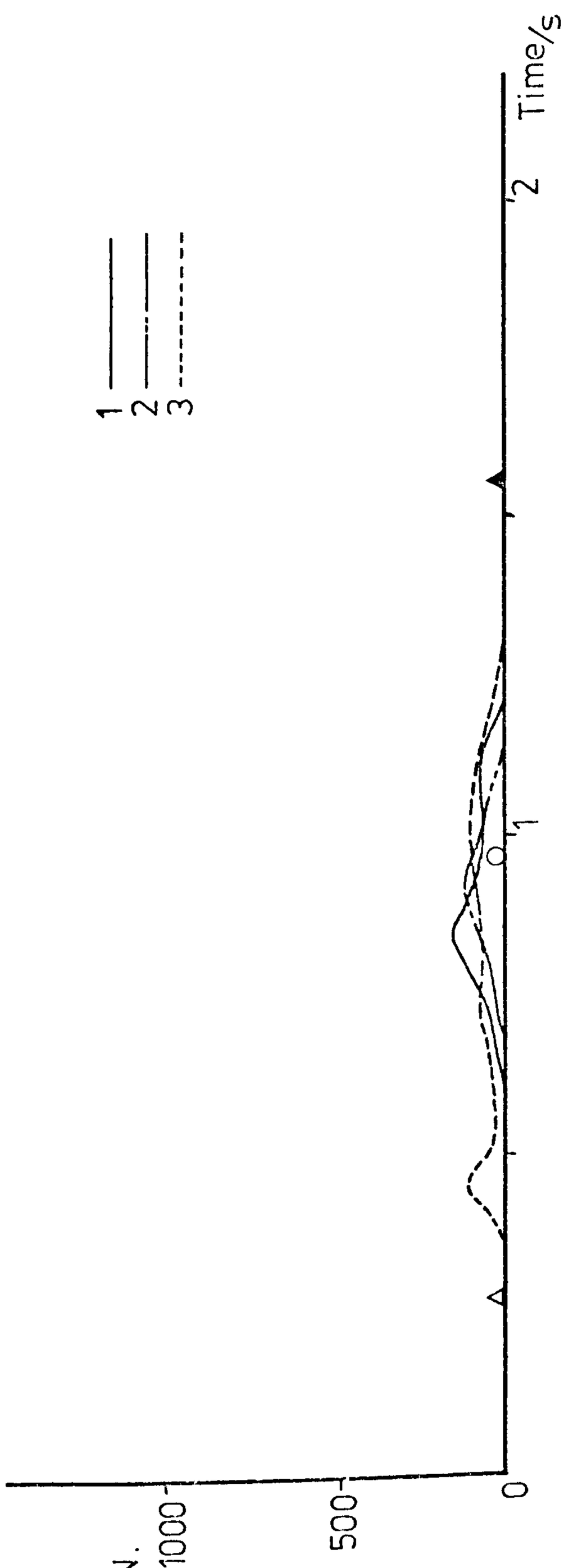

Figure 7·14: Lateral ligament tension — "eating" activity.

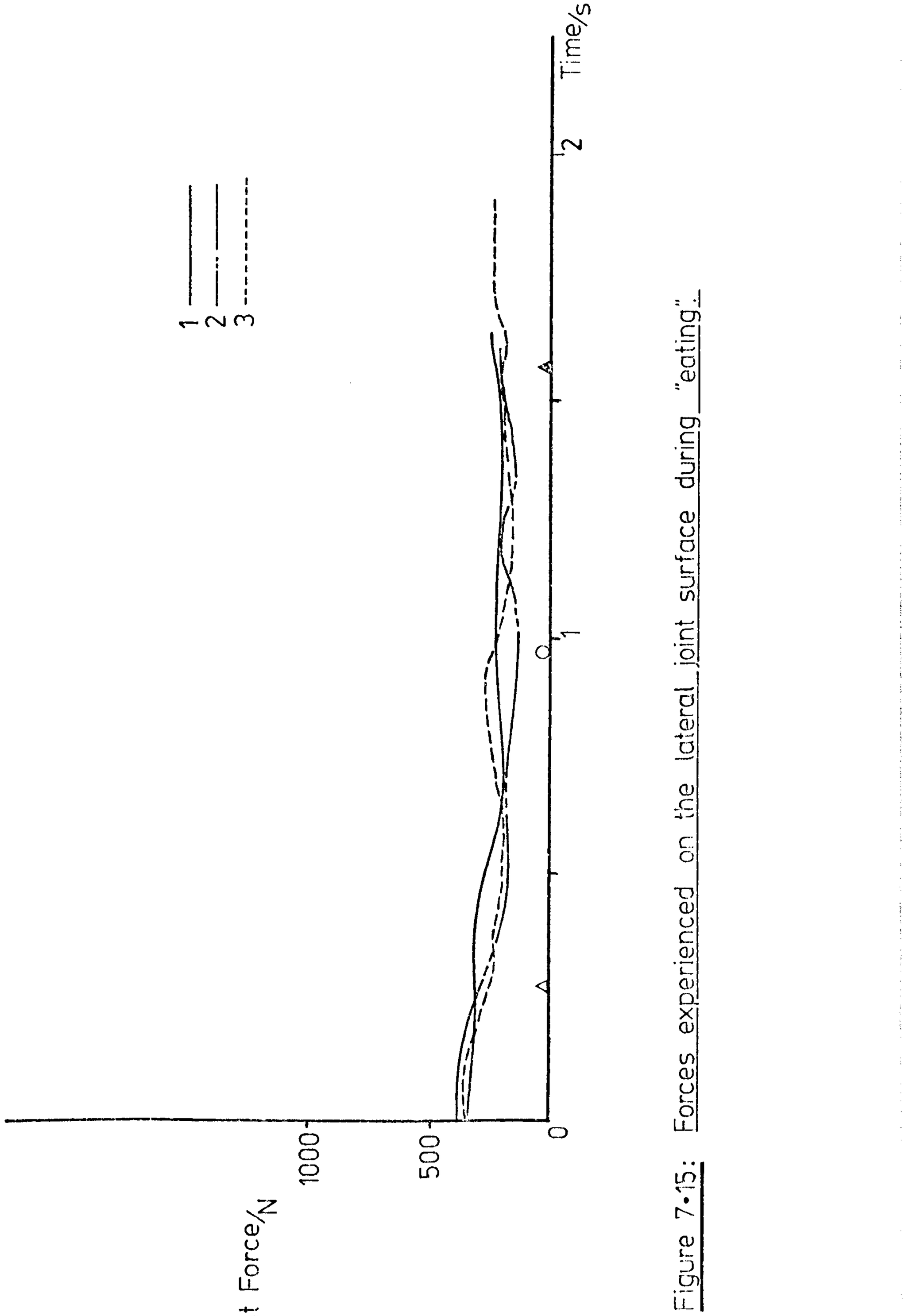

Figure 7•15: Forces experienced on the lateral joint surface during "eating"

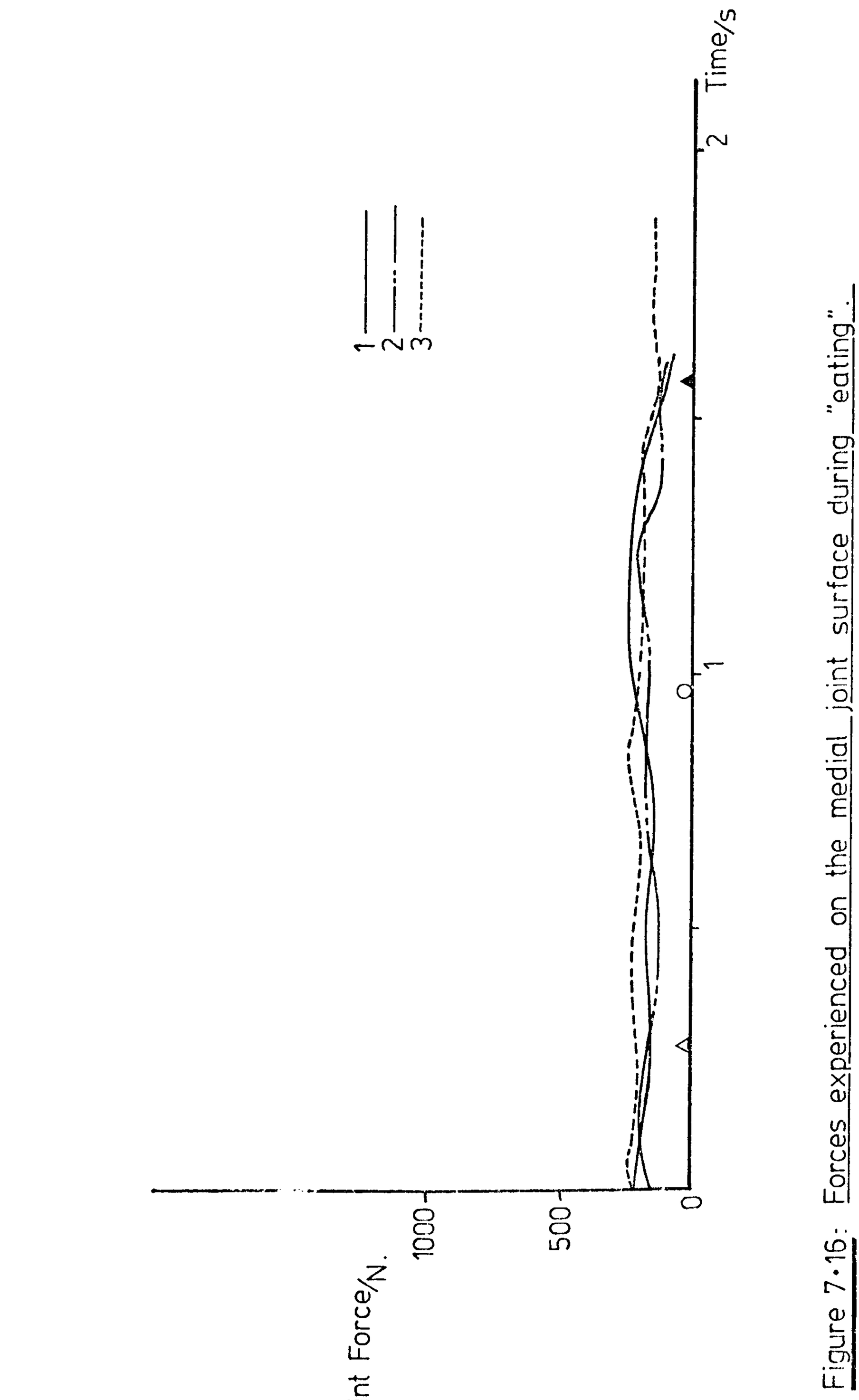

Forces experienced on the medial joint surface during "eating".

Figure 7·16: F

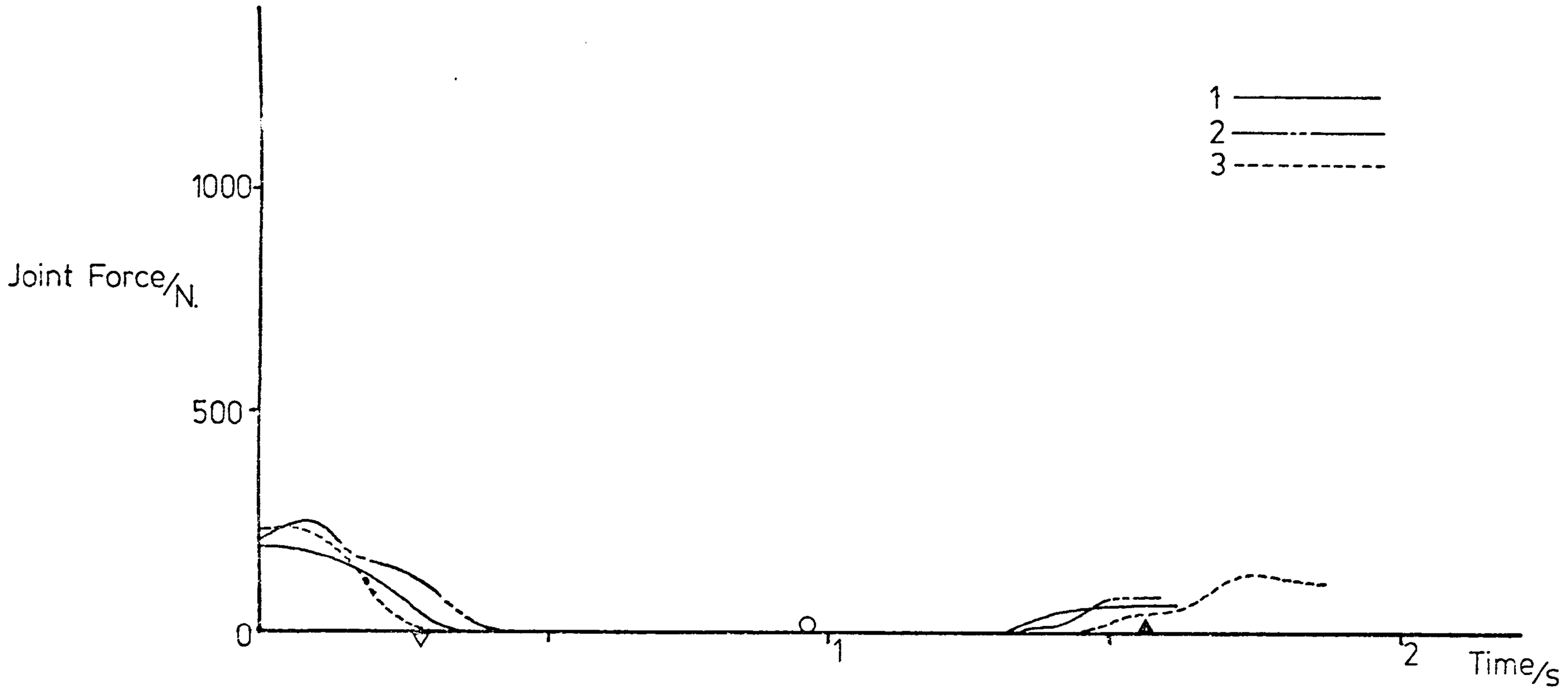

Figure 7·17: Forces experienced on the radial head during "eating".

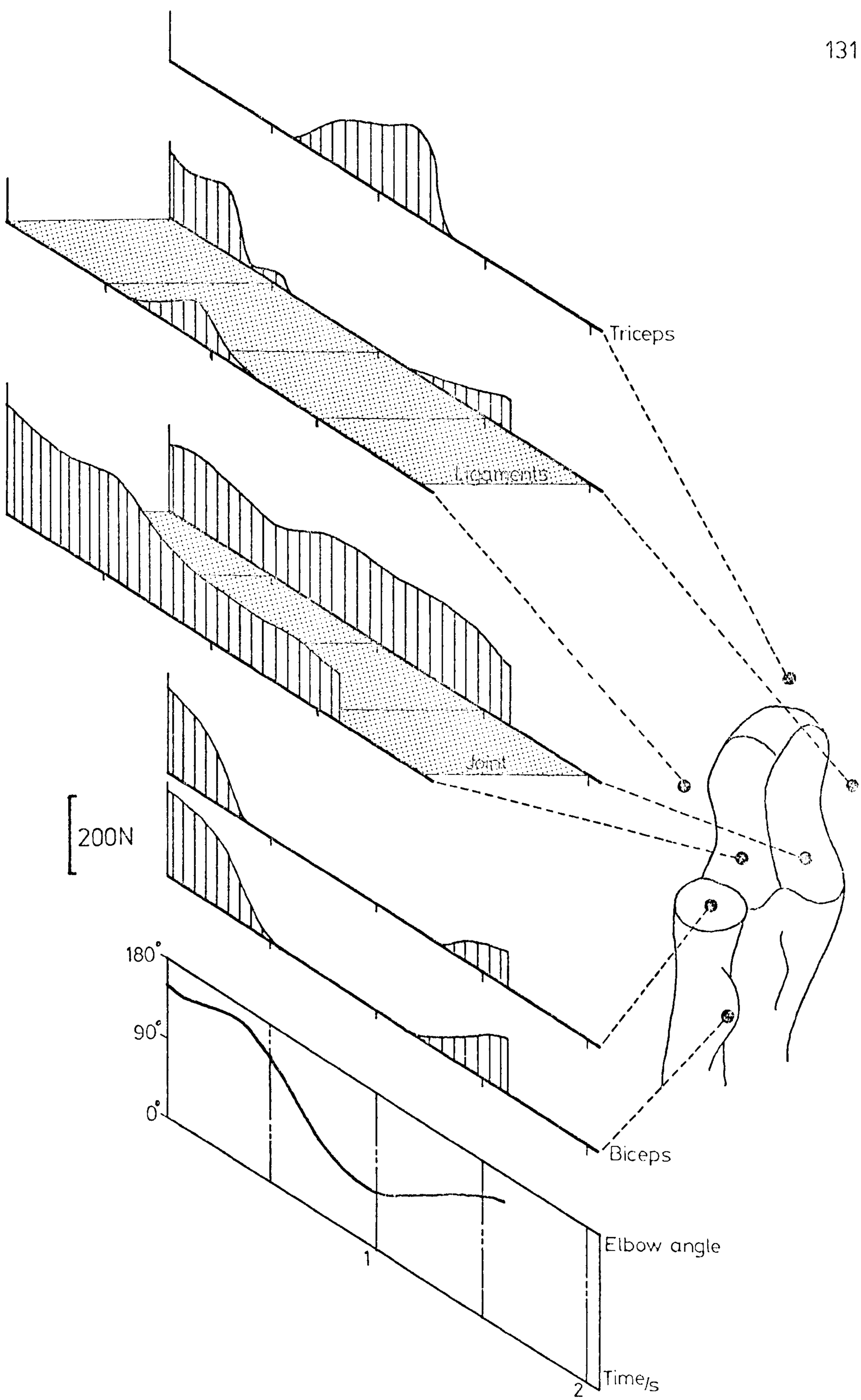

Figure 7·18: Force analysis. [subject 1—"eating"]

131a

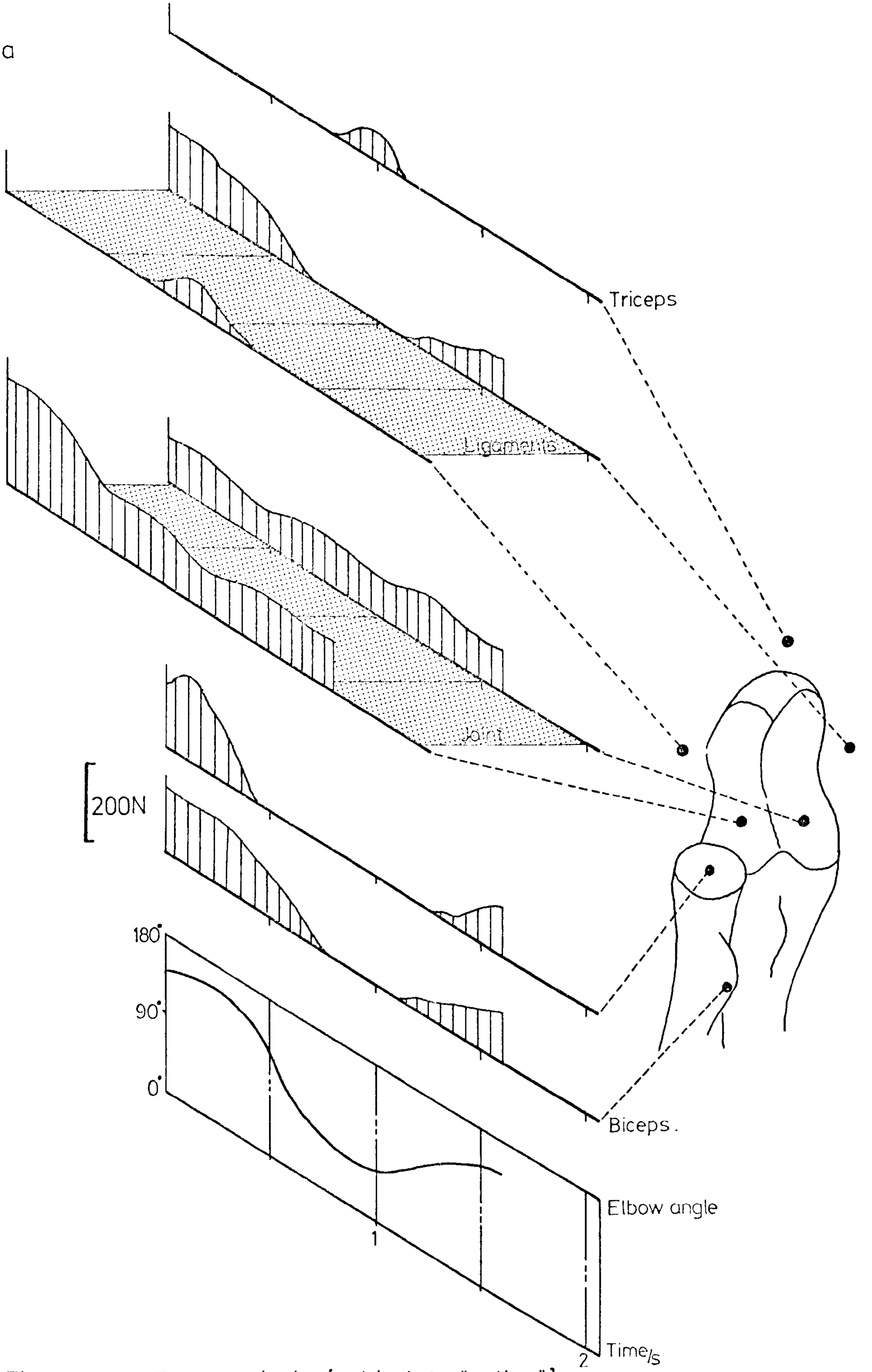

Figure 7·19: Force analysis. [subject 2—"eating"]

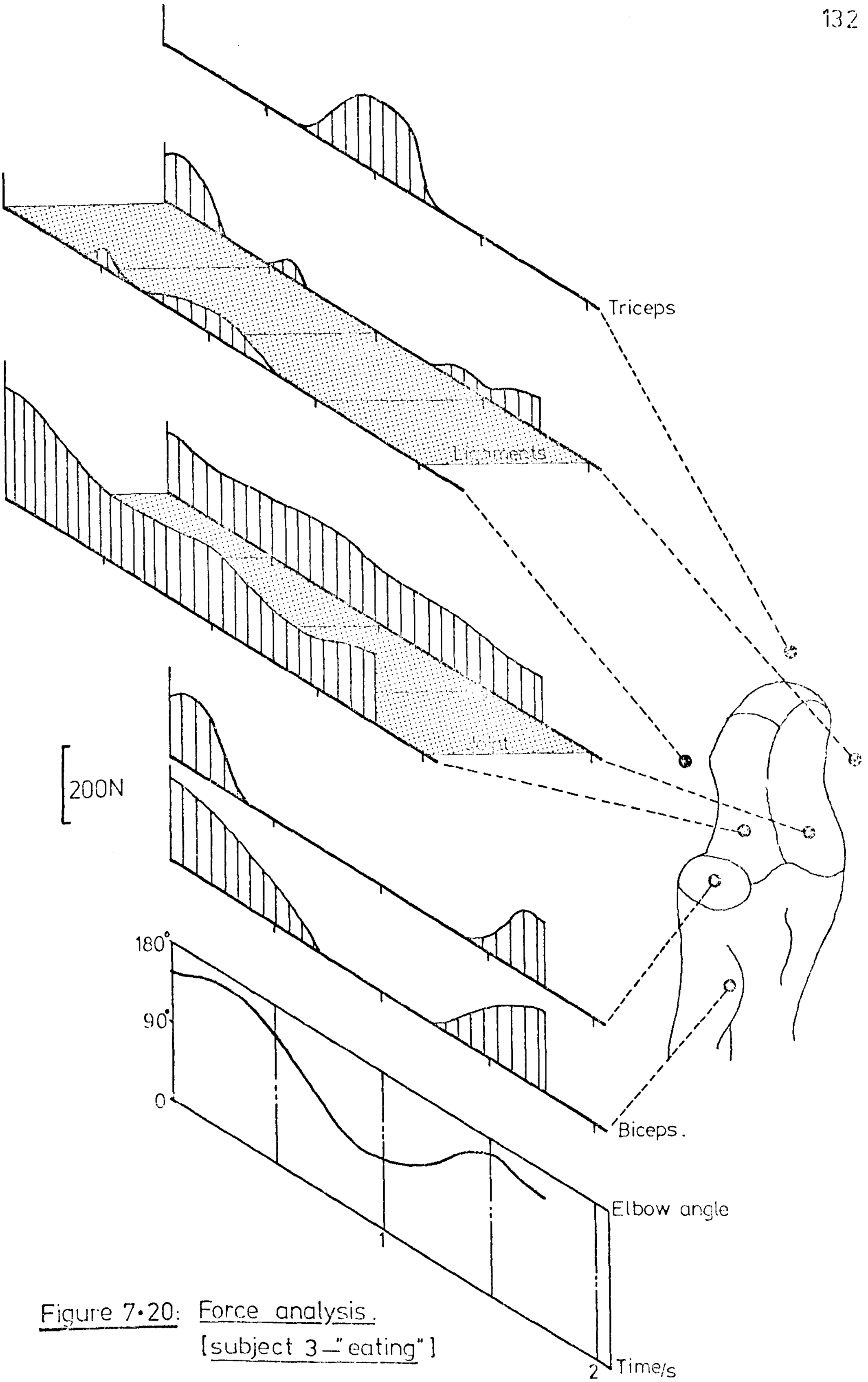

Figure 7·20: Force analysis.
[subject 3 — "eating"]

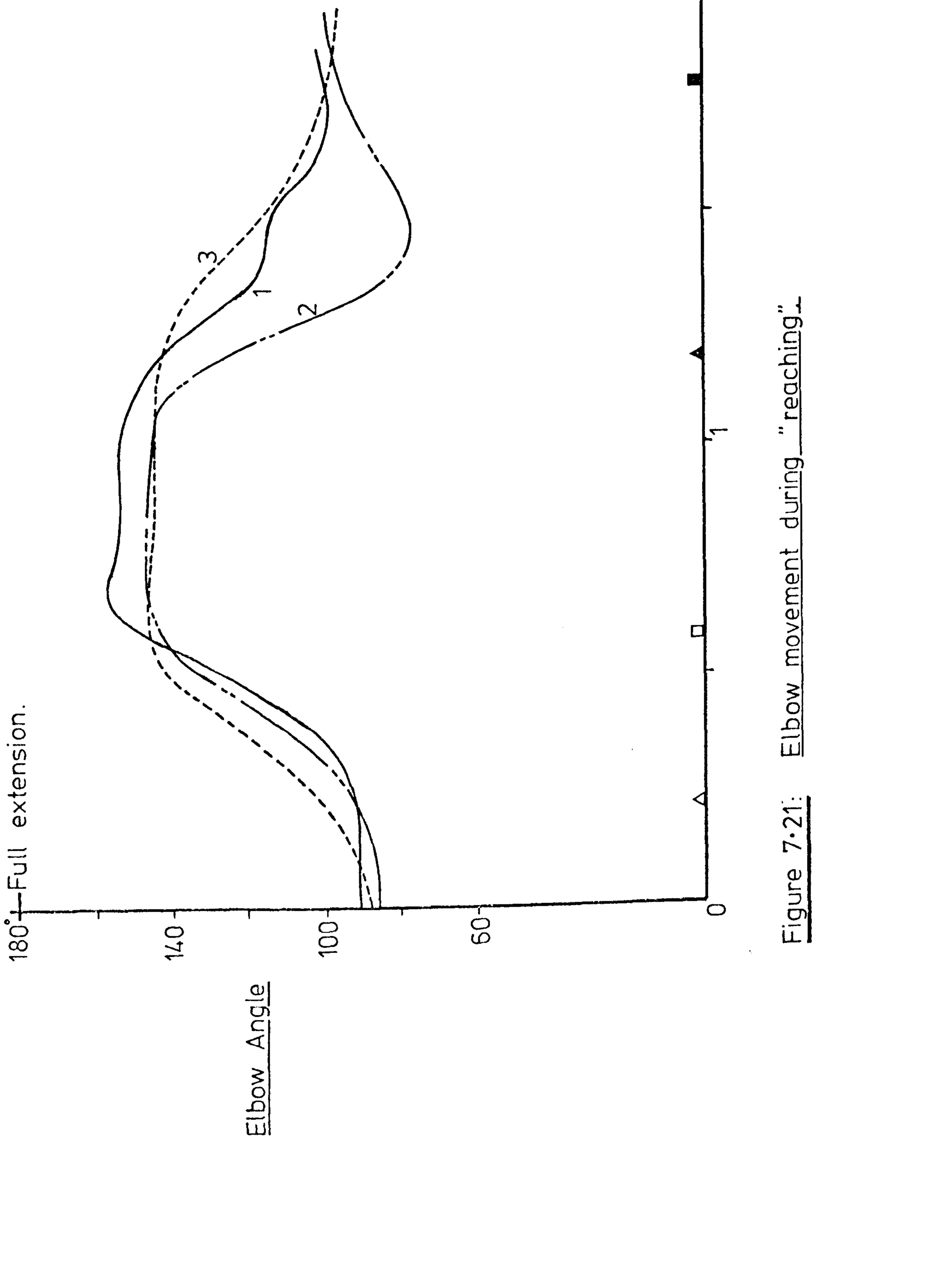

Figure 7·21: Elbow movement during "reaching".

7.3 "Reaching" Activity:

Four distinct time instants became apparent during the analysis of the "reaching" activity

a) Initiation of elbow extension. (△)

b) Termination of elbow extension. (□)

c) Initiation of elbow flexion. (▲)

d) Termination of elbow flexion. (■)

Although the timing of this activity was not as closely controlled as the timing of the "eating" activity the relative differences in duration between the three subjects were slight. The graphs were therefore labelled for the "average" of such time instants using the symbols shown in parenthesis.

7.3.1 Movement: Figure 7.21 shows the variation of the elbow angle for the three subjects analysed and it can be seen that the same overall range of movement was covered by each subject. Elbow extension was performed at an approximate rate of 4 rad/s and the fully outstretched position was obtained at $t = 0.3$ s. Throughout the "changeover" period from shoulder abduction to shoulder adduction the elbow angle was held constant in all cases. During the return movement Subject No.3 experienced a smooth return to the original elbow position whereas Subject No.2 overshot the finishing position and performed 11^{o} of elbow extension at $t = 1.5$ s. Subject No.1 performed the return movement in two stages and the elbow angle was held constant for 0.15 s. A slight amount of elbow extension was again necessary (at $t = 1.7$ s) to bring the limb to the final position. In general however, the duration of each movement was relatively constant at 1.85, 1.95 and 1.95s.

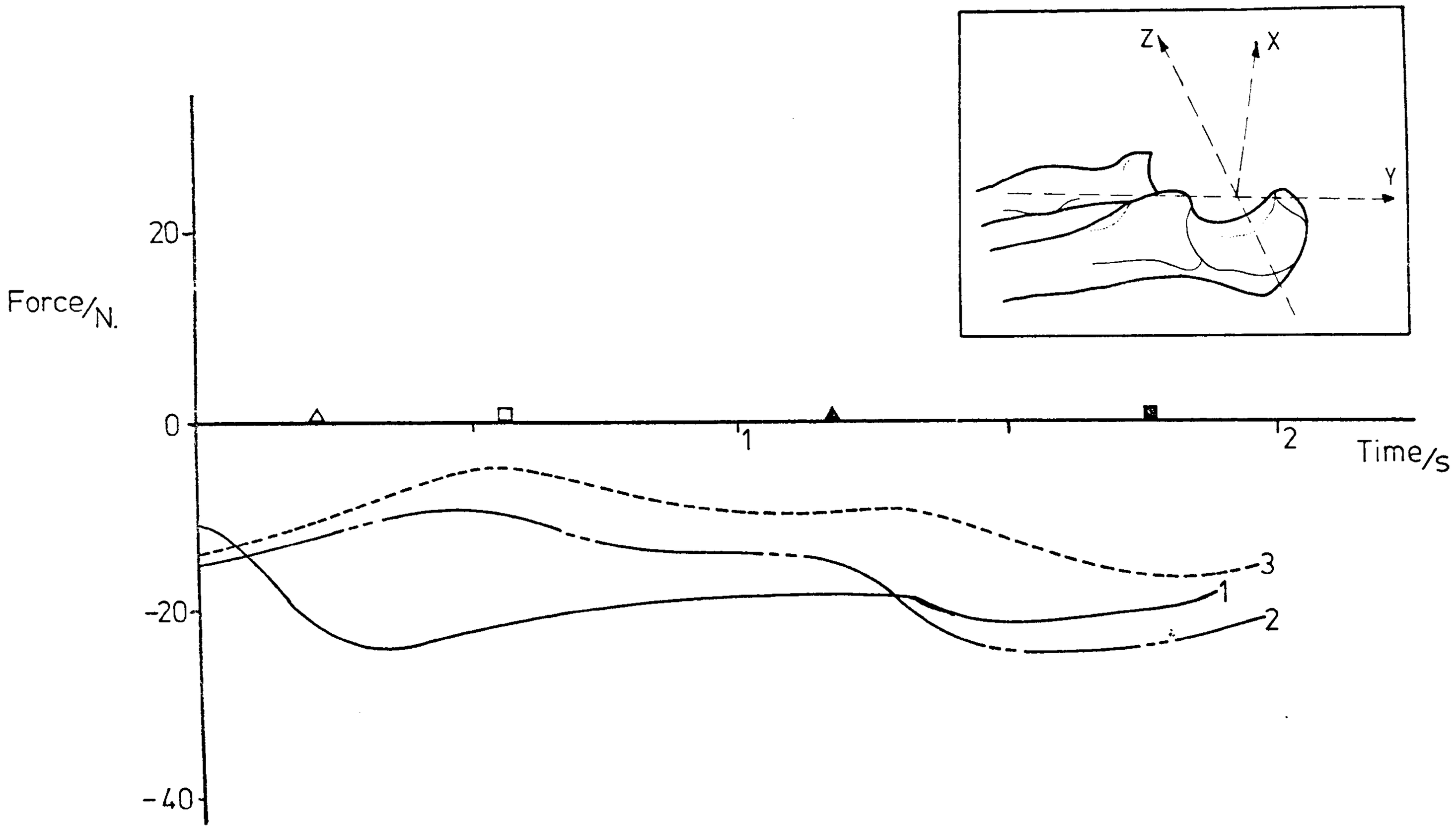

Figure 7·22: Forces acting along Xu during "reaching".

7.3.2 External force system: Referring to figure 5.14, the orientation of the X-axis of the ulna was always positively upwards. For this reason, the X-forces acting on the elbow joint were negative throughout the movement as shown in figure 7.22. In a similar manner, the forces in the Y_u direction were positive (see figure 7.23) and represented an axial "thrust" on the forearm. When the long axis of the forearm (Y_u) approached the horizontal position at the beginning and end of the movement, this thrust of 20 N was very small in comparison to the forces experienced in other directions.

Concurrent with the X_u force actions on the forearm, large negative forces were calculated to be acting in the lateral direction (Z_u) at the beginning and end of the movement (see figure 7.24). When the arm was decelerated just before t = 0.6, the inertial forces generated in the Z_u direction balanced the gravitational effects and the net force approached zero.

As experienced in section 7.2.2, the moments in the X_u and Z_u directions were dependent on the forces produced in the Z_u and X_u directions respectively (see figures 7.25 and 7.27). However, the magnitudes of the moments occurring in the Y_u and Z_u directions (Figures 7.26 and 7.27) were small compared to the moments calculated to be acting in the X_u direction. Maximum values of 9 Nm were recorded.

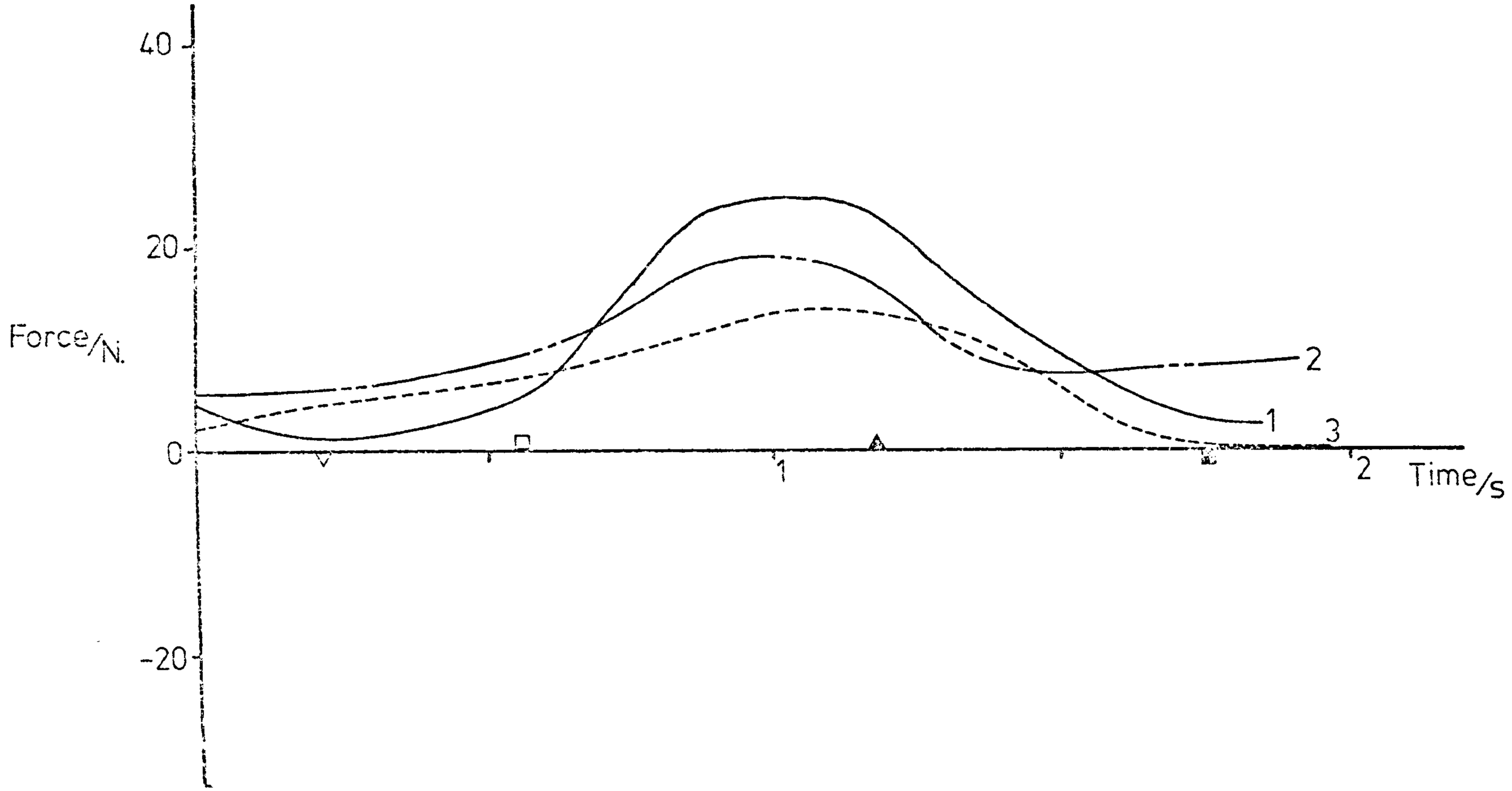

Figure 7·23: Forces acting along Y_U during "reaching".

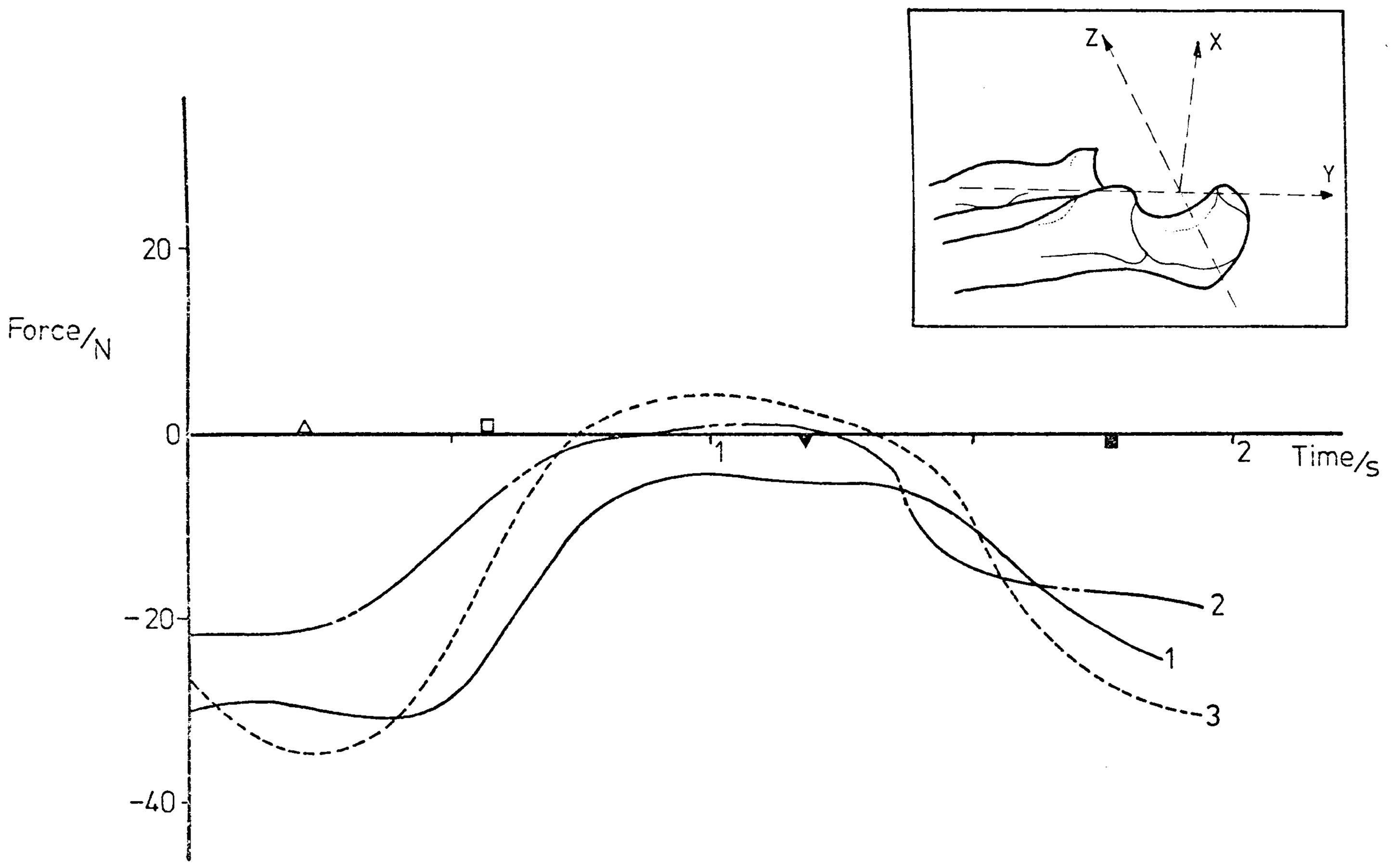

Figure 7·24: Forces acting along Z_u during "reaching".

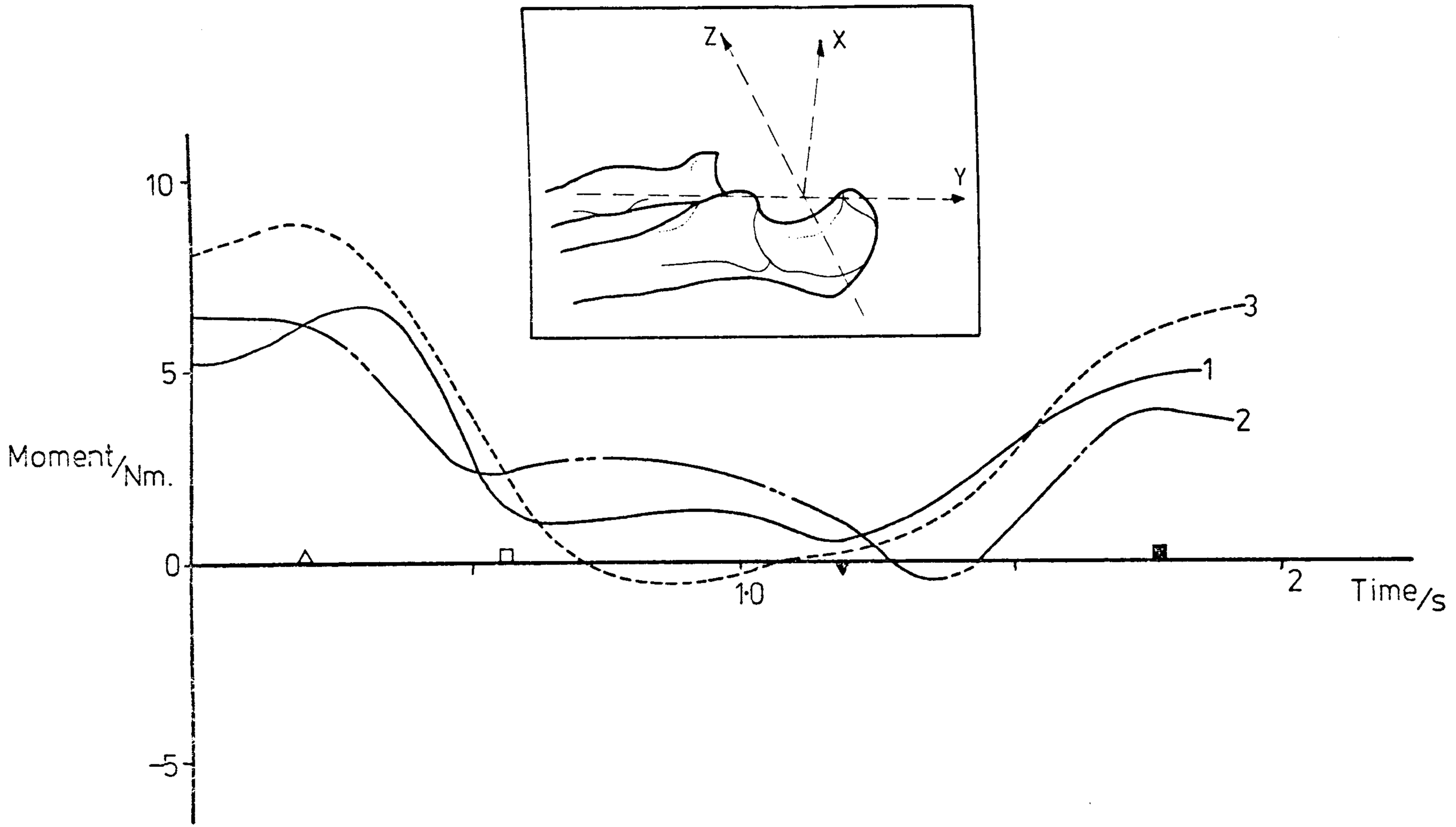

Figure 7·25: Moments acting about X_U during "reaching".

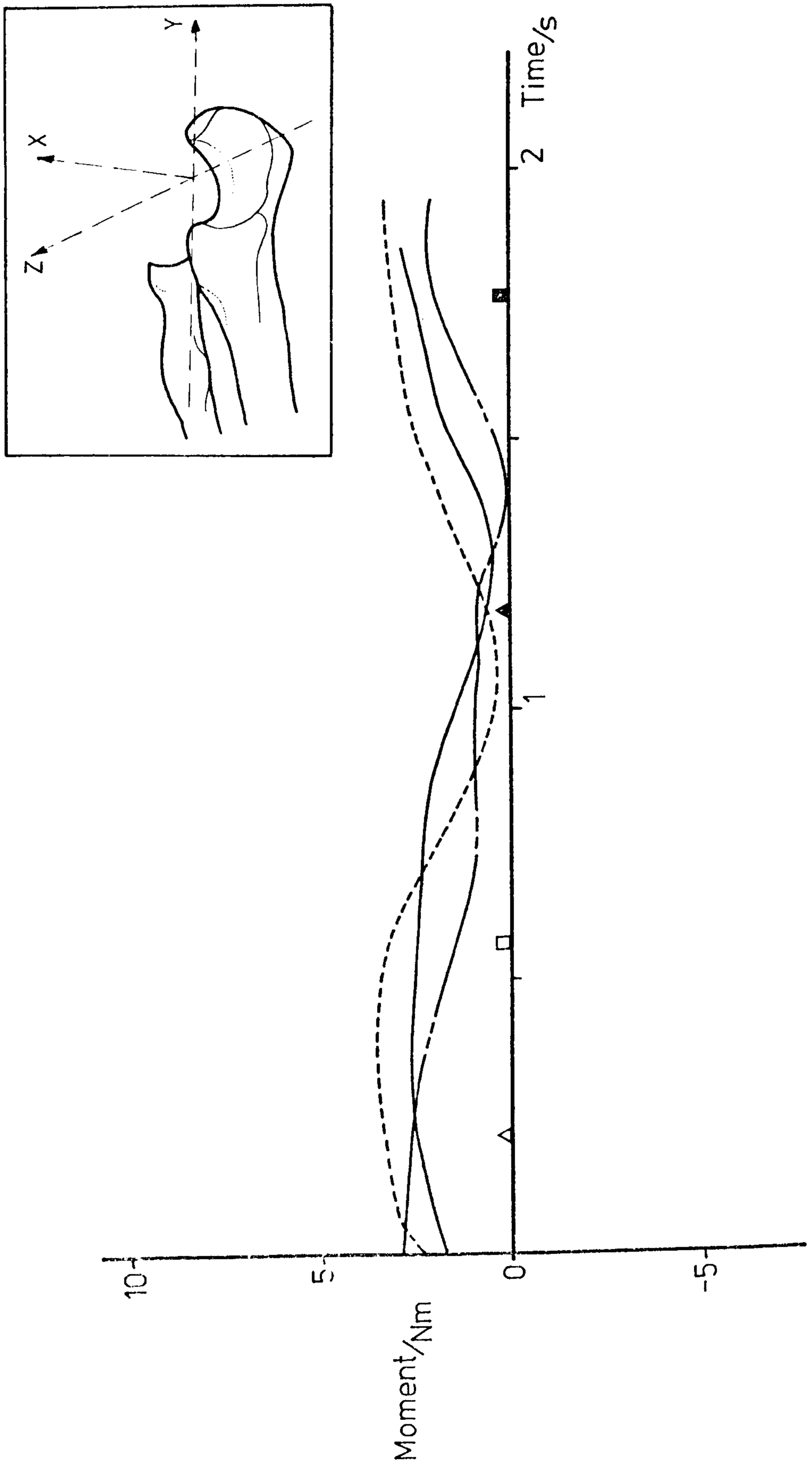

Figure 7·26: Moments acting about Y_u during "reaching"

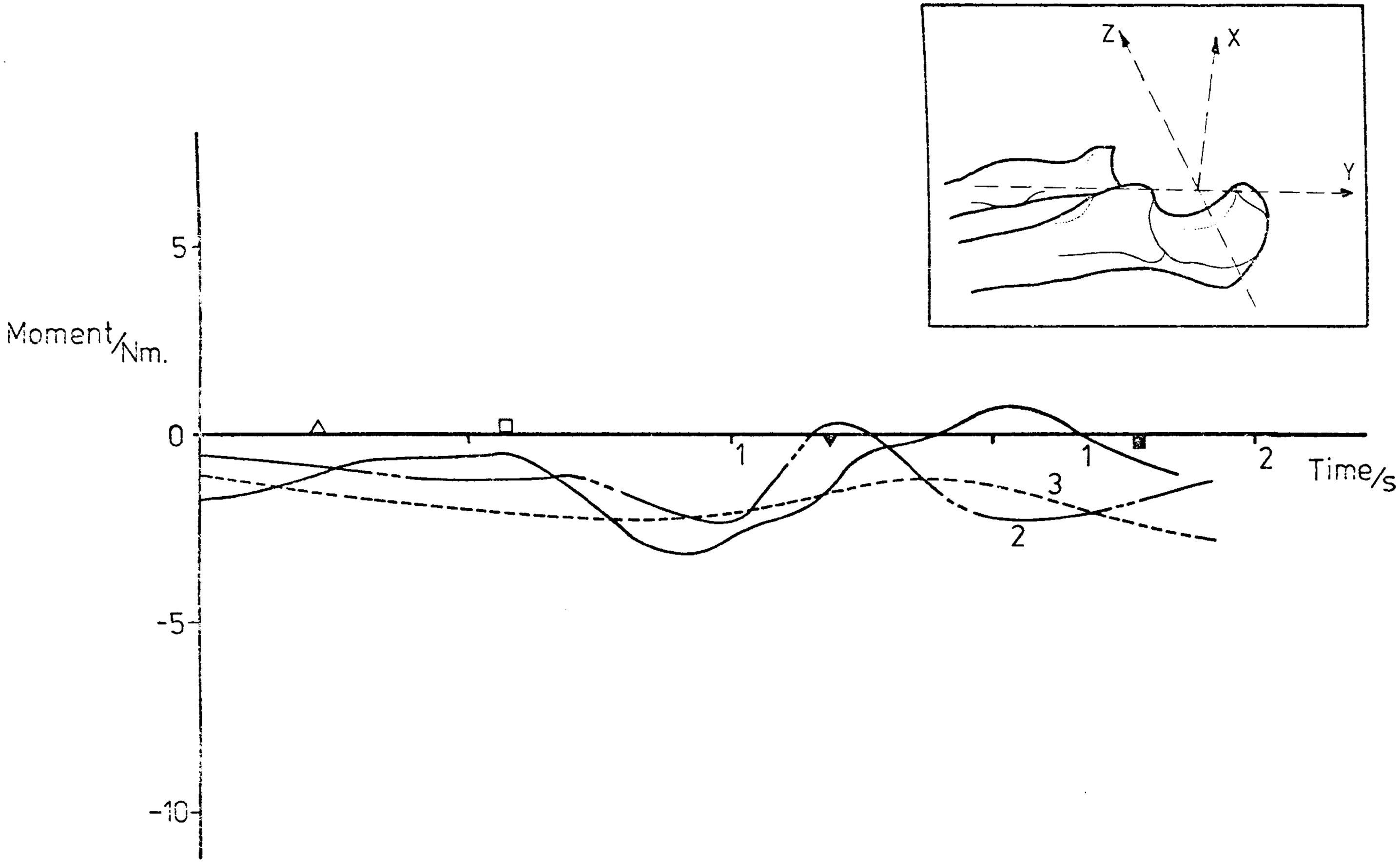

Figure 7·27: Moments acting about Z_U during "reaching".

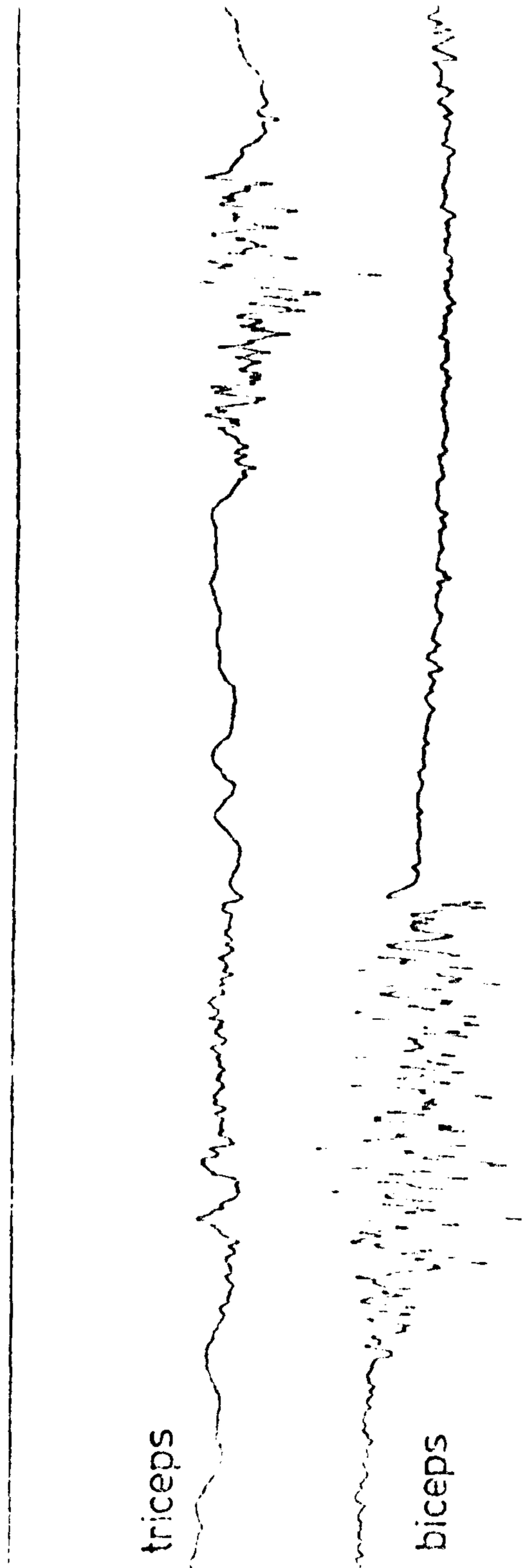

Figure 7.28: Muscle activity recorded during "reaching" (pen recording)

7.3.3 Muscle forces: Flexor activity was found to be dominant throughout most of the movement as shown in figure 7.29. During the first half of the exercise the flexor group resisted the extensive action of the inertial effects which occurred in the $-X_U$ direction. At the initiation of elbow flexion, the acceleration of the forearm involved increased flexor activity up to 200 N. As the arm was returned to the initial position the outburst of flexor activity was quickly followed by greatly reduced muscle tension. In one case (Subject No.2), a short burst of triceps action was experienced (see figure 7.30) which was attributable to gravitational effects.

Subject No.1 experienced triceps tension of 100 N at the end of the movement (t = 1.5s) which corresponded to the 11^{o} of elbow extension described in section 7.3.1.

7.3.4 Ligament forces: Throughout the "reaching" activity, the tension experienced in the lateral collateral ligament was very small. Figure 7.31 indicates that the tension in the lateral ligament coincided with the triceps activity of Subject Nos. 1 and 2. In general however, the majority of the relevant force actions were transmitted by the medial ligament. Tensions up to 200 N were computed (see figure 7.32).

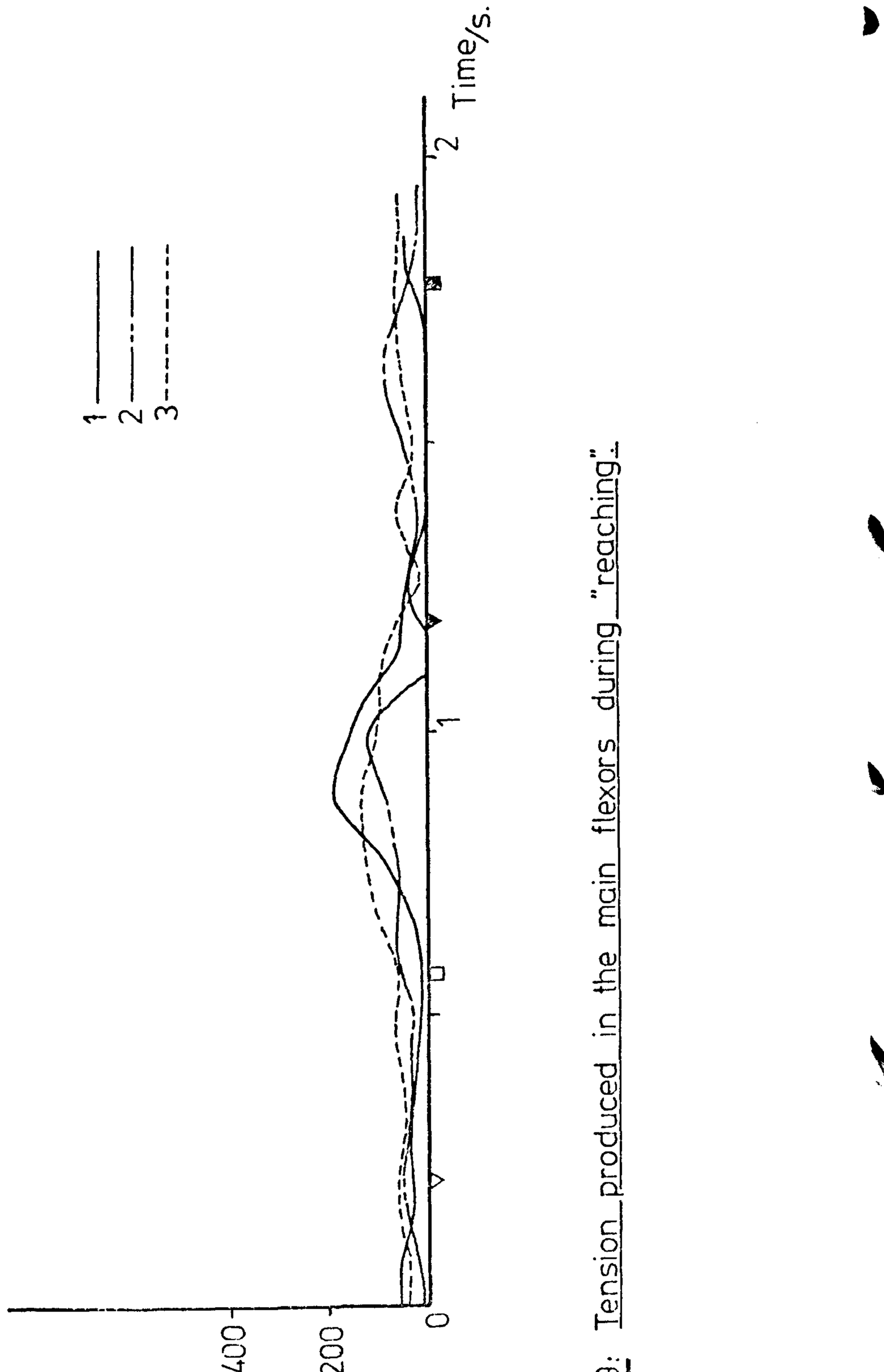

Figure 7·29: Tension produced in the main flexors during "reaching".

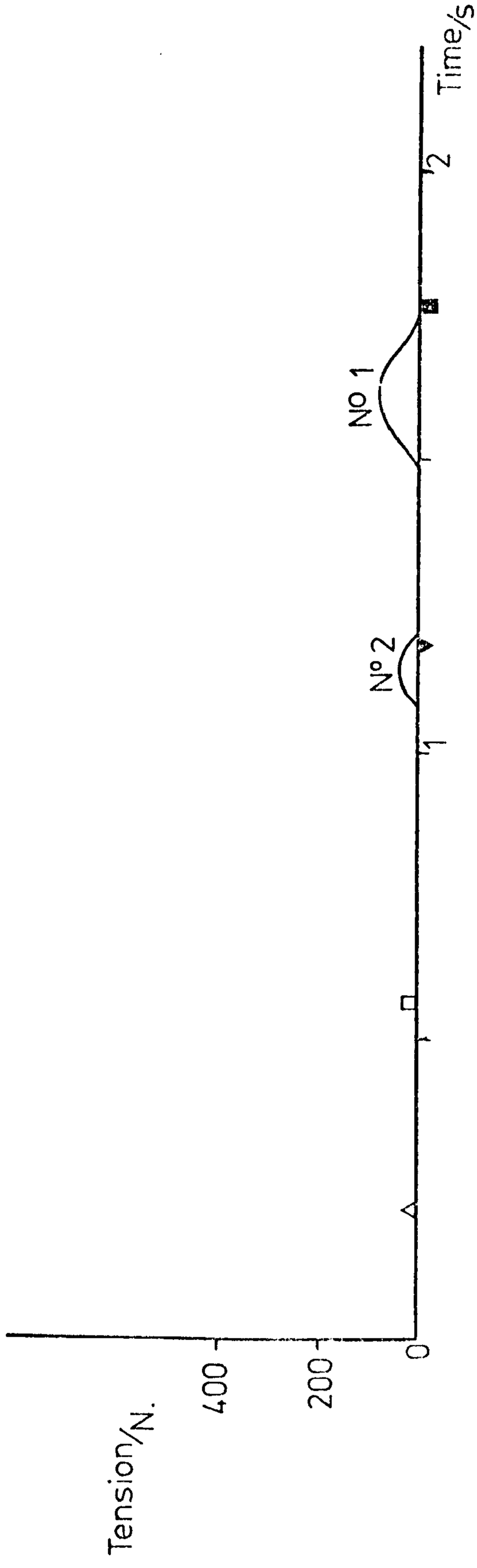
Tension/N.
400
200
0
Triceps tension produced during "reaching".
No 1
No 2
1
2
Time/s

Figure 7·30:

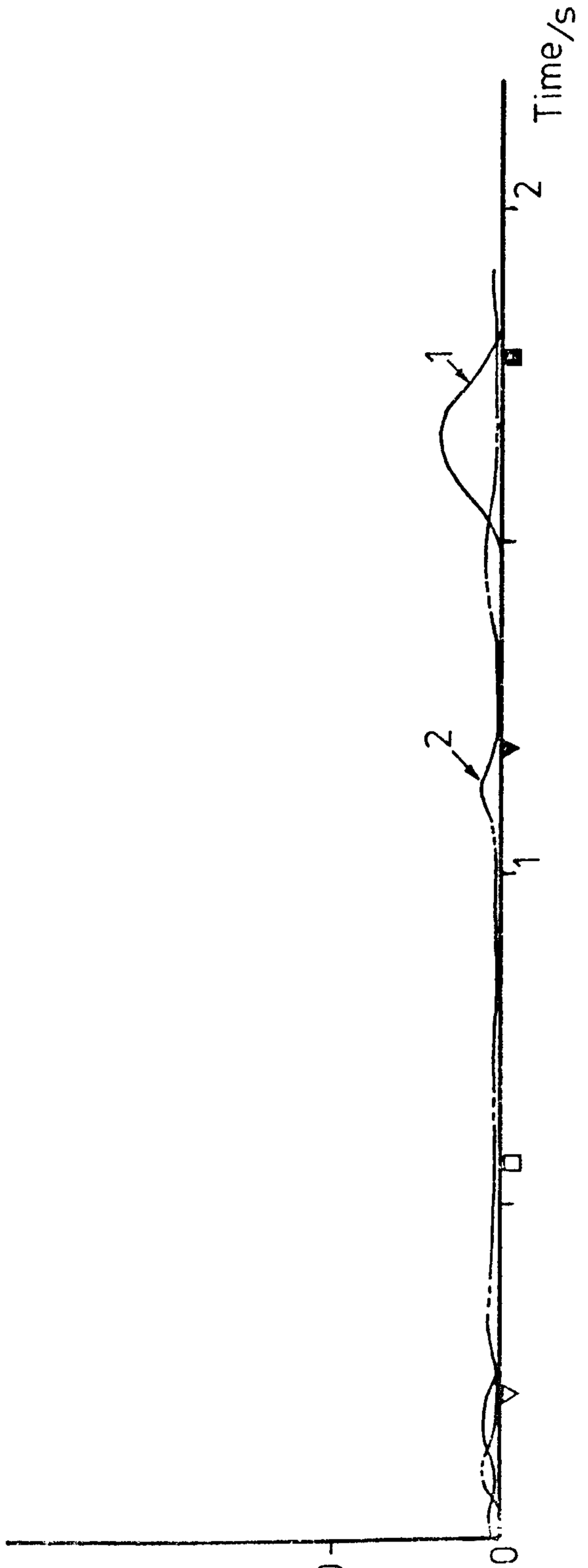

Figure 7·31: Lateral ligament tension — "reaching" activity.

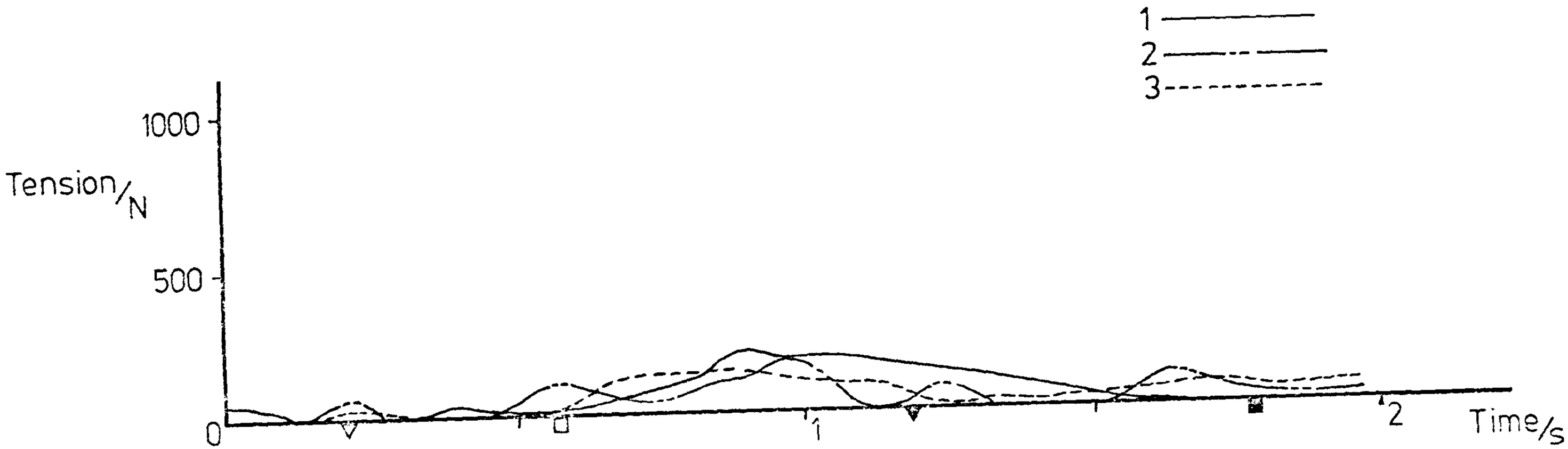

Figure 7·32: Medial ligament tension — "reaching" activity.

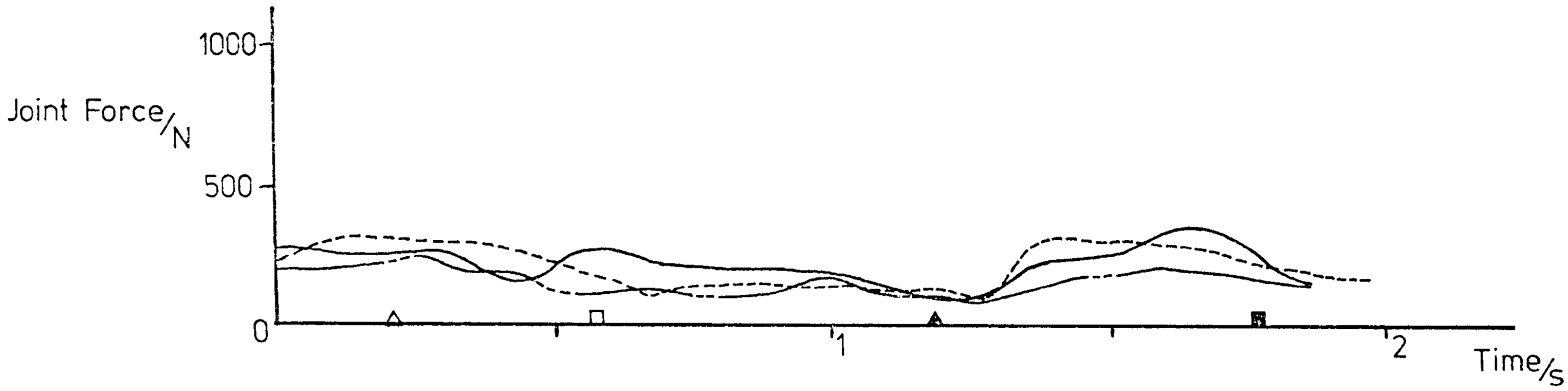

Figure 7·33: Forces experienced on the medial joint surface during "reaching".

7.3.5 Joint forces: In keeping with tension in the medial ligament, the resultant compressive force on the lateral surface of the trochlear notch was slightly greater than the force experienced on the medial surface. Figures 7.33 and 7.34 show the medial and lateral joint forces respectively and it can be seen that the variation in the magnitude of these forces corresponds to the fluctuation of muscle tensions.

An interesting situation occurred at the changeover period when the elbow was fully extended (t = 0.6s). To cater for the large moments in a coronal plane (Z_U - Y_U) the radial head and the capitulum were subjected to considerable contact pressure. Figure 7.35 shows that compressive forces of 200 N occurred at that time.

Figures 7.36, 7.37 and 7.38 contain the complete "internal" force systems for Subject Nos. 1, 2 and 3 respectively.

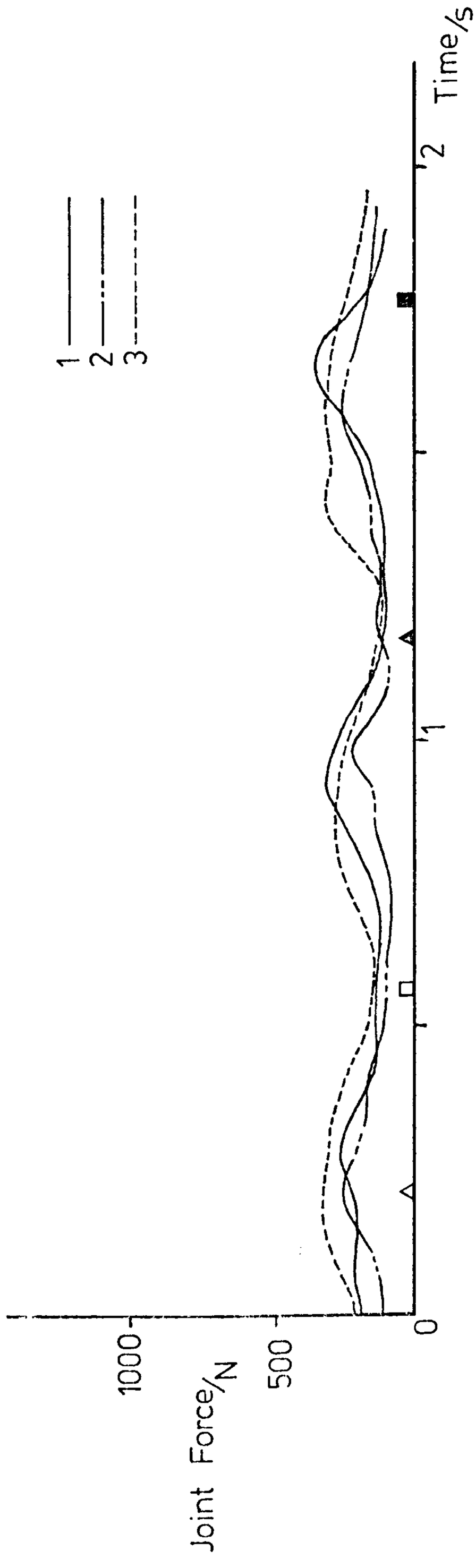

Figure 7·34: Forces experienced on the lateral joint surface during "reaching".

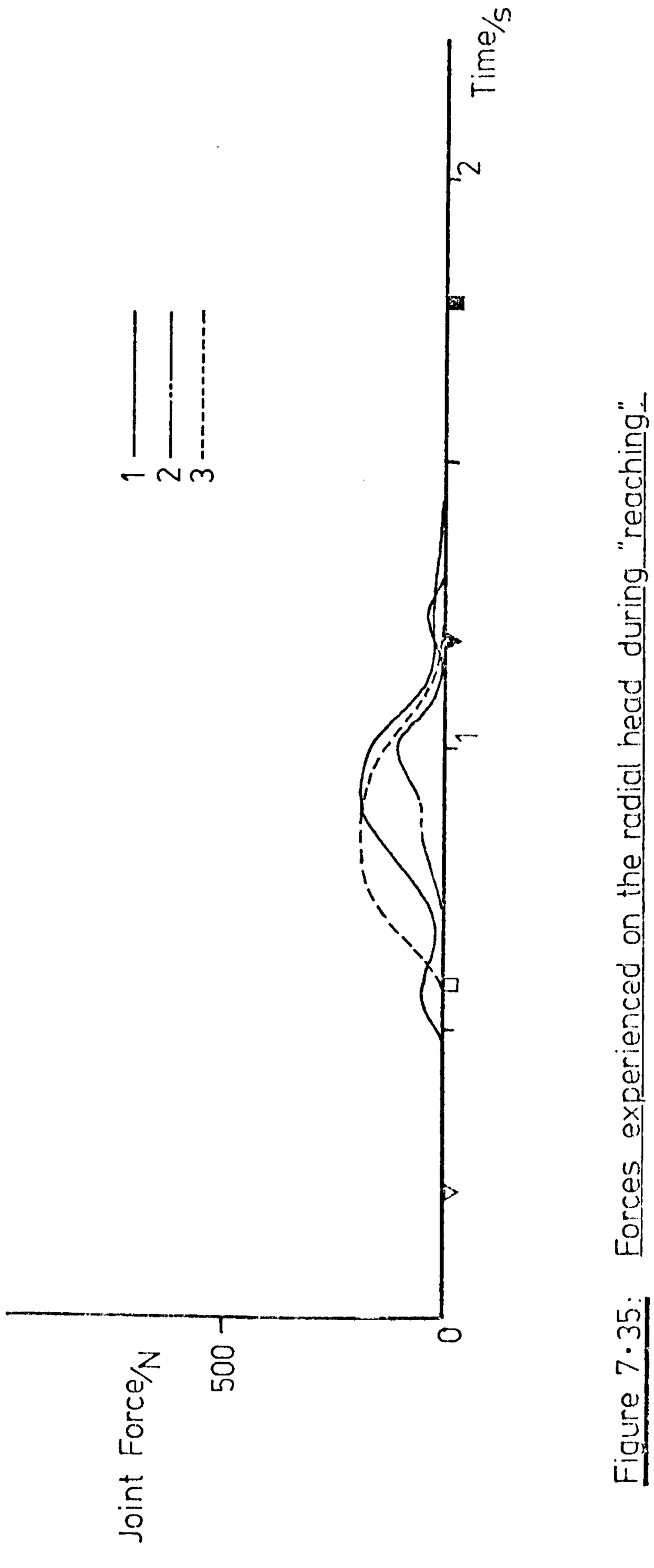

Forces experienced on the radial head during "reaching".

Figure 7·35:

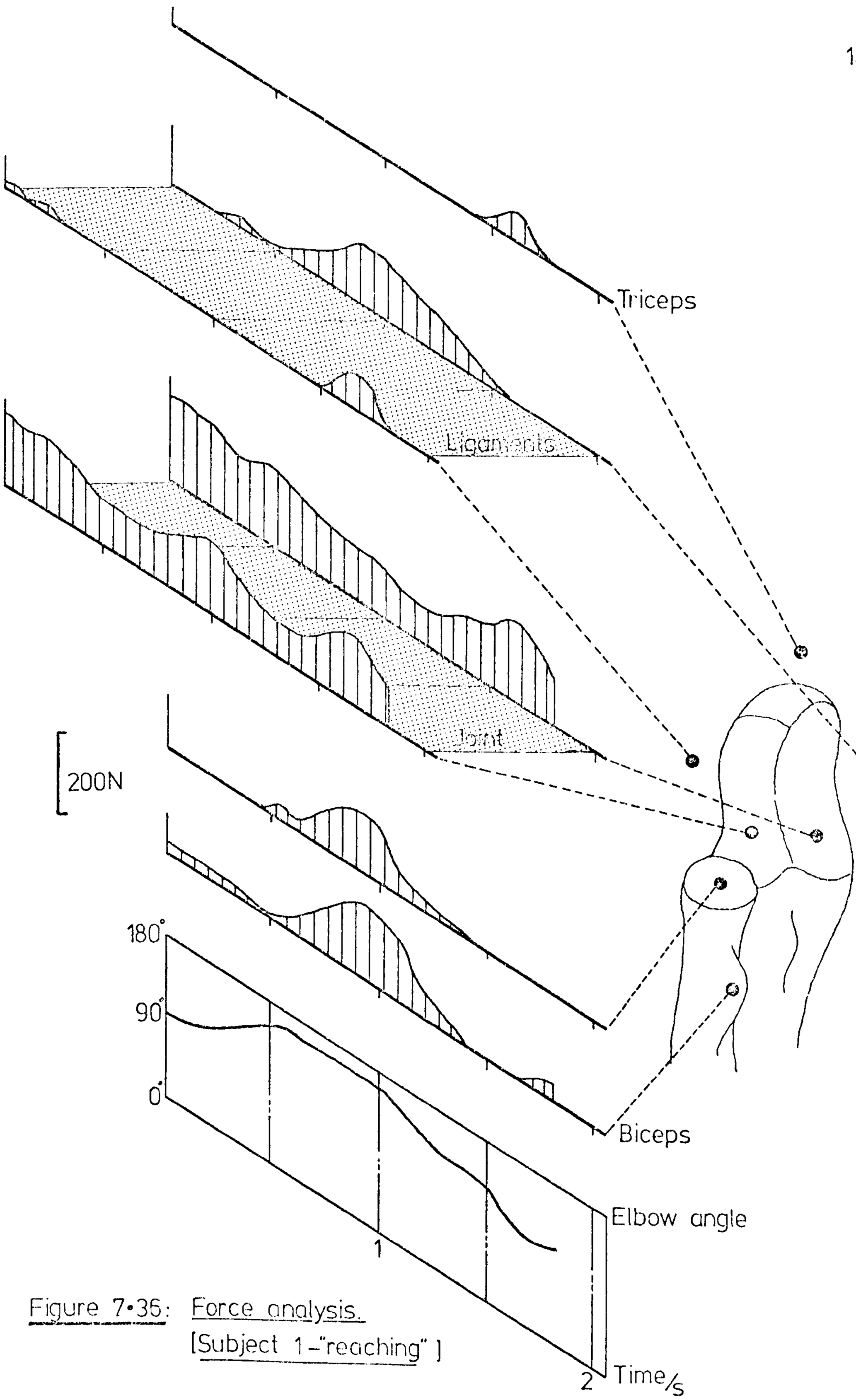

Figure 7·36: Force analysis.
[Subject 1–"reaching"]

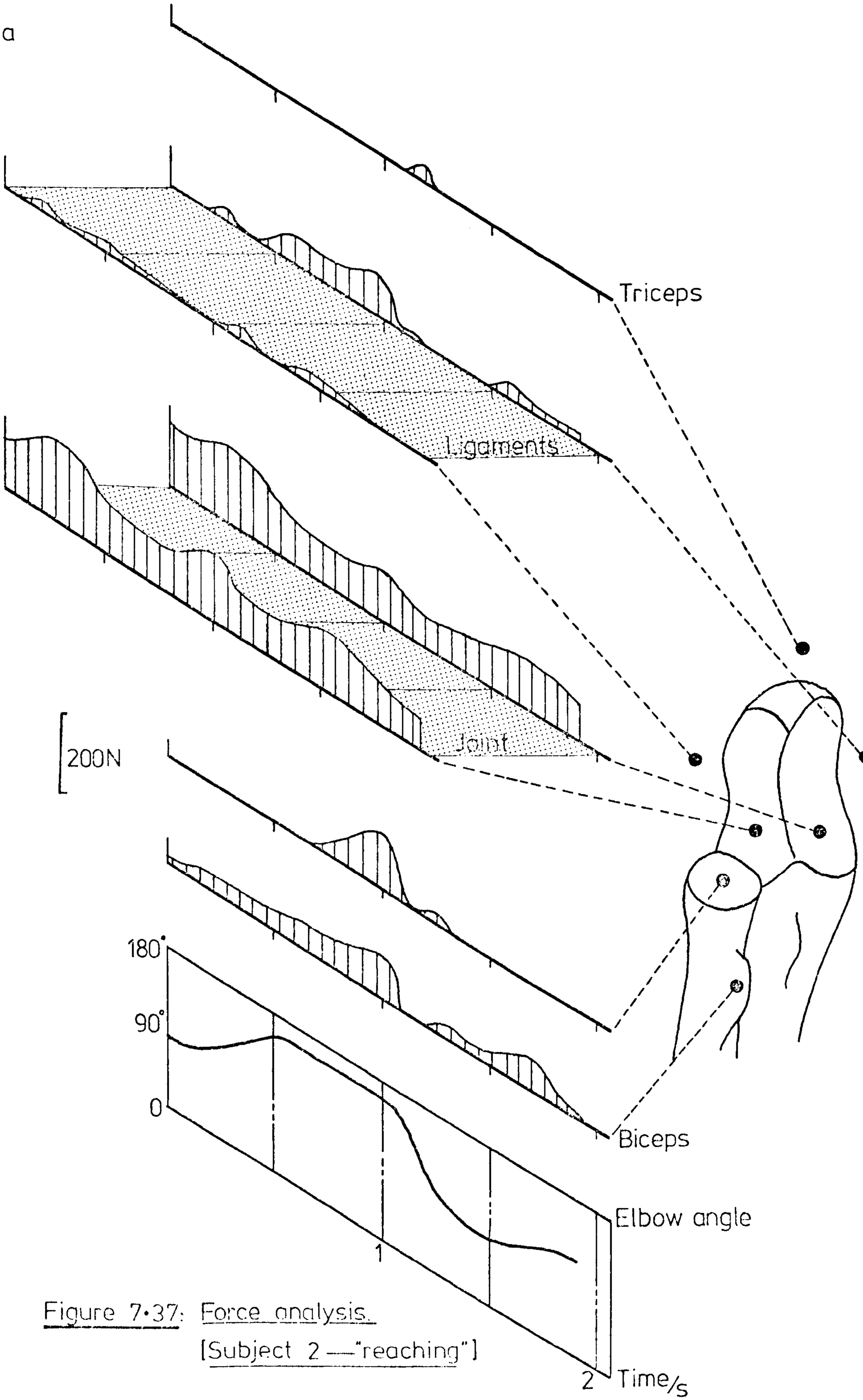

Figure 7·37: Force analysis.
[Subject 2 — "reaching"]

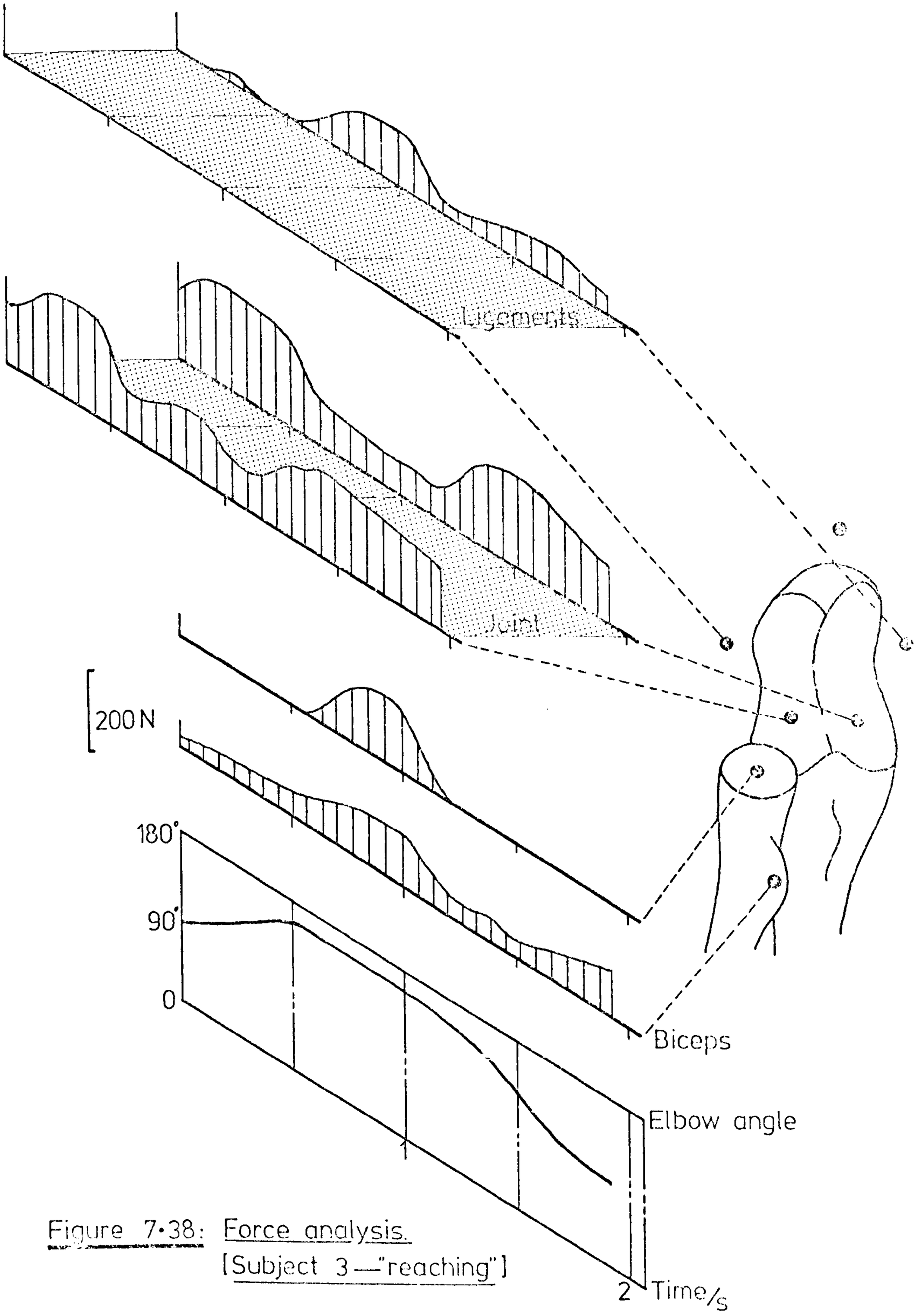

Figure 7·38: Force analysis.
[Subject 3—"reaching"]

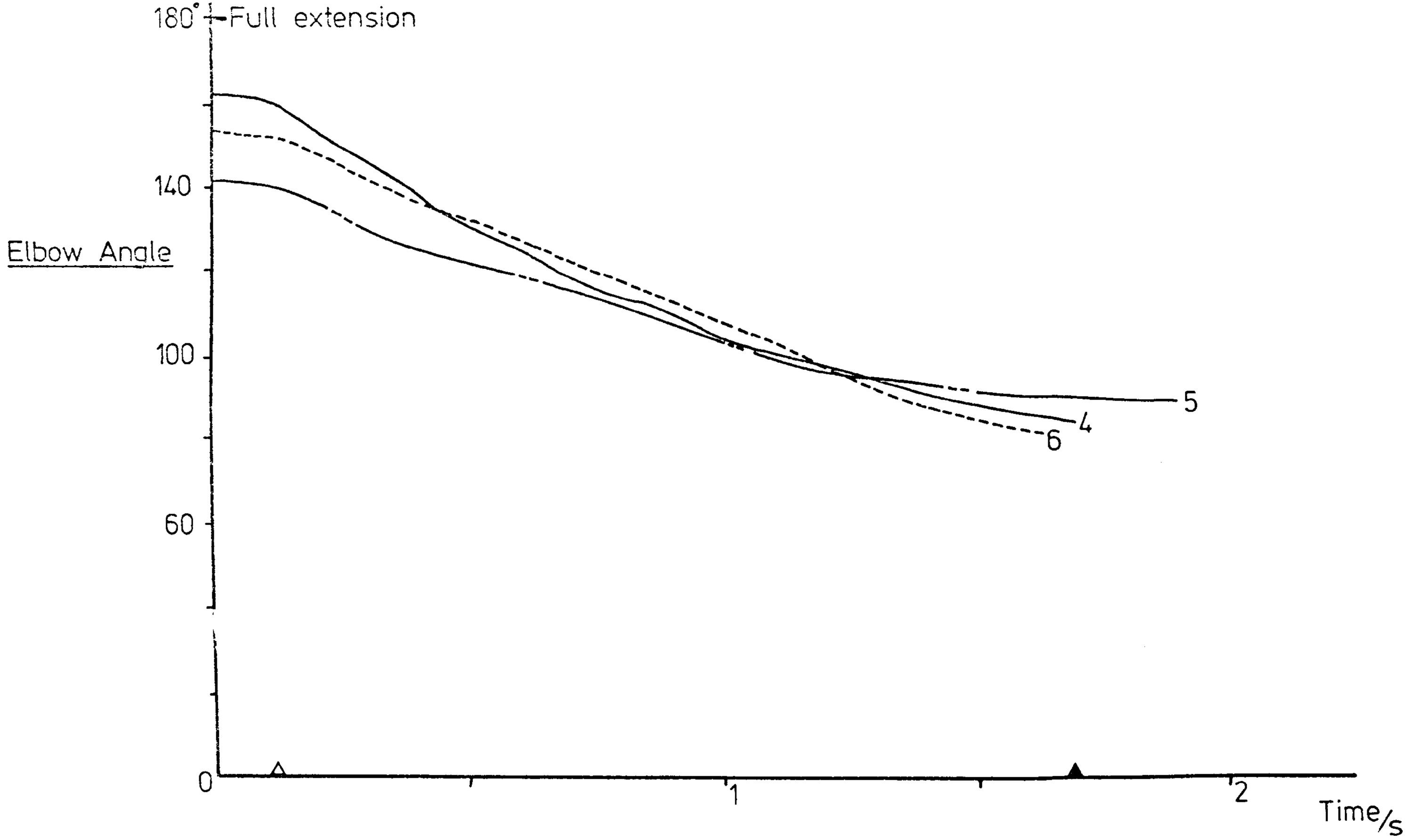

Figure 7·41: Elbow movement during "pulling".

7.4 "Table-pull" Exercise:

The "table-pull" exercise was found to have been the most strenuous activity of the four movements analysed. Speed variations between Subject No.4, 5 and 6 were minimal and this produced close agreement in the forces calculated to be acting on the anatomical structures. Labels △ and ▲ indicate the initiation and the termination of the movement of the table respectively.

7.4.1 Movement: Referring to figure 7.41, the elbow angle for all three subjects decreased in a linear fashion during the exercise. A variation of some 20^{o} was evident in the starting position but the overall range of movement was typically 80^{o}. A limit of 90^{o} was imposed on the elbow angle and the forearm was held in a horizontal position throughout the movement. No significant movements of the trunk were recorded (see figure 5.17).

The horizontal motion of the table is presented in figure 7.42. A range of 320 to 380 mm was obtained.

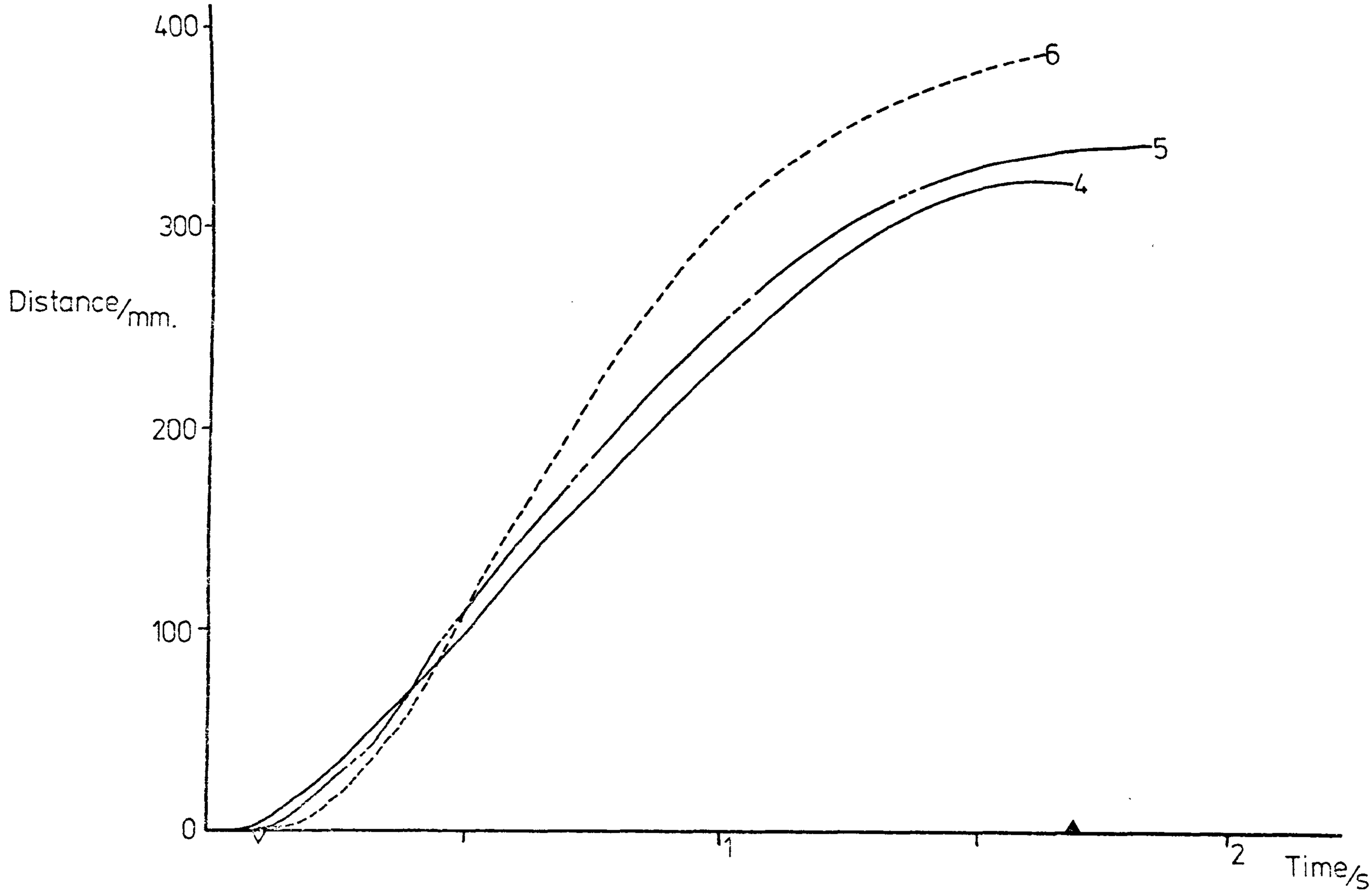

Figure 7·42: Horizontal displacement of the transducer during "pulling".

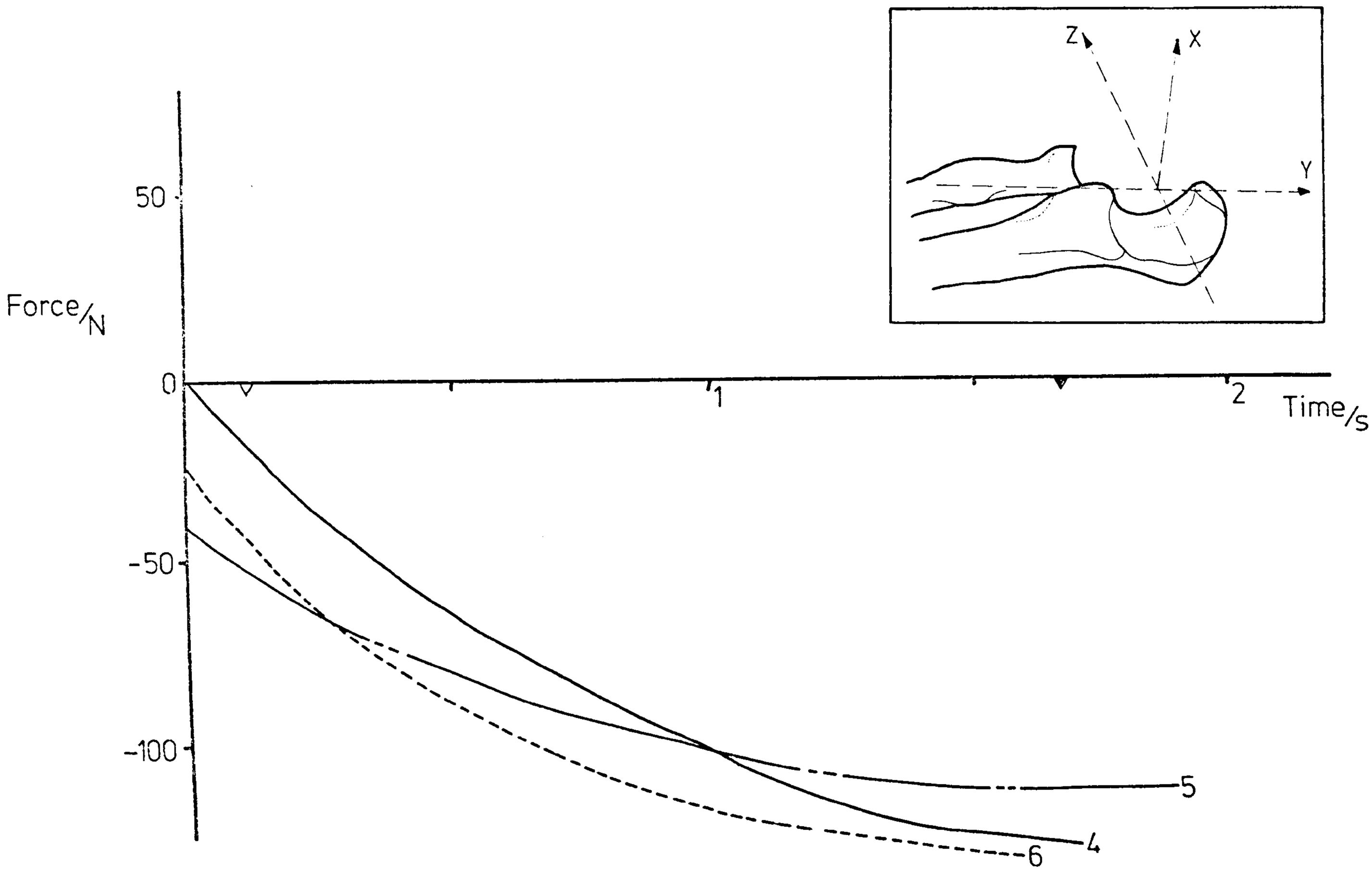

Figure 7·43: Forces acting along X_U during "pulling".

7.4.2 External force system: Figures 7.43 to 7.48 show the forces and moments acting on the elbow joint in terms of the ulnar axis system. Figure 7.43 represents the degree of "lift" applied to the table and the axial "pull" on the forearm is shown in figure 7.44. The forces in the Z_U direction (see figure 7.45) created considerable moments in the X_U direction as shown in figure 7.46. Maximum values of -45 Nm were obtained whereas the moments in the Y and Z directions of the ulnar axis system reached maxima of 30 Nm and -25 Nm respectively (see figures 7.47 and 7.48). The moments in the Y_U direction represented an axial torque about the long axis of the forearm. No such action was required for the movement of the table and this effect was therefore superfluous to the exercise as a whole.

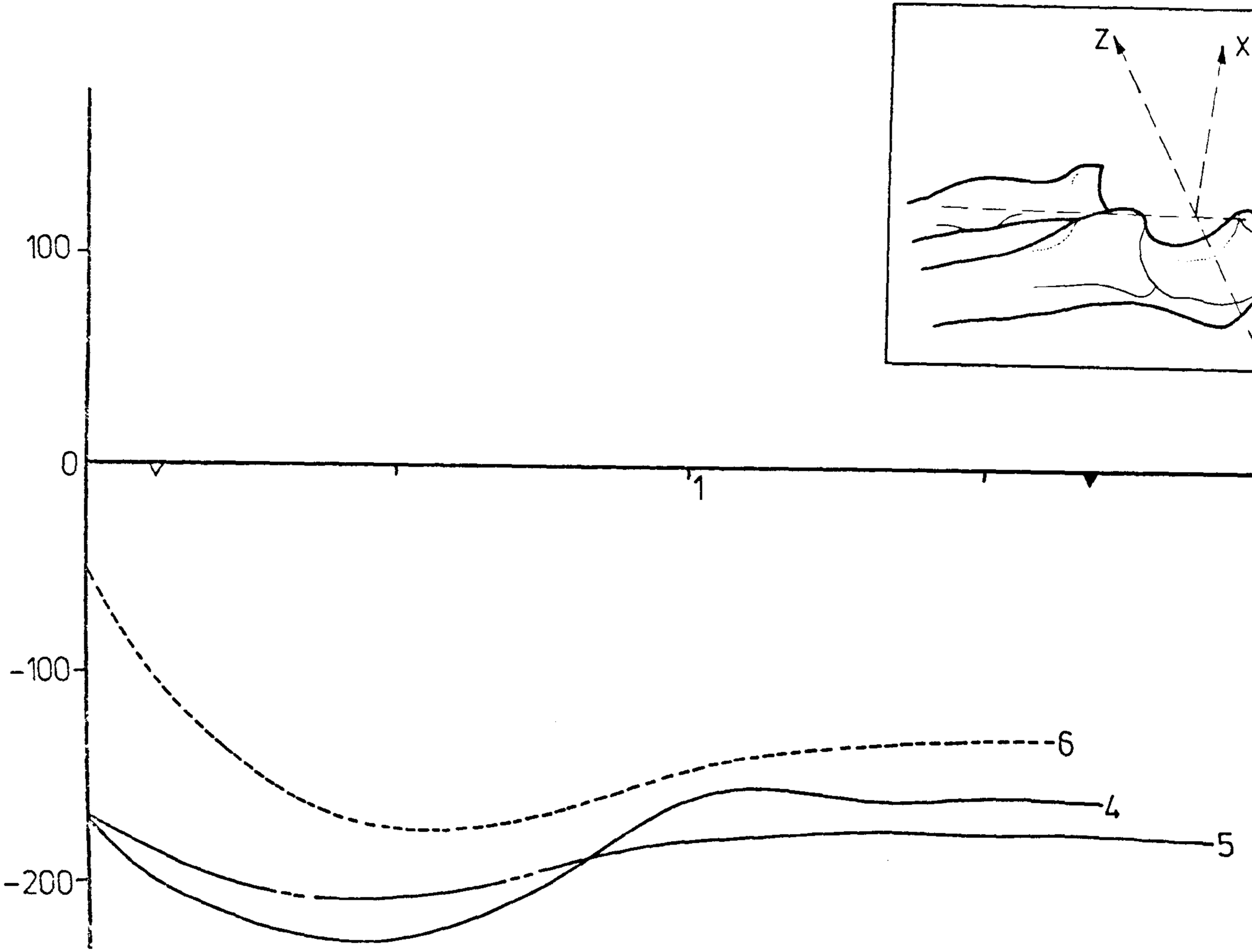

Figure 7·44: Forces acting along Yu during "pulling"

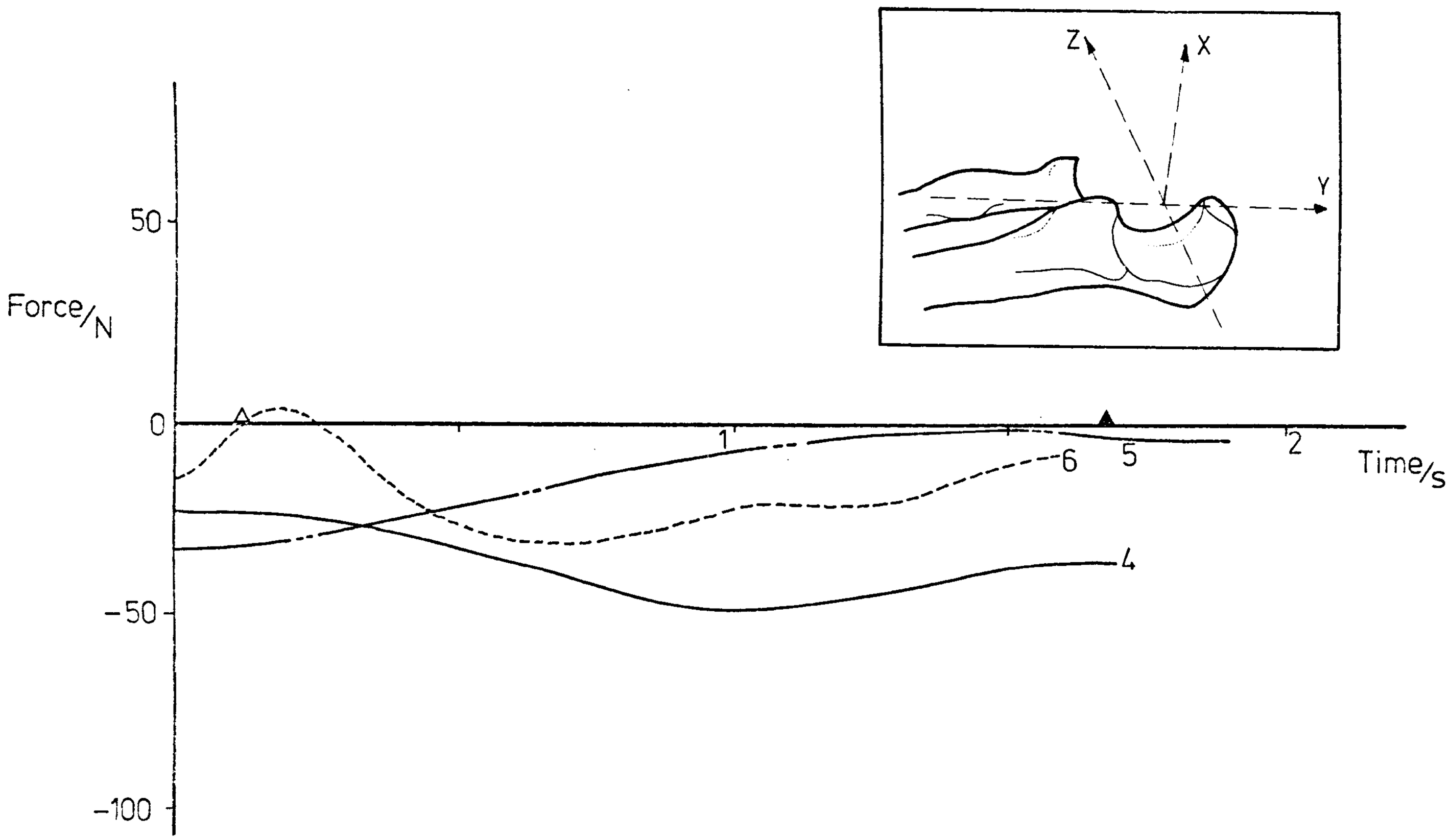

Figure 7·45: Forces acting along Z_U during "pulling".

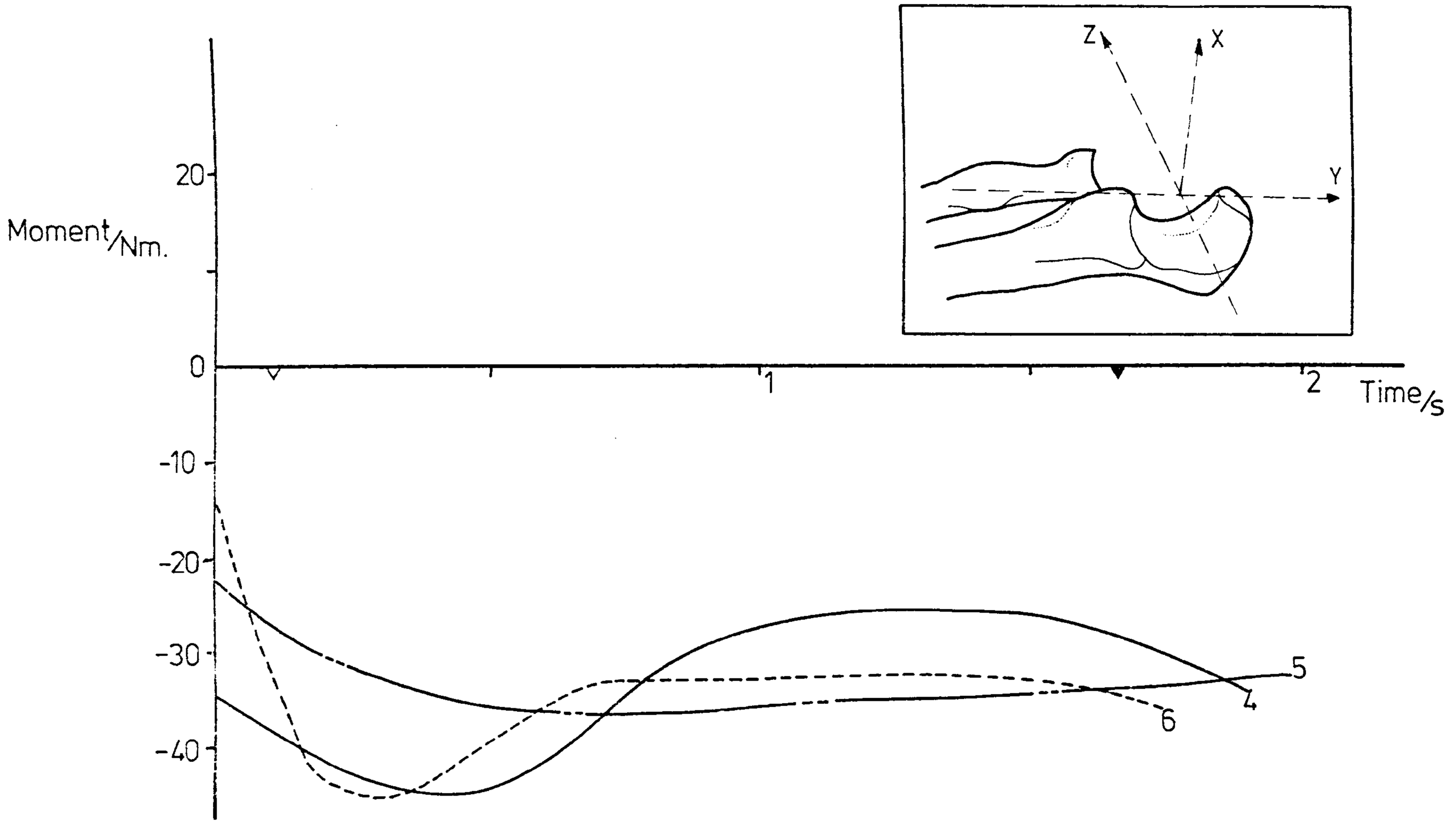

Figure 7·46: Moments acting about X_u during "pulling".

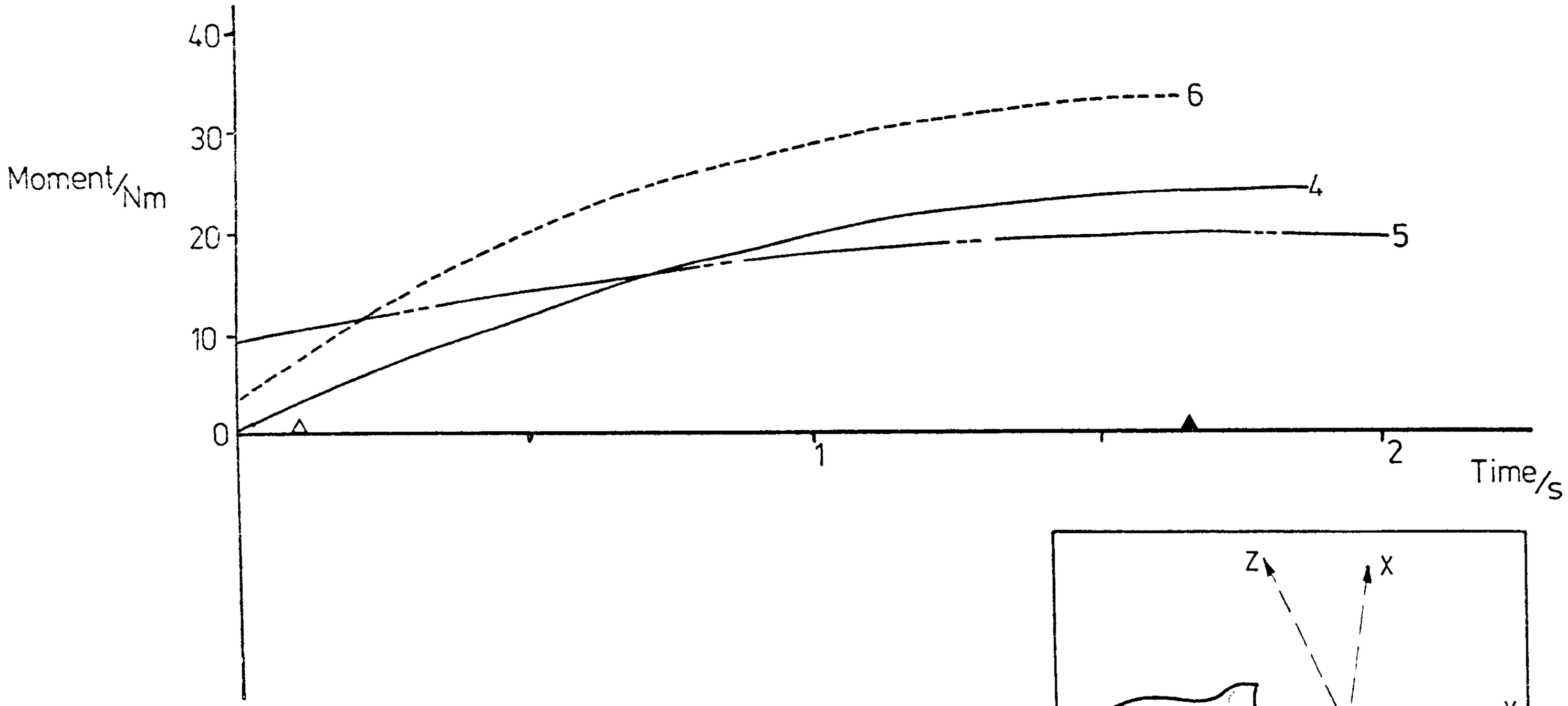

Figure 7·47: Moments acting about Y_U during "pulling".

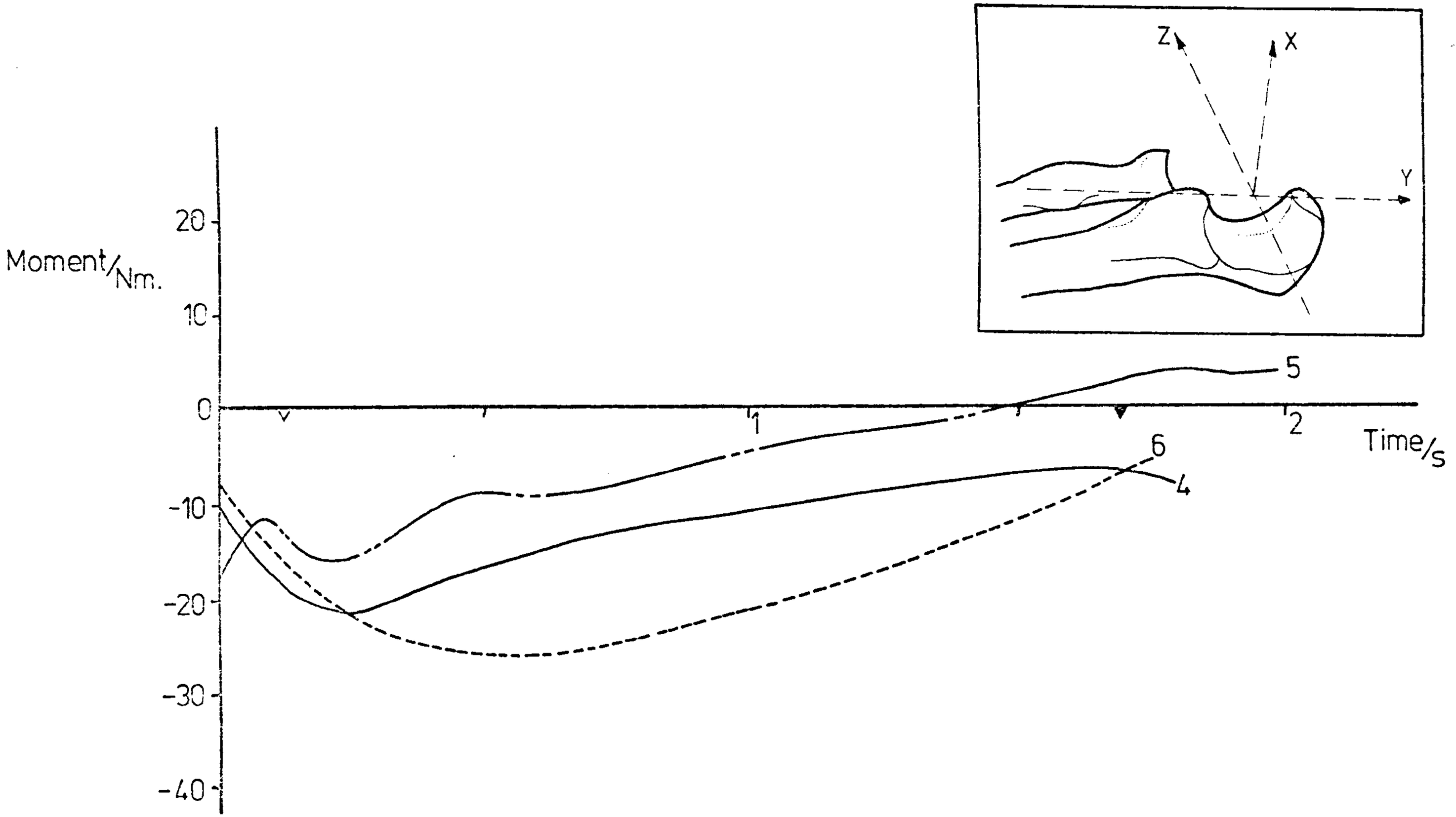

Figure 7·48: Moments acting about Z_U during "pulling".

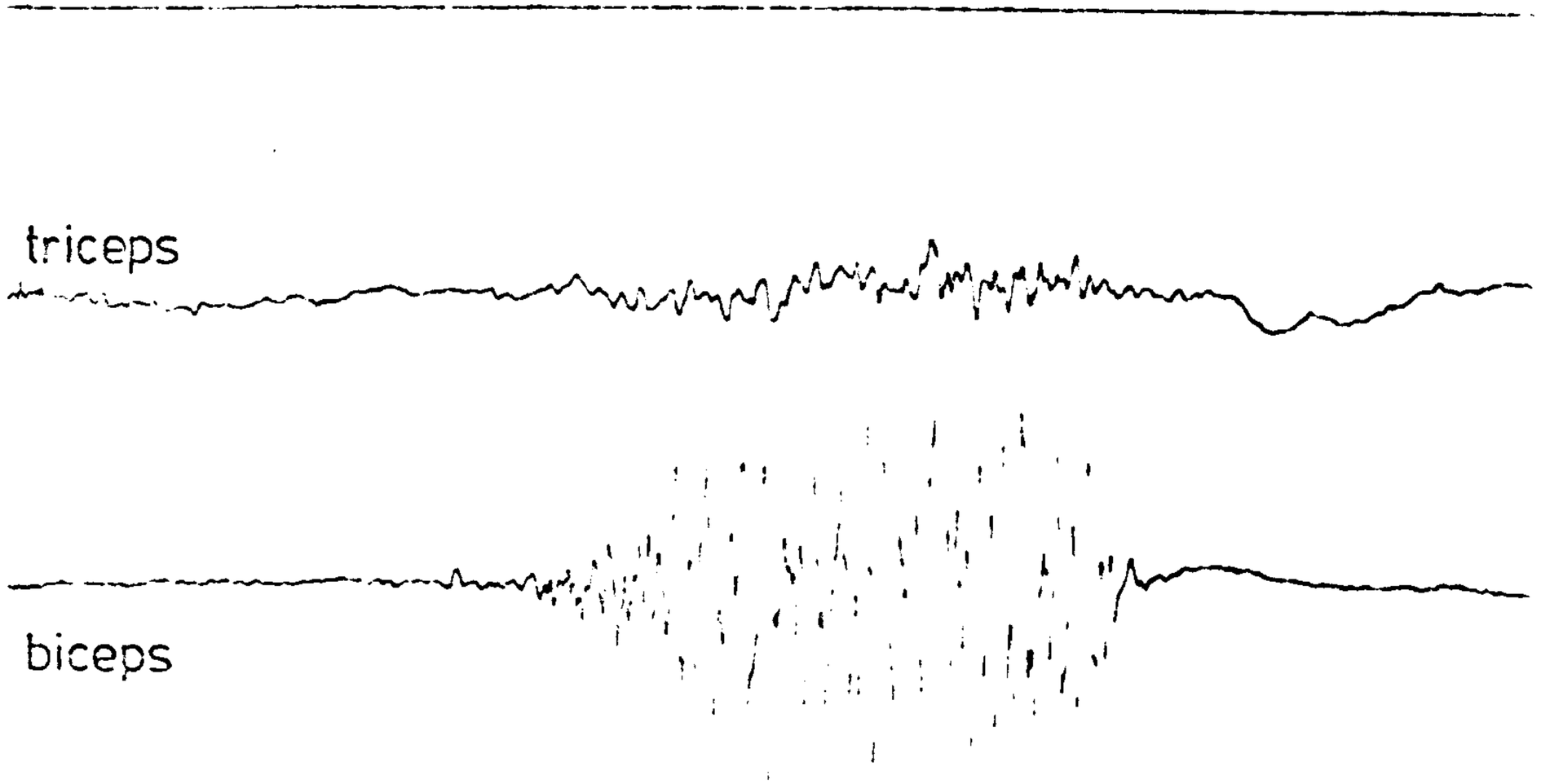

Figure 7·49: Muscle activity during the "table pull" exercise.

7.4.3 Muscle forces: The electromyograph recordings obtained during the pulling exercise showed that both the flexor and extensor groups were active throughout the movements. Figure 7.49 shows a typical trace of muscle activity and the antagonistic activity can be explained as follows.

Consider a simplified model (figure 7.50) which represents the skeletal and muscular structure of the upper limb. The "LOAD" can be overcome by applying tension to the flexor muscle and by applying a counterclockwise moment (M) to the shoulder joint.

From a basic model of the shoulder complex, the long head of triceps can act as a flexor and adductor of the gleno-humeral joint. Since the resultant moment at the elbow joint must tend to produce flexion, the effects of the flexor muscle must exceed those produced by the triceps group. The antagonistic muscle activity is therefore a result of the complex control which applies to bi-articular muscle groups.

Figure 7.51 shows the tension which was developed in the flexor group muscles. An initial peak of 750 to 1000 N was experienced by each subject and represented the effort required to overcome the "static" friction between the floor and the table. Following this situation, the muscle forces were reduced to low values at the end of the movement.

Subject No.6 experienced significantly higher muscle forces than the two other subjects and this was due to the "supination" torque (M_y) applied to the transducer. Triceps activity was involved in the latter part of the exercise in one case (Subject No.5) and corresponded to shoulder flexion and approximately zero angular velocity of elbow flexion. (see Figure 7.52).

7.4.4 Ligament forces: In keeping with strong flexor activity (biceps), the medial ligament transmitted considerable tension throughout the pulling exercise. Forces of 1500 - 2000 N were typical of all three subjects as shown in figure 7.53. Zero tension was computed for the lateral ligament.

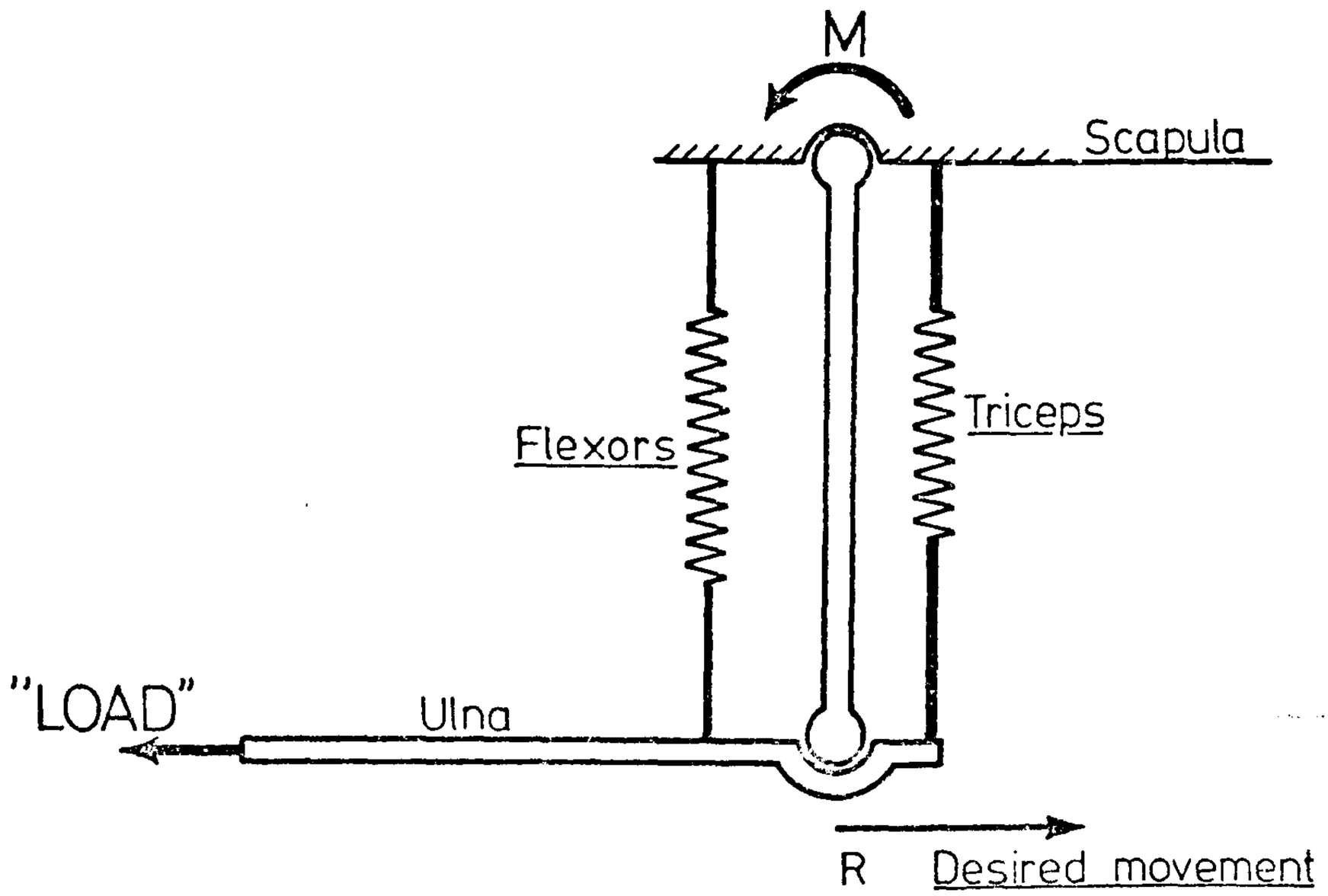

Figure 7·50: Simplified model of antagonistic muscle action.

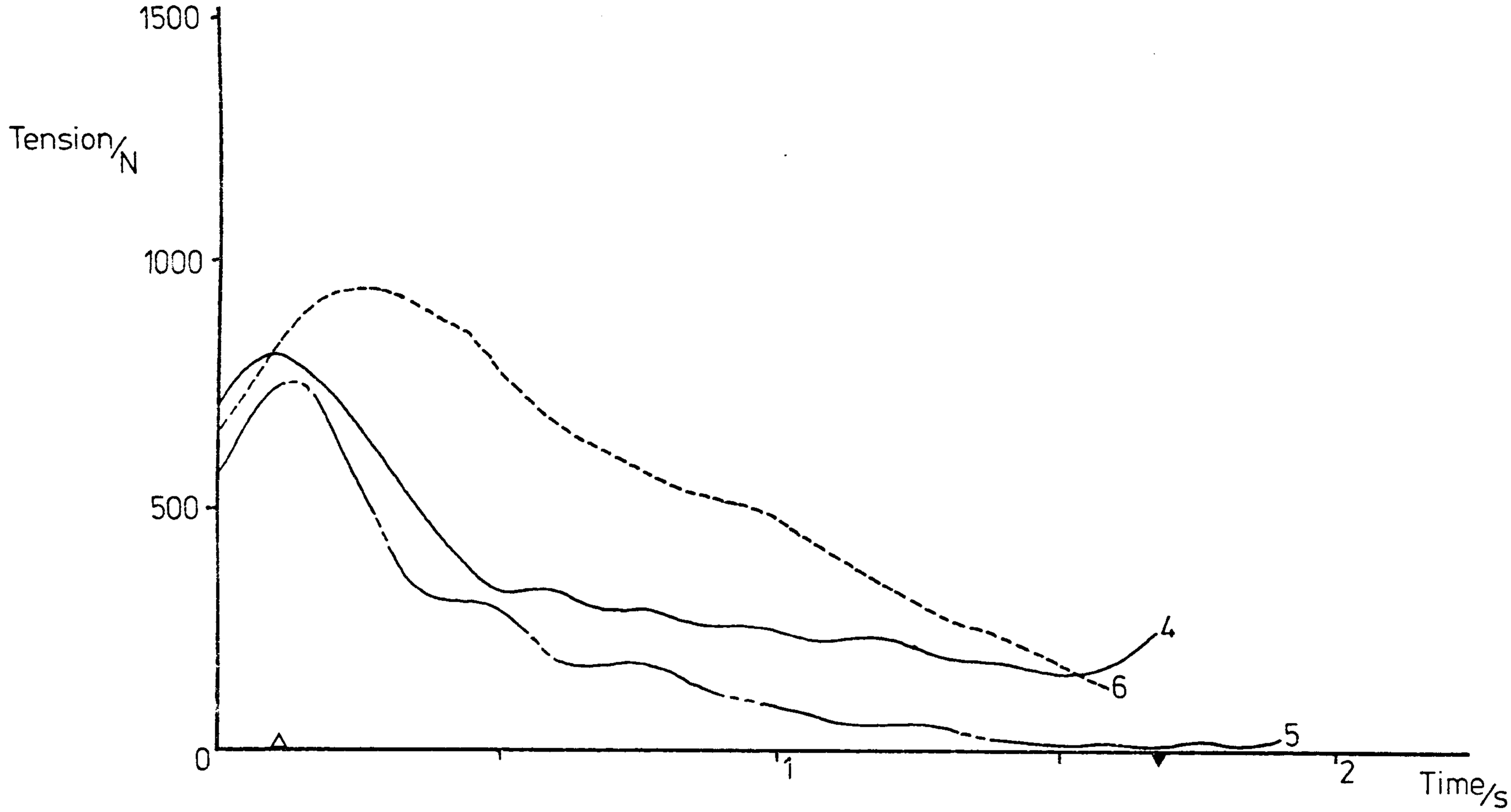

Figure 7·51: Tensions produced in the main flexors during "pulling".

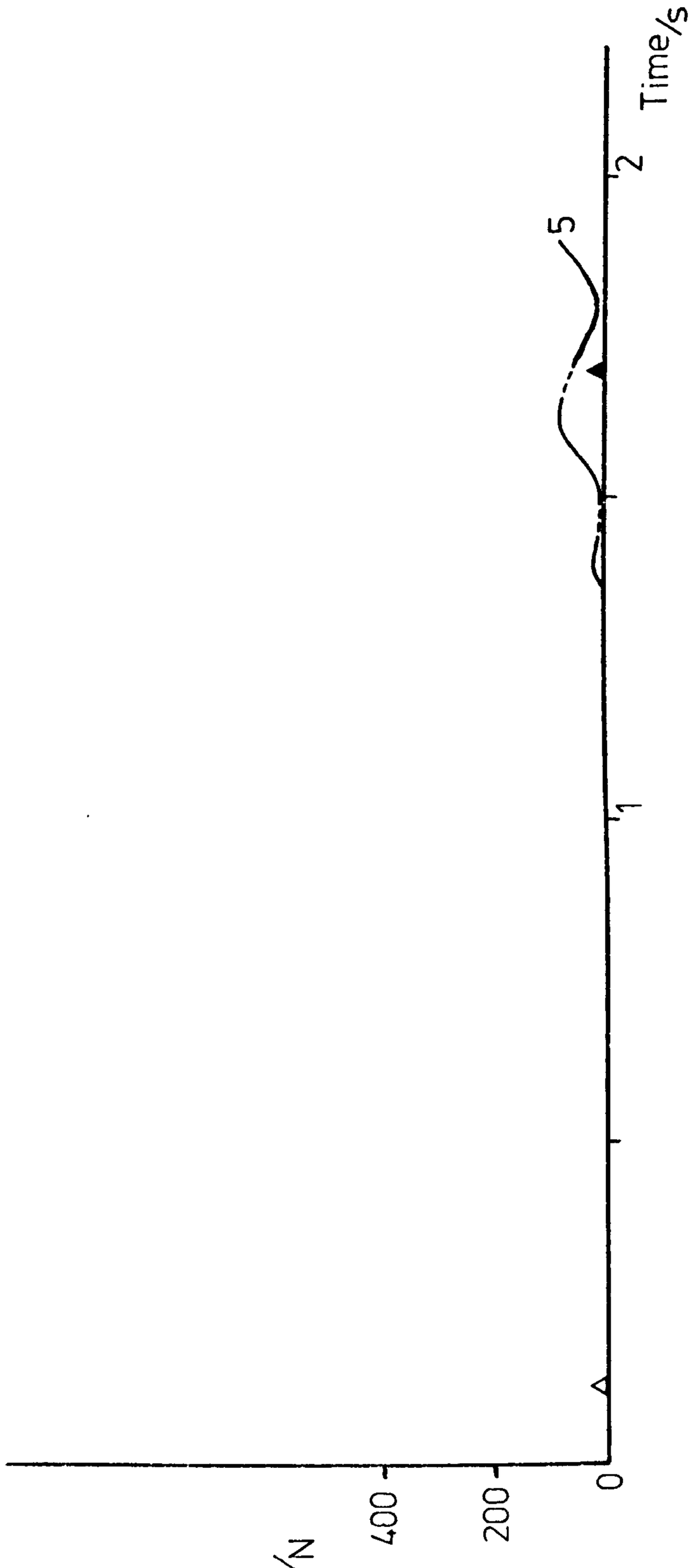

Figure 7·52: Triceps tension produced during "pulling".

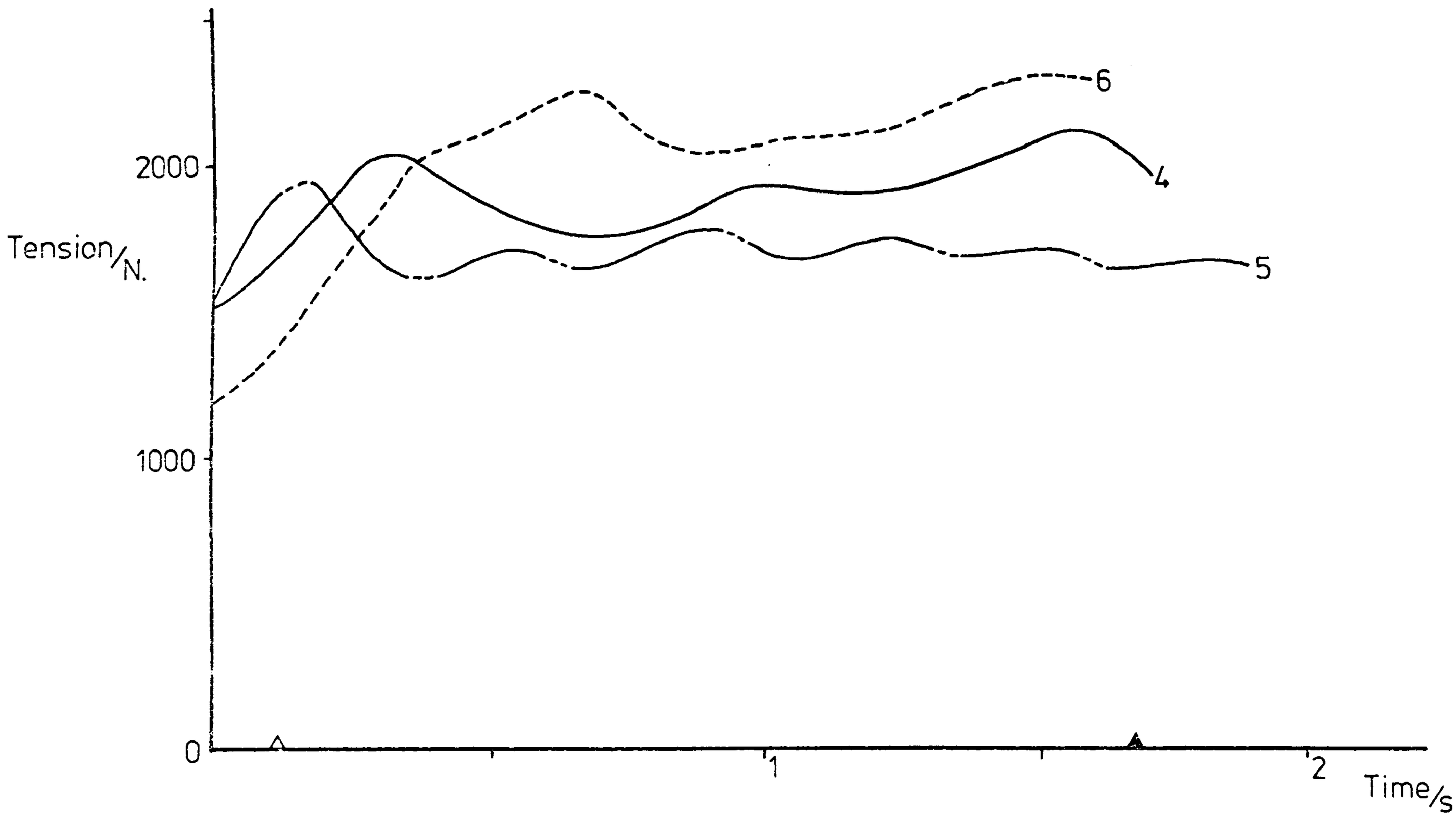

Figure 7·53: Medial ligament tension —"table-pull" activity.

7.4.5 Joint forces: The lateral surface of the trochlear notch was subjected to greater compressive forces than those experienced on the medial side of the joint. Joint forces of 2450 N and 1900 N were obtained respectively (see figures 7.54 and 7.55).

The humero-radial articulation transmitted a considerable amount of force at the higher values of elbow angle ($t \leqslant 0.25$ s) as shown in figure 7.56. As the elbow was flexed, the contributions of biceps and brachialis muscles to the radial head force became reduced. However, the effects of tension in the brachioradialis muscle on this joint force became increased as the elbow angle approached 90^{o} and maintained a compressive force of approximately 500 N.

The force actions experienced by each subject are illustrated in figures 7.57, 7.58 and 7.59.

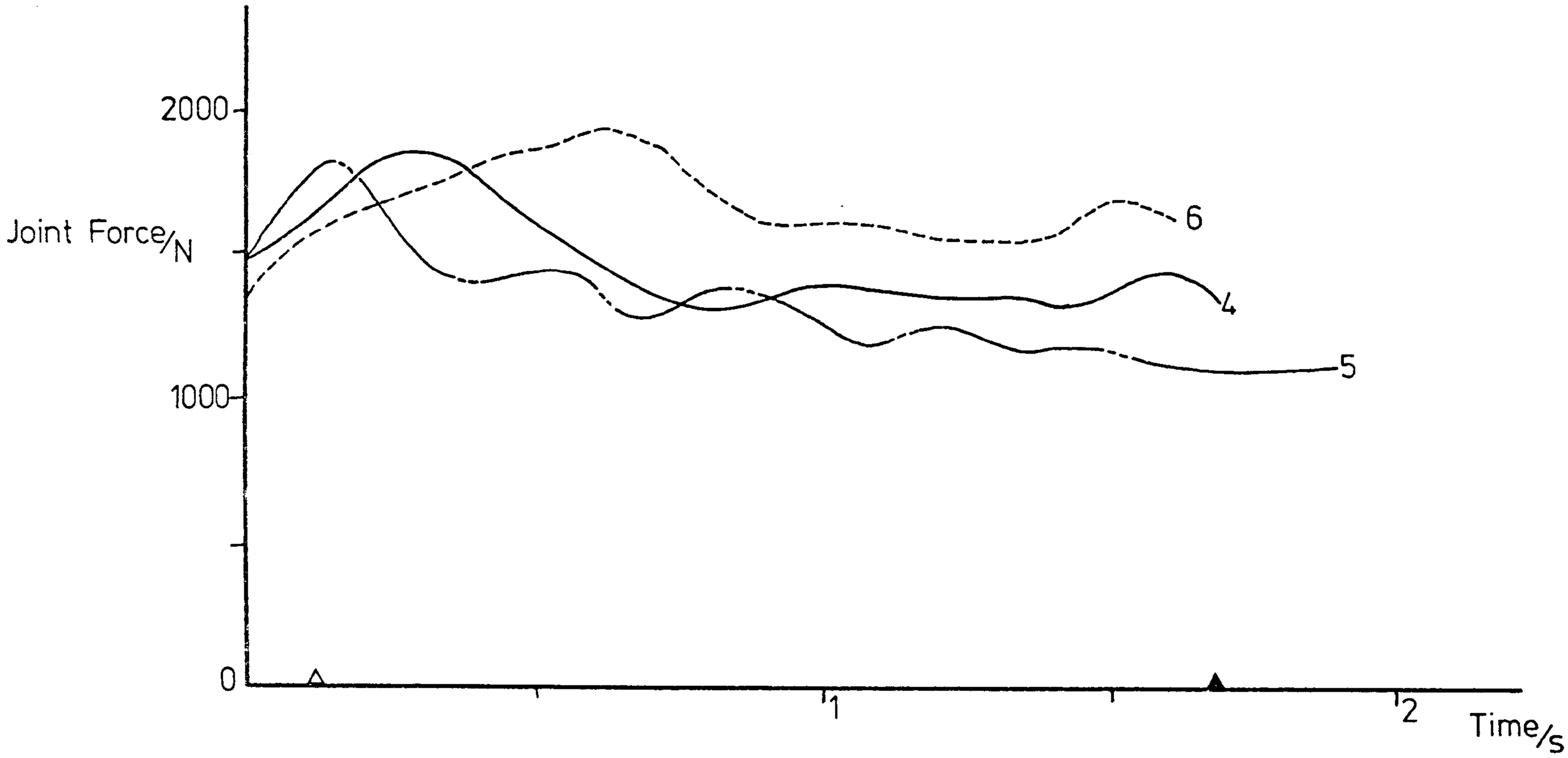

Figure 7·54: Forces experienced on the medial joint surface during "pulling".

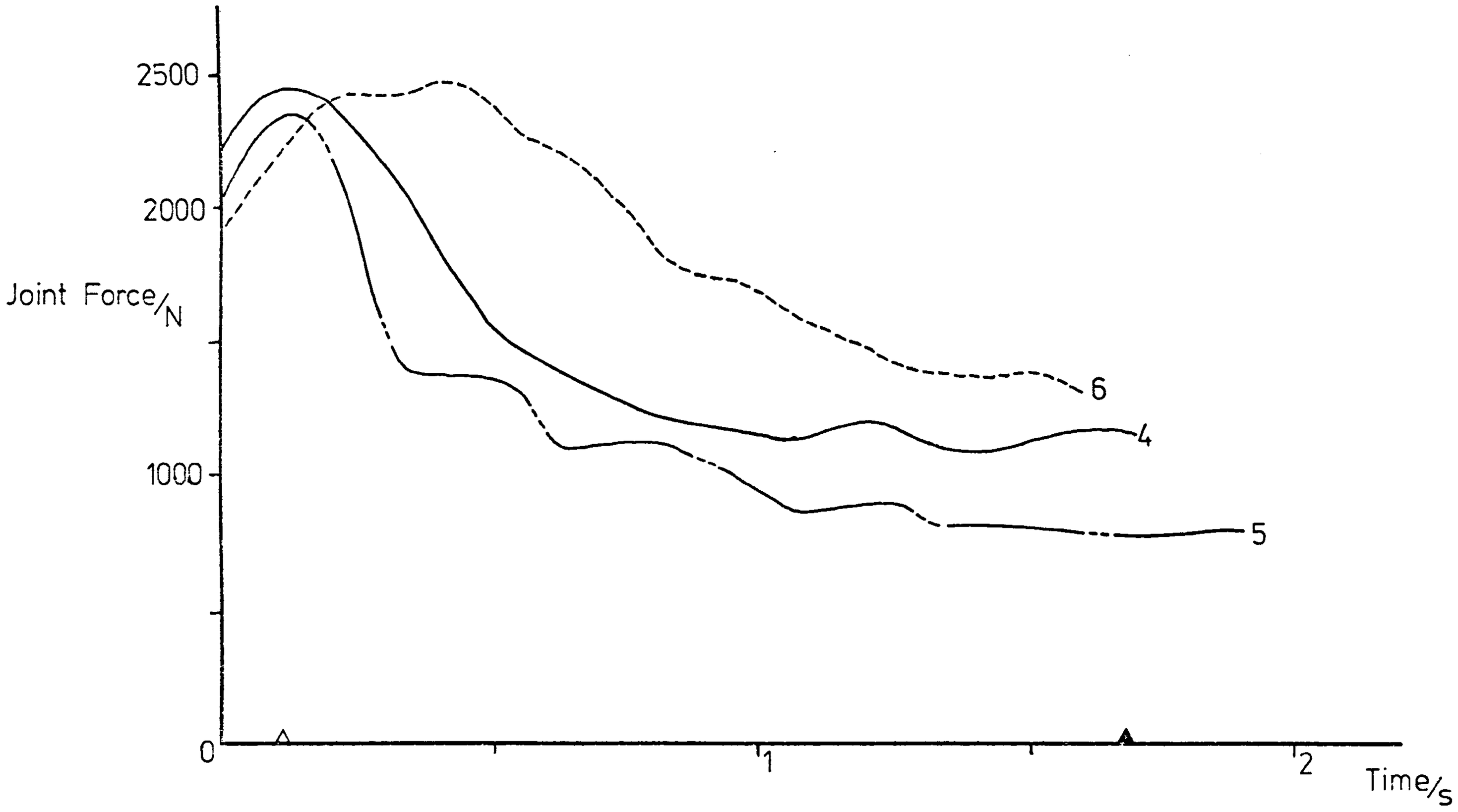

Figure 7·55: Forces experienced on the lateral joint surface during "pulling".

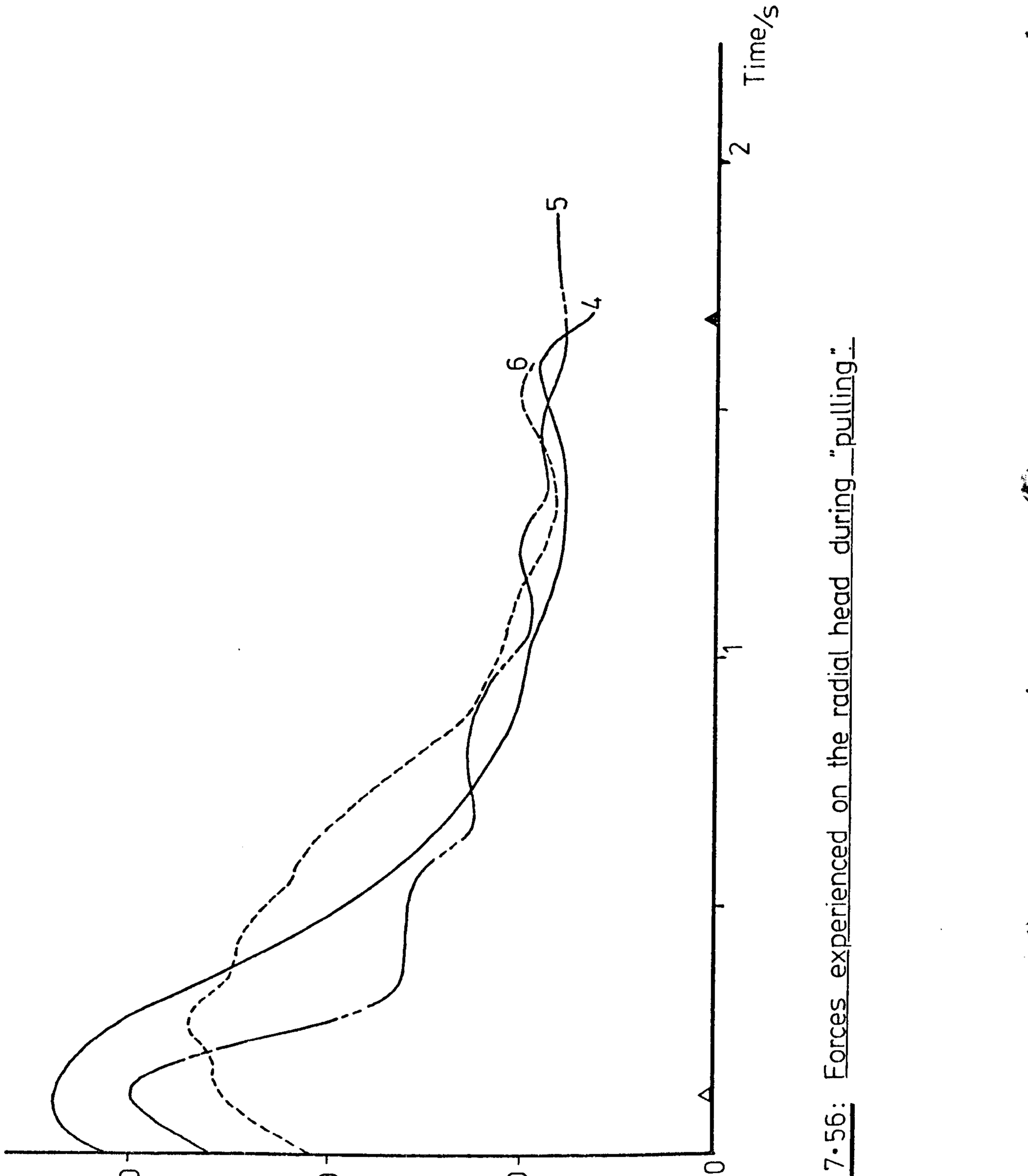

Forces experienced on the radial head during "pulling".

Figure 7·56: F

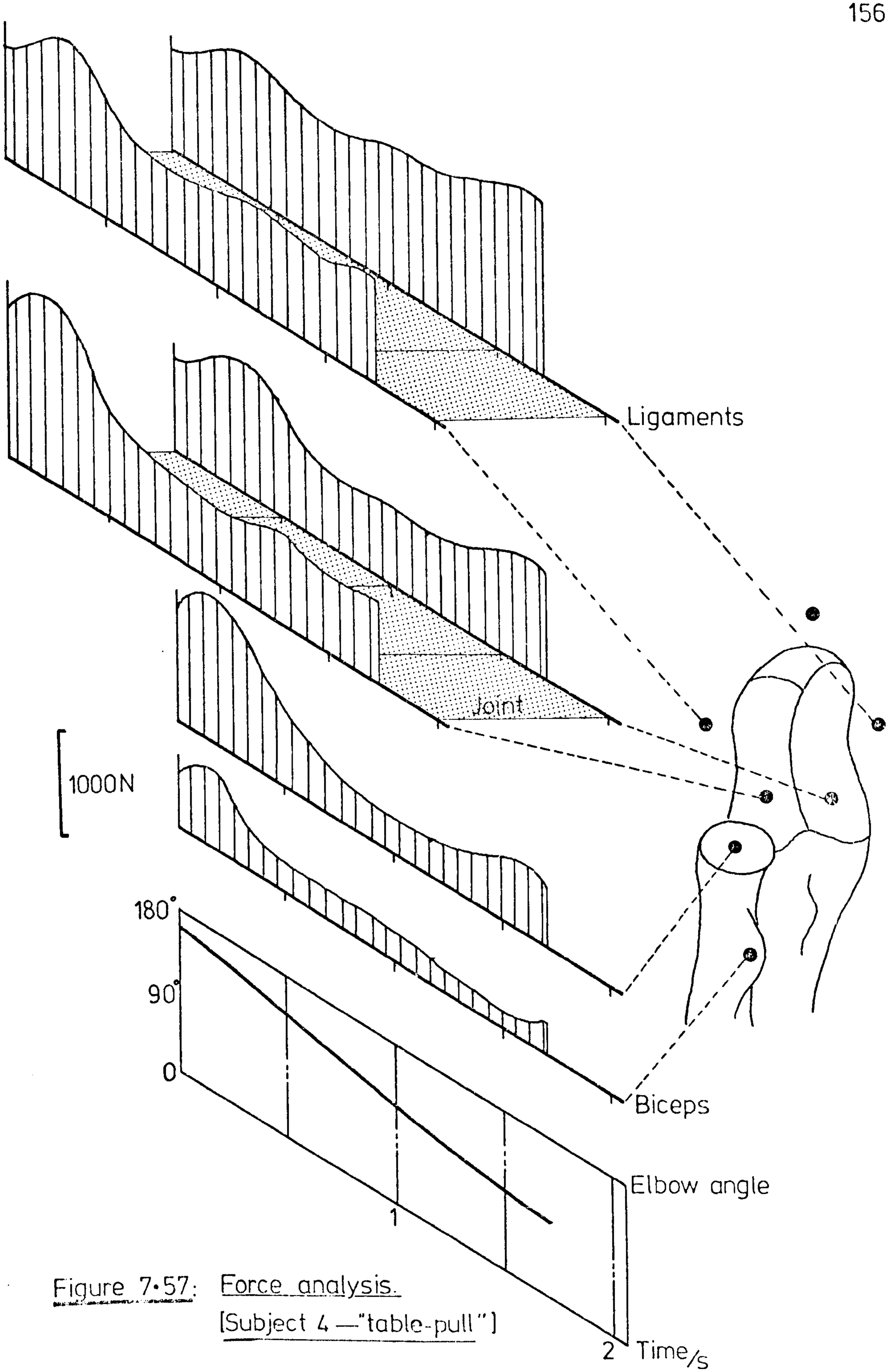

Figure 7·57: Force analysis.
[Subject 4 —"table-pull"]

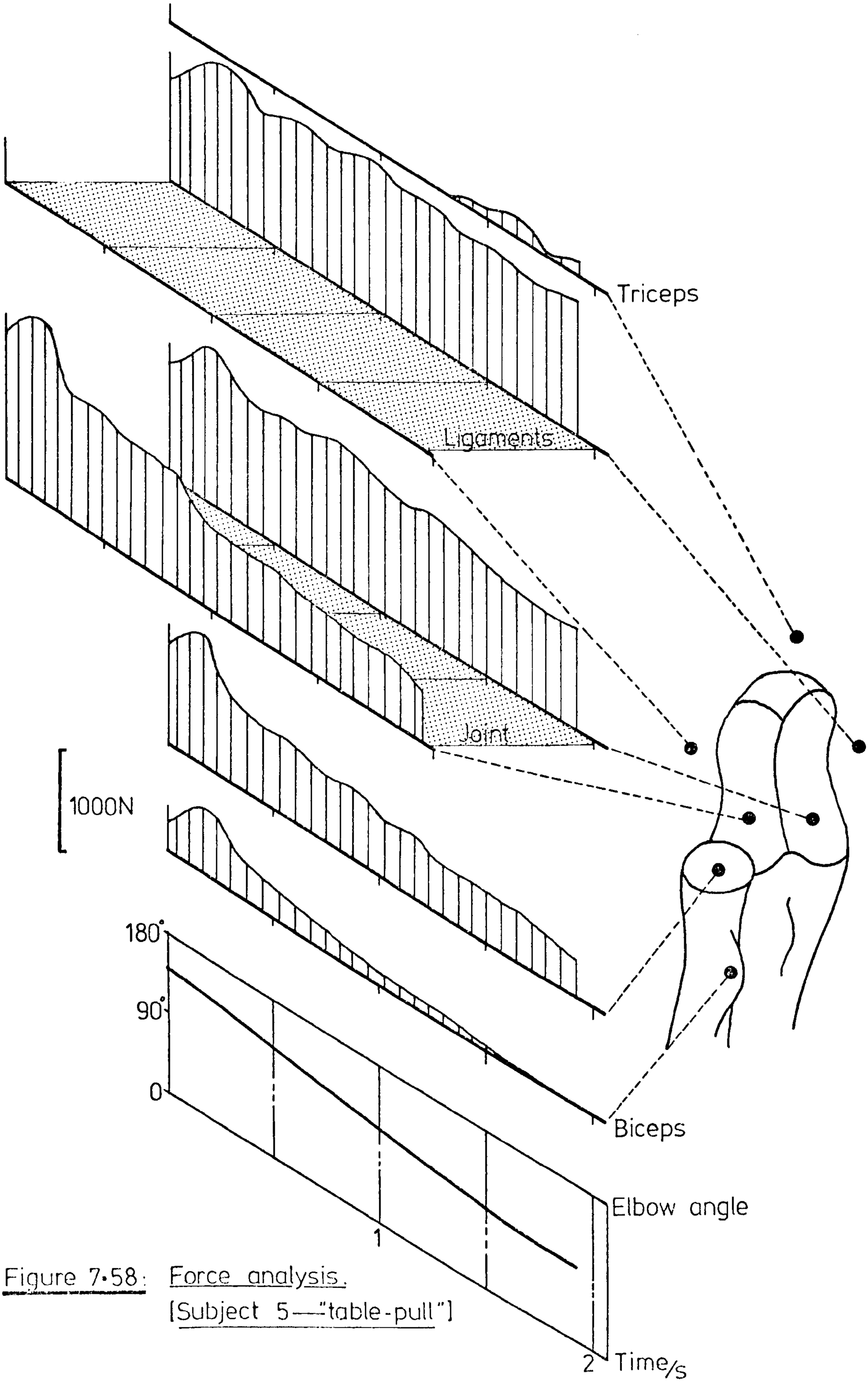

Figure 7·58: Force analysis.
[Subject 5—"table-pull"]

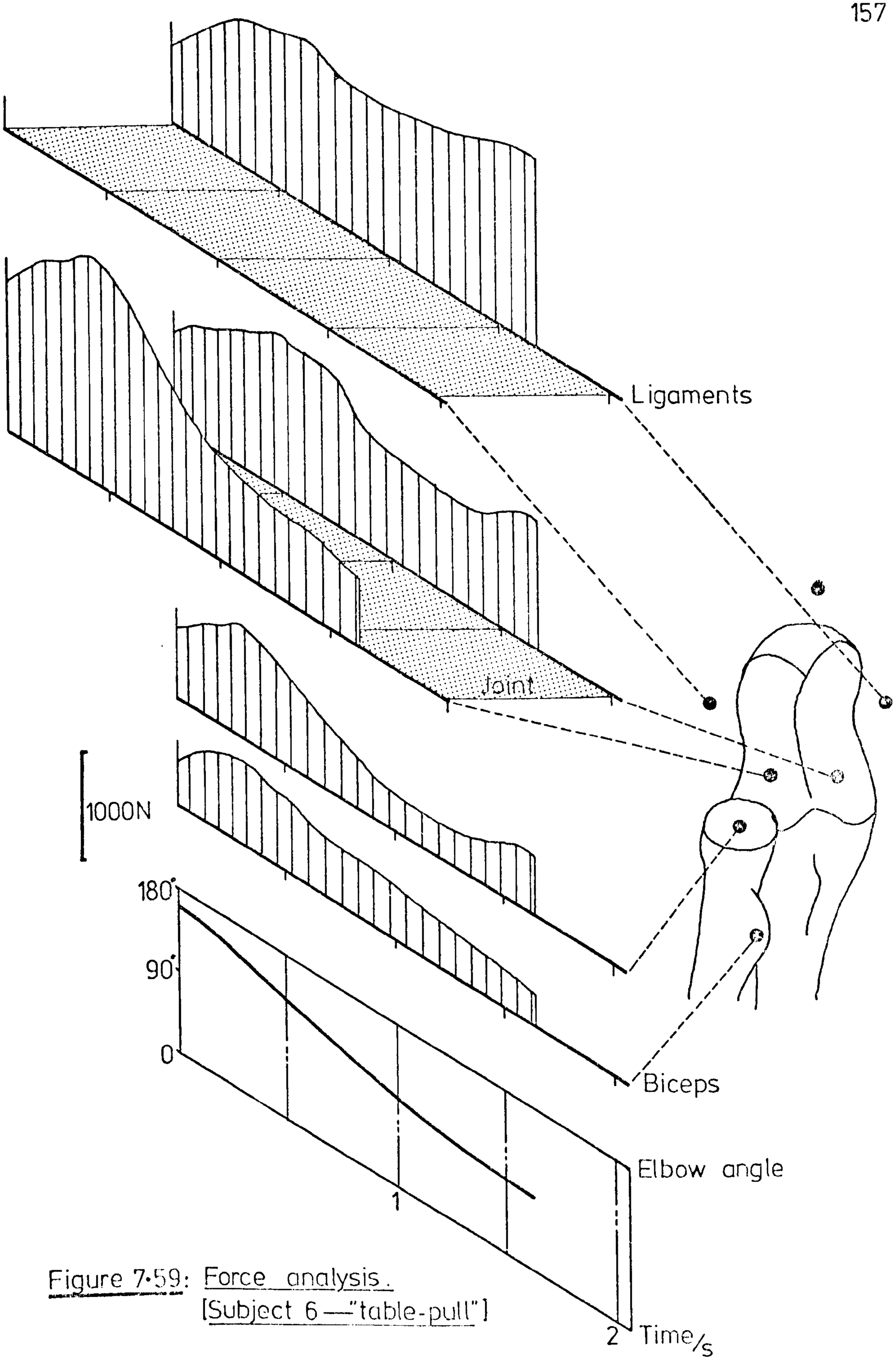

Figure 7·59: Force analysis.
[Subject 6 — "table-pull"]

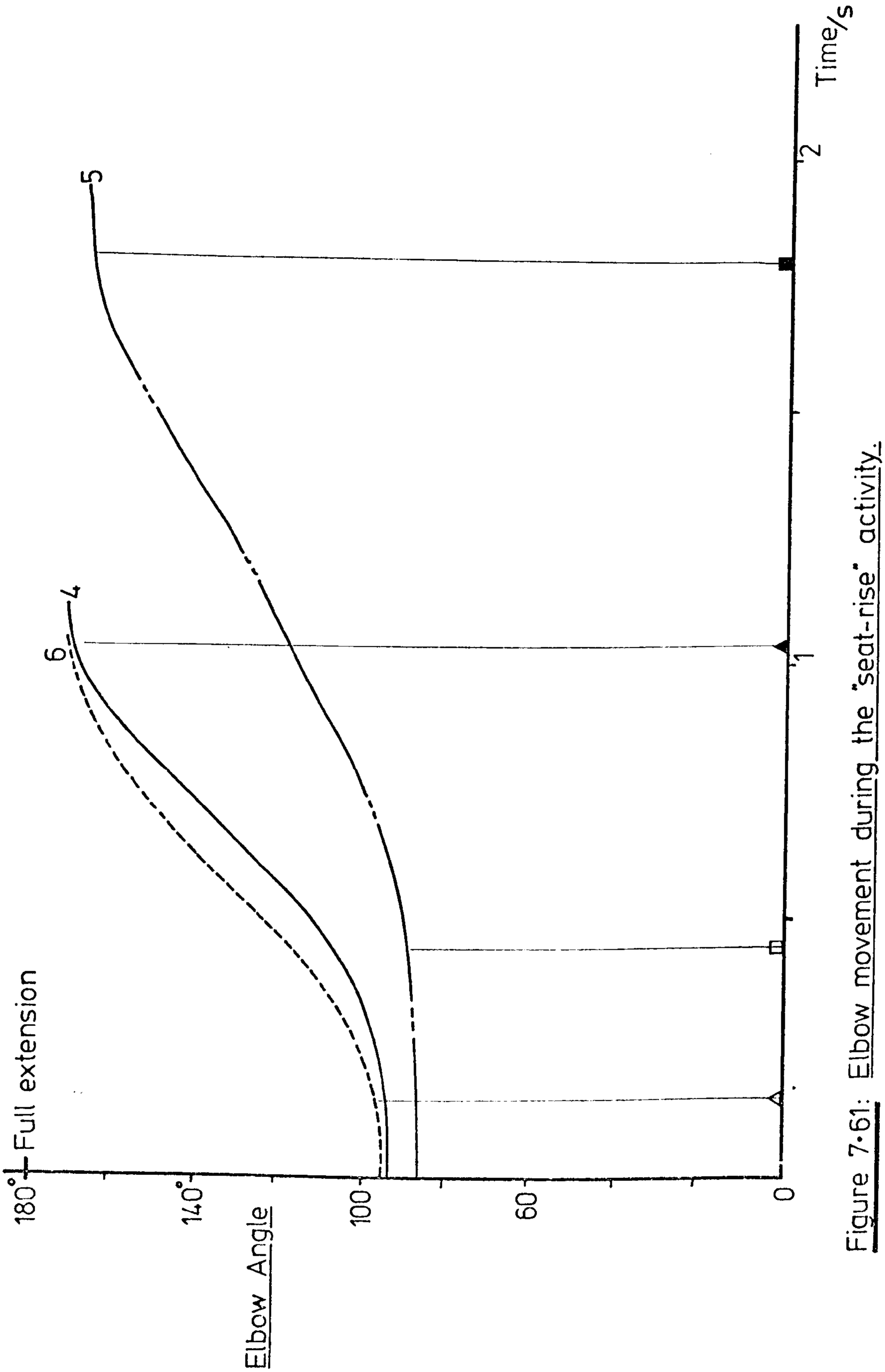

Figure 7·61: Elbow movement during the "seat-rise" activity.

7.5 "Seat-rise" Exercise:

In general, Subject Nos. 4, 5 and 6 performed the "seat-rise" movement with the same range of elbow extension but the duration of the activity varied from 1.0 s (Subjects 4 and 6) to 1.9 (Subject 5). This inconsistency presented problems regarding the indication of specific time related events. It was therefore decided to use the symbols △ and ▲ to signify the initiation and termination of the body movement for Subject Nos. 4 and 6. The symbols □ and ■ were adopted for the designation of the corresponding events for Subject No.5.

7.5.1 Movement: The analysis of the cine films was started just prior to the detection of arm movement on the film record. Although the upper limb was "mobile" at that time, it can be seen from figure 7.61 that the elbow angle was unchanged until t = 0.1 s. The vertical displacement of the shoulder joint was similarly delayed as shown in figure 7.62.

Subject Nos. 4 and 6 executed the ascent phase with uniform velocity of flexion (2.1 rad/s) and uniform vertical displacement of the shoulder (approx. 310 mm/s). Subject No.5, however, experienced much slower movements with "average" velocities of 1.15 rad/s and 200 mm/s.

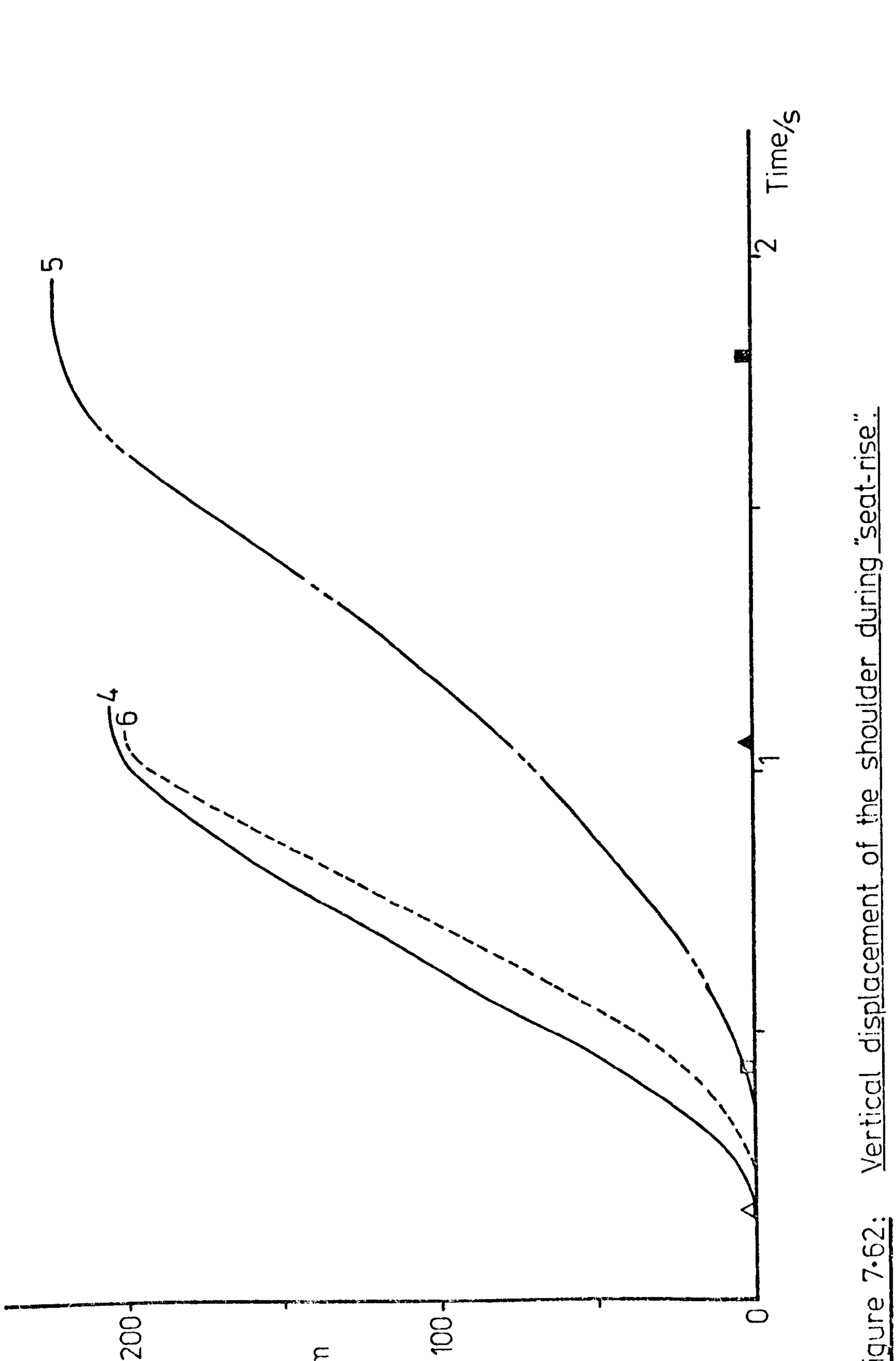

Figure 7·62: Vertical displacement of the shoulder during "seat-rise".

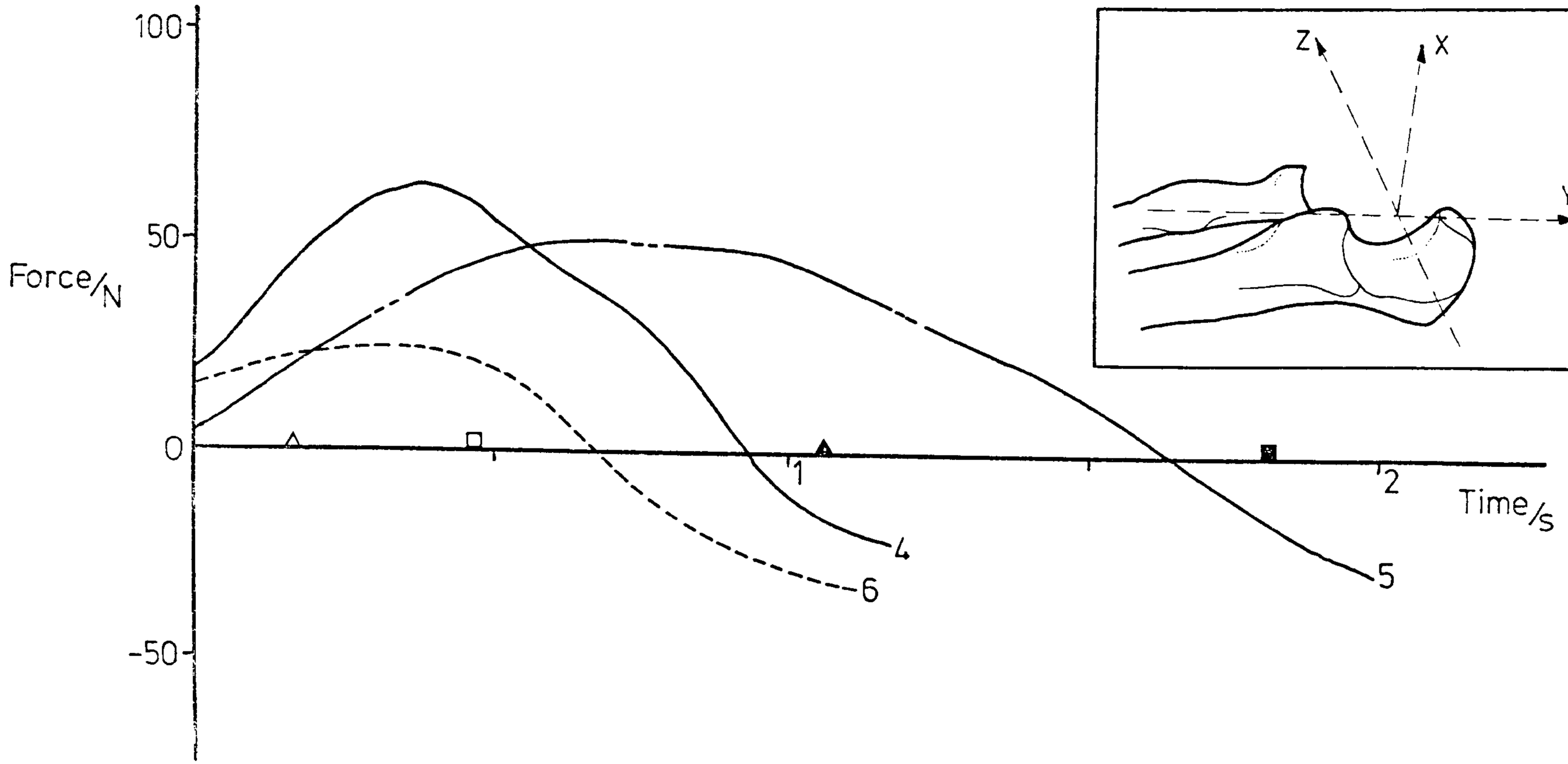

Figure 7·63: Forces acting along X_u during "seat-rise".

7.5.2 External force actions: The external forces and moments acting on the elbow joint are presented in figures 7.63 to 7.68.

Referring back to figure 5.15, the orientation of the forearm, during the seat-rise exercise, was such that the X-axis of the ulna was directed towards the trunk whereas the Z_U axis pointed in a forward direction. In addition, the long axis of the forearm (Y_U) was held in a vertical position and the elbow was flexed to approximately 90° at the beginning of the movement.

Figure 7.63 shows that the "inward" push exerted by the arm of the chair was of the order of 50 N at the initiation of the ascent phase. The negative forces at the finish of the activity corresponded to forced adduction of the shoulder joint. This action attempted to bring the arm into a vertical position and reduce the total muscular activity necessary for the maintenance of the body position. The axial "thrust" transmitted by the forearm reached 200 N in the fully extended elbow joint (see figure 7.64) and represented 30% of the total weight of the body. Figure 7.65 contains the "fore and aft" shear which existed between the upper limb and the arm of the chair. The arm was found to exert reactive forces in a backward direction which reached a maximum of 62 N (Subject No.4).

As experienced with the "table-pull" exercise, the moments calculated for the Y_U and Z_U directions were small compared to moments in the X_U direction. Figure 7.66 shows a maximum moment about the X_U axis of 38 Nm whereas figures 7.67 and 7.68 are bounded by $\pm$ 10 Nm (M_{yu} and M_{zu} respectively).

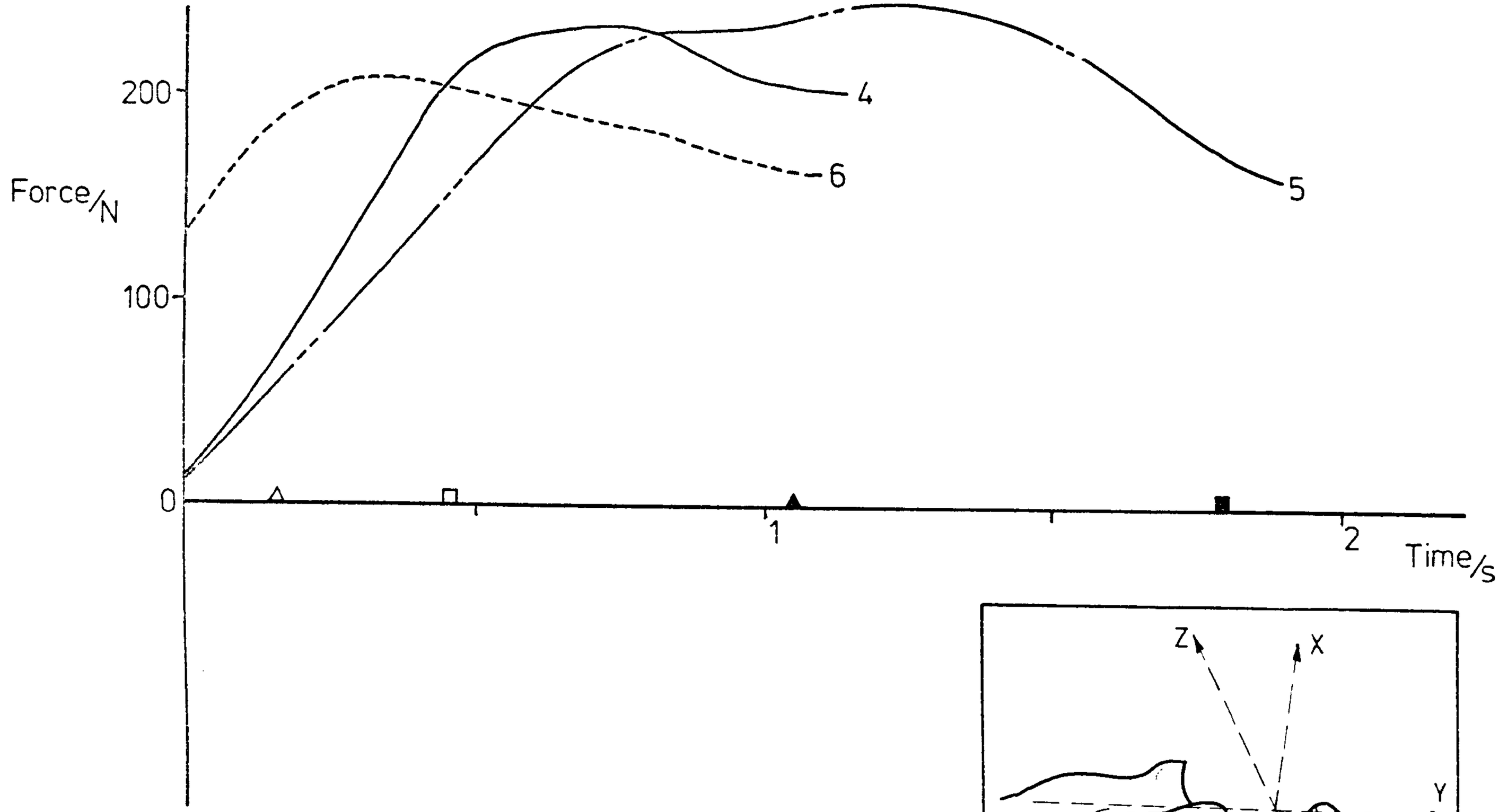

Figure 7·64: Forces acting along Y_u during "seat-rise".

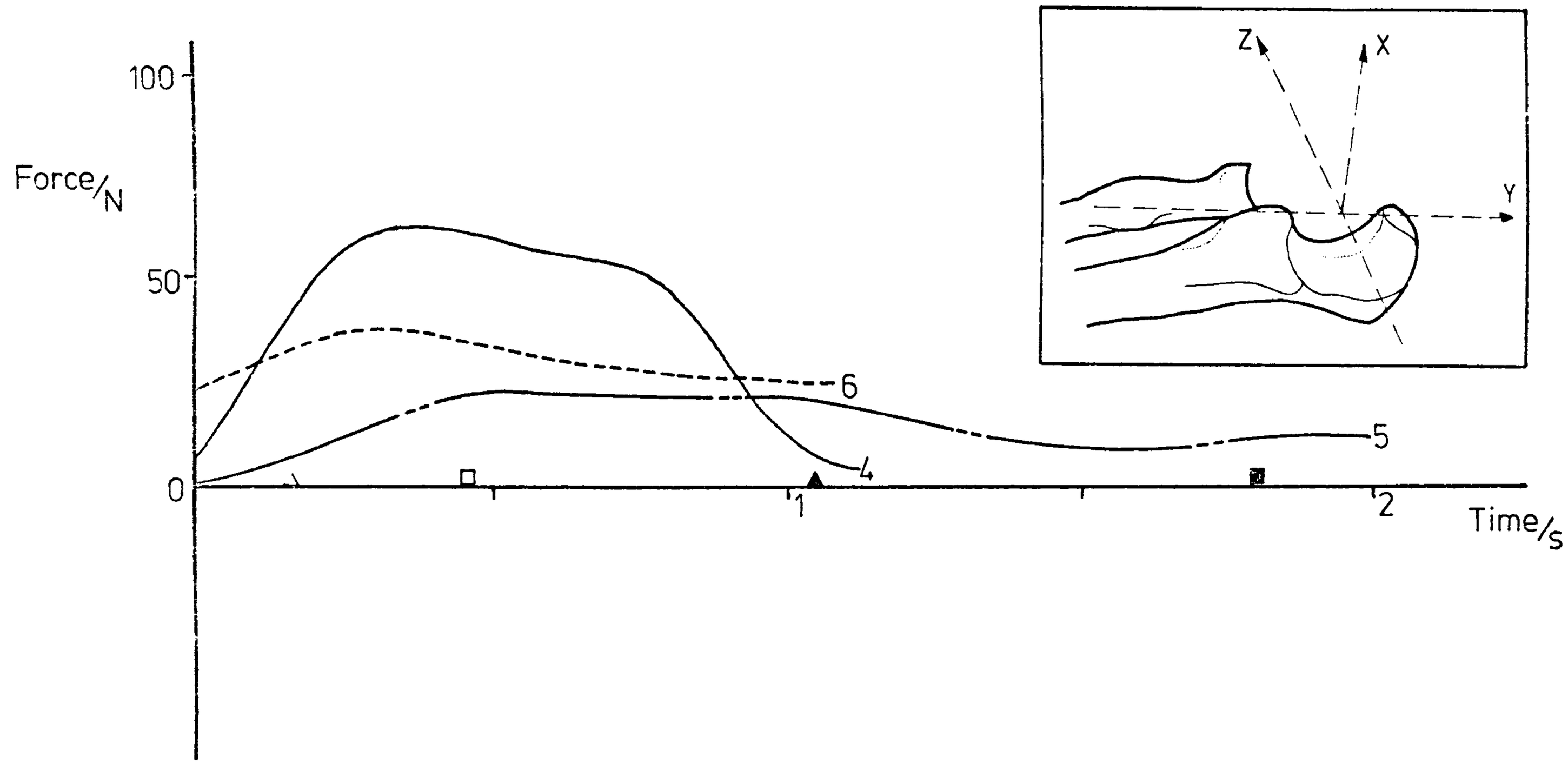

Figure 7·65: Forces acting along Z_u during "seat-rise".

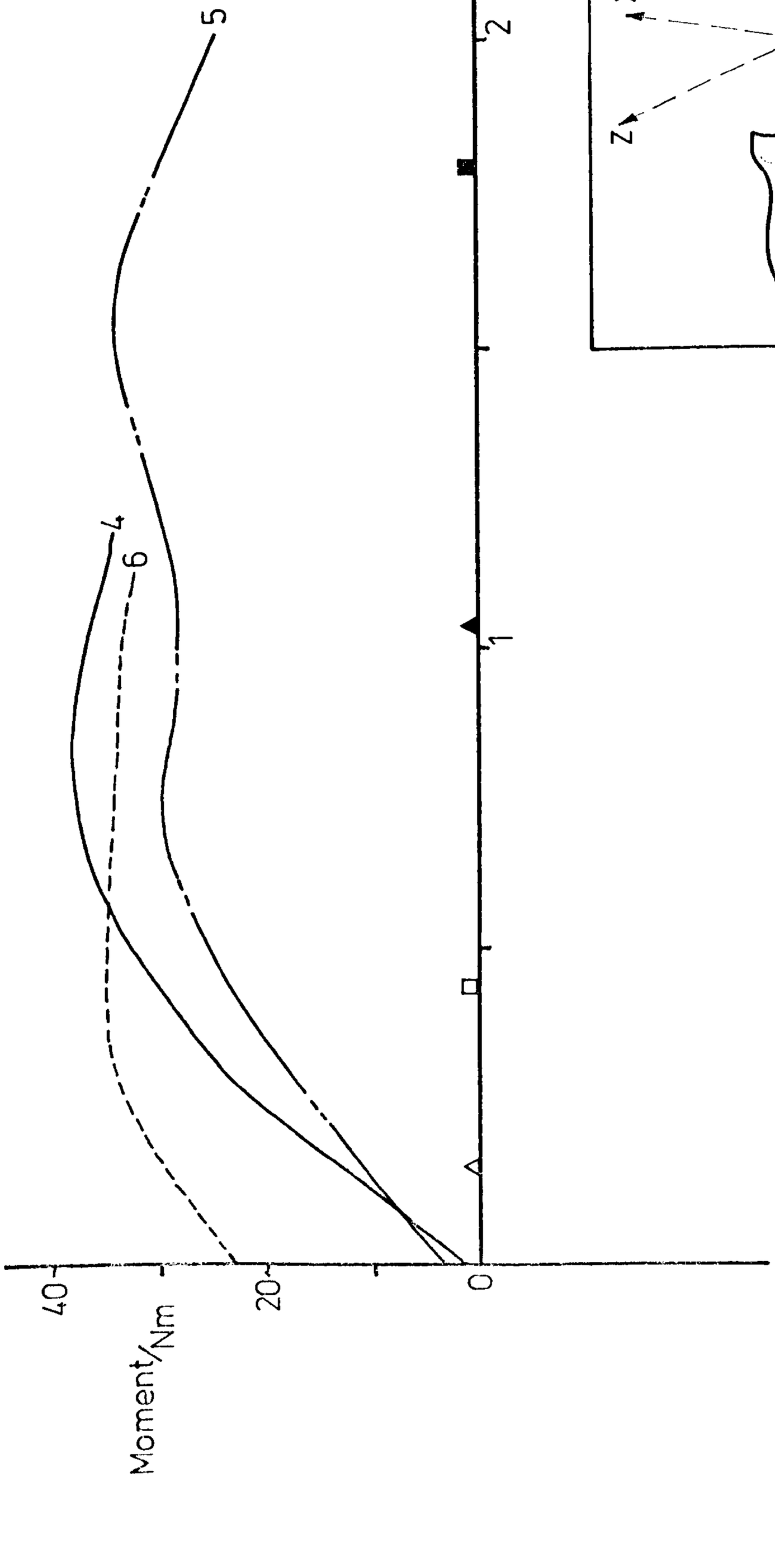

Moments acting about X_u during "seat-rise".

Figure 7.66: Moments acting about X_u during "seat-rise".

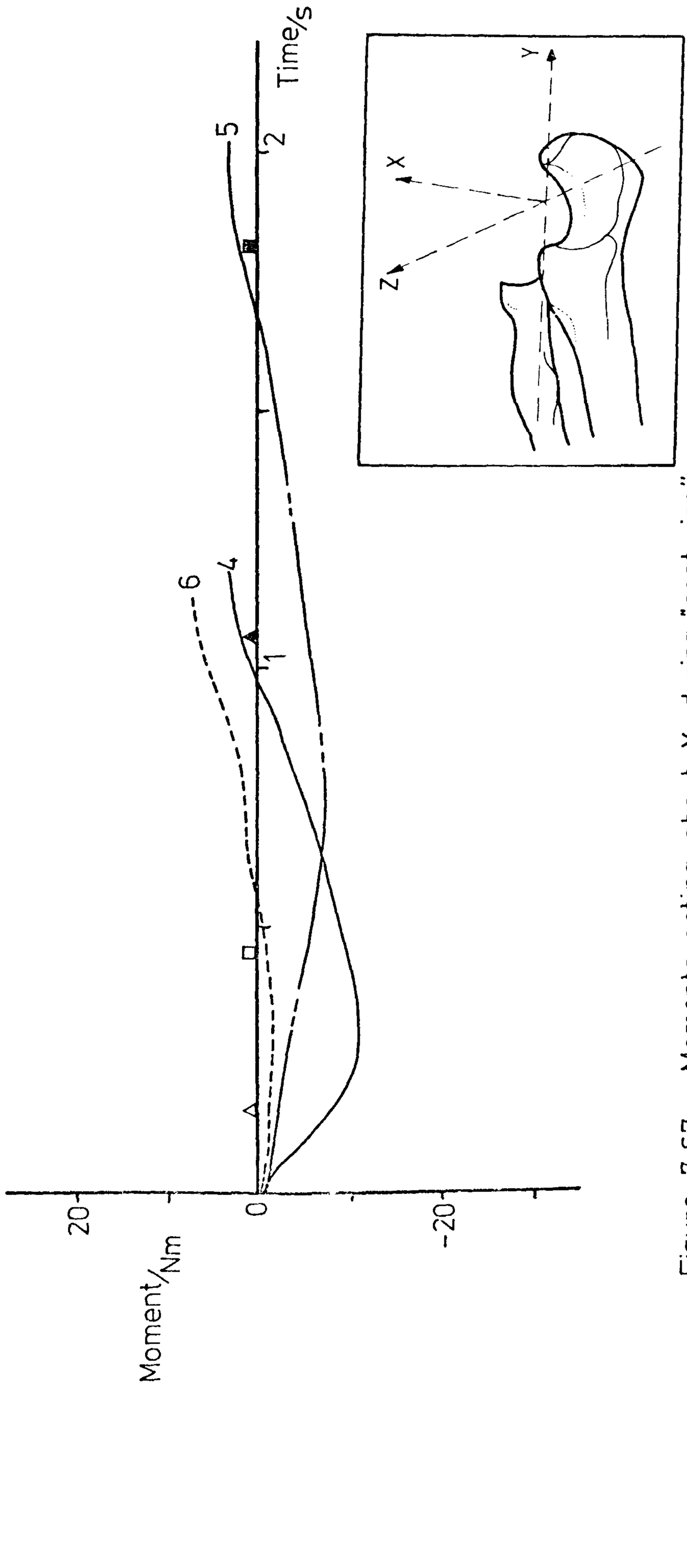

Figure 7·67: Moments acting about Y_U during "seat-rise".

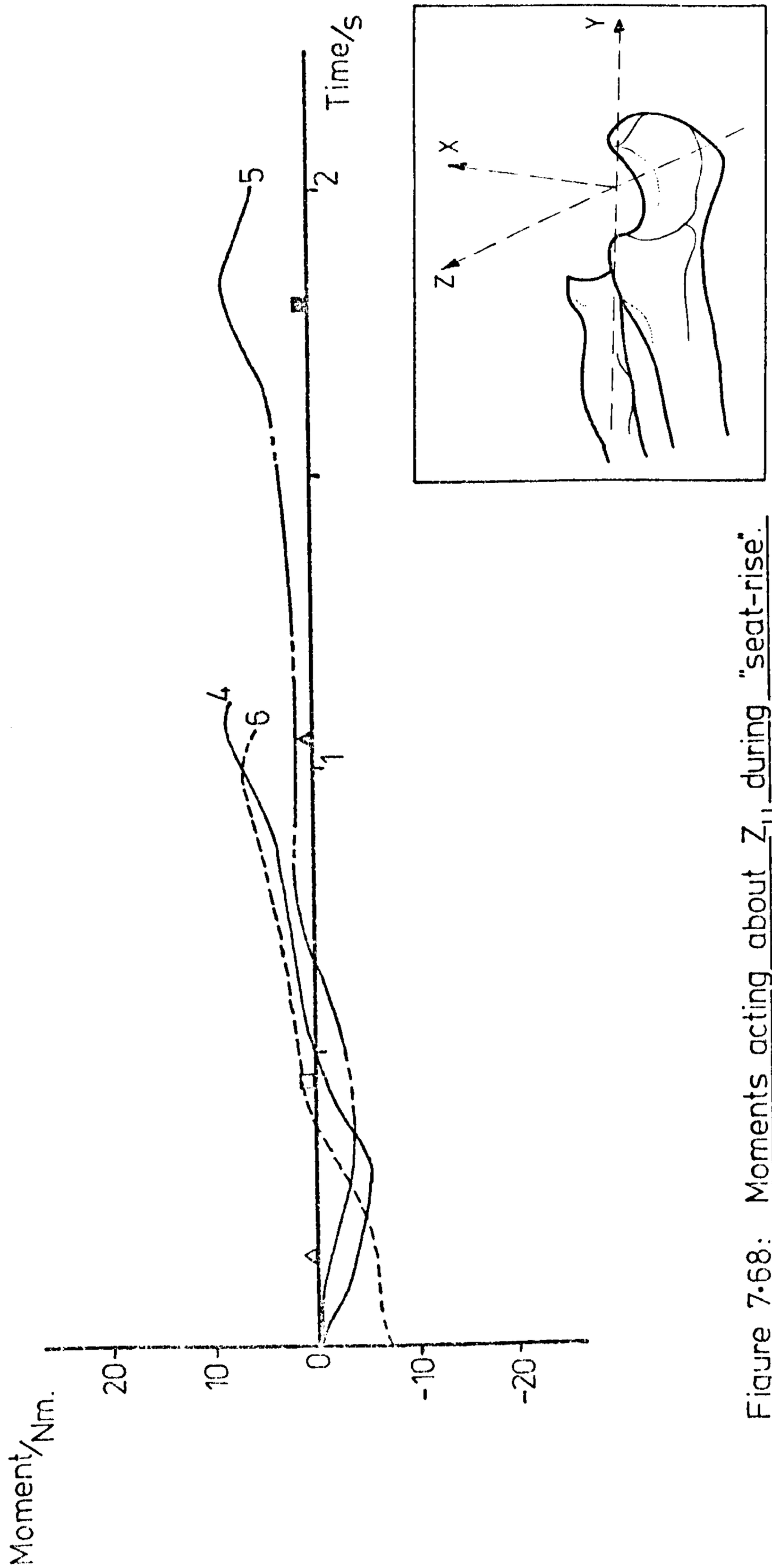

Figure 7.68: Moments acting about Z_u during "seat-rise".

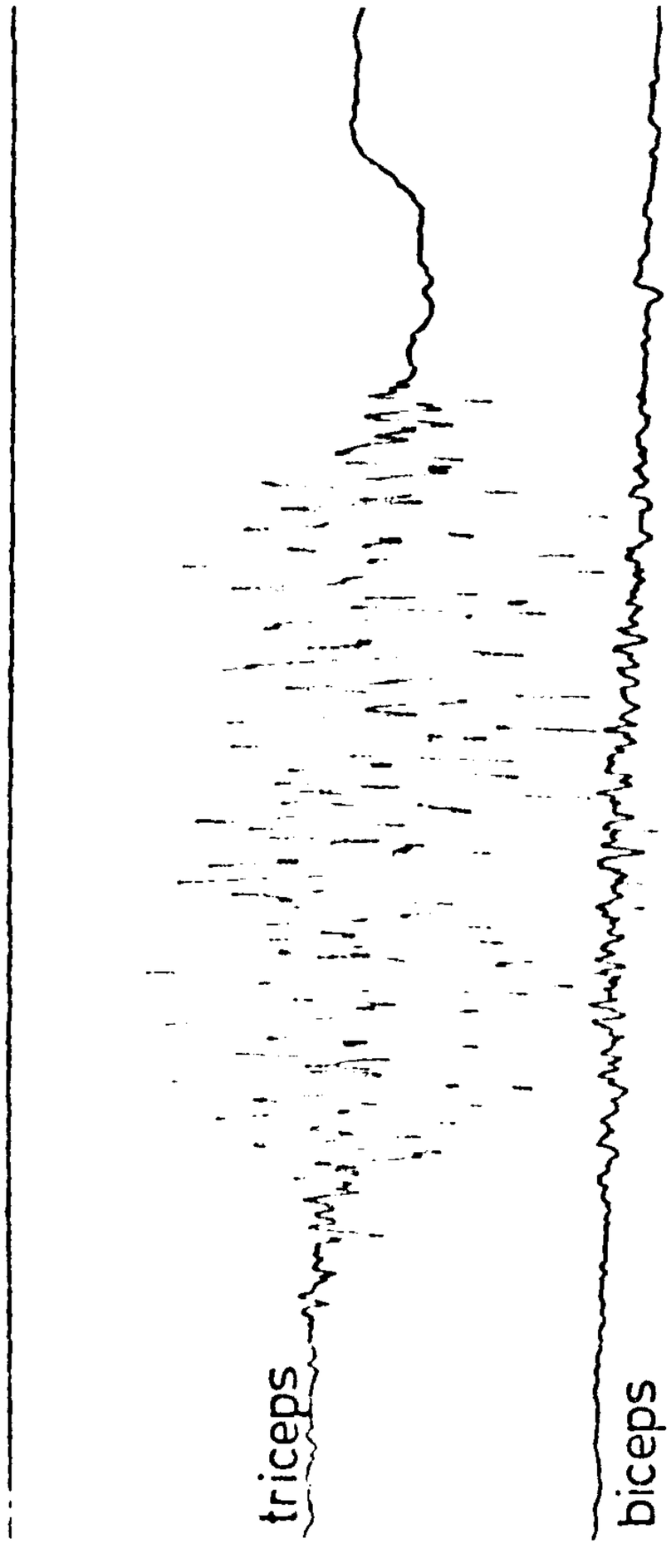

Figure 7·69: Muscle activity during the "seat rise" exercise.

7.5.3 Muscle forces: The electromyograph records indicated the existence of antagonistic muscle activity throughout the exercise as shown by figure 7.69.

At the start of the exercise, the effects of the flexor group were dominant as the arm was brought into a suitable starting position as opposed to the static position shown in figure 5.15. Figure 7.70 shows that tensions up to 100 N were experienced in the flexor group muscles during the first 0.5 s. Once the arm was in the "preferred" position, the moment produced by the extensor group (triceps) became dominant and, in turn, produced extension of the elbow joint (see figure 7.71).

The maximum values of triceps tension coincided with the completion of elbow extension at the end of the exercise and the slight reduction in muscle tension was characteristic of the stable position provided by the geometry of the elbow joint at full extension. The muscle action served only to supplement this aspect whereas previous muscle action had produced gross movement of the body and had required larger values of muscle tension.

7.5.4 Ligament forces: As a result of the negative moments experienced in the Y_U direction (figure 7.67) together with the external force actions at the interface of hand and chair, the lateral ligament transmitted tension throughout the whole activity. Subject No.4 developed tensions as high as 800 N but tensions of 500 N were characteristic of the other subjects (see figure 7.72).

7.55 Joint forces: Figures 7.73 and 7.74 show the resultant force actions on the medial and lateral surfaces of the trochlear notch. The lateral joint forces were typically 500 N but the medial force increased from 500 N to maxima of 1250 N.

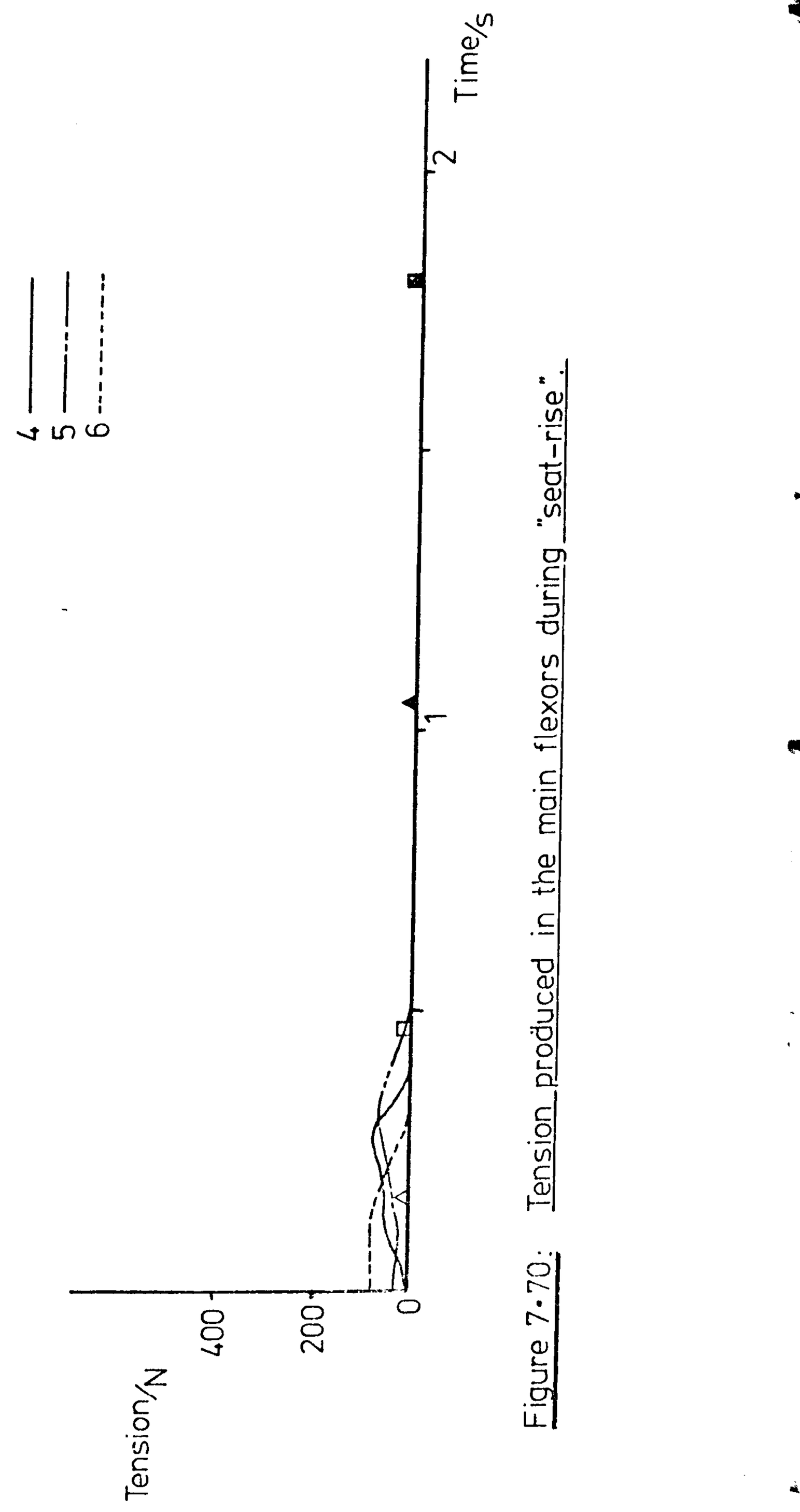

Figure 7·70: Tension produced in the main flexors during "seat-rise".

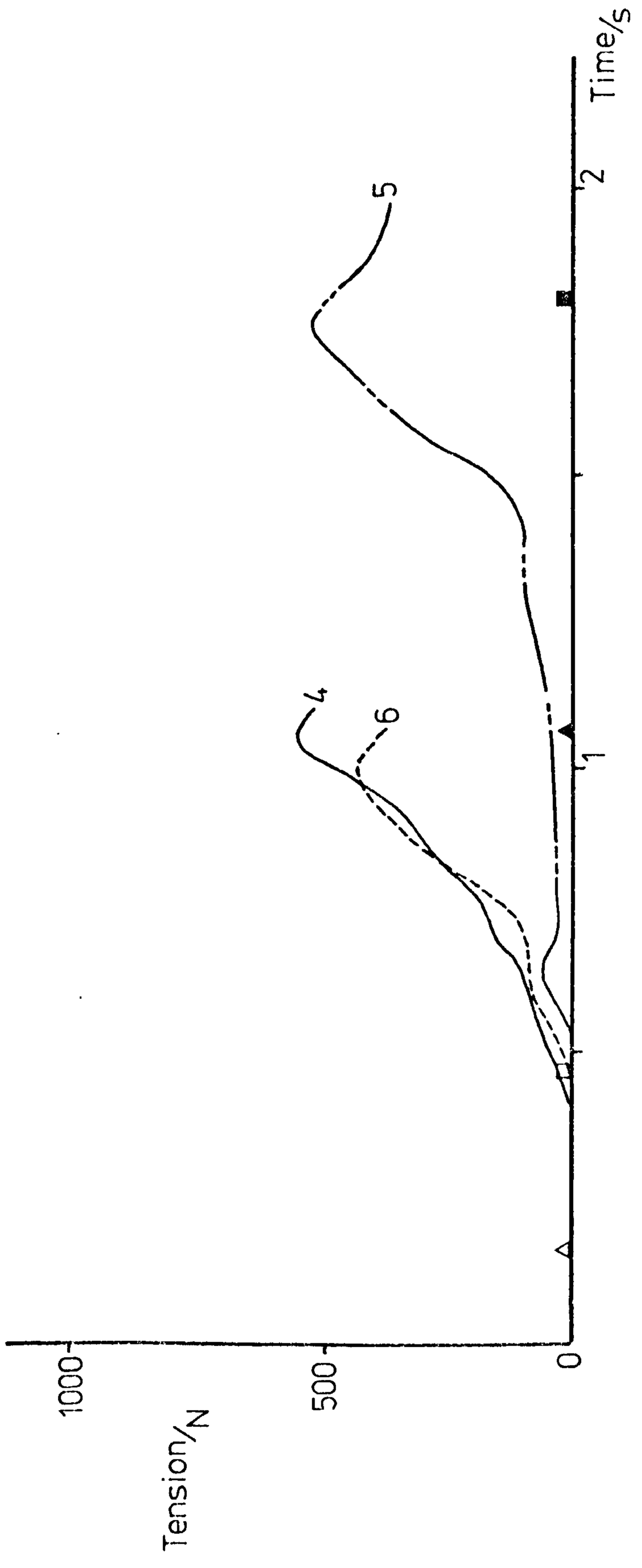

Figure 7·71: Triceps tension produced during "seat rise".

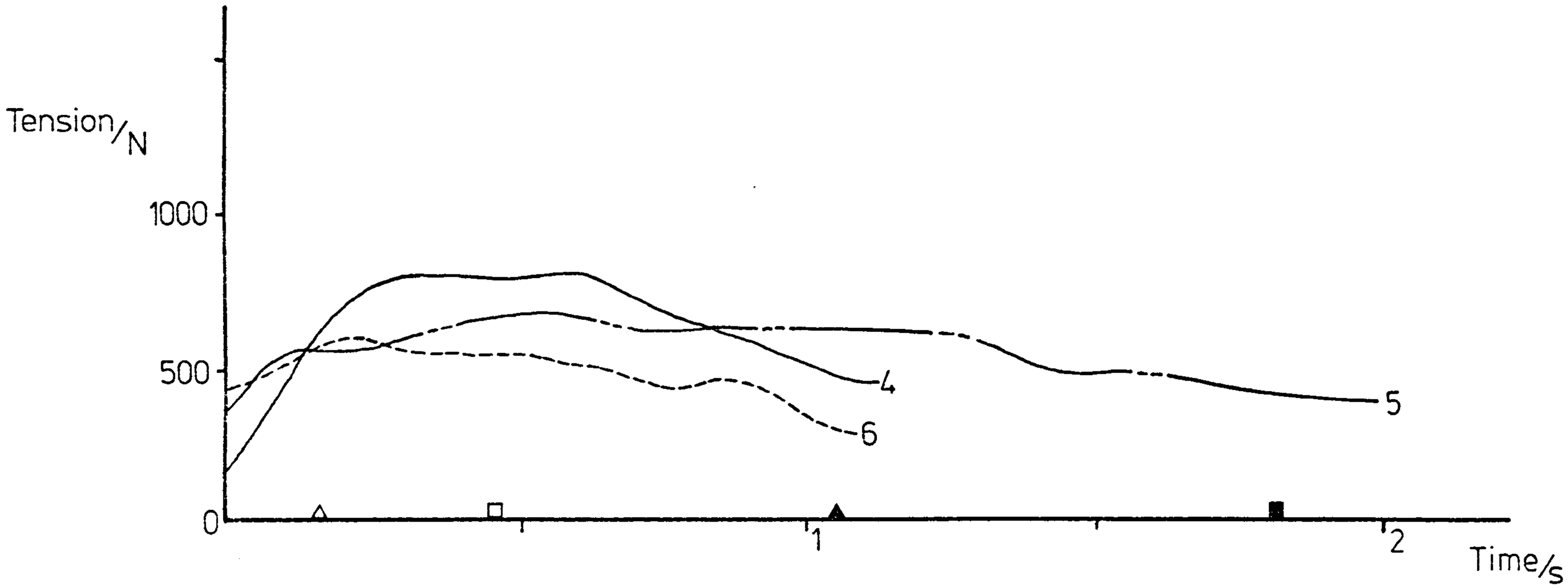

Figure 7·72: Lateral ligament tension —"seat-rise" activity.

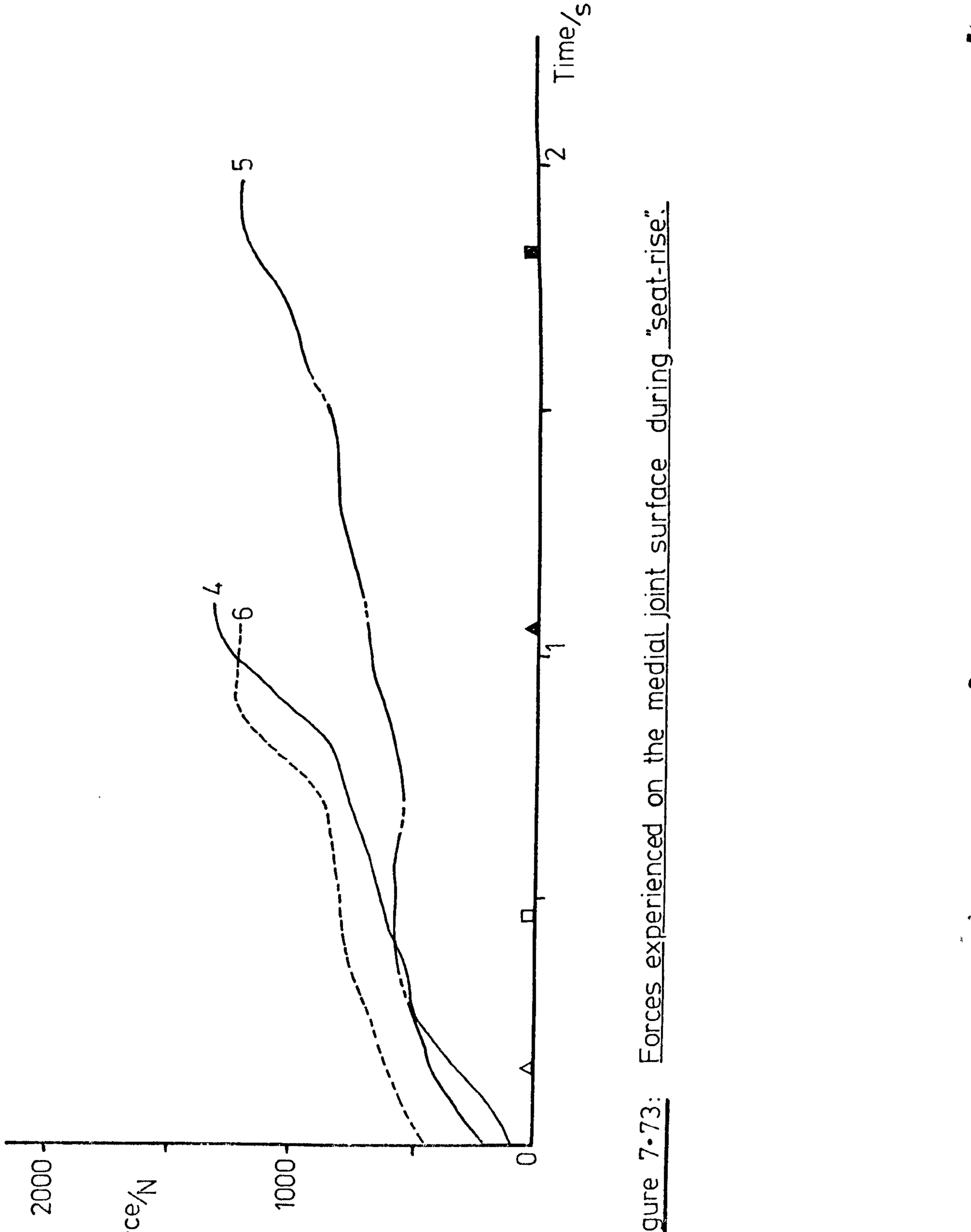

Figure 7·73: Forces experienced on the medial joint surface during "seat-rise".

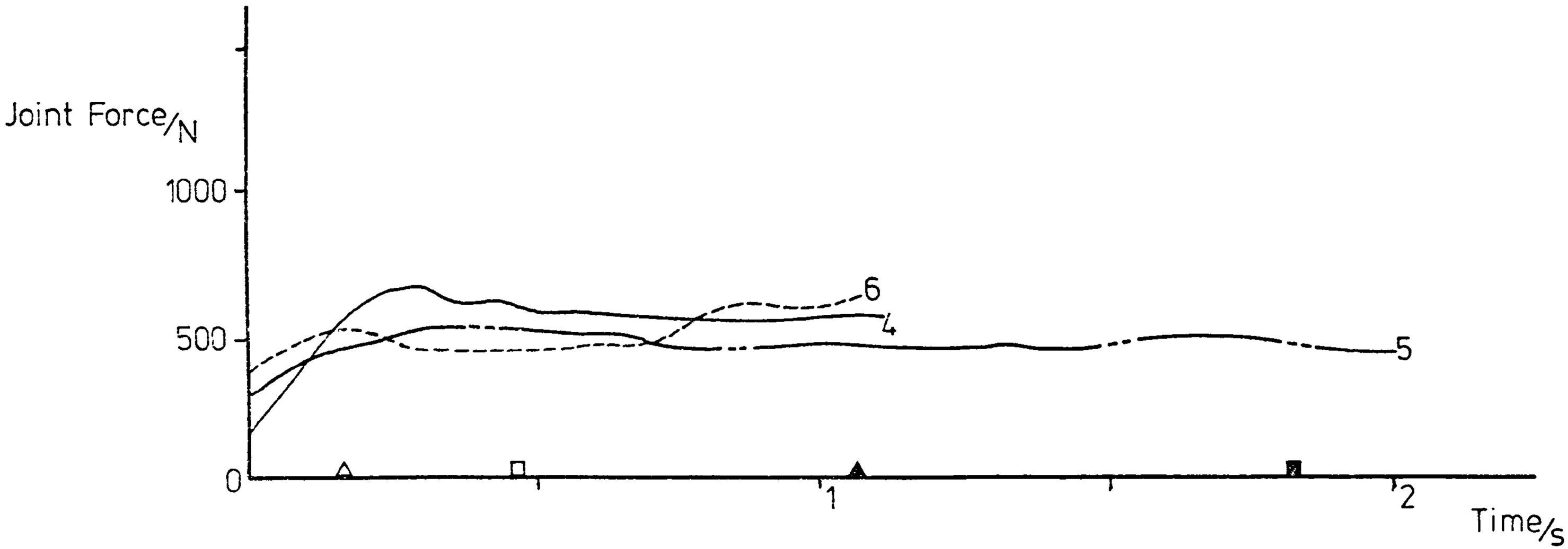

Figure 7·74: Forces experienced on the lateral joint surface during "seat-rise".

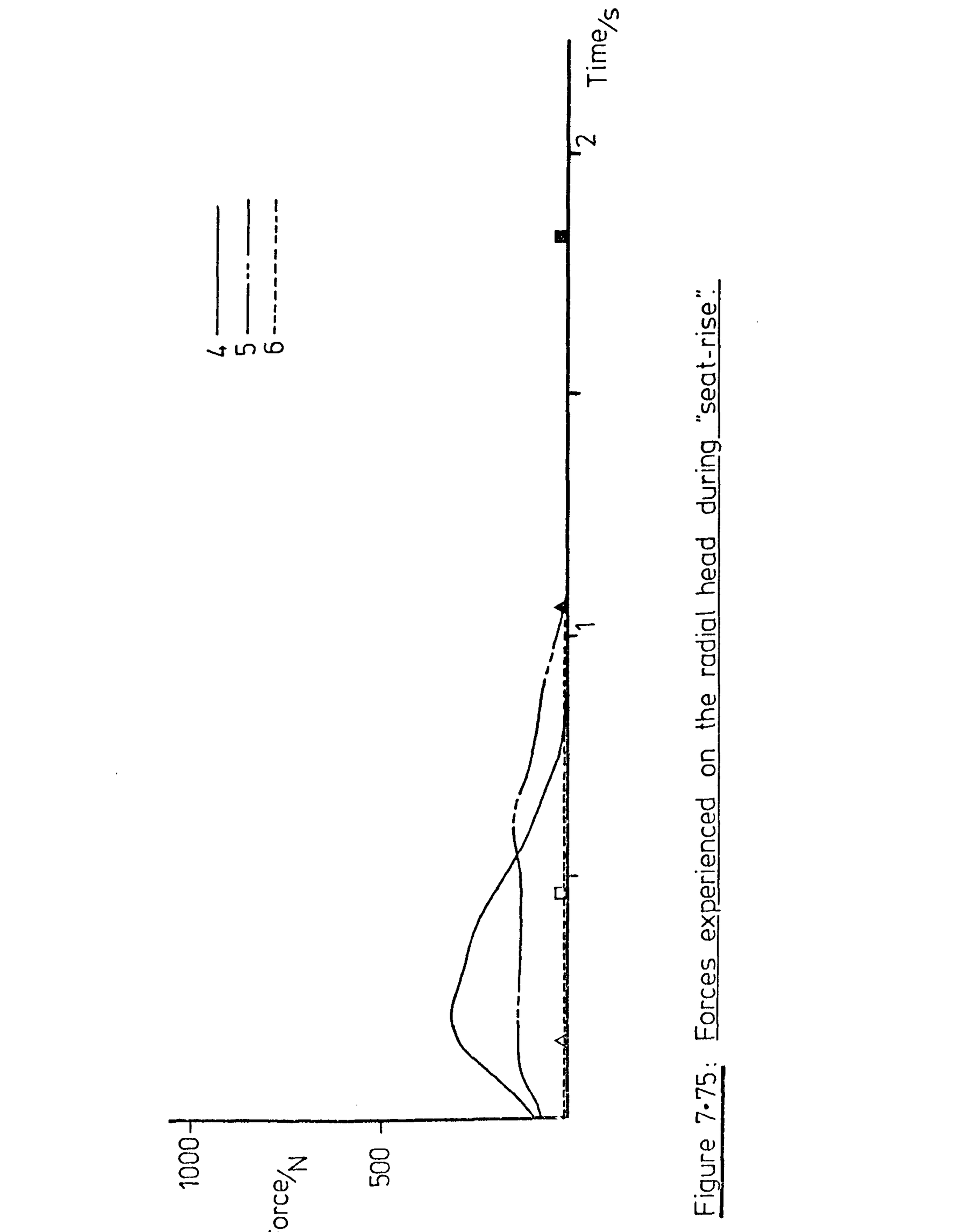

Figure 7·75: Forces experienced on the radial head during "seat-rise".

Contact between the capitulum and the head of the radius was evident in two subjects. For Subject No.4, contact was experienced throughout the complete movement and a peak of 300 N was reached as shown in figure 7.75. Compressive forces of 150 N were calculated for Subject No.5 during the first half of the exercise whereas no contact was experienced by Subject No.6. It was postulated that the position of the hands in relation to the rest of the body was responsible for this difference.

The complete system of force actions for each subject is detailed in figures 7.76, 7.77 and 7.78.

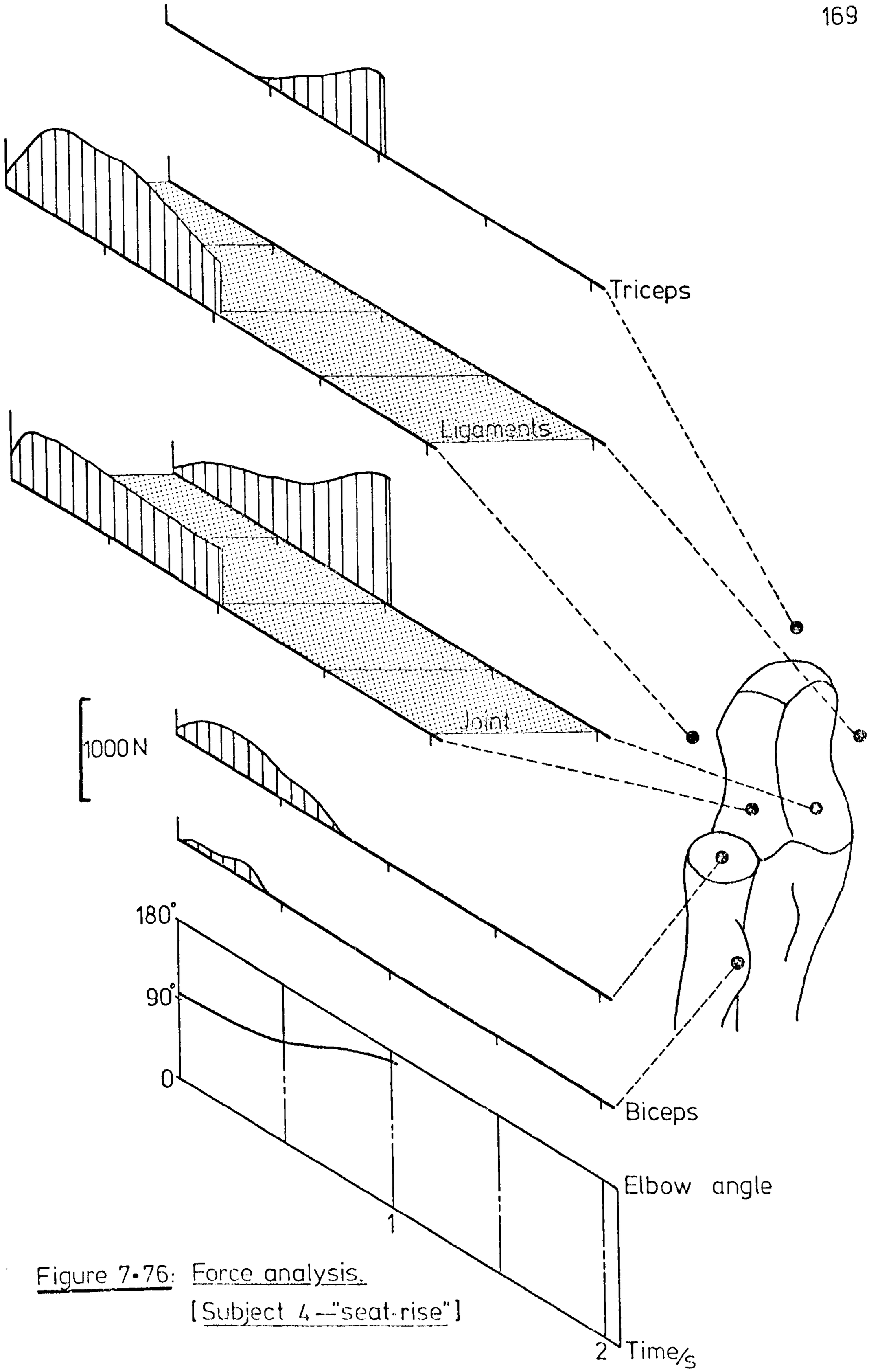

Figure 7·76: Force analysis.
[Subject 4 -- "seat-rise"]

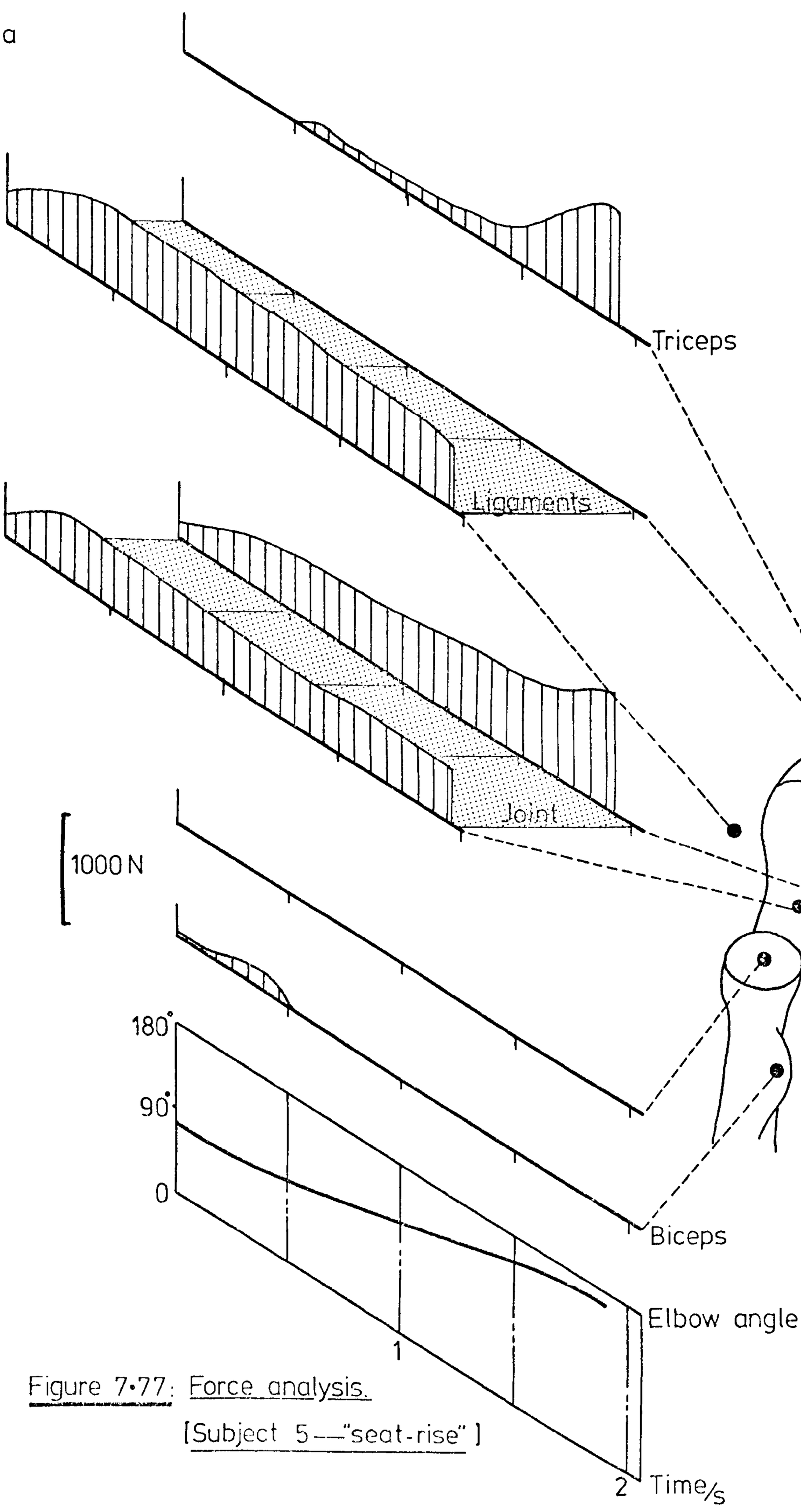

Figure 7·77: Force analysis.

[Subject 5 —"seat-rise"]

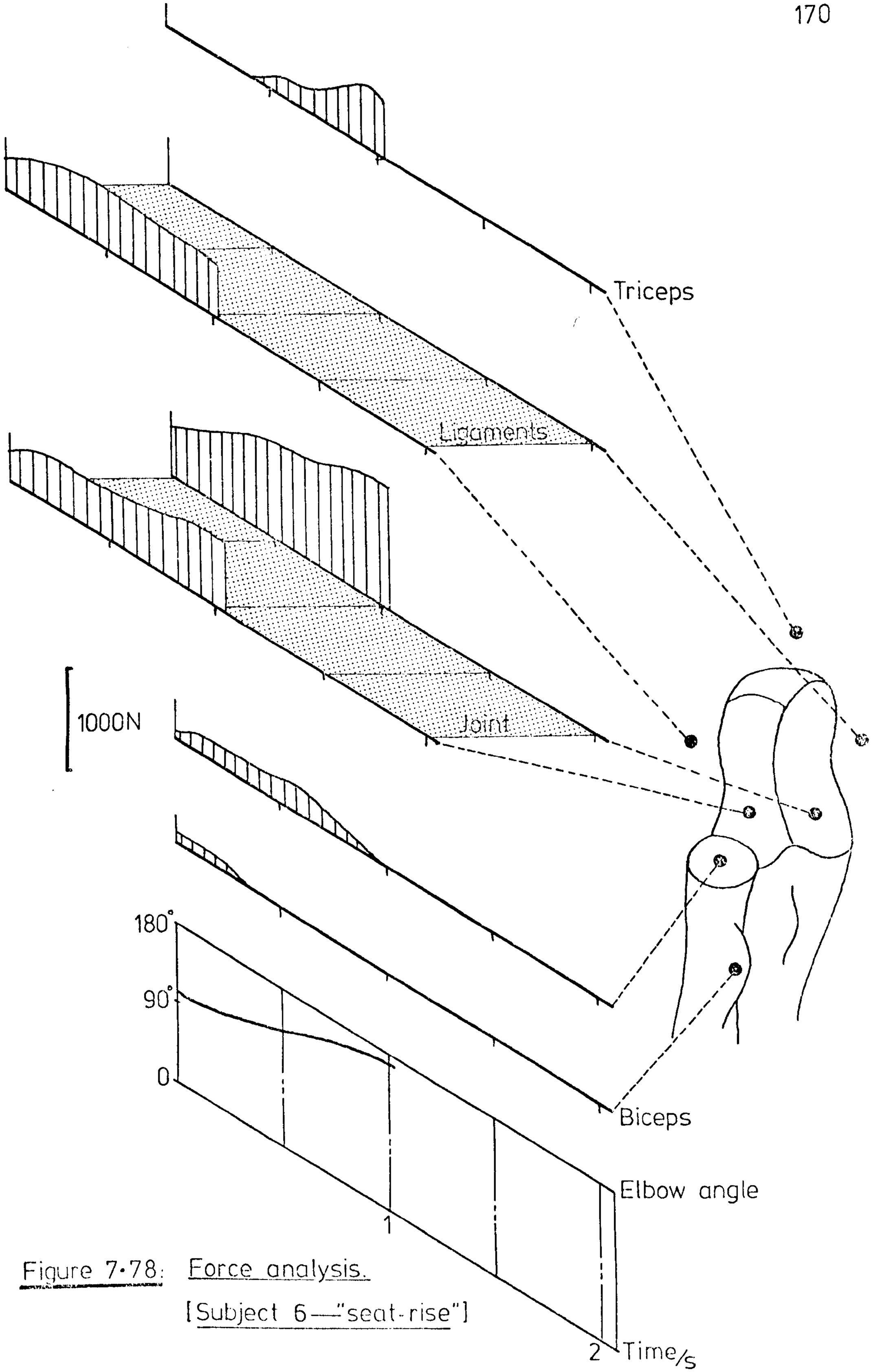

Figure 7·78: Force analysis.

[Subject 6—"seat-rise"]

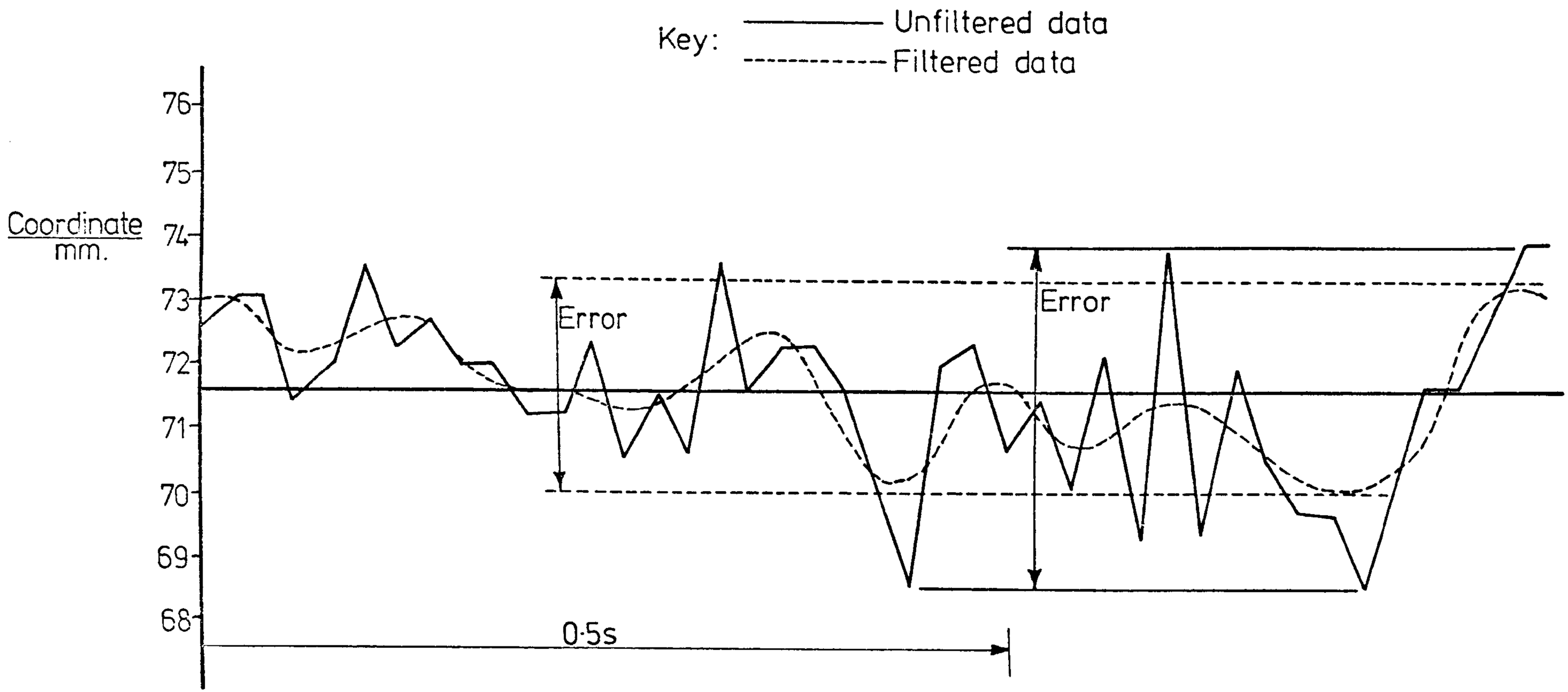

Figure 7·80: The effect of filtering procedures on the coordinates of a stationary point.

7.6 Sources of Error:

Several sources of error were discovered and are described as follows.

7.6.1 Cadaveric measurements: As previously mentioned in section 5.2.1 the measurement of the three-dimensional coordinates of relevant anatomical structures incurred an error of $\pm$ 1 mm. To obtain an estimate of the resulting "error", each coordinate was altered by 2 mm in the program "XNICOLPROG" so that the final joint forces would be increased to a maximum value. For example, the muscle coordinates were decreased by 2 mm in order to increase the muscle tension necessary to balance the unaltered moment M_{zu}. Ligament coordinates were similarly altered but the geometry of the articular surfaces was not included in the perturbation routine.

7.6.2 Film measurements: The synchronisation errors between the three cine cameras were small (<0.02 sec). The constant errors of up to several centimetres in certain displacements were considered to have a minor contribution to the error in the final elbow joint forces and were not analysed. However, fluctuating errors in the measurement of the marker points were significant and a study was undertaken in order to establish the effects these errors had on the coordinates of each marker joint.

During the "seat-rise" activity, the position of the transducer markers (Nos. 10, 11, 12 and 13) did not alter and the x-coordinate of marker No.13 was chosen as the reference coordinate for the error study. The choice of x, y or z was immaterial since the distances of each camera from the reference grid origin ensured a standard image size (dependent on the focal length of the lens and the camera-object distance). Figure 7.80 shows the measured values together with the "filtered" data. An "error" of + 2 mm and - 3 mm was evident for the unprocessed data but the "error" involved with the filtered data was reduced to $\pm$ 1.5 mm. This latter value was taken to be characteristic of the whole measurement sequence. The mean value of the coordinate remained unaltered at 71.52 mm for both sets of data.

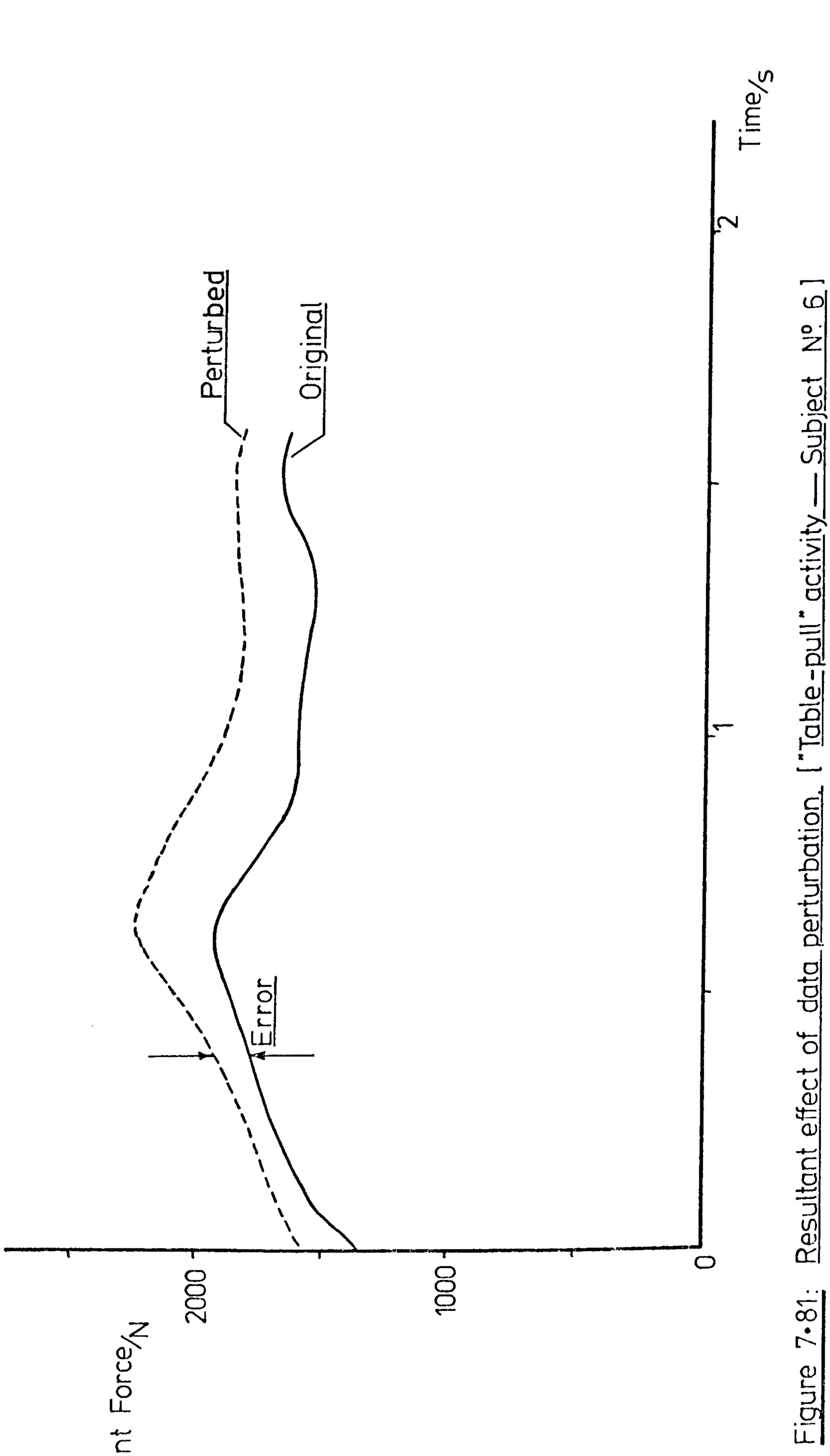

Resultant effect of data perturbation. ["Table-pull" activity — Subject No: 6]

Figure 7•81: R

Since the calculation of subcutaneous points involved two marker points, coordinates were altered by 3 mm to study the error in the loadings on the elbow region.

7.6.3 Analytical procedure: For the purpose of this thesis, the determination of errors which could be attributed to the mathematical procedures involved in the theoretical analysis was considered to be too time consuming. Reference is therefore made to Andrews (1976) for information related to the "accuracy" of various theoretical analyses.

7.6.4 Results: The perturbation routines applied to the above-mentioned coordinates produced joint forces which were considerably higher than those calculated from the original data. Figure 7.81 shows the original and the "processed" joint forces acting on the medial surface of the trochlear notch during the table-pull exercise (Subject No.6.).

A maximum difference of 390 N was recorded and this represented an error of 20.5%. It is estimated, however, that consideration of antagonistic muscle activity would result in larger alterations to the original computations.

It is interesting to note that Paul (1967) calculated a standard error of 24% for the forces acting at the hip joint during walking. The analytical method used in this thesis was similar to that used by Paul and agreement on this aspect was expected.

7.7 Summary:

The following points were concluded from the preceding work.

I) The maximum angular velocities of elbow flexion occurred during the eating and reaching activities. Values of 2.95 rad/s and 4.8 rad/s were experienced respectively.

2) The rate of elbow extension was greatest in the eating and reaching activities with angular velocities of 4.35 rad/s and 3.65 rad/s respectively.

3) Maximum joint forces of 350 N were produced between the ulna and the humerus during the two inertial activities (eating and reaching).

4) The maximum value of muscle force calculated during the table-pull exercise was 950 N acting in the biceps and brachialis muscles. Half this value was generated in the brachioradialis muscle.

5) Joint forces at the elbow joint during the table-pull exercise were typically 1500 N. A maximum value of 2450 N was obtained for two subjects (Nos. 4 and 6) at the start of the activity.

6) During the seat-rise exercise, maximum triceps tension of 560 N was obtained for two subjects (Nos. 4 and 5).

7) A maximum joint force of 1300 N was calculated for the medial surface of the elbow joint during the seat rise activity. Typical contact forces of 500 N were experienced on the lateral surface of the joint.

8) Maximum ligament tensions of 800 N (lateral) and 2290 N (medial) were generated during the seat-rise and table-pull exercises respectively. During the eating and reaching activities, the ulnar collateral ligament transmitted, in general, 30% more tension than the radial collateral ligament.

Activity	Angular velocity (rads/s)	Joint force (N)	Sliding velocity (mm/s)	"P_*V" (Nm/s)
"Eating"	4.35 0.5	240 400	52.2 6.0	12.5 2.4
"Reaching"	4.8 0	140 400	57.6 0	8.06 0
"Table-pull"	1.25 1.25	2450 2450	15 15	36.75 36.75
"Seat Rise"	2.1 0.85	700 1300	25.2 10.2	17.6 13.26
Normal gait (hip joint)	2.6 0.87	3200 4800	41.6 13.9	133 67

Table 7.1: Summary of Maximal Results.

9) Forces calculated to be acting in the medio-lateral direction (Z_U) were of secondary importance to the design of an elbow prosthesis. The maximum value obtained for this "residual" force was 1064 N during the "table-pull" exercise and represented 24% of the total joint force.

Table 7.1 contains the maximum joint forces and the maximum angular velocities for the four activities together with the corresponding angular velocities and joint forces respectively. Taking an "average" radius of 12 mm for the articular surfaces of the elbow joint, the articular "sliding velocities" were calculated from the angular velocities of elbow flexion and extension. The product of this sliding velocity and the corresponding joint force ($P * V$) is becoming accepted as a criterion in the design of joint prostheses and the appropriate values are presented. A maximum value of 36.75 Nm/s was obtained during the "table-pull" exercise which has previously been described as the most "strenuous" of the four activities (section 7.4).

Using data from Tooth (1976) the product of force and sliding velocity at the hip joint was calculated at the instants of maximum joint force and maximum angular motion of the hip joint. Values of 67 and 133 Nm/s were obtained respectively (see Table 7.1) which were very much greater than the corresponding values computed for the elbow joint. It can therefore be expected that the joint surfaces of the proposed elbow prosthesis will be capable of handling the full range of load actions from "everyday" activities.

7.8 Recommendations for Further Work:

One of the most important aspects of biomechanical analyses is its contribution to the development of prosthetic and/or orthotic components. In this case, the analysis was undertaken to aid the development of an improved elbow prosthesis. Chapter 9 is essentially a report of the design study and contains details of the advanced prototype total elbow prosthesis.

Before further studies of upper limb function are undertaken, it would be advantageous to fully investigate the precise activities which can be selected for analysis. Although liaison was established with physiotherapists and physical education personnel during the experiment design stage of this project, the complete requirements of arthritic patients should be considered in future.

A natural extension of the project would be an investigation into the biomechanics of the elbow joint/upper limb for arthritic and paraplegic patients. In these groups, the arms are frequently used to supplement the reduced muscle activity of the lower limb or to provide total body motion and this leads to a greater dependency on the correct performance of the upper limb. A secondary project should also be undertaken to study the muscular "strength" of patients compared to healthy subjects.

In order to obtain a greater understanding of the movements of the elbow joint, the kinematics of the shoulder complex should be analysed. Antagonistic activity of the bi-articular muscles (biceps and triceps) could then be studied in relation to the E.M.G. recordings and the motion of the elbow and shoulder joints. In addition, sophisticated quantitative electromyography would enable the derivation of the relative contributions from individual muscle groups (see Bankov and Jorgensen, 1969) and could lead to a deeper knowledge of the mechanics of human muscle.

8. REVIEW OF ELBOW PROSTHESES

8. REVIEW OF ELBOW PROSTHESES

8.1 Introduction:

The commendable success of total joint replacement for the lower limb in recent years (see Appendices 3 and 4) has encouraged researchers to undertake the design and development of prosthetic joints for the upper limb. As a prelude to the "design study" described in Chapter 9, this section presents a brief description of the important developments over the past thirty years in the design of elbow prostheses.

8.2 Distal Humerus:

Mellen and Phalen (1947) manufactured methylmethacrylate models of the distal humerus. The design of the articular surfaces did not correspond to the anatomical geometry of the trochlea but did allow painless elbow movement. The prostheses was bound to the remaining bone by loops of tantalum wire. Four patients were treated and flexion of 50-150° was obtained.

Venable (1952) formed an all-metal (Vitallium) component from a "jigsaw" of bone pieces taken from a comminuted fracture. To obtain correct articulation the olecranon had to be fractured since errors in x-ray sizing had resulted in the production of an excessively large trochlea. Fixation to the humerus was achieved by an intramedullary stem and two external "leaves". Good flexion movements were obtained free of pain.

Nylon was used by MacAusland (1953) to replace the distal humerus in four patients but the results are of little relevance due to current restrictions of biocompatibility.

From a cast of a cadaveric humerus, Barr and Eaton (1965) produced a Vitallium component with a diamond section intramedullary stem and two transverse bone screws for fixation. Small loops were provided at the epicondyles for attachment of muscle tendons and ensured correct forearm function. Minimisation of weight was an important design feature and the hollow prosthesis was trimmed where possible. Initial range of movement was 30° - 125° but after four years strenuous use the distal fixation screw had fractured and a considerable

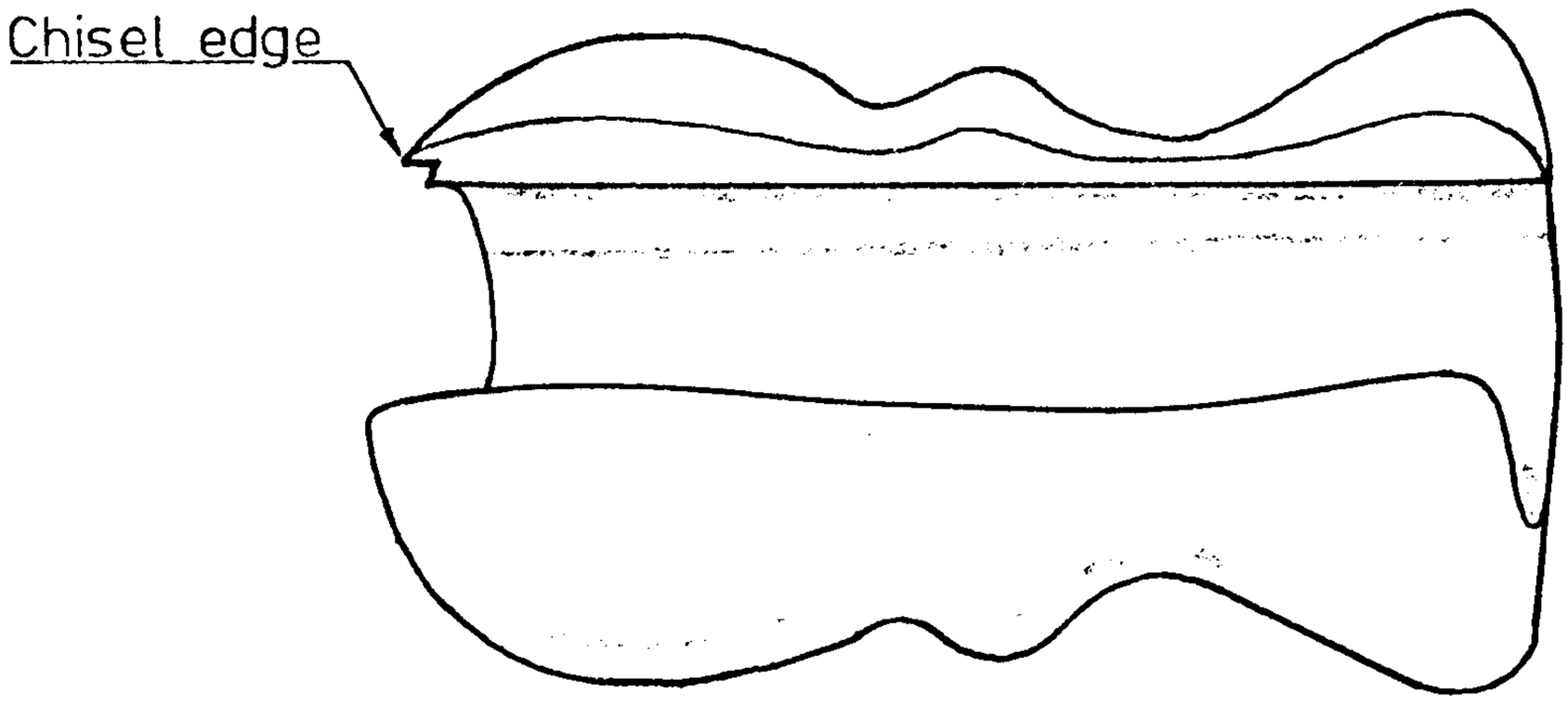

Figure 8·1: Shape of humeral prosthesis [Street and Stevens]

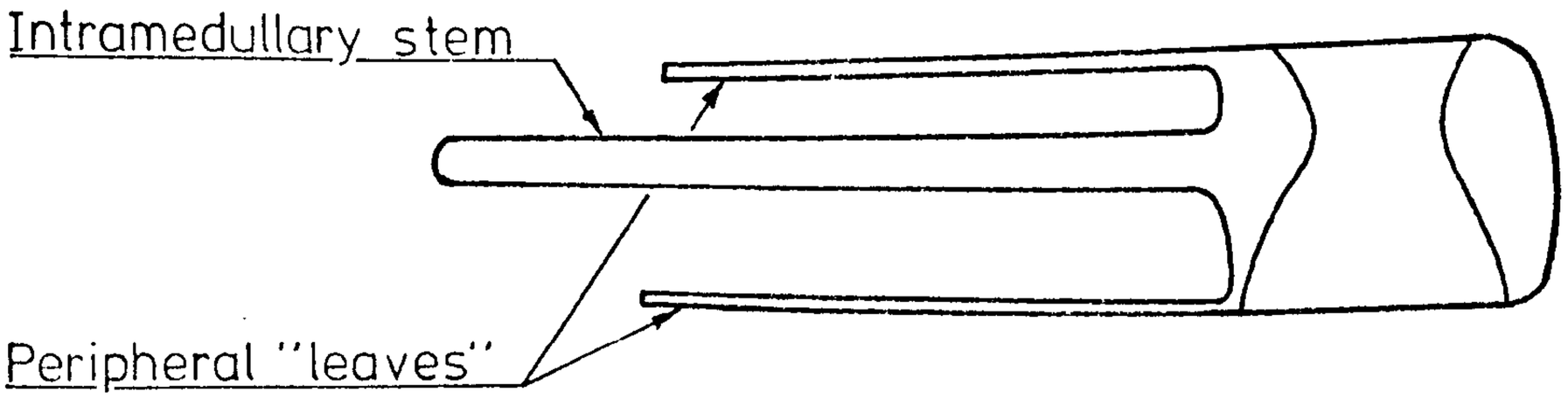

Figure 8·2: Sketch of ulnar prosthesis [Johnson and Schlein]

degree of pain was experienced.

Using roentgenogram measurements of the opposite humerus, Dunn (1971) reconstructed a distal humerus with a Vitallium component. An intramedullary stem and two extracortical flanges provided fixation to the remaining bone mass. In addition, three screws were driven transversely through the humerus and stem to prevent rotation of the unit. The forearm flexor and extensor groups were attached to the prosthesis by means of loops (cf. Barr and Eaton) and a very stable joint was obtained with 30° - 120° flexion and no pain.

More recently, Street and Stevens (1974) reported a long term follow-up of a humeral component to replace both the trochlea and the capitulum. The units were made from stainless steel or titanium and were formed from a solid of revolution as shown in figure 8.1. Fixation was provided by the hole/slot arrangement since the slot width was less than the diameter of the central hole. A chisel edge at one end enabled the prosthesis to be driven across the prepared bone end and good fixation was obtained without the use of acrylic bone cement. Several fixation problems were experienced from patients with "active" rheumatoid arthritis or abundant bone formation. Of the ten cases reported, six were considered to be satisfactory.

8.3 Radial Head:

The radial head is often excised in cases of arthritic elbow problems to reduce pain and increase the range of forearm rotation. Very few post-operative problems arise regarding elbow joint stability but Silastic implants have been used to replace the radial head. No novel development work is currently in progress.

8.4 Proximal Ulna:

Johnson and Schlein (1970) described the reconstruction of the proximal ulna following a shotgun injury. The irreparable radial head was removed and the proximal ulna replaced by a Vitallium prosthesis with an "I" - section intramedullary stem. Two peripheral plates were "fitted and fixed" to the

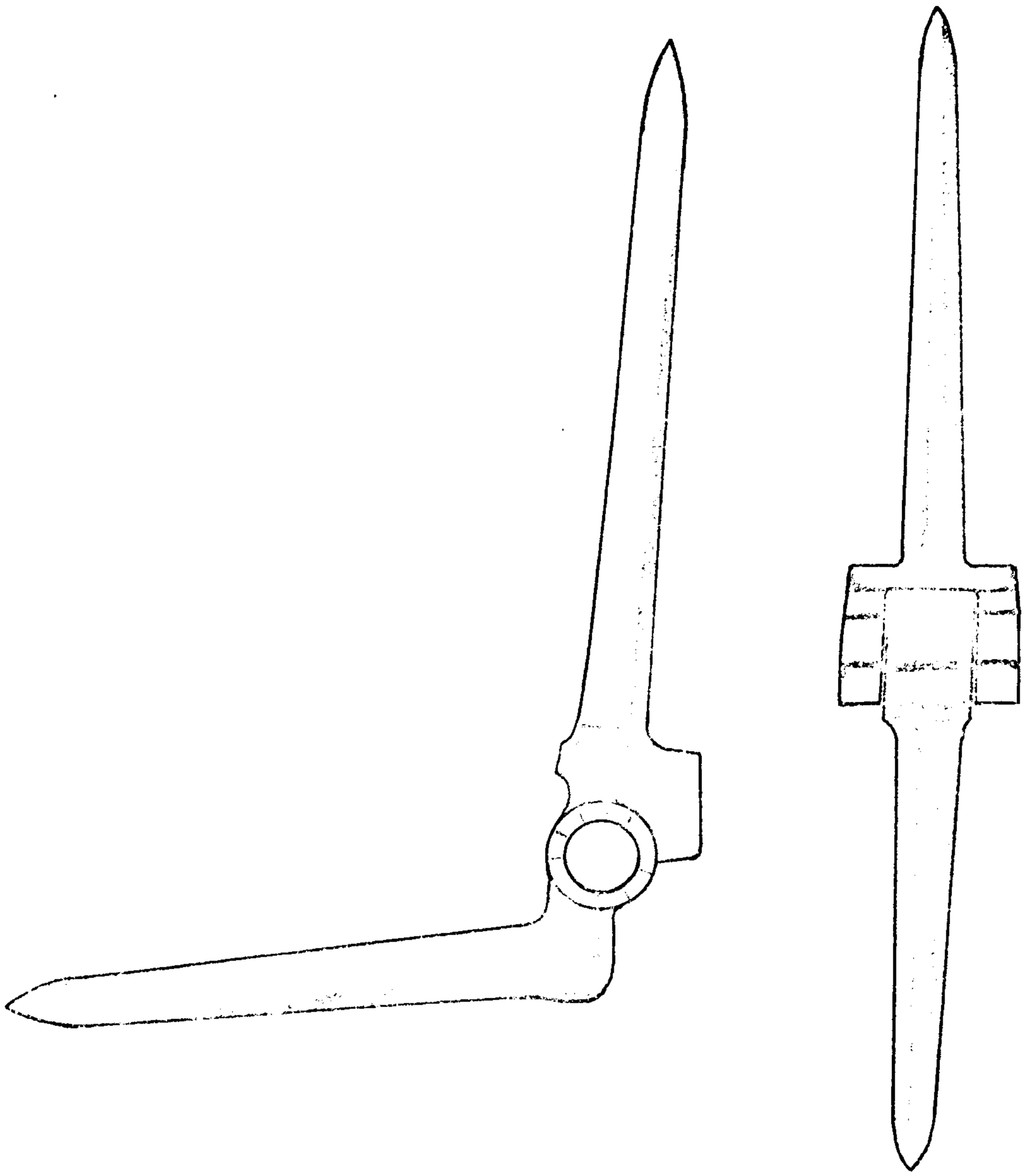

Figure 83: The "Shiers" elbow hinge

ulnar shaft using transverse screws (see figure 8.2). Erosion of the humerus occurred post operatively and it was discovered that the anatomically shaped trochlear notch had excessive height at the coronoid process. Enlargement of the semi-lunar notch and reduction of the coronoid process were recommended for future procedures.

8.5 Hinged Elbow Prostheses:

In the early 1970's, three hinge replacements were available for the elbow joint; namely, the Shiers, McKee and Dee.

The Shiers elbow prosthesis consisted of a pin hinge with straight intramedullary stems as shown in figure 8.3. In an attempt to model the anatomical configuration of the elbow joint the prosthesis flexion axis was offset from the line of the ulnar stem. Originally the prosthesis was relatively large and had long straight stems. Problems were encountered when the stems were inserted into small bones and the prosthesis was suitably modified to cater for the full range of sizes required.

Although basically the same design as the above, the McKee elbow prosthesis had a much neater hinge unit. Reduction in the length and section of the stems was also necessary to accommodate patients of small stature. In addition, the ulnar stem was curved slightly to follow the lines of the ulnar cavity.

Although the McKee prosthesis gained more acceptance than did the Shiers elbow, both units were difficult to insert due to their size and the length of the stems. By far the greatest advance in the design of an elbow prosthesis at that time was made by Dee (1972).

The "Dee" prosthesis had short curved stems of rectangular cross section as shown in figure 8.4. The ulnar stem was designed to follow the medullary cavity of the ulna and allow the use of a standard reamer for its insertion. The olecranon was left intact and the ulnar component was slotted into the ulna from an anterior position which prevented skin/metal contact and ensured correct function of the triceps muscle.

For the humeral component, the distal humerus was excised above the supracondylar ridges and the prosthesis cemented in place. The intramedullary stem was again curved but in this case a straight stem would have sufficed

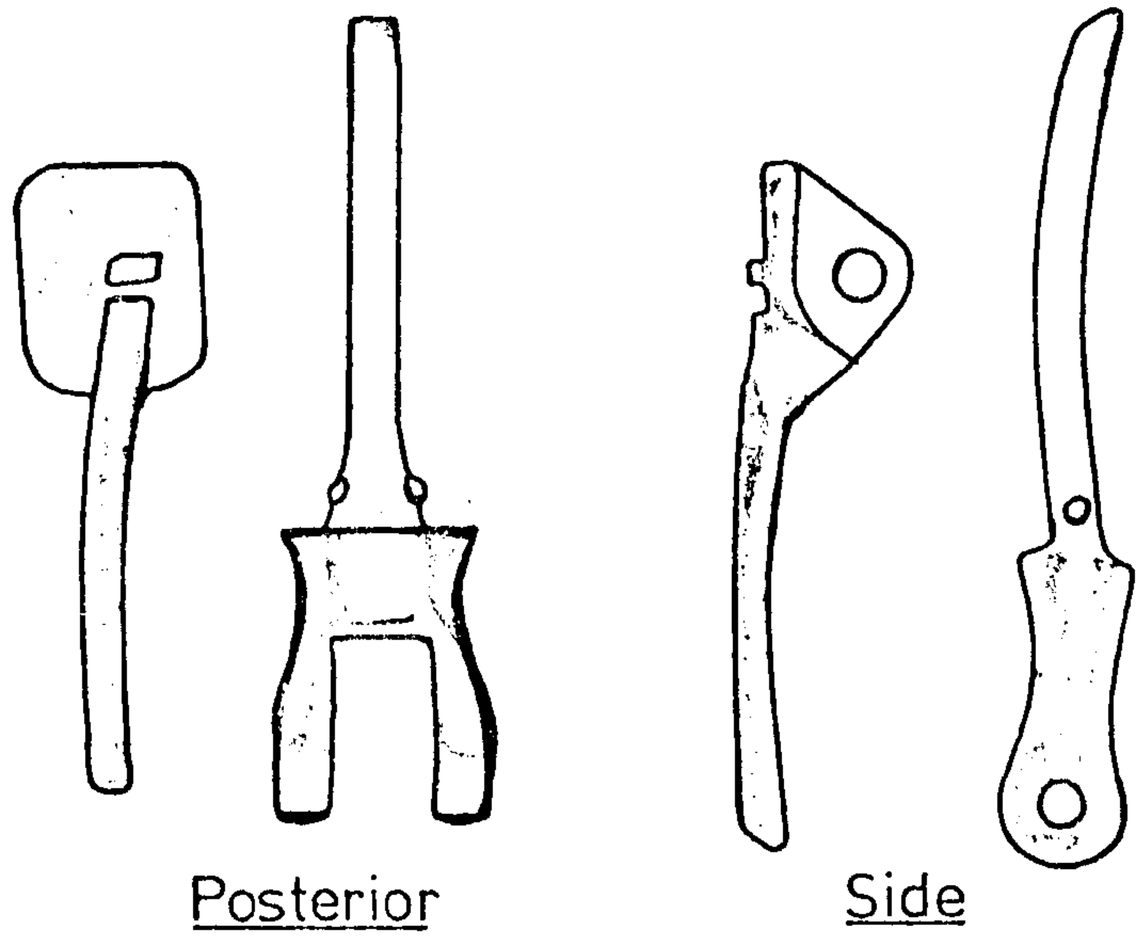

Figure 8·4: Components of the "Dee" elbow prosthesis

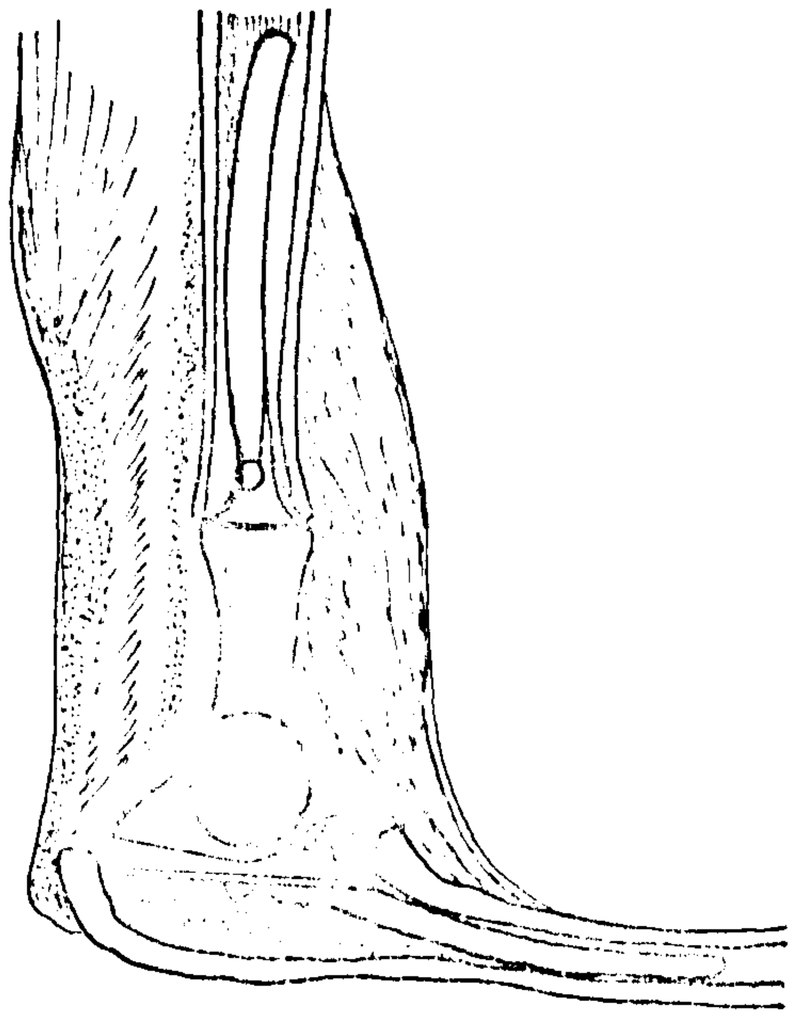

Figure 8·5: The "Dee" prosthesis in situ

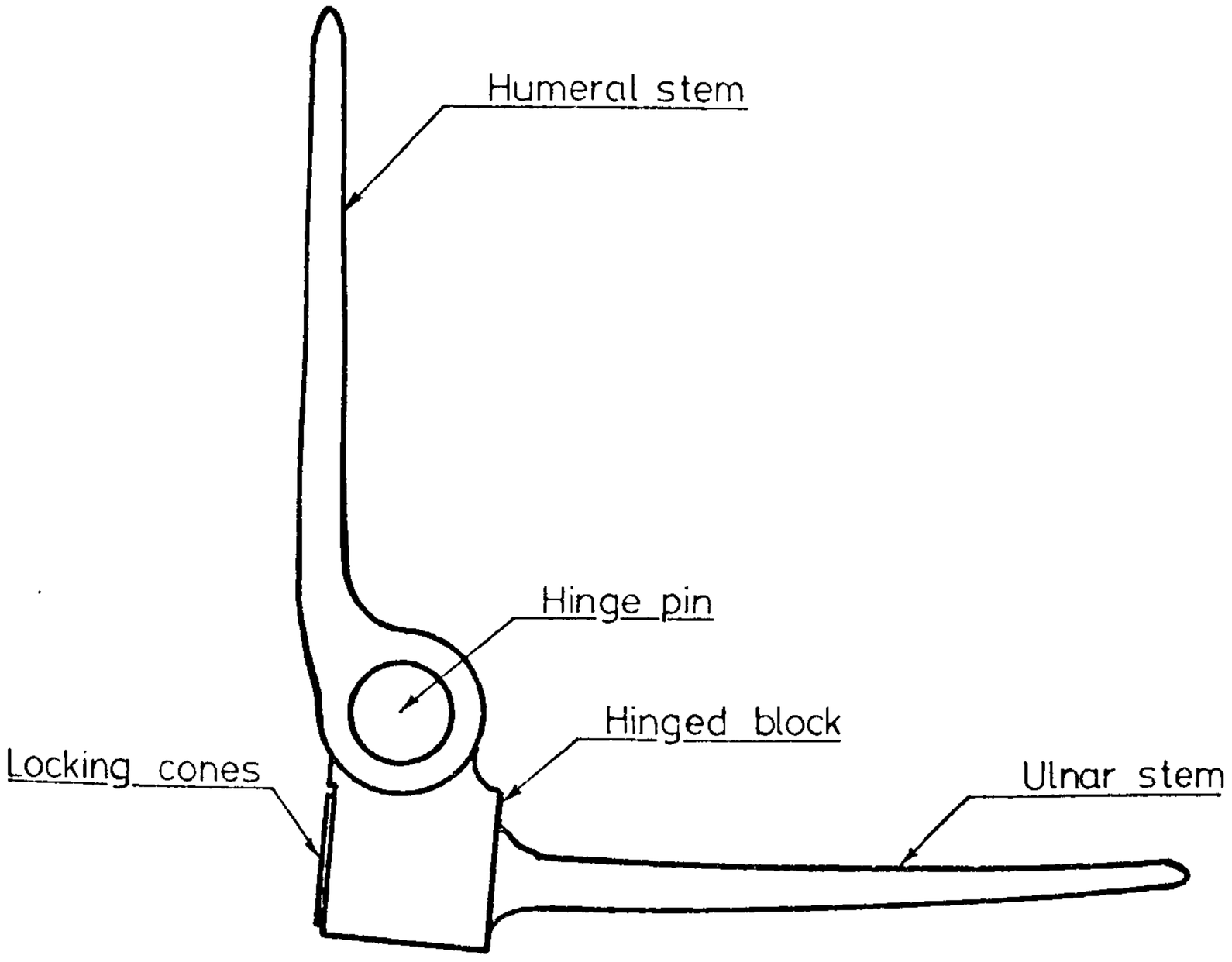

Figure 8·6: Side view of the "GSB" elbow prosthesis

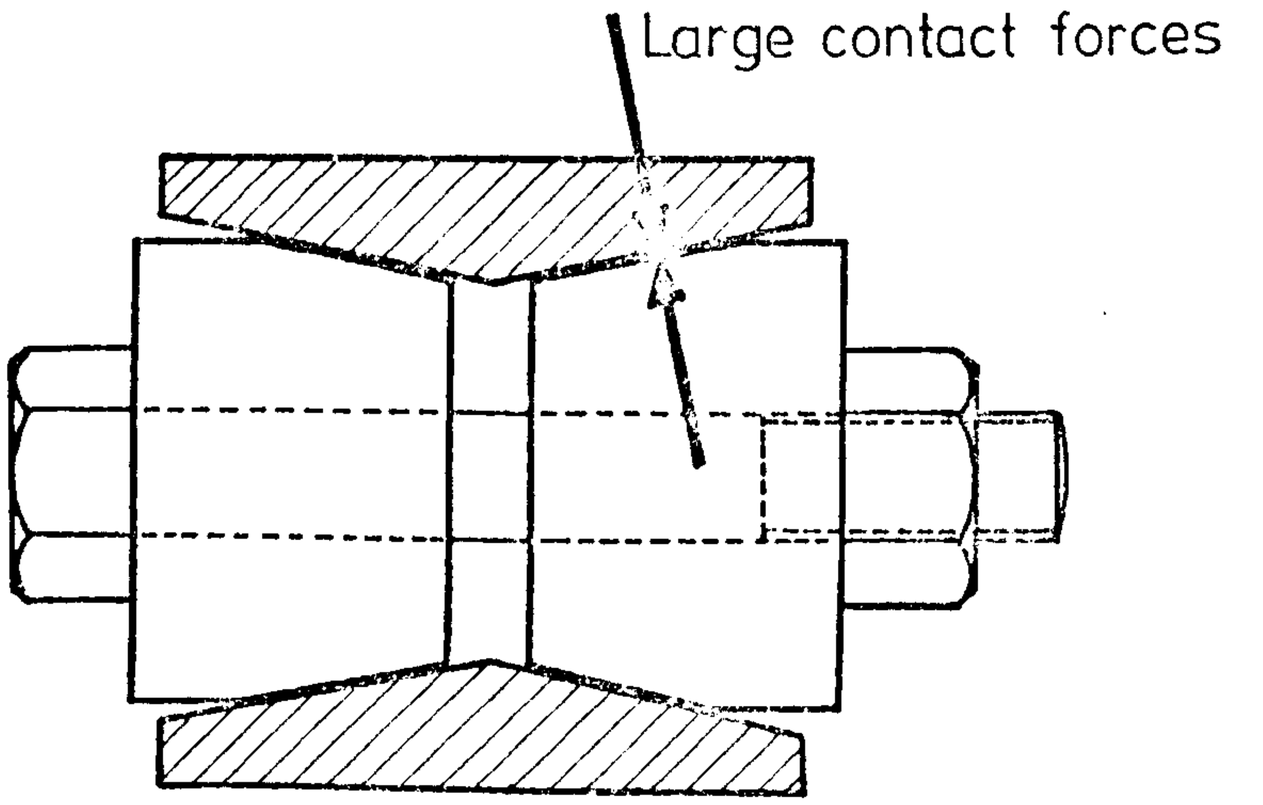

Figure 8·7: Frictional locking mechanism of conical surfaces

(see figure 8.5).

The two components were joined with a hinge pin and the assembly was made secure by flaring one end of the pin with a G-clamp device. The major drawback to the prosthesis, however, was the low salvage potential. In the event of component removal, the amount of bone removed from the humerus excluded the use of normal reconstruction techniques. Consequently, several patients had to contend with flail elbow joints.

Disturbed by the failure rate of the various hinged elbow prostheses, Souter (1973) reviewed the postoperative results of twenty five total elbow replacements. A "considerable number" of complications were described and it was advised that hinge arthroplasty should be approached with great caution. It was also stated that loosening of the humeral stem was a frequent occurrence and that it was probably due to high torsional loads transmitted along the long axis of the humerus.

One of the first attempts to reduce the degree of bone resection was made by Trillat et al (1972). For the humerus, the trochlea, capitulum and epicondyles were removed and the specially designed stem cemented into the medullary cavity. The ulna was left intact except for the hollowing of the medullary cavity to accommodate a short ulnar stem. Correct positioning of the ulnar component was achieved by registering the base of the unit with the articular surface of the trochlear notch. The articulated joint possessed 10° valgus inclination and the stems were suitably curved to match the anatomical bone cavities.

Three case studies were reported of which two were considered to be "satisfactory". The third case history presented several complications involving bone resorption and it was stated that subsequent operations were limited to elderly patients.

A further development in the design of a total elbow prosthesis was reported by Gschwend and Scheir (1974) regarding the "GSB" prosthesis. Four components were involved in the complete assembly with the humeral component carrying the main hinge unit as shown in figure 8.6. The "mobile" unit of the hinge mechanism was securely locked to the ulnar component by a screw based on the double-cone principle (figure 8.7). The "GSB" device provided a simple method of joining the ulnar and humeral components in a position of

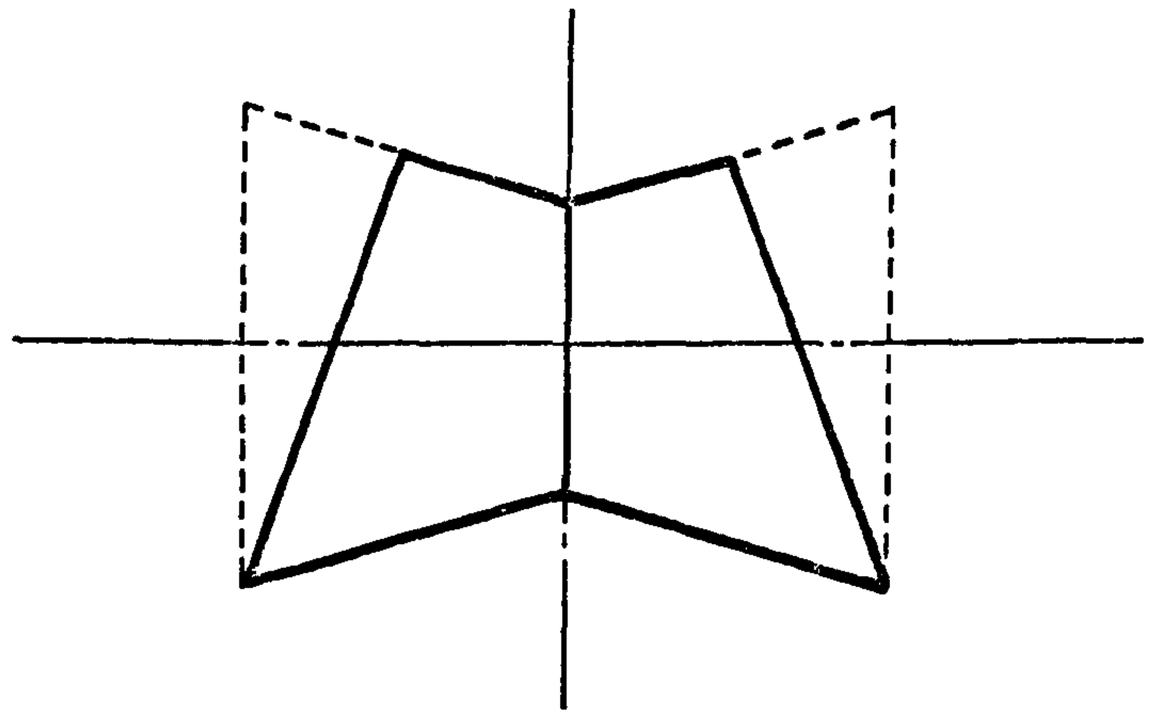

Figure 8·8: Conical surfaces of the "Liverpool" prosthesis [humeral]

correct alignment. To cater for left and right elbows and individual variations in carrying angle the stems were made from "Protasul-10". This alloy allowed the stems to be bent to suit particular requirements with no risk of fracture. Under certain conditions the action of the collateral ligaments was retained and the minimal bone removal provided a safe "line of retreat" in the event of severe complications.

Post operative results of the first seventeen elbow replacements indicated that an extension of the indication for the operation was justified. No fractures or loosening of the prosthesis were reported. Increased mobility and reduced pain were typical of the results. However, a slight deficiency of elbow extension remained in patients with a long history of anhylosis.

8.6 Unrestrained Elbow Prostheses:

During recent years the progress of elbow prostheses has followed similar trends to the development of the total knee prostheses. The problems encountered with loosening of the humeral component have led to attempts to reconstruct the elbow joint and retain the normal load carrying capacity of the collateral ligaments. Although several research establishments have been working on the design of a non-restrained elbow prosthesis only two reports have been published to date.

From Liverpool, Wright et al (1975) have developed a metal-on-plastic elbow prosthesis which replaces the humero-ulnar articulation. The geometry of the anatomical joint surfaces was grossly simplified with the humeral component originating from a solid of revolution in the form of two straight sided "frustro-cones" (see figure 8.8). Stability was achieved by the use of inclined ends and the fixation of the unit in a wedge-shaped cavity between the capitulum and medical epicondyle. The ulnar component was formed from a 160° sector of a complementary bearing surface. A small peg protruded from the base of the device and provided a "key" for the bone cement. For cases of severe erosion of the olecranon a bone screw was inserted from the olecranon and passed through the peg to provide additional support. Although the form of this prosthesis is relatively basic, the preliminary clinical trials have encountered no major complications and the use of the prosthesis was to be extended.

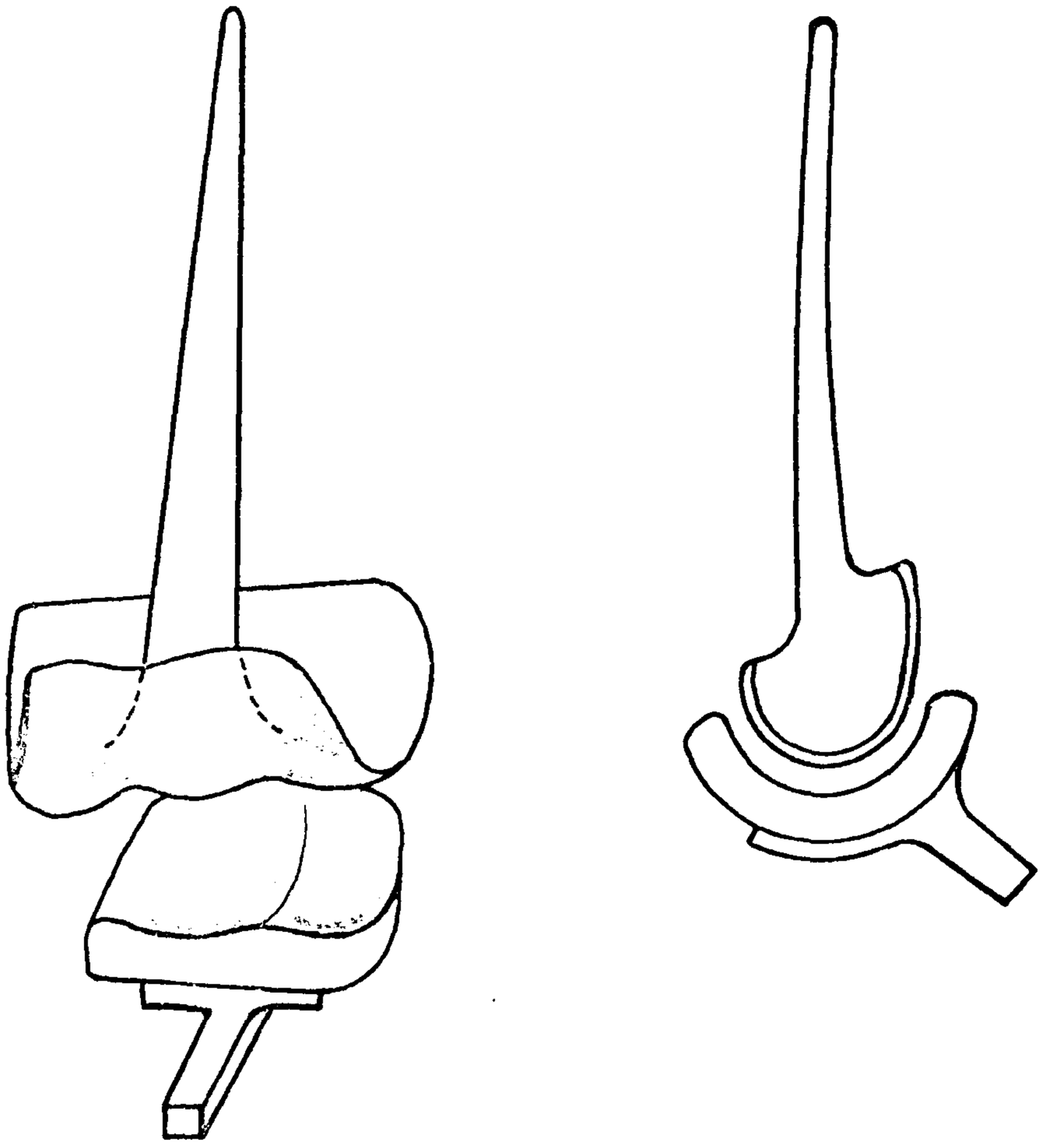

Figure 8·9: Two sketches of Ewald's elbow prosthesis

From a completely different viewpoint, another metal-on-plastic elbow prosthesis has been developed in America by Ewald (1975). A functional articular surface for the polyethylene ulnar component was obtained by moulding a suitably modified distal humerus in dental casting wax. The dimensions and orientation of the ulnar fixation plug were obtained from radiographic measurements. Good stability in the M-L direction was provided by retaining the trochlear groove and by a medial polyethylene lip (see figure 8.9).

The metal humeral component consisted of an intramedullary stem and a modified casting of the anatomical trochlea and capitulum. The articular surface was made in the form of a shell to simplify the insertion procedure. In addition, a certain amount of laxity was incorporated in the prosthesis which allowed some of the torque and shear forces across the joint to be transmitted by the capsule and collateral ligaments.

The early results of a limited number of joint replacements were described as "encouraging". It was stated that cases with a history of joint sepsis or ligament resection could not be dealt with since the ligaments must be functionally normal (cf. Coventry and Bryan 1974).

Several reports have been published on the design of new elbow prostheses including Ananthakrishnan and Easwaran (1975) and Burrough (1973). To date no clinical trials have been performed and for this reason, description of these prostheses is not included.

From the previous reviews it can be seen that the development of elbow prostheses is following similar lines to the various stages involved in knee prosthesis development (see Appendix 4). With this in mind, a project was undertaken to study the design criteria suitable for a non-restrained prosthesis and to develop and test a prototype joint using the results of the biomechanical analysis of section 7.

9. DEVELOPMENT OF A NEW ELBOW PROSTHESIS

9. DEVELOPMENT OF A NEW ELBOW PROSTHESIS

9.1 Introduction:

In recent years, a great deal of interest has been shown in relation to the development of new total elbow prostheses. To the author's knowledge none of the presently available elbow replacements has undergone a rigorous programme of "laboratory" evaluation. For this reason, most designers have become dependent on the results of clinical trials for the assessment of new design concepts.

It was therefore decided to undertake a design study for a new elbow prosthesis and make use of the analytical results presented in Chapter 7. This section discusses the reasoning behind several design aspects and describes the implementation of the various stages involved in the development of a novel elbow prosthesis.

9.2 Design Criteria:

9.2.1 Introduction: The original design concepts of the proposed elbow replacement were formulated by Mr W.A. Souter of Princess Margaret Rose Orthopaedic Hospital, Edinburgh. In 1973, liaison was established with the Bioengineering Unit at the University of Strathclyde and a development programme was arranged for the introduction of a prototype elbow prosthesis. The various design factors considered in the study are presented in this section with reference to the criteria laid down, in the following order by Elloy et al (1976):

a) Appropriate articulation
b) Good stability
c) Adequate strength
d) Good fixation
e) Correct choice of materials
f) Low friction forces
g) Acceptable wear rate
h) Good salvage potential
i) Fail safe feature

j) Standardisation

k) Sterilisation

l) Cost effectiveness

m) Surgical Instrumentation.

9.2.2 Articulation: The geometry of the joint surfaces was initially specified as a "close copy" of the anatomical articular surfaces. From preliminary investigations it was found that a straightforward cast of the trochlea produced a joint surface for which the area of humero-ulnar contact was not acceptable for non-cartilagenous materials. It was therefore decided to design the joint surfaces with geometrically specified contours which would retain the proper function of the collateral ligaments. In addition, a range of movement of 30° to 120° was considered to be the minimum for post operative elbow flexion. A fuller range of 0° to 150° was consequently specified for the prosthesis. It was finally stipulated that the overall dimensions of the joint surfaces should be such that no impingement could occur between the prosthesis and body tissues.

9.2.3 Stability: Of the three articulations at the elbow joint, the humero-radial and radio-ulnar joints were not included in the design proposal. Since favourable results have been obtained from procedures involving radial head excision (Souter, 1975), the overall stability of the elbow joint should not be greatly affected by this exclusion.

The stability characteristics of the proposed prosthesis therefore depended on the detailed geometry of the humero-ulnar joint surfaces. In the engineering sense, the anatomical joint is not "tight" but permits a certain degree of "release-glide" to effect ligament tension. To cater for this phenomenon the anatomical joint surfaces were carefully studied and the prosthetic surfaces designed accordingly.

The coronal outlines of the joint surfaces of 15 cadaveric humeri were obtained by moulding fine solder wire across the trochlea and capitulum. The pieces of wire were taped to a sheet of card and photocopies were produced.

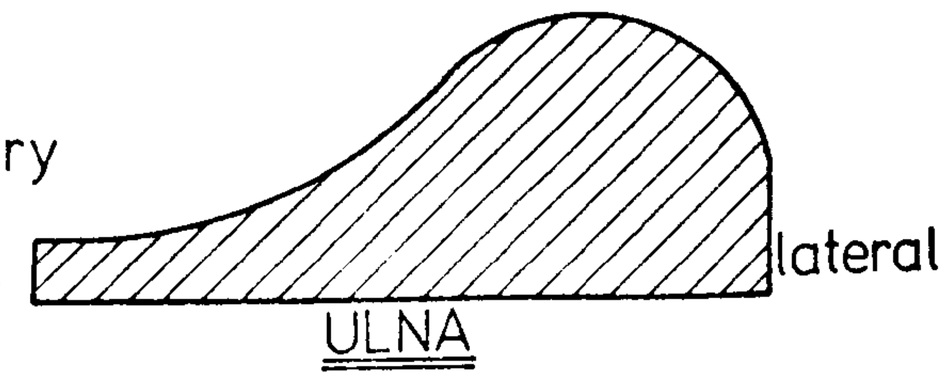

Figure 9·1: Original surface geometry

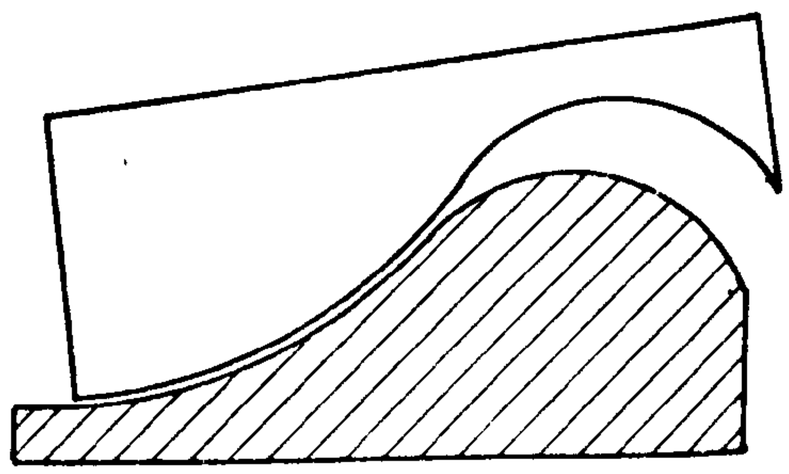

Figure 9·2: Medial "toppling"

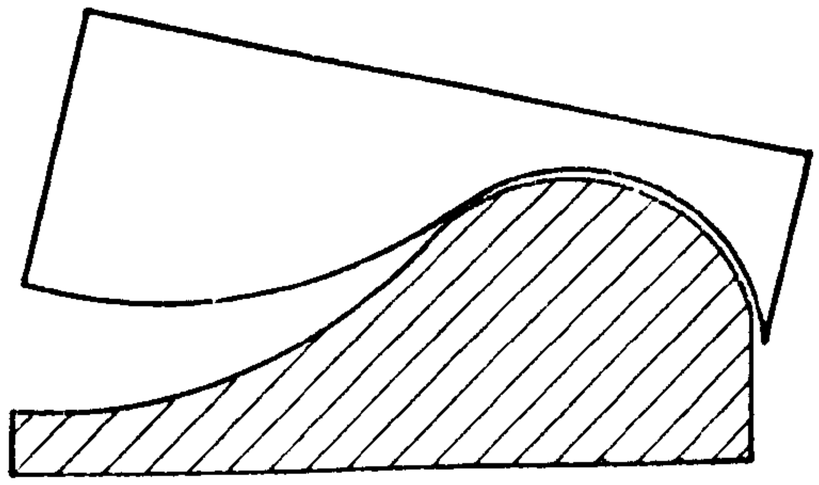

Figure 9·3: Lateral "toppling"

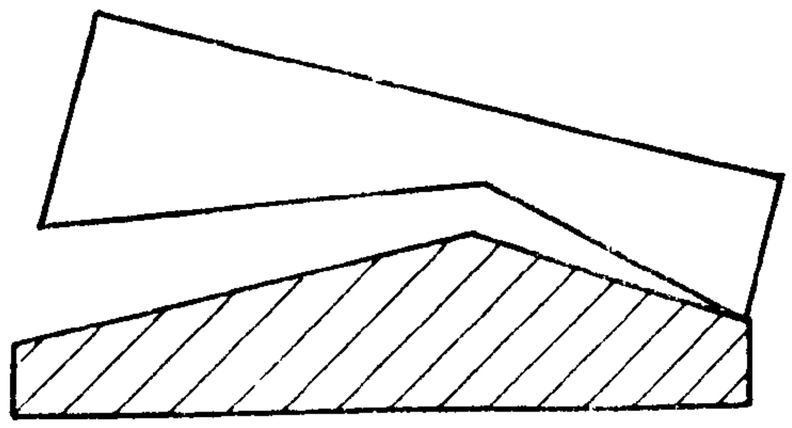

Figure 9·4: Effect of straight sides on the contact area during toppling movements.

Standard radii were used to determine the transverse geometry of the trochlea and it was found that the medial surface was convex whereas the lateral surface was slightly concave. A wooden model of the joint was constructed having concave and convex conical surfaces as shown in figure 9.1. It was noticed that the medial surface allowed the trochlea to tilt over and create tension in the lateral ligament. A similar situation occurred with the lateral surface for the opposite movement of the humerus. Figures 9.2 and 9.3 show both positions of the joint surfaces.

With a mutually articulating pair of curved surfaces the bearing area of the joint was more or less constant throughout the range of movement shown. However a straight-sided joint surface would have produced very high contact pressures at the perimeter of the joint as shown in figure 9.4. To ensure good lateral stability and correct articulation, a small amount of clearance was specified at the apex of the concave and convex surfaces.

In the coronal plane, the provision of "release glide" was considered essential and the model was therefore progressively trimmed to give a controlled degree of instability. The precise amount of "give" will be discussed later.

9.2.4 Strength: Although the strength of an implant is an important factor in the design criteria, it was considered to be of secondary importance to the fixation characteristics of the assembly. From the outset it was realised that the fixation "strength" of the prosthesis/bone interface would be a fraction of the mechanical strength of the prosthesis itself. Therefore, in place of direct strength testing, a series of tests was organised to study the effectiveness of fixation members under selected load actions (see section 9.3).

9.2.5 Fixation: The basic fixation criterion was taken to be the "maximum use of the existing bone structure for support of the prosthesis". Cadaveric bone specimens of the proximal ulna and distal humerus were dissected in such a way that the internal bone structure was revealed (see figure 9.5). In effect, a bone "prosthesis" was produced which represented the maximum available

Figure 9.5: Bone specimens used to determine the fixation cavities.

space that any fixation member could occupy.

These fixation cavities were studied in detail and the models were suitably modified before the manufacture of wax patterns. A metal-on-plastic prototype was subsequently produced by casting the humeral component in Cr-Co alloy and machining the ulnar unit from high density polyethylene (HDP). These components (called "No.1 Prototype") were implanted into post mortem material and subjected to predetermined load actions using an Instron material testing machine and special adaptors. Full details of the test procedures are given in section 9.3.2.

9.2.6 Material selection: The original concept of the prosthesis specified a metal-on-plastic joint. Modern standards therefore limited the selection procedure to Cr-Co alloy, stainless steel alloys, Titanium and high density polyethylene. In the preliminary stages of the development, a decision had to be taken concerning the relative position of metal and plastic. Two factors were considered:

From strength considerations the metal component should be used in the compartment which is subjected to the greater stresses. For the elbow joint it was envisaged that the weakest sections of the prosthesis would be the supracondylar arch of the humeral component and the intramedullary stem of the ulnar unit. Since the cross-sectional area of the supracondylar arch was extremely small, it was decided to have a metal humeral component.

From a durability point of view, it is accepted engineering practice to combine metal and plastic in such a way that the "male" unit is metallic. The reasoning for this is twofold.

In the undesirable situation of edge contact shown in figure 9.6, the region of contact will deform as indicated by the dotted line. If component A were plastic, the circular bearing journal may become permanently damaged under high joint loads. If the journal were to come in contact with other parts of the bearing, incorrect articulation would occur as shown in figure 9.7. On

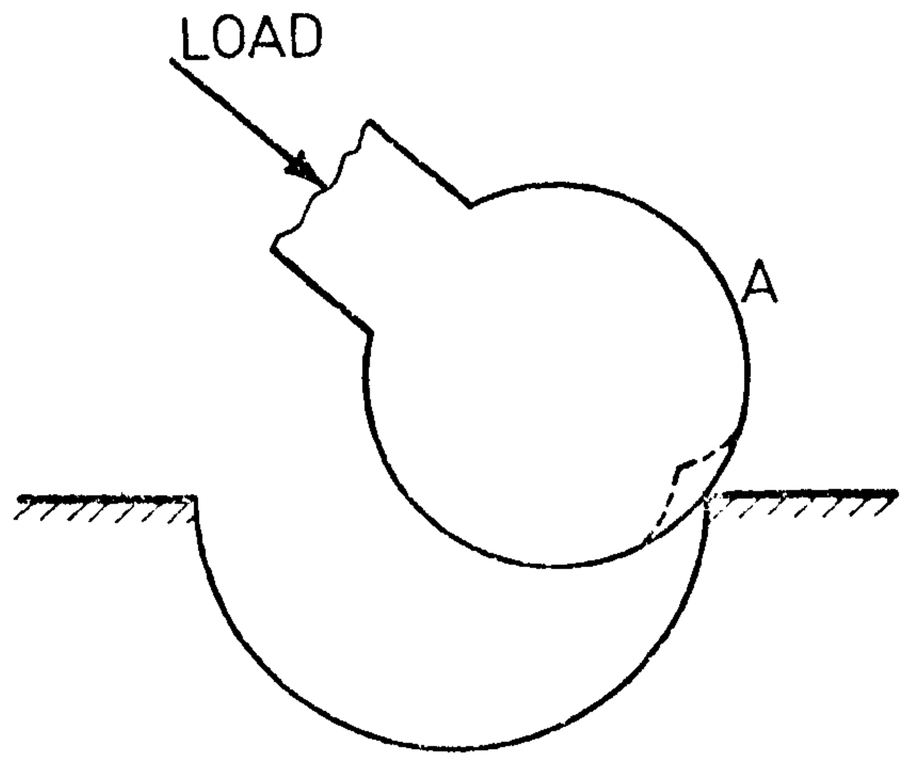

Figure 9·6: Effect of edge loading situation.

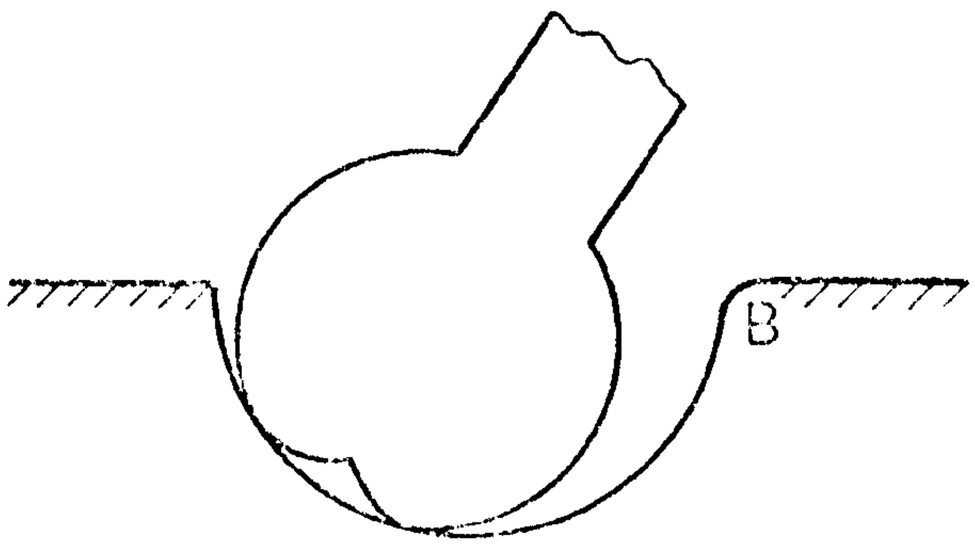

Figure 9·7: Damaged journal and subsequent contact area.

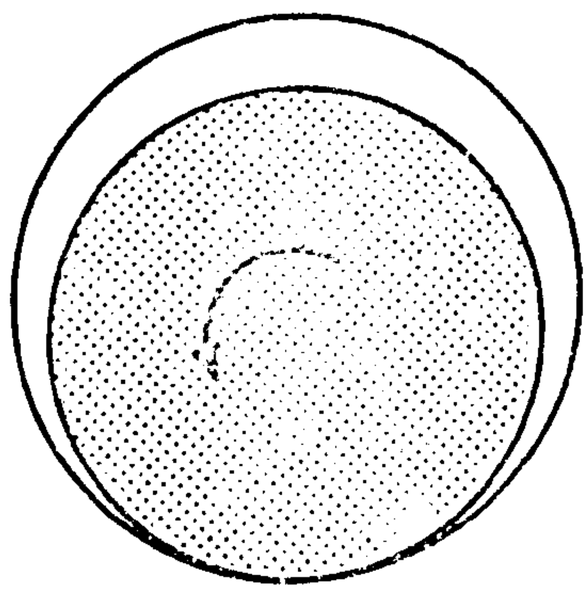

Figure 9-8: Normal bearing

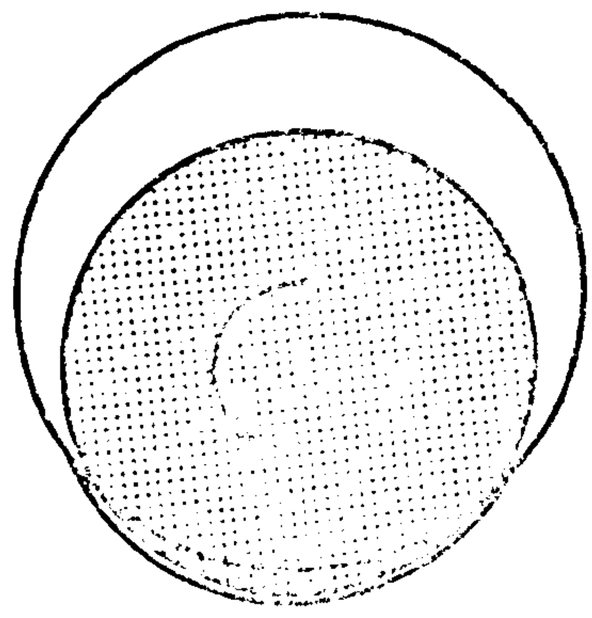

Figure 9-9: Shaft "bedded-in"

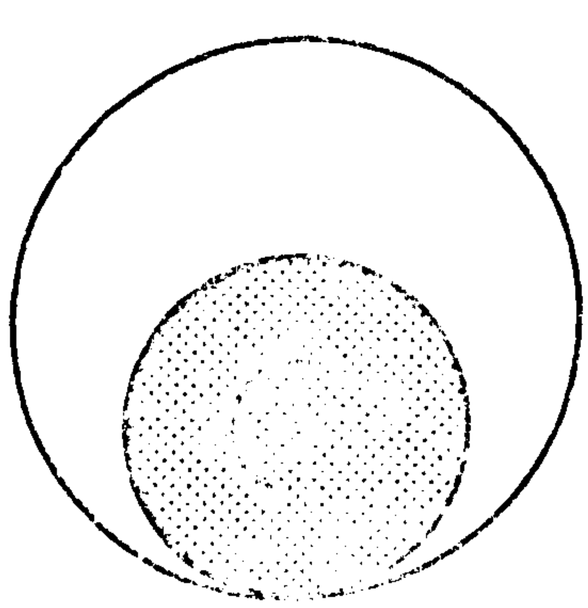

Figure 9-10: Shaft badly worn

the other hand, if the journal was made of metal, edge contact would deform the corner of the base material but would not affect surface contact in subsequent joint positions. The long term effect of this combination would therefore be a slight increase in the radius of corner B.

Secondly, wear characteristics must be considered. In all engineering applications, the bearing journal is made from a hard material compared to the bush material, to cater for wear in the direction of loading. Figures 9.8 and 9.9 show the effect of wear on a typical bearing and it can be seen that joint contact exists over a reasonable area after the "bedding-in" period. For an inverse combination the journal would tend to "wear-out" and give a poor area of contact as shown in figure 9.10.

9.2.7 Friction: Factors which affect the frictional torque at a prosthetic joint include material selection and journal diameter. In this particular situation both factors were satisfactorily fulfilled by other design criteria and no further consideration was necessary.

9.2.8 Wear resistance: Several studies have been performed on the rate of wear in hip and knee prostheses during locomotion (Charnley, 1975). The joint pressures and sliding velocities experienced in certain hip and knee prostheses were tabulated and compared to the estimated service conditions for the proposed elbow replacement. Joint loadings and angular velocities at the hip and knee joints were obtained from Paul (1967) and Tooth (1976) respectively and are listed in Table 9.1. Table 9.2 contains the theoretical joint pressures for a "Charnley" hip, a "Mueller" hip and "Leeds" knee prosthesis. (See Appendices 3 and 4).

Seedhom et al (1974) studied the contact areas of plastic models of the Leeds knee prosthesis and obtained the slightly higher values of 2 to 5 MN/m^2. Subsequent measurements of the contact areas for the prototype components

	"Toe-off"		"Heel strike"	
	Load	Ang. vel.	Load	Ang. vel.
Hip	2200 N	3.5 s^{-1}	4400 N	2.1 s^{-1}
Knee	2000 N	7 s^{-1}	1400 N	1.9 s^{-1}

Table 9.1: Joint loadings for lower limb during normal locomotion.

Prosthesis	Projected area (mm^2)	Pressure (toe off) (MN/m^2)	Pressure (heel strike) (MN/m^2)
Charnley hip	380	5.8	11.6
Mueller hip	800	2.75	5.5
Leeds knee	1400	1.5	1.0

Table 9.2: Contact pressures for three prostheses (corresponding to figures from Table 9.1).

returned contact pressures of 3 to 8 MN/m^2. It was postulated that the higher pressures were due to some loss in the conformity between the components during the manufacturing process.

Similar theoretical calculations were performed for the elbow prosthesis using the joint forces and angular velocities experienced during the "seat-rise" and "table-pull" activities. Joint loads of 1400 N at 1.75 rad/s and 2000 N at 0.88 rad/s were obtained. The projected contact area of one side of the joint surface was taken to be 200 mm^2 and this resulted in contact pressures of 7 MN/m^2 and 10 MN/m^2.

These values are of the same order of magnitude as the joint pressures calculated for the Charnley hip prosthesis. When account is taken of the effective radii of both units (11 mm for the hip and 13 mm for the elbow) the sliding velocities are also similar. It was not possible to compare the angular velocities of knee and elbow prosthesis due to the complex combination of rolling and sliding at the articular surfaces of the knee joint.

It must be emphasised that the elbow joint pressures represented "strenuous" activities whereas the pressures calculated for the joints of the lower limb were characteristic of normal level walking. For this reason, the loadings imposed on the elbow prosthesis were considered to be effectively less than load actions on lower limb prostheses during general activity. Metal-on-plastic articular surfaces were therefore adopted for the proposed elbow prosthesis.

9.2.9 Salvage potential: With the poor history of complications arising from hinged elbow prostheses, one of the major considerations for a new prosthesis was "minimal bone removal" so that a secondary intervention could be performed if necessary. It was therefore essential to keep the length of the ulnar stem and the height of the supracondylar arch to a minimum. The development of these fixation members is described in section 9.4.

9.2.10 Fail safe: Two "fail safe" characteristics were considered during the design stages. As previously mentioned, a certain degree of release-glide was incorporated in the prosthesis to cater for torsion in a coronal plane. In addition to this, the height of the olecranon region of the ulnar component must be suitably controlled to allow "pull-out" and subsequent ligament tension.

9.2.11 Others: The four remaining design criteria (standardisation, sterilisation, cost effectiveness and surgical instrumentation) were considered to be of secondary importance during the preliminary design stages and their consideration was therefore postponed until clinical trials had commenced. It was realised, however, that a certain amount of special instrumentation would be required.

9.3 Evaluation Procedure:

9.3.1 Introduction: A total joint replacement can only be termed "successful" after an extensive period of clinical evaluation. Almost all of the currently available prostheses have undergone some technical modifications during clinical trials and this extends the "probationary" period quite considerably. It is therefore advantageous, for both developmental and ethical viewpoints to evaluate a proposed prosthesis, as far as possible before the introduction of clinical undertakings. Several factors are of importance to the elbow prosthesis and these include surgical procedure, articulation characteristics and fixation strengths.

The technical complications involved in the two former items can be overcome during a series of post mortem "operations". The surgeon will have time to obtain sufficient experience in the handling of the prosthesis to ensure unimpeded insertion of the components.

The most difficult problem to overcome, however, concerns the fixation strength of each component. Long term effects of bone growth/resorption can only be realised after many years of post operative performance. It must therefore be accepted that short term testing can only provide an indication

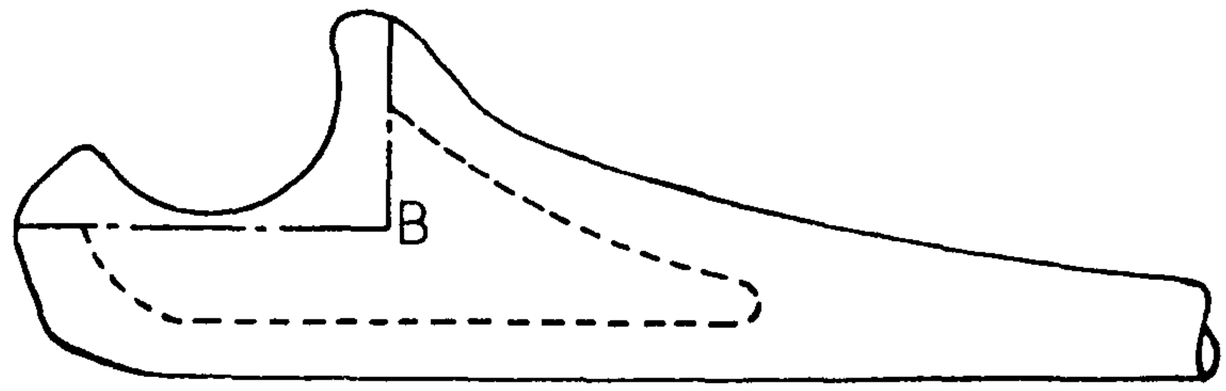

Figure 9·11: Required excavation of the ulna

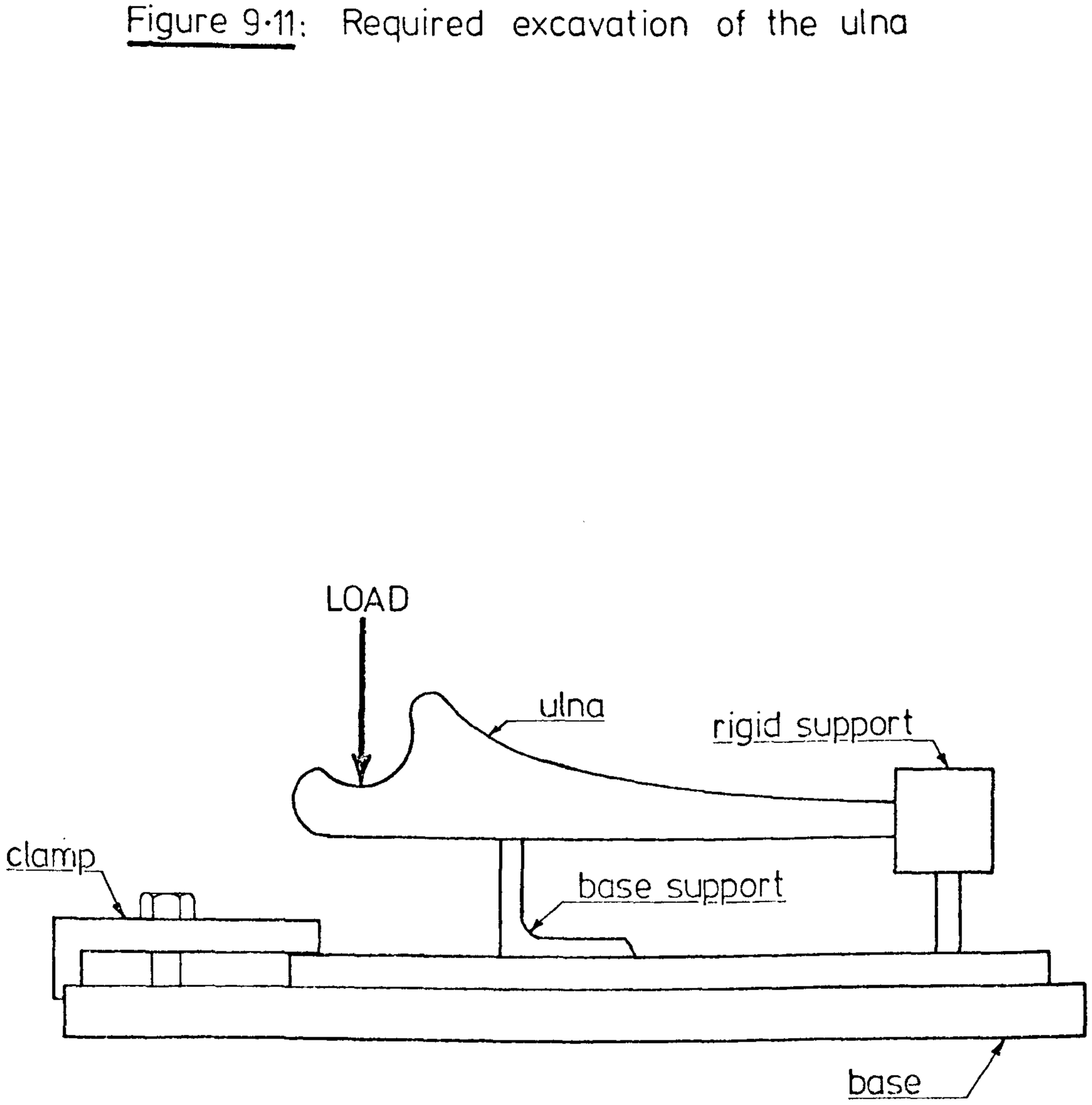

Figure 9·13: Elements of the lower part of the test rig.

of the initial mechanical security of the assemblies.

To assess the efficiency of the intended fixation members, the post mortem bone/prosthesis structures were mechanically tested under selected loading conditions. The following section describes these routines.

9.3.2 Test specifications: In ideal situations it is desirable to study the load actions applied to any structure and to investigate the load/deflection relationships for certain "critical" cross sections and loading directions. Difficulties involving the anisotropic nature of the bone/cement/prosthesis assembly and the accurate measurement of strain make such test procedures impracticable. It is therefore necessary to adopt "fracture" techniques and this, in turn, necessitates the selection of a single "critical" loading direction for each component.

For the ulnar implant it was specified that the articular surfaces of the trochlear notch should be excised as shown in figure 9.11. The resulting cross section at "B" was consequently very weak under bending loads. Moments and forces in the remaining directions were partly transmitted by ligament action and were considered to be of secondary importance. It was therefore decided to perform 3-point bending tests on the ulnar assembly in order to evaluate the fixation characteristics of the ulnar stem. An "Instron TTC" materials testing machine was employed for the application and measurement of loads on the prosthetic components (see figure 9.12). Fully adjustable supports were manufactured to ensure unidirectional loading of the specimen as shown in figure 9.13. The "base support" provided ground reaction in place of flexor muscle tension from the coronoid process and the radio-ulnar joint (transmission of biceps effort). Despite the abnormal loading of the bone structure, the base support was positioned below the ulna and in line with the cartilaginous area forming the radio-ulnar joint. A strip of acrylic cement was moulded to the form of the ulna to reduce the local pressures at this region.

Loads were applied to the ulnar specimen by downward pressure on the trochlear notch using the distal end of the humerus as shown in figure 9.15.

Figure 9.12: The Instron testing machine.

Figure 9.15: Vertical loading of the ulnar assembly.

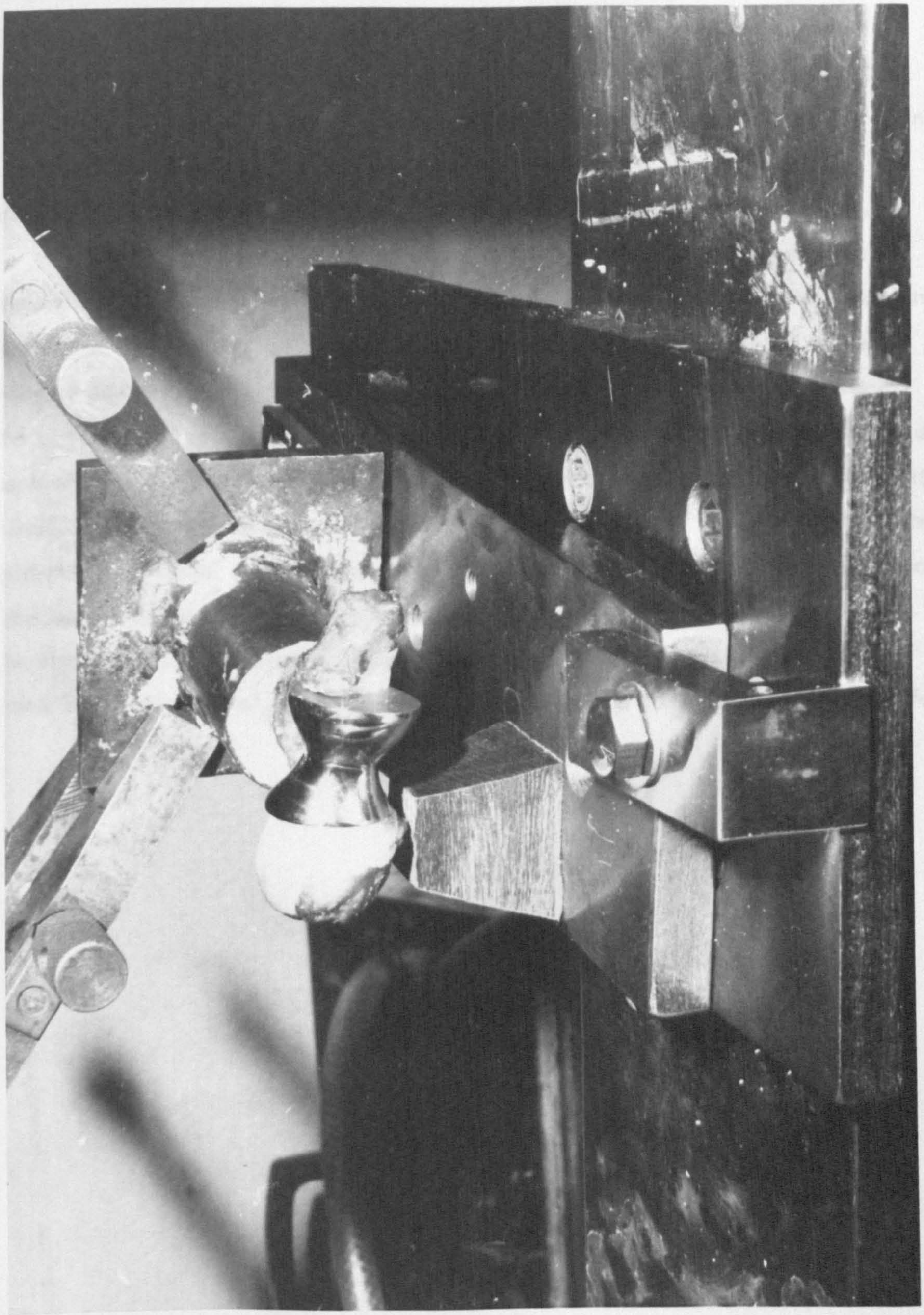

Figure 9.16: Torsional loading of the humeral assembly.

The metal tube was inclined to the vertical axis to bring the centre of the trochlea directly below the central region of the top platform. Careful positioning of the humerus was necessary to ensure normal articulation with the ulna in a coronal plane. Two hard steel rollers were positioned between the machine head and the top platform and provided a vertical loading direction at all times in the event of deflection of the ulnar component.

Following the completion of ulnar tests, the base plate supports were rearranged and the humeral component was clamped in the horizontal position shown in figure 9.16. Torsional effects about the long axis of the humerus were taken to be the most critical load actions for the humeral component. In a transverse section of the distal humerus the posterior surfaces of the medial epicondyle and medial supracondylar ridge were considered to be the weakest areas of the excavated bone. Vertical load actions were applied to the anterior side of the medial edge of the metal "trochlea" while the posterior surface of the capitulum was supported by a block of hard wood (afrormosia) as shown in figure 9.23. An acrylic cement "applicator" was moulded to the form of medial anterior lip of the trochlea and was attached to a serrated "top platform".

9.4 Prosthesis Evaluation:

9.4.1 Reference data: Before "in vitro" evaluation of the prosthesis could be conducted, it was essential to investigate the mechanical strength of intact ulnar and humeral specimens. Two normal bone specimens were therefore tested under similar test conditions to those previously described for the prosthetic components.

Fracture of the proximal ulnae occurred in a longitudinal direction from the base of the trochlear notch and failure loads of 1400 N and 1900 N were recorded. The comparatively high variation in the ulnar bending strength was explained by a corresponding difference in the gross dimensions of the two specimens.

Several difficulties were encountered during the torsional testing of the intact humerus. Very high torques were required and it was realised that machine loads in excess of 2000 N would probably damage the clamping system (refer to figure 9.16). In addition, it was envisaged that failure of the intact humerus would occur as torsional fracture of the bone shaft and not as collapse of the medial supracondylar ridge. It would therefore be impossible to obtain a definite value for the ultimate strength of the intact specimen and the figure of 2000 N was taken to be characteristic of the anatomical structure.

9.4.2 Prototype "No.1": Several wax models of the ulnar and humeral components were manufactured using the bone models (section 9.2.5) as patterns. The ulnar component was machined from a block of high density polyethylene and completed by hand. A mould was made from the wax model of the humeral component and a Cr-Co casting produced. During the finishing stages for both components, the original bone specimens were consulted with regard to the intricacies of the fixation members and articular surfaces.

The ulnar component consisted of a replica of the trochlear notch and had flat posterior and inferior surfaces to correspond to the excision lines shown in figure 9.11. A straight stem of dovetail section protruded from the base of the

component and was inclined to the sagittal plane. The anterior surface of the stem joined the main body of the implant near the "coronoid" process as shown in figure 9.20.

The humeral implant included a casting of the anatomical trochlea, epicondylar fixation plugs, and a supracondylar fixation arch as shown in figure 9.21. The square sectioned lateral "peg" fitted loosely into the excavated capitulum whereas the supracondylar arch followed the perimeter of the coronoid and olecranon fossae and became wider at the medial side of the "trochlea" to form the medial flange. A certain degree of anterior concavity was incorporated in the arch which was offset posteriorly from the centre line of the trochlea. Since the unit was cast from a bone specimen, the joint surfaces were neither uniaxial or perfectly smooth but these imperfections were of little relevance during the preliminary evaluation programme.

9.4.3 Test results: It must be stated that the availability of post mortem material was somewhat limited and for this reason a small number of fracture tests were performed.

The first prototype (No.1) was implanted on two occasions. Unfortunately, one of the "operations" was performed under low temperatures and difficulties were experienced regarding the hardening of the acrylic cement. The resulting fixation strengths were exceptionally low and the results were discarded.

The second procedure was performed under normal conditions and satisfactory results were obtained from subsequent testing. Bend tests on the ulnar assembly produced first stage fracture at 1040 N as the cement separated from the hard tissue underlying the coronoid process. On further deflection, the ulna fractured along a line joining the corner of the bone excision ("B" in figure 9.11) and the point of support as shown in figure 9.22. A load of 600 N was recorded.

When the humeral component was inserted into the excavated humerus, it was found that the prosthesis was very unstable during the cement curing period. It was postulated that this inferior fixation procedure was responsible for the low torsional resistance of 540 N. The failure mechanism involved the

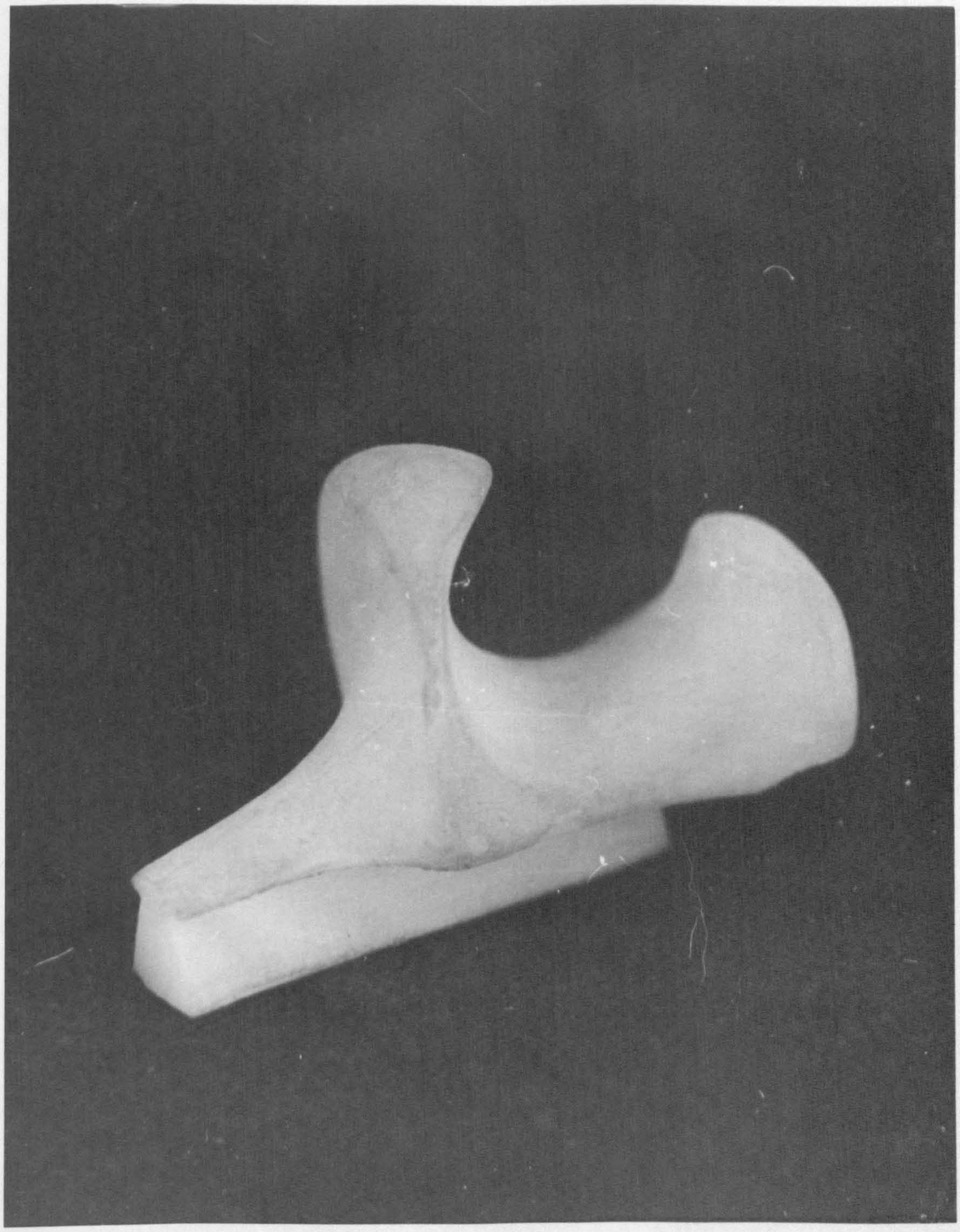

Figure 9.20: Prototype No 1: Ulnar component.

Figure 9.21: Prototype No 1; Humeral component.

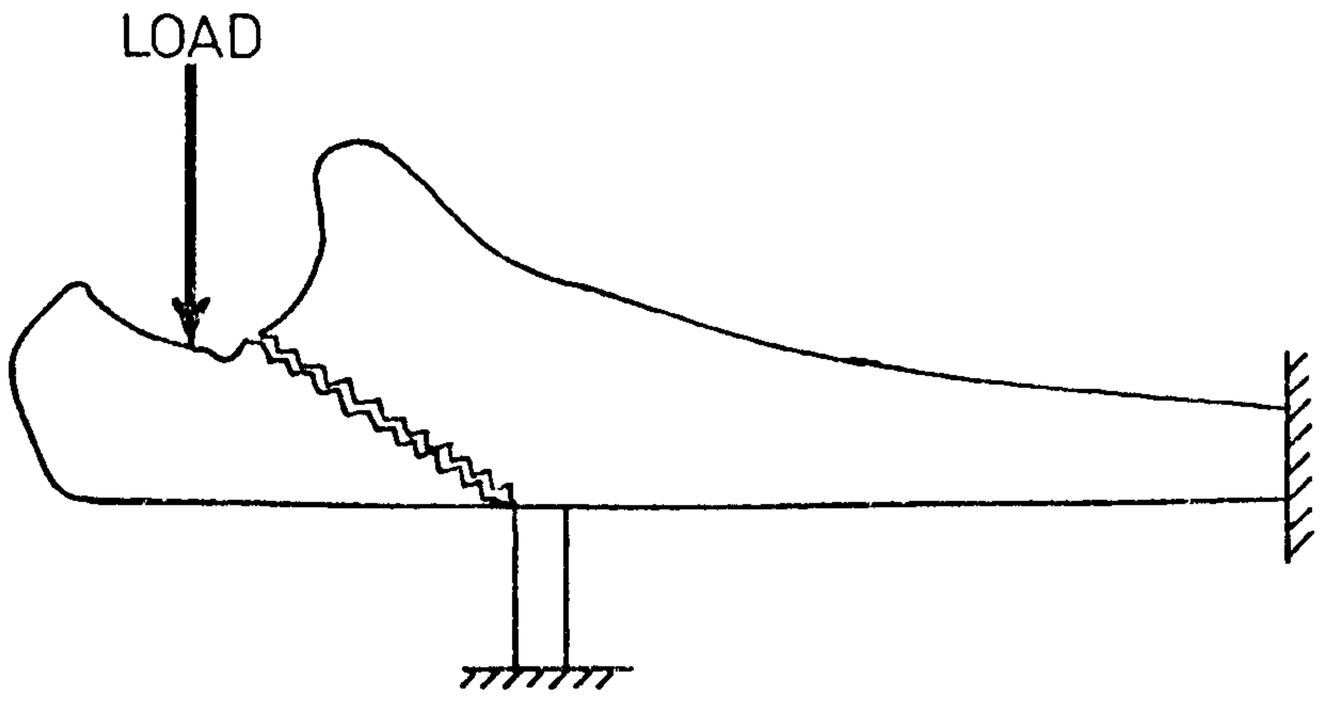

Figure 9·22: Crack formation during fracture of the ulna.[intact]

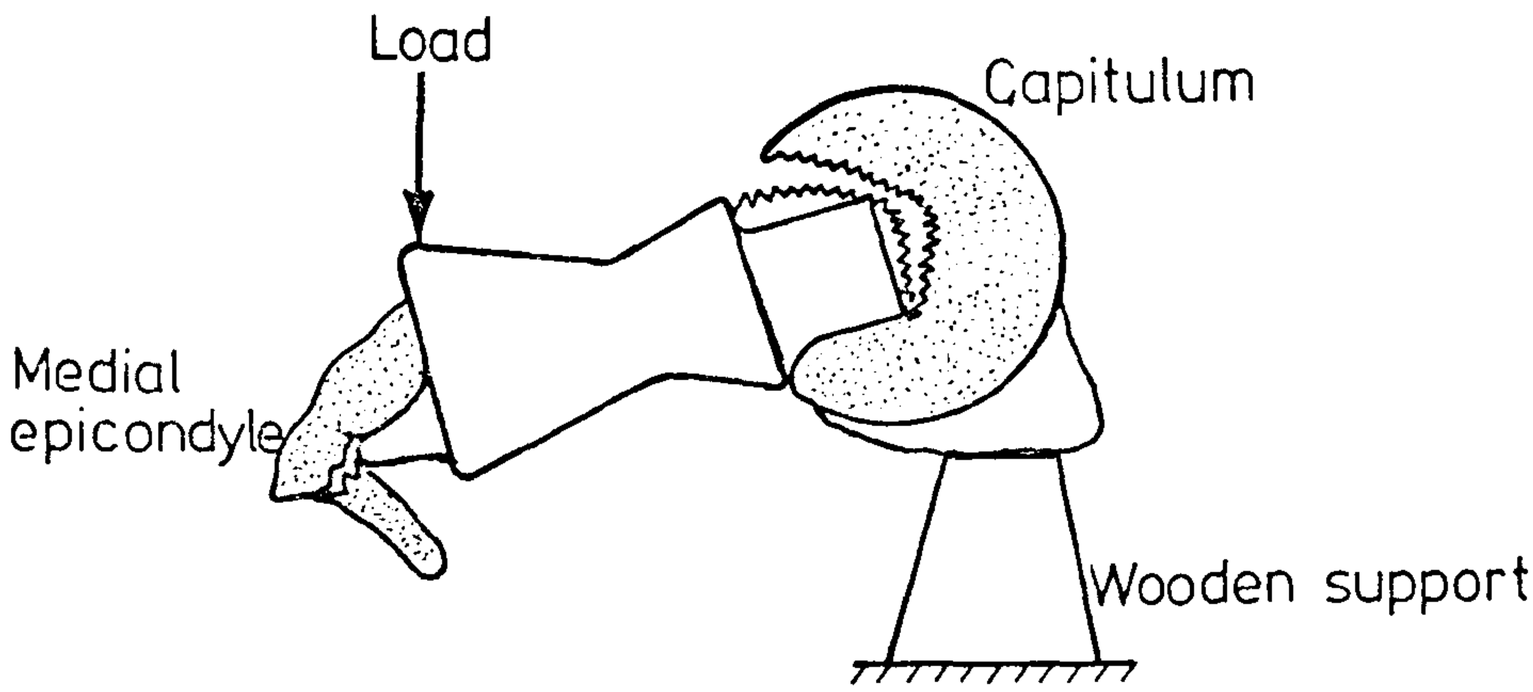

Figure 9·23: Failure of humeral fixation under load

collapse of the posterior structure of the medial epicondyle and fracture of the cement plug surrounding the lateral peg (see figure 9.23).

9.4.4 Prototype "No.2": To overcome the stability problems experienced during the fixation of the humeral component, it was decided to incorporate a stabilizing "protrusion" at the apex of the arch. A 10 mm extension "spike" was brazed on to the existing arch and suitably contoured as shown in figure 9.24.

An extra 8 mm was added to the length of the ulnar stem to increase the rigidity of the component under bending loads.

The modified units were inserted into post mortem material and tested as before. Significant improvements were obtained for the fixation strength of the ulnar and humeral units. Failure of the specimens was recorded at loads of 1500 N and 900 N respectively.

After careful consideration of all other aspects of the second prototype it was agreed that the prosthesis was suitable for clinical evaluation. Detailed drawings of the prototype were drawn up and presented for patent applications.

Figure 9.24: Prototype No 2: Humeral component.

9.5 Development of a "Clinical Prototype":

9.5.1 X-Ray sizing: With the completion of the development of a prototype prosthesis it became necessary to determine the range of sizes required for general use before clinical trials could be performed.

A total of 94 full size X-rays were obtained which included anterior and lateral aspects of the elbow joint (see figures 9.25 and 9.26 respectively). The x-rays were obtained from the patient population at Princess Margaret Rose Orthopaedic Hospital and were considered to be representative of rheumatoid sufferers. Several characteristic dimensions were measured from the x-rays and are shown in figure 9.27(a) and (b). Sample measurements are listed in Table 9.3.

The results were punched on computer cards and analysed by statistical routines to study the distributions of various dimensions and the correlation between selected parameters. Initial results showed that the dimensions examined were not normally distributed and further analysis produced very low correlation coefficients between the dimensions measured and the "reference" epicondylar width. The distribution of epicondylar width, ulnar width and trochlear width are shown in figures 9.28, 9.29 and 9.30 respectively.

In conclusion, the statistical results were not considered to add anything of relevance to the relationship between individual dimensions of the elbow joint.

9.5.2 Template sizing: As an alternative sizing procedure, the distribution of the epicondylar width was studied and found to vary from 48 mm to 72 mm. It was generally accepted that the model prototype would be suitable for "small" elbow joints and it was estimated that a range of epicondylar widths of 48 mm to 56 mm would suit such a size. The remaining sizes were split into groups of two and three and ratios of 1.00; 1.275 and 1.00; 1.18; 1.366 were obtained respectively (1.00 signifies the "small" prosthesis). The front elevations of the ulnar and humeral components were enlarged using a "PLAN Variograph", and transparent perspex templates were manufactured to the above sizes. A pair of templates corresponding to a ratio of 0.90 was also produced as a precaution

Figure 9.25: An A-P X-ray of the elbow joint.

Figure 9.26: Lateral X-ray of the elbow joint.

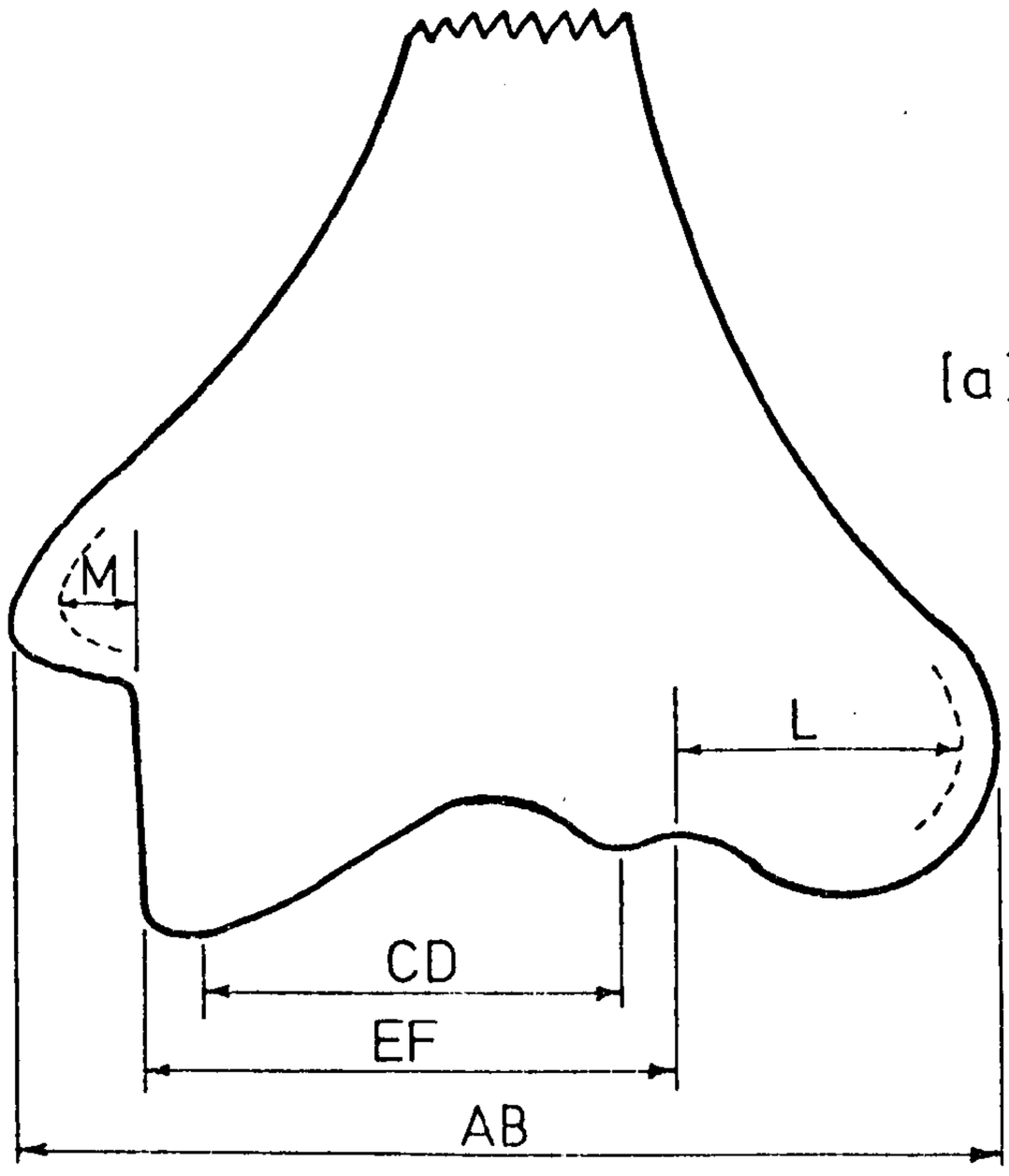

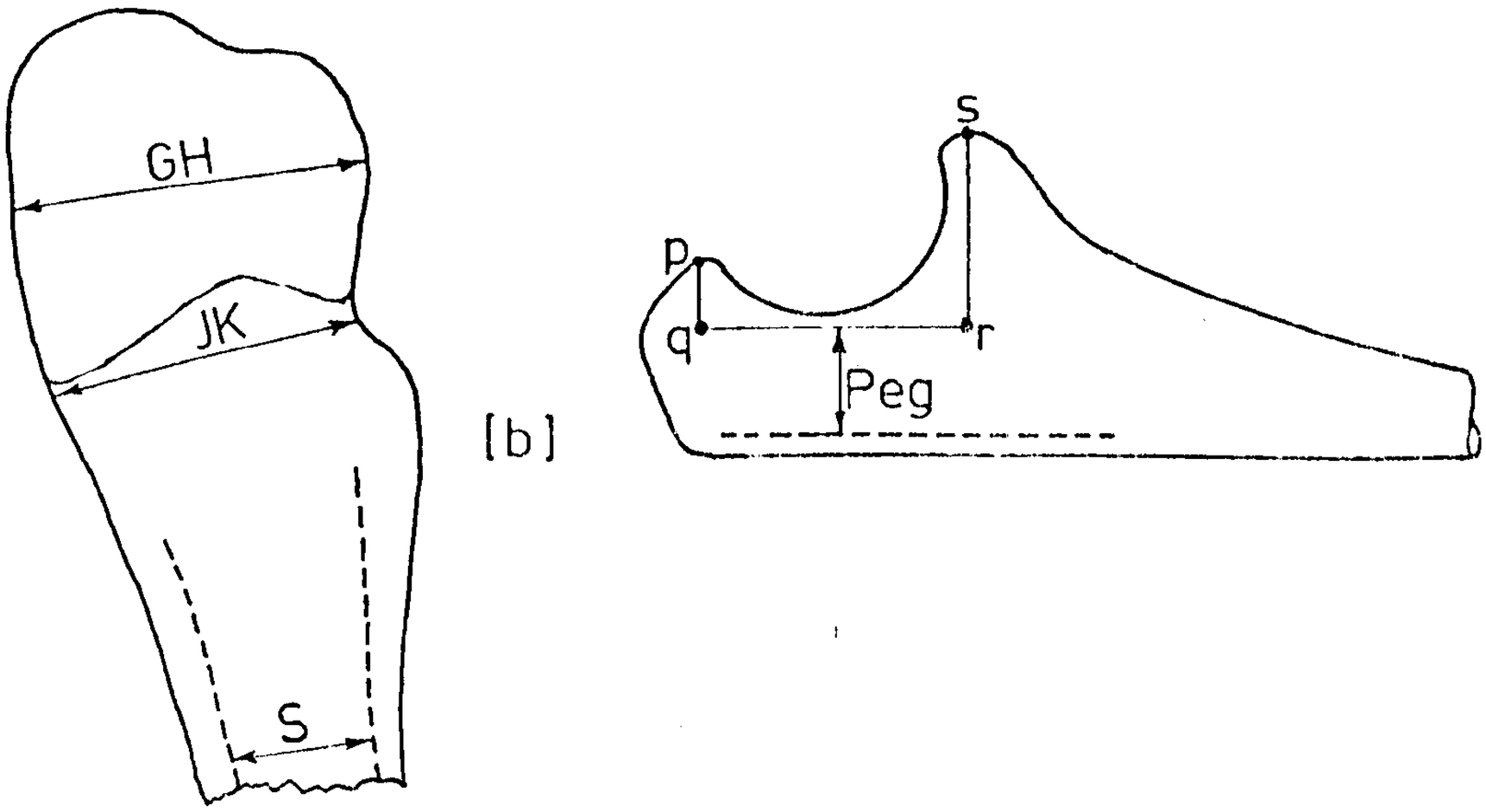

Figure 9·27: Characteristic humeral [a] and ulnar [b] dimensions

AB	CD	EF	GH	JK	S	pq	qr	rs	Peg	M	L
70	20	32	28	17	12	11	27	21	10	12	15
54	19	30	20	17	10	9	25	18	9	9	10
64	21	35	23	18	10	11	26	20	10	8	10
71	24	36	26	23	13	11	28	27	12	11	16
66	25	37	25	21	14	12	30	25	11	10	10

Table 9·3: Sample X-Ray measurements [see figure 9·27] in mm.

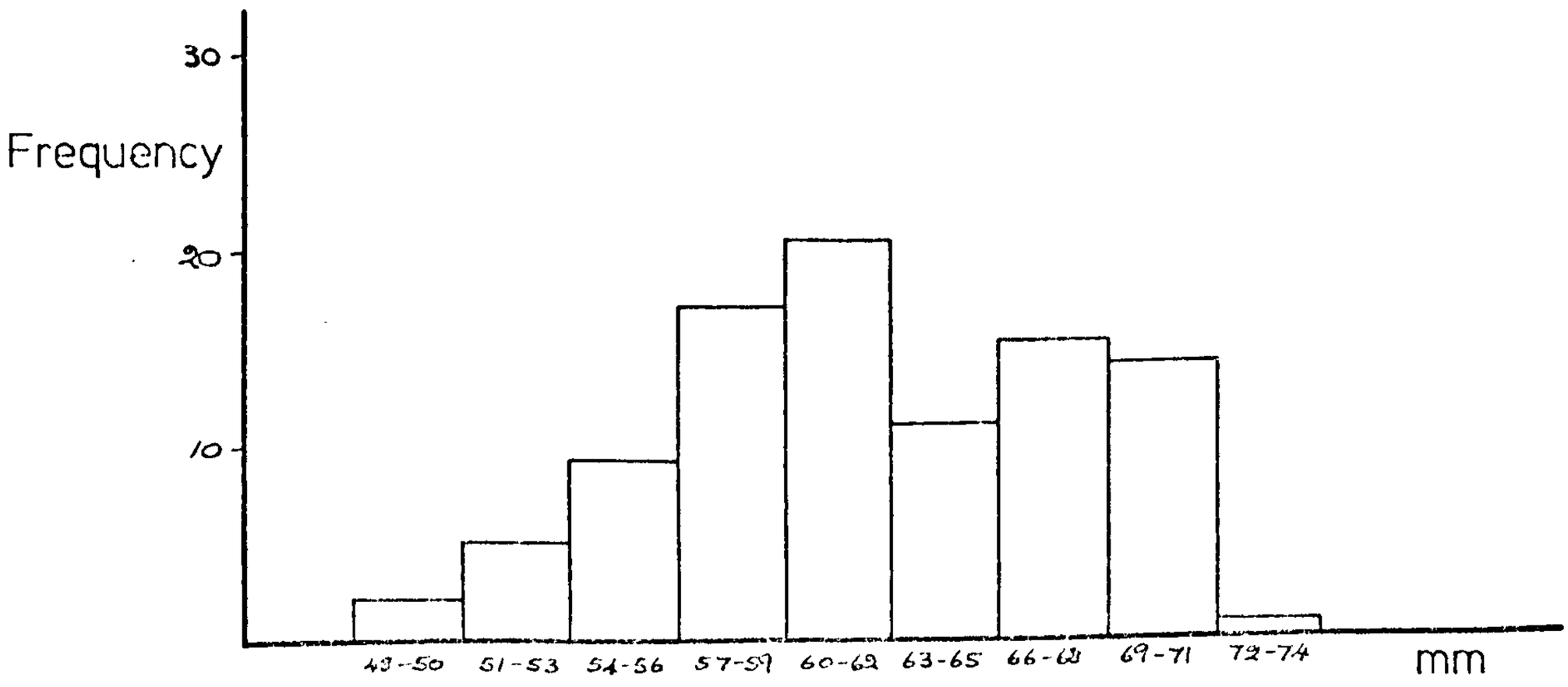

Figure 9·28: Distribution of epicondylar width

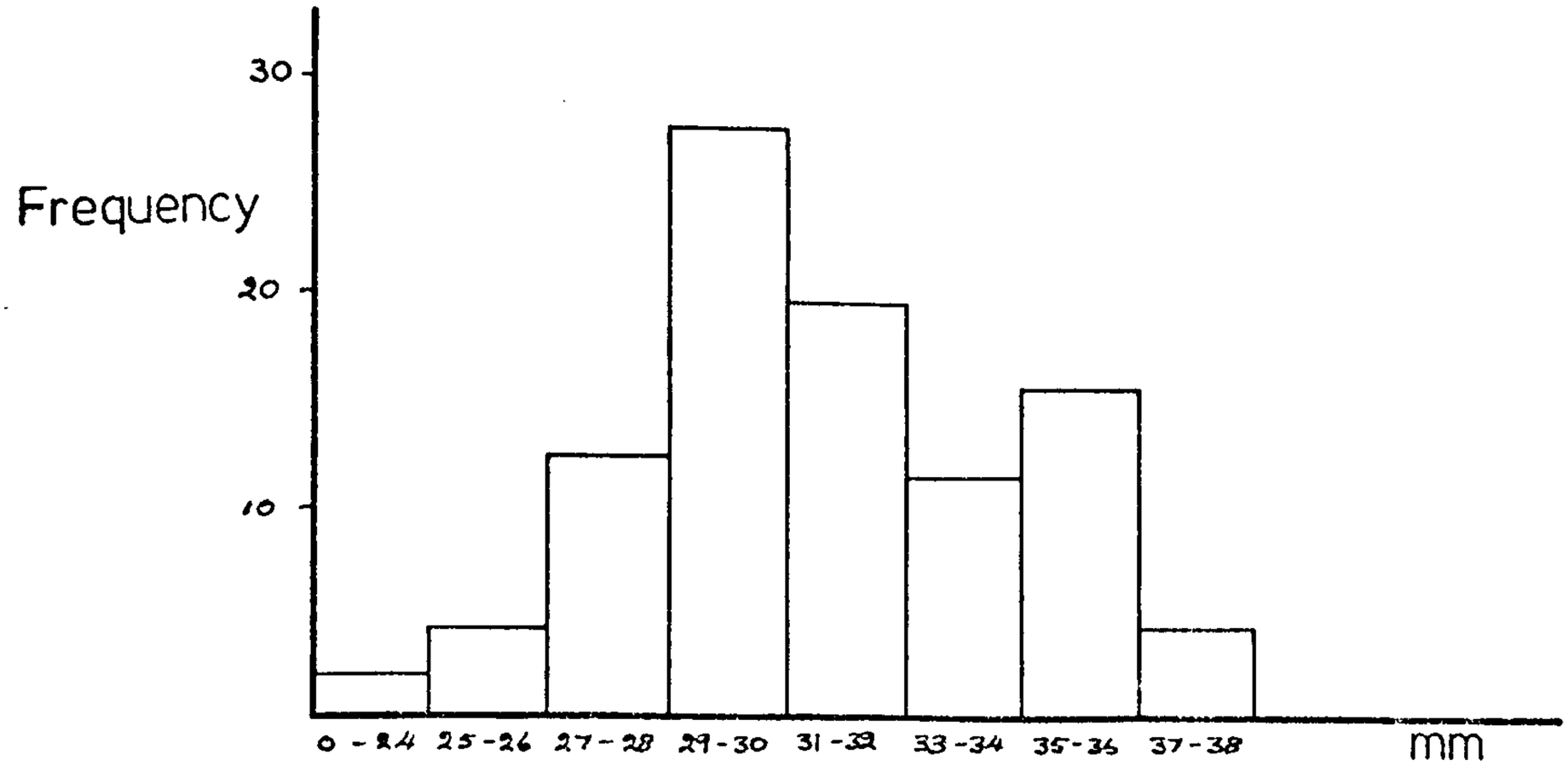

Figure 9·29: Distribution of ulnar width

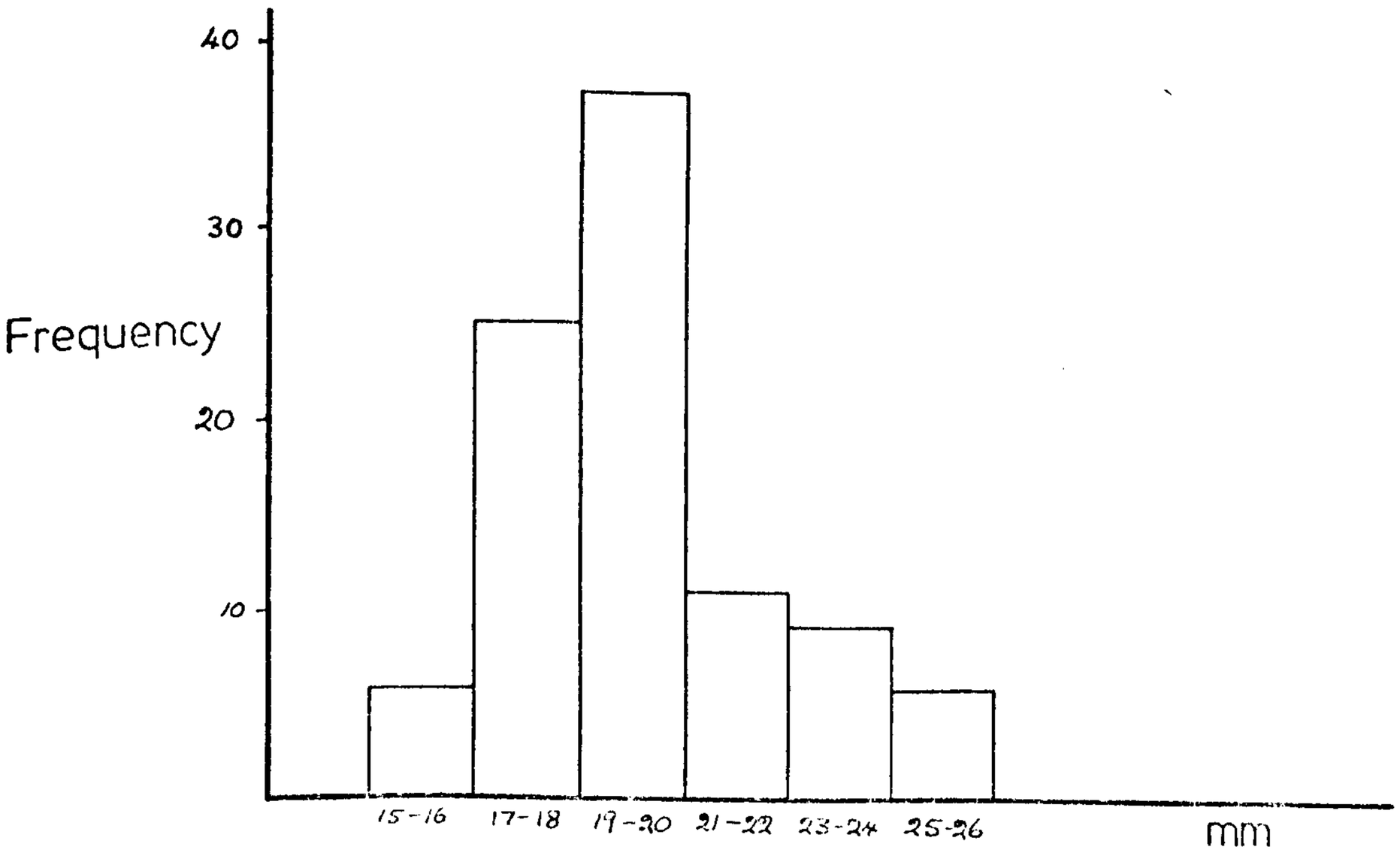

Figure 9·30: Distribution of trochlear width

against the occurrence of exceptionally small joints.

The templates were matched to the full size x-rays and it was found that a selection of a "two-size" group could not satisfy the geometrical restraints with respect to fixation cavities. No elbow joints required the extra small size of "0.90" and the model prototype was therefore taken to be the "smallest" size (rather than the "small" size). The three sizes 1.00, 1.18 and 1.366 were consequently selected as the required range. The appropriate templates were again matched to the x-rays and two modifications were found to be necessary:

(a) The size of the humeral supracondylar arch was not directly proportional to the size of the trochlea. The reduction in width, at the level of the supracondylar ridges, was found to be more pronounced in the larger elbows than in the small sizes. The medial contour of the arch was suitably modified for the "medium" and "large" templates.

(b) The inclination of the ulnar stem (8.5^{o}) was considered to be insufficient and the positioning of the stem was modified accordingly.

Detailed drawings of the "medium" size of prosthesis are contained in figures 9.31 and 9.32.

9.6 Current Status:

At the time of publication the development of the elbow prosthesis had reached the "manufacturing" stage. The construction of a preproduction model was underway in order to verify the efficacy of the final modifications.

Production problems were being discussed and these included tolerances, quantities and number of sizes. It was planned to manufacture a limited number of prostheses for clinical evaluation and to delay full-scale production until satisfactory post-operative results had been realised.

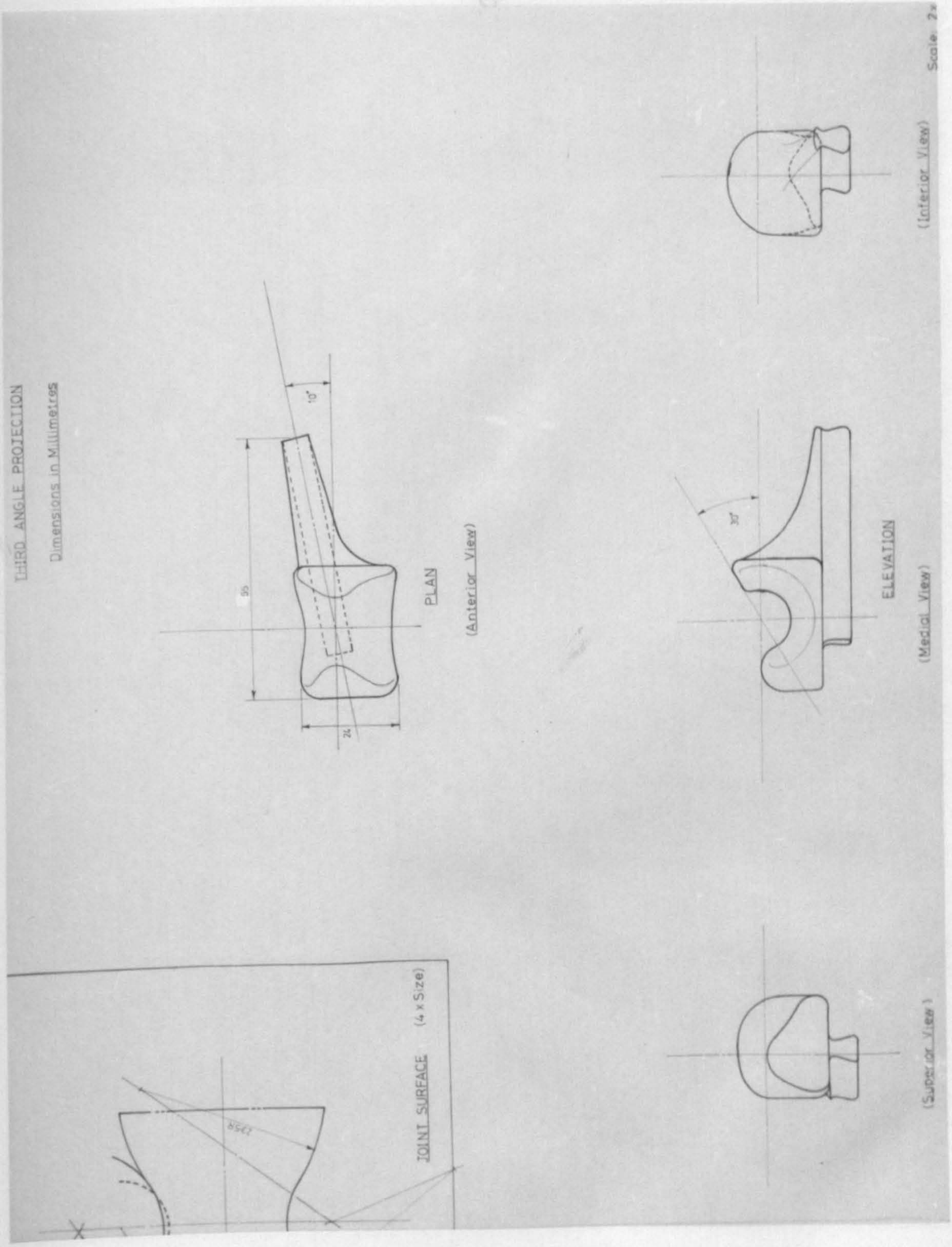

Figure 9.31: Clinical prototype: Ulnar component.

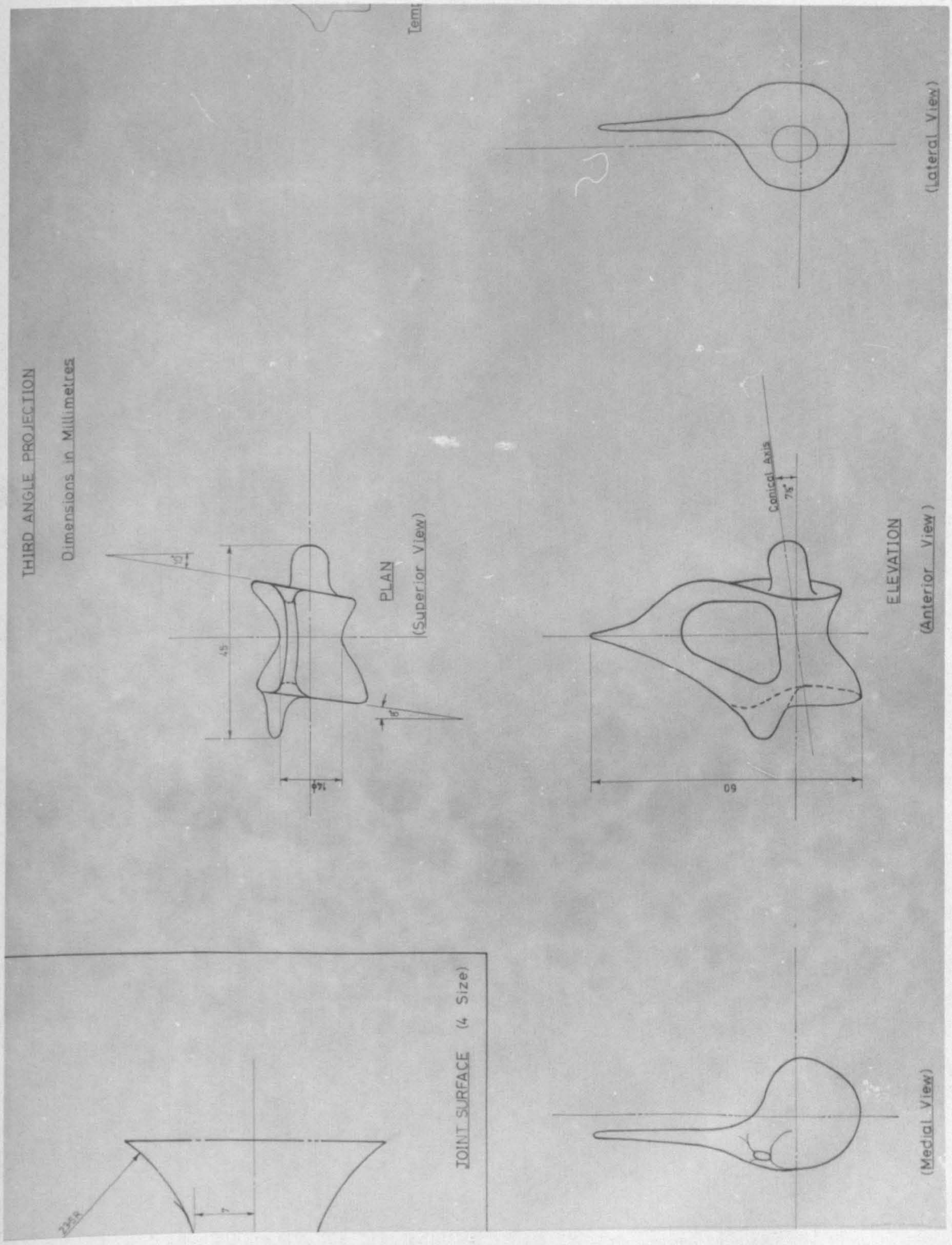

Figure 9.32: Clinical prototype: Humeral component.

APPENDICES

APPENDIX I

BIBLIOGRAPHY

ANANTHAKRISHNAN, C.V. and Easwaran, C.V. (1975). "Arthroplasty of the elbow: a new approach". Eng. in Med. 4 : No.4, pp3-5.

ANDREWS, B.J. (1975). Ph.D. Thesis: University of Strathclyde. To be published.

ATTENBOROUGH, G.G. (1974). "Total Knee Replacement using a stabilised gliding prosthesis". Conf. on Total Knee Replacement, pp.92-95, Inst. Mech. Eng. (C257/74).

AYOUB, M.A., Ayoub, M.M. and Ramsey, J.D. (1970). "A stereometric system for measuring human motion". Human Factors 12 : 523-535.

BANKOV, S. and Jorgensen, K. (1969). "Maximum strength of Elbow Flexors with pronated and supinated forearm". Communications from the Danish National Association for Infantile Paralysis No.29.

BARBENEL, J.C. (1972). "The Biomechanics of the Temperomandibular Joint: a theortical study". J. Biomechanics 5 : 251-256.

BARNETT, C.H., Davies, D.V. and MacConnail, M.A. (1961). "Synovial Joints - Their structure and mechanics". Longmans, 1961.

BARR, J.S. and Eaton, R.G. (1965). "Elbow Reconstruction with a new prosthesis to replace the distal end of the humerus". J. Bone Joint Surg. 47A : 1408.

BASMAJIAN, J.V. (1973). "Electrodes and Electrode Connectors". From Desmedt, J.E. (1973).

BASMAJIAN, J.V. (1974). "Muscles Alive". 3rd edition. Williams and Wilkins (Baltimore).

BASMAJIAN, J.V. and Latif, (1957). "Integrated actions and functions of the chief flexors of the elbow". J. Bone Joint Surg. 39A: 1106-1118.

BECKETT, R. and Chang, K. (1968). "An evaluation of the kinematics of gait by minimum energy". J. Biomechanics 1 : 147-159.

BERME, N., Lawes, P., Solomonidis, S. and Paul, J.P. (1975). "A shorter pylon transducer for measurement of prosthetic forces and moments during amputee gait". Eng. in Med. 4 : No.4 pp.6-8.

BIGLAND, B. and Lippold, O.C.J. (1954). "The relation between force, velocity and integrated electrical activity in human muscles". J. Physiol. (Lond.) 123 : 214-224.

BOURNE, G.H. (editor) (1972). "The structure and function of muscle". Vol. I, 2nd edition. Academic Press (London).

BRESLER, B. and Frankel, J.P. (1950). "The forces and moments in the leg during level walking". Trans. A.S.M.E. 72 : paper No. 48-A-62 pp.27-36.

BYERS, P.D. (1969). "The pathology of rheumatic diseases". In Arthritis and Physical Medicine by S. Licht: Waverly Press (USA).

CARLSOO, S. and Johansson, O. (1962). "Stabilisation of and load on the elbow joint in some protective movements". Acta Anat. (Basel) 48 : 224-231.

CARSON-DICK, W. (1972). "An introduction to Clinical Rheumatology". Livingstone Medical Text.

CHARNLEY, J. (1970). "Total Hip Replacement by low-friction arthroplasty". Clin. Orthop. 72 : 7.

CHARNLEY, J. (1975). "The wear of plastic materials in the hip joint". Conf. on Plastics in Medicine and Surgery. Plastics and Rubber Institute (in press).

CNOCKAERT, J.C., Lensel, G. and Pertuzon, E. (1975). "Relative contribution of individual muscles to the isometric contraction of a muscular group". J. Biomechanics 8 : 191-197.

CONTINI, R. and Drillis, R. (1966). "Body Segment Mass Properties". Technical Report No. 1166.03. New York University.

COVENTRY, M.B. and Bryan, R.S. (1974). "Technical Pitfalls in the poly-centric and geometric total knee arthroplasties". Conf. on Total Knee Replacement pp. 163-168. Inst. Mech. Eng. (C257/74).

CURREY, J.D. (1959). "Differences in the tensile strength of bone of different histological types". J. Anat. 93 : 87-95.

CURREY, J.D. (1970). "The mechanical properties of bone". Clin. Orthop. 73 : 210-232.

CURRIER, D.P. (1972). Maximal isometric tension of the elbow extensors at varied positions. I. Assessment by cable tensiometer. Phys. Ther. 52 : 1043-9.

DEE, R. (1972). "Total Replacement Arthroplasty of the elbow for rheumatoid arthritis". J. Bone Joint. Surg. 54B : 88-95.

DERN, R.J., Levene, J.M. and Blair, H.A. (1947). "Forces exerted at different velocities in human arm movements". Am. J. Physiol. 151 : 415-437.

DESMEDT, J.E. (editor) (1973). "New developments in E.M.G. and Clinical Neurophysiology". Vol. I. pp. 502-510. S. Karger (Basel).

DOSS, W.S. and Karpovich, P.V. (1965). "A comparison of concentric, eccentric and isometric strength of elbow flexors". J. Appl. Physiol. 20 : 351-353.

DOWSON, D. (1973). "Lubrication and wear of joints". Physioltherapy 59 : 104.

DUNN, A.W. (1971). "A distal humeral prosthesis". Clin. Orthop. 77: 199-202.

ELFTMAN, H. (1939). "The function of the arms in walking". Human Biol. 11 : 529-535.

ELFTMAN, H. (1966). "Biomechanics of muscle". J. Bone Joint Surg. 48A : 363.

ELLOY, M.A., Wright, J.T.M. and Cavendish, M.E. (1976). "The basic requirements and design criteria for total joint prostheses". Acta Orthop. Scand. 47 : 193-202.

ENGEN, T.J. and Spencer, W.A. (1968). "Method of kinematic study of normal upper extremity movements". Arch. Phys. Med. 49 : 9-12.

EVANS, F.G. (1957). "Stress and strain in bones". Thomas (Illinois).

EWALD, F.C. (1975). "Total elbow replacement". Orthop. Clin. of N. America 6 : 685-696.

FREEMAN, M.A.R. (1972). "The pathogenesis of primary ostcoarthrosis: an hypothesis". in: Modern Trends in Orthopaedics 6. Ed. A.G. Apley (Butterworth).

FREEMAN, M.A.R., Swanson, S.A.V. and Todd, R. (1974). "Replacement of the knee with the Freeman-Swanson prosthesis; current developments and the results of a clinical trial with a standard prosthesis". Conf. on Total Knee Replacement pp. 102-107. Inst. Mech. Eng. (C257/74).

GRAY, H. (1973). "Gray's Anatomy". 35th edition. Longman.

GRIEVE, D.W., Miller, D., Mitchelson, D., Paul, J.P. and Smith, A.J. (1975). "Techniques for the analysis of human movement". Lepus Books (London).

GROH, H. (1973). "Proceedings I: Elbow fractures in the adult. General : Anatomy, biomechanics. Biomechanics of the elbow joint". Hefte Unfallheilkd 114 : 13-20.

GSCHWEND, N. and Scheier, H. (1974). "Elbow arthroplasty with the new GSB prosthesis". Scand. J. Rheumatol. 3 : 177-182.

GUTEWORT, W. (1971). "The numerical presentation of kinematics of human body motions". in: Biomechanics Vol. II. pp.290-298. University Park Press.

HALLS, A.A. and Travill, A. (1964). "Transmission of pressures across the elbow joint". Anat. Rec. 150 : 243-247.

HILL, A.V. (1938). "The heat of shortening and the dynamic constants of muscle". Proc. Roy. Soc. B126 : 136.

HILL, A.V. (1950). "The series elastic component of muscle". Proc. Roy. Soc. B137 : 273-280.

HILL, A.V. (1951). "The mechanics of voluntary muscle". Lancet 261 : 947.

HILL, A.V. (1970). "First and last experiments in muscle mechanics". Cambridge University Press.

HUNSICKER, P.A. (1955). "Arm strength at selected degrees of elbow flexion". WADC Technical report 54-543. Project No. 7214.

IKAI, M. and Fukunaga, T. (1968). "Calculation of muscle strength per unit cross sectional area of human muscle by means of ultrasonic measurement". Int. Z. angew. Physiol. einschl. Arbeitsphysiol. 26 : 26-32.

INMAN, V.T., Ralston, H.J., Saunders, J.B., Feinstein, B. and Wright, E.W. (1952). "Relation of human electromyogram to muscular tension". EEG Clin. Neurophysiol. 4 : 187-194.

JARRETT, M.O. (1976). "A television/computer system for human locomotion analysis". Ph.D. Thesis : University of Strathclyde.

JOHNSON, E.W. and Schlein, A.P. (1970). "Vitallium prosthesis for the olecranon and proximal part of the ulna". J. Bone Joint Surg. 52A : 721.

KATZ, B. (1966). "Nerve, Muscle and Synapse". McGraw-Hill.

KENDALL, H.O., Kendall, F.P. and Wadsworth, G.E. (1971). "Muscles: their Testing and Function". 2nd edition, Williams and Wilkins.

KINZEL, G.L., Hall, A.S. and Hillberry, B.M. (1972). "Measurement of the total motion between two body segments. II. Description of application". J. Biomechanics 5 : 283-293.

LAMOREUX, L.M. (1971). "Kinematic measurement in the study of human walking". Bull. Prosthetics Research (Spring) pp.3-85.

LARSON, C.L. and Nelson, R.C. (1969). "An analysis of strength, speed and acceleration of elbow flexion". Arch. Phys. Med. 50 : 274-278.

LARSON, R.F. (1969). "Forearm positioning on maximal elbow flexor force". Phys. Ther. 49 : 748-756.

LAWES, P. (1975). "Personal communication".

LIPPOLD, O.C.J. (1952). "The relation between integrated action potentials in a human muscle and its isometric tension". J. Physiol. (Lond.) 117 : 492-99.

MACAUSLAND, W.R. (1953). "Nylon prosthesis in lesions of the shoulder, elbow and finger". Am. J. Surg. 85 : 164-173.

MACCONAIL, M.A. (1967). "Basic anatomy of weight bearing joints". Proc. Inst. Mech. Eng. 181, 3J : 1-7.

McELHANEY, J.H. (1966). "Dynamic response of bone and muscle tissue". J. Appl. Physiol. 21 : 1231.

MARMOR, L. (1967). "Surgery of rheumatoid arthritis". Henry Kimpton (London).

MATSUMOTO, Y. (1966). "Validity of the force-velocity for muscle contraction in the length region $L < L_o$". J. of General Physiol. 50 : 1125.

MELLEN, R.H. and Phalen, G.S. (1947). "Arthroplasty of the elbow by replacement of the distal portion of the humerus with an acrylic prosthesis". J. Bone Joint Surg. 29 : 348-353.

MESSIER, R.H., Duffy, J., Litchman, H.M., Pasley, P.R., Soechting, J.F. and Stewart, P.A. (1971). "The EMG as a measure of tension in the human biceps and triceps muscles". Int. J. of Mech. Sci. 13 : 585.

MITCHELSON, D. (1975). "Recording of movement without photography". in: Grieve et al. (1975).

MORREY, B.F. and Chao, E.Y.S. (1976). "Passive motion of the elbow joint". J. Bone Joint Surg. 58A : 501-508.

MORRIS, J.R.W. (1973). "Accelerometry - a technique for the measurement of human body movements". J. Biomechanics 6 : 729-736.

MORRISON, J.B. (1968). "Bioengineering analysis of force actions transmitted by the knee joint". Biomed. Eng. 3 : 164-170.

MORRISON, J.B. (1970). "The mechanics of muscle function in locomotion". J. Biomechanics 3 : 431-451.

NELSON, R.C., Petak, K.L. and Pechar, G.S. (1969). "Use of stroboscopic-photographic techniques in biomechanics research". Res. Quart. 40 : 424-426.

NUBAR, Y. and Contini, R. (1961). "A minimal principle in biomechanics". Bull. of Math. Biophysics 23 : 377-391.

O'CONNELL, A.L. and Gardner, E.B. (1962). "The use of electromyography in kinesiological research". Res. Quart. 34 : 166-184.

PAUL, J.P. (1967). "Forces at the human hip joint". Ph.D. Thesis : University of Glasgow.

PAUL, J.P. (1975). "Instruments for force measurement". in: Grieve et al (1975).

PEAT, M., Grahame, R., Fulford, R. and Quanbury, A.O. (1976). "An electrogoniometer for the measurement of single plane movements". J. Biomechanics 9 : 423-424.

PRITCHARD, J.J. (1972). "General histology of bone". in Bourne (1972).

PROVINS, K.A. and Salter, N. (1955). "Maximum torque exerted about the elbow joint". J. Appl. Physiol. 7 : 393-398.

PUGH, J.W., Rose, R.M. and Radin, E.L. (1973). "A structural model for the mechanical behaviour of trabecular bone". J. Biomechanics 6 : 657-670.

RALSTON, H.J., Inman, V.T., Strait, L.A. and Shaffrath, M.D. (1947). "Mechanics of human, isolated voluntary muscle". Amer. J. Physiol. 151 : 612-620.

RALSTON, H.J., Pollisar, M.J., Inman, V.T., Close, J.R. and Feinstein, B. (1948). "Dynamic features of human isolated voluntary muscle in isometric and free conditions". J. Appl. Physiol. 1 : 526.

RASCH, P.J. and Burke, R.K. (1974). "Kinesiology and applied anatomy". 5th edition, Lea and Febiger (Philadelphia).

RASCH, P.J. and Pierson, W.R. (1960). "Relationship between maximum isometric tension and breaking strength of forearm flexors". Res. Quart. 31 : 534-535.

ROMANES, G.J. (1969). "Cunningham's Manual of Practical Anatomy". Oxford University Press.

SAHA, S. (1973). "Anisotropic analysis of bone - some 2-dimensional problems". J. Biomechanics 6 : 641-650.

SAHA, A.K., Saha, M.R. and Chakravarty (1957). "Anatomical and mechanical observations on the gleno-humeral joint". Calcutta Med. J. 54 : 48.

SCHLEIN, A.P. (1974). "Prosthesis for total arthroplasty of the elbow joint". U.S. Patent 3,816,854.

SEEDHOM, B.B., Longton, E.B., Wright, V. and Dowson, D. (1972a). "Dimensions of the knee". Ann. Rheum. Dis. 31 : 54-58.

SEEDHOM, B.B., Longton, E.B., Dowson, D. and Wright, V. (1974). "The Leeds Knee". Conf. on Total Knee Replacement pp.108-114. Inst. Mech. Eng. (C257/74).

SEIREG, A. and Arvikar, R.J. (1973). "Mathematical model for evaluation of the forces in the lower extremities of the musculo-skeletal system". J. Biomechanics 6 : 313-326.

SEMLITSCH, M. (1974). "Technical progress in artificial hip joints". Eng. in Med. 3 : No.4, pp.10-19.

SHIERS, L.P.G. (1974). "Total knee hinge replacement". Conf. on Total Knee Replacement. pp.44-49. Inst. Mech. Eng. (C257/74).

SIMPSON, D. (1975). "An examination of the design of an endoprosthesis for the elbow". M.Sc. Thesis, University of Strathclyde.

SOUTER, W.A. (1973). "Arthroplasty of the elbow". Orthop. Clin. of N. America 4 : No.2 pp.395-413.

SOUTER, W.A. (1975). "Personal communication".

STREET, D.M. and Steven, P.S. (1974). "A humeral replacement prosthesis for the elbow". J. Bone Joint. Surg. 56A : 1147-1158.

SUTHERLAND, D. and Hagy, J. (1972). "Measurement of gait movements from motion picture film". J. Bone Joint Surg. 54A : 787-797.

SWANSON, S.A.V. (1975). "Lubrication in joints". in: Recent Advances in Orthopaedics by B. McKibbin (Churchill-Livingstone).

SWEENEY, A.W., Kroon, R.P. and Byres, R.K. (1965). "Mechanical characteristics of bone and its constituents". ASME 65-WA/HUF-7, 1965.

TOOTH, R. (1976). "The biomechanics of arthrodesis and arthroplasty in the human leg". Ph.D. Thesis: University of Strathclyde.

TRILLAT, A., Dejour, H. and Bousquet, G. (1972). "A new type of elbow prosthesis". Lyon Chir. 68 : 311-315.

VENABLE, C.S. (1952). "An elbow and an elbow prosthesis - Case of complete loss of lower third of humerus". Am. J. Surg. 83 : 271-274.

WALKER, P.S. (1973). "Trends in knee prosthesis development". Eng. Med. 2 : 76-81.

WALKER, P.S. (1975). Deflection of the radio-humeral joint. Data to be published.

WITVOET, J. and Aubriot, J.H. (1974). "The Guepar total knee prosthesis". Conf. on Total Knee Replacement pp. 144-152. Inst. Mech. Eng. (C257/74).

WRIGHT, J.T.M., Elloy, M.A. and Cavendish, M.E. (1975). "New total joint prostheses for fingers, elbow and ankle". 15th Anniversary Conference (Edinburgh). Biological Engineering Society.

WRIGHT, V., Dowson, D. and Unsworth, A. (1971a). "The lubrication and stiffness of joints". in: Modern Trends in Rheumatology. by A. Hill (editor) : Butterworths.

WRIGHT, V., Dowson, D. and Sellar, P.C. (1971b). "Bioengineering aspects of synovial fluid and cartilage". in : Modern Trends in Rheumatology.

WRIGHT, V. and Amis, A. (1975). Personal Communication.

YAMADA, H. (1970). "Strength of biological materials". Williams and Wilkins.

YEO, B.P. (1976). "Investigation concerning the principle of minimal total muscular force". J. Biomechanics 9 : 413-416.

APPENDIX 2

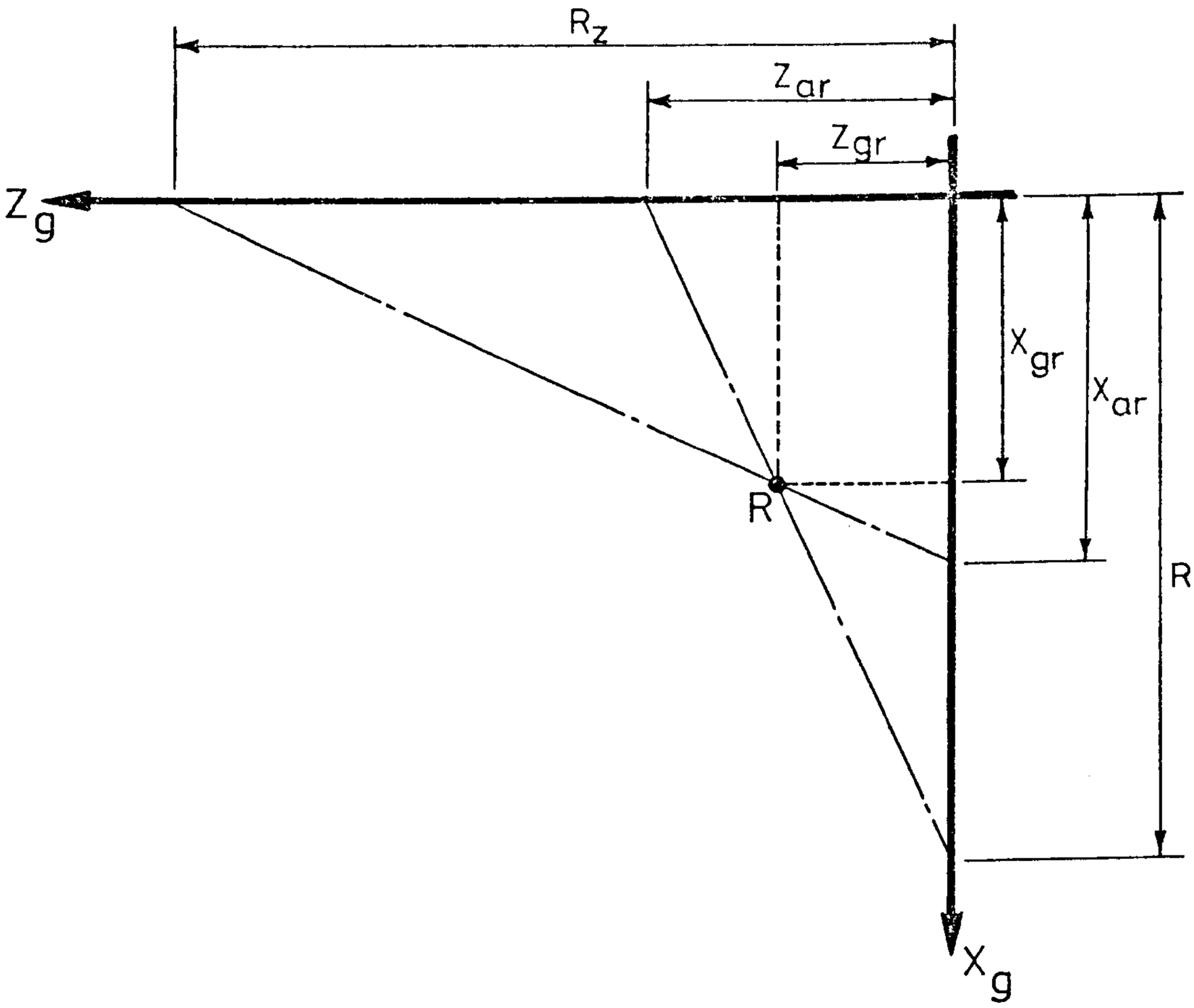

Figure A2·1: Plan view of parallax errors.

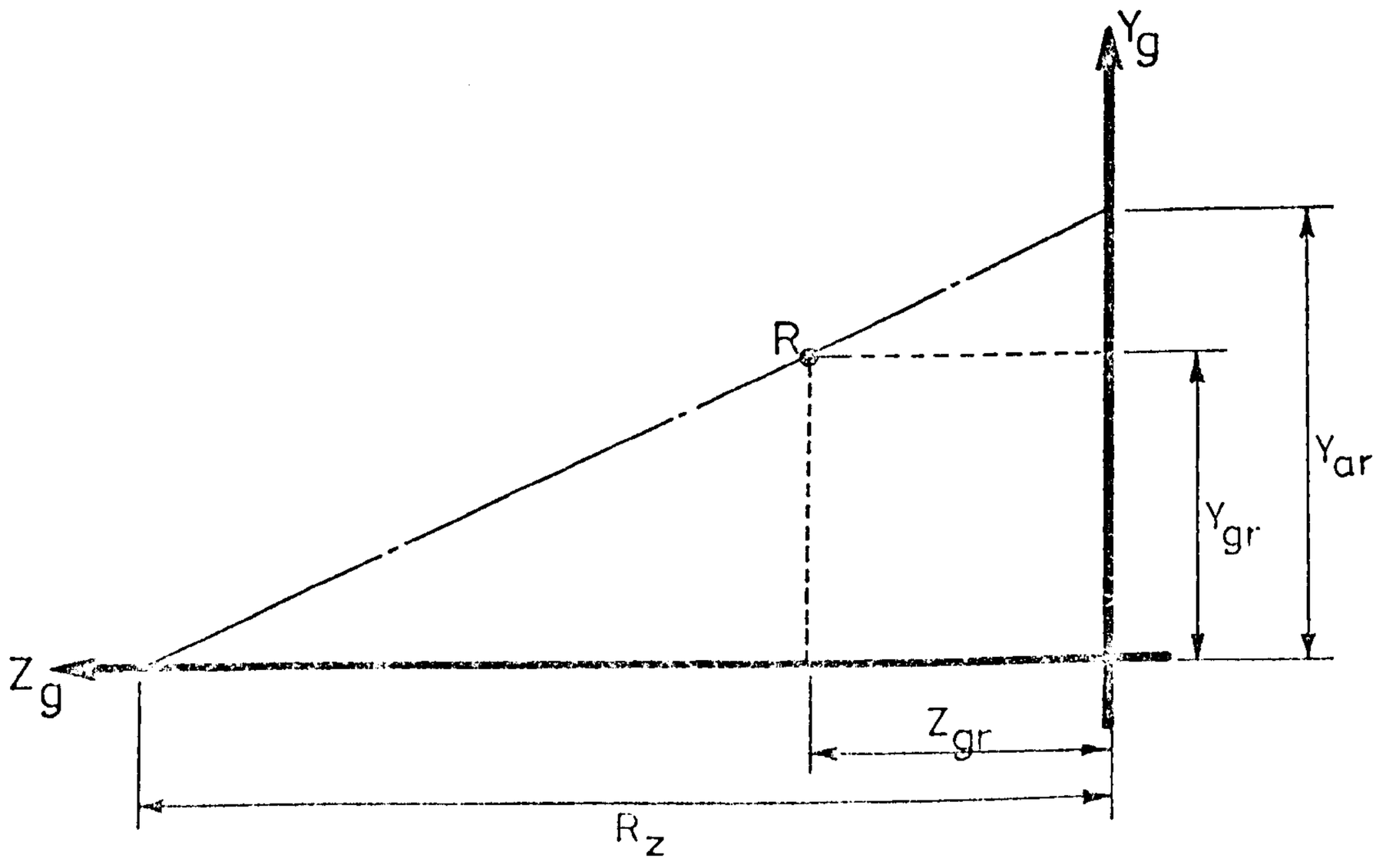

Figure A2·2: Calculation of the error in Y_g

A2.1 Derivation of Parallax Equations:

The camera arrangements are shown diagrammatically in figures A2.1 and A2.2. Equations 6.2a,b,c and d were derived as follows.

From figure A2.1:

$$\frac{Z_{gr}}{Z_{ar}} = \frac{R_{xl} - X_{gr}}{R_{xl}}$$

$$\therefore \quad Z_{gr} = Z_{ar} - \frac{Z_{ar} \cdot X_{gr}}{R_{xl}} \qquad \text{A2.1}$$

And:

$$\frac{X_{gr}}{R_z - Z_{gr}} = \frac{X_{ar}}{R_z}$$

$$\therefore \quad X_{gr} = \frac{X_{ar}(R_z - Z_{gr})}{R_z}$$

Substituting eqn. A2.1 for Z_{gr}:-

$$X_{gr} = \frac{X_{ar}.R_z - X_{ar}.Z_{ar}}{R_z} + \frac{X_{ar}.Z_{ar}.X_{gr}}{R_z.R_{xl}}$$

$$\therefore \quad X_{gr}\left(\frac{R_z.R_{xl} - X_{ar}.Z_{ar}}{R_z.R_{xl}}\right) = \frac{X_{ar}.R_z - X_{ar}.Z_{ar}}{R_z}$$

$$\therefore \quad X_{gr} = \frac{X_{ar}(R_z.R_{xl} - Z_{ar}.R_{xl})}{R_z.R_{xl} - X_{ar}.Z_{ar}}$$

From eqn. A2.1:

$$Z_{gr} = Z_{ar}\left(1 - \frac{X_{gr}}{R_{xl}}\right)$$

For Z coordinates obtained from the right hand camera, R_{x2} lies in the negative X_g direction. Hence:

$$Z_{gr} = Z_{ar}\left(1 + \frac{X_{gr}}{R_{x2}}\right)$$

From figure A2.2:

$$\frac{Y_{gr}}{Y_{ar}} = \frac{(R_z - Z_{gr})}{R_z}$$

$$\therefore \quad Y_{gr} = \frac{Y_{ar}(R_z - Z_{gr})}{R_z}$$

A2.2 4th Order Butterworth Filter:

This filter was incorporated in an ALGOL 60 procedure which was named "BUT4" and is listed overleaf. The procedure format is BUT4 (Q, NT, FCUT, T, WI, AD, W).

Where:

Q	Input matrix (one dimensional).
NT	Total number of samples.
FCUT	"Cut-off" frequency (Hz).
T	Time interval between samples (s).
WI	Output matrix (one dimensional).
AD	Work array.
W	Work array.

```
'PROCEDURE' BUT4(Q,NT,FCUT,T,W1,AD,W);
'INTEGER' NT;
'REAL' FCUT,T;
'ARRAY' Q,W1,AD,W;
'BEGIN'
AMEN:=0.0;
'FOR' K:=1 'STEP' 1 'UNTIL' NT 'DO'
AMEN:=AMEN+Q[K]/NT;
LINTR:=Q[NT]-Q[1];
PI:=3.14159265;
T1:=SIN(PI*FCUT*T);
T2:=COS(PI*FCUT*T);
TT:=T1/T2;
A:=COS(PI/8.0)*TT;
B:=SIN(PI/8.0)*TT;
C1:=2.0*(A+B);
C2:=2.0*(A+B)↑2;
C3:=((A↑2+B↑2)*(B+A))*2.0;
C4:=(A↑2+B↑2)↑2;
C5:=1+C1+C2+C3+C4;
C6:=-4.0+4.0*C4-2.0*C1+2.0*C3;
C7:=6.0+6.0*C4-2.0*C2;
C8:=-4.0+2.0*C1-2.0*C3+4.0*C4;
C9:=1.0-C1+C2+C4-C3;
N1:=NT+24;
'FOR' K:=NT 'STEP' 1 'UNTIL' 150 'DO'
AD[K]:=0.0;
'FOR' K:=1 'STEP' 1 'UNTIL' NT 'DO'
AD[K+4]:=Q[K]-Q[1]-(K-1)*LINTR/NT;
'FOR' K:=1 'STEP' 1 'UNTIL' 4 'DO'
'BEGIN'
AD[K]:=0.0;
W[K]:=0.0;
'END';
'FOR' K:=1 'STEP' 1 'UNTIL' NT+20 'DO'
W[K+4]:=(C4*(AD[K+4]+4*AD[K+3]+6*AD[K+2]+4*AD[K+1]+AD[K])-
(W[K+3]*C6+W[K+2]*C7+W[K+1]*C8+W[K]*C9))/C5;

'FOR' JKJ:=1 'STEP' 1 'UNTIL' NT+20 'DO'
W[JKJ]:=W[JKJ+4];
'FOR' K:=1 'STEP' 1 'UNTIL' 4 'DO'
'BEGIN'
K4:=N1-K;
W1[K4+1]:=0.0;
W[K4+1]:=0.0;
'END';
'FOR' K:=1 'STEP' 1 'UNTIL' NT+20 'DO'
'BEGIN'
K5:=N1-K;
W1[K5-3]:=(C4*(W[K5-3]+4*W[K5-2]+6*W[K5-1]+4*W[K5]+W[K5+1]
)-(W1[K5-2]*C6+W1[K5-1]*C7+W1[K5]*C8+W1[K5+1]*C9))/C5;
'END';
'FOR' K:=1 'STEP' 1 'UNTIL' NT 'DO'
W1[K]:=W1[K]+Q[1]+(K-1)*LINTR/NT;
'END';
```

A2.3 Axis Orientations:

The various axes were defined in relation to grid coordinates as follows:

Humerus (see figure 6.9).

Axis lengths:

$$DX = \sqrt{[(X_5 - X_B)^2 + (Y_5 - Y_B)^2 + (Z_5 - Z_B)^2]}$$

$$DY = \sqrt{[(X_B - X_{SS})^2 + (Y_B - Y_{SS})^2 + (Z_B - Z_{SS})^2]}$$

$$DZ = \sqrt{[(X_B - X_3)^2 + (Y_B - Y_3)^2 + (Z_B - Z_3)^2]}$$

$$\therefore \quad LGH1 = (X_B - X_5)/DX.$$

$$MGH1 = (Y_B - Y_5)/DX.$$

$$NGH1 = (Z_B - Z_5)/DX.$$

$$LGH2 = (X_{SS} - X_B)/DY.$$

$$MGH2 = (Y_{SS} - Y_B)/DY.$$

$$NGH2 = (Z_{SS} - Z_B)/DY.$$

$$LGH3 = (X_3 - X_B)/DZ.$$

$$MGH3 = (Y_3 - Y_B)/DZ.$$

$$NGH3 = (Z_3 - Z_B)/DZ.$$

LGHI, MGHI and NGHI were recalculated using orthogonality relations since marker no.5 was considered to be placed inaccurately.

Ulna (see figure 6.10).

Axis lengths

$$DX = \sqrt{[(X_6 - X_{EC})^2 + (Y_6 - Y_{EC})^2 + (Z_6 - Z_{EC})^2]}$$

$$DY = \sqrt{[(X_w - X_{EC})^2 + (Y_w - Y_{EC})^2 + (Z_w - Z_{EC})^2]}$$

$\therefore$ $LGUI = (X_{EC} - X_6)/DX.$

$MGUI = (Y_{EC} - Y_6)/DX.$

$NGUI = (Z_{EC} - Z_6)/DX.$

$LGU2 = (X_{EC} - X_w)/DY.$

$MGU2 = (Y_{EC} \mid Y_w)/DY.$

$NGU2 = (Z_{EC} - Z_w)/DY.$

The direction cosines of Z_u relative to the grid axes were calculated from orthogonality relations (see Appendix A2.4).

Transducer: (see figure 6.11).

Axis Lengths

$$DX = \sqrt{[(X_{12} - X_{13})^2 + (Y_{12} - Y_{13})^2 + (Z_{12} - Z_{13})^2]}$$

$$DY = \sqrt{[(X_{13} - X_{11})^2 + (Y_{13} - Y_{11})^2 + (Z_{13} - Z_{11})^2]}$$

$$DZ = \sqrt{[(X_{10} - X_p)^2 + (Y_{10} - Y_p)^2 + (Z_{10} - Z_p)^2]}$$

$\therefore$ $LGPI = (X_{13} - X_{12})/DX$

$MGPI = (Y_{13} - Y_{12})/DX$

$NGPI = (Z_{13} - Z_{12})/DX$

$LGP2 = (X_{11} - X_{13})/DY$

$MGP2 = (Y_{11} - Y_{13})/DY$

$NGP2 = (Z_{11} - Z_{13})/DY$

$$LGP3 = (X_{10} - X_p)/DZ$$

$$MGP3 = (Y_{10} - Y_p)/DZ$$

$$NGP3 = (Z_{10} - Z_p)/DZ$$

2.4 Derivation of Orthogonality Relations:

For right hand orthogonality, we define:

$$X_H = Y_H \wedge Z_H$$

and: $$Z_U = X_U \wedge Y_U$$

For X_H:

$$Y_H \wedge Z_H = \begin{vmatrix} X_g & Y_g & Z_g \\ LGH2 & MGH2 & NGH2 \\ LGH3 & MGH3 & NGH3 \end{vmatrix}$$

$$= X_g\,(MGH2.NGH3 - NGH2.MGH3)$$
$$+ Y_g\,(NGH2.LGH3 - NGH3.LGH2)$$
$$+ Z_g\,(LGH2.MGH3 - MGH2.LGH3)$$

By definition:

$$X_H = X_g * LGHI + Y_g * MGHI + Z_g * NGHI$$

$$\therefore LGHI = (MGH2.NGH3 - NGH2.MGH3)$$

$$\therefore MGHI = (NGH2.LGH3 - NGH3.LGH2)$$

$$\therefore NGHI = (LGH2.MGH3 - MGH2.LGH3)$$

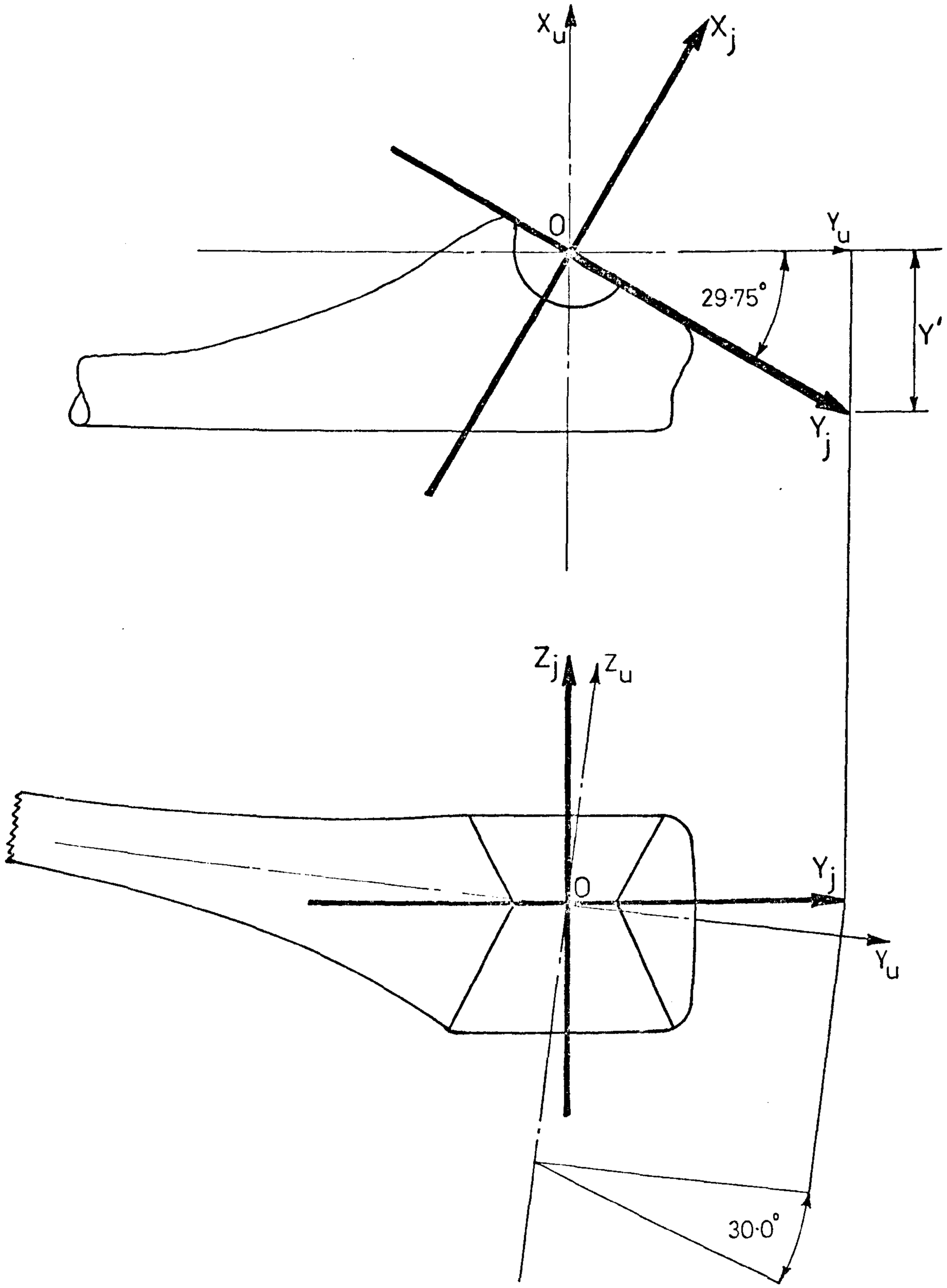

Figure A2·3: Position of the "joint" axis system in relation to the ulnar axes

For X_u:

$$X_u \wedge Y_u = \begin{vmatrix} X_g & Y_g & Z_g \\ LGUI & MGUI & NGUI \\ LGU2 & MGU2 & NGU2 \end{vmatrix}$$

$$= X_g(MGUI.NGU2 - NGUI.MGU2)$$
$$+ Y_g(NGUI.LGU2 - LGUI.NGU2)$$
$$+ Z_g(LGUI.NGU2 - NGUI.LGU2)$$

By definition:

$$Z_u = X_g * LGU3 + Y_g * MGU3 + Z_g * NGU3$$

$\therefore$ LGU3 = (MGUI.NGU2 - NGUI.MGU2)

MGU3 = (NGUI.LGU2 - LGUI.NGU2)

NGU3 = (LGUI.NGU2 - NGUI.LGU2)

A2.5 Joint-Ulna Relationships:

For the purpose of this analysis, it was assumed that the joint axes, relative to the ulna, were positioned as shown in figure A2.3.

By definition:

$$X_u \hat{O} X_i = 30^\circ$$

And $Y' = 0.5 * \cos 7^\circ$

$= 0.4962$

For X_i:

$\therefore X_i \hat{O} Y_u = 60.25$ MUJI = 0.4962

$\therefore$ NUJ1 = 0.06089

$\therefore$ $X_i \hat{O} Z_u = 86.5^\circ$

For Y_i:

$Y_i \hat{O} X_u = 120^\circ$ LUJ2 = -0.50

$Y_i \hat{O} Z_u$ = ?

$Y_i \hat{O} Y_u$ = ?

For Z_i:

$Z_i \hat{O} Z_u = 7^\circ$ (approximately)

$\therefore$ NUJ3 = 0.9925

$Z_i \hat{O} X_u$ = 90

$\therefore$ LUJ3 = 0.0

$\therefore$ MUJ3 = $\sqrt{(1 - 0.9925^2)}$

= 0.122 ($Z_i \hat{O} Y_u$ = 82.99)

But $Z_i \hat{O} Y = 180 - 82.99$

$\therefore$ MUJ3 = -0.122

From orthogonality relations:

LUJ2 = -0.50

MUJ2 = 0.8595

NUJ2 = 0.1055

Therefore, the matrix [DCJU] becomes

$$\begin{bmatrix} 0.866 & 0.4692 & 0.06089 \\ -0.50 & 0.8595 & 0.1055 \\ 0.0 & -0.122 & 0.9925 \end{bmatrix}$$

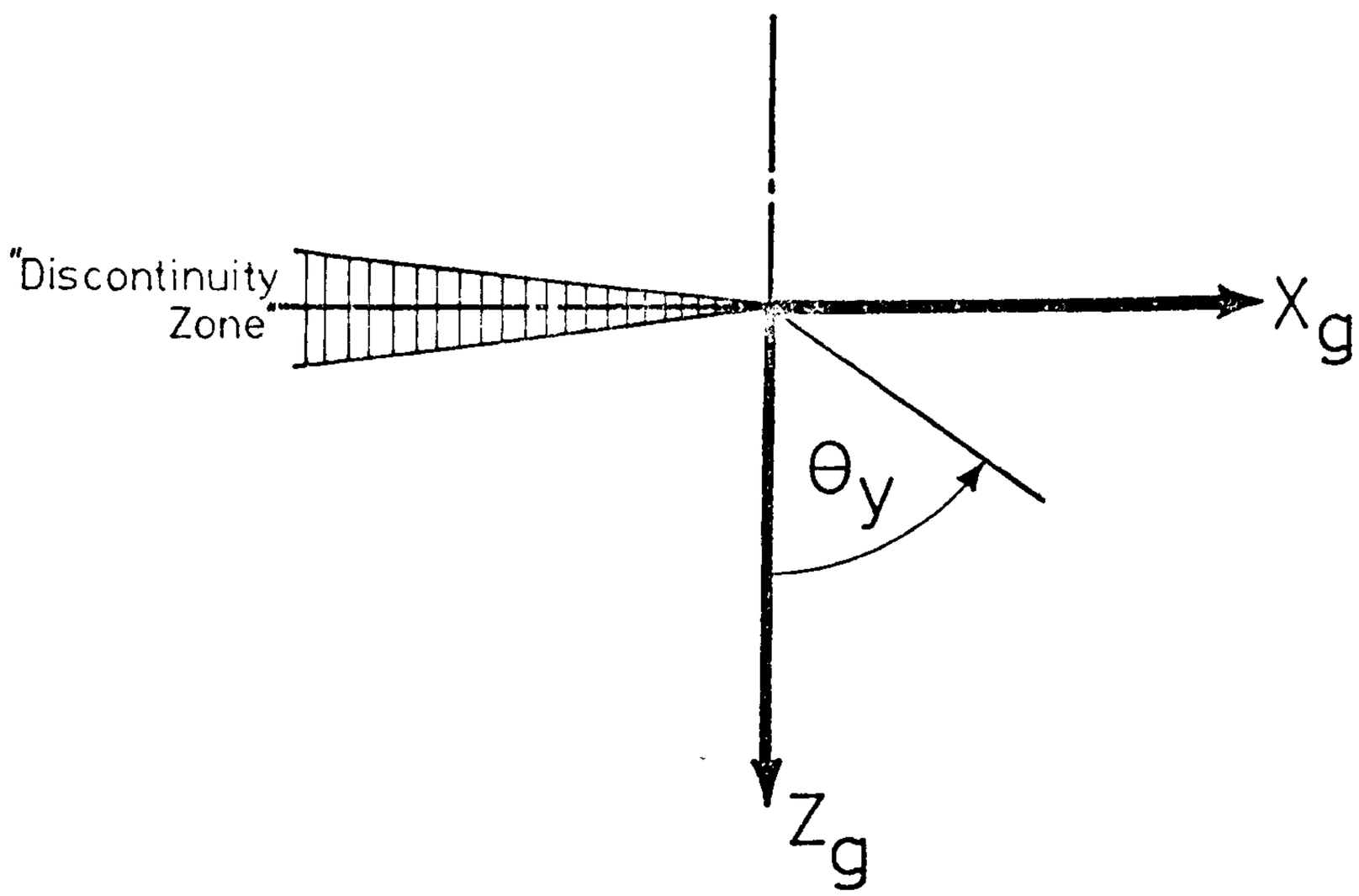

Figure A2·4: Definition of θ_y for forearm orientation.

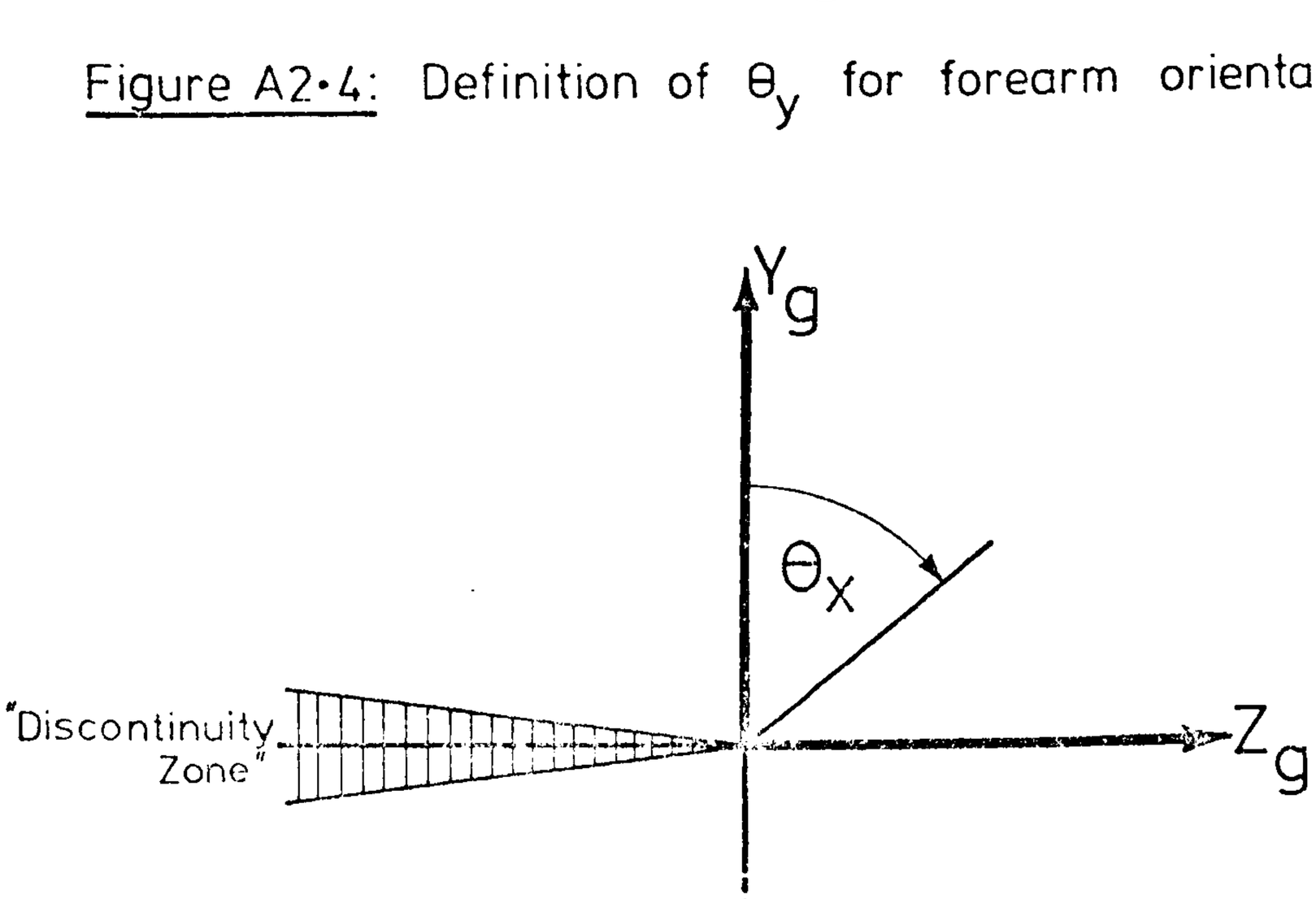

Figure A2·5: Definition of θ_x for forearm orientation.

A2.6 Forearm Orientation:

With the computer functions limiting $\tan^{-1}\Theta$ solutions to $-\frac{\pi}{2} < \Theta < \frac{\pi}{2}$ critical directions were defined to avoid discontinuities as previously described (section 6.9). The probable positions of the long axis of the forearm (Y_u) were therefore carefully studied to select the critical directions pertaining to rotations about X_g, Y_g and Z_g.

Details for θ_z have already been presented in section 6.9. For θ_y, the most unlikely position of the forearm in the $X_g - Z_g$ plane was considered to be the "$-X_g$" direction (see figure A2.4). θ_y was consequently determined from the following logic:

$$\Delta Z > 0,\ \Delta X > 0 \Rightarrow \theta_y := \theta_y$$

$$\Delta Z > 0,\ \Delta X < 0 \Rightarrow \theta_y := \theta_y$$

$$\Delta Z < 0,\ \Delta X < 0 \Rightarrow \theta_y := \theta_y + \pi$$

$$\Delta Z < 0,\ \Delta X > 0 \Rightarrow \theta_y := \theta_y + \pi$$

For θ_x, the critical direction was chosen as "$-Z_g$". Reffering to figure A2.5, θ_x was evaluated using the following:

$$\Delta Y > 0,\ \Delta Z > 0 \Rightarrow \theta_x := \theta_x$$

$$\Delta Y > 0,\ \Delta Z < 0 \Rightarrow \theta_x := \theta_x$$

$$\Delta Y < 0,\ \Delta Z > 0 \Rightarrow \theta_x := \theta_x + \pi$$

$$\Delta Y < 0,\ \Delta Z < 0 \Rightarrow \theta_x := \theta_x + \pi$$

A2.7 Geometry of Joint Surfaces:

The shape and size of the analytical joint surfaces were obtained from the results of the bone-sectioning experiments described in section 5.2.2. The trochlear notch was considered to be semi-circular in section having a 130° "V" form transversely (see figure 6.20). Dimensions were calculated with

Epicondylar Width [EP] = 100

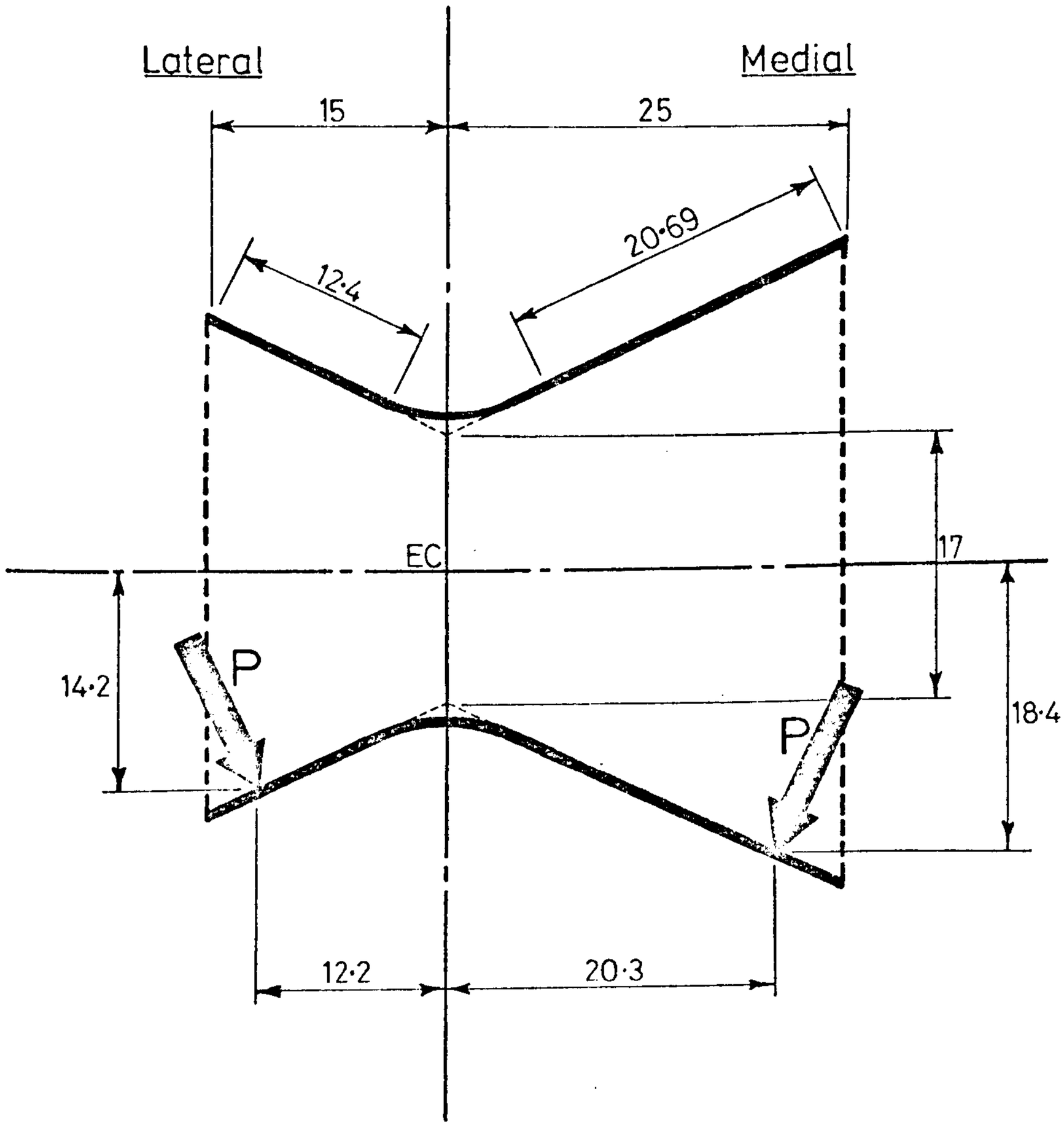

Figure A2·6: Geometric details of the "analytical" joint surfaces.

respect to the epicondylar width "EP" and the apex of the "V" was curved, as shown, for a quarter of the joint width on each side. From standard pressure distributions for conical surfaces, the position of the effective force "P" approximated to 3/4 of the remaining joint width. Referring to figure A2.6, the force quantities became:

For the medial side:

Z component of P = 0.422

Y component of P = 0.906

Moment arm of P = $[(0.906 * 0.203) + (0.423 * 0.184)] * EP$

= $0.26 * EP$

For the lateral side:

Z component of P = 0.422

Y component of P = 0.906

Moment arm of P = $[(0.906 * 0.122) + (0.423 * 0.142)] * EP$

= $0.171 * EP$.

APPENDIX 3

"Important characteristics of hip prostheses" (Semlitsch, 1974).

Hip joint replacement began in the 1940's with the introduction of the Judet brother's femoral head prosthesis made from Plexiglas. Though the Plexiglas was compatible with the body, it suffered heavy abrasion from the continual rubbing movement against the natural hip joint socket and its use was subsequently abandonned. Around 1950 an intramedullary stem was used for the fixation of the "Moore" and the "Thompson" femoral head prostheses and subsequently proved to be the basis of most of the successful hip replacements to date.

In 1956 the McKee-Farrar total hip replacement was introduced and methyl methacrylate cement was utilised for the fixation of the two-component joint. Good fixation was obtained initially but in the early post operative period the prostheses often worked loose. These loosening phenomena were the result of joint seizure from deformation of the thin-walled metal socket and the inclusion of foreign particles between the articulating surfaces. A clearance of some 0.2 mm solved this problem and the McKee-Farrar hip prosthesis is still in current use.

A novel modification to the all metal hip joint was introduced by Mueller in 1965. Three plastic bearing pads were inserted into the acetabular component and acted as a "frictionless" joint surface during initial post operative use. The plastic pads were designed to reduce the stress on the fixation interfaces. After a few months the plastic had worn away and the abrasion resistant metal-on-metal joint remained. With the introduction of low-friction metal-on-plastic hip replacements however, Mueller's design became redundant.

Having encountered several biocompatibility problems with various metal alloys and plastic materials, Charnley (1970) succeeded in developing a low friction arthroplasty using high density polyethylene. Charnley used a 22 mm diameter metal sphere bearing upon a polyethylene acetabular cup. The resulting friction was very low and it was claimed that this factor was responsible for the low incidence of post-operative complications. The "Charnley" hip

prosthesis has undergone many years of development and is now available in many forms to cater for different surgical requirements.

Of the many additional hip prostheses based on Charnley's design, the Mueller metal on plastic prosthesis is of particular interest. To reduce the contact pressure and subsequent wear of the plastic socket, Mueller increased the diameter of the sphere to 32 mm. Despite the slight increase in frictional torque with this arrangement its magnitude was small compared to all-metal joints. Mueller also modified the intramedullary stem to simplify the technique of insertion. A more pronounced flange and a greater radius of curvature ensured correct valgus positioning of the femoral component. "Protasul-10" alloy was later used for the stem and provided high resistance to the dynamic loadings imposed on the implant during activity.

Total hip joint replacement is now accepted as a "successful" procedure for the majority of patients. Enormous effort was required during the development of materials, instrumentation and surgical techniques for such procedures and must surely contribute greatly to the realisation of satisfactory upper limb endoprotheses.

A4 APPENDIX 4

IMPORTANT CHARACTERISTICS OF KNEE PROSTHESES

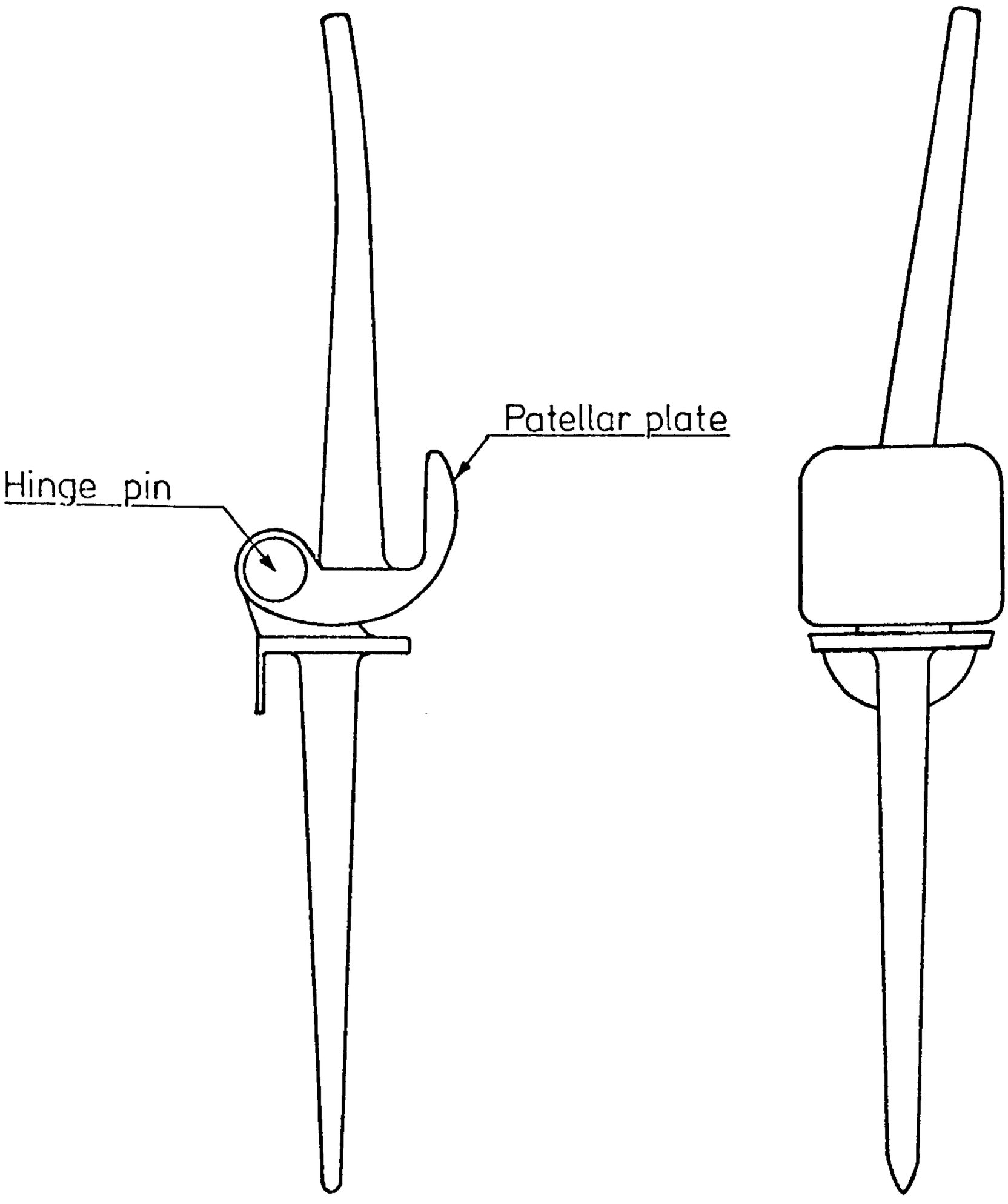

Figure A4·1: The "GUEPAR" total knee prosthesis

APPENDIX 4

A4.1 Introduction:

During recent years, the development programme for total knee prostheses has involved three fundamental designs; namely, the "traditional" hinge, totally unconnected joint surfaces and the so-called "link" prostheses. It should be noted that all three types of total knee replacement are presently in use for the treatment of a variety of knee joint conditions.

A4.2 Restrained Hinges:

The Shiers knee, introduced twenty five years ago, was based on a fully constrained hinge mechanism and used long straight stems of trifin section. The length of the stems presented some initial surgical problems but a more serious complication arose with the frequent occurrence of fracture at the base of the stem. The development of Cr - Co alloys and methyl methacrylate bone cement overcame these problems and the present design has remained unchanged for more than five years (Shiers, 1974).

In the late 1960's the "Guepar" total knee prosthesis was introduced and is shown in figure A4.1. (Witvoet and Aubriot, 1974). Unlike the Shiers knee prosthesis, the long stems are of I-section and oriented to suit the anatomical layout of the femur and tibia. A trochlear plate allows retention of the patella which, in turn, ensures correct muscle function. Both the trochlear plate and the tibial plate provide resistance to rotation of the prosthetic components.

A4.3 Unconnected Prostheses:

Although hinged knee prostheses are necessary when no stability can be provided by ligamentous structures it is now possible to use the collateral and cruciate ligaments, where available, for joint stability. From studies of articular surface geometry, "non-restrained" knee prostheses have been developed for use in patients with serviceable ligaments. Two fundamental varieties are available; "polycentric" and "geometric".

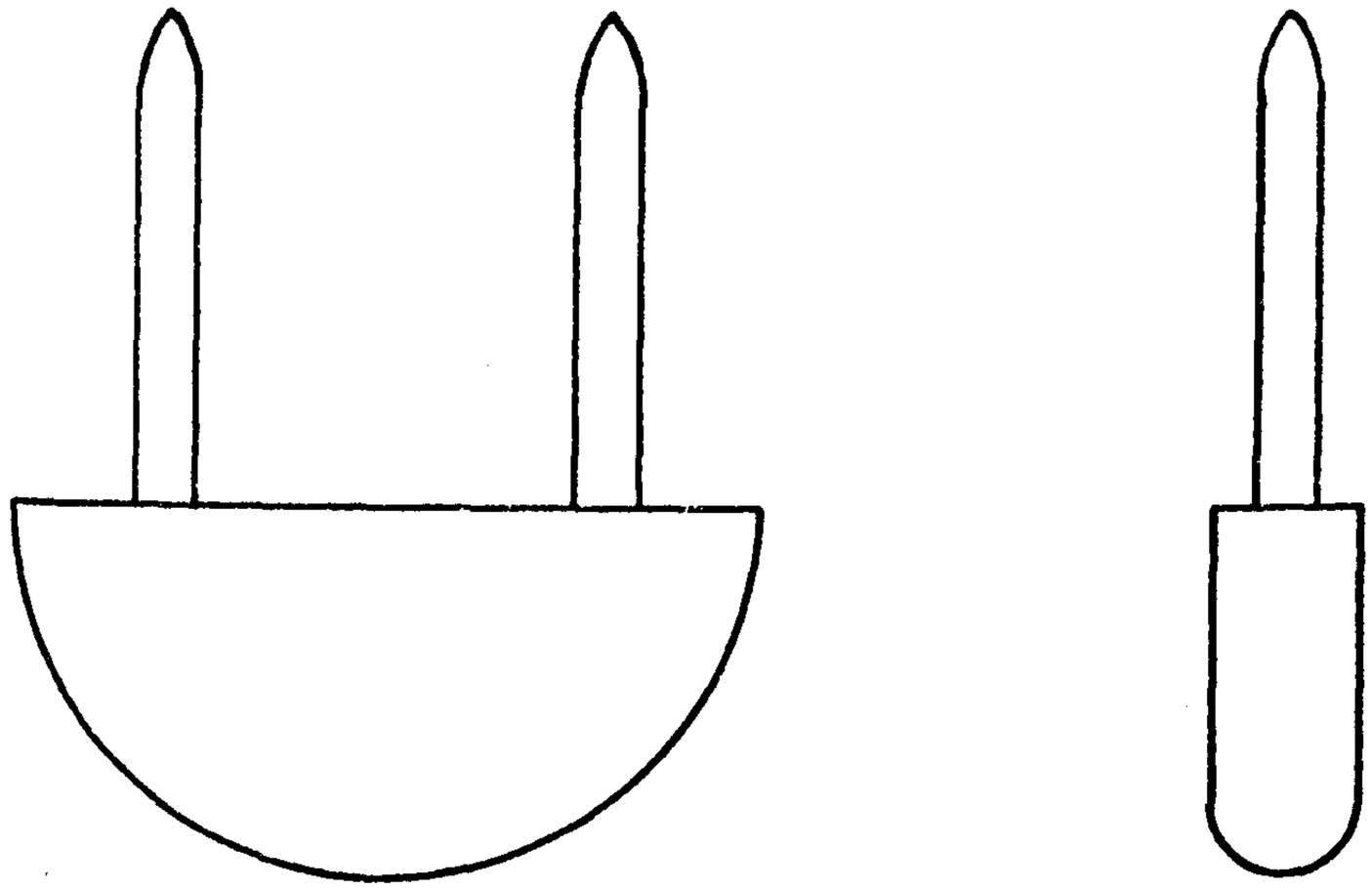

Figure A4·2: Generalized component of "polycentric" prostheses

The polycentric prosthesis involves the replacement of each side of the articulating surfaces using slim discs as shown in figure A4.2. The femoral components are cemented into slots cut in the femoral condyles and their sizes can be chosen to produce normal alignment of the knee joint. High density polyethylene tibial units are cemented into the tibial plateau and can be similarly aligned. Care must be taken to ensure that the slots for both components are cut accurately. Coventry and Bryan (1974) have shown that the gap filling properties of acrylic bone cement are low. Manufacturers provide the necessary jigs and alignment devices to aid insertion but, in cases with gross deformity, the surgeon must use his own judgement in component positioning. The above authors performed 713 polycentric knee replacements and reported only six cases of tibial loosening. Several problems of subluxation were experienced and it was suggested that prolific rheumatoid arthritis was affecting the important ligamentous structures.

The geometric prosthesis, on the other hand, replaces the whole of the articular surface and was designed to retain the functional stability arising from the collateral and cruciate ligaments.

From rigorous studies of knee geometry and loading, Seedhom et al (1974) designed a condylar prosthesis, the surface of which closely resembled the anatomical articulation. It was found that the anatomical knee joint lacked congruity and that the high contact pressures between the femur and the tibia were partly transmitted by the action of the menisci. Moreover, stability in the anterio-posterior (A-P) and medio-lateral (M-L) directions was achieved by the action of the two cruciate and two collateral ligaments respectively.

To cater for the above criteria, the prosthesis was designed to give inherent stability with low surface contact pressures. The plastic tibial component consisted of two platforms with concavity in both the A-P and M-L directions. The metal femoral component was designed in the form of a shell to give a congruent fit in most positions of knee flexion. The gross shape of the prosthesis ensures the normal function of all four ligaments and allows the patella to slide over the femoral component.

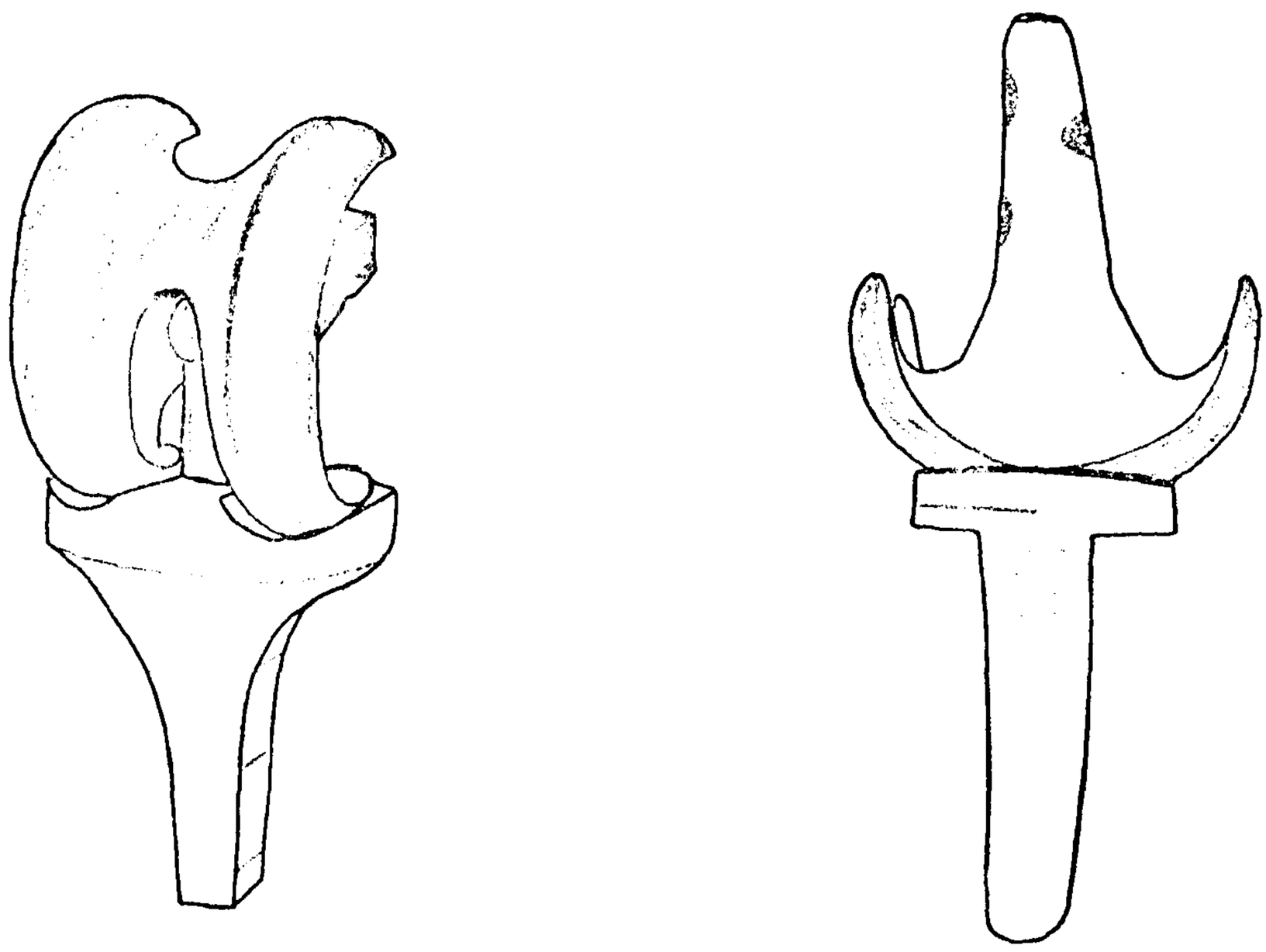

Figure A4·4: Stabilized gliding knee prosthesis [Attenborough, 1974]

Other researchers have developed similar prostheses (Walker, 1973; Freeman et al, 1974) and the now "long-term" results suggest that the use of normal ligamentous structures for joint stability is desirable whenever possible.

A4.4 Link Prostheses:

As a compromise between the totally unrestrained knee prostheses and the "rigid" hinged units, Attenborough (1974) has developed a third generation of knee prosthesis which provides normal joint mobility with a certain degree of inherent stability. In general, the design resembles a conventional geometric knee prosthesis but a central "link" is provided which acts in place of the cruciate ligaments and in place of, or in addition to the collateral ligaments (see figure A4.4). A hollow is provided at the base of the femoral stem into which a ball on a rounded stem is fitted (the link pin). The ball is free to rotate and its stem runs in a gap between the posterior halves of the femoral surfaces. This gap widens towards the end of the joint surfaces and provides lateral mobility of the knee joint in positions of flexion. Rotational movements are possible (after 20° flexion position) due to the curvature of the femoral condyles.

Early results have shown that the combination of joint laxity, joint stability and ligament action overcomes some of the theoretical and practical problems associated with other total knee replacements.

APPENDIX 5

Computer Programs

PROGRAM	RUN	DATA	ANTRHOPOMETRIC	RESULTS
FILTERPROG	FILTXKET20	XKET21, 22+23	XKET20A	XFTKET20
SANDYPROG	RUNXKET20	XFTKE T20	XKET20B	XKETDATA20
FORCEPROG	RUNXKET20	KETSR2	-	FXKET20
XNICOLPROG	RUNXGIL20	XKETDATA20 FXKET20	XKET20C	PLOTXGIL20
PLOTPROG	XGIL20PLOT	PLOTXGIL20	-	"Graphs"

Table A5.1: Computer nomenclature used for one Subject.

APPENDIX 5

Computer Programs

The numerous calculations involved in the theoretical analysis of Chapter 6 were executed using four computer programs. All the programs were written in "ALGOL 60 " and run on an "ICL 1904S" computer housed in the Computing Centre of the University of Strathclyde. Logical nomenclature was applied to all data files and running files as shown in Table A5.1. The terms "KET" and "GIL" refer to the first three letters of the subjects' forename and surname respectively. The numerals 20, 21, 22, 23 and "SR2" refer to the second 'seat-rise' activity. Letter 'x' before the "KET" or "GIL" character signifies a transducer test whereas no letter was required for inertial tests.

The four programs are described as follows:

"FILTERPROG". Used to reduce the film data and to correct the subsequent co-ordinates for parallax errors. Figure A5.1 shows the sequence of events in flow chart form. The 'running' file is detailed in figure A5.2 and the format of the three "D-MAC" (cine film measurements) files is given in figures A5.3, A5.4 and A5.5. The subjects' anthropometric data file is detailed in figure A5.6. The results of this program were used as input to "SANDYPROG" and the complete program is listed on pages 250 - 258.

"SANDYPROG" Used to calculate the co-ordinates of the numerous subcutaneous landmarks and the direction cosines of all the axes. Figure A5.8 (page 259) lists the sequence of events and figure A5.9 details the 'running' file used during data processing. The anthropometric data file is listed in figure A5.10 (page 260) and the complete

program is presented on pages 261-269. The results produced by this program were used as input data to "XNICOLPROG"

"FORCEPROG"

This program used the digital output from the PDP-12 computer to calculate the actual force actions applied to the transducer. Figure A5.12 (page 269a) contains the flow chart for the program and figure A5.13 (page 270a) lists the 'running' file. The required format of the PDP-12 data file is shown in figure A5.14 (page 271) and the complete program is listed in pages 272 - 278. The results produced from "FORCEPROG" were used as input for "XNICOLPROG".

"XNICOLPROG"

This program performed the main analytical procedures and is shown in flow chart form on pages 278a - 281 (figure A5.16). The required running file is shown in figure A5.17 (page 281a) and the anthropometric data set is given in figure A5.18. The complete program is listed in pages 283 - 306. The results produced by this program were presented on "line printer" output and also used as input data for a special plotting program called PLOTPROG. The running file for plotting is shown in figure A5.20 (page 306a) and the program is listed on pages 307 - 313. A graphical output was obtained for the principal force actions.

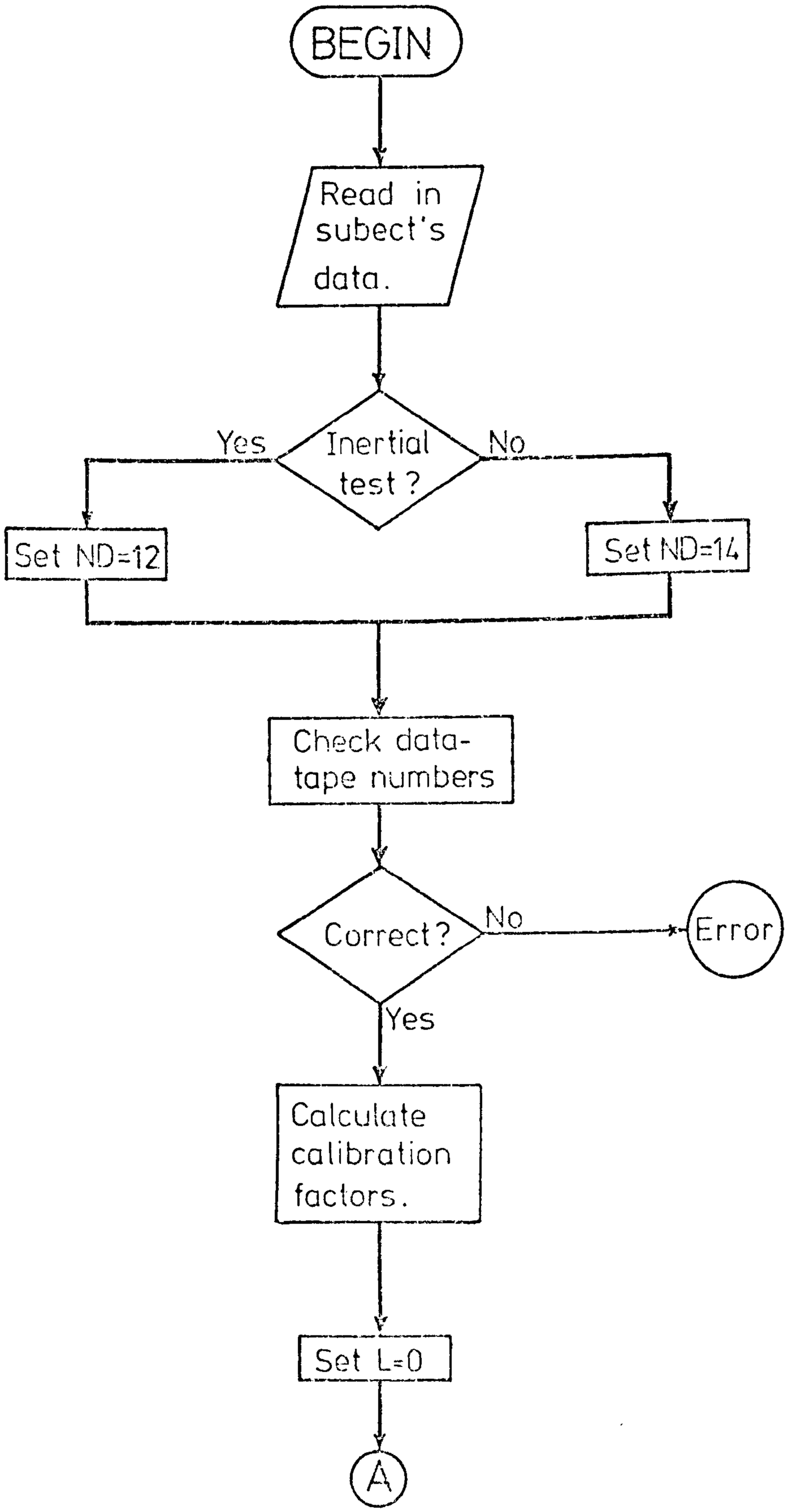
BEGIN
Read in subect's data.
Inertial test ?
Yes
No
Set ND=12
Set ND=14
Check data-tape numbers
Correct?
No
Error
Yes
Calculate calibration factors.
Set L=0
A

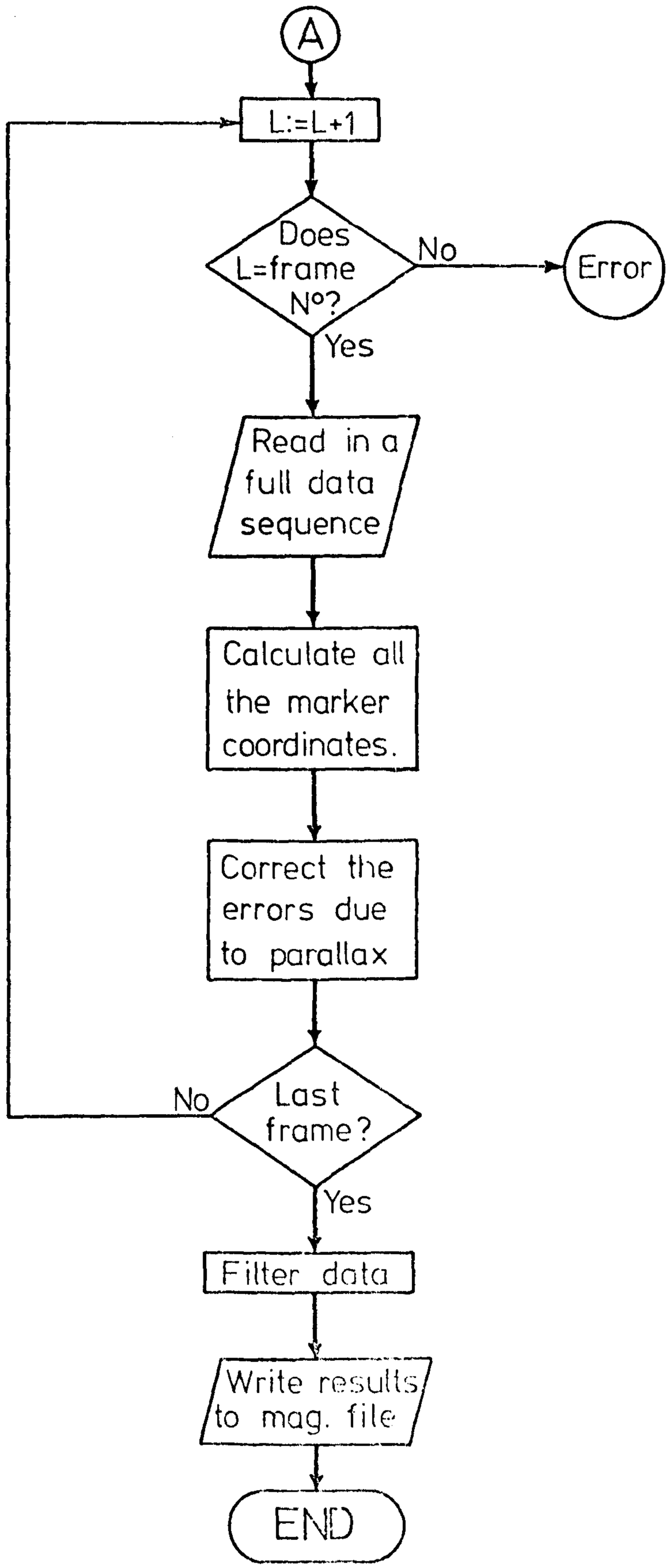

Figure A5·1: Sequence of events for "FILTERPROG"

```
ER RXFILTKG20
SALGOLRUN FILTERPROGB,*TR(0,XKET21),*TR(1,XKET22),*TR(2,XKET23),-
*TR(3,XKET20A),*LP(0,RXFILTKG20),*MT(0,XFTKET20(WRITE,LIMIT10000)),-
PMDPOSTFILE
LF RXFILTKG20,*LP
EJ
****
```

Figure A5.2: Running file: FILTXKET20.

```
1064
5287  2002  3938  3363  2608  2021  3937  0659
1  0
3938  2019  4390  2250  4473  2075  3928  1715  4088  1658  4168
3921  1364
4037  1441  3879  1234  4017  1146  3630  0546  4085  0306  4082
4084  0474
```

N data sets.

```
4172  1722  3907  1178  4059  1168  3626  0550  4086  0312  4081
4081  0479
55  0
3939  2028  4339  2756  4433  2581  4075  1859  4215  1852  4189
4043  1790
4176  1722  3911  1185  4057  1172  3628  0554  4086  0317  4082
4081  0485
9999
9999
```

Figure A5.3: Film measurement file: XKET21.

```
1064
5177   1930   3810   3295   2471   1932   3823   0831

1  0
3823   1929   3475   2154   3447   1977   3212   1572   3143   1507   2938   1560
2821   1118
2939   1235   3581   1122   3507   1020   3682   0375   4020   0248   4258   0414
4018   0418
```

N data sets.

```
55  0
3822   1940   3859   2646   3805   2477   3862   1772   3732   1771   3520   1840
3321   1673
3458   1625   3696   1068   3579   1048   3683   0379   4020   0259   4259   0423
4017   0422
9999
```

Figure A5.4: Film measurement file: XKET22.

```
1064

5287  2002  3938  3363  2608  2021  3937  0659
1  0

3938  2019  4390  2250  4473  2075  3928  1715  4088  1658  4168  12
3921  1364
4037  1441  3879  1234  4017  1146  3630  0546  4085  0306  4082  04
4084  0474

                    N  data sets.

3939  2028  4339  2756  4433  2581  4075  1859  4215  1852  4189  19
4043  1790
4176  1722  3911  1185  4057  1172  3628  0554  4086  0317  4082  04
4081  0485
9999
```

Figure A5.5: Film measurement file: XKET23.

```
?XFTKET20;
1064
55
57.0
1735
94
34
70
68
26
50
451
331

1.00
6135
2565
3846
1092
10.00
0.020
```

Figure A5.6: Anthropometric data file: XKET20A.

```
'PMD'(ED,POSTFILE)
'DUMPON'(ED)
'RUN'
'PROGRAM' (FILTER)
'INPUT' 0=TR0
'INPUT' 1=TR1
'INPUT' 2=TR2
'INPUT' 3=TR3
'OUTPUT' 0=LP0
'TRACE' 2

'BEGIN' 'PROCEDURE' WRITEBINARY(CHANNEL NUMBER,ARRAY,ARRAY
 NAME);
              'VALUE' CHANNEL NUMBER;
'INTEGER' CHANNEL NUMBER;
'ARRAY' ARRAY;
'STRING' ARRAY NAME;
'EXTERNAL';
         'PROCEDURE' CREATE(CHANNEL NUMBER,FILE NAME);
'VALUE' CHANNEL NUMBER;
'INTEGER' CHANNEL NUMBER;
'ARRAY' FILE NAME;
'EXTERNAL';
         'PROCEDURE' INSTRARR(S,A);
'STRING' S;
'ARRAY' A;
'EXTERNAL';
'INTEGER' TN1,TN2,TN3,I,J,K,L,M,N,P;
'INTEGER' FN1,FN2,FN3,MARK;
'ARRAY' CAL[1:4,1:2],XC,YC[1:3],I1,I2,I3[1:14,1:2],A[1:3],
C[1:3];
SELECT INPUT(3);
WARNING: M:=READCH;
'IF' M 'NE' CODE('('?')') 'THEN' 'GOTO' WARNING;
INSTRARR('(';')',A);CREATE(40,A);

'COMMENT' NOW READS IN SUBJECT DATA STARTING WITH SUBJECT
NUMBER
THEN NUMBER OF FRAMES THEN DISTANCE AND HEIGHT OF CAMERAS;
'BEGIN'
'INTEGER' SN,N,ND;
'REAL' MT,HT,DA,EL,KL,EP,BT,W,BET,FB,EB,M2,ZUHLE,BF,GRAV,L
EQ,M1,M,L1,L2,FCUT,T,
RZ,RX,H,ITOT,RX1,RX2;
GRAV:=9.81*1000;
SN:=READ;
N:=READ;
MT:=READ;
HT:=READ;
DA:=READ;
```

FILTERPROG continued

```
EL:=READ;
EP:=READ;
BT:=READ;
W:=READ;
BET:=READ;
FB:=READ;
EB:=READ;
M2:=READ;
RZ:=READ;
RX1:=READ;
RX2:=READ;
H:=READ;
FCUT:=READ;
T:=0.020;
'IF' SN 'GT' 1000 'THEN' ND:=14 'ELSE' ND:=12;
M1:=0.024*MT;
L1:=0.42*FB;
L2:=EB;
M:=M1+M2;
LEQ:=(L1*M1+L2*M2)/M;
KL:=0.25*FB;
ITOT:=M1*(KL↑2+(LEQ-L1)↑2)+(M2*(L2-LEQ)↑2);
ITOT:=ITOT*10↑(-6);
ZUHLE:=3*EP/7;
BF:=FB/465;
PAPERTHROW;
WRITETEXT('('('6S')'G'('10S')'SN'('9S')'N'('10S')'MT'('9S
')'
HT'('9S')'D'('10S')'EL'('9S')'EP'('9S')'BT'('9S')'W'('2C')
'')');
PRINT(GRAV,5,3);
PRINT(SN,4,3);
PRINT(N,4,3);
PRINT(MT,4,3);
PRINT(HT,4,3);
PRINT(DA,4,3);
PRINT(EL,4,3);
PRINT(EP,4,3);
PRINT(BT,4,3);
PRINT(W,4,3);
NEWLINE(4);
WRITETEXT('('('7S')'B'('9S')'FB'('9S')'EB'('9S')'M2'('9S'
)'
RZ'('9S')'RX1'('8S')'RX2'('8S')'H'('2C')'')');
PRINT(BET,5,3);
PRINT(FB,4,3);
PRINT(EB,4,3);
PRINT(M2,4,3);
```

FILTERPROG continued

```
PRINT(RZ,4,3);
PRINT(RX1,4,3);
PRINT(RX2,4,3);
PRINT(H,4,3);
NEWLINE(4);
WRITETEXT('('''('6S')'M1'('9S')'L1'('9S')'L2'('9S')'M'('9S'
)')LEQ
'('8S')'KL'('7S')'ITOT'('7S')'ZUHLE'('8S')'BF'('4C')'')');
PRINT(M1,5,3);
PRINT(L1,4,3);
PRINT(L2,4,3);
PRINT(M,4,3);
PRINT(LEQ,4,3);
PRINT(KL,4,3);
PRINT(ITOT,4,3);
PRINT(ZUHLE,4,3);
PRINT(BF,4,3);
NEWLINE(4);

'COMMENT' READS AND CHECKS TEST NUMBER;
PAPERTHROW;
SELECT INPUT(0);
TN1:=READ;
SELECT INPUT(1);
TN2:=READ;
SELECT INPUT(2);
TN3:=READ;
'IF' TN1 'NE' TN2 'THEN' 'GOTO' ERROR1;
'IF' TN2 'NE' TN3 'THEN' 'GOTO' ERROR2;
PAPERTHROW;
PRINT(TN1,4,0);
NEWLINE(2);

'COMMENT' READS,THEN CALCULATES AND PRINTS CALIBRATION
FACTORS;
K:=0;
REPEAT: SELECT INPUT(K);
'FOR' I:=1 'STEP' 1 'UNTIL' 4 'DO'
'FOR' J:=1 'STEP' 1 'UNTIL' 2 'DO'          CAL[I,J]:=READ;
XC[K+1]:=1000/(CAL[1,1]-CAL[3,1]);
YC[K+1]:=1000/(CAL[2,2]-CAL[4,2]);
K:=K+1;
'IF' K 'LE' 2 'THEN' 'GOTO' REPEAT;
'FOR' I:=1 'STEP' 1 'UNTIL' 3 'DO'
'BEGIN' PRINT(XC[I],4,3);
        PRINT(YC[I],4,3);
       NEWLINE(1);
'END';
```

FILTERPROG continued

```
'COMMENT' READS AND CHECKS FRAME NOS. AND READS IN COORDS
FOR FIRST FRAME;
SELECT INPUT(0);
'BEGIN'
'REAL' PI,T1,T2,TT,A,B,C1,C2,C3,C4,C5,C6,C7,C8,C9,AMEN,LIN
TR;
'INTEGER' NT,N1,JKJ,K4,K5;
'REAL' 'ARRAY' AGRID[1:150,1:14,1:3],GRID[1:14,1:3],WA1[1:
150],WA2[1:150],AD[1:200],WA[1:200];
'ARRAY' RE[1:14,1:3],CRC[1:21,1:3];

'PROCEDURE' BUT4(Q,NT,FCUT,T,W1,AD,W);
'INTEGER' NT;
'REAL' FCUT,T;
'ARRAY' Q,W1,AD,W;
'BEGIN'
AMEN:=0.0;
'FOR' K:=1 'STEP' 1 'UNTIL' NT 'DO'
AMEN:=AMEN+Q[K]/NT;
LINTR:=Q[NT]-Q[1];
PI:=3.14159265;
T1:=SIN(PI*FCUT*T);
T2:=COS(PI*FCUT*T);
TT:=T1/T2;
A:=COS(PI/8.0)*TT;
B:=SIN(PI/8.0)*TT;
C1:=2.0*(A+B);
C2:=2.0*(A+B)↑2;
C3:=((A↑2+B↑2)*(B+A))*2.0;
C4:=(A↑2+B↑2)↑2;
C5:=1+C1+C2+C3+C4;
C6:=-4.0+4.0*C4-2.0*C1+2.0*C3;
C7:=6.0+6.0*C4-2.0*C2;
C8:=-4.0+2.0*C1-2.0*C3+4.0*C4;
C9:=1.0-C1+C2+C4-C3;
N1:=NT+24;
'FOR' K:=NT 'STEP' 1 'UNTIL' 150 'DO'
AD[K]:=0.0;
'FOR' K:=1 'STEP' 1 'UNTIL' NT 'DO'
AD[K+4]:=Q[K]-Q[1]-(K-1)*LINTR/NT;
'FOR' K:=1 'STEP' 1 'UNTIL' 4 'DO'
'BEGIN'
AD[K]:=0.0;
W[K]:=0.0;
'END';
'FOR' K:=1 'STEP' 1 'UNTIL' NT+20 'DO'
W[K+4]:=(C4*(AD[K+4]+4*AD[K+3]+6*AD[K+2]+4*AD[K+1]+AD[K])-
(W[K+3]*C6+W[K+2]*C7+W[K+1]*C8+W[K]*C9))/C5;
```

FILTERPROG continued

```
'FOR' JKJ:=1 'STEP' 1 'UNTIL' NT+20 'DO'
W[JKJ]:=W[JKJ+4];
'FOR' K:=1 'STEP' 1 'UNTIL' 4 'DO'
'BEGIN'
K4:=N1-K;
W1[K4+1]:=0.0;
W[K4+1]:=0.0;
'END';
'FOR' K:=1 'STEP' 1 'UNTIL' NT+20 'DO'
'BEGIN'
K5:=N1-K;
W1[K5-3]:=(C4*(W[K5-3]+4*W[K5-2]+6*W[K5-1]+4*W[K5]+W[K5+1]
)-(W1[K5-2]*C6+W1[K5-1]*C7+W1[K5]*C8+W1[K5+1]*C9))/C5;
'END';
'FOR' K:=1 'STEP' 1 'UNTIL' NT 'DO'
W1[K]:=W1[K]+Q[1]+(K-1)*LINTR/NT;
'END';

FN1:=READ;
MARK:=READ;
L:=0;
'COMMENT' MARK=0 MEANS BICEPS, MARK=1 MEANS TRICEPS;
AGAIN:
L:=L+1;
'IF' L 'NE' FN1 'THEN' 'GOTO' ERROR3;
'FOR' I:=1 'STEP' 1 'UNTIL' ND 'DO'
'FOR' J:=1 'STEP' 1 'UNTIL' 2 'DO' 'BEGIN' I1[I,J]:=READ;
                                           'END';
SELECT INPUT(1);
FN2:=READ;
MARK:=READ;
'FOR' I:=1 'STEP' 1 'UNTIL' ND 'DO'
'FOR' J:=1 'STEP' 1 'UNTIL' 2 'DO' I2[I,J]:=READ;
SELECT INPUT(2);
FN3:=READ;
MARK:=READ;
'FOR' I:=1 'STEP' 1 'UNTIL' ND 'DO'
'FOR' J:=1 'STEP' 1 'UNTIL' 2 'DO' I3[I,J]:=READ;
'IF' FN1 'NE' FN2 'THEN' 'GOTO' WRONG1;
'IF' FN2 'NE' FN3 'THEN' 'GOTO' WRONG2;
NEWLINE(2);
'COMMENT' TRANSFORMS ORIGINAL VALUES USING GRID ORIGIN
AND CALIBRATION FACTORS;
'COMMENT' IF Z-COORD COMES FROM TAPE 3, 5000 IS ADDED TOIT
S VALUE;
RE[1,1]:=FN1;
RE[1,2]:=MARK;
```

FILTERPROG continued

```
'FOR' I:=2 'STEP' 1 'UNTIL' ND 'DO'
'BEGIN'
RE[I,1]:=(I2[I,1]-I2[1,1])*XC[2];
RE[I,2]:=(I2[I,2]-I2[1,2])*YC[2];
'IF' I1[I,2] 'LT' 8000 'THEN' 'GOTO' TONE 'ELSE' 'GOTO'
T3;
TONE:
RE[I,3]:=-(((I1[I,1]-I1[1,1])*XC[1])+(7+0.007*RE[I,2]));
'GOTO' BACK;
T3:
RE[I,3]:=(I3[I,1]-I3[1,1])*XC[3]+5000-(7+0.007*RE[I,2]);
BACK:
'END';
'COMMENT' PRINTS RESULTS ARRAY;
RE[1,3]:=99999;

NEXTPART:

'BEGIN'
'REAL' XS,YS,ZS,XB,YB,ZB,XW,YW,ZW,XM,YM,ZM,F,G,E,TTHX,TTHY
,TTHZ,
DX,DY,DZ,CAL,DXU,DYU,X3,Y3,Z3,X1,Y1,Z1,X2,Y2,Z2,DXH,DYH,DZ
H,
DC3,DC4,LH3,MH3,NH3,LH4,MH4,NH4;
'COMMENT' GRID VALUES ARE NOW READ IN AND AMENDED FROM
EACH FRAME IN
TURN AND STORED IN ARRAY GRID;
AGRID[L,1,1]:=RE[1,1];
AGRID[L,1,2]:=RE[1,2];
AGRID[L,1,3]:=RE[1,3];
'COMMENT' THIS IS CODE FOR BICEPS(0) OR TRICEPS(1);
'FOR' I:=2 'STEP' 1 'UNTIL' ND 'DO'
'BEGIN'
'IF' RE[I,3] 'LT' 2500 'THEN' 'GOTO' LEFTCAM 'ELSE' 'GOTO'
 RICAM;
LEFTCAM:
AGRID[L,I,1]:=(RE[I,1]*(RZ*RX1-RE[I,3]*RX1))/(RZ*RX1-RE[I,
3]*RE[I,1]);
AGRID[L,I,3]:=RE[I,3]*(1-(AGRID[L,I,1]/RX1));
'GOTO' ZEAD;
RICAM:
RE[I,3]:=RE[I,3]-5000;
AGRID[L,I,1]:=(RE[I,1]*(RZ*RX1-RE[I,3]*RX1))/(RZ*RX1-RE[I,
3]*RE[I,1]);
AGRID[L,I,3]:=RE[I,3]*(1+AGRID[L,I,1]/RX2);
ZEAD:
AGRID[L,I,2]:=RE[I,2]*(RZ-AGRID[L,I,3])/RZ;
'END';
```

FILTERPROG continued

```
'IF' SN 'GT' 1000 'THEN' 'GOTO' SKIP;
'FOR' J:= 1 'STEP' 1 'UNTIL' 3 'DO'
'BEGIN'
AGRID[L,13,J]:=1111;
AGRID[L,14,J]:=1111;
RE[9,J]:=AGRID[L,12,J];
RE[10,J]:=AGRID[L,9,J];
RE[12,J]:=AGRID[L,10,J];
AGRID[L,9,J]:=RE[9,J];
AGRID[L,10,J]:=RE[10,J];
AGRID[L,12,J]:=RE[12,J];
'END';
SKIP:
SELECT INPUT(0);
FN1:=READ;
MARK:=READ;
'IF' FN1 'NE' 9999 'THEN' 'GOTO' AGAIN;

'COMMENT'                    CHECK PRINTOUT OF DATA;

'FOR' L:=1 'STEP' 1 'UNTIL' N 'DO'
'BEGIN'
PRINT(L,3,0);

'FOR' I:=2 'STEP' 1 'UNTIL' 14 'DO'
PRINT(AGRID[L,I,1],3,1);
NEWLINE(1);
'END';
NEWLINE(10);

'FOR' L:=1 'STEP' 1 'UNTIL' N 'DO'
'BEGIN'
PRINT(L,3,0);
'FOR' I:=2 'STEP' 1 'UNTIL' 14 'DO'
PRINT(AGRID[L,I,2],3,1);
NEWLINE(1);
'END';
NEWLINE(10);

'FOR' L:=1 'STEP' 1 'UNTIL' N 'DO'
'BEGIN'
PRINT(L,3,0);
'FOR' I:=2 'STEP' 1 'UNTIL' 14 'DO'
PRINT(AGRID[L,I,3],3,1);
NEWLINE(1);
'END';
NEWLINE(10);
```

FILTERPROG continued

```
'COMMENT'          FILTERING TAKES PLACE HERE!!!!!!!!!!!!;
'COMMENT'           CYRIL'S BUTTERWORTH;
'FOR' J:=1 'STEP' 1 'UNTIL' 3 'DO'
'BEGIN'
'FOR' I:=2 'STEP' 1 'UNTIL' 14 'DO'
'BEGIN'
'FOR' L:=1 'STEP' 1 'UNTIL' N 'DO'
WA1[L]:=AGRID[L,I,J];
BUT4(WA1,N,FCUT,T,WA2,AD,WA);
'FOR' L:=1 'STEP' 1 'UNTIL' N 'DO'
AGRID[L,I,J]:=WA2[L];
'END';
'END';

NEWLINE(30);

'FOR' L:=1 'STEP' 1 'UNTIL' N 'DO'
'BEGIN'
PRINT(L,3,0);
'FOR' I:=2 'STEP' 1 'UNTIL' 14 'DO'
PRINT(AGRID[L,I,1],3,1);
NEWLINE(1);
'END';
NEWLINE(10);

'FOR' L:=1 'STEP' 1 'UNTIL' N 'DO'
'BEGIN'
PRINT(L,3,0);
'FOR' I:=2 'STEP' 1 'UNTIL' 14 'DO'
PRINT(AGRID[L,I,2],3,1);
NEWLINE(1);
'END';
NEWLINE(10);

'FOR' L:=1 'STEP' 1 'UNTIL' N 'DO'
'BEGIN'
PRINT(L,3,0);
'FOR' I:=2 'STEP' 1 'UNTIL' 14 'DO'
PRINT(AGRID[L,I,3],3,1);
NEWLINE(1);
'END';
NEWLINE(10);

'COMMENT'          TRANSFER OF RESULTS MATRIX ONTO MAG
TAPE.........;
L:=0;
```

FILTERPROG continued

```
WRITE:
L:=L+1;
'FOR' I:=1 'STEP' 1 'UNTIL' 14 'DO'
'BEGIN'
'FOR' J:=1 'STEP' 1 'UNTIL' 3 'DO'
GRID[I,J]:=AGRID[L,I,J];
'END';
WRITEBINARY(40,GRID,'('UNIT')');
'IF' L 'LT' N 'THEN' 'GOTO' WRITE;
'GOTO' STOP;
'END';


WRONG1: WRITETEXT('(''('1C')'FRAME%NOS.%ON%TAPES%1%AND%
2%DO%NOT%MATCH')');
PRINT(FN1,4,6);
PRINT(FN2,4,6);
'GOTO' STOP;
ERROR3:
WRITETEXT('(''('1C')'FRAME%NO%AND%MATRIX%NO%DO%NOT%MATCH')
');
PRINT(FN1,4,6);
PRINT(L,4,6);
'GOTO' STOP;
WRONG2: WRITETEXT('(''('1C')'FRAME%NOS.%ON%TAPES%2%AND%3
%DO%NOT%MATCH')');
PRINT(FN2,4,6);
PRINT(FN3,4,6);
'GOTO' STOP;
'END';
ERROR1: WRITETEXT('(''('1C')'SUBJECT%NUMBERS%ON%TAPES%1%AN
D%2
%DO%NOT%MATCH'('1C')'')');
'GOTO' STOP;
ERROR2: WRITETEXT('(''('1C')'SUBJECT%NO.%ON%TAPES%2%AND%3
%DO%NOT%MATCH')');
'GOTO' STOP;
'END';
STOP: 'END';
```

FILTERPROG concluded.

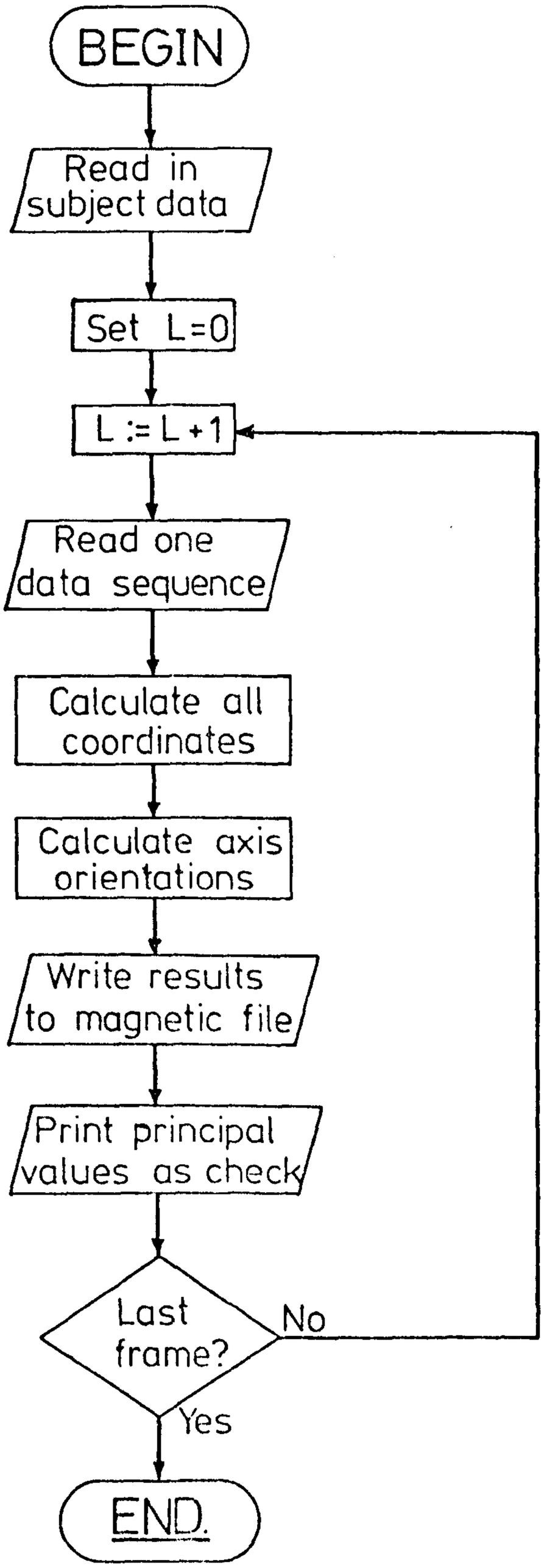

Figure A5·8: Sequence of events for "SANDYPROG".

```
ER RXKEITH20
SALGOLRUN SANDYPROGB,*TR(0,XKET21),*TR(1,XKET22),*TR(2,XKET23),-
*TR(3,XKET20B),*LP(0,RXKEITH20),*MT(0,XFTKET20),-
*MT(1,XKETDATA20(WRITE,LIMIT10000)),PMDPOSTFILE
LF RXKEITH20,*LP
EJ
****
```

Figure A5.9: Running file: RUNXKET20.

```
?XFTKET20;

XKETDATA20;
1064
55
57.0
1735
94
34
70
68
26
50
451
331

1.00
6135
2565
3846
1092
10.000
0.020
```

Figure A5.10: Anthropometric data file: XKET20B

```
'PMD'(ED,POSTFILE)
'DUMPON'(ED)
'RUN'
'PROGRAM' (XXXXSANDY)
'INPUT' 3=TR3
'OUTPUT' 0=LP0
'TRACE' 2

'BEGIN' 'PROCEDURE' WRITEBINARY(CHANNEL NUMBER,ARRAY,ARRAY
 NAME);
              'VALUE' CHANNEL NUMBER;
'INTEGER' CHANNEL NUMBER;
'ARRAY' ARRAY;
'STRING' ARRAY NAME;
'EXTERNAL';

        'PROCEDURE' CREATE(CHANNEL NUMBER,FILE NAME);
'VALUE' CHANNEL NUMBER;
'INTEGER' CHANNEL NUMBER;
'ARRAY' FILE NAME;
'EXTERNAL';

'PROCEDURE' READBINARY(CHANNEL NUMBER,ARRAY,ARRAY NAME);
'VALUE' CHANNEL NUMBER;
'INTEGER' CHANNEL NUMBER;
'ARRAY' ARRAY;
'STRING' ARRAY NAME;
'EXTERNAL';

'PROCEDURE' INPUT(CHANNEL NUMBER,FILE NAME);
'VALUE' CHANNEL NUMBER;
'INTEGER' CHANNEL NUMBER;
'ARRAY' FILE NAME;
'EXTERNAL';

        'PROCEDURE' INSTRARR(S,A);
'STRING' S;
'ARRAY' A;
'EXTERNAL';

'INTEGER' TN1,TN2,TN3,I,J,K,M,P;
'INTEGER' FN1,FN2,FN3,MARK;
'ARRAY' CAL[1:4,1:2],XC,YC[1:3],I1,I2,I3[1:12,1:2],A[1:3],
APDIST[1:5],REDIST[1:5],C[1:3];
SELECT INPUT(3);
WARNING: M:=READCH;
'IF' M 'NE' CODE('('?')') 'THEN' 'GOTO' WARNING;
INSTRARR('(';')',A);INPUT(40,A);
LOOKING:
P:=READCH;
```

SANDYPROG continued

```
'IF' P 'NE' CODE('('EL')') 'THEN' 'GOTO' LOOKING;
INSTRARR('(':')',C);CREATE(41,C);


'COMMENT' NOW READS IN SUBJECT DATA STARTING WITH SUBJECT
NUMBER
THEN NUMBER OF FRAMES THEN DISTANCE AND HEIGHT OF CAMERAS;
'BEGIN'
'INTEGER' SN,N;
'REAL' MT,HT,DA,EL,KL,EP,BT,W,BET,FB,EB,M2,ZUHLE,BF,GRAV,L
EQ,M1,M,L1,L2,
RZ,RX,H,ITOT,RX1,RX2;
GRAV:=9.81*1000;
SN:=READ;
N:=READ;
MT:=READ;
HT:=READ;
DA:=READ;
EL:=READ;
EP:=READ;
BT:=READ;
W:=READ;
BET:=READ;
FB:=READ;
EB:=READ;
M2:=READ;
RZ:=READ;
RX1:=READ;
RX2:=READ;
H:=READ;
M1:=0.024*MT;
L1:=0.42*FB;
L2:=EB;
M:=M1+M2;
LEQ:=(L1*M1+L2*M2)/M;
KL:=0.25*FB;
ITOT:=M1*(KL↑2+(LEQ-L1)↑2)+(M2*(L2-LEQ)↑2);
ITOT:=ITOT*10↑(-6);
ZUHLE:=3*EP/2;
BF:=FB/465;
'BEGIN'
'ARRAY' WRX,WRY,WRZ,ECX,ECY,ECZ,BX,BY,BZ,LAL,UAL[1:150],
TTX,TTY,TTZ,SSX,SSY,SSZ,SIXX,SIXY,SIXZ,PYX,PYY,PYZ[1:150];
NEXTPART:
'BEGIN'
'REAL' XS,YS,ZS,XB,YB,ZB,XW,YW,ZW,XM,YM,ZM,F,G,E,TTHX,TTHY
,TTHZ,
DX,DY,DZ,CAL,DXU,DYU,X3,Y3,Z3,X1,Y1,Z1,X2,Y2,Z2,DXH,DYH,DZ
```

SANDYPROG continued

```
H,

DC3,DC4,LH3,MH3,NH3,LH4,MH4,NH4,DXP,DYP,DZP;
'REAL' 'ARRAY' CRC[1:21,1:3],GRID[1:14,1:3];

'PROCEDURE' CALCULATION;
'BEGIN'
X2:=(CRC[3,1]*X1)+(CRC[3,2]*Y1)+(CRC[3,3]*Z1);
Y2:=(CRC[4,1]*X1)+(CRC[4,2]*Y1)+(CRC[4,3]*Z1);
Z2:=(CRC[5,1]*X1)+(CRC[5,2]*Y1)+(CRC[5,3]*Z1);
F:=(CRC[8,1]*X2)+(CRC[9,1]*Y2)+(CRC[10,1]*Z2);
G:=(CRC[8,2]*X2)+(CRC[9,2]*Y2)+(CRC[10,2]*Z2);
E:=(CRC[8,3]*X2)+(CRC[9,3]*Y2)+(CRC[10,3]*Z2);
'END';

'PROCEDURE' AMEND(DC3,DC4);
'REAL' DC3,DC4;
'BEGIN'
'IF' DC4 'GE' 0 'AND' DC3 'GE' 0 'THEN' DC3:=DC4;
'IF' DC4 'GE' 0 'AND' DC3 'LT' 0 'THEN' DC3:=DC4*(-1);
'IF' DC4 'LT' 0 'AND' DC3 'LT' 0 'THEN' DC3:=DC4;
'IF' DC4 'LT' 0 'AND' DC3 'GE' 0 'THEN' DC3:=DC4*(-1);
'END';

'COMMENT'                    NOW READ IN MAG TAPE FILE;
'COMMENT' CALCULATES VBLES AND STORES THEM IN ARRAYS FOR
LATER
CALCULATIONS;
K:=0;
AGAIN:
K:=K+1;

READBINARY(40,GRID,'('UNIT')');

'IF' K 'GT' N 'THEN' 'GOTO' FINAL;
CRC[1,1]:=GRID[1,1];
CRC[1,2]:=GRID[1,2];
CRC[1,3]:=GRID[1,3];
CAL:=(180+DA)/150;
CRC[2,1]:=GRID[2,1]+(GRID[3,1]-GRID[2,1])*CAL;
CRC[2,2]:=GRID[2,2]+(GRID[3,2]-GRID[2,2])*CAL;
CRC[2,3]:=GRID[2,3]+(GRID[3,3]-GRID[2,3])*CAL;
CAL:=(200+BT)/150;
XB:=GRID[4,1]+(GRID[5,1]-GRID[4,1])*CAL;
YB:=GRID[4,2]+(GRID[5,2]-GRID[4,2])*CAL;
ZB:=GRID[4,3]+(GRID[5,3]-GRID[4,3])*CAL;
DXH:=SQRT((GRID[6,1]-XB)↑2+(GRID[6,2]-YB)↑2+(GRID[6,3]-ZB)
↑2);
```

SANDYPROG continued

```
DYH:=SQRT((XB-CRC[2,1])↑2+(YB-CRC[2,2])↑2+(ZB-CRC[2,3])↑2)
;
DZH:=SQRT((XB-GRID[4,1])↑2+(YB-GRID[4,2])↑2+(ZB-GRID[4,3])
↑2);
LH3:=(XB-GRID[6,1])/DXH;
MH3:=(YB-GRID[6,2])/DXH;
NH3:=(ZB-GRID[6,3])/DXH;
CRC[3,2]:=(CRC[2,1]-XB)/DYH;
CRC[4,2]:=(CRC[2,2]-YB)/DYH;
CRC[5,2]:=(CRC[2,3]-ZB)/DYH;
CRC[3,3]:=(GRID[4,1]-XB)/DZH;
CRC[4,3]:=(GRID[4,2]-YB)/DZH;
CRC[5,3]:=(GRID[4,3]-ZB)/DZH;
CRC[3,1]:=CRC[4,2]*CRC[5,3]-CRC[4,3]*CRC[5,2];
CRC[4,1]:=-CRC[3,2]*CRC[5,3]+CRC[3,3]*CRC[5,2];
CRC[5,1]:=CRC[3,2]*CRC[4,3]-CRC[3,3]*CRC[4,2];

CAL:=(100+EL)/75;
CRC[6,1]:=GRID[7,1]+(GRID[8,1]-GRID[7,1])*CAL;
CRC[6,2]:=GRID[7,2]+(GRID[8,2]-GRID[7,2])*CAL;
CRC[6,3]:=GRID[7,3]+(GRID[8,3]-GRID[7,3])*CAL;
CAL:=(180+W)/150;
CRC[7,1]:=GRID[9,1]+(GRID[10,1]-GRID[9,1])*CAL;
CRC[7,2]:=GRID[9,2]+(GRID[10,2]-GRID[9,2])*CAL;
CRC[7,3]:=GRID[9,3]+(GRID[10,3]-GRID[9,3])*CAL;
'IF' SN 'GT' 1000 'THEN' 'GOTO' WSKIP;
CRC[7,1]:=GRID[12,1]+(GRID[9,1]-GRID[12,1])*CAL;
CRC[7,2]:=GRID[12,2]+(GRID[9,2]-GRID[12,2])*CAL;
CRC[7,3]:=GRID[12,3]+(GRID[9,3]-GRID[12,3])*CAL;
WSKIP:

DXU:=SQRT((GRID[7,1]-CRC[6,1])↑2+(GRID[7,2]-CRC[6,2])↑2
+(GRID[7,3]-CRC[6,3])↑2);
DYU:=SQRT((CRC[7,1]-CRC[6,1])↑2+(CRC[7,2]-CRC[6,2])↑2+(CRC
[7,3]-CRC[6,3])↑2);
CRC[8,1]:=(CRC[6,1]-GRID[7,1])/DXU;
CRC[9,1]:=(CRC[6,2]-GRID[7,2])/DXU;
CRC[10,1]:=(CRC[6,3]-GRID[7,3])/DXU;
CRC[8,2]:=(CRC[6,1]-CRC[7,1])/DYU;
CRC[9,2]:=(CRC[6,2]-CRC[7,2])/DYU;
CRC[10,2]:=(CRC[6,3]-CRC[7,3])/DYU;
LH3:=CRC[3,3];
MH3:=CRC[4,3];
NH3:=CRC[5,3];
CRC[8,3]:=CRC[9,1]*CRC[10,2]-CRC[10,1]*CRC[9,2];
CRC[9,3]:=CRC[10,1]*CRC[8,2]-CRC[8,1]*CRC[10,2];
CRC[10,3]:=CRC[8,1]*CRC[9,2]-CRC[9,1]*CRC[8,2];
'IF' SN 'GT' 1000 'THEN' 'GOTO' SKIP;
```

SANDYPROG continued

```
CAL:=(110+BET)/60;
XM:=GRID[11,1]+(GRID[12,1]-GRID[11,1])*CAL;
YM:=GRID[11,2]+(GRID[12,2]-GRID[11,2])*CAL;
ZM:=GRID[11,3]+(GRID[12,3]-GRID[11,3])*CAL;
CAL:=LEQ/EB;
CRC[11,1]:=CRC[6,1]+(XM-CRC[6,1])*CAL;
CRC[11,2]:=CRC[6,2]+(YM-CRC[6,2])*CAL;
CRC[11,3]:=CRC[6,3]+(ZM-CRC[6,3])*CAL;
'GOTO' SKIP1;
SKIP:
'FOR' J:=1 'STEP' 1 'UNTIL' 3 'DO'
CRC[11,J]:=1111;
SKIP1:
DX:=CRC[7,1]-CRC[6,1];
DY:=CRC[7,2]-CRC[6,2];
DZ:=CRC[7,3]-CRC[6,3];
TTHX:=DZ/DY;
TTHY:=DX/DZ;
TTHZ:=DY/DX;
'COMMENT' TO OBTAIN QUADRANT OF THETA;
'IF' DY 'GE' 0 'AND' DX 'GE' 0 'THEN' CRC[12,3]:=ARCTAN(TT
HZ);
'IF' DY 'GE' 0 'AND' DX 'LT' 0 'THEN' CRC[12,3]:=ARCTAN(TT
HZ)+3.142;
'IF' DY 'LT' 0 'AND' DX 'LT' 0 'THEN' CRC[12,3]:=ARCTAN(TT
HZ)-3.142;
'IF' DY 'LT' 0 'AND' DX 'GE' 0 'THEN' CRC[12,3]:=ARCTAN(TT
HZ);
'IF' DX 'GE' 0 'AND' DZ 'GE' 0 'THEN' CRC[12,2]:=ARCTAN(TT
HY);
'IF' DX 'GE' 0 'AND' DZ 'LT' 0 'THEN' CRC[12,2]:=ARCTAN(TT
HY)+3.142;
'IF' DX 'LT' 0 'AND' DZ 'LT' 0 'THEN' CRC[12,2]:=ARCTAN(TT
HY)+3.142;
'IF' DX 'LT' 0 'AND' DZ 'GE' 0 'THEN' CRC[12,2]:=ARCTAN(TT
HY);
'IF' DZ 'GE' 0 'AND' DY 'GE' 0 'THEN' CRC[12,1]:=ARCTAN(TT
HX);
'IF' DZ 'GE' 0 'AND' DY 'LT' 0 'THEN' CRC[12,1]:=ARCTAN(TT
HX)+3.142;
'IF' DZ 'LT' 0 'AND' DY 'GE' 0 'THEN' CRC[12,1]:=ARCTAN(TT
HX);
'IF' DZ 'LT' 0 'AND' DY 'LT' 0 'THEN' CRC[12,1]:=ARCTAN(TT
HX)+3.142;
DX:=DX↑2;
DY:=DY↑2;
DZ:=DZ↑2;
CAL:=DX+DY+DZ;
```

SANDYPROG continued

```
CRC[13,1]:=(DY+DZ)/CAL;
CRC[13,2]:=(DX+DZ)/CAL;
CRC[13,3]:=(DX+DY)/CAL;
'COMMENT' LIMB DIMENSIONS FOLLOW;
X1:=EL*0.6263;
Y1:=EB*1.105;
Z1:=EP*0.1252;
CALCULATION;
CRC[14,1]:=F/1000;
CRC[14,2]:=G/1000;
CRC[14,3]:=E/1000;
X1:=-EL*0.7621;
Y1:=EB*0.8095;
Z1:=-EP*0.1384;
CALCULATION;
CRC[15,1]:=F/1000;
CRC[15,2]:=G/1000;
CRC[15,3]:=E/1000;
X1:=EL*0.1091;
Y1:=EB*0.0579;
Z1:=EP*0.3212;
CALCULATION;
CRC[16,1]:=F/1000;
CRC[16,2]:=G/1000;
CRC[16,3]:=E/1000;
X1:=EL*0.4941;
Y1:=EB*0.5890;
Z1:=EP*0.0148;
CALCULATION;
CRC[21,1]:=F/1000;
CRC[21,2]:=G/1000;
CRC[21,3]:=E/1000;
'IF' SN 'LT' 1000 'THEN' 'GOTO' CARRYON;
CRC[17,1]:=GRID[13,1]+(GRID[14,1]-GRID[13,1])*205/90;
CRC[17,2]:=GRID[13,2]+(GRID[14,2]-GRID[13,2])*205/90;
CRC[17,3]:=GRID[13,3]+(GRID[14,3]-GRID[13,3])*205/90;
DXP:=SQRT((GRID[13,1]-GRID[14,1])↑2+(GRID[13,2]-GRID[14,2]
)↑2+(GRID[13,3]-GRID[14,3])↑2);
CRC[18,1]:=(GRID[14,1]-GRID[13,1])/DXP;
CRC[19,1]:=(GRID[14,2]-GRID[13,2])/DXP;
CRC[20,1]:=(GRID[14,3]-GRID[13,3])/DXP;
DYP:=SQRT((GRID[14,1]-GRID[12,1])↑2+(GRID[14,2]-GRID[12,2]
)↑2+(GRID[14,3]-GRID[12,3])↑2);
CRC[18,2]:=(GRID[12,1]-GRID[14,1])/DYP;
CRC[19,2]:=(GRID[12,2]-GRID[14,2])/DYP;
CRC[20,2]:=(GRID[12,3]-GRID[14,3])/DYP;
DZP:=SQRT((GRID[11,1]-CRC[17,1])↑2+(GRID[11,2]-CRC[17,2])↑
2+(GRID[11,3]-CRC[17,3])↑2);
```

SANDYPROG continued

```
CRC[18,3]:=(GRID[11,1]-CRC[17,1])/DZP;
CRC[19,3]:=(GRID[11,2]-CRC[17,2])/DZP;
CRC[20,3]:=(GRID[11,3]-CRC[17,3])/DZP;
CARRYON:
WRX[K]:=CRC[7,1];
WRY[K]:=CRC[7,2];
WRZ[K]:=CRC[7,3];
ECX[K]:=CRC[6,1];
ECY[K]:=CRC[6,2];
ECZ[K]:=CRC[6,3];
BX[K]:=XB;
BY[K]:=YB;
BZ[K]:=ZB;
SSX[K]:=CRC[2,1];
SSY[K]:=CRC[2,2];
SSZ[K]:=CRC[2,3];
SIXX[K]:=GRID[6,1];
SIXY[K]:=GRID[6,2];
SIXZ[K]:=GRID[6,3];
UAL[K]:=SQRT((SSX[K]-ECX[K])↑2+(SSY[K]-ECY[K])↑2+(SSZ[K]-E
CZ[K])↑2);
LAL[K]:=SQRT((WRX[K]-ECX[K])↑2+(WRY[K]-ECY[K])↑2+(WRZ[K]-E
CZ[K])↑2);
'IF' SN 'LT' 1000 'THEN' 'GOTO' SKIP2;
PYX[K]:=CRC[17,1];
PYY[K]:=CRC[17,2];
PYZ[K]:=CRC[17,3];
SKIP2:

TTX[K]:=CRC[12,1];
TTY[K]:=CRC[12,2];
TTZ[K]:=CRC[12,3];

WRITEBINARY(41,CRC,'('UNIT')');

'GOTO' AGAIN;


FINAL:
'FOR' I:=1 'STEP' 1 'UNTIL' 21 'DO'
'FOR' J:=1 'STEP' 1 'UNTIL' 3 'DO' CRC[I,J]:=999999;
WRITEBINARY(41,CRC,'('UNIT')');


'FOR' K:=1 'STEP' 1 'UNTIL' N-1 'DO'
'BEGIN'
PRINT(K,3,0);
PRINT(WRX[K],4,3);
```

SANDYPROG continued

```
PRINT(WRY[K],4,3);
PRINT(WRZ[K],4,3);
PRINT(ECX[K],4,3);
PRINT(ECY[K],4,3);
PRINT(ECZ[K],4,3);
PRINT(BX[K],4,3);
PRINT(BY[K],4,3);
PRINT(BZ[K],4,3);
NEWLINE(1);
'END';
NEWLINE(6);
'FOR' K:=1 'STEP' 1 'UNTIL' N-1 'DO'
'BEGIN'

PRINT(K,3,0);
PRINT(SSX[K],3,3);
PRINT(SSY[K],3,3);
PRINT(SSZ[K],3,3);
PRINT(SIXX[K],3,3);
PRINT(SIXY[K],3,3);
PRINT(SIXZ[K],3,3);
'IF' SN 'LT' 1000 'THEN' 'GOTO' SKIP3;
PRINT(PYX[K],3,3);
PRINT(PYY[K],3,3);
PRINT(PYZ[K],3,3);
SKIP3:
NEWLINE(1);
'END';

NEWLINE(6);
'FOR' K:=1 'STEP' 1 'UNTIL' N 'DO'
'BEGIN'
PRINT(K,8,0);
PRINT(TTX[K],2,4);
PRINT(TTY[K],2,4);
PRINT(TTZ[K],2,4);
PRINT(LAL[K],20,4);
PRINT(UAL[K],8,4);
NEWLINE(1);
'END';

'GOTO' STOP;
'END';

WRONG1: WRITETEXT('('''('1C')'FRAME%NOS.%ON%TAPES%1%AND%
```

SANDYPROG continued

```
2%DO%NOT%MATCH')');
PRINT(FN1,4,6);
PRINT(FN2,4,6);
'GOTO' STOP;
WRONG2: WRITETEXT('(''('1C')'FRAME%NOS.%ON%TAPES%2%AND%3
%DO%NOT%MATCH')');
PRINT(FN2,4,6);
PRINT(FN3,4,6);
'GOTO' STOP;
'END';
ERROR1: WRITETEXT('(''('1C')'SUBJECT%NUMBERS%ON%TAPES%1%AN
D%2
%DO%NOT%MATCH'('1C')'')');
'GOTO' STOP;
ERROR2: WRITETEXT('(''('1C')'SUBJECT%NO.%ON%TAPES%2%AND%3
%DO%NOT%MATCH')');
'GOTO' STOP;
'END';
STOP: 'END';
```

SANDYPROG concluded.

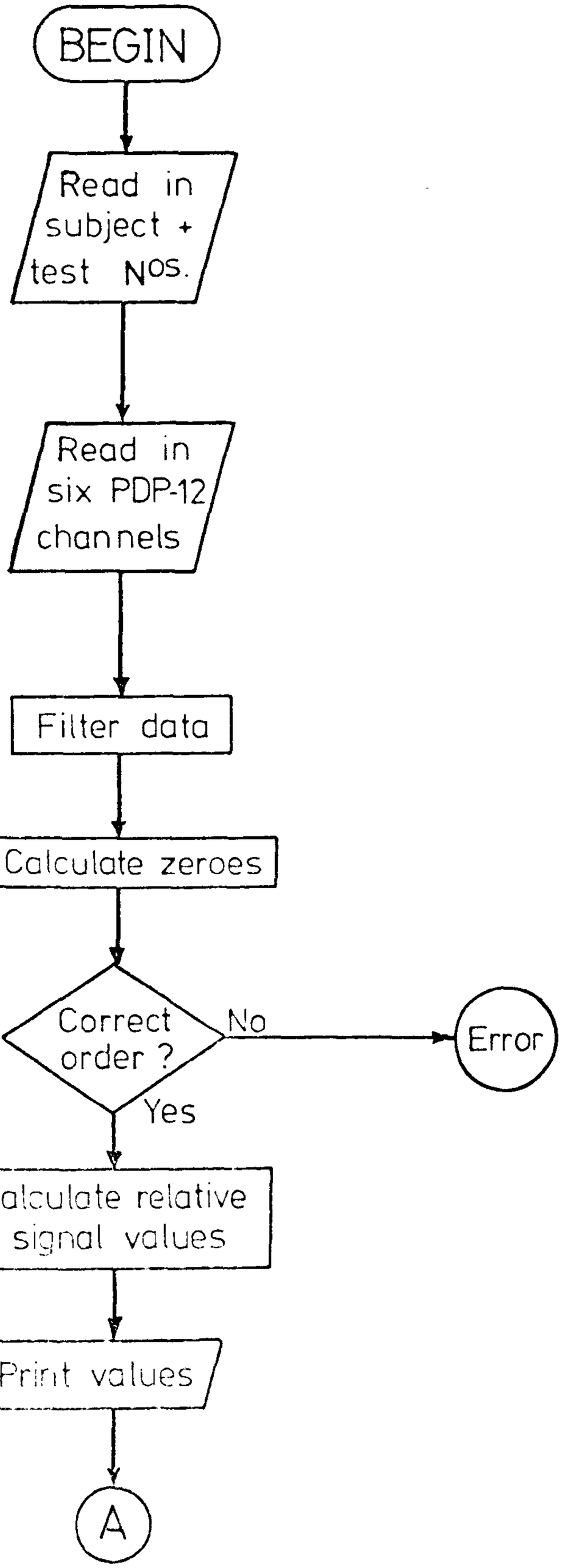
BEGIN
Read in subject + test NOS.
Read in six PDP-12 channels
Filter data
Calculate zeroes
Correct order ?
No
Error
Yes
Calculate relative signal values
Print values
A

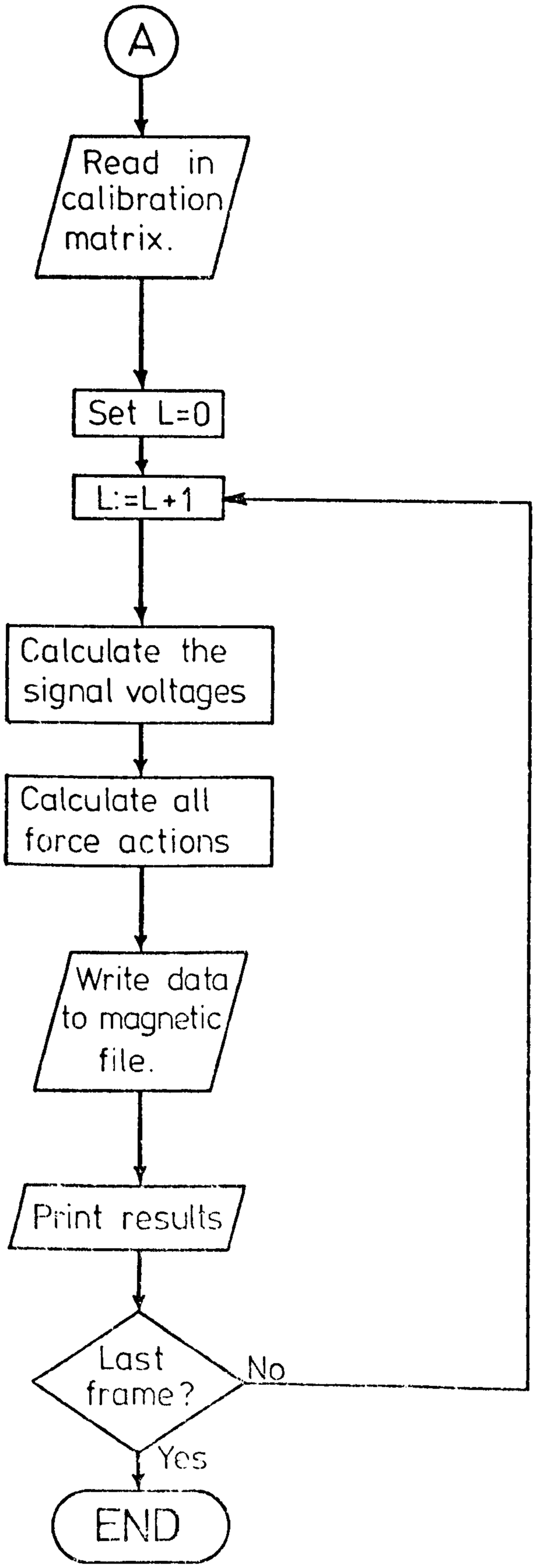

Figure A5·12: Sequence of events for "FORCEPROG"

```
ER RFORCKG20
SALGOLRUN FORCEPROGB,*TR(0,KETSR2),*LP(0,RFORCKG20),-
*MT(0,FXKET20(WRITE,LIMIT10000)),PMDPOSTFILE
LF RFORCKG20,*LP
EJ
****
```

Figure A5.13: Running file: RUNFXKET20.

```
?FXKET20;

1064
55
20
5.00

   0      251

 -25     -82     -82     -82

 -86     -78     -77     -78

        N  data sets.

  -70     -67     -66     -61

-68  -69  -68

888888

9.15    0    0    -3.526    2.37    1.077
0.05    -0.928    0    0.928    -0.66    -1.14

0    0    9.06    0.684    -9.56    3.67
0    0    0    -55.4    0    0
0      0      0      0      137      0
0      0      0      0      0      23.3
```

Figure A5.14: "PDP-12" output data file: KETSR2.

```
'PMD'(ED,POSTFILE)
'DUMPON'(ED)
'RUN'
'LIBRARY'(ED,SUBGROUPNGFA)
'LIBRARY'(ED,SUBGROUPNGPA)
'PROGRAM' (FORCES)
'INPUT' 0=TR0
'OUTPUT' 0=LP0
'TRACE' 2

'BEGIN'

'PROCEDURE' WRITEBINARY(CHANNEL NUMBER,ARRAY,ARRAY NAME);
'VALUE' CHANNEL NUMBER;
'INTEGER' CHANNEL NUMBER;
'ARRAY' ARRAY;
'STRING' ARRAY NAME;
'EXTERNAL';

'PROCEDURE' CREATE(CHANNEL NUMBER,FILE NAME);
'VALUE' CHANNEL NUMBER;
'INTEGER' CHANNEL NUMBER;
'ARRAY' FILE NAME;
'EXTERNAL';

'PROCEDURE' INSTRARR(S,A);
'STRING' S;
'ARRAY' A;
'EXTERNAL';


'REAL' PI,T1,T2,TT,T,FCUT,Q,B,C1,C2,C3,C4,C5,C6,C7,C8,C9,A
MEN,LINTR;
'INTEGER' M,NTOT,K,K4,K5,JKJ,N,N1;
'ARRAY' A[1:3];
COMMENCE:
M:=READCH;
'IF' M 'NE' CODE('('?')') 'THEN' 'GOTO' COMMENCE;
INSTRARR('(':')',A);CREATE(40,A);

'BEGIN'

'REAL' A,ZERO1,ZERO2,ZERO3,ZERO4,ZERO5,ZERO6;
'INTEGER' I,J,K,Z10,SN,DELAY,START1,START2,START3,START4,S
TART5,START6,LENGTH1,LENGTH2,LENGTH3,LENGTH4,LENGTH5,LENGT
H6,CHECK,POINT,ORDER,FAIL,IFAIL,E,F,G,OPT,P;
```

FORCEPROG continued

```
'REAL' 'ARRAY' CH1F,CH2F,CH3F,CH4F,CH5F,CH6F[1:512],
CH1,CH2,CH3,CH4,CH5,CH6[1:512],
CAL[1:6,1:6],SIG,PFORCE[1:6,1:1],FORCE[1:6],AD[1:550],W[1:
550];


'PROCEDURE' BUT4(Q,N,FCUT,T,W1,AD,W);

'INTEGER' N;
'REAL' FCUT,T;
'ARRAY' Q,W1,AD,W;
'BEGIN'
AMEN:=0.0;
'FOR' K:=1 'STEP' 1 'UNTIL' N 'DO'
AMEN:=AMEN+Q[K]/N;
LINTR:=Q[N]-Q[1];
PI:=3.14159265;
T1:=SIN(PI*FCUT*T);
T2:=COS(PI*FCUT*T);
TT:=T1/T2;
A:=COS(PI/8.0)*TT;
B:=SIN(PI/8.0)*TT;
C1:=2*(A+B);
C2:=2*(A+B)↑2;
C3:=((A↑2+B↑2)*(B+A))*2;
C4:=(A↑2+B↑2)↑2;
C5:=1+C1+C2+C3+C4;
C6:=-4.0+4.0*C4-2.0*C1+2.0*C3;
C7:=6.0+6.0*C4-2.0*C2;
C8:=-4+2*C1-2*C3+4*C4;
C9:=1.0-C1+C2+C4-C3;
N1:=N+24;
'FOR' K:=N 'STEP' 1 'UNTIL' N+30 'DO'
AD[K]:=0.0;
'FOR' K:=1 'STEP' 1 'UNTIL' N 'DO'
AD[K+4]:=Q[K]-Q[1]-(K-1)*LINTR/N;
'FOR' K:=1 'STEP' 1 'UNTIL' 4 'DO'
'BEGIN'
AD[K]:=0.0;
W[K]:=0.0;
'END';
'FOR' K:=1 'STEP' 1 'UNTIL' N+20 'DO'
W[K+4]:=(C4*(AD[K+4]+4*AD[K+3]+6*AD[K+2]+4*AD[K+1]+AD[K])-
(W[K+3]*C6+W[K+2]*C7+W[K+1]*C8+W[K]*C9))/C5;
'FOR' JKJ:=1 'STEP' 1 'UNTIL' N+20 'DO'
W[JKJ]:=W[JKJ+4];
'FOR' K:=1 'STEP' 1 'UNTIL' 4 'DO'
'BEGIN'
```

FORCEPROG continued

```
K4:=N1-K;
W1[K4+1]:=0.0;
W[K4+1]:=0.0;
'END';
'FOR' K:=1 'STEP' 1 'UNTIL' N+20 'DO'
'BEGIN'
K5:=N1-K;
W1[K5-3]:=(C4*(W[K5-3]+4*W[K5-2]+6*W[K5-1]+4*W[K5]+W[K5+1]
)-(W1[K5-2]*C6+W1[K5-1]*C7+W1[K5]*C8+W1[K5+1]*C9))/C5;
'END';
'FOR' K:=1 'STEP' 1 'UNTIL' N 'DO'
W1[K]:=W1[K]+Q[1]+(K-1)*LINTR/N;
'END';



'PROCEDURE' F01AAA(A,N,IFAIL);
'VALUE' N;
'INTEGER' N,IFAIL;
'ARRAY'A;
'ALGOL';

'PROCEDURE' F01CKA(A,B,C,N,P,M,OPT,IFAIL);
'VALUE' N,P,M,OPT;
'INTEGER' N,P,M,OPT,IFAIL;
'ARRAY' A,B,C;
'ALGOL';


SN:=READ;
N:=READ;
DELAY:=READ;

FCUT:=READ;
T:=0.020;
START1:=READ;
LENGTH1:=READ;
'FOR' K:=1 'STEP' 1 'UNTIL' LENGTH1 'DO'
CH1F[K]:=READ;

START2:=READ;
LENGTH2:=READ;
'FOR' K:=1 'STEP' 1 'UNTIL' LENGTH2 'DO'
CH2F[K]:=READ;

START3:=READ;
LENGTH3:=READ;
'FOR' K:=1 'STEP' 1 'UNTIL' LENGTH3 'DO'
```

FORCEPROG continued

```
CH3F[K]:=READ;

START4:=READ;
LENGTH4:=READ;
'FOR' K:=1 'STEP' 1 'UNTIL' LENGTH4 'DO'
CH4F[K]:=READ;

START5:=READ;
LENGTH5:=READ;
'FOR' K:=1 'STEP' 1 'UNTIL' LENGTH5 'DO'
CH5F[K]:=READ;

START6:=READ;
LENGTH6:=READ;
'FOR' K:=1 'STEP' 1 'UNTIL' LENGTH6 'DO'
CH6F[K]:=READ;
'FOR' K:=1 'STEP' 1 'UNTIL' LENGTH1 'DO'
'BEGIN'
PRINT(K,8,0);
PRINT(CH1F[K],4,2);
PRINT(CH2F[K],4,2);
PRINT(CH3F[K],4,2);
PRINT(CH4F[K],4,2);
PRINT(CH5F[K],4,2);
PRINT(CH6F[K],4,2);
NEWLINE(1);
'END';
NEWLINE(10);

BUT4(CH1F,LENGTH1,FCUT,T,CH1,AD,W);
BUT4(CH2F,LENGTH2,FCUT,T,CH2,AD,W);
BUT4(CH3F,LENGTH3,FCUT,T,CH3,AD,W);
BUT4(CH4F,LENGTH4,FCUT,T,CH4,AD,W);
BUT4(CH5F,LENGTH5,FCUT,T,CH5,AD,W);
BUT4(CH6F,LENGTH6,FCUT,T,CH6,AD,W);

'IF' LENGTH1 'NE' LENGTH2 'OR' LENGTH2 'NE' LENGTH3 'OR'
LENGTH3 'NE' LENGTH4 'THEN' 'GOTO' ERROR1;
'IF' LENGTH4 'NE' LENGTH5 'OR' LENGTH5 'NE' LENGTH6 'THEN'
 'GOTO' ERROR1;
'FOR' K:=1 'STEP' 1 'UNTIL' LENGTH1 'DO'
'BEGIN'
PRINT(K,8,0);
PRINT(CH1[K],4,2);
PRINT(CH2[K],4,2);
PRINT(CH3[K],4,2);
PRINT(CH4[K],4,2);
PRINT(CH5[K],4,2);
```

```
PRINT(CH6[K],4,2);
NEWLINE(1);
'END';
NEWLINE(10);

ZERO1:=0.0;
ZERO2:=0.0;
ZERO3:=0.0;
ZERO4:=0.0;
ZERO5:=0.0;
ZERO6:=0.0;

Z10:=LENGTH1-9;

'FOR' K:=Z10 'STEP' 1 'UNTIL' LENGTH1 'DO'
'BEGIN'
ZERO1:=ZERO1+CH1[K]/10;
ZERO2:=ZERO2+CH2[K]/10.0;
ZERO3:=ZERO3+CH3[K]/10.0;
ZERO4:=ZERO4+CH4[K]/10.0;
ZERO5:=ZERO5+CH5[K]/10.0;
ZERO6:=ZERO6+CH6[K]/10.0;
'END';

POINT:=START1+START2+START3-START4-START5-START6;

'IF' POINT 'NE' 0 'THEN' 'GOTO' ERROR2;

J:=DELAY-START1-1;

'FOR' K:=1 'STEP' 1 'UNTIL' N 'DO'
'BEGIN'
CH1[K]:=CH1[J+K]-ZERO1;
CH2[K]:=CH2[J+K]-ZERO2;
CH3[K]:=CH3[J+K]-ZERO3;
CH4[K]:=CH4[J+K]-ZERO4;
CH5[K]:=CH5[J+K]-ZERO5;
CH6[K]:=CH6[J+K]-ZERO6;
'END';
PRINT(ZERO1,4,2);
PRINT(ZERO2,4,2);
PRINT(ZERO3,4,2);
PRINT(ZERO4,4,2);
PRINT(ZERO5,4,2);
PRINT(ZERO6,4,2);
NEWLINE(3);
PRINT(J,9,0);
NEWLINE(3);
```

```
'FOR' K:=1 'STEP' 1 'UNTIL' N 'DO'
'BEGIN'
PRINT(K,8,0);
PRINT(CH1[K],4,2);
PRINT(CH2[K],4,2);
PRINT(CH3[K],4,2);
PRINT(CH4[K],4,2);
PRINT(CH5[K],4,2);
PRINT(CH6[K],4,2);
NEWLINE(1);
'END';
NEWLINE(10);

CHECK:=READ;
'IF' CHECK 'NE' 888888 'THEN' 'GOTO' ERROR3;

'COMMENT'      THE VALUE OF CHECK IS A CHECK ON THE END
OF THE PDP-12TAPE DATA.................;
'COMMENT'                          NOW READS IN THE CALIBRATION
MATRIX FOR CONVERSION OF PYLON SIGNALS;

'FOR' I:=1 'STEP' 1 'UNTIL' 6 'DO'
'FOR' J:=1 'STEP' 1 'UNTIL' 6 'DO'
CAL[I,J]:=READ;
ORDER:=6;
FAIL:=0;

F01AAA(CAL,ORDER,FAIL);

'COMMENT' CALIBRATION MATRIX NOW INVERTED;
WRITETEXT('('('1C')'INVERSE%OF%CALIBRATION%MATRIX'('1C')'
')');
'FOR' I:=1 'STEP' 1 'UNTIL' 6 'DO'
'BEGIN'
NEWLINE(1);
'FOR' J:=1 'STEP' 1 'UNTIL' 6 'DO'
PRINT(CAL[I,J],4,4);
'END';

E:=6;
F:=1;
G:=6;
OPT:=1;
IFAIL:=0;
K:=0;
WRITETEXT('('('2C')'FRAME'('4S')'APSHR'('4S')'AXIAL'('4S'
)'MLSHR'('4S')'MLBEND'('4S')'TORQUE'('4S')'APBEND'('2C')''
)');
```

FORCEPROG continued

```
AGAIN:

K:=K+1;
SIG[1,1]:=CH6[K]*1.953;
SIG[2,1]:=CH3[K]*1.953;
SIG[3,1]:=CH2[K]*1.953;
SIG[4,1]:=CH5[K]*1.953;
SIG[5,1]:=CH1[K]*1.953;
SIG[6,1]:=CH4[K]*1.953;
FD1CKA(PFORCE,CAL,SIG,E,F,G,OPT,IFAIL);

PRINT(K,5,0);
'FOR' J:=1 'STEP' 1 'UNTIL' 6 'DO'
'BEGIN'
FORCE[J]:=PFORCE[J,1];
PRINT(FORCE[J],5,2);
'END';
NEWLINE(1);

WRITEBINARY(40,FORCE,'('UNIT')');

'IF' K 'LT' N 'THEN' 'GOTO' AGAIN;

'FOR' J:=1 'STEP' 1 'UNTIL' 6 'DO'
FORCE[J]:=9999;
WRITEBINARY(40,FORCE,'('UNIT')');
'GOTO' STOP;

ERROR1:
WRITETEXT('('('1C')'LENGTH1%IS%NOT%COMMON%TO%ALL%CHANNELS
'('1C')'')');
'GOTO' STOP;

ERROR2:
WRITETEXT('('('1C')'STARTING%CURSORS%ON%PDP-12%SCREEN%MUS
T%HAVE%SHIFTED%A%BIT'('1C')'')');
'GOTO' STOP;

ERROR3:
WRITETEXT('('('2C')'START%OF%CALIBRATION%MATRIX%MISPLACED
%IN%DATA%BLOCK'('1C')'')');
'GOTO' STOP;

STOP:
'END';
'END';
```

FORCEPROG concluded.

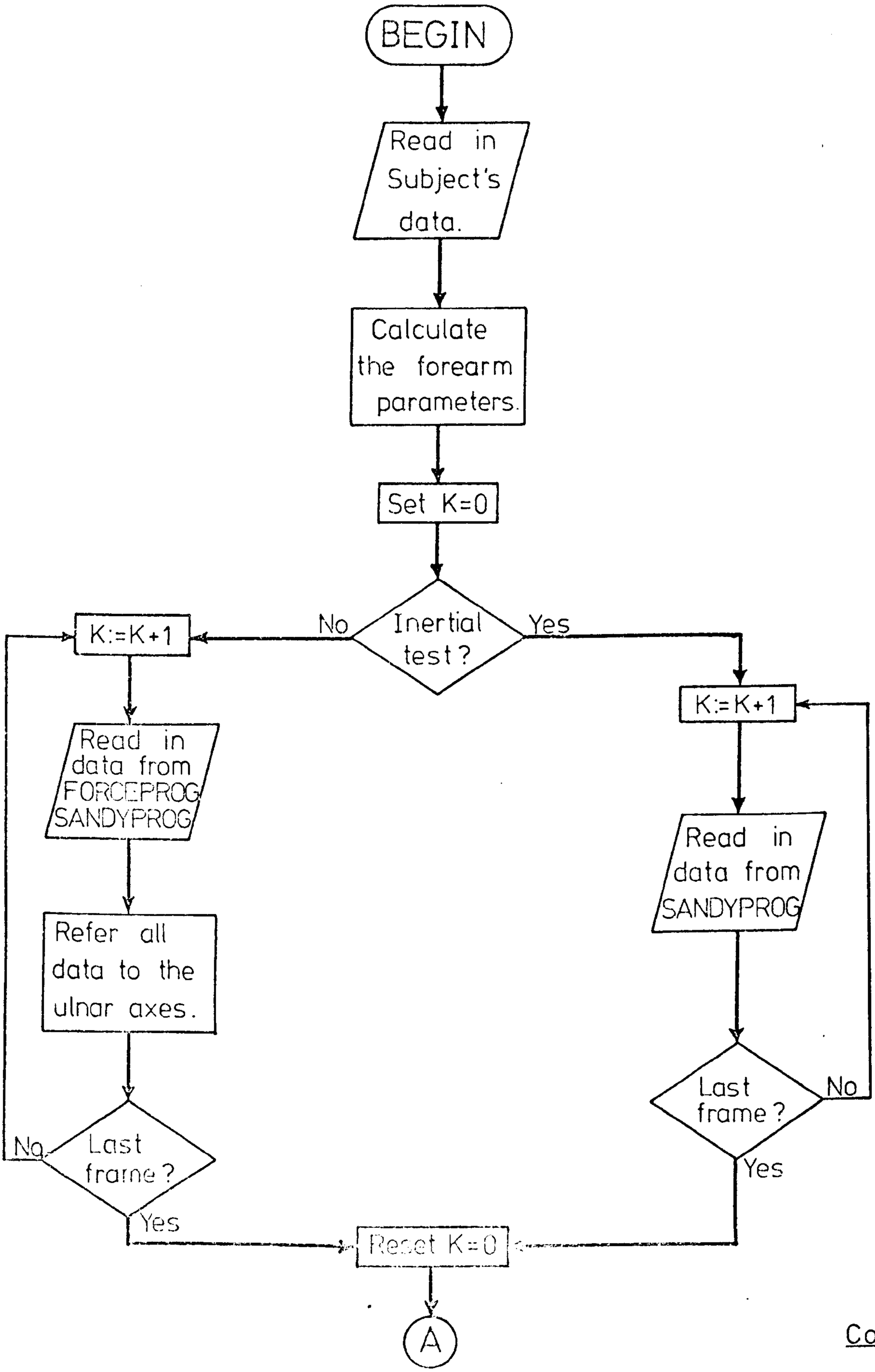
BEGIN
Read in Subject's data.
Calculate the forearm parameters.
Set K=0
Inertial test?
No
Yes
K:=K+1
Read in data from FORCEPROG SANDYPROG
Refer all data to the ulnar axes.
Last frame?
No
Yes
K:=K+1
Read in data from SANDYPROG
Last frame?
No
Yes
Reset K=0
A

Continued

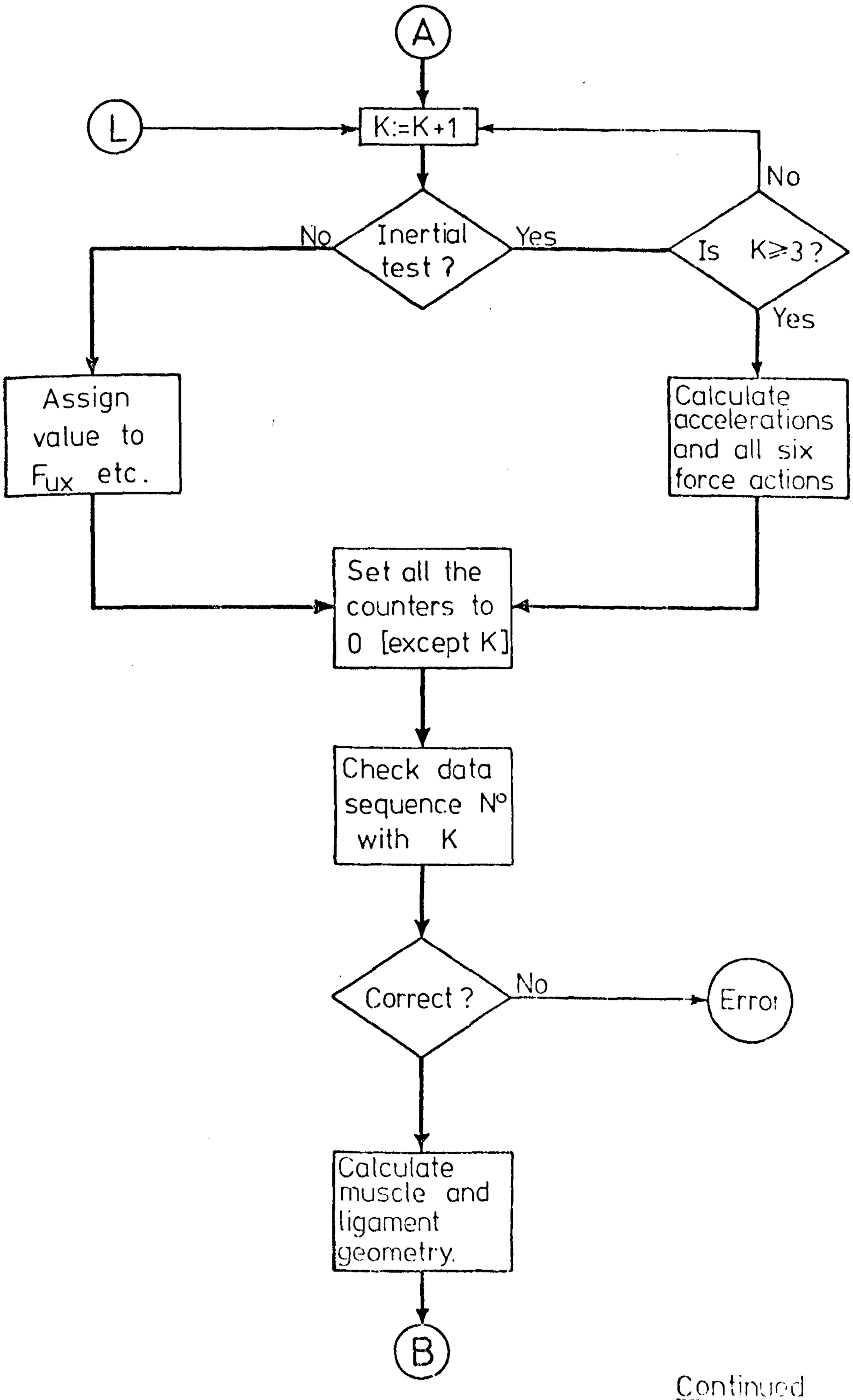
A
L
K:=K+1
No
Inertial test ?
No
Yes
Is K≥3 ?
Yes
Assign value to Fux etc.
Calculate accelerations and all six force actions
Set all the counters to 0 [except K]
Check data sequence N° with K
Correct ?
No
Error
Calculate muscle and ligament geometry.
B

Continued

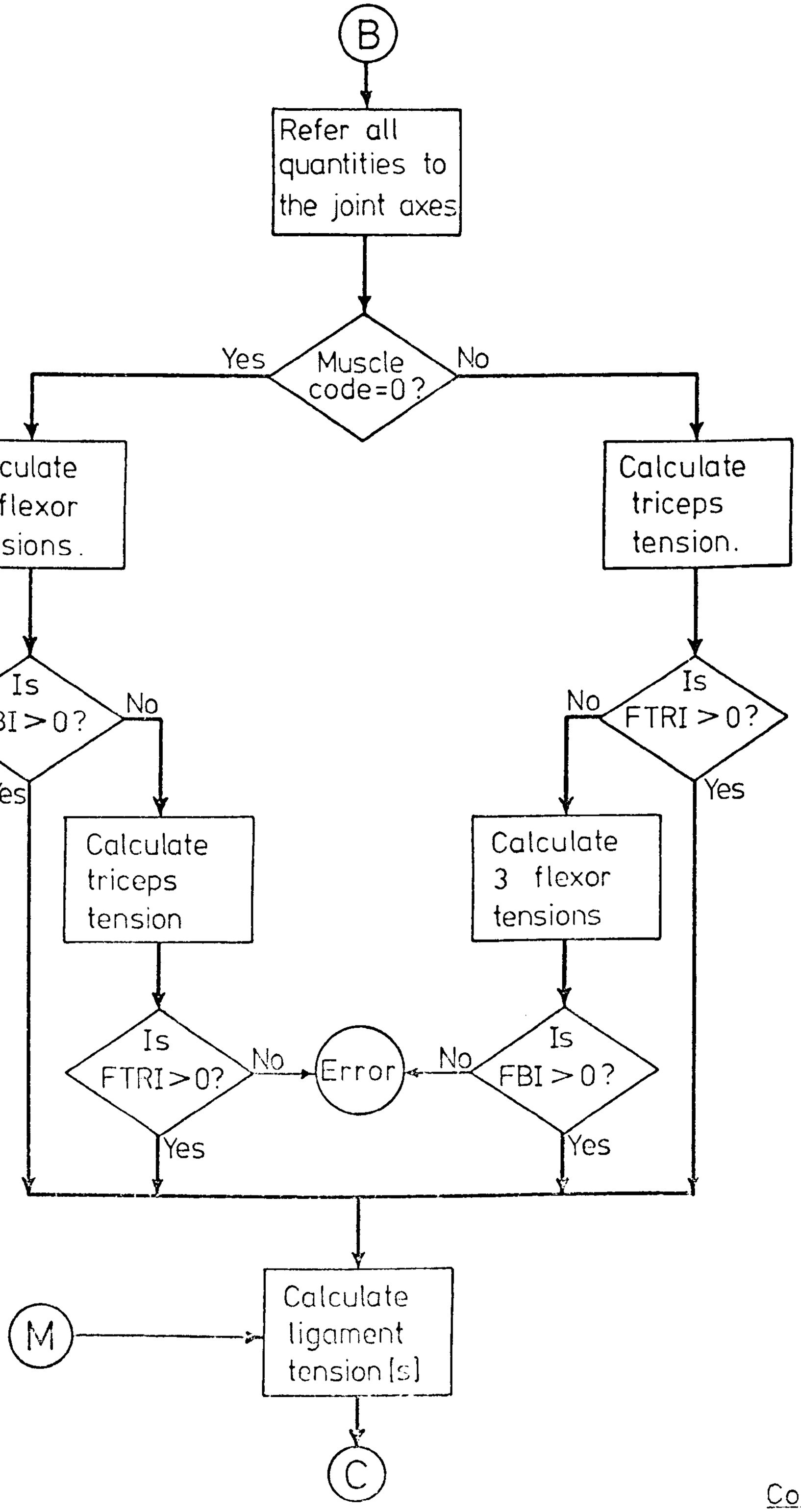
B
Refer all quantities to the joint axes
Muscle code=0?
Yes
No
Calculate 3 flexor tensions.
Calculate triceps tension.
Is FBI>0?
No
Yes
Is FTRI>0?
No
Yes
Calculate triceps tension
Calculate 3 flexor tensions
Is FTRI>0?
No
Error
No
Is FBI>0?
Yes
Yes
M
Calculate ligament tension [s]
C

Cont'd

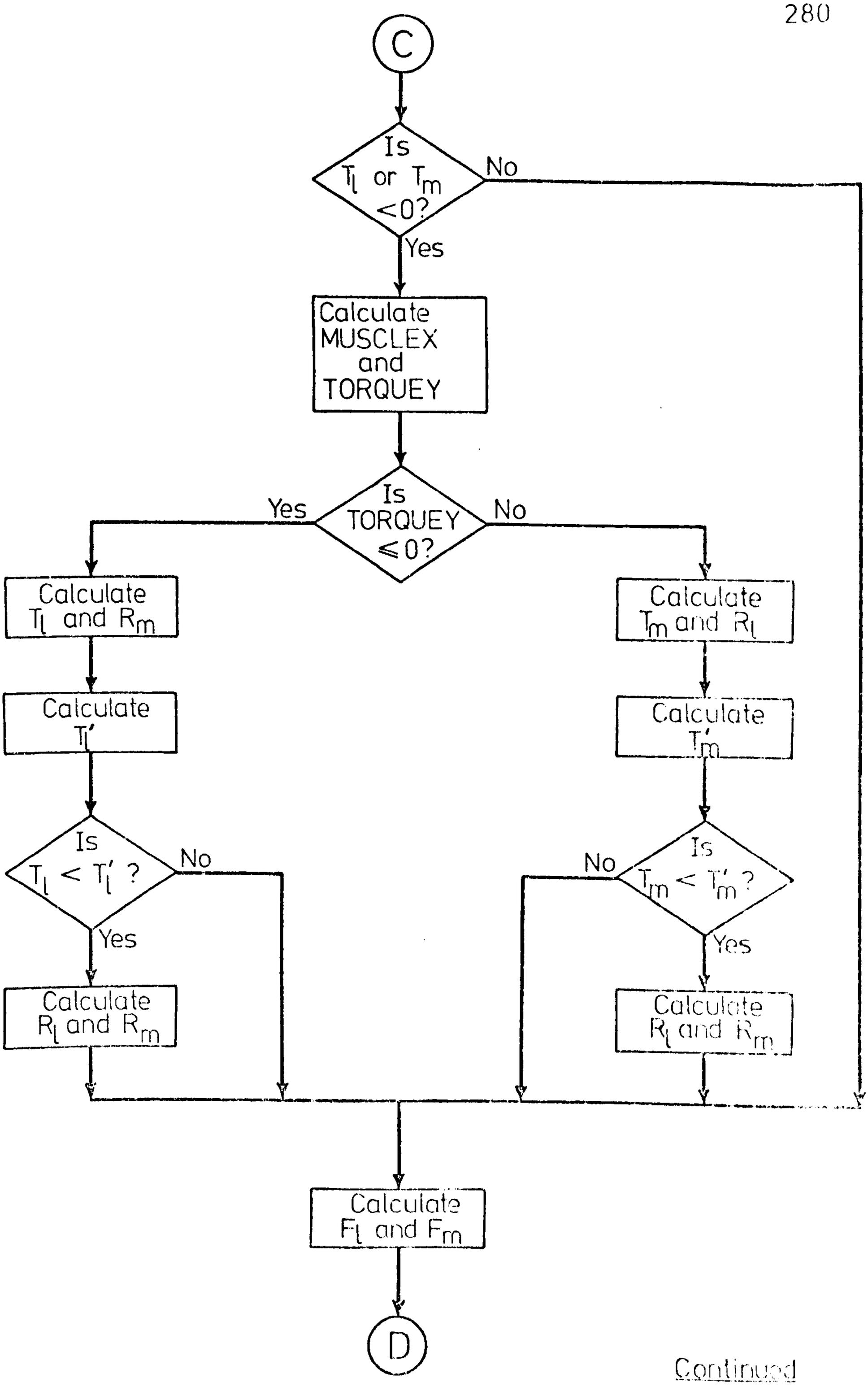
C
Is T_l or T_m <0?
No
Yes
Calculate MUSCLEX and TORQUEY
Is TORQUEY ≤0?
Yes
No
Calculate T_l and R_m
Calculate T_l'
Is $T_l < T_l'$?
No
Yes
Calculate R_l and R_m
Calculate T_m and R_l
Calculate T_m'
Is $T_m < T_m'$?
No
Yes
Calculate R_l and R_m
Calculate F_l and F_m
D

Continued

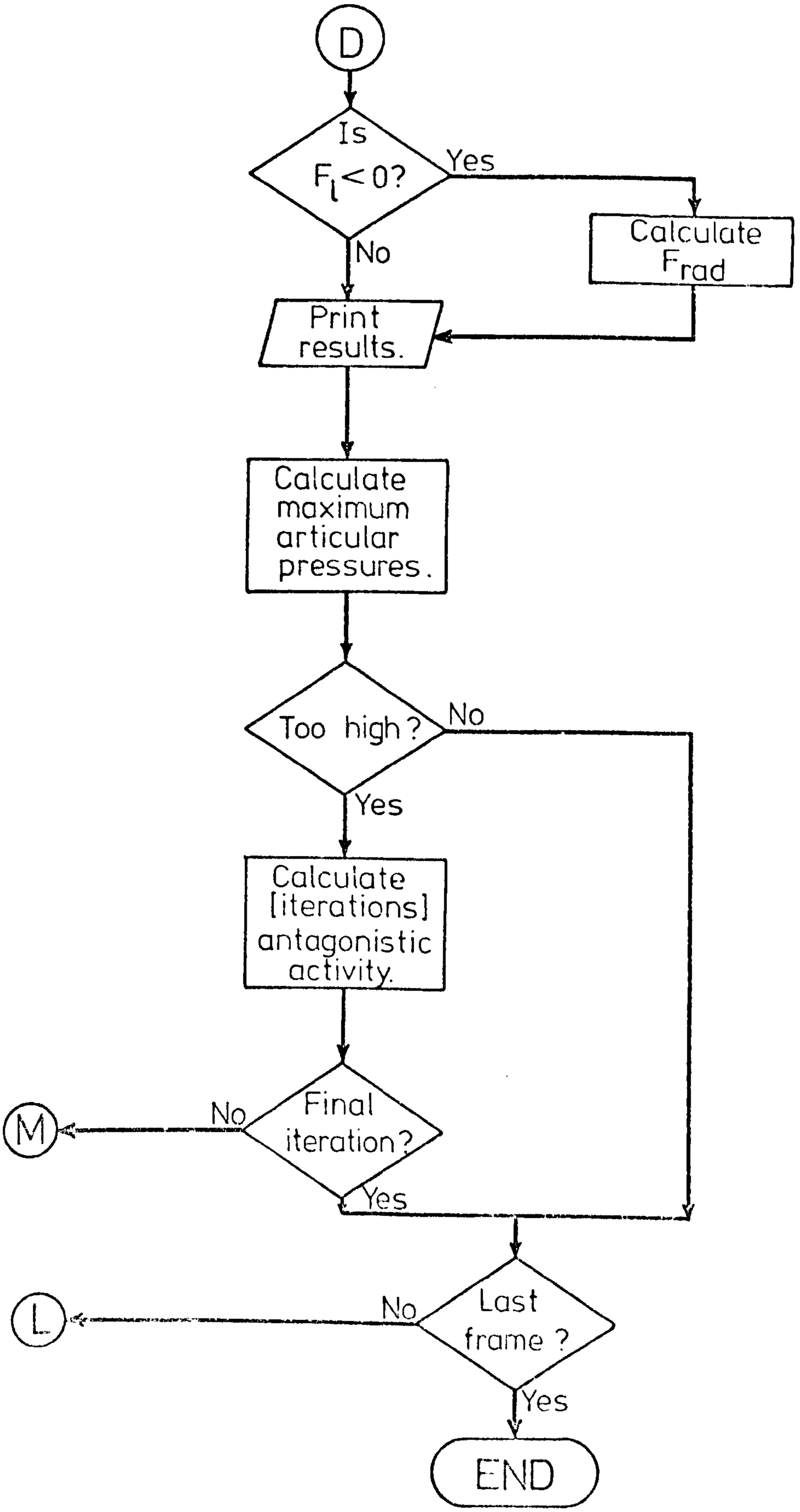

Figure A5·16: Sequence of events for "XNICOLPROG".

```
ER RXGIL20
SALGOLRUN XNICOLPROGB,*TR(0,XKET20C),*LP(0,RXGIL20),-
*MT(0,XKETDATA20),*MT(1,FXKET20),*MT(2,PLOTXGIL20(WRITE,LIMIT 10000)),-
PMDNICPOST,SECONDS 550
LF RXGIL20,*LP
EJ
****
```

Figure A5.17: Running file: RUNXGIL20.

```
?XKETDATA20;

FXKET20;

PLOTXGIL20;

1064
55
57.0
1735
94
34
70
68
26
50
451
331

1.00
6135
2565
3846
1092
10.00
0.020
4.00
50.0
```

Figure A5.18: Anthropometric data file: XKET20C.

```
'PMD'(ED,NICPOST)
'DUMPON'(ED)
'RUN'
'LIBRARY'(ED,SUBGROUPNGFA)
'LIBRARY'(ED,SUBGROUPNGPA)
'PROGRAM' (XXXXNICOL)
'INPUT'0=TR0
'OUTPUT'0=LP0
'TRACE'2

'BEGIN'
'PROCEDURE' WRITEBINARY(CHANNEL NUMBER,ARRAY,ARRAY NAME);
'VALUE' CHANNEL NUMBER;
'INTEGER' CHANNEL NUMBER;
'ARRAY' ARRAY;
'STRING' ARRAY NAME;
'EXTERNAL';

'PROCEDURE' CREATE(CHANNEL NUMBER,FILE NAME);
'VALUE' CHANNEL NUMBER;
'INTEGER' CHANNEL NUMBER;
'ARRAY' FILE NAME;
'EXTERNAL';

'PROCEDURE' READBINARY(CHANNEL NUMBER,ARRAY,ARRAY NAME);
'VALUE' CHANNEL NUMBER;
'INTEGER' CHANNEL NUMBER;
'ARRAY' ARRAY;
'STRING' ARRAY NAME;
'EXTERNAL';

'PROCEDURE' REWIND(CHANNEL NUMBER);
'VALUE' CHANNEL NUMBER;
'INTEGER' CHANNEL NUMBER;
'EXTERNAL';

'PROCEDURE' INSTRARR(S,A);
'STRING' S;
'ARRAY' A;
'EXTERNAL';

'PROCEDURE' INPUT(CHANNEL NUMBER,FILE NAME);
'VALUE' CHANNEL NUMBER;
'INTEGER' CHANNEL NUMBER;
'ARRAY' FILE NAME;
'EXTERNAL';


'ARRAY' C[1:3],D[1:3],E[1:3];
'INTEGER' K,I,J,P,M;
```

XNICOLPROG continued

```
WARNING:  P:=READCH;
'IF' P 'NE' CODE('('?')') 'THEN' 'GOTO' WARNING;
INSTRARR('(':')',C);
INPUT(40,C);
WARN2:
K:=READCH;
'IF' K 'NE' CODE('('EL')') 'THEN' 'GOTO' WARN2;
INSTRARR('(':')',D);
INPUT(41,D);
LOOKING:
M:=READCH;
'IF' M 'NE' CODE('('EL')') 'THEN' 'GOTO' LOOKING;
INSTRARR('(':')',E);
CREATE(42,E);


'COMMENT' NOW READS IN SUBJECT DATA STARTING WITH SUBJECT
NUMBER
THEN NUMBER OF FRAMES THEN DISTANCE AND HEIGHT OF CAMERAS;

'BEGIN'
'INTEGER' SN,N;
'REAL' MT,HT,DA,EL,KL,EP,BT,W,BET,FB,EB,M2,ZUHLE,BF,GRAV,L
EQ,M1,M,L1,L2,FCUT,TIME,
UUCLX,UUCLY,UUCLZ,URCLX,URCLY,URCLZ,UBIX,UBIY,UBIZ,UTIX,UT
IY,UTIZ,UBAX,UBAY,UBAZ,
FLIM,UXS,UYS,UZS,X2,Y2,Z2,UCX,UCY,UCZ,
RZ,RX,H,ITOT,RX1,RX2;
GRAV:=9810;

SN:=READ;
N:=READ;
MT:=READ;
HT:=READ;
DA:=READ;
EL:=READ;
EP:=READ;
BT:=READ;
W:=READ;
BET:=READ;
FB:=READ;
EB:=READ;
M2:=READ;
RZ:=READ;
RX1:=READ;
RX2:=READ;
H:=READ;
FCUT:=READ;
```

```
TIME:=READ;
RX:=READ;
FLIM:=READ;
M1:=0.024*MT;
L1:=0.42*FB;
L2:=EB;
M:=M1+M2;
LEQ:=(L1*M1+L2*M2)/M;
KL:=0.25*FB;
ITOT:=M1*(KL↑2+(LEQ-L1)↑2)+(M2*(L2-LEQ)↑2);
ITOT:=ITOT*10↑(-6);
ZUHLE:=3*EP/7;
BF:=FB/465;
EP:=EP/1000;
EB:=EB/1000;
EL:=EL/1000;


'BEGIN'

'REAL' 'ARRAY' MARK[1:N],CG[1:N,1:3],THETA[1:N,1:3],CRC[1:
21,1:3],LINACC[1:N,1:3],ANGACC[1:N,1:3];
'REAL' 'ARRAY' ZI[1:N],FORCE[1:6],LOT[1:17],CGX,CGY,CGZ,CG
X1,CGY1,CGZ1[1:200],
THETAX,THETAY,THETAZ,THETAX1,THETAY1,THETAZ1[1:200];


'BEGIN'
'REAL' AN,ANSQ,ACX,ACY,ACZ,AX,AY,AZ,FX,FY,FZ,FUX,FUY,FUZ,M
X,MY,MZ,MOMUX,MOMUY,MOMUZ,AA,BB,CC,XXX,YYY,ZZZ;
'REAL' AVZ,AVY,AVX,ANGVEL,DFORCE,AMEN,LINTR,PI,T1,T2,TT,B,
A,C1,C2,C3,C4,C5,C6,C7,C8,C9,FGX,FGY,FGZ;
'INTEGER' OPT,FAIL,E,F,G,K4,K5,JKJ,N1;
'REAL' 'ARRAY' PLDC,UNDC,TOTDC[1:3,1:3],FORPY,FORUL,MOMPY,
MOMUL,GOPT,ULPT[1:3,1:1],ACT1[1:200],
ACT2[1:200],ACT3[1:200],ACT4[1:200],ACT5[1:200],ACT6[1:200
],FACT1[1:200],FACT2[1:200],
FACT3[1:200],FACT4[1:200],FACT5[1:200],FACT6[1:200],WK1[1:
250],WK2[1:250];

'PROCEDURE' F01CKA(A,B,C,N,P,M,OPT,IFAIL);
'VALUE' N,P,M,OPT;
'INTEGER' N,P,M,OPT,IFAIL;
'ARRAY' A,B,C;
'ALGOL';
'COMMENT' DIGITAL FILTER FOLLOWS++++++++++;

'PROCEDURE' BUT4(Q,N,FCUT,T,W1,AD,W);
```

XNICOLPROG continued

```
'INTEGER' N;
'REAL' FCUT,T;
'ARRAY' Q,W1,AD,W;
'BEGIN'
AMEN:=0.0;
'FOR' K:=1 'STEP' 1 'UNTIL' N 'DO'
AMEN:=AMEN+Q[K]/N;
LINTR:=Q[N]-Q[1];
PI:=3.14159265;
T1:=SIN(PI*FCUT*T);
T2:=COS(PI*FCUT*T);
TT:=T1/T2;
A:=COS(PI/8.0)*TT;
B:=SIN(PI/8.0)*TT;
C1:=2*(A+B);
C2:=2*(A+B)↑2;
C3:=((A↑2+B↑2)*(B+A))*2;
C4:=(A↑2+B↑2)↑2;
C5:=1+C1+C2+C3+C4;
C6:=-4.0+4.0*C4-2.0*C1+2.0*C3;
C7:=6.0+6.0*C4-2.0*C2;
C8:=-4+2*C1-2*C3+4*C4;
C9:=1.0-C1+C2+C4-C3;
N1:=N+24;
'FOR' K:=N 'STEP' 1 'UNTIL' N+30 'DO'
AD[K]:=0.0;
'FOR' K:=1 'STEP' 1 'UNTIL' N 'DO'
AD[K+4]:=Q[K]-Q[1]-(K-1)*LINTR/N;
'FOR' K:=1 'STEP' 1 'UNTIL' 4 'DO'
'BEGIN'
AD[K]:=0.0;
W[K]:=0.0;
'END';
'FOR' K:=1 'STEP' 1 'UNTIL' N+20 'DO'
W[K+4]:=(C4*(AD[K+4]+4*AD[K+3]+6*AD[K+2]+4*AD[K+1]+AD[K])-
(W[K+3]*C6+W[K+2]*C7+W[K+1]*C8+W[K]*C9))/C5;
'FOR' JKJ:=1 'STEP' 1 'UNTIL' N+20 'DO'

'FOR' K:=1 'STEP' 1 'UNTIL' 4 'DO'
'BEGIN'
K4:=N1-K;
W1[K4+1]:=0.0;
W[K4+1]:=0.0;
'END';
'FOR' K:=1 'STEP' 1 'UNTIL' N+20 'DO'
'BEGIN'
K5:=N1-K;
W1[K5-3]:=(C4*(W[K5-3]+4*W[K5-2]+6*W[K5-1]+4*W[K5]+W[K5+1]
```

XNICOLPROG continued

```
)-(W1[K5-2]*C6+W1[K5-1]*C7+W1[K5]*C8+W1[K5+1]*C9))/C5;


'END';
'FOR' K:=1 'STEP' 1 'UNTIL' N 'DO'
W1[K]:=W1[K]+Q[1]+(K-1)*LINTR/N;
'END';
NEWLINE(9);
WRITETEXT('('('4S')'FRAME'('6S')'FTRI'('7S')'FBI'('7S')'F
RCL'('7S')'FUCL'('9S')'RF'('9S')'FL'('9S')'FM'('8S')'DFORC
E'('6S')'DIFF'('3S')'FRADIUS'('2C')')');
WRITETEXT('('('4S')'FRAME'('4S')'FUX'('7S')'FUY'('7S')'FU
Z'('6S')'MOMUX'('5S')'MOMUY'('5S')'MOMUZ'('2C')')');
K:=0;

'IF' SN 'LT' 1000 'THEN' 'GOTO' NEXT;

'COMMENT' THIS IS THE SECTION FOR TRANSDUCER STUDIES >>>>>
>>>>>>>;

AGAIN:
K:=K+1;
READBINARY(40,CRC,'('UNIT')');
READBINARY(41,FORCE,'('UNIT')');
'IF' FORCE[1] 'EQ' 9999 'AND' CRC[1,1] 'EQ' 999999 'THEN'
'GOTO' FILTERING;
'IF' CRC[1,1] 'EQ' 999999 'THEN' 'GOTO' ERROR6;
'IF' FORCE[1] 'EQ' 9999 'THEN' 'GOTO' ERROR6;

'BEGIN'


'FOR' J:=1 'STEP' 1 'UNTIL' 3 'DO'
'BEGIN'
PLOC[1,J]:=CRC[18,J];
PLOC[2,J]:=CRC[19,J];
PLOC[3,J]:=CRC[20,J];
GOPT[J,1]:=CRC[17,J];
UNOC[J,1]:=CRC[8,J];
UNOC[J,2]:=CRC[9,J];
UNOC[J,3]:=CRC[10,J];
'END';
'FOR' J:=1 'STEP' 1 'UNTIL' 3 'DO'
'BEGIN'
FORPY[J,1]:=-FORCE[J];
MOMPY[J,1]:=-FORCE[J+3];
'END';

OPT:=1;
FAIL:=0;
```

XNICOLPROG continued

```
E:=3;
F:=3;
G:=3;
FO1CKA(TOTDC,UNDC,PLDC,E,F,G,OPT,FAIL);
F:=1;
FO1CKA(FORUL,TOTDC,FORPY,E,F,G,OPT,FAIL);
FO1CKA(MOMUL,TOTDC,MOMPY,E,F,G,OPT,FAIL);
FO1CKA(ULPT,UNDC,GOPT,E,F,G,OPT,FAIL);
FGX:=-CRC[9,1]*M1*9.81;
FGY:=-CRC[9,2]*M1*9.81;
FGZ:=-CRC[9,3]*M1*9.81;
FUX:=FORUL[1,1];
FUY:=FORUL[2,1];
FUZ:=FORUL[3,1];
ACT4[K]:=MOMUL[1,1]+(FUZ*ULPT[2,1]-FUY*ULPT[3,1]-FGZ*L1)*0
.001;
ACT5[K]:=MOMUL[2,1]+(FUX*ULPT[3,1]-FUZ*ULPT[1,1])*0.001;
ACT6[K]:=MOMUL[3,1]+(FUY*ULPT[1,1]-FUX*ULPT[2,1]-FGX*L1)*0
.001;

ACT1[K]:=FUX+FGX;
ACT2[K]:=FUY+FGY;
ACT3[K]:=FUZ+FGZ;

'IF' K 'NE' 30 'THEN' 'GOTO' AGAIN;
'FOR' I:=1 'STEP' 1 'UNTIL' 3 'DO'
'BEGIN'
PRINT(K,8,0);
PRINT(TOTDC[I,1],2,4);
PRINT(TOTDC[I,2],2,4);
PRINT(TOTDC[I,3],2,4);
PRINT(MOMUL[I,1],14,2);
PRINT(ULPT[I,1],14,2);
NEWLINE(1);
'END';
'GOTO' AGAIN;
'FOR' J:=1 'STEP' 1 'UNTIL' N 'DO'
'BEGIN'

PRINT(K,6,0);
PRINT(ACT1[K],4,2);
PRINT(ACT2[K],4,2);
PRINT(ACT3[K],4,2);
PRINT(ACT4[K],4,2);
PRINT(ACT5[K],4,2);
PRINT(ACT6[K],4,2);
NEWLINE(1);
'END';
```

XNICOLPROG continued

```
FILTERING:
CRC[1,1]:=0.0;
BUT4(ACT1,N,FCUT,TIME,FACT1,WK1,WK2);
BUT4(ACT2,N,FCUT,TIME,FACT2,WK1,WK2);
BUT4(ACT3,N,FCUT,TIME,FACT3,WK1,WK2);
BUT4(ACT4,N,FCUT,TIME,FACT4,WK1,WK2);
BUT4(ACT5,N,FCUT,TIME,FACT5,WK1,WK2);
BUT4(ACT6,N,FCUT,TIME,FACT6,WK1,WK2);
NEWLINE(10);

'FOR' J:=1 'STEP' 1 'UNTIL' N 'DO'
'BEGIN'
PRINT(J,6,0);
PRINT(FACT1[J],4,2);
PRINT(FACT2[J],4,2);
PRINT(FACT3[J],4,2);
PRINT(FACT4[J],4,2);
PRINT(FACT5[J],4,2);
PRINT(FACT6[J],4,2);
NEWLINE(1);

'END';

'GOTO' RESTART;
'COMMENT' THE INERTIAL STUDIES ARE HERE HERE>>>>>>>>>>>>>>>>
>>>:


NEXT:

K:=K+1;
'IF' K 'GT' N 'THEN' 'GOTO' ACCELERATION;


READBINARY(40,CRC,'('UNIT')');
X2:=CRC[3,1]*CRC[2,1]+CRC[3,2]*CRC[2,2]+CRC[3,3]*CRC[2,3];
Y2:=CRC[4,1]*CRC[2,1]+CRC[4,2]*CRC[2,2]+CRC[4,3]*CRC[2,3];
Z2:=CRC[5,1]*CRC[2,1]+CRC[5,2]*CRC[2,2]+CRC[5,3]*CRC[2,3];
UXS:=CRC[8,1]*X2+CRC[9,1]*Y2+CRC[10,1]*Z2;
UYS:=CRC[8,2]*X2+CRC[9,2]*Y2+CRC[10,2]*Z2;
UZS:=CRC[8,3]*X2+CRC[9,3]*Y2+CRC[10,3]*Z2;

CG[K,1]:=CRC[11,1];

CG[K,2]:=CRC[11,2];
```

```
CG[K,3]:=CRC[11,3];

THETA[K,1]:=CRC[12,1];

THETA[K,2]:=CRC[12,2];

THETA[K,3]:=CRC[12,3];
'IF' K 'LT' 28 'OR' K 'GT' 32 'THEN' 'GOTO' NEXT;
PRINT(K,8,0);
PRINT(X2,3,4);
PRINT(Y2,3,4);
PRINT(Z2,3,4);
PRINT(UXS,20,4);
PRINT(UYS,3,4);
PRINT(UZS,3,4);
NEWLINE(1);
'GOTO' NEXT;

ACCELERATION:
'FOR' K:=1 'STEP' 1 'UNTIL' N 'DO'
'BEGIN'
CGX[K]:=CG[K,1];
CGY[K]:=CG[K,2];
CGZ[K]:=CG[K,3];
THETAX[K]:=THETA[K,1];
THETAY[K]:=THETA[K,2];
THETAZ[K]:=THETA[K,3];
'END';

'FOR' K:=1 'STEP' 1 'UNTIL' N 'DO'
'BEGIN'
PRINT(K,3,0);
PRINT(CG[K,1],4,3);
PRINT(CG[K,2],4,3);
PRINT(CG[K,3],4,3);
PRINT(THETA[K,1],2,3);
PRINT(THETA[K,2],2,3);
PRINT(THETA[K,3],2,3);
NEWLINE(1);
'END';


BUT4(CGX,N,FCUT,TIME,CGX1,WK1,WK2);
BUT4(CGY,N,FCUT,TIME,CGY1,WK1,WK2);
BUT4(CGZ,N,FCUT,TIME,CGZ1,WK1,WK2);
BUT4(THETAX,N,FCUT,TIME,THETAX1,WK1,WK2);
BUT4(THETAY,N,FCUT,TIME,THETAY1,WK1,WK2);
```

XNICOLPROG continued

```
BUT4(THETAZ,N,FCUT,TIME,THETAZ1,WK1,WK2);

'FOR' K:=1 'STEP' 1 'UNTIL' N 'DO'
'BEGIN'
CG[K,1]:=CGX1[K];
CG[K,2]:=CGY1[K];
CG[K,3]:=CGZ1[K];
THETA[K,1]:=THETAX1[K];
THETA[K,2]:=THETAY1[K];
THETA[K,3]:=THETAZ1[K];
'END';


NEWLINE(10);
'FOR' K:=1 'STEP' 1 'UNTIL' N 'DO'
'BEGIN'
PRINT(K,3,0);
PRINT(CG[K,1],4,3);
PRINT(CG[K,2],4,3);
PRINT(CG[K,3],4,3);
PRINT(THETA[K,1],2,3);
PRINT(THETA[K,2],2,3);
PRINT(THETA[K,3],2,3);
NEWLINE(1);

'END';


RESTART:

REWIND(40);
NEWLINE(9);
WRITETEXT('('''('4S')'FRAME'('6S')'FTRI'('7S')'FBI'('7S')'F
RCL'('7S')'FUCL'('9S')'RF'('9S')'FL'('9S')'FM'('8S')'RRFFF
'('8S')'DIFF'('7S')'FRAD'('2C')'')');
K:=0;
NEXTFRAME:

'IF' K 'EQ' N 'THEN' 'GOTO' TERMINATION;
INERTIAL:

K:=K+1;
READBINARY(40,CRC,'('UNIT')');
AN:=CRC[3,2]*CRC[8,2]+CRC[4,2]*CRC[9,2]+CRC[5,2]*CRC[10,2]
;
ANSQ:=AN*AN;
ZI[K]:=ARCTAN(SQRT((1/ANSQ)-1));
'IF' AN 'GT' 0.0 'THEN' ZI[K]:=180-(ZI[K]*180/3.14159);
```

XNICOLPROG continued

```
'IF' AN 'LE' 0.0 'THEN' ZI[K]:=ZI[K]*180/3.14159;


'IF' SN 'GT' 1000 'THEN' 'GOTO' FORCES;
'IF' K 'LT' 3 'THEN' 'GOTO' INERTIAL;
'IF' K 'GT' N-2 'THEN' 'GOTO' TERMINATION1;
'IF' CRC[1,1] 'EQ' 999999 'THEN' 'GOTO' TERMINATION;

'GOTO' ROBSONE;

'COMMENT' 999999 POINT DIFFERENTIATOR!!;
ACCEL(CG):

ACX:=F;

ACY:=G;

ACZ:=E;

ACCEL(THETA):

AX:=F;

AY:=G;

AZ:=E;

ROBSONE:

'COMMENT' THIS IS THE NEWTONIAN DIFFERENTIATOR!!**!!;
ACX:=(-CG[K-2,1]+16*CG[K-1,1]-30*CG[K,1]+16*CG[K+1,1]-CG[K
+2,1])/(12*0.0004);
ACY:=(-CG[K-2,2]+16*CG[K-1,2]-30*CG[K,2]+16*CG[K+1,2]-CG[K
+2,2])/(12*0.0004);
ACZ:=(-CG[K-2,3]+16*CG[K-1,3]-30*CG[K,3]+16*CG[K+1,3]-CG[K
+2,3])/(12*0.0004);

AX:=(-THETA[K-2,1]+16*THETA[K-1,1]-30*THETA[K,1]+16*THETA[
K+1,1]-THETA[K+2,1])/(12*0.0004);
AY:=(-THETA[K-2,2]+16*THETA[K-1,2]-30*THETA[K,2]+16*THETA[
K+1,2]-THETA[K+2,2])/(12*0.0004);
AZ:=(-THETA[K-2,3]+16*THETA[K-1,3]-30*THETA[K,3]+16*THETA[
K+1,3]-THETA[K+2,3])/(12*0.0004);

FX:=-M*ACX*10↑(-3);
```

XNICOLPROG continued

```
LINACC[K,1]:=ACX;
LINACC[K,2]:=ACY;
LINACC[K,3]:=ACZ;
ANGACC[K,1]:=AX;
ANGACC[K,2]:=AY;
ANGACC[K,3]:=AZ;
FY:=-M*(ACY+GRAV)*10↑(-3);

FZ:=-M*ACZ*10↑(-3);

MZ:=-(ITOT*AZ*CRC[13,3])-M*((ACY+GRAV)*(CG[K,1]-CRC[6,1])-
(ACX*(CG[K,2]

-CRC[6,2]))}*10↑(-6);

MY:=-(ITOT*AY*CRC[13,2])-M*(ACX*(CG[K,3]-CRC[6,3])-(ACZ*(C
G[K,1]

-CRC[6,1])))*10↑(-6);

MX:=-(ITOT*AX*CRC[13,1])-M*(ACZ*(CG[K,2]-CRC[6,2])-(ACY+GR
AV)*(CG[K,3]

-CRC[6,3]))*10↑(-6);

FUX:=(CRC[8,1]*FX)+(CRC[9,1]*FY)+(CRC[10,1]*FZ);

FUY:=(CRC[8,2]*FX)+(CRC[9,2]*FY)+(CRC[10,2]*FZ);

FUZ:=(CRC[8,3]*FX)+(CRC[9,3]*FY)+(CRC[10,3]*FZ);

MOMUX:=(CRC[8,1]*MX)+(CRC[9,1]*MY)+(CRC[10,1]*MZ);

MOMUY:=(CRC[8,2]*MX)+(CRC[9,2]*MY)+(CRC[10,2]*MZ);

MOMUZ:=(CRC[8,3]*MX)+(CRC[9,3]*MY)+(CRC[10,3]*MZ);

'GOTO' ANALYSIS;
NEWLINE(20);
PRINT(FX,4,3);
PRINT(FY,4,3);
PRINT(FZ,4,3);
PRINT(MX,14,5);
PRINT(MY,3,5);
PRINT(MZ,3,5);
NEWLINE(3);
PRINT(K,8,0);
```

XNICOLPROG continued

```
PRINT(FUX,4,2);
PRINT(FUY,4,2);
PRINT(FUZ,4,2);
PRINT(MOMUX,3,4);
PRINT(MOMUY,3,4);
PRINT(MOMUZ,3,4);
NEWLINE(3);
'FOR' I:=3 'STEP' 1 'UNTIL' 30 'DO'
'BEGIN'
PRINT(I,4,0);
'FOR' J:=1 'STEP' 1 'UNTIL' 3 'DO'
PRINT(LINACC[I,J],6,4);
'FOR' J:=1 'STEP' 1 'UNTIL' 3 'DO'
PRINT(ANGACC[I,J],4,4);
NEWLINE(1);
'END';
'GOTO' ANALYSIS;
FORCES:
FUX:=FACT1[K];
FUY:=FACT2[K];
FUZ:=FACT3[K];
MOMUX:=FACT4[K];
MOMUY:=FACT5[K];
MOMUZ:=FACT6[K];
ANALYSIS:
'COMMENT' PROGRAM NOW SOLVES SIMULTANEOUS EQUATIONS WITH
BRANCHES FOR BICEPS OR TRICEPS;
'BEGIN'
'REAL' EPS,TRIL,BIL,FTRI,FBI,FBR,BRL,XFT,YFT,ZFT,XFB,YFB,Z
FB,XFR,
PRESSL1,PRESSM1,DFORCEM,DFORCEL,PRESSL,PRESSM,AREAL,AREAM,
ZYEL,ZYEM,
X3,Y3,Z3,LLX,LLY,LLZ,MLX,MLY,MLZ,FBC,XFC,YFC,ZFC,BRAL,SITB
IC,RATIOL,RATIOM,BVAL,
YFR,ZFR,RATIO,FRCL,FUCL,CONDTRI,CONDBIC,RF,FL,FM,DIFF,TM,F
RAD,UCLL,RCLL,RFF,FUCLM,FRCLM;
'INTEGER' R,S,T,ANERROR,COUNT,TIMES,MUSCLE,REVS,TURNS;
'ARRAY' A[1:5,1:5],B[1:5,1:5],X[1:5,1:2],A1[1:4,1:4],B1[1:
4,1:4],
X1[1:4,1:2],V[1:7,1:9],W[1:7,1:9];

'PROCEDURE' F04AMA(A,X,B,M,N,P,EPS,ANERROR);
'VALUE' M,N,P,EPS;
'INTEGER' M,N,P,ANERROR;
'REAL' EPS;
'ARRAY' A,X,B;
'ALGOL';
```

XNICOLPROG continued

```
EPS:=2↑(-37);
ANERROR:=0;
R:=2;
S:=2;
T:=1;
'BEGIN'

'PROCEDURE' JTROT(AA,BB,CC);
'REAL' AA,BB,CC;
'BEGIN'
XXX:=0.866*AA+0.4962*BB+0.06089*CC;
YYY:=-0.50*AA+0.8595*BB+0.1055*CC;
ZZZ:=-0.12187*BB+0.9925*CC;
AA:=XXX;
BB:=YYY;
CC:=ZZZ;
'END';


'PROCEDURE' PRFORCE;
'BEGIN'
PRINT(K,4,3);
PRINT(FTRI,4,3);
PRINT(FBI,4,3);
PRINT(FRCL,4,3);
PRINT(FUCL,4,3);
PRINT(RF,4,2);
PRINT(FL,4,2);
PRINT(FM,4,2);
PRINT(RFF,4,2);
PRINT(DIFF,4,2);
PRINT(FRAD,4,2);
NEWLINE(1);
'GOTO' BREAK;
PRINT(UBIX,2,2);
PRINT(UBIY,2,2);
PRINT(UBIX,1,3);
PRINT(UBIY,1,3);
PRINT(UBIZ,1,3);
PRINT(UCX,1,3);
PRINT(UCY,1,3);
PRINT(UCZ,1,3);
PRINT(UTIX,1,3);
PRINT(UTIY,1,3);
PRINT(UTIZ,1,3);
PRINT(MOMUX,5,4);
PRINT(MOMUY,3,4);
```

XNICOLPROG continued

```
PRINT(MOMUZ,3,4);
NEWLINE(1);
BREAK:
LOT[1]:=K;

LOT[2]:=FTRI;
LOT[3]:=FBI;
LOT[4]:=FRCL;
LOT[5]:=FUCL;
LOT[6]:=RF;
LOT[7]:=FL;
LOT[8]:=FM;
LOT[9]:=RFF;
LOT[10]:=DIFF;
LOT[11]:=FRAD;
LOT[12]:=PRESSM;
LOT[13]:=PRESSL;
LOT[14]:=DFORCEM;
LOT[15]:=DFORCEL;
LOT[16]:=ZI[K];
LOT[17]:=SN;

WRITEBINARY(42,LOT,'('UNIT')');
'END';
SINMULTANEOUS:

TURNS:=0;
REVS:=0;
COUNT:=0;
MUSCLE:=0;
TIMES:=0;
DFORCE:=0.0;
'COMMENT'    COUNT MEANS------0----BOTH LIGS +VE
                                   0----ONE LIG +VE
                                   1----OTHER LIG +VE
                                   2----"RF" LATERAL
                                   3----"RF" MEDIAL;
'IF' CRC[1,1] 'EQ' 999999 'THEN' 'GOTO' TERMINATION;
'IF' CRC[1,1] 'NE' K 'THEN' 'GOTO' ERROR4;
MARK[K]:=CRC[1,2];
FRAD:=0.0;
DFORCE:=0.0;
FBI:=0.0;
FTRI:=0.0;
RF:=0.0;
RFF:=0.0;
DIFF:=0.0;
```

XNICOLPROG continued

```
DFORCEM:=0.0;
DFORCEL:=0.0;
PRESSM:=0.0;
PRESSL:=0.0;

PRESSM1:=0.0;
PRESSL1:=0.0;

UUCLX:=-EL*0.3238;
UUCLY:=-EB*0.01078;
UUCLZ:=-EP*0.2597;
URCLX:=-EL*0.3283;
URCLY:=-EB*0.07843;
URCLZ:=EP*0.5053;
UBIX:=-EL*0.3291;
UBIY:=-EB*0.1264;
UBIZ:=-EP*0.2018;
UTIX:=-EL*0.4131;
UTIY:=EB*0.07769;
UTIZ:=-EP*0.09406;
UBAX:=EL*0.1615;
UBAY:=-EB*0.7164;
UBAZ:=EP*0.1345;
UCX:=EL*0.2295;
UCY:=-EB*0.0559;
UCZ:=EP*0.02467;
```

```
X3:=CRC[14,1];
X3:=X3-UBIX;
Y3:=CRC[14,2]-UBIY;
Z3:=CRC[14,3]-UBIZ;
BIL:=SQRT(X3↑2+Y3↑2+Z3↑2);
XFB:=X3/BIL;
YFB:=Y3/BIL;
ZFB:=Z3/BIL;
'IF' YFB 'GE' 0.80 'THEN' YFB:=0.80;

'IF' XFB 'LE' 0.606 'AND' YFB 'GT' 0.0 'THEN' XFB:=0.606;
X3:=CRC[21,1]-UCX;
Y3:=CRC[21,2]-UCY;
Z3:=CRC[21,3]-UCZ;
BRAL:=SQRT(X3↑2+Y3↑2+Z3↑2);
XFC:=X3/BRAL;
YFC:=Y3/BRAL;
ZFC:=Z3/BRAL;
X3:=CRC[16,1]-UBAX;
Y3:=CRC[16,2]-UBAY;
```

```
Z3:=CRC[16,3]-UBAZ;
BRL:=SQRT(X3↑2+Y3↑2+Z3↑2);
XFR:=X3/BRL;
YFR:=Y3/BRL;
ZFR:=Z3/BRL;
X3:=CRC[15,1]-UTIX;
Y3:=CRC[15,2]-UTIY;
Z3:=CRC[15,3]-UTIZ;
TRIL:=SQRT(X3↑2+Y3↑2+Z3↑2);
XFT:=X3/TRIL;
YFT:=Y3/TRIL;
ZFT:=Z3/TRIL;
'IF' YFT 'LE' 0.00 'THEN' YFT:=0.00;
'IF' XFT 'LE' 1.00 'AND' YFT 'LE' 0.00 'THEN' XFT:=1.00;
MLZ:=-(EP*0.4105)-UUCLZ;
UCLL:=SQRT(MLZ↑2+UUCLY↑2+UUCLX↑2);
MLX:=-UUCLX/UCLL;
MLY:=-UUCLY/UCLL;
MLZ:=MLZ/UCLL;

LLZ:=(EP*0.5893)-URCLZ;
RCLL:=SQRT(LLZ↑2+URCLY↑2+URCLX↑2);
LLX:=-URCLX/RCLL;
LLY:=-URCLY/RCLL;
LLZ:=LLZ/RCLL;

'COMMENT'                    JOINT ROTATION NOW
                            THIRTY DEGREES THETAZ
                             SEVEN DEGREES THETAX;

JTROT(XFB,YFB,ZFB);
JTROT(XFR,YFR,ZFR);
JTROT(XFC,YFC,ZFC);
JTROT(XFT,YFT,ZFT);

JTROT(MOMUX,MOMUY,MOMUZ);
JTROT(FUX,FUY,FUZ);

JTROT(MLX,MLY,MLZ);
JTROT(LLX,LLY,LLZ);

JTROT(UUCLX,UUCLY,UUCLZ);
JTROT(URCLX,URCLY,URCLZ);
JTROT(UBIX,UBIY,UBIZ);
JTROT(UBAX,UBAY,UBAZ);
JTROT(UCX,UCY,UCZ);
JTROT(UTIX,UTIY,UTIZ);
```

```
'IF' MARK[K]=1 'THEN' 'GOTO' TRICALC;
'IF' MARK[K]=0 'THEN' 'GOTO' BICALC 'ELSE'
'GOTO' ERROR1;

TRICALC:
FTRI:=MOMUZ/((XFT*UTIY-YFT*UTIX));
'IF' FTRI 'LT' 0.0 'AND' MARK[K]=1 'THEN' 'GOTO' BICALC;
'IF' FTRI 'LT' 0.0 'AND' MARK[K]=0 'THEN' FTRI:=0.0;
FBI:=0.0;
FBR:=0.0;
FBC:=0.0;
MUSCLE:=100;
'GOTO' CARR;

BICALC:
'COMMENT' BICEPS=BRACHIALIS=BRACHIORADIALIS/2;
FBI:=MOMUZ/(XFB*UBIY-YFB*UBIX+XFR*UBAY/2-YFR*UBAX/2+XFC*UC
Y-YFC*UCX);
FBR:=FBI/2;
FBC:=FBI;
FTRI:=0.0;
'IF' FBI 'LT' 0.0 'AND' MARK[K]=0 'THEN' 'GOTO' TRICALC;
'IF' FBI 'LT' 0.0 'AND' MARK[K]=1 'THEN' FBI:=0.0;
MUSCLE:=10;
'GOTO' CARR;
RECALCT:
BVAL:=XFB*UBIY-YFB*UBIX+XFC*UCY-YFC*UCX+XFR*UBAY/2-YFR*UBA
X/2;
FTRI:=(MOMUZ-FBI*BVAL)/((XFT*UTIY-YFT*UTIX));
'IF' FTRI 'LT' 0.0 'THEN' FTRI:=0.0;
'GOTO' CARR;


RECALCB:
'COMMENT' BICEPS=BRACHIALIS=BRACHIORADIALIS*2;

FBI:=(MOMUZ-FTRI*(XFT*UTIY-YFT*UTIX))/(XFB*UBIY-YFB*UBIX+(
XFR*UBAY/2-YFR*UBAX/2)+(XFC*UCY-YFC*UCX));
'IF' FBI 'LT' 0.0 'THEN' FBI:=0.0;
FBR:=FBI/3;
FBC:=FBI;
CARR:

TURNS:=TURNS+1;
'IF' TURNS 'GT' 30 'THEN' 'GOTO' NEXTFRAME;
```

XNICOLPROG continued

```
'COMMENT' BOTH LIGAMENTS ACT;
RF:=0.0;
A[1,1]:=MLX;
A[1,2]:=LLX;
A[2,1]:=MLX*UUCLZ-MLZ*UUCLX;
A[2,2]:=LLX*URCLZ-LLZ*URCLX;
B[1,1]:=-FUX-(XFB+XFC+XFR/2)*FBI-XFT*FTRI;
B[2,1]:=-MOMUY-(XFB*UBIZ-ZFB*UBIX+(XFR*UBAZ-ZFR*UBAX)/2+XF
C*UCZ-ZFC*UCX)*FBI-(XFT*UTIZ-ZFT*UTIX)*FTRI;
F04AMA(A,X,B,R,S,T,EPS,ANERROR);
FUCL:=X[1,1];
FRCL:=X[2,1];
'IF' FUCL 'LE' 0.0 'OR' FRCL 'LE' 0.0 'THEN' 'GOTO' CARRYO
N1 'ELSE'
A1[1,1]:=0.906;
A1[1,2]:=0.906;
A1[2,1]:=-0.144*EP;
A1[2,1]:=-0.171*EP;
A1[2,2]:=0.26*EP;
B1[1,1]:=-FUY-MLY*FUCL-LLY*FRCL-(YFB+YFC+YFR/2)*FBI-YFT*FT
RI;
B1[2,1]:=(-MLZ*UUCLY+MLY*UUCLZ)*FUCL+(LLY*URCLZ-LLZ*URCLY)
*FRCL
+((-ZFB*UBIY+YFB*UBIZ-(ZFR*UBAY-YFR*UBAZ)/2-ZFC*UCY+YFC*UC
Z)*FBI)-MOMUX+(YFT*UTIZ-ZFT*UTIY)*FTRI;
F04AMA(A1,X1,B1,R,S,T,EPS,ANERROR);
FL:=X1[1,1];
FM:=X1[2,1];
DIFF:=FUZ+LLZ*FRCL+MLZ*FUCL-0.423*ABS(FL)+0.423*ABS(FM)
+(ZFB+ZFC+ZFR/2)*FBI+ZFT*FTRI;
PREFORCE;
'GOTO' NEXTFRAME;
CARRYON1:
SITBIC:=(ZFB*UBIY-YFB*UBIZ+ZFC*UCY-YFC*UCZ+
(ZFR*UBAY-YFR*UBAZ)/2)*FBI+(ZFT*UTIY-YFT*UTIZ)*FTRI;
CONDBIC:=MOMUY+(-ZFB*UBIX+XFB*UBIZ
-ZFC*UCX+XFC*UCZ+(XFR*UBAZ/2)-(ZFR*UBAX/3))*FBI+(XFT*UTIZ-
ZFT*UTIX)*FTRI;
'IF' CONDBIC 'LT' 0.0 'THEN' 'GOTO' BILAT 'ELSE' 'GOTO'
BIMED;
BIMED:


'COMMENT' MEDIAL LIGAMENT ACTS;
'GOTO' BIMED2;
BIMED1:
COUNT:=1;
BIMED2:
```

XNICOLPROG continued

```
TIMES:=TIMES+1;
FRCL:=0.0;
A[1,1]:=MLX;
A[1,2]:=-0.906;
A[2,1]:=-MLZ*UUCLX+MLX*UUCLZ;
A[2,2]:=-0.171*EP;
B[1,1]:=-FUX-((XFB+XFC+XFR/2)*FBI)-XFT*FTRI;
B[2,1]:=-CONDBIC;
F04AMA(A,X,B,R,S,T,EPS,ANERROR);
FUCL:=X[1,1];
RF:=X[2,1];
FUCLM:=CONDBIC/((MLZ*UUCLX-MLX*UUCLZ));
'IF' FUCL 'GE' FUCLM 'THEN' 'GOTO' CARRYON2 'ELSE'
FUCL:=FUCLM;
RF:=(-B[1,1]+MLX*FUCL)/1.504;
RFF:=RF/1.52;
'COMMENT' RFF IS THE BALANCING FORCE FOR SMALL MOMENTS;
CARRYON2:
A1[1,1]:=0.906;
A1[1,2]:=0.906;
A1[2,1]:=-0.171*EP;
A1[2,2]:=0.26*EP;
B1[1,1]:=-FUY-(MLY*FUCL)-(YFB+YFC+YFR/2)*FBI-YFT*FTRI;
B1[2,1]:=(-MLZ*UUCLY+MLY*UUCLZ)*FUCL-MOMUX-SITBIC;
F04AMA(A1,X1,B1,R,S,T,EPS,ANERROR);
FL:=X1[1,1];
FM:=X1[2,1];
RATIOL:=FL/RF;
'IF' RFF 'GT' 0.0 'THEN' RATIOM:=FM/RFF 'ELSE' RATIOM:=RX;
DFORCEM:=SQRT(FM↑2+RFF↑2);
DFORCEL:=SQRT(FL↑2+RF↑2);
DIFF:=(-0.423*(RF-RFF+ABS(FL)-ABS(FM))+FUZ+MLZ*FUCL
+(ZFB+ZFC+ZFR/2)*FBI)+ZFT*FTRI;
'IF' FL 'GT' 0.0 'THEN' 'GOTO' APRIN 'ELSE'
A1[1,1]:=-1.00;
A1[2,1]:=0.30*EP;
F04AMA(A1,X1,B1,R,S,T,EPS,ANERROR);
FRAD:=X1[1,1];
FM:=X1[2,1];
DFORCEL:=SQRT(FRAD↑2+RF↑2);
DFORCEM:=SQRT(FM↑2+RFF↑2);
RATIOL:=RX;
RATIOM:=FM/RFF;
'IF' RFF 'GT' 0.0 'THEN' RATIOM:=FM/RFF 'ELSE' RATIOM:=RX;
DIFF:=(-0.423*(RF-RFF-ABS(FM))+FUZ+MLZ*FUCL+(ZFB+ZFC+ZFR/2
)*FBI)+ZFT*FTRI;
APRIN:
PRFORCE;
```

XNICOLPROG continued

```
ZYEL:=ARCTAN(ABS(RATIOL));
ZYEM:=ARCTAN(ABS(RATIOM));
AREAL:=2*0.0088*ZYEL*EP↑2;
AREAM:=2*0.0189*ZYEM*EP↑2;
PRESSL:=DFORCEL/AREAL;
PRESSM:=DFORCEM/AREAM;
'IF' FL 'LT' 0.0 'THEN' PRESSL:=5000;
'IF' REVS 'GT' 0 'THEN' 'GOTO' ANTAGONISM;
'IF' PRESSL 'GT' 1250000 'OR' PRESSM 'GT' 1250000 'THEN'
'GOTO' ANTAGONISM;
'GOTO' NEXTFRAME;
BILAT:


'COMMENT' LATERAL LIGAMENT ACTS;
'GOTO' BILAT2;
BILAT1:
COUNT:=1;
BILAT2:
TIMES:=TIMES+1;
FUCL:=0.0;
A[1,1]:=LLX;
A[1,2]:=-0.906;
A[2,1]:=LLX*URCLZ-LLZ*URCLX;
A[2,2]:=0.26*EP;
B[1,1]:=-FUX-(XFB+XFC+XFR/2)*FBI-XFT*FTRI;
B[2,1]:=-CONDBIC;
F04AMA(A,X,B,R,S,T,EPS,ANERROR);
FRCL:=X[1,1];
RF:=X[2,1];
FRCLM:=-CONDBIC/((LLX*URCLZ-LLZ*URCLX));
'IF' FRCL 'GE' FRCLM 'THEN' 'GOTO' CARRYON3 'ELSE'
FRCL:=FRCLM;
RF:=(-B[1,1]+LLX*FRCL)/2.27;
RFF:=1.52*RF;
CARRYON3:
A1[1,1]:=0.906;
A1[1,2]:=0.906;
A1[2,1]:=-0.171*EP;
A1[2,2]:=0.26*EP;
B1[1,1]:=-FUY-LLY*FRCL-(YFR+YFC+YFR/2)*FBI-YFT*FTRI;
B1[2,1]:=(LLY*URCLZ-LLZ*URCLY)*FRCL-MOMUX-SITBIC;
F04AMA(A1,X1,B1,R,S,T,EPS,ANERROR);
FL:=X1[1,1];
FM:=X1[2,1];
RATIOM:=FM/RF;
'IF' RFF 'GT' 0.0 'THEN' RATIOL:=FL/RFF 'ELSE' RATIOL:=RX;
DFORCEL:=SQRT(FL↑2+RFF↑2);
```

XNJCOLPROG continued

```
DFORCEM:=SQRT(FM↑2+RF↑2);
DIFF:=(FUZ+0.423*(RF-RFF+ABS(FM)-ABS(FL))+LLZ*FRCL
+(ZFB+ZFC+ZFR/2)*FBI)+ZFT*FTRI;
'IF' FL 'GT' 0.0 'THEN' 'GOTO' PRINTL 'ELSE'
A1[1,1]:=-1.00;
A1[2,1]:=0.30*EP;
F04AMA(A1,X1,B1,R,S,T,EPS,ANERROR);
FRAD:=X1[1,1];
FM:=X1[2,1];
RATIOM:=FM/RF;
RATIOL:=RX;
DFORCEL:=SQRT(FRAD↑2+RFF↑2);
DFORCEM:=SQRT(FM↑2+RF↑2);
DIFF:=FUZ+0.423*(RF-RFF+ABS(FM))+LLZ*FRCL+(ZFB+ZFC+ZFR/2)*
FBI+ZFT*FTRI;
PRINTL:
PRFORCE;
'IF' FM 'LT' FLIM*(-2) 'AND' FM 'LE' 0.0 'THEN' RATIOM:=RX
;
ZYEL:=ARCTAN(ABS(RATIOL));
ZYEM:=ARCTAN(ABS(RATIOM));
AREAL:=2*0.0088*ZYEL*EP↑2;
AREAM:=2*0.0189*ZYEM*EP↑2;
PRESSL:=DFORCEL/AREAL;
PRESSM:=DFORCEM/AREAM;
'IF' FL 'LT' 0.0 'THEN' PRESSL:=5000;
'IF' REVS 'GT' 0 'THEN' 'GOTO' ANTAGONISM;
'IF' PRESSL 'GT' 1250000 'OR' PRESSM 'GT' 1250000 'THEN'
'GOTO' ANTAGONISM;
'GOTO' NEXTFRAME;



ANTAGONISM:
'IF' PRESSL 'GE' PRESSL1 'OR' PRESSM 'GE' PRESSM1 'THEN'
'GOTO' NEXTFRAME;
PRESSL1:=PRESSL;
PRESSM1:=PRESSM;

REVS:=REVS+1;
'IF' MUSCLE=10 'THEN' 'GOTO' BICEPS;
'IF' MUSCLE=100 'THEN' 'GOTO' TRICEPS 'ELSE' 'GOTO' ERROR1
;

BICEPS:
'COMMENT'                TRICEPS PROVIDES THE ANTAGONISM....
..........;
'IF' COUNT 'GT' 1 'THEN' 'GOTO' ATTENUATB;
```

```
'IF' PRESSL 'LE' 1250000 'AND' PRESSM 'LE' 1250000 'AND'
COUNT 'LT' 2 'THEN' 'GOTO' STARTATB;
'IF' PRESSL 'LE' 1250000 'AND' PRESSM 'LE' 1250000 'THEN'
'GOTO' ATTENUATB 'ELSE'
FTRI:=FTRI+20.0;
'GOTO' RECALCB;

STARTATB:
COUNT:=1;
ATTENUATB:
COUNT:=COUNT*2;
'IF' COUNT 'GT' 18 'THEN' 'GOTO' LAST 'ELSE'
'IF' PRESSL 'GT' 1250000 'OR' PRESSM 'GT' 1250000 'THEN'
FTRI:=FTRI+(20/COUNT);
'IF' PRESSL 'LE' 1250000 'AND' PRESSM 'LE' 1250000 'THEN'
FTRI:=FTRI-(20/COUNT);
'GOTO' RECALCB;


TRICEPS:
'IF' COUNT 'GT' 1 'THEN' 'GOTO' ATTENUATT;
'IF' PRESSL 'LE' 1250000 'AND' PRESSM 'LE' 1250000 'AND'
COUNT 'LT' 2 'THEN' 'GOTO' STARTATT;
'IF' PRESSL 'LE' 1250000 'AND' PRESSM 'LE' 1250000 'THEN'
'GOTO' ATTENUATT 'ELSE'
FBI:=FBI+20.0;
'GOTO' RECALCT;

STARTATT:
COUNT:=1;
ATTENUATT:
COUNT:=COUNT*2;
'IF' COUNT 'GT' 18 'THEN' 'GOTO' LAST 'ELSE'
'IF' PRESSL 'GT' 1250000 'OR' PRESSM 'GT' 1250000 'THEN'
FBI:=FBI+(20/COUNT);
'IF' PRESSL 'LE' 1250000 'AND' PRESSM 'LE' 1250000 'THEN'
FBI:=FBI-(20/COUNT);
'GOTO' RECALCT;


LAST:
PREFORCE;
'GOTO' NEXTFRAME;
```

XNICOLPROG continued

```
ERROR1: WRITETEXT('('MARKER%NOT%EQUAL%TO%1%OR%0%IN%FRAME%N
UMBER')');
PRINT(K,8,0);
NEWLINE(4);
'GOTO' NEXTFRAME;

ERROR2: WRITETEXT('('FORCE%LESS%THAN%ZERO%IN%FRAME%NUMBER'
)');
PRINT(K,8,0);
WRITETEXT('(''('2C')'MARKER%=%')');
PRINT(MARK[K],8,0);
NEWLINE(1);
'GOTO' NEXTFRAME;

ERROR3:
WRITETEXT('('NO%LIGAMENT%ACTION%IN%FRAME')');
PRINT(K,4,0);
NEWLINE(1);
'GOTO' NEXTFRAME;

ERROR5:
WRITETEXT('('SOMETHING%UP%WITH%RF%IN%FRAME')');
PRINT(K,3,0);
NEWLINE(1);
'GOTO' NEXTFRAME;

ERROR7:
WRITETEXT('('FM%AND%FL%ARE%NEGATIVE%IN%FRAME%')');
PRINT(K,4,0);
NEWLINE(1);
PREFORCE;
'GOTO' NEXTFRAME;
'END';

ERROR4:
WRITETEXT('('MISMATCHED%FRAME%TAPE%NUMBERS')');
'END';
NEWLINE(6);
'END';

ERROR6:
WRITETEXT('('DIFFERENT%DATA%LENGTHS')');
PRINT(K,8,0);
PRINT(FORCE[1],10,0);
PRINT(CRC[1,1],10,0);
NEWLINE(1);
```

XNICOLPROG continued

```
TERMINATION:
NEWLINE(20);
'FOR' K:=1 'STEP' 1 'UNTIL' N 'DO'
'BEGIN'
PRINT(K,8,0);
PRINT(ZI[K],4,4);
NEWLINE(1);
'END';
'GOTO' TERMINATE;
TERMINATION1:
'FOR' K:=3 'STEP' 1 'UNTIL' N-2 'DO'
'BEGIN'
PRINT(K,8,0);
PRINT(ZI[K],4,4);
NEWLINE(1);
'END';

TERMINATE:

'FOR' I:=1 'STEP' 1 'UNTIL' 17 'DO'
LOT[I]:=999999;

'END';
'GOTO' STOP;
FRAMEERROR: WRITETEXT('('''('2C')'FRAME%NUMBER%ERROR%AT%FRA
ME%')');
PRINT(K,4,0);
STOP:
'END';
'END';
'END';
```

XNICOLPROG concluded.

```
LO PLOTPROGB
TIME 450
AS *TRO,XKET20
AS *MT1,PLOTXGIL20
AS *LPO,XGIL20
LF XGIL20,*LP
RUN PLOT=XKET20
PICTURE XKET20,NARROW,KEEP,PLOTON
EJ
****
```

Figure A5.20: Running file: XGIL20PLOT.

```
'LIBRARY'(ED,SUBGROUPGOST)
'PROGRAM' (PLOTTER)
'INPUT'0=TR0
'OUTPUT'0=LP0
'TRACE'2
'BEGIN'
'PROCEDURE' PLOTCL(X,Y,PH,NC);
'VALUE' X,Y,NC;
'REAL' X,Y;
'INTEGER' PH,NC;
'EXTERNAL';
'INTEGER' 'ARRAY' D[1:2];
'PROCEDURE' READBINARY(CHANNEL NUMBER,ARRAY,ARRAY NAME);
'VALUE' CHANNEL NUMBER;
'INTEGER' CHANNEL NUMBER;
'ARRAY' ARRAY;
'STRING' ARRAY NAME;
'EXTERNAL';
'PROCEDURE' INSTRARR(S,A);
'STRING' S;
'ARRAY' A;
'EXTERNAL';
'PROCEDURE' INPUT(CHANNEL NUMBER,FILE NAME);
'VALUE' CHANNEL NUMBER;
'INTEGER' CHANNEL NUMBER;
'ARRAY' FILE NAME;
'EXTERNAL';
'PROCEDURE' BORDER;
'EXTERNAL';
'PROCEDURE' CRSET(NOSET);
'VALUE' NOSET;
'INTEGER' NOSET;
'EXTERNAL';
'PROCEDURE' CRSIZE(HEIGHT);
'VALUE' HEIGHT;
'REAL' HEIGHT;
'EXTERNAL';
'PROCEDURE' FRAME;
'EXTERNAL';
'PROCEDURE' LIMITS(XMIN,XMAX,YMIN,YMAX);
'VALUE' XMIN,XMAX,YMIN,YMAX;
'REAL' XMIN,XMAX,YMIN,YMAX;
'EXTERNAL';
'PROCEDURE' PLOTAS(X,Y,PHRASE);
'VALUE' X,Y;
'REAL' X,Y;
'STRING' PHRASE;
'EXTERNAL';
'PROCEDURE' PTPLOT(XV,YV,M,N,NC);
'VALUE' M,N,NC;
```

PLOTPROG continued

```
'REAL' 'ARRAY' XV,YV;
'INTEGER' M,N,NC;
'EXTERNAL';
'PROCEDURE' REGION(XMIN,XMAX,YMIN,YMAX);
'VALUE' XMIN,XMAX,YMIN,YMAX;
'REAL' XMIN,XMAX,YMIN,YMAX;
'EXTERNAL';
'PROCEDURE' POINT(X,Y);
'VALUE' X,Y;
'REAL' X,Y;
'EXTERNAL';
'PROCEDURE' GREND;
'EXTERNAL';
'INTEGER' K,M,N,P,SN;
'PROCEDURE' AXESSI(SPINCX,SPINCY);
'VALUE' SPINCX,SPINCY;
'REAL' SPINCX,SPINCY;
'EXTERNAL';
'ARRAY' C[1:3];
 'COMMENT' READ IN MAGTAPE NAME AS STRING
           THEN SUBJECT NO. AS STRING
           THEN SUBJECT NO. AND NO. OF FRAMES AS NUMBERS;
WARNING: P:=READCH;
'IF' P 'NE' CODE('('?')') 'THEN' 'GOTO' WARNING;
INSTRARR('(';')',C);
INPUT(40,C);

WARN2:P:=READCH;
'IF' P 'NE' CODE('('?')') 'THEN' 'GOTO' WARN2;
INSTRARR('(':')',D);
SN:=READ;
N:=READ;

'BEGIN'
'REAL' 'ARRAY' FNO,FBI,FTRI,FRCL,FUCL,RF,FL,FM,RFF,FRAD,DF
M,
DFL,ZI[1:N],LOT[1:17];
K:=0;
'IF' SN 'LT' 1000 'THEN' K:=2;
NEXTFRAME:
K:=K+1;
'IF' K 'GT' N 'THEN' 'GOTO' CALLPROC;
READBINARY(40,LOT,'('UNIT')');
'IF' LOT[1] 'NE' K 'THEN' 'GOTO' ERROR1;
'IF' LOT[12] 'NE' SN 'THEN' 'GOTO' ERROR2;
FNO[K]:=LOT[1];
FBI[K]:=LOT[3];
FTRI[K]:=LOT[2];
```

PLOTPROG continued

```
FRCL[K]:=LOT[4];
FUCL[K]:=LOT[5];
RF[K]:=LOT[6];
FL[K]:=LOT[7];
FM[K]:=LOT[8];
RFF[K]:=LOT[9];
FRAD[K]:=LOT[11];
DFM[K]:=LOT[14];
DFL[K]:=LOT[15];
ZI[K]:=LOT[16];
'GOTO' NEXTFRAME;
CALLPROC: 'COMMENT' ALL PLOTTING FILES ARE FULL
                    START TO CREATE PICTURE FILE NOW;
REGION(0.0,120.0,-100.0,1800.0);
LIMITS(0.0,8.0,0.0,5.5);
FRAME;


AXESSI(25.0,200.0);

CRSIZE(80.0);
CRSET(0);

PLOTCL(4.0,1400.0,D[1],4);
PLOTAS(4.0,1200.0,'('FBI')');
CRSET(4);
PTPLOT(FNO,FBI,1,N,57);
FRAME;
AXESSI(25.0,200.0);
CRSET(0);
PLOTCL(4.0,1400.0,D[1],4);
PLOTAS(2.0,1200.0,'('FTRI')');
CRSET(4);
PTPLOT(FNO,FTRI,1,N,57);

FRAME;
REGION(0.0,120.0,-100.0,3000.0);

AXESSI(25.0,200.0);

CRSET(0);
PLOTCL(4.0,1400.0,D[1],4);
PLOTAS(2.0,1700.0,'('FRCL')');
CRSET(4);
PTPLOT(FNO,FRCL,1,N,57);
FRAME;
AXESSI(25.0,200.0);
```

PLOTPROG continued

```
CRSET(0);
PLOTCL(4.0,1900.0,D[1],4);
PLOTAS(2.0,1700.0,'('FUCL')');
CRSET(4);
PTPLOT(FNO,FUCL,1,N,57);
'GOTO' BREAK;
FRAME;
AXESSI(25.0,200.0);
CRSET(0);
PLOTCL(4.0,1900.0,D[1],4);
PLOTAS(2.0,1700.0,'('RF')');
CRSET(4);
PTPLOT(FNO,RF,1,N,57);

FRAME;
REGION(0.0,120.0,-3000.0,2500.0);

CRSIZE(240.0);

AXESSI(25.0,500.0);
CRSET(0);
PLOTCL(4.0,2300.0,D[1],4);
PLOTAS(2.0,2100.0,'('FL')');
CRSET(4);
PTPLOT(FNO,FL,1,N,57);

FRAME;
REGION(0.0,120.0,-3000.0,5000.0);

AXESSI(25.0,500.0);
CRSET(0);
PLOTCL(4.0,4900.0,D[1],4);
PLOTAS(2.0,4700.0,'('FM')');
CRSET(4);
PTPLOT(FNO,FM,1,N,57);

FRAME;
REGION(0.0,120.0,-100.0,2000.0);

CRSIZE(80.0);

AXESSI(25.0,200.0);
CRSET(0);
PLOTCL(4.0,1900.0,D[1],4);
PLOTAS(2.0,1700.0,'('RFF')');
CRSET(4);
PTPLOT(FNO,RFF,1,N,57);
```

PLOTPROG continued

```
BREAK:
FRAME;
REGION(0.0,120.0,-100.0,2000.0);

AXESSI(25.0,200.0);
CRSET(0);

PLOTCL(4.0,1400.0,D[1],4);
PLOTAS(2.0,1200.0,'('FRAD')');
CRSET(4);
PTPLOT(FNO,FRAD,1,N,57);

FRAME;
REGION(0.0,120.0,-300.0,3000.0);

CRSIZE(160.0);

AXESSI(25.0,500.0);
CRSET(0);
PLOTCL(4.0,2900.0,D[1],4);
PLOTAS(2.0,2700.0,'('DFM')');
CRSET(4);
PTPLOT(FNO,DFM,1,N,57);

FRAME;
AXESSI(25.0,500.0);
CRSET(0);
PLOTCL(4.0,2900.0,D[1],4);
PLOTAS(2.0,2700.0,'('DFL')');
CRSET(4);
PTPLOT(FNO,DFL,1,N,57);

FRAME;
REGION(0.0,120.0,-20.0,180.0);

CRSIZE(6.0);

AXESSI(25.0,20.0);
CRSET(0);
PLOTCL(4.0,170.0,D[1],4);
PLOTAS(2.0,150.0,'('ZI')');
CRSET(4);
PTPLOT(FNO,ZI,1,N,57);

FRAME;
REGION(0.0,180.0,-100.0,1500.0);
```

PLOTPROG continued